AWARD NUMBER: W81XWH-14-1-0504

TITLE: The Oviduct and Serous Cancer Risk Assessment

PRINCIPAL INVESTIGATOR: Christopher P. Crum, MD

CONTRACTING ORGANIZATION: The Brigham and Women's Hospital, Inc
Boston, MA 02115

REPORT DATE: October 2015

TYPE OF REPORT: Annual

PREPARED FOR: U.S. Army Medical Research and Materiel Command
Fort Detrick, Maryland 21702-5012

DISTRIBUTION STATEMENT: Approved for Public Release;
Distribution Unlimited

REPORT DOCUMENTATION PAGE

Form Approved
OMB No. 0704-0188

1. REPORT DATE October 2015	**2. REPORT TYPE** Annual	**3. DATES COVERED** 30 Sep 2014 - 29 Sep 2015

4. TITLE AND SUBTITLE

The Oviduct and Serous Cancer Risk Assessment

5a. CONTRACT NUMBER

5b. GRANT NUMBER
W81XWH-14-1-0504

5c. PROGRAM ELEMENT NUMBER

6. AUTHOR(S)
Christopher P. Crum, MD

E-Mail: ccrum@partners.org

5d. PROJECT NUMBER

5e. TASK NUMBER

5f. WORK UNIT NUMBER

7. PERFORMING ORGANIZATION NAME(S) AND ADDRESS(ES)

The Brigham and Women's
Hospital, Inc
75 Francis Street
Boston MA 02115-61110

8. PERFORMING ORGANIZATION REPORT NUMBER

9. SPONSORING / MONITORING AGENCY NAME(S) AND ADDRESS(ES)

U.S. Army Medical Research and Materiel Command
Fort Detrick, Maryland 21702-5012

10. SPONSOR/MONITOR'S ACRONYM(S)

11. SPONSOR/MONITOR'S REPORT NUMBER(S)

12. DISTRIBUTION / AVAILABILITY STATEMENT

Approved for Public Release; Distribution Unlimited

13. SUPPLEMENTARY NOTES

14. ABSTRACT

The proposal was designed to address three issues. First could we identify stem cells from the fallopian tube, including from patients with high grade serous cancer (HGSC). Second, could we link the molecular abnormalities in cancer associated stem cells and validate them in pathologic material, specifically in what we feel are stem cell outgrowths or SCOUTs and third could we identify molecular alterations that would place the oviduct or the patient at risk for HGSC. In essence we wished to drill down to the cell of origin and link it to cancer risk, identifying an assay that could predict the presence of cancer by analyzing lower genital tract fluids or other samples.

15. SUBJECT TERMS

HGSC = high grade serous cancer; Fallopian tube; BRCA; Tp53, SCOUT = stem cell outgrowth; STIC = serous tubal intraepithelial carcinoma; STIN = serous tubal intraepithelial neoplasia.

16. SECURITY CLASSIFICATION OF:			**17. LIMITATION OF ABSTRACT**	**18. NUMBER OF PAGES**	**19a. NAME OF RESPONSIBLE PERSON** USAMRMC
a. REPORT Unclassified	**b. ABSTRACT** Unclassified	**c. THIS PAGE** Unclassified	Unclassified	293	**19b. TELEPHONE NUMBER** *(include area code)*

Standard Form 298 (Rev. 8-98)
Prescribed by ANSI Std. Z39.18

Table of Contents

Page

1. INTRODUCTION: The proposal was designed to address three issues. First could we identify stem cells from the fallopian tube, including from patients with high grade serous cancer (HGSC). Second, could we link the molecular abnormalities in cancer associated stem cells and validate them in pathologic material, specifically in what we feel are stem cell outgrowths or SCOUTs and third could we identify molecular alterations that would place the oviduct or the patient at risk for HGSC. In essence we wished to drill down to the cell of origin and link it to cancer risk, identifying an assay that could predict the presence of cancer by analyzing lower genital tract fluids or other samples.

KEYWORDS: HGSC = high grade serous cancer ; Fallopian tube; BRCA; Tp53, SCOUT = stem cell outgrowth; STIC = serous tubal intraepithelial carcinoma; STIN = serous tubal intraepithelial neoplasia.

2. ACCOMPLISHMENTS: All three goals were addressed in the past year with some modifications that will be addressed under part 5.

What were the major goals of the project?
The specific aims were as follows:

AIM 1: To grow stem cells from the tubes in culture from patients with and without malignancy and compare them.

AIM 2: Link the molecular disturbances seen in cancer associated stem cells and validate them in pathologic material specifically an entity we have described called the stem cell outgrowth or SCOUT.

AIM 3: Exploit the molecular alterations to make molecular probes that will detect those alterations that place women at risk for the disease, either in the fallopian tubes or lower genital tract fluids.

What was accomplished under these goals?

AIM 1: 1) Major activity: grow and identify fallopian stem cells in culture. 2) The specific objective was to identify stem cell characteristics that distinguished tumor associated (but normal appearing) stem cells from normal controls. 3) Significant results: a) We successfully cloned stem cells from normal fallopian tubes and showed that these cells were capable of both ciliated and squamous differentiation, in parallel with the histology of the fallopian tube (Figure 1). b) We generated a "stem cell" specific signature by comparing gene expression between undifferentiated stem cells and those grown on an air-liquid interface, which permitted ciliated differentiation. This was the first ever successful cloning, propagation and maturation of fallopian tube stem cells (Ning et al 2015). What we have <u>not</u> accomplished is to show that stem cells from normal tubal epithelium in cancers can be distinguished from epithelium from normal controls. b) An additional achievement, however, was to identify potential stem cell markers that were novel and might be used to unearth potential stem cells in the general pool of non-ciliated tubal epithelium (Yamamoto et al 2015). Moreover, we showed remarkable parallels between stem cells and putative stem cell outgrowths as well as HGSC precursors. c) Another added achievement was to demonstrate a parallel between immortalized and transformed stem cells and precursor and malignant HGSCs in the fallopian tube (Figures 2&3). D) Still another added achievement was a successful experiment focusing on propagating potential cancer stem cells. In this study we identified subpopulations that were Taxane resistant and were able to identify the same cells in Taxane naive cell cultures (Ning et al, submitted). This suggests that there is a small population of chemo-resistant cells that is inborn and not created by chemotherapy per se.

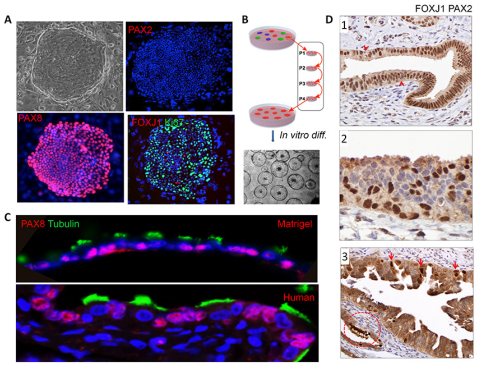

Figure 1. In-vivo propagation of fallopian tube stem cells with tissue correlates (See Ning 2015).

AIM 2 1) Major activity: Translating the *in vitro* findings to histopathology. 2) Objective : To link the disturbances in cancer associated stem cells and validate them in pathologic material. 3) Significant results: Although we have not yet shown that stem cells in cancer-associated tubes differ from normal, the expression profile of normal stem

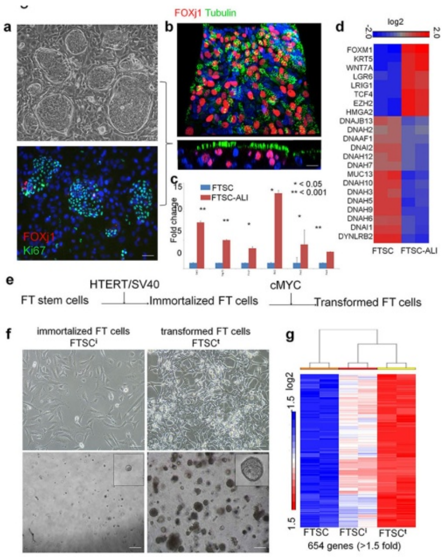

Figure 2. Upper panels show demonstrate differences in expression between putative stem cells and cell undergoing ciliated differentiation in vitro. Lower panel depicts progressive change of gene expression among FTSC, and immortalized and transformed FTSCs (See Yamamoto 2015).

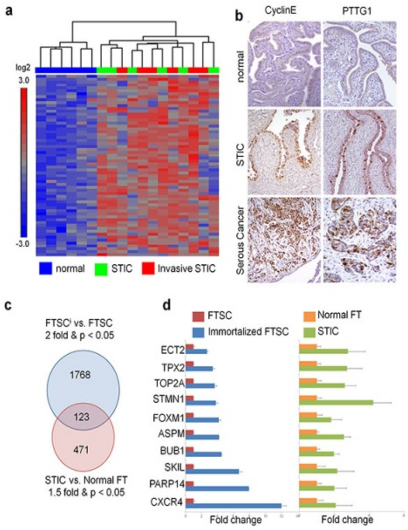

Figure 3. Overlapping gene expression between immortalized fallopian tube stem cells and serous carcinoma (See Yamamoto 2015).

cells closely resembles what we are seeing in so-called stem cell outgrowths (SCOUTs) as well as serous cancer precursors (STICs). This was shown in the papers by Ning et al and Yamamoto et al. Additional achievements: During these studies we took the opportunity to address an issue fundamental to the aims, which is the origin of HGSC. Because a high grade precancerous process (or STIC) can only be uncovered in subset of cancers, we felt it important to address this issue, the goal being to better understand the potential origins of these neoplasms. This was done in series of studies. First, we showed a potential dualistic model for HGSC with a lower association with STIC seen for tumors with certain morphologic features (Howitt 2015). This suggests that there could be more than one pathway to HGSC including one where STIC is not the primary predecessor. Second, we showed that certain histologic patterns were associated with specific gene mutations (Ritterhouse et al submitted) again suggesting more than one pathogenetic route to HGSC. Third, we recently sequenced cases with bilateral STICs and have shown them to contain *identical* p53 mutations. This raises the critical question that not all STICs develop *de novo* but may signify mucosal metastases from either the opposite tube or another site (Meserve et al unpublished). Fourth, we have concluded the preliminary phase of an ambitious project that has exhaustively analyzed fallopian tubes of women with HGSC but no STIC. In these tubes we have seen non-cancerous epithelium with p53 mutations. On comparing the p53 mutations status between these non-cancerous epithelia and the associated (and physically removed) HGSCs we have discovered identical mutations. This suggests the possibility that pelvic HGSCs could be derived from minor atypias within genetically altered stem cell proliferations (Figure 4). This has potentially profound implications in that it suggests that the serous carcinogenic sequence can initiate in the tube but continue beyond the confines of the oviduct at an unknown pelvic location (Soong et al unpublished).

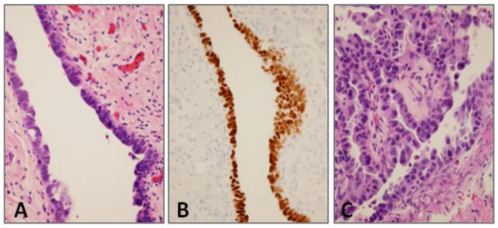

Figure 4. Mild tubal atypia (A) associated staining for p53 (B) is associated with a pelvic HGSC (C). Both lesions shared the same Tp53 mutation.

AIM3: 1) Major activity: To develop a means to detect the presence of biomarkers unique to serous cancer or serous cancer risk in the uterus or lower genital tract. Objective: To employ second generation sequencing (deep sequencing) to identify p53 mutations in the lower genital tract tissues or fluids that would indicate the presence of an upper genital tract neoplasm. Significant results: We decided to use a novel approach to this problem by first identifying cases of HGSC and then searching the archive for prior formalin-fixed, paraffin embedded endometrial specimens from diagnostic procedures. DNA from serial sections of this material was extracted and then analyzed on a platform targeting p53 mutations. These mutations were compared to those found in the tumors at a later date. We identified 5 samples in which information was available. In two (40%) we detected p53 mutation in prior endometrial samples that matched those found in the subsequent tumor (Figure 5). The intervals from detecting the mutations to the diagnosis of the tumors were 2 weeks and 2 months.

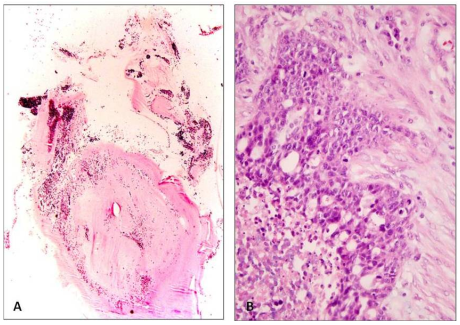

Figure 5. (A) An endometrial sample contains mostly mucus and a few cells. Extracted DNA from this archival sample revealed a p53 mutation identical to that found in a HGSC diagnosed over 2 months later.

What opportunities for training and professional development has the project provided?

This project has provided extensive training opportunities. Dr. Brooke Howitt, a co-investigator, is a junior attending (instructor) who was actively involved in study design and execution. Moreover, she was engaged in project planning with four resident/fellows (Kyle Strickland, Lauren Ritterhouse, Emily Meserve, Rinda Soong) and supervised them on these projects. Fellows were introduced to DNA extraction, data analysis, second generation sequencing etc. and three are interested in a career in academic gynecologic pathology. All of these individuals have presented their data at the USCAP meeting (in Boston in 2015) and/or have abstracts submitted on the above projects to the USCAP meeting scheduled for Seattle in 2016. They also will present their results in a departmental seminar scheduled for February 2016. The list of abstracts presented an d planned is below.

The contributions of two additional members of the team were supported partially by this grant. The first was a summer college (From Washington University) student, Brennan Beeler, who is planning a career in research. A second is a Danish medical student taking a year off for research, Helena Dietzel. She has been working closely with Dr. Howitt, creating an important opportunity for Ms Dietzel as well as for Dr. Howitt to mentor a younger colleague.

How were the results disseminated to communities of interest?

The PI has participated in an outreach program to disseminate information on ovarian cancer. (http://www.brighamandwomens.org/Departments_and_Services/obgyn/Services/ovarian-cancer-treatment.aspx) Dr. Howitt has spent time in both Rwanda and Haiti performing outreach activities in the past year.

What do you plan to do during the next reporting period to accomplish the goals?

For year two the following projects are planned.

AIM1: We have a series of stem cell markers that have been unearthed by the in vitro comparison of FTSCs and FTSCs in an air-liquid interface. The protein atlas will be surveyed and 20 candidates will be identified and used to probe normal fallopian tube mucosa. We will focus primarily on markers that overlap in the same cells or region in an effort to find a consistently reproducible putative stem cell signature. Once we accomplish this we will do the following: 1) Map the distribution of putative stem cells in the fallopian tube as a function of location and age including reproductive status. The goal will be to determine if putative stem cells concentrate in particular areas of the fallopian tube and whether their distribution and frequency are altered by factors such as hormones, pregnancy, and menopause. 2) Confirm the presence of stem cell markers in lesions at variable stages of serous carcinogenesis. This will entail analysis of p53 signatures, tubal intraepithelial neoplasms and STICs.

AIM2: We are going to further explore the concept that early atypias in the fallopian tube are capable of spreading to the peritoneum. Our plan will be to analyze 25 cases of HGSC with negative fallopian tubes and concentrate on identifying early p53 mutations signatures that can be linked to HGSC. To accomplish this we will 1) microdissect non-malignant p53 positive clonal expansions in the tube and determine the nature of their mutations by next generation sequencing. The mutations will be compared to those of the concurrent serous carcinomas. 2) We will compare this group with 25 cases of HGSC associated with STICs that co-exist with less marked atypias, i.e. STICs most likely to represent primary tubal precursors. The goal will be to determine if BRCA status, the age of tumor presentation and distribution of tumor between the two groups highlights important differences.

AIM3: We will further expand the concept that archival material can be probed for p53 mutations to predict the presence of an intraabdominal HGSC. We will expand the pilot to 30 cases of HGSC that were preceded by a normal curetting and assess both HGSC and the prior material for matching mutations. This will be accomplished by next generation sequencing.

4. IMPACT: The PI and his colleagues were the first to provide solid evidence that a high percentage of high-grade serous carcinomas (HGSC) in the pelvis arise in the fallopian tube. This work began in 2005 and has been associated with a paradigm shift in this field. A testimony to the extent and speed of this evolution can be seen in the sudden increase in programs targeting the fallopian tube and funding opportunities (many from the DOD) that have been placed on this conceptual framework. This pilot project was designed specifically to address the concept that there is an underpinning of unique stem cell biology that confers risk of HGSC. If such is true, we would expect to see unique differences between normal tubes associated with HGSCs and controls. We have yet to answer this particular question but we have made major advances in our understanding of the stem cell populations in the fallopian tube, which is a necessary prerequisite to any such endeavors. Taking into account the additional studies supported by this pilot, the areas of potential impact can be summarized as follows.

Impact on the principle and other disciplines

1. Stem cell biology: If we assume that stem cells are the vulnerable targets in serous carcinogenesis we must identify them and then determine if their numbers are increased in patients with cancer and map their distribution in the fallopian tubes throughout reproductive and postmenopausal life. The recent papers by Ning et al and Yamamoto et al provide the research community ("the principle discipline") with abundant evidence for further development of this concept. Other disciplines have clearly received benefit as evidenced by the parallel studies performed in the pulmonary and gastrointestinal tract by our collaborators Wa Xian and Frank McKeon. This concept of "stem cell" has been re-named "ground state" cells in their studies.

2. The origins of HGSC: The additional projects that query the role of the fallopian tube in the genesis of a serous carcinogenic sequence are vital to our understanding of where these tumors come from. The questions we pose are STICs really a primary process or an intramucosal metastasis and are we overestimating the importance of STICs?" and is there some other source of HGSC that we need to understand before we pursue prophylactic salpingectomy? It is highly likely that not all STICS are primary tubal neoplasm (i.e. they could in some instances represent tumor that migrates from another site) but this re-emphasized the need to determine where in the carcinogenic sequence that *tumorigenesis* initiates. The general assumption is that STICs develop and then invade or spread to pelvic surfaces. Another possibility is that altered stem cells invade or spread prior to becoming STICs and emerge suddenly in an *extra-ovarian* site. We have initiated studies to answer both of these questions and the answers to both are germane to the notion that prophylactic salpingectomy will have the desired effect of preventing HGSC.

3. The potential discovery of gene mutations in archival material prior to the onset of HGSC: We have preliminary data that supports the possibility that the simple screening of an archival specimen will detect mutations that indicate the presence of an undiagnosed HGSC. The degree to which this will interrupt the natural history of this disease remains unclear but it adds to emerging data indicating that early diagnosis of HGSC is possible by analyzing routine specimens from the lower genital tract.

What was the impact on technology transfer?
Nothing to report

What was the impact on society beyond science and technology?

2. Origins of HGSC: The management of women with germ-line mutations in BRCA1 and BRCA2 is in a state of flux as the question remains as to the degree of benefit that can be expected from prophylactic salpingo-oophorectomy. This population has been keenly aware of the data emerging in this field and is making decisions about cancer prevention around the concept that most of these tumors could originate from the fallopian tube.

3. The potential discovery of gene mutations in archival material prior to the onset of HGSC: Any lay person can imagine the potential value of a test for ovarian cancer that can be applied to their endometrial biopsy.

5. CHANGES/PROBLEMS:

Changes in the direction and scope of the projects

AIM 1: No significant changes. The original goal was to identify alterations in fallopian tube stem cells that distinguish tubes associated with HGSCs from those of control fallopian tubes. We did not demonstrate this in the data obtained so far but we have identified a stem-cell signature (albeit one that will require pruning). While it is unlikely that we will identify differences in stem cell between cancer associated and control tubes, we have the tools to more precisely morphologically define stem or "ground state" cells in the tube. If we accomplish this then we can determine whether these cells are in greater abundance in the fimbria. If not we will be positioned to retrieve genetic information from these disparate stem cell populations and search for factors that influence stem cell vulnerability. No delays or problems are anticipated and there will be no change in expenditures.

AIM2: We have succeeded in translating in vitro fallopian tube stem cells to histopathology for the most part. We will plan to shift our emphasis to address whether early precursor lesions that emerge from these stem cell are able to initiate a progression sequence to HGSC in or beyond the tube. There will be no delays or human subject issues. We do however anticipate some increase in costs that were incurred in the first year of funding. Because of the exhaustive sampling of multiple fallopian tubes to unearth the small foci suspected of being precursors to HGSC we have incurred considerable costs for tissue sectioning.

AIM3: This is essentially unchanged other than the novel approach to detecting mutations in *archival* material. This material is readily available and we anticipate no changes in cost.

Changes in funding for which we are requesting approval

No changes in funding are anticipated.

6. PRODUCTS: List any products resulting from the project during the reporting period. Examples of products include:

Publications

Yamamoto Y, Ning G, Howitt BE, Mehra K, Wu L, Wang X, Hong Y, Kern F, Wei TS, Zhang T, Nagarajan N, Basuli D, Torti S, Brewer M, Choolani M, McKeon F, Crum CP, Xian W. In Vitro and In Vivo Correlates of Physiologic and Neoplastic Human Fallopian Tube Stem Cells. J Pathol. 2015 Sep 28. [Epub ahead of print]

Novak M, Lester J, Karst AM, Parkash V, Hirsch MS, Crum CP, Karlan BY, Drapkin R. Stathmin 1 and p16INK4A are sensitive adjunct biomarkers for serous tubal intraepithelial carcinoma. Gynecol Oncol. 2015 Jul 20.. [Epub ahead of print]

Worley MJ Jr, Liu S, Hua Y, Kwok JS, Samuel A, Hou L, Shoni M, Lu S, Sandberg EM, Keryan A, Wu D, Ng SK, Kuo WP, Parra-Herran CE, Tsui SK, Welch W, Crum C, Berkowitz RS, Ng SW. Molecular changes in endometriosis-associated ovarian clear cell carcinoma. Eur J Cancer. 2015 Sep;51(13):1831-42.

Wang X, Yamamoto Y, Wilson LH, Zhang T, Howitt BE, Farrow MA, Kern F, Ning G, Hong Y, Khor CC, Chevalier B, Bertrand D, Wu L, Nagarajan N, Sylvester FA, Hyams JS, Devers T, Bronson R, Lacy DB, Ho KY, Crum CP, McKeon F, Xian W. Cloning and variation of ground state intestinal stem cells. Nature. 2015 Jun 11;522(7555):173-8.

Ivanova A, Loo A, Tworoger S, Crum CP, Fan I, McLaughlin JR, Rosen B, Risch H, Narod SA, Kotsopoulos J. Ovarian cancer survival by tumor dominance, a surrogate for site of origin. Gynecol Oncol, in press.

Howitt BE, Hanamornroongruang S, Lin DI, Conner JE, Schulte S, Horowitz N, Crum CP, Meserve EE. Evidence for a Dualistic Model of High-grade Serous Carcinoma: BRCA Mutation Status, Histology, and Tubal Intraepithelial Carcinoma. Am J Surg Pathol. 2015 Mar;39(3):287-93. PMID:25581732

Zuo W, Zhang T, Wu DZ, Guan SP, Liew AA, Yamamoto Y, Wang X, Lim SJ, Vincent M, Lessard M, Crum CP, Xian W, McKeon F. p63(+)Krt5(+) distal airway stem cells are essential for lung regeneration. Nature. 2015 Jan 29;517(7536):616-20. PMID:25383540

Ning G, Bijron JG, Yamamoto Y, Wang X, Howitt BE, Herfs M, Yang E, Hong Y, Cornille M, Wu L, Hanamornroongruang S, McKeon FD, Crum CP, Xian W. The PAX2-null immunophenotype defines multiple lineages with common expression signatures in benign and neoplastic oviductal epithelium. J Pathol. 2014 Dec;234(4):478-87. PMID:25130537

Books or non-periodical publications

Berek JS, Crum C, Friedlander M. Cancer of the ovary, fallopian tube, and peritoneum.
Int J Gynaecol Obstet. 2015 Oct;131 Suppl 2:S111-22.

Poole EM, Rice MS, Crum CP, Tworoger SS. Salpingectomy as a potential ovarian cancer risk-reducing procedure. J Natl Cancer Inst. 2015 Jan 27;107(2). PMID:25628373

Kaspar HG, Crum CP. The utility of immunohistochemistry in the differential diagnosis of gynecologic disorders. Arch Pathol Lab Med. 2015 Jan;139(1):39-54. PMID:25549143 Review

Presentations, conference publications

Past presentations

Jelena Mirkovic, Amy DiVasta, Stacey Missmer, Brooke Howitt, Christopher Crum, Marc Laufer, Sara Vargas. The Histologic Spectrum of Adolescent Endometriosis. USCAP meeting, Boston, March 2015

Andre Pinto, Brooke Howitt, Christopher Crum. The Variable Spectrum of Tubal Intraepithelial Neoplasia in Women With High Grade Serous Carcinoma. USCAP meeting, Boston, March 2015

Lauren Ritterhouse, Christopher Crum, Lynette Sholl, Neal Lindeman, Brooke Howitt. Morphologic and Molecular Evaluation of Extra-Uterine Mullerian Carcinoma. USCAP meeting, Boston, March 2015

Submitted presentations for the USCAP 2016 meeting

Kyle C Strickland, Emily Meserve, Helena M Ditzel, Frank Campbell , Alexander Miron, Christopher P Crum, and Brooke E Howitt. Detection of Tumor Specific TP53 Signatures from Archival Endometrial Biopsies Prior to the Diagnosis of HighGrade Serous Carcinoma.

Emily E Meserve, Alexander Miron, Helena Ditzel, Andre Pinto, Frank Campbell, Brooke E Howitt, Christopher P Crum. Identical TP53 mutation in “bilateral” serous tubal intraepithelial carcinoma (STIC)

Emily E Meserve, Jelena Mirkovic, James R Conner , Eric Yang, Brooke E Howitt, Christopher P Crum. Detection of serous tubal intraepithelial carcinoma (STIC) in incidentally removed fallopian tubes from low-risk women.

Thing Rinda Soong, Christopher P Crum, Brooke E Howitt. Serial Sectioning of Distal Fallopian Tubes and its Role in the Discovery of Occult Serous Tubal Intraepithelial Carcinoma in Women with High Grade Ovarian Serous Carcinoma.

7. PARTICIPANTS & OTHER COLLABORATING ORGANIZATIONS

Individuals who worked on the project

Collaboration with Wa Xian at the Jackson Laboratory: We have a long-standing collaboration with Wa Xian who was at the Jackson Laboratory the past year. Her group received de-identified specimens for cell culture under an IRB approved protocol (included). Her laboratory was funded by the Jackson Laboratory and she did not receive funds from this grant. She has now moved to the University of Texas at Houston. We are currently not sending specimens pending the approval of an MTA, after which an amendment will be issued to the IRB.

Changes in active other support of the PD/PI(s) or senior/key personnel since the last reporting period?

None

What other organizations were involved as partners?
Nothing to report.

8. SPECIAL REPORTING REQUIREMENTS: None

9. APPENDIX:

Selected Manuscripts:

Yamamoto Y, Ning G, Howitt BE, Mehra K, Wu L, Wang X, Hong Y, Kern F, Wei TS, Zhang T, Nagarajan N, Basuli D, Torti S, Brewer M, Choolani M, McKeon F, Crum CP, Xian W. In Vitro and In Vivo Correlates of Physiologic and Neoplastic Human Fallopian Tube Stem Cells. J Pathol. 2015 Sep 28. [Epub ahead of print]

Wang X, Yamamoto Y, Wilson LH, Zhang T, Howitt BE, Farrow MA, Kern F, Ning G, Hong Y, Khor CC, Chevalier B, Bertrand D, Wu L, Nagarajan N, Sylvester FA, Hyams JS, Devers T, Bronson R, Lacy DB, Ho KY, Crum CP, McKeon F, Xian W. Cloning and variation of ground state intestinal stem cells. Nature. 2015 Jun 11;522(7555):173-8.

Howitt BE, Hanamornroongruang S, Lin DI, Conner JE, Schulte S, Horowitz N, Crum CP, Meserve EE. Evidence for a Dualistic Model of High-grade Serous Carcinoma: BRCA Mutation Status, Histology, and Tubal Intraepithelial Carcinoma. Am J Surg Pathol. 2015 Mar;39(3):287-93. PMID:25581732

Ning G, Bijron JG, Yamamoto Y, Wang X, Howitt BE, Herfs M, Yang E, Hong Y, Cornille M, Wu L, Hanamornroongruang S, McKeon FD, Crum CP, Xian W. The PAX2-null immunophenotype defines multiple lineages with common expression signatures in benign and neoplastic oviductal epithelium. J Pathol. 2014 Dec;234(4):478-87. PMID:25130537

In Vitro and In Vivo Correlates of Physiologic and Neoplastic Human Fallopian Tube Stem Cells

Journal:	*The Journal of Pathology*
Manuscript ID:	Draft
Wiley - Manuscript type:	Original Research Article
Date Submitted by the Author:	n/a
Complete List of Authors:	Crum, Christopher; Brigham and Women's Hospital, Pathology yamamoto, yusuke; Jackson laboratory, Genomic Medicine Ning, Gang; Jackson laboratory, Genomic Medicein; Jackson laboratory, Genomic Medicine Howitt, Brooke; Brigham and Women's Hospital, Pathology Mehra, Karishma; Yale University Hospital, Medicine Wu, Lingyan; Genome Institute of Singapore, Stem Cell Biology Wang, Xia; Jackson Laboratory, Genomic Medicine Hong, Yue; Jackson Laboratory, Genomic Medicine Kern, Florian; Genome Institute of Singapore, Stem Cell Biology Wei, Tay; Genome Institute of Singapore, Stem Cell Biology Zhang, Ting; Genome Institute of Singapore, Stem Cell Biology Nagarajan, Niranjan ; Genome Institute of Singapore, Stem Cell Biology Torti, Suzy; UCONN Health Center, Molecular microbial and structural biology Brewer, Mollie; UCONN Health Center, OB GYN Choolani, Mahesh; National University of Singapore, Ob Gyn McKeon, Frank; Genome Institute of Singapore, Stem Cell Biology Xian, Wa; UCONN Health Center, Genetics and Developmental Biology
Tissue:	
Pathology:	
Technique:	

In Vitro and *In Vivo* Correlates of Physiologic and Neoplastic Human Fallopian Tube Stem Cells

Yusuke Yamamoto[1,10*], Gang Ning[1,10], Brooke E. Howitt[2], Karishma Mehra[2], Lingyan Wu[3], Xia Wang[1], Yue Hong[1], Florian Kern[3], Tay Seok Wei[3], Ting Zhang[3], Niranjan Nagarajan[3], , Suzy Torti[4], Molly Brewer[5], Mahesh Choolani[6], Frank McKeon[1,3,7,8]^, Christopher P. Crum[2,^] and Wa Xian[1,2,7,9,^]

[1]The Jackson Laboratory for Genomic Medicine, Farmington, CT USA; [2]Department of Pathology, Brigham and Women's Hospital, Boston, MA USA; [3]Genome Institute of Singapore, A-STAR, Singapore; [4]Departments of Molecular, Microbial and Structural Biology, University of Connecticut Health Center, Farmington, CT, USA; [5]Department of Obstetrics and Gynecology, University of Connecticut Health Center, Farmington, CT, USA; [6]Division of Obstetrics and Gynecology, National University of Singapore; [7]MultiClonal Therapeutics, Inc., Farmington, CT, USA; [8]Department of Microbiology, National University of Singapore; [9]Department of Genetics and Developmental Biology, University of Connecticut Health Center, Farmington, CT, USA;

[10]these authors contributed equally to this work.

[*]present affiliation: Division of Molecular and Cellular Medicine, National Cancer Center Research Institute, Tokyo, Japan

^senior authors

Word count: 3819; pages 11, Figures 5, Supplemental Figures 2, Supplemental Tables 2

Abstract

High-grade serous cancer (HGSC) progresses to advanced stages without symptoms and the 5-year survival rate is a dismal 30%. Recent studies of ovaries and fallopian tubes in patients with BRCA1 or BRCA2 mutations have documented a pre-metastatic intramucosal neoplasm that is found almost exclusively in the fallopian tube termed “serous tubal intraepithelial carcinoma” or STIC. Moreover, other proliferations, termed p53 signatures, secretory cell outgrowths (SCOUTs) and lower grade serous tubal intraepithelial neoplasms (STINs) fall short of STIC but share similar alterations in expression, in keeping with an underpinning of genomic disturbances involved in - or occurring in parallel with serous carcinogenesis. To gain insight into the cellular origins of this unique tubal pathway to high-grade serous cancer, we cloned and both immortalized and transformed fallopian tube stem cells (FTSC). We demonstrated that pedigrees of FTSCs were capable of multi-potent differentiation and that the tumors derived from the transformed FTSC shared the same histological and molecular features with HGSC. We also demonstrated that altered expression of some biomarkers seen in transformed FTSCs and HGSCs (Stathmin, EZH2, CXCR4, CXCL12 and FOXM1) could be seen as well in immortalized cells and their *in vivo* counterparts SCOUTs and STINs. Thus, a whole-genome transcriptome analysis comparing FTSC, immortalized FTSC, and transformed FTSC showed a clear molecular progression sequence that is recapitulated by the spectrum of accumulated perturbations characterizing the range of proliferations seen *in vivo*. Biomarkers unique to STIC relative to normal tubal epithelium provide a basis for novel detection approaches to early HGSC, but must be viewed critically given their potential expression in lesser proliferations. Perturbations shared by both immortalized and transformed FTSCs may provide unique early targets for prevention strategies. Central to these efforts has been the ability to clone and perpetuate multi-potent FTSCs.

Introduction

Epithelial ovarian cancer (EOC) is the fifth most common cause of death from cancer in women, and the most common type – high grade serous carcinoma or HGSC – is the most lethal. One in 200 women will develop ovarian cancer between their 50th and 70th birthday. Worldwide, there are 225,000 new cases of ovarian cancer diagnosed annually, and an estimated 140,163 disease-related deaths[1]. Up to 80% of women present with Stages III/IV disease, and the 5-year survival rate is a dismal 30%. Mortality for this disease has not markedly changed since the 1930s[2] and this is because ovarian cancer cannot be detected at low stage by current screening programs. Resolving this dilemma will require effective tools and methods to interrupt the carcinogenic sequence at a point that permits either cure or prevention of tumor-specific mortality.

There is cogent clinical and molecular evidence to suggest that many if not all cases of HGSCs arise from the fallopian tube. From the clinical end, it has been known that reducing risk of BRCA1 and BRCA2 patients required removing the fallopian tube in addition to the ovary[3]. Molecular analyses have shown that HGSC has gene expression profiles more akin to those of fallopian tube epithelium than to ovarian surface epithelium[4]. Finally, and most significantly, the pathological examination of risk reduction salpingo-oophorectomies for germ-line BRCA1 and BRCA2 mutations has uncovered pre-metastatic stages of HGSC (serous tubal intraepithelial carcinoma or STIC) as well as premalignant tubal intraepithelial neoplasia (or serous tubal intraepithelial lesions) [5 6]. In the fallopian tube model, STIC is considered the earliest morphologic manifestation of serous carcinoma. STICs are composed of ‘‘secretory cells,’’ the non-ciliated population of the endosalpinx. These cells, when neoplastic, exhibit features including variable stratification, increased proliferation and loss of nuclear polarity[7].

Most STICs are marked by mutant p53, same as their metastatic form, high-grade serous cancer. Further analyses of BRCA1/BRCA2 mutation-associated fallopian tubes have revealed the presence as well of a “latent precancer” - the “p53 signature”, which has mutant p53 overexpression but retains cell polarity and lacks excessive cell proliferation. Interestingly, p53 signatures have been found adjacent to STICs and in several revealing examples have been shown to share the same p53 mutation as HGSC suggesting a lineage relationship[8]. These compelling results demonstrate that the fallopian tube is a site of origin of HGSC, the development of which follows the classic multi-step carcinogenesis model. Importantly, latent precancers are common in tubes of women who are not at genetic risk and between 40-60% of the serous cancers in BRCA mutation-negative women also co-exist with STIC[7 8] with a genetic link between the two[9 10]. Thus, STIC represents the earliest phase of most pelvic serous cancers and targeted treatment or prevention of STIC is a valid goal in cancer prevention. In parallel with the serous carcinogenic sequence is the one characterized by putative stem cell outgrowths or SCOUTs. These proliferations lack p53 mutations but share many attributes with intraepithelial neoplasms, altered expression levels of certain genes, including ALDH1, PAX2, EZH2, LEF1 and others. The impression from these collective entities is that the tube is prone to both self-limited and potentially malignant intraepithelial proliferations.

HGSCs presumably arise from non-ciliated cells of the fallopian tube (secretory cells) but the precise relationship between these cells and stem cells in the tube is not understood, in part because of a lack of detailed *in vitro* studies of putative stem cells. Herein, we report a fallopian tube stem cell model based on a cell culture paradigm of both limited (immortalization) and aggressive (transformation) cell outgrowth. This model is superimposed on a similar *in vivo* paradigm of proliferative lesions seen in the fallopian tube. The goal of this exercise is to not only divine molecular perturbations marking the transition from STIC to metastatic disease but also those that highlight the loss of growth control in the early phases of neoplasia.

Methods

Case material

This study was approved by the Brigham and Women's Human Investigation Committee and involved the use of discarded fresh and archived tissues. Case material for gene expression analysis and histology consisted of the following epithelia/lesions: (1) normal oviduct and HGSC paired samples (n = 10) and (2) normal oviduct, STIC and invasive HGSC lesions from each patient section (n = 6). Cases for immunohistochemistry were selected by one of us (CPC) using criteria that have been previously described[10].

Stem cell culture and differentiation

Fallopian tube tissue was obtained from discarded surgical specimens of women undergoing benign procedures. Discarded fetal fallopian tube tissues were obtained under an approved IRB protocol. Disaggregated cells were cultivated onto a feeder layer of lethally irradiated 3 T3-J2 cells in stem cell culturing media (SCM-6F8) [11]. Clonal analysis and *in vitro* ALI differentiation were based on previously described methods for lung epithelial stem cells[12].

Xenografts of transformed FTSCs

Fallopian tube stem cells were infected with retroviruses expressing c-Myc, hTERT, and SV40 large T antigen (SV40 large T and hTERT for immortalization, and SV40 large T, hTERT and c-Myc for transformation). In brief, 200,000 stem cells were plated onto a lawn of feeder cells in 3cm culture dishes and transduced three days later. After 48hr, cells were split 1:5 onto new lawns and grown and passaged for four weeks before plating onto culture plates without feeder cells for an additional four weeks. Individual colonies were selected and tested for growth in soft agar, and positive colonies selected for expansion and transplantation. Two thousand transformed cells (expressing SV40 large T antigen, hTERT and c-myc) were injected subcutaneously into six-week-old female NSG (NOD.Cg-*Prkdc*^{scid} *Il2rg*^{tm1Wjl}/SzJ) mice following the protocols approved by BRC IACUC #110643 at the Agency for Science Technology and Research (A*STAR) Singapore. Visible tumors appeared typically at two weeks and were harvested following euthanasia and analyzed by histology and expression microarray.

Histology and immunofluorescence

Histology, immunohistochemistry (IHC), and immunofluorescence (IF) were performed following standard lab protocols. For IF and IHC staining, 4% paraformaldehyde-fixed slides were subjected to antigen retrieval in citrate buffer (pH 6.0, Sigma-Aldrich, USA) at 120 °C for 20 min, and blocking procedure was performed with 5 % bovine serum albumin (BSA, Sigma-Aldrich, USA) and 0.05 % Triton X-100 (Sigma-Aldrich, USA) in DPBS(-) (Gibco, USA) at room temperature for 1 hr. Cells cultured on 3T3 and air-liquid interface culture were fixed with 4% formaldehyde at 4°C overnight and directly used in staining. All primary antibodies used in this study and staining condition were summarized in Supplemental Table 1. For IHC, detection was completed with the Vectastain ABC kit (Cat No PK-6102; Vector Laboratories, Inc, Burlingame, CA, USA) with a liquid DAB-plus substrate kit (Cat No 00-2020). Slides were counterstained with Hematoxylin Stain 3 (Cat No CS402-1D). Stained slides were stored at 4 °C in the dark and all images for section slides were captured by using the Inverted Eclipse Ti-Series (Nikon, Japan) microscope with Lumencor SOLA light engine and Andor Technology Clara Interline CCD camera and NIS-Elements Advanced Research v.4.13 software (Nikon, Japan) or LSM 780 confocal microscope (Carl Zeiss, Germany) with LSM software. Bright field cell culture images were obtained on an Eclipse TS100 microscope (Nikon, Japan) with Digital Sight DSFi1camera (Nikon, Japan) and NIS-Elements F3.0 software (Nikon, Japan).

Laser captured microdissection

Fresh surgical specimens from 10 independent women for normal oviduct and HGSC and 6 independent women for normal, STIC and invasive STIC were embedded in OCT, sectioned on a cryostat, and stained with hematoxylin to morphologically identify each region. Twelve serial frozen sections of each tissue sample were microdissected using a PALM microbeam instrument (Carl Zeiss, Germany), and each selected cell population from different slides of the same patient were pooled. Total RNAs were extracted using the Pico Pure RNA extraction kit (Life technologies, USA).

Microarray

For normal fallopian tube epithelium and paired HGSC samples from 10 patients and FTSC (stem cells, immortalized, transformed and xenograft) samples, total RNA processing and hybridization were performed on Affymetrix human U133 plus 2.0 Array chips (Affymetrix, CA, USA). For normal fallopian tube epithelium, STIC and invasive STIC from 6 patients, total RNAs were amplified using the WT Pico RNA Amplification System V2 and Encore Biotin Module (NuGEN Technologies, USA). Amplified DNA samples were prepared according to manufacturer's instructions and hybridized onto GeneChip Human Exon 1.0 ST Array (Affymetrix, CA, USA). GeneChip operating software was used to process all the Cel files and calculate probe intensity values. To validate sample quality, quality check was conducted using Affymetrix Expression Console software. The intensity values were log2-transformed and imported into the Partek Genomics Suite 6.6 (Partek Incorporated, MO, USA). For GeneChip Human Exon 1.0 ST Array, exons were summarized to genes and a 1-way ANOVA was performed to identify differentially expressed genes. P-values and fold-change numbers were calculated for each analysis.

Bioinformatics for gene expression

Unsupervised clustering and heatmap generation were performed with sorted datasets by Euclidean distance on average linkage clustering with selected probe sets by Partek Genomics Suite 6.6. Gene Set Enrichment Analysis (GSEA; Subramanian et al., 2005) was performed to compare 1) STIC with invasive STIC, and 2) immortalized FTSC and FTSC, respectively. To find enriched pathways, DAVID bioinformatics resources (http://david.abcc.ncifcrf.gov/) were used[13].

Accession numbers

Datasets generated for this study have been submitted to the National Center for Biotechnology Information Gene Expression Omnibus (GEO) database under GSE69428 for normal oviduct and HGSC from 10 patients, GSE69453 for FTSC-ALI, and transformed FTSCs (stem cell, immortalized, transformed and xenografts) and GSE69429 for normal fallopian tubal epithelium, STIC and invasive STIC from 6 patients.

Results

Cloning, immortalizing and transforming the fallopian tube stem cells.

If the fallopian tube is the origin of serous cancer, one possible mechanism for the evolution of cancer is a dysregulation of indigenous stem cells. We therefore set out to clone the stem cells of the fallopian tube using methods to clone columnar epithelial stem cells such as human intestinal stem cells[11]. Using this method, we were able to generate clones of fallopian tube stem cells that contain many small, undifferentiated and highly proliferative (Ki67 +) cells that can propagate through multiple passages (Figure 1a). These stem cell clones show strong and consistent staining with markers of fallopian tube epithelial cells (PAX8) (Figure 2a). In our recent work on cloning adult stem cells from human airway and human intestine[11 12],we established a pedigree analysis method to examine the multipotential differentiation ability from a single stem cell. The high clonogenic capacity of fallopian tube stem cells allowed us to use the same approach to rapidly generate single cell "pedigree" lines of expansion and characterization of their lineage fates upon induced differentiation in air-liquid interface (ALI) cultures. Following FTSC differentiation, we found through immune-staining with specific antibodies and RT-PCR with specific primers that one single fallopian tube stem cell (Foxj1-, acetylated tubulin-, TAp73-, Sall2-, BCL2-, PAX2-) can give rise to both ciliated cells (Foxj1+, acetylated tubulin+, TAp73+, Sall2+) and secretory cells (Foxj1-, acetylated tubulin-, BCL2+, PAX2+)[14] (Figure 1b and c). Moreover, the same FTSC pedigree line can be induced to differentiate into squamous metaplasia (p63+/Krt5+) in 3D Matrigel assay[15]. We next compared the FTSCs and their differentiated structure in ALI by gene expression. FTSCs showed high expression of several known adult stem cell markers such as Lrig1[16], Lgr6[17] and regulators of self-renewal such as EZH2[18] and FOXM1[19], TCF4[20]. Interestingly, we did not find high expression of Lgr5[21] in FTSCs. While the differentiated cells lost the expression of stem cell markers, they showed significantly increased expression of genes associated with ciliated cell and secretory cell differentiation such as genes in the Dynein family[22] and MUC13[23] (Figure 1d).

To examine whether the fallopian tube stem cells are the cell of origin of high-grade serous cancer, we introduced SV40/ hTERT or SV40/hTERT/c-MYC into these cells by retroviral infection to induce immortalization or transformation of these cells (Figure 1e). We showed while both immortalized and transformed FTSCs gained the new property of growing without the support of irradiated 3T3-J2 fibroblast feeder, the transformed FTSCs lost contact inhibition and showed fibroblast like morphology in the petri dish (Figure 1f, upper). Moreover, both immortalized and transformed FTSCs formed sphere structures in growth-factor-reduced Matrigel in 5 days, but transformed FTSCs generated the irregular structures around 10 times larger in comparison with small and round spheres derived from immortalized FTSCs (Figure 1f, lower). A heat map of differentially expressed genes in whole-genome transcriptome analysis of FTSCs, immortalized and transformed FTSCs showed distinct expression profile differences between normal FTSCs and transformed FTSCs (Figure 1d and supplementary table 2). Interestingly, immortalized FTSCs expressed at the moderate level many genes that are highly expressed in transformed FTSCs (Figure 1g). Gene ontology Analysis was performed to identify the gene pathways significantly enriched in transformed cells including DNA replication and DNA repair (Supplemental Figure 1a). In addition, a highly amplified gene in ovarian cancer, c-MYC was used as the transforming agent[24]. Consistently, we observed that downstream genes of c-MYC are highly enriched in transformed FTSCs but not in immortalized FTSCs (Supplemental Figure 1b).

Transformed fallopian tube stem cells gave rise to high-grade serous cancer.

In order to examine whether the transformed fallopian tube stem cells belong in the serous carcinogenic pathway, we injected subcutaneously two thousand transformed fallopian tube stem cells into the immunodeficient (NOD.Cg-Prkdc^{scid} Il2rg^{tm1Wjl}/SzJ) mice[25] and observed the formation of palpable tumor in two weeks. The xenografted tumors demonstrate all the pathological and immunological hallmarks of human high-grade serous cancer, such as gain of p53, EZH2 and MUC4 expression (Figure 2a) [15] [26] [27]. To understand whether FTSC^{t} xenograft tumors resemble human high-grade serous cancer at the level of gene expression, we first compared RNA from ten microdissected histologically normal fallopian tube epithelium and paired high-grade serous cancer tumor samples on expression microarray chips. These data revealed a significant two-or-more-fold alteration (P<0.5) of the expression in 2395 genes that is presented in a heatmap (Figure 2b and supplementary table 3). Of the 2395 genes, 1017 genes are up-regulated, and in contrast, 1378 genes are down regulated in tumor samples. The further analysis showed that FTSC^t xenograft tumors, just like HGSC, also expressed these HGSC related genes in a similar manner.

To clarify the function of the genes that we identified in the study and uncover the pathways that conceivably could be targeted to lead to tumor cell death for the therapeutic purpose, we uncovered a number of druggable targets in HGSC such as Enhancer of Zeste Homolog 2. (EZH2). EZH2 is a histone methyl transferase (HMT) and a member of the polycomb group of genes (PcG) regulating (suppressing) transcription through nucleosome modification, chromatin remodeling, and interaction with other transcription factors. Several studies have demonstrated that EZH2 is involved in oncogenesis and consistently, high EZH2 transcript and protein levels have been associated with aggressive tumor behavior, chemo-resistant tumor stem-like side populations and overall poor clinical outcome in ovarian, breast, prostate and bladder cancer patients[28]. We showed that the protein expression of EZH2 is upregulated in precancerous lesion of HSGC (p53 signature[29], STIC, invasive serous cancer and FTSC^t xenograft tumors (Figure 2c). Consistent with the increased expression of EZH2 in HGSC and xenograft tumor, the expression of downstream targets of EZH2 was significantly down regulated compared with normal fallopian tube epithelium (Figure 2d). Moreover, treating the transformed fallopian tube stem cells with EZH2 inhibitor that specifically blocks EZH2 activity[30] led to dramatically decreased cell proliferation based on the diminished Ki67 antibody staining and drastic decreased structure size in the Matrigel (Figure 2e).

Resolving molecular alterations in STIC and its progression to invasive serous cancer.

Although advanced serous cancer has been proposed to result from STIC progression, there has not been transcriptome analysis to demonstrate the molecular progression from STIC to advanced serous cancer. To better understand potential links between these entities via markers of progression, we used the LCM approach to isolate normal fallopian tube epithelium, STIC and advance serous cancer from the same patient (Figure 3a). A heatmap of differentially expressed genes in these datasets showed distinct expression profile between normal fallopian tubal epithelium and advanced serous cancer among six patients. In contrast, STIC showed significant overlap with both normal epithelium and advanced cancer (Figure 3b). Gene Set Enrichment Analysis (GSEA) was performed to identify the gene pathways significantly enriched in both STIC and advanced cancer or uniquely changed in advanced serous cancer. The pathways involved in cell proliferation, genomic instability and survival are aberrantly expressed at the early stage of serous carcinogenesis and are followed by deregulation of the pathways involved in angiogenesis and cell adhesion (Figure 3c).

Furthermore, we particularly focused on the secreted proteins that are highly expressed in STIC or invasive serous cancer with the goal to use them as biomarkers for early detection of HGSC. We identified eight genes significantly upregulated in invasive cancer and three of them are already upregulated in the localized tubal tumor (STIC) (Figure 3d). Among them, SPP1 (osteopontin), SPARC (Osteonectin) and VCAN (Versican) have been reported to be overexpressed in various human cancers. Particularly, osteopontin levels in plasma were significantly higher in patients with epithelial ovarian cancer compared with those of healthy controls and patients with other gynecologic cancers[31].

Uncovering early molecular changes associated with STIC

The data presented here support the existing hypothesis that the fallopian tube is the site of origin of high-grade serous cancer and the STIC is the non-invasive, pre-metastatic form of high-grade serous cancer. A heatmap including 62 genes (>2 folds, $p<0.05$) was generated to show the genes that were aberrantly upregulated in common between STIC and matched invasive cancer (Figure 4a and supplementary table 4). Among these 62 genes, Pituitary tumor transforming gene (PTTG1) and Cyclin E1 (CCNE1) (Supplemental Figure 2a) are particularly interesting because they have been implicated in early oncogenesis through their driving role in cellular transformation[32 33]. In order to validate some of these genes, we next performed the immunohistochemistry using the specific antibodies for PTTG1 and CCNE1 on patient-matched sections of normal fallopian tube epithelium, STIC and invasive cancer. While the protein expression of these two markers is barely detectable in normal fallopian tube epithelium, they are highly expressed in STIC and invasive cancer (Figure 4b).

We next hypothesized that among aberrantly expressed genes in STIC, there is a group of genes expressing during cellular immortalization, which is the first step towards malignancy[34]. In order to test this hypothesis, we compared upregulated genes in immortalized FTSCs and STIC and uncovered 123 genes (>2 folds, $p<0.05$) that overlap in these two entities (Figure 4c and supplementary table 5). Among them, genes such as Stathmin1, a microtubule destabilizing protein[35], Ect2, a Rho guanine nucleotide exchange factor[36], Forkhead Box M1 (FOXM1), a transcription factor regulating cell cycle[37] have been suggested playing critical roles in tumor initiation of HGSC (Figure 4d and supplementary Figure 2b).

Discussion

The perception of ovarian epithelial carcinogenesis is changing rapidly since the proposal of the hypothesis that many of these tumors appear to originate in the fallopian tube[29]. In 2012, Gilbert and colleagues further supported this hypothesis. Among their patients with “early” HGSC 78% the cancer had originated from the fallopian tube, peritoneum, or both[38]. Recently another report noted that in the general patient population, incidentally discovered non-uterine high-grade serous carcinomas arise in the fallopian tube in most cases: further evidence for the tubal origin of high-grade serous carcinomas[39].

In this study, we cloned stem cells from human fallopian tube and demonstrated that transformed fallopian tube stem cells can develop to aggressive HGSC in mouse xenograft models in a short time. The xenografted tumor shared all the hallmark features with HGSC, further supporting the fallopian tube as the site of origin of serous cancer (Figure 5). Attempts to culture oviductal epithelial cells have been made previously, including efforts to model HGSC[14 40 41]. However this study is the first to show that stem cells of fallopian tube can be maintained in culture in their elemental state and using the pedigree approach, are capable of multipotent differentiation from one single stem cell in the fallopian tube. Importantly, this platform of culturing FTSCs faithfully and robustly *in vitro* provided us a unique opportunity of functionally studying putative oncogenes or tumor suppressors discovered in recent cancer genome analysis through genetic editing of patient-derived FTSCs. Moreover, in this study we found that several putative oncogenes were significantly overexpressed at the step of FTSC immortalization prior to the occurrence of transformation. Among them, Stathmin 1 has been proposed as a marker expressed in early pelvic serous cacinomas[35]; CXCR4 and its ligand CXCL12 have been suggested as the key determinants of tumor initiation and metastasis of ovarian cancer[42]; Forkhead Box M1 (FOXM1) has been reported as a key regulator of tumorigenesis by increasing proliferative activity and leading to uncontrolled cell division[37]. EZH2, a negative regulator of transcription was also upregulated two-fold with immortalization. Interestingly, our previous study showed the PAX2-null progenitor

cell growth (secretory cell outgrowth, SCOUTs) in the fallopian tube also expressed strongly both EZH2 and Stathmin 1[15]. This correlation led us to propose the link between FTSC immortalization and the development of early proliferations in the tube, either SCOUTs or lower grade STINs. Based on these correlations it appears that these gene perturbations associated with immortalization might occur prior to or even in the absence of the serous cancer, in which case their value as predictors of malignancy could be limited by their lack of specificity as actionable values. However, they could conceivably be targeted as co-determinants of neoplastic progression with the goal of depriving the serous carcinogenic sequence of a participating pathway.

The stage at which an ovarian cancer is detected is the single most important factor influencing outcome and interrupting ovarian cancer when it is curable will require addressing early disease in the distal fallopian tube. Early molecular signatures that are specific for these neoplasms are of paramount importance given their potential value in detecting neoplasia via analysis of fluids in the lower genital tract [43]. Given the fact that many STICs do not have a HGSC outcome, we believe that there is a window of opportunity where patients with potentially lethal precursors can be identified through screening and spared a death from this malignancy.

It would be hoped that a molecular analysis of early lesions might provide an array of targets that are either secreted by these cells or presented on the cell surface for screening and therapeutic value, respectively. Monoclonal antibodies to secreted proteins have the potential to form the basis of population-wide screening methods from blood or cervical fluid for those at risk who might benefit from salpingectomy. Monoclonal antibodies to cell surface markers in these lesions might assist in alternative detection via imaging technologies as the technology evolves. An important question that must be addressed is whether the parallels between immortalized cells *in vitro* and proliferations *in vivo* signify a background of accrued biologic events that both precede - and are needed for - progression to malignancy. Thus the challenge will be to tease out those molecular events that are biologically significant and when intervened will prevent subsequent malignancy.

Acknowledgements

This work was supported by grants from Connecticut Innovations (WX, FM), the Joint Council Office of the Agency for Science Technology Research Agency (ASTAR), Singapore (WX, FM), the National Medical Research Council, Singapore (BnB11dec063 to NN, MC, FM and WX), the Department of Defense (W81XWH-10-1-0289 to CPC) and NIH (R01 CA188025 to ZT). We thank J. Hammer for assistance of figure preparation and the Division of Gynecologic Oncology at Brigham and Women's Hospital and Dana Farber Cancer Institute for their contribution to the study. We also thank Drs. Ju Yuan and In Young Hwang for the assistance in cell culture.

This paper has not been previously published. Preliminary findings with clonogenic tubal epithelial cells have been previously described by Ning et al[15]. The authors have no conflicts of interest or relevant financial relationships. This study was approved by the Brigham and Women's Hospital Institutional Review Board. Array data is displayed in Supplemental Figure 2.

Abbreviations

STIC - serous tubal intraepithelial carcinoma; FTSC - fallopian tube stem cells;
HGSC – high grade serous cancer; ALI – air-liquid interface culture

Contribution of the coauthors are as follows:

Author	Design	Data collection	Data analysis	Data Interpretation	Literature search	Figures	Manuscript writing

Yamamoto	X	X	X	X	X		X
Ning	X	X	X	X			
Howitt		X	X	X			
Mehra		X	X	X			
Wu		X	X	X			
Wang		X	X	X			
Hong		X	X	X			
Tay		X	X	X			
Zhang		X	X	X			
Kern		X	X	X			
Nagarajan			X	X			
Choolani	X		X	X	X		X
Torti			X	X			X
Brewer			X	X			X
McKeon	X		X	X	X	X	X
Crum	X		X	X	X	X	X
Xian	X	X	X	X	X	X	X

Illustrations

Figure 1. Cloning, immortalization and transformation of the fallopian tube stem cells. a. Cloned FTSC marked with proliferation marker Ki67 (green) and occasional expression of ciliated marker FOXJ1 (red). b ALI differentiation culture of FTSC stained with FOXJ1 (red) and acetylated tubulin (green). c. RT-PCR of selected markers. d. Heatmap of selected genes from whole-genome transcriptome analysis. e. Schematic of FTSC immortalization and transformation *in vitro*. f. Morphological difference of FTSC^i and FTSC^t on plastic culture dishes and in 3D Matrigel assay. g. Progressive change of gene expression among FTSC, FTSC^i and FTSC^t (n = 2, each). Genes with increased expression (>1.5 fold and $p < 0.05$ in each, 654 genes) following transformation were selected for heatmap production.

Figure 2. FTSC^t xenograft tumor resembles human high-grade serous cancer. a. *Upper panel*, 2K FTSC^t cells (PAX8, red) were injected into NSG mice and palpable tumor was observed in two weeks. *Lower panel*, Xenograft tumor expressed HGSC hallmark genes MUC4, p53 and PAX8. b. A heatmap showing FTSC^t xenograft tumors and invasive SC

shared similar gene expression profile (FTSC^t tumor: n = 3; invasive SC: n = 10 and paired normal oviduct: n = 10; 2395 genes selected, > 2 folds and $p < 0.05$). c. EZH2 protein expressed in multiple stages of HGSC development including lower grade serous tubal intraepithelial neoplasia and secretory cell outgrowths[15]. d. EZH2 target genes were downregulated in FTSC^t xenograft tumors and invasive SC. e. Selective inhibition of EZH2 by its inhibitor (3-Deazaneplanocin A) blocked FTSC^t cell proliferation in a matrigel culture. Ki67 (red) stained for proliferating cells. Dapi (blue) stained nuclei.

Figure 3. Molecular correlates of progression from STIC to invasive cancer. a. *Left,* Histology of the sections used for Laser captured microdissection (LCM) of normal fallopian tube epithelium, STIC and invasive cancer; *Right*, p53 antibody staining showing prominent expression of p53 protein in STIC and invasive cancer. b. Six heatmaps showing the progressive gene expression from STIC to invasive cancer in individual patients (genes differentially expressed in invasive cancer compared with normal FT epithelium were selected, >2 folds and $p<0.05$). c. Gene set enrichment analysis (GSEA) of invasive cancer vs. STIC highlighting angiogenesis and regulation of cell adhesion in invasive cancer. d. Dot plots of selected genes highly expressed in STIC and invasive cancer (normal fallopian tube: n = 6; STIC: n = 6; invasive SC: n = 6).

Figure 4. Early molecular changes associated with FTSC immortalization and STIC. a. A heatmap showing 62 genes (>2 folds, $p<0.05$) commonly overexpressed between STIC and matched invasive serous cancer. b. Representative images of CCNE1 and PTTG1 immunostaining on normal FT epithelium, STIC and invasive serous cancer. c. Venn diagram of genes overexpressed in STIC (>1.5 fold, $p<0.05$) and immortalized FTSC (>2 fold, $p < 0.05$). 123 genes were overlapped. d. Selected overlapping genes and fold change.

Figure 5. *In vitro* and *in vivo* correlations proposing a model of multi-step development of HGSC originated from fallopian tube stem cells.

Supplementary Figure 1. a. Pathways enriched in immortalized and transformed FTSCs compared with normal FTSC ($p < 0.05$) are listed in the table. b. GSEA showed enrichment of MYC target genes in transformed nut not immortalized FTSC.

Supplementary figure 2. a. Dot plots of PTTG1 and CCNE1 expression in normal fallopian tube epithelium, STIC and invasive SC. b. Pathway analysis showed significantly enriched pathways ($p < 0.05$) in immortalized FTSCs and STIC.

References

1. Auersperg N, Wong AS, Choi KC, *et al*. Ovarian surface epithelium: biology, endocrinology, and pathology. *Endocr Rev* 2001; **22:** 255–288.
2. Vaughan S, Coward JI, Bast RC Jr, *et al*. Rethinking ovarian cancer: recommendations for improving outcomes. *Nat Rev Cancer* 2011; **11:** 719–725.
3. Piek JM, van Diest PJ, Zweemer RP, *et al*. Dysplastic changes in prophylactically removed fallopian tubes of women predisposed to developing ovarian cancer. *J Pathol* 2001; **195:** 451–456.
4. Marquez RT, Baggerly KA, Patterson AP, *et al*. Patterns of gene expression in different histotypes of epithelial ovarian cancer correlate with those in normal fallopian tube, endometrium, and colon. *Clin Cancer Res* 2005; **11:** 6116-6126.
5. Finch A, Shaw P, Rosen B, *et al*. Clinical and pathologic findings of prophylactic salpingo-oophorectomies in 159 BRCA1 and BRCA2 carriers. *Gynecol Oncol* 2006; **100:** 58–64.
6. Lowell CB, Swisher EM, Cass I, *et al.* Long term follow up of BRCA1 and BRCA2 mutation carriers with unsuspected neoplasia identified at risk reducing salpingo-oophorectomy. *Gynecol Oncol* 2013; **129:** 364-371.
7. Carlson JW, Miron A, Jarboe EA, *et al*. Serous tubal intraepithelial carcinoma: Its potential role in primaryperitoneal serous carcinoma and serous cancer prevention. *J Clin Oncol* 2008; **26:** 4160–4165.

8. Kindelberger DW, Lee Y, Miron A, *et al*. Intraepithelial carcinoma of the fimbria and pelvic serous carcinoma: evidence for a causal relationship. *Am J Surg Pathol* 2007; **31:** 161–169.
9. Salvador S, Rempel A, Soslow RA, *et al.* Chromosomal instability in fallopian tube precursor lesions of serous carcinoma and frequent monoclonality of synchronous ovarian and fallopian tube mucosal serous carcinoma. *Gynecol Oncol* 2008; **110:** 408-417.
10. Mehrad M, Ning G, Chen EY, *et al.* A pathologist's road map to benign, precancerous, and malignant intraepithelial proliferations in the fallopian tube. *Adv Anat Pathol* 2010; **17:** 293-302.
11. Wang X, Yamamoto Y, Wilson LH, et al. Cloning and variation of ground state intestinal stem cells. *Nature* 2015; DOI 10.1038/nature14484
12. Kumar PA, Hu Y, Yamamoto Y, *et al*. Distal airway stem cells yield alveoli in vitro and during lung regeneration following H1N1 influenza infection. *Cell* 2011; **147:** 525-538.
13. Huang da W, Sherman BT, Lempicki RA. Systematic and integrative analysis of large gene lists using DAVID bioinformatics resources. *Nat Protoc* 2009; **4:** 44-57.
14. Levanon K, Ng V, Piao HY, *et al.* Primary ex vivo cultures of human fallopian tube epithelium as a model for serous ovarian carcinogenesis. *Oncogene* 2010; **29:** 1103-1113.
15. Ning G, Bijron J, Yamamoto Y, *et al.* The PAX2-null immunophenotype defines multiple lineages with common expression signatures in benign and neoplastic oviductal epithelium. *J Pathol* 2014; **234:** 478-87.
16. Wong VW, Stange DE, Page ME, *et al.* Lrig1 controls intestinal stem-cell homeostasis by negative regulation of ErbB signalling. *Nat Cell Biol* 2012; **14:** 401-408.
17. Oeztuerk-Winder F, Guinot A, Ochalek A, *et al.* Regulation of human lung alveolar multipotent cells by a novel p38α MAPK/miR-17-92 axis. *EMBO J* 2012; **31:** 3431-3441.
18. Juan AH, Derfoul A, Feng X, *et al.* Polycomb EZH2 controls self-renewal and safeguards the transcriptional identity of skeletal muscle stem cells. *Genes Dev* 2011; **25:** 789-794.

19. Bella L, Zona S, Nestal de Moraes G, *et al.* FOXM1: A key oncofoetal transcription factor in health and disease. *Semin Cancer Biol* 2014; **29:** 32-39.
20. van Es JH, Haegebarth A, Kujala P, *et al.* A critical role for the Wnt effector Tcf4 in adult intestinal homeostatic self-renewal. *Mol Cell Biol* 2012; **32:** 1918-1927.
21. Ng A, Tan S, Singh G, *et al.* Lgr5 marks stem/progenitor cells in ovary and tubal epithelia. *Nat Cell Biol* 2014; **16:** 745-757.
22. Kikkawa M. Big steps toward understanding dynein. *J Cell Biol* 2013; **202:** 15-23.
23. Chauhan SC, Vannatta K, Ebeling MC, *et al.* Expression and functions of transmembrane mucin MUC13 in ovarian cancer. *Cancer Res* 2009; **69:** 765-774.
24. Hahn WC1, Counter CM, Lundberg AS, *et al*. Creation of human tumour cells with defined genetic elements. *Nature* 1999; 400: 464-468.
25. Shultz LD, Goodwin N, Ishikawa F, *et al.* Human cancer growth and therapy in immunodeficient mouse models. *Cold Spring Harb Protoc* 2014; **7:** 694-708.
26. Crum CP, Herfs M, Gang N, *et al.* Through the glass darkly: intraepithelial neoplasia, top down differentiation, and the road to ovarian cancer. *J Pathol* 2013; **231:** 402-412.
27. Chauhan SC, Singh AP, Ruiz F, *et al.* Aberrant expression of MUC4 in ovarian carcinoma: diagnostic significance alone and in combination with MUC1 and MUC16 (CA125). *Mod Pathol* 2006; **9:**1386-1394.
28. Rizzo S, Hersey JM, Mellor P, *et al.* Ovarian cancer stem cell-like side populations are enriched following chemotherapy and overexpress EZH2. *Mol Cancer Ther* 2011; **10:** 325-335.
29. Lee Y, Miron A, Drapkin R, *et al.* A candidate precursor to serous carcinoma that originates in the distal fallopian tube. *J Pathol* 2007; **211:** 26–35.
30. Sun F, Chan E, Wu Z, *et al.* Combinatorial pharmacologic approaches target EZH2-mediated gene repression in breast cancer cells. *Mol Cancer Ther* 2009; **8:** 3191-3202.
31. Kim JH, Skates SJ, Uede T, *et al.* Osteopontin as a potential diagnostic biomarker for ovarian cancer. *JAMA* 2002; **287:** 1671-1679.
32. Pei L, Melmed S. Isolation and characterization of a pituitary tumor-transforming gene (PTTG). *Mol Endocrinol* 1997; **11:** 433–441.

33. Karst AM, Jones PM, Vena N, *et al.* Cyclin E1 deregulation occurs early in secretory cell transformation to promote formation of fallopian tube-derived high-grade serous ovarian cancers. *Cancer Res* 2014; **74:** 1141-1152.
34. Hanahan D, Weinberg RA. Hallmarks of cancer: the next generation. *Cell* 2011; **144:** 646-674.
35. Karst AM, Levanon K, Duraisamy S, *et al*. Stathmin 1, a marker of PI3K pathway activation and regulator of microtubule dynamics, is expressed in early pelvic serous carcinomas. *Gynecol Oncol* 2011; **123:** 5-12.
36. Huff LP, Decristo MJ, Trembath D, *et al*. The Role of Ect2 Nuclear RhoGEF Activity in Ovarian Cancer Cell Transformation. *Genes Cancer* 2013; **4:** 460-475.
37. Wierstra I, Alves J. FOXM1, a typical proliferation-associated transcription factor. *Biol Chem* 2007; **388:** 1257–1274.
38. Gilbert L, Basso O, Sampalis J, *et al.* Assessment of symptomatic women for early diagnosis of ovarian cancer: results from the prospective DOvE pilot project. *Lancet Oncol* 2012; **13:** 285-291.
39. Gilks CB, Irving J, Köbel M, *et al*. Incidental nonuterine high-grade serous carcinomas arise in the fallopian tube in most cases: further evidence for the tubal origin of high-grade serous carcinomas. *Am J Surg Pathol* 2015; **39:** 357-364.
40. Kervancioglu ME, Saridogan E, Martin JE *et al.* A simple technique for the long-term non-polarised and polarised culture of human fallopian tube epithelial cells. *Biol Cell* 1994; **82:** 103–107.
41. Karst AM, Levanon K, Drapkin R. Modeling high-grade serous ovarian carcinogenesis from the fallopian tube. *Proc Natl Acad Sci U S A* 2011; **108:** 7547-7552.
42. Kajiyama H, Shibata K, Terauchi M, *et al*. Involvement of SDF-1alpha/CXCR4 axis in the enhanced peritoneal metastasis of epithelial ovarian carcinoma. *Int J Cancer* 2008; **122:** 91-99.
43. Kinde I, Bettegowda C, Wang Y, *et al*. Evaluation of DNA from the Papanicolaou test to detect ovarian and endometrial cancers. *Sci Transl Med* 2013; **5:** 167ra4

Figure 1

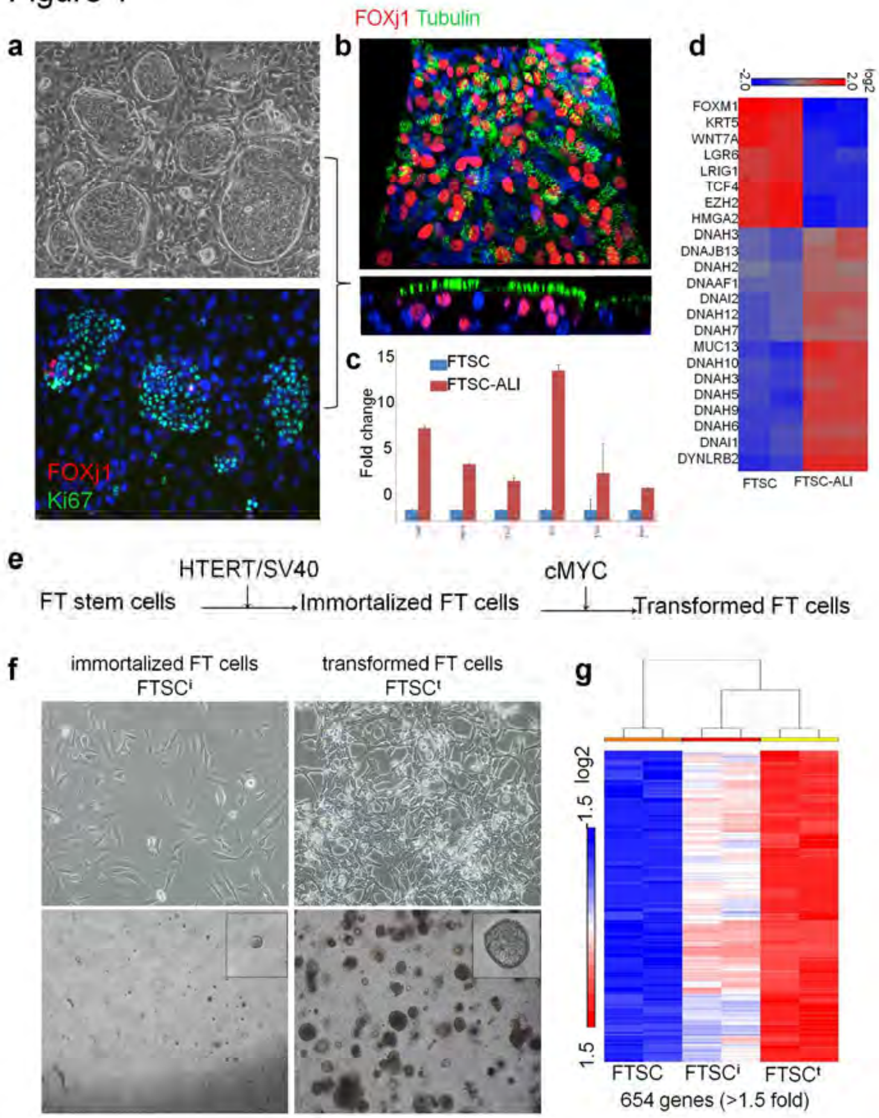

Figure 1. Cloning, immortalization and transformation of the fallopian tube stem cells. a. Cloned FTSC marked with proliferation marker Ki67 (green) and occasional expression of ciliated marker FOXJ1 (red). b ALI differentiation culture of FTSC stained with FOXJ1 (red) and acetylated tubulin (green). c. RT-PCR of selected markers. d. Heatmap of selected genes from whole-genome transcriptome analysis. e. Schematic of FTSC immortalization and transformation in vitro. f. Morphological difference of FTSCi and FTSCt on plastic culture dishes and in 3D Matrigel assay. g. Progressive change of gene expression among FTSC, FTSCi and FTSCt (n = 2, each). Genes with increased expression (>1.5 fold and p < 0.05 in each, 654 genes) following transformation were selected for heatmap production.
571x762mm (96 x 96 DPI)

Figure 2

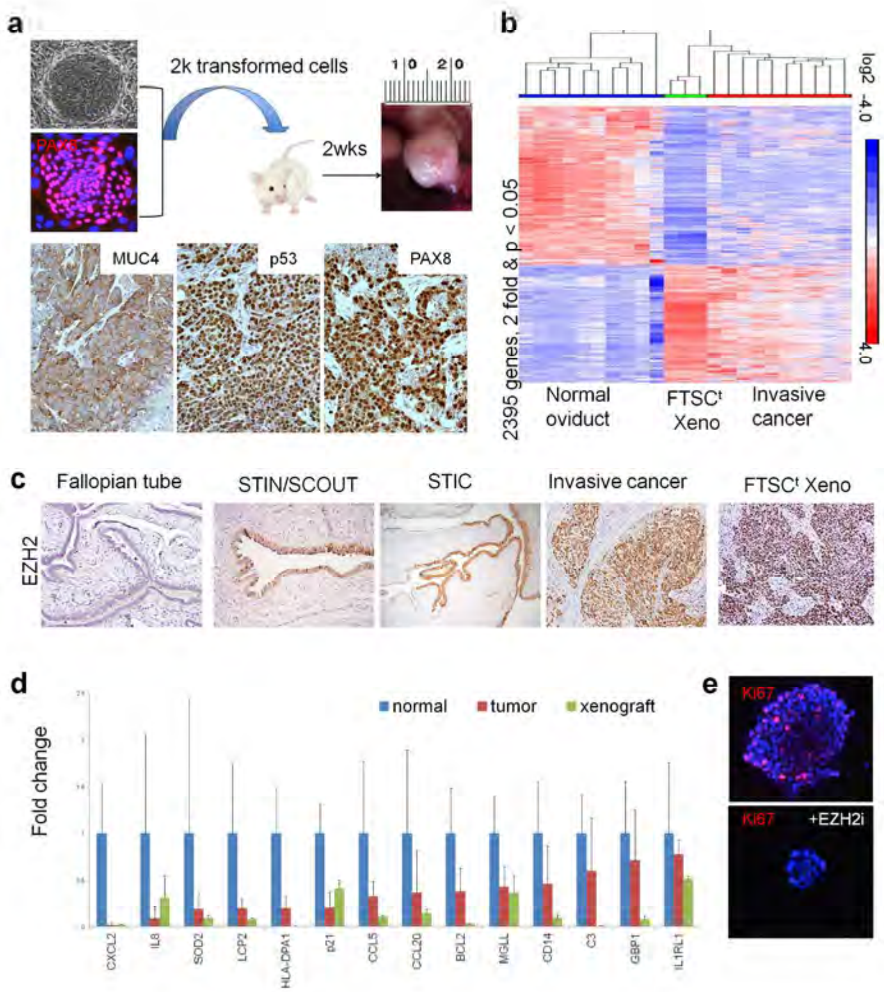

Figure 2. FTSCt xenograft tumor resembles human high-grade serous cancer. a. Upper panel, 2K FTSCt cells (PAX8, red) were injected into NSG mice and palpable tumor was observed in two weeks. Lower panel, Xenograft tumor expressed HGSC hallmark genes MUC4, p53 and PAX8. b. A heatmap showing FTSCt xenograft tumors and invasive SC shared similar gene expression profile (FTSCt tumor: n = 3; invasive SC: n = 10 and paired normal oviduct: n = 10; 2395 genes selected, > 2 folds and p < 0.05). c. EZH2 protein expressed in multiple stages of HGSC development including lower grade serous tubal intraepithelial neoplasia and secretory cell outgrowths15. d. EZH2 target genes were downregulated in FTSCt xenograft tumors and invasive SC. e. Selective inhibition of EZH2 by its inhibitor (3-Deazaneplanocin A) blocked FTSCt cell proliferation in a matrigel culture. Ki67 (red) stained for proliferating cells. Dapi (blue) stained nuclei.
571x762mm (96 x 96 DPI)

Figure 3

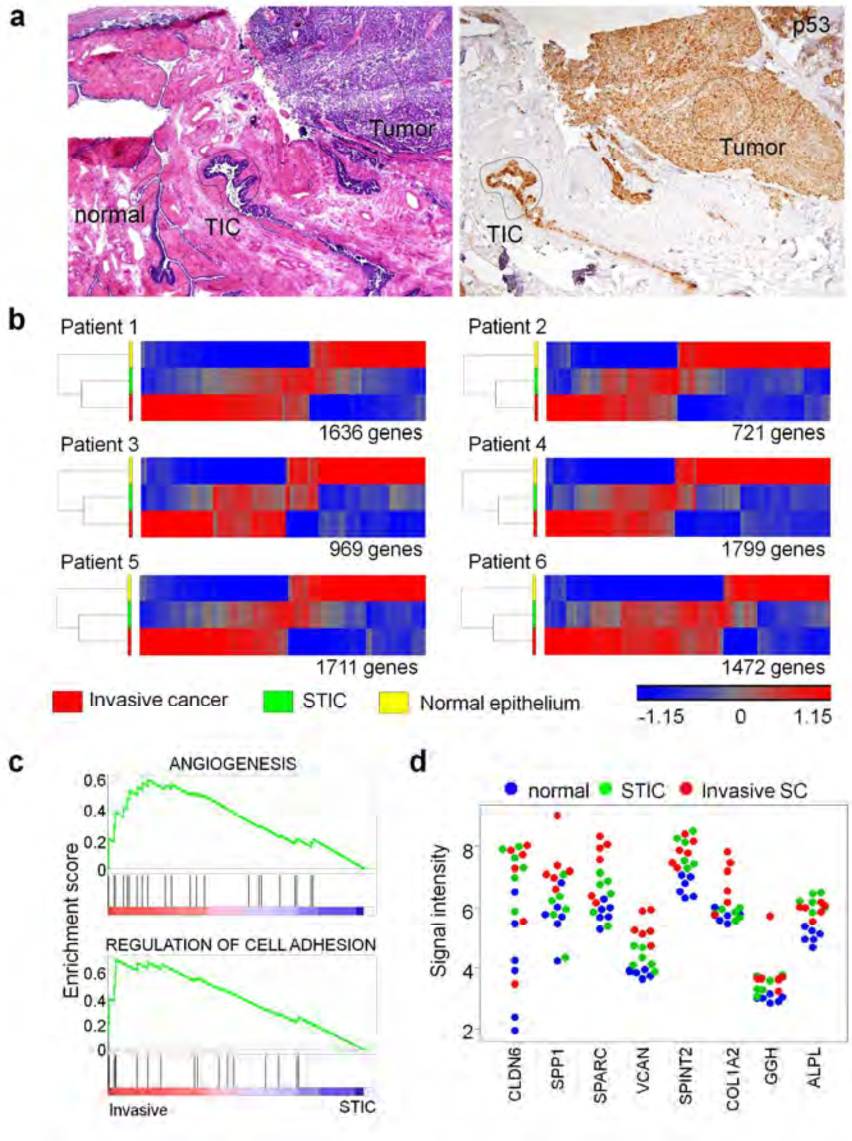

Figure 3. . Molecular correlates of progression from STIC to invasive cancer. a. Left, Histology of the sections used for Laser captured microdissection (LCM) of normal fallopian tube epithelium, STIC and invasive cancer; Right, p53 antibody staining showing prominent expression of p53 protein in STIC and invasive cancer. b. Six heatmaps showing the progressive gene expression from STIC to invasive cancer in individual patients (genes differentially expressed in invasive cancer compared with normal FT epithelium were selected, >2 folds and $p<0.05$). c. Gene set enrichment analysis (GSEA) of invasive cancer vs. STIC highlighting angiogenesis and regulation of cell adhesion in invasive cancer. d. Dot plots of selected genes highly expressed in STIC and invasive cancer (normal fallopian tube: n = 6; STIC: n = 6; invasive SC: n = 6).

571x762mm (96 x 96 DPI)

Figure 4

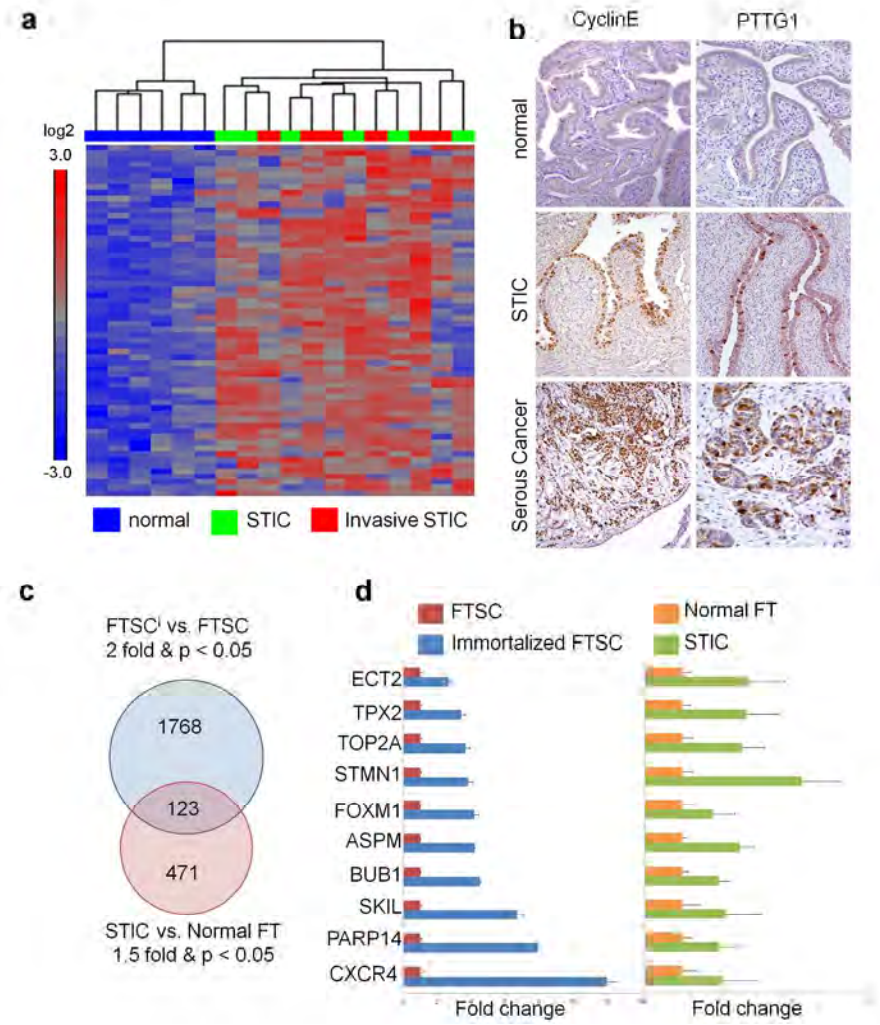

Figure 4. Figure 4. Early molecular changes associated with FTSC immortalization and STIC. a. A heatmap showing 62 genes (>2 folds, p<0.05) commonly overexpressed between STIC and matched invasive serous cancer. b. Representative images of CCNE1 and PTTG1 immunostaining on normal FT epithelium, STIC and invasive serous cancer. c. Venn diagram of genes overexpressed in STIC (>1.5 fold, p<0.05) and immortalized FTSC (>2 fold, p < 0.05). 123 genes were overlapped. d. Selected overlapping genes and fold change.
571x762mm (96 x 96 DPI)

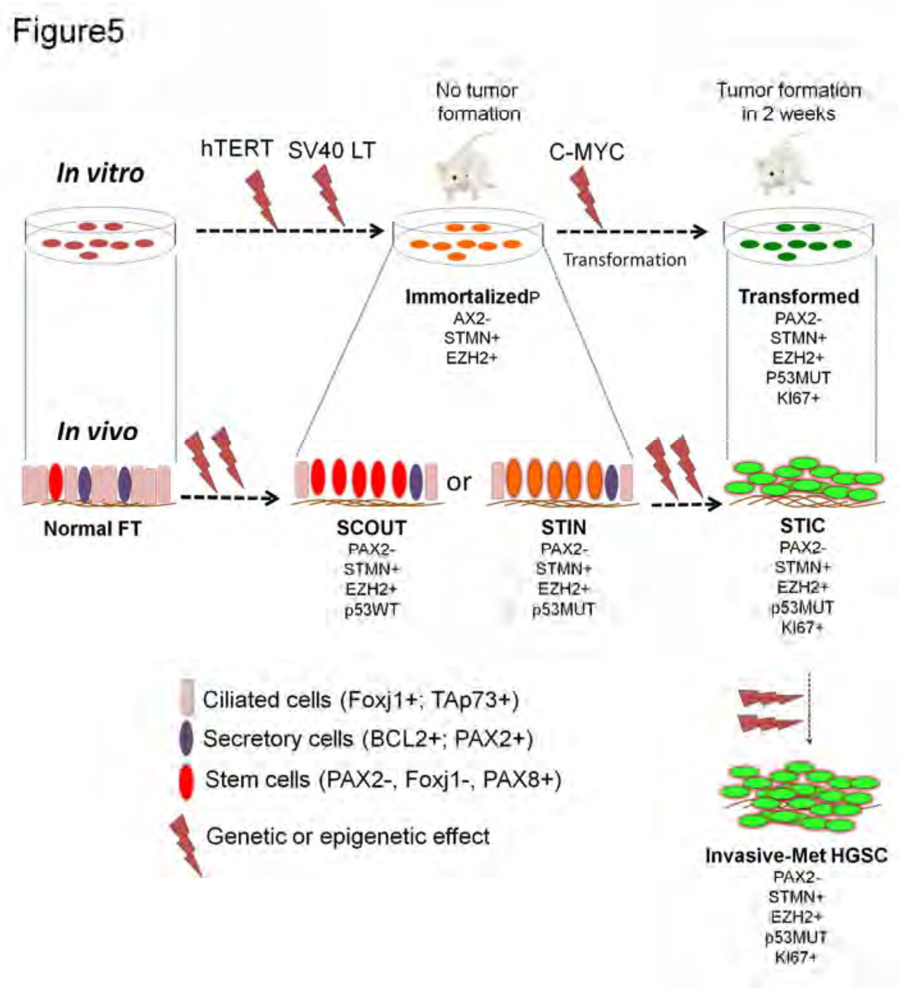

Figure 5. In vitro and in vivo correlations proposing a model of multi-step development of HGSC originated from fallopian tube stem cells.

571x762mm (96 x 96 DPI)

Supplemental Figure 1

a

Category	Count	PValue
DNA replication	10	1.52E-07
Cell cycle	14	1.13E-05
Aminoacyl-tRNA biosynthesis	8	5.70E-05
One carbon pool by folate	4	0.006716
Mismatch repair	4	0.018706
TGF-beta signaling pathway	7	0.020951
Nucleotide excision repair	5	0.023315
Glycine, serine and threonine metabolism	4	0.041123

b

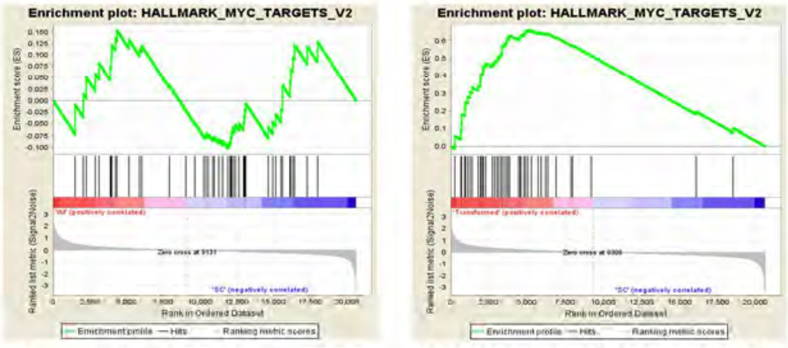

Immortalized FTSC vs. FTSC Transformed FTSC vs. FTSC

Supplemenatary Figure 1. a. Pathways enriched in immortalized and transformed FTSCs compared with normal FTSC ($p < 0.05$) are listed in the table. b. GSEA showed enrichment of MYC target genes in transformed nut not immortalized FTSC.
571x762mm (96 x 96 DPI)

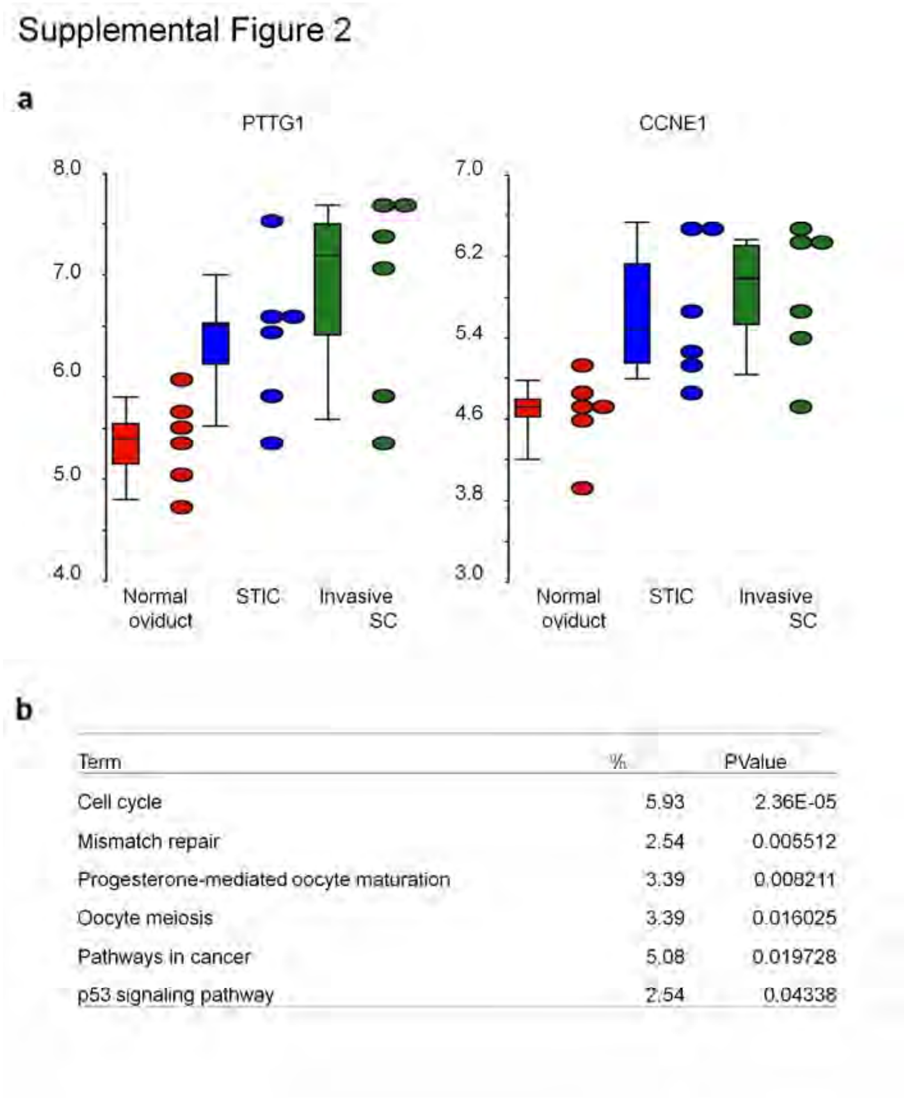

Term	%	PValue
Cell cycle	5.93	2.36E-05
Mismatch repair	2.54	0.005512
Progesterone-mediated oocyte maturation	3.39	0.008211
Oocyte meiosis	3.39	0.016025
Pathways in cancer	5.08	0.019728
p53 signaling pathway	2.54	0.04338

Supplementary Figure 2. a. Dot plots of PTTG1 and CCNE1 expression in normal fallopian tube epithelium, STIC and invasive SC. b. Pathway analysis showed significantly enriched pathways ($p < 0.05$) in immortalized FTSCs and STIC.
571x762mm (96 x 96 DPI)

Supplemental Table 1. Antibodies used

Antibody	Manufacturers	Cat. No.	Working Dilution
Alpha-Tubulin	Sigma-Aldrich	T9026	1:3000
CyclinE1	Abcam	ab3927	1:1600
EZH2	Leica Biosystems	NCL-L-EZH2	1:500
Foxj1	Sigma-Aldrich	HPA005714	1:500
MUC4	Invitrogen	18-2322	1:800
P53	Caibiochem	OP43	1:500
PAX8	Protein Tech	10336-1-AP	1:400
PTTG1	Sigma-Aldrich	HPA008890	1:1000

Supplementary Table 2 incrementally expressed

Probeset ID	Gene Symbol
210587_at	INHBE
203548_s_at	LPL
1554242_a_at	COCH
235020_at	TAF4B
239352_at	SLC6A15
219295_s_at	PCOLCE2
226695_at	PRRX1
219911_s_at	SLCO4A1
240419_at	SLC6A15
214651_s_at	HOXA10-HOXA9 /// HOXA9
204394_at	SLC43A1
204794_at	DUSP2
206376_at	SLC6A15
203387_s_at	TBC1D4
219985_at	HS3ST3A1
210143_at	ANXA10
232263_at	SLC6A15
203386_at	TBC1D4
205885_s_at	ITGA4
223721_s_at	DNAJC12
1558404_at	LOC644242
207536_s_at	TNFRSF9
213113_s_at	SLC43A3
206261_at	ZNF239
236302_at	PPM1E
220615_s_at	FAR2
223722_at	DNAJC12
212813_at	JAM3
205884_at	ITGA4
206172_at	IL13RA2
238681_at	GDPD1
235343_at	VASH2
218976_at	DNAJC12
201578_at	PODXL
225516_at	SLC7A2
204521_at	FAM216A
235548_at	APCDD1L
1569582_at	LOC201651
207219_at	ZNF643
242931_at	LONRF3
1554918_a_at	ABCC4
218541_s_at	C8orf4
228956_at	UGT8

219969_at	TXLNG
200841_s_at	EPRS
210692_s_at	SLC43A3
232291_at	MIR17HG /// MIR18A /// M
238831_at	TMEM33
1554640_at	PALM2
213416_at	ITGA4
1555606_a_at	GDPD1
230763_at	SPATA17
226890_at	WDR35
236313_at	CDKN2B
205429_s_at	MPP6
218590_at	C10orf2
221648_s_at	AGMAT
222062_at	IL27RA
221586_s_at	E2F5
225285_at	BCAT1
229437_at	MIR155 /// MIR155HG
231984_at	MTAP
235644_at	CCDC138
238990_x_at	TRIM61
219262_at	SUV39H2
204956_at	MTAP
229596_at	AMDHD1
206085_s_at	CTH
225421_at	PM20D2
229715_at	B7H6
209406_at	BAG2
212816_s_at	CBS
236219_at	SLC35G1
209892_at	FUT4
208264_s_at	EIF3J
227892_at	PRKAA2
1553972_a_at	CBS
227607_at	STAMBPL1
236075_s_at	LOC100506676
202684_s_at	RNMT
212706_at	RASA4 /// RASA4B
214452_at	BCAT1
220251_at	DIEXF
228962_at	PDE4D
227896_at	BCCIP
219616_at	ACSS3
227932_at	ARIH2
242905_at	PNO1
235177_at	METTL21A
235733_at	GXYLT2

202920_at	ANK2
220346_at	MTHFD2L
221088_s_at	PPP1R9A
243502_at	GJC1
228494_at	PPP1R9A
233737_s_at	LOC284561
242037_at	ASPH
212894_at	SUPV3L1
226517_at	BCAT1
238452_at	FCRLB
236917_at	LRRC34
1555882_at	SPIN3
212290_at	SLC7A1
218599_at	REC8
218936_s_at	CCDC59
217127_at	CTH
203163_at	KATNB1
207057_at	SLC16A7
229435_at	GLIS3
219731_at	CC2D2B
205047_s_at	ASNS
1559993_at	SFXN3
227916_x_at	EXOSC3
220370_s_at	USP36
222305_at	HK2
205541_s_at	GSPT2
212036_s_at	PNN
220698_at	MGC4294
205668_at	LY75
225100_at	FBXO45
230097_at	GART
204700_x_at	DIEXF
1552430_at	WDR17
224873_s_at	MRPS25
227606_s_at	STAMBPL1
233655_s_at	HAUS6
200790_at	ODC1
1555562_a_at	ZCCHC7
206613_s_at	TAF1A
1569183_a_at	CHM
228378_at	C12orf29
222624_s_at	ZNF639
201228_s_at	ARIH2
225142_at	JHDM1D
204491_at	PDE4D
1552625_a_at	TRNT1
235610_at	ALKBH8

203622_s_at	PNO1
227856_at	C4orf32
226876_at	FAM101B
241866_at	SLC16A7
206204_at	GRB14
230258_at	GLIS3
223700_at	MND1
200975_at	PPT1
230166_at	KIAA1958
227037_at	PLD6
218591_s_at	NOL10
222736_s_at	TMEM38B
208541_x_at	TFAM
231973_s_at	ANAPC1 /// LOC100653327
204603_at	EXO1
236609_at	PMS1
203223_at	RABEP1
233985_x_at	PPP1R9A
203177_x_at	TFAM
242294_at	FBXO45
210188_at	GABPA
223221_at	SCO1
238576_at	MOCOS
242370_at	MTHFD2L
205053_at	PRIM1
244822_at	GART
223570_at	MCM10
219751_at	SETD6
228434_at	BTNL9
1554249_a_at	ZNF638
220651_s_at	MCM10
231292_at	EID3
235109_at	ZBED3
221540_x_at	GTF2H2 /// GTF2H2B /// GT
203199_s_at	MTRR
223758_s_at	GTF2H2
220265_at	GPR107
235949_at	TTC26
238441_at	PRKAA2
226905_at	FAM101B
241985_at	JMY
235661_at	POU2F2
223092_at	ANKH
209893_s_at	FUT4
230954_at	C20orf112
206847_s_at	HOXA7
241908_at	BROX

206112_at	ANKRD7
221020_s_at	SLC25A32
229975_at	BMPR1B
209676_at	TFPI
201083_s_at	BCLAF1
214507_s_at	EXOSC2
204128_s_at	RFC3
219983_at	HRASLS
1560579_s_at	LOC100506392
228402_at	ZBED3
214390_s_at	BCAT1
227749_at	POU2F2
235371_at	GXYLT2
228343_at	POU2F2
222528_s_at	SLC25A37
235707_at	C6orf228
226875_at	DOCK11
235406_x_at	TMEM161B-AS1
204042_at	WASF3
235779_at	ZNF790-AS1
1559942_at	MDFIC
242663_at	LOC148189
228702_at	FLJ43663
226481_at	VPRBP
226446_at	HES6
230047_at	ARHGAP42
235977_at	LONRF2
207891_s_at	HAUS7 /// TREX2
242579_at	BMPR1B
230177_at	GTF2H2B
209239_at	NFKB1
203176_s_at	TFAM
220512_at	DLC1
226901_at	C17orf58
207039_at	CDKN2A
220841_s_at	AHI1
235753_at	HOXA7
225996_at	LONRF2
205282_at	LRP8
1555167_s_at	NAMPT
1554155_at	MCPH1
207038_at	SLC16A6
210089_s_at	LAMA4
236518_at	KIAA1984
205969_at	AADAC
226881_at	GRPEL2
202510_s_at	TNFAIP2

219634_at	CHST11
220892_s_at	PSAT1
226179_at	SLC25A37
238443_at	TFAM
221621_at	LINC00338 /// SCARNA16
205909_at	POLE2
228416_at	ACVR2A
1557945_at	TCTE3
228191_at	FLVCR1
229141_at	SFT2D3 /// WDR33
242900_at	ALG10B
219880_at	LOC100507619
221920_s_at	SLC25A37
202637_s_at	ICAM1
227699_at	C14orf149
211575_s_at	UBE3A
218794_s_at	TXNL4B
1552306_at	ALG10
215223_s_at	LOC100129518 /// SOD2
226135_at	UHRF1BP1
208795_s_at	MCM7
219000_s_at	DSCC1
203716_s_at	DPP4
1559052_s_at	PAK2
213262_at	SACS
225550_at	CNST
209644_x_at	CDKN2A
202780_at	OXCT1
231894_at	SARS
206173_x_at	GABPB1
1564651_at	C6orf228
228752_at	EFCAB4B
204699_s_at	DIEXF
233234_at	KCTD16
225472_at	GPANK1
204327_s_at	ZNF202
210807_s_at	SLC16A7
232899_at	RPL23AP7 /// RPL23AP82
228955_at	LRP8
219595_at	LOC100287515 /// ZNF26
230588_s_at	LOC285074
228245_s_at	LOC100509445 /// LOC7287
215722_s_at	SNRPA1
227514_at	ITPRIPL2
240239_at	ZNF566
233827_s_at	SUPT16H
210664_s_at	TFPI

1557217_a_at	FANCB
1555760_a_at	RBM15
223595_at	TMEM133
1555004_a_at	RBL1
204059_s_at	ME1
227954_at	ITPRIPL2
200956_s_at	SSRP1
214193_s_at	DIEXF
226368_at	CHST11
235117_at	CHAC2
235931_at	LOC100506290 /// LOC1006
220399_at	LINC00115
201869_s_at	TBL1X
218579_s_at	DHX35
213556_at	LOC390940
210983_s_at	MCM7
223251_s_at	ANKRD10
220094_s_at	CCDC90A
223296_at	SLC25A33
1552822_at	TMX3
221778_at	JHDM1D
212110_at	SLC39A14
37433_at	PIAS2
204127_at	RFC3
219558_at	ATP13A3
1554572_a_at	SUV39H2
238069_at	LOC100506090
232063_x_at	FARSB
202453_s_at	GTF2H1
227406_at	GABPB1-AS1
229432_at	NAGS
214913_at	ADAMTS3
213608_s_at	SRRD
214552_s_at	RABEP1
242690_at	ATP11C
1568597_at	LOC646762
218866_s_at	POLR3K
239302_s_at	LOC100506922
1553528_a_at	TAF5
240983_s_at	CARS
1554660_a_at	CNST
202345_s_at	FABP5
208931_s_at	ILF3
1557755_at	CEP128
228308_at	FKBP11
204695_at	CDC25A
209754_s_at	TMPO

1553167_a_at	SEPSECS
202979_s_at	CREBZF
219131_at	UBIAD1
1554424_at	FIP1L1
210053_at	TAF5
223556_at	HELLS
1553338_at	SDE2
227559_at	NDUFAF4
226680_at	IKZF5
210389_x_at	TUBD1
202451_at	GTF2H1
220085_at	HELLS
201490_s_at	PPIF
241534_at	LOC100505549
236126_at	ACVR2B
229090_at	ZEB1-AS1
202470_s_at	CPSF6
218768_at	NUP107
214690_at	TAF1B
1555225_at	C1orf43
234304_s_at	IPO11
223624_at	ZFAND4
236431_at	U2SURP
212060_at	U2SURP
227105_at	CSPP1
202402_s_at	CARS
1555350_at	PPHLN1
225841_at	HENMT1
229091_s_at	CCNJ
231853_at	TUBD1
225470_at	NUP35
209804_at	DCLRE1A
225919_s_at	C9orf72
209457_at	DUSP5
222529_at	SLC25A37
225970_at	DDHD1
214141_x_at	SRSF7
1553725_s_at	ZNF644
232489_at	TRMT13
202819_s_at	TCEB3
204126_s_at	CDC45
223352_s_at	C17orf80
230678_at	RGS5
221606_s_at	HMGN5
224825_at	DNTTIP1
1554099_a_at	SPIN3
48808_at	DHFR

241661_at	JMJD1C
229855_at	RNF34
222748_s_at	TXNL4B
227623_at	CACNA2D1
205085_at	ORC1
200692_s_at	HSPA9
223211_at	HACL1
208447_s_at	PRPS1
242230_at	ATXN1
224200_s_at	RAD18
1553169_at	LRRN4
234942_s_at	DNTTIP1
220885_s_at	CENPJ
223898_at	ZNF670
204492_at	ARHGAP11A
217767_at	C3
210541_s_at	TRIM27
243531_at	ORAOV1
204510_at	CDC7
236918_s_at	LRRC34
228341_at	NUDT16
1567013_at	NFE2L2
207528_s_at	SLC7A11
218331_s_at	FAM208B
201795_at	LBR
219118_at	FKBP11
221909_at	RNFT2
201229_s_at	ARIH2
225551_at	CNST
1555803_a_at	C11orf57
241024_at	C6orf147 /// KHDC1
227101_at	ZNF800
218517_at	PHF17
214144_at	POLR2D
213157_s_at	LOC339166 /// WSCD1
238848_at	OTUD4
244790_at	MTCP1
222891_s_at	BCL11A
226372_at	CHST11
221571_at	TRAF3
209421_at	MSH2
209799_at	PRKAA1
214962_s_at	NUP160
212118_at	TRIM27
228566_at	RPRD1A
212022_s_at	MKI67
233255_s_at	BIVM

241706_at	CPNE8
203358_s_at	EZH2
210555_s_at	NFATC3
222632_s_at	LZTFL1
215101_s_at	CXCL5
202534_x_at	DHFR
234863_x_at	FBXO5
235409_at	MGA
216237_s_at	MCM5
203843_at	RPS6KA3
210813_s_at	XRCC4
228902_at	NUP214
201489_at	PPIF
223195_s_at	SESN2
41469_at	PI3
219270_at	CHAC1
235791_x_at	CHD1
228365_at	CPNE8
226315_at	ZNF830
204233_s_at	CHKA
210665_at	TFPI
229751_s_at	PUS7L
222735_at	TMEM38B
65493_at	HEATR6
200628_s_at	WARS
235356_at	NHLRC2
233387_s_at	PCNT
212654_at	TPM2
225786_at	HNRNPU-AS1
1565149_at	DYNC2H1
219178_at	QTRTD1
213373_s_at	CASP8
212142_at	MCM4
233924_s_at	EXOC6
1555834_at	UCHL1
219660_s_at	ATP8A2
202034_x_at	RB1CC1
225237_s_at	MSI2
237005_at	LOC442075
1554661_s_at	CNST
236626_at	ALG1
226947_at	GUSBP1 /// GUSBP4
227164_at	SRSF1
226475_at	FAM118A
219117_s_at	FKBP11
204258_at	CHD1
231791_at	ASAH2B

219258_at	TIPIN
227767_at	CSNK1G3
219576_at	MAP7D3
219637_at	ARMC9
212092_at	PEG10
201791_s_at	DHCR7
206288_at	PGGT1B
221025_x_at	PUS7L
203115_at	FECH
218468_s_at	GREM1
209418_s_at	THOC5
235315_at	TSC22D1
201101_s_at	BCLAF1
204977_at	DDX10
234759_at	LOC100287497 /// LOC1002
211478_s_at	DPP4
206308_at	TRDMT1
234976_x_at	MTHFD2
217508_s_at	C18orf25
235158_at	TMEM209
1553171_x_at	LRRN4
233970_s_at	TRMT6
227650_at	HSPA14
204244_s_at	DBF4
1554036_at	ZBTB24
1555384_a_at	LARP4
201867_s_at	TBL1X
223305_at	TMEM216
209257_s_at	SMC3
1557218_s_at	FANCB
228868_x_at	CDT1
225577_at	HCG18
242866_x_at	POU2F2
201555_at	MCM3
226980_at	DEPDC1B
223759_s_at	GSG2
215985_at	ZNRD1-AS1
208875_s_at	PAK2
234701_at	ANKRD11
235333_at	B4GALT6
222037_at	MCM4
204058_at	ME1
229429_x_at	LOC728855 /// LOC728875
220060_s_at	PARPBP
219056_at	RNASEH2B
213155_at	LOC339166 /// WSCD1
227214_at	GOPC

218469_at	GREM1
1552978_a_at	SCAMP1
209753_s_at	TMPO
203804_s_at	LUC7L3
210255_at	RAD51B
223407_at	C16orf48
223530_at	TDRKH
1554020_at	BICD1
208693_s_at	GARS
219130_at	TRMT13
1555450_a_at	NAA16
206232_s_at	B4GALT6
1554037_a_at	ZBTB24
214446_at	ELL2
201266_at	TXNRD1
208103_s_at	ANP32E
238867_at	TMEM182
227561_at	DDR2
207564_x_at	OGT
203234_at	UPP1
228249_at	C11orf74
226924_at	LOC400657
210530_s_at	NR2C1
229622_at	FAM132B
226352_at	JMY
221925_s_at	CSPP1
203526_s_at	APC
202003_s_at	ACAA2
209017_s_at	LONP1
204640_s_at	SPOP
204033_at	TRIP13
222680_s_at	DTL
202124_s_at	TRAK2
223988_x_at	METTL17
230629_s_at	EP400
239579_at	EPHX4
228287_at	ING5
211376_s_at	NSMCE4A
219698_s_at	METTL4
218138_at	MKKS
225064_at	RABEP1
212655_at	ZCCHC14
205655_at	MDM4
241713_s_at	DYX1C1 /// DYX1C1-CCPG1
241820_at	RIF1
203068_at	KLHL21
218772_x_at	TMEM38B

232504_at	LOC285628 /// MIR146A
230721_at	C16orf52
225399_at	TSEN15
218754_at	NOL9
217771_at	GOLM1
209693_at	ASTN2
219399_at	LIN7C
218875_s_at	FBXO5
203378_at	PCF11
223172_s_at	MTFP1
204224_s_at	GCH1
207147_at	DLX2
221701_s_at	STRA6
203210_s_at	RFC5
233245_at	UHRF1BP1
233208_x_at	CPSF2
1559393_at	ALDH1L2
223275_at	PRMT6
1565269_s_at	ATF1
212945_s_at	MGA
222626_at	RBM26
203496_s_at	MED1
1558093_s_at	MATR3 /// SNHG4
1559064_at	NUP153
1552812_a_at	SENP1
217739_s_at	NAMPT
204080_at	TOE1
242916_at	CNTRL
226909_at	ZNF518B
226574_at	PSPC1
218366_x_at	METTL17
203194_s_at	NUP98
212133_at	NIPA2
222685_at	HAUS6
212116_at	TRIM27
202147_s_at	IFRD1
211220_s_at	HSF2
206108_s_at	SRSF6
214729_at	TWISTNB
238821_at	CSTF2
222697_s_at	ABHD10
205588_s_at	FGFR1OP
241343_at	RNASEH1
1556308_at	PRRT3
223686_at	TPK1
242996_at	MTRF1
222001_x_at	LOC728855 /// LOC728875

227633_at	RHEB
200690_at	HSPA9
1555874_x_at	MGC21881
225538_at	ZCCHC9
220744_s_at	IFT122
223735_at	ARL6
236526_x_at	C5orf44
218395_at	ACTR6
239343_at	LOC728705
217403_s_at	ZNF227
202638_s_at	ICAM1
239282_at	CCDC41
214881_s_at	UBTF
226576_at	ARHGAP26
228597_at	MIS18A
219004_s_at	MIS18A
220397_at	MDM1
239835_at	KBTBD8
1555125_at	GCFC1
225030_at	BOD1
226335_at	RPS6KA3
226284_at	ZBTB2
214095_at	SHMT2
235089_at	FBXL20
243092_at	PAN3-AS1
228367_at	ALPK2
226229_s_at	SSU72
1556361_s_at	ANKRD13C
210298_x_at	FHL1
209281_s_at	ATP2B1
212317_at	TNPO3
235119_at	TAF3
231999_at	ANKRD11
231149_s_at	ULK4
238506_at	LRRC58
218926_at	MYNN
229793_at	ASAH2B
218256_s_at	NUP54
201475_x_at	MARS
205068_s_at	ARHGAP26
242639_at	NARG2
223575_at	KIAA1549
225887_at	PROSER1
201962_s_at	RNF41
224740_at	C5orf43
213672_at	MARS
238526_at	RAB3IP

genes (1.5 fold and $p < 0.05$) during progression (FTSC -> FTSCi -> FTSCt) 654 probes

Gene Title
inhibin, beta E
lipoprotein lipase
coagulation factor C homolog, cochlin (Limulus polyphemus)
TAF4b RNA polymerase II, TATA box binding protein (TBP)-associated factor, 105kDa
solute carrier family 6 (neutral amino acid transporter), member 15
procollagen C-endopeptidase enhancer 2
paired related homeobox 1
solute carrier organic anion transporter family, member 4A1
solute carrier family 6 (neutral amino acid transporter), member 15
HOXA10-HOXA9 readthrough /// homeobox A9 /// microRNA 196b
solute carrier family 43, member 1
dual specificity phosphatase 2
solute carrier family 6 (neutral amino acid transporter), member 15
TBC1 domain family, member 4
heparan sulfate (glucosamine) 3-O-sulfotransferase 3A1
annexin A10
solute carrier family 6 (neutral amino acid transporter), member 15
TBC1 domain family, member 4
integrin, alpha 4 (antigen CD49D, alpha 4 subunit of VLA-4 receptor)
DnaJ (Hsp40) homolog, subfamily C, member 12
uncharacterized LOC644242
tumor necrosis factor receptor superfamily, member 9
solute carrier family 43, member 3
zinc finger protein 239
protein phosphatase, Mg2+/Mn2+ dependent, 1E
fatty acyl CoA reductase 2
DnaJ (Hsp40) homolog, subfamily C, member 12
junctional adhesion molecule 3
integrin, alpha 4 (antigen CD49D, alpha 4 subunit of VLA-4 receptor)
interleukin 13 receptor, alpha 2
glycerophosphodiester phosphodiesterase domain containing 1
vasohibin 2
DnaJ (Hsp40) homolog, subfamily C, member 12
podocalyxin-like
solute carrier family 7 (cationic amino acid transporter, y+ system), member 2
family with sequence similarity 216, member A
adenomatosis polyposis coli down-regulated 1-like
arylacetamide deacetylase (esterase) pseudogene
zinc finger protein 643
LON peptidase N-terminal domain and ring finger 3
ATP-binding cassette, sub-family C (CFTR/MRP), member 4
chromosome 8 open reading frame 4
UDP glycosyltransferase 8

taxilin gamma
glutamyl-prolyl-tRNA synthetase
solute carrier family 43, member 3
miR-17-92 cluster host gene (non-protein coding) /// microRNA 18a /// microRNA 19a ///
transmembrane protein 33
paralemmin 2
integrin, alpha 4 (antigen CD49D, alpha 4 subunit of VLA-4 receptor)
glycerophosphodiester phosphodiesterase domain containing 1
spermatogenesis associated 17
WD repeat domain 35
cyclin-dependent kinase inhibitor 2B (p15, inhibits CDK4)
membrane protein, palmitoylated 6 (MAGUK p55 subfamily member 6)
chromosome 10 open reading frame 2
agmatine ureohydrolase (agmatinase)
interleukin 27 receptor, alpha
E2F transcription factor 5, p130-binding
branched chain amino-acid transaminase 1, cytosolic
microRNA 155 /// MIR155 host gene (non-protein coding)
methylthioadenosine phosphorylase
coiled-coil domain containing 138
tripartite motif containing 61
suppressor of variegation 3-9 homolog 2 (Drosophila)
methylthioadenosine phosphorylase
amidohydrolase domain containing 1
cystathionase (cystathionine gamma-lyase)
peptidase M20 domain containing 2
B7 homolog 6
BCL2-associated athanogene 2
cystathionine-beta-synthase
solute carrier family 35, member G1
fucosyltransferase 4 (alpha (1,3) fucosyltransferase, myeloid-specific)
eukaryotic translation initiation factor 3, subunit J
protein kinase, AMP-activated, alpha 2 catalytic subunit
cystathionine-beta-synthase
STAM binding protein-like 1
uncharacterized LOC100506676
RNA (guanine-7-) methyltransferase
RAS p21 protein activator 4 /// RAS p21 protein activator 4B
branched chain amino-acid transaminase 1, cytosolic
digestive organ expansion factor homolog (zebrafish)
phosphodiesterase 4D, cAMP-specific
BRCA2 and CDKN1A interacting protein
acyl-CoA synthetase short-chain family member 3
ariadne homolog 2 (Drosophila)
partner of NOB1 homolog (S. cerevisiae)
methyltransferase like 21A
glucoside xylosyltransferase 2

ankyrin 2, neuronal
methylenetetrahydrofolate dehydrogenase (NADP+ dependent) 2-like
protein phosphatase 1, regulatory subunit 9A
gap junction protein, gamma 1, 45kDa
protein phosphatase 1, regulatory subunit 9A
uncharacterized LOC284561
aspartate beta-hydroxylase
suppressor of var1, 3-like 1 (S. cerevisiae)
branched chain amino-acid transaminase 1, cytosolic
Fc receptor-like B
leucine rich repeat containing 34
spindlin family, member 3
solute carrier family 7 (cationic amino acid transporter, y+ system), member 1
REC8 homolog (yeast)
coiled-coil domain containing 59
cystathionase (cystathionine gamma-lyase)
katanin p80 (WD repeat containing) subunit B 1
solute carrier family 16, member 7 (monocarboxylic acid transporter 2)
GLIS family zinc finger 3
Coiled-coil and C2 domain containing 2B
asparagine synthetase (glutamine-hydrolyzing)
Sideroflexin 3
exosome component 3
ubiquitin specific peptidase 36
hexokinase 2
G1 to S phase transition 2
pinin, desmosome associated protein
uncharacterized MGC4294
lymphocyte antigen 75
F-box protein 45
phosphoribosylglycinamide formyltransferase, phosphoribosylglycinamide synthetase, phos
digestive organ expansion factor homolog (zebrafish)
WD repeat domain 17
mitochondrial ribosomal protein S25
STAM binding protein-like 1
HAUS augmin-like complex, subunit 6
ornithine decarboxylase 1
zinc finger, CCHC domain containing 7
TATA box binding protein (TBP)-associated factor, RNA polymerase I, A, 48kDa
choroideremia (Rab escort protein 1)
chromosome 12 open reading frame 29
zinc finger protein 639
ariadne homolog 2 (Drosophila)
jumonji C domain containing histone demethylase 1 homolog D (S. cerevisiae)
phosphodiesterase 4D, cAMP-specific
tRNA nucleotidyl transferase, CCA-adding, 1
alkB, alkylation repair homolog 8 (E. coli)

partner of NOB1 homolog (S. cerevisiae)
chromosome 4 open reading frame 32
family with sequence similarity 101, member B
solute carrier family 16, member 7 (monocarboxylic acid transporter 2)
growth factor receptor-bound protein 14
GLIS family zinc finger 3
meiotic nuclear divisions 1 homolog (S. cerevisiae)
palmitoyl-protein thioesterase 1
KIAA1958
phospholipase D family, member 6
nucleolar protein 10
transmembrane protein 38B
transcription factor A, mitochondrial
anaphase promoting complex subunit 1 /// anaphase-promoting complex subunit 1-like ///
exonuclease 1
PMS1 postmeiotic segregation increased 1 (S. cerevisiae)
rabaptin, RAB GTPase binding effector protein 1
protein phosphatase 1, regulatory subunit 9A
transcription factor A, mitochondrial
F-box protein 45
GA binding protein transcription factor, alpha subunit 60kDa
SCO cytochrome oxidase deficient homolog 1 (yeast)
molybdenum cofactor sulfurase
methylenetetrahydrofolate dehydrogenase (NADP+ dependent) 2-like
primase, DNA, polypeptide 1 (49kDa)
phosphoribosylglycinamide formyltransferase, phosphoribosylglycinamide synthetase, phos
minichromosome maintenance complex component 10
SET domain containing 6
butyrophilin-like 9
zinc finger protein 638
minichromosome maintenance complex component 10
EP300 interacting inhibitor of differentiation 3
zinc finger, BED-type containing 3
general transcription factor IIH, polypeptide 2, 44kDa /// general transcription factor
5-methyltetrahydrofolate-homocysteine methyltransferase reductase
general transcription factor IIH, polypeptide 2, 44kDa
G protein-coupled receptor 107
tetratricopeptide repeat domain 26
protein kinase, AMP-activated, alpha 2 catalytic subunit
family with sequence similarity 101, member B
junction mediating and regulatory protein, p53 cofactor
POU class 2 homeobox 2
ankylosis, progressive homolog (mouse)
fucosyltransferase 4 (alpha (1,3) fucosyltransferase, myeloid-specific)
chromosome 20 open reading frame 112
homeobox A7
BRO1 domain and CAAX motif containing

ankyrin repeat domain 7
solute carrier family 25 (mitochondrial folate carrier) , member 32
bone morphogenetic protein receptor, type IB
tissue factor pathway inhibitor (lipoprotein-associated coagulation inhibitor)
BCL2-associated transcription factor 1
exosome component 2
replication factor C (activator 1) 3, 38kDa
HRAS-like suppressor
uncharacterized LOC100506392
zinc finger, BED-type containing 3
branched chain amino-acid transaminase 1, cytosolic
POU class 2 homeobox 2
glucoside xylosyltransferase 2
POU class 2 homeobox 2
solute carrier family 25 (mitochondrial iron transporter), member 37
chromosome 6 open reading frame 228
dedicator of cytokinesis 11
TMEM161B antisense RNA 1 (non-protein coding)
WAS protein family, member 3
ZNF790 antisense RNA 1 (non-protein coding)
MyoD family inhibitor domain containing
Uncharacterized LOC148189
uncharacterized LOC378805
Vpr (HIV-1) binding protein
hairy and enhancer of split 6 (Drosophila)
Rho GTPase activating protein 42
LON peptidase N-terminal domain and ring finger 2
HAUS augmin-like complex, subunit 7 /// three prime repair exonuclease 2
bone morphogenetic protein receptor, type IB
general transcription factor IIH, polypeptide 2B (pseudogene)
nuclear factor of kappa light polypeptide gene enhancer in B-cells 1
transcription factor A, mitochondrial
deleted in liver cancer 1
chromosome 17 open reading frame 58
cyclin-dependent kinase inhibitor 2A
Abelson helper integration site 1
homeobox A7
LON peptidase N-terminal domain and ring finger 2
low density lipoprotein receptor-related protein 8, apolipoprotein e receptor
nicotinamide phosphoribosyltransferase
microcephalin 1
solute carrier family 16, member 6 (monocarboxylic acid transporter 7)
laminin, alpha 4
KIAA1984
arylacetamide deacetylase (esterase)
GrpE-like 2, mitochondrial (E. coli)
tumor necrosis factor, alpha-induced protein 2

carbohydrate (chondroitin 4) sulfotransferase 11
phosphoserine aminotransferase 1
solute carrier family 25 (mitochondrial iron transporter), member 37
transcription factor A, mitochondrial
long intergenic non-protein coding RNA 338 /// small Cajal body-specific RNA 16
polymerase (DNA directed), epsilon 2, accessory subunit
activin A receptor, type IIA
T-complex-associated-testis-expressed 3
feline leukemia virus subgroup C cellular receptor 1
SFT2 domain containing 3 /// WD repeat domain 33
asparagine-linked glycosylation 10, alpha-1,2-glucosyltransferase homolog B (yeast)
uncharacterized LOC100507619
solute carrier family 25 (mitochondrial iron transporter), member 37
intercellular adhesion molecule 1
chromosome 14 open reading frame 149
ubiquitin protein ligase E3A
thioredoxin-like 4B
asparagine-linked glycosylation 10, alpha-1,2-glucosyltransferase homolog (S. pombe)
uncharacterized LOC100129518 /// superoxide dismutase 2, mitochondrial
UHRF1 binding protein 1
minichromosome maintenance complex component 7
defective in sister chromatid cohesion 1 homolog (S. cerevisiae)
dipeptidyl-peptidase 4
p21 protein (Cdc42/Rac)-activated kinase 2
spastic ataxia of Charlevoix-Saguenay (sacsin)
consortin, connexin sorting protein
cyclin-dependent kinase inhibitor 2A
3-oxoacid CoA transferase 1
seryl-tRNA synthetase
GA binding protein transcription factor, beta subunit 1
chromosome 6 open reading frame 228
EF-hand calcium binding domain 4B
digestive organ expansion factor homolog (zebrafish)
potassium channel tetramerisation domain containing 16
G patch domain and ankyrin repeats 1
zinc finger protein 202
solute carrier family 16, member 7 (monocarboxylic acid transporter 2)
ribosomal protein L23a pseudogene 7 /// ribosomal protein L23a pseudogene 82
low density lipoprotein receptor-related protein 8, apolipoprotein e receptor
zinc finger protein 26-like /// zinc finger protein 26
anaphase promoting complex subunit 1 pseudogene
uncharacterized LOC100509445 /// ovostatin homolog 2-like /// ovostatin 2
small nuclear ribonucleoprotein polypeptide A'
inositol 1,4,5-trisphosphate receptor interacting protein-like 2
zinc finger protein 566
suppressor of Ty 16 homolog (S. cerevisiae)
tissue factor pathway inhibitor (lipoprotein-associated coagulation inhibitor)

Fanconi anemia, complementation group B
RNA binding motif protein 15
transmembrane protein 133
retinoblastoma-like 1 (p107)
malic enzyme 1, NADP(+)-dependent, cytosolic
inositol 1,4,5-trisphosphate receptor interacting protein-like 2
structure specific recognition protein 1
digestive organ expansion factor homolog (zebrafish)
carbohydrate (chondroitin 4) sulfotransferase 11
ChaC, cation transport regulator homolog 2 (E. coli)
uncharacterized LOC100506290 /// uncharacterized LOC100653153 /// methyltransferase lik
long intergenic non-protein coding RNA 115
transducin (beta)-like 1X-linked
DEAH (Asp-Glu-Ala-His) box polypeptide 35
uncharacterized protein ENSP00000244321
minichromosome maintenance complex component 7
ankyrin repeat domain 10
coiled-coil domain containing 90A
solute carrier family 25 (pyrimidine nucleotide carrier), member 33
thioredoxin-related transmembrane protein 3
jumonji C domain containing histone demethylase 1 homolog D (S. cerevisiae)
solute carrier family 39 (zinc transporter), member 14
protein inhibitor of activated STAT, 2
replication factor C (activator 1) 3, 38kDa
ATPase type 13A3
suppressor of variegation 3-9 homolog 2 (Drosophila)
uncharacterized LOC100506090
phenylalanyl-tRNA synthetase, beta subunit
general transcription factor IIH, polypeptide 1, 62kDa
GABPB1 antisense RNA 1 (non-protein coding)
N-acetylglutamate synthase
ADAM metallopeptidase with thrombospondin type 1 motif, 3
SRR1 domain containing
rabaptin, RAB GTPase binding effector protein 1
ATPase, class VI, type 11C
uncharacterized LOC646762
polymerase (RNA) III (DNA directed) polypeptide K, 12.3 kDa
uncharacterized LOC100506922
TAF5 RNA polymerase II, TATA box binding protein (TBP)-associated factor, 100kDa
cysteinyl-tRNA synthetase
consortin, connexin sorting protein
fatty acid binding protein 5 (psoriasis-associated)
interleukin enhancer binding factor 3, 90kDa
centrosomal protein 128kDa
FK506 binding protein 11, 19 kDa
cell division cycle 25 homolog A (S. pombe)
thymopoietin

Sep (O-phosphoserine) tRNA:Sec (selenocysteine) tRNA synthase
CREB/ATF bZIP transcription factor
UbiA prenyltransferase domain containing 1
FIP1 like 1 (S. cerevisiae)
TAF5 RNA polymerase II, TATA box binding protein (TBP)-associated factor, 100kDa
helicase, lymphoid-specific
SDE2 telomere maintenance homolog (S. pombe)
NADH dehydrogenase (ubiquinone) complex I, assembly factor 4
IKAROS family zinc finger 5 (Pegasus)
tubulin, delta 1
general transcription factor IIH, polypeptide 1, 62kDa
helicase, lymphoid-specific
peptidylprolyl isomerase F
uncharacterized LOC100505549
activin A receptor, type IIB
ZEB1 antisense RNA 1 (non-protein coding)
cleavage and polyadenylation specific factor 6, 68kDa
nucleoporin 107kDa
TATA box binding protein (TBP)-associated factor, RNA polymerase I, B, 63kDa
chromosome 1 open reading frame 43
importin 11
zinc finger, AN1-type domain 4
U2 snRNP-associated SURP domain containing
U2 snRNP-associated SURP domain containing
centrosome and spindle pole associated protein 1
cysteinyl-tRNA synthetase
periphilin 1
HEN1 methyltransferase homolog 1 (Arabidopsis)
cyclin J
tubulin, delta 1
nucleoporin 35kDa
DNA cross-link repair 1A
chromosome 9 open reading frame 72
dual specificity phosphatase 5
solute carrier family 25 (mitochondrial iron transporter), member 37
DDHD domain containing 1
serine/arginine-rich splicing factor 7
zinc finger protein 644
tRNA methyltransferase 13 homolog (S. cerevisiae)
transcription elongation factor B (SIII), polypeptide 3 (110kDa, elongin A)
cell division cycle 45 homolog (S. cerevisiae)
chromosome 17 open reading frame 80
regulator of G-protein signaling 5
high mobility group nucleosome binding domain 5
deoxynucleotidyltransferase, terminal, interacting protein 1
spindlin family, member 3
dihydrofolate reductase

jumonji domain containing 1C
ring finger protein 34, E3 ubiquitin protein ligase
thioredoxin-like 4B
calcium channel, voltage-dependent, alpha 2/delta subunit 1
origin recognition complex, subunit 1
heat shock 70kDa protein 9 (mortalin)
2-hydroxyacyl-CoA lyase 1
phosphoribosyl pyrophosphate synthetase 1
ataxin 1
RAD18 homolog (S. cerevisiae)
leucine rich repeat neuronal 4
deoxynucleotidyltransferase, terminal, interacting protein 1
centromere protein J
zinc finger protein 670
Rho GTPase activating protein 11A
complement component 3
tripartite motif containing 27
oral cancer overexpressed 1
cell division cycle 7 homolog (S. cerevisiae)
leucine rich repeat containing 34
nudix (nucleoside diphosphate linked moiety X)-type motif 16
nuclear factor (erythroid-derived 2)-like 2
solute carrier family 7 (anionic amino acid transporter light chain, xc- system), membe
family with sequence similarity 208, member B
lamin B receptor
FK506 binding protein 11, 19 kDa
ring finger protein, transmembrane 2
ariadne homolog 2 (Drosophila)
consortin, connexin sorting protein
chromosome 11 open reading frame 57
chromosome 6 open reading frame 147 /// KH homology domain containing 1
zinc finger protein 800
PHD finger protein 17
polymerase (RNA) II (DNA directed) polypeptide D
uncharacterized LOC339166 /// WSC domain containing 1
OTU domain containing 4
mature T-cell proliferation 1
B-cell CLL/lymphoma 11A (zinc finger protein)
carbohydrate (chondroitin 4) sulfotransferase 11
TNF receptor-associated factor 3
mutS homolog 2, colon cancer, nonpolyposis type 1 (E. coli)
protein kinase, AMP-activated, alpha 1 catalytic subunit
nucleoporin 160kDa
tripartite motif containing 27
Regulation of nuclear pre-mRNA domain containing 1A
antigen identified by monoclonal antibody Ki-67
basic, immunoglobulin-like variable motif containing

copine VIII
enhancer of zeste homolog 2 (Drosophila)
nuclear factor of activated T-cells, cytoplasmic, calcineurin-dependent 3
leucine zipper transcription factor-like 1
chemokine (C-X-C motif) ligand 5
dihydrofolate reductase
F-box protein 5
MAX gene associated
minichromosome maintenance complex component 5
ribosomal protein S6 kinase, 90kDa, polypeptide 3
X-ray repair complementing defective repair in Chinese hamster cells 4
nucleoporin 214kDa
peptidylprolyl isomerase F
sestrin 2
peptidase inhibitor 3, skin-derived
ChaC, cation transport regulator homolog 1 (E. coli)
chromodomain helicase DNA binding protein 1
copine VIII
zinc finger protein 830
choline kinase alpha
tissue factor pathway inhibitor (lipoprotein-associated coagulation inhibitor) pseudouridylate synthase 7
homolog (S. cerevisiae)-like
transmembrane protein 38B
HEAT repeat containing 6
tryptophanyl-tRNA synthetase
NHL repeat containing 2
pericentrin
tropomyosin 2 (beta)
HNRNPU antisense RNA 1 (non-protein coding)
dynein, cytoplasmic 2, heavy chain 1
queuine tRNA-ribosyltransferase domain containing 1
caspase 8, apoptosis-related cysteine peptidase
minichromosome maintenance complex component 4
exocyst complex component 6
Ubiquitin carboxyl-terminal esterase L1 (ubiquitin thiolesterase)
ATPase, aminophospholipid transporter, class I, type 8A, member 2
RB1-inducible coiled-coil 1
musashi homolog 2 (Drosophila)
uncharacterized LOC442075
consortin, connexin sorting protein
asparagine-linked glycosylation 1, beta-1,4-mannosyltransferase homolog (S. cerevisiae) glucuronidase, beta
pseudogene 1 /// glucuronidase, beta pseudogene 4
serine/arginine-rich splicing factor 1
family with sequence similarity 118, member A
FK506 binding protein 11, 19 kDa
chromodomain helicase DNA binding protein 1
N-acylsphingosine amidohydrolase (non-lysosomal ceramidase) 2B

TIMELESS interacting protein
casein kinase 1, gamma 3
MAP7 domain containing 3
armadillo repeat containing 9
paternally expressed 10
7-dehydrocholesterol reductase
protein geranylgeranyltransferase type I, beta subunit
pseudouridylate synthase 7 homolog (S. cerevisiae)-like
ferrochelatase
gremlin 1
THO complex 5
TSC22 domain family, member 1
BCL2-associated transcription factor 1
DEAD (Asp-Glu-Ala-Asp) box polypeptide 10
uncharacterized LOC100287497 /// uncharacterized LOC100287934
dipeptidyl-peptidase 4
tRNA aspartic acid methyltransferase 1
methylenetetrahydrofolate dehydrogenase (NADP+ dependent) 2, methenyltetrahydrofolate c
chromosome 18 open reading frame 25
transmembrane protein 209
leucine rich repeat neuronal 4
tRNA methyltransferase 6 homolog (S. cerevisiae)
heat shock 70kDa protein 14
DBF4 homolog (S. cerevisiae)
zinc finger and BTB domain containing 24
La ribonucleoprotein domain family, member 4
transducin (beta)-like 1X-linked
transmembrane protein 216
structural maintenance of chromosomes 3
Fanconi anemia, complementation group B
Chromatin licensing and DNA replication factor 1
HLA complex group 18 (non-protein coding)
POU class 2 homeobox 2
minichromosome maintenance complex component 3
DEP domain containing 1B
germ cell associated 2 (haspin)
ZNRD1 antisense RNA 1 (non-protein coding)
p21 protein (Cdc42/Rac)-activated kinase 2
ankyrin repeat domain 11
UDP-Gal:betaGlcNAc beta 1,4- galactosyltransferase, polypeptide 6
minichromosome maintenance complex component 4
malic enzyme 1, NADP(+)-dependent, cytosolic
uncharacterized LOC728855 /// uncharacterized LOC728875
PARP1 binding protein
ribonuclease H2, subunit B
uncharacterized LOC339166 /// WSC domain containing 1
golgi-associated PDZ and coiled-coil motif containing

gremlin 1
secretory carrier membrane protein 1
thymopoietin
LUC7-like 3 (S. cerevisiae)
RAD51 homolog B (S. cerevisiae)
chromosome 16 open reading frame 48
tudor and KH domain containing
bicaudal D homolog 1 (Drosophila)
glycyl-tRNA synthetase
tRNA methyltransferase 13 homolog (S. cerevisiae)
N(alpha)-acetyltransferase 16, NatA auxiliary subunit
UDP-Gal:betaGlcNAc beta 1,4- galactosyltransferase, polypeptide 6
zinc finger and BTB domain containing 24
elongation factor, RNA polymerase II, 2
thioredoxin reductase 1
acidic (leucine-rich) nuclear phosphoprotein 32 family, member E
transmembrane protein 182
discoidin domain receptor tyrosine kinase 2
O-linked N-acetylglucosamine (GlcNAc) transferase
uridine phosphorylase 1
chromosome 11 open reading frame 74
uncharacterized LOC400657
nuclear receptor subfamily 2, group C, member 1
family with sequence similarity 132, member B
junction mediating and regulatory protein, p53 cofactor
centrosome and spindle pole associated protein 1
adenomatous polyposis coli
acetyl-CoA acyltransferase 2
lon peptidase 1, mitochondrial
speckle-type POZ protein
thyroid hormone receptor interactor 13
denticleless E3 ubiquitin protein ligase homolog (Drosophila)
trafficking protein, kinesin binding 2
methyltransferase like 17
E1A binding protein p400
epoxide hydrolase 4
inhibitor of growth family, member 5
non-SMC element 4 homolog A (S. cerevisiae)
methyltransferase like 4
McKusick-Kaufman syndrome
rabaptin, RAB GTPase binding effector protein 1
zinc finger, CCHC domain containing 14
Mdm4 p53 binding protein homolog (mouse)
dyslexia susceptibility 1 candidate 1 /// DYX1C1-CCPG1 readthrough (non-protein coding)
RAP1 interacting factor homolog (yeast)
kelch-like 21 (Drosophila)
transmembrane protein 38B

uncharacterized LOC285628 /// microRNA 146a
chromosome 16 open reading frame 52
tRNA splicing endonuclease 15 homolog (S. cerevisiae)
nucleolar protein 9
golgi membrane protein 1
astrotactin 2
lin-7 homolog C (C. elegans)
F-box protein 5
PCF11, cleavage and polyadenylation factor subunit, homolog (S. cerevisiae)
mitochondrial fission process 1
GTP cyclohydrolase 1
distal-less homeobox 2
stimulated by retinoic acid gene 6 homolog (mouse)
replication factor C (activator 1) 5, 36.5kDa
UHRF1 binding protein 1
cleavage and polyadenylation specific factor 2, 100kDa
aldehyde dehydrogenase 1 family, member L2
protein arginine methyltransferase 6
activating transcription factor 1
MAX gene associated
RNA binding motif protein 26
mediator complex subunit 1
matrin 3 /// small nucleolar RNA host gene 4 (non-protein coding)
nucleoporin 153kDa
SUMO1/sentrin specific peptidase 1
nicotinamide phosphoribosyltransferase
target of EGR1, member 1 (nuclear)
centriolin
zinc finger protein 518B
paraspeckle component 1
methyltransferase like 17
nucleoporin 98kDa
non imprinted in Prader-Willi/Angelman syndrome 2
HAUS augmin-like complex, subunit 6
tripartite motif containing 27
interferon-related developmental regulator 1
heat shock transcription factor 2
serine/arginine-rich splicing factor 6
TWIST neighbor
cleavage stimulation factor, 3' pre-RNA, subunit 2, 64kDa
abhydrolase domain containing 10
FGFR1 oncogene partner
Ribonuclease H1
proline-rich transmembrane protein 3
thiamin pyrophosphokinase 1
mitochondrial translational release factor 1
uncharacterized LOC728855 /// uncharacterized LOC728875

Ras homolog enriched in brain
heat shock 70kDa protein 9 (mortalin)
uncharacterized locus MGC21881
zinc finger, CCHC domain containing 9
intraflagellar transport 122 homolog (Chlamydomonas)
ADP-ribosylation factor-like 6
chromosome 5 open reading frame 44
ARP6 actin-related protein 6 homolog (yeast)
uncharacterized LOC728705
zinc finger protein 227
intercellular adhesion molecule 1
coiled-coil domain containing 41
upstream binding transcription factor, RNA polymerase I
Rho GTPase activating protein 26
MIS18 kinetochore protein homolog A (S. pombe)
MIS18 kinetochore protein homolog A (S. pombe)
Mdm1 nuclear protein homolog (mouse)
kelch repeat and BTB (POZ) domain containing 8
GC-rich sequence DNA-binding factor 1
biorientation of chromosomes in cell division 1
ribosomal protein S6 kinase, 90kDa, polypeptide 3
zinc finger and BTB domain containing 2
serine hydroxymethyltransferase 2 (mitochondrial)
F-box and leucine-rich repeat protein 20
PAN3 antisense RNA 1 (non-protein coding)
alpha-kinase 2
SSU72 RNA polymerase II CTD phosphatase homolog (S. cerevisiae)
ankyrin repeat domain 13C
four and a half LIM domains 1
ATPase, Ca++ transporting, plasma membrane 1
transportin 3
TAF3 RNA polymerase II, TATA box binding protein (TBP)-associated factor, 140kDa
ankyrin repeat domain 11
unc-51-like kinase 4 (C. elegans)
leucine rich repeat containing 58
myoneurin
N-acylsphingosine amidohydrolase (non-lysosomal ceramidase) 2B
nucleoporin 54kDa
methionyl-tRNA synthetase
Rho GTPase activating protein 26
NMDA receptor regulated 2
KIAA1549
proline and serine rich 1
ring finger protein 41
chromosome 5 open reading frame 43
methionyl-tRNA synthetase
RAB3A interacting protein (rabin3)

	FTSCi vs. FTSC		FTSCi vs. FTSCt	
RefSeq Transcript ID	p-value	Fold-Change	p-value	Fold-Change
NM_031479	0.00063466	4.47907	0.00011722	-14.0452
NM_000237	0.0131274	1.76946	0.000156224	-13.4391
NM_001135058 /// NM_0040	0.0162055	1.61273	0.000153534	-10.6209
NM_005640 /// XM_0034036	0.0191241	1.58515	0.000178229	-10.0019
NM_001146335 /// NM_0180	0.0105459	2.59215	0.00102089	-8.43969
NM_013363	0.00305735	2.05335	0.00013755	-7.76648
NM_006902 /// NM_022716	0.00180276	1.87496	5.79E-05	-7.35897
NM_016354	0.000204472	3.5843	5.84E-05	-6.96513
NM_001146335 /// NM_0180	0.037793	3.59134	0.0127751	-6.82613
NM_152739 /// NR_029911 //	0.00976867	2.11093	0.000667088	-6.54988
NM_001198810 /// NM_0036	0.00449467	2.75125	0.000787765	-6.2531
NM_004418	0.00106929	1.67057	2.40E-05	-6.24194
NM_001146335 /// NM_0180	0.000211709	11.0668	0.000549682	-5.72656
NM_014832	0.0106757	1.93074	0.000634044	-5.68462
NM_006042	0.0122319	2.26689	0.00148915	-5.47793
NM_007193	0.00132816	3.27592	0.000495115	-5.23638
NM_001146335 /// NM_0180	6.25E-05	7.98439	0.000152631	-4.67199
NM_014832	0.000711087	1.69076	3.07E-05	-4.50536
NM_000885	0.00288285	3.6754	0.00192927	-4.45159
NM_021800 /// NM_201262	5.35E-05	4.09336	4.53E-05	-4.43831
NR_036540	0.012274	2.99782	0.00539301	-4.34267
NM_001561	0.000837259	5.11388	0.00114579	-4.33945
NM_014096 /// NM_017611 /	6.19E-05	6.44123	0.000127631	-4.31804
NM_001099282 /// NM_0010	0.00241823	2.46865	0.000594205	-4.28094
NM_014906 /// NR_048561	0.000575669	4.27946	0.000581963	-4.25678
NM_018099	0.000320981	8.46914	0.0010498	-4.19331
NM_021800 /// NM_201262	0.00428715	2.17319	0.000710089	-4.18842
NM_001205329 /// NM_0328	0.00415698	1.60154	0.000168486	-4.03007
NM_000885	0.000555189	2.75336	0.000222183	-3.96463
NM_000640	0.000156605	17.5483	0.00148009	-3.83944
NM_001165993 /// NM_0011	0.00291364	2.87724	0.00149129	-3.7743
NM_001136474 /// NM_0011	0.00194104	2.15487	0.000383515	-3.77305
NM_021800 /// NM_201262	0.000769521	5.86935	0.0018147	-3.75622
NM_001018111 /// NM_0053	0.000516371	1.67003	3.09E-05	-3.7319
NM_001008539 /// NM_0011	0.000240162	1.74941	1.89E-05	-3.69546
NM_013300	0.000539073	2.23343	0.00012699	-3.68719
NM_153360	0.00363714	1.82295	0.000372349	-3.67211
NR_026915	0.000325162	4.23953	0.000453272	-3.63997
NM_023070	0.000189272	3.33401	0.000155038	-3.6232
NM_001031855 /// NM_0247	2.13E-06	6.24795	6.21E-06	-3.60359
NM_001105515 /// NM_0058	0.0310334	1.56143	0.00161066	-3.57561
NM_020130	0.00166867	2.637	0.000750887	-3.5631
NM_001128174 /// NM_0033	0.0140875	1.92193	0.00211459	-3.55385

NM_001168683 /// NM_0183	0.0191046	1.78848	0.00210053	-3.54116
NM_004446	0.0331087	1.70171	0.00311908	-3.46836
NM_014096 /// NM_017611 /	0.000822018	2.98108	0.000560762	-3.46446
NR_027349 /// NR_027350 //	0.00408478	3.68229	0.00503027	-3.36273
NM_018126	0.000693866	1.77011	7.43E-05	-3.34663
NM_001037293 /// NM_0530	0.000726468	3.8613	0.00101561	-3.34174
NM_000885	7.92E-05	11.8713	0.000704556	-3.28298
NM_001165993 /// NM_0011	0.0315555	1.62724	0.00261211	-3.28091
NM_138796	0.0113527	1.68461	0.00105663	-3.27148
NM_001006657 /// NM_0207	0.00772359	2.54	0.00416161	-3.17951
NM_004936 /// NM_078487	0.000250821	2.32403	9.85E-05	-3.16758
NM_016447	0.0279302	1.99346	0.00701231	-3.12972
NM_001163812 /// NM_0011	0.0210729	1.52625	0.00138443	-3.00133
NM_024758	0.000398925	3.28164	0.000503589	-3.00067
NM_004843	0.000288241	2.427	0.000154511	-2.98216
NM_001083588 /// NM_0010	0.0220728	1.8732	0.00483948	-2.94767
NM_001178091 /// NM_0011	0.00173067	2.39224	0.00092015	-2.94618
NR_001458 /// NR_030784	0.000105734	10.8253	0.00119618	-2.86971
NM_002451	0.00416762	1.66505	0.00049305	-2.8675
NM_144978	0.00866037	1.68121	0.00111525	-2.86529
NM_001012414	0.00112834	3.02887	0.00131713	-2.86223
NM_001193424 /// NM_0011	0.016303	1.92782	0.0043606	-2.85139
NM_002451	0.00969203	1.7786	0.00173004	-2.84699
NM_152435	0.00877474	1.55224	0.000710225	-2.83618
NM_001190463 /// NM_0019	0.000498646	14.2116	0.00771832	-2.82886
NM_001010853	0.0146196	1.79481	0.00284339	-2.82851
NM_001009913 /// NM_0012	0.000772337	2.98865	0.000901498	-2.82678
NM_004282	0.00473948	1.90698	0.00118131	-2.82492
NM_000071 /// NM_0011780	0.000188095	3.88182	0.000417843	-2.8229
NM_001134658 /// NM_1532	0.00486072	2.61877	0.00391508	-2.82248
NM_002033	0.0110379	1.90883	0.00286235	-2.81807
NM_003758	0.00505745	1.68683	0.000726672	-2.75615
NM_006252	0.000467916	1.9408	0.000131903	-2.75601
NM_000071 /// NM_0011780	0.00119818	3.01119	0.00156242	-2.73851
NM_020799	5.38E-05	6.6908	0.000360185	-2.73436
XR_109352 /// XR_109353 ///	0.009435	2.35498	0.00613506	-2.70979
NM_003799	0.00204196	2.23351	0.00108856	-2.70467
NM_001079877 /// NM_0069	0.0107778	1.58535	0.00118858	-2.68527
NM_001178091 /// NM_0011	0.000187637	6.60506	0.0013051	-2.67214
NM_014388	0.00306528	1.82265	0.000719961	-2.67015
NM_001104631 /// NM_0011	0.00816016	2.02134	0.00318482	-2.65505
NM_016567 /// NM_078468 /	0.00057257	2.18437	0.000296402	-2.65058
NM_024560	0.00644622	1.58069	0.000708264	-2.65027
NM_006321	0.00864154	1.57502	0.000952046	-2.63875
NM_020143	0.00823243	1.69414	0.0014386	-2.61813
NM_001127395 /// NM_1452	0.0433475	1.71245	0.00952125	-2.58109
NM_001080393	0.000330274	2.29404	0.000225712	-2.56861

NM_001127493 /// NM_0011	0.000125647	15.3348	0.00295129	-2.56258
NM_001004346 /// NM_0011	0.000227211	3.99391	0.000723962	-2.55525
NM_001166160 /// NM_0011	0.00349031	3.42279	0.0077023	-2.54484
NM_001080383 /// NM_0054	0.0124754	2.11209	0.0067535	-2.53415
NM_001166160 /// NM_0011	0.00145068	7.27677	0.0129271	-2.52925
XR_110828 /// XR_112106	0.00311139	1.85646	0.00095139	-2.52454
NM_001164750 /// NM_0011	0.0469918	1.85414	0.0164046	-2.51949
NM_003171	0.0369583	1.53649	0.0046082	-2.50101
NM_001178091 /// NM_0011	0.000450889	2.48127	0.00044943	-2.48373
NM_001002901	0.0101577	1.61988	0.00165711	-2.47034
NM_001172779 /// NM_0011	0.00571494	3.54471	0.0147565	-2.46736
NM_001010862 /// NR_0271	0.019748	1.79838	0.00610417	-2.44583
NM_003045	0.000313056	1.84303	0.000101403	-2.43956
NM_001048205 /// NM_0051	0.0197574	1.79332	0.00612467	-2.43318
NM_014167 /// NR_033192	0.0181265	1.53603	0.00230098	-2.42905
NM_001190463 /// NM_0019	0.000483805	26.5228	0.0210033	-2.42389
NM_005886	0.043365	1.75362	0.0131283	-2.41703
NM_004731	0.00252403	6.45052	0.0210054	-2.41337
NM_001042413 /// NM_1526	0.00547258	7.32928	0.0495364	-2.41334
NM_001001732 /// NM_0011	0.00452493	1.59394	0.000717432	-2.3953
NM_001178075 /// NM_0011	0.000135484	4.54944	0.000719672	-2.37491
NM_030971	0.0079964	1.60354	0.00139542	-2.3683
NM_001002269 /// NM_0160	0.0165645	1.56152	0.00258135	-2.35638
NM_025090	0.0123931	2.01927	0.00721546	-2.34397
NM_000189	0.00285691	2.0464	0.00172109	-2.34294
NM_018094	0.00265826	2.69731	0.00416898	-2.33937
NM_002687	0.0114346	2.13188	0.00827534	-2.33822
XR_109628 /// XR_112170	0.0179112	1.64274	0.0039839	-2.3309
NM_002349	0.00905109	1.81287	0.00333536	-2.32285
NM_001105573	0.0164246	1.82426	0.0063852	-2.32243
NM_000819 /// NM_0011360	0.000353907	2.16532	0.000273583	-2.32162
NM_014388	0.000115198	2.88666	0.000230481	-2.31745
NM_170710 /// NM_181265	0.00790502	1.73697	0.00235919	-2.3155
NM_022497	0.0119601	2.6073	0.017315	-2.31115
NM_020799	0.00241798	3.52234	0.00790851	-2.30453
NM_017645	0.0238987	2.32179	0.0245577	-2.30192
NM_002539	0.00459841	1.93659	0.00234236	-2.30165
NM_032226	0.049075	1.63478	0.0122774	-2.29743
NM_001201536 /// NM_0056	0.00417297	2.2937	0.00415649	-2.29631
NM_000390 /// NM_0010373	0.0381292	1.66308	0.010253	-2.29293
NM_001009894	0.0107222	1.55	0.00171921	-2.28709
NM_016331	0.00268468	1.69544	0.000723994	-2.27915
NM_006321	0.0146743	1.67168	0.00389625	-2.27202
NM_030647	0.00062285	3.53997	0.00225564	-2.26446
NM_001104631 /// NM_0011	0.023319	1.5898	0.00481276	-2.26296
NM_016000 /// NM_182916	0.00443791	1.83685	0.00188298	-2.26173
NM_138775	0.00560761	2.38545	0.00675275	-2.25843

NM_020143	3.14E-05	1.64671	7.23E-06	-2.25694
NM_152400	0.000981883	2.118	0.000786039	-2.24573
NM_182705	0.00130802	4.63123	0.00841306	-2.2405
NM_004731	0.00644407	3.02676	0.0156829	-2.23941
NM_004490	0.000596815	2.45693	0.000828983	-2.23592
NM_001042413 /// NM_1526	0.000702157	4.83719	0.00504626	-2.23493
NM_001253861 /// NM_0321	0.00425605	2.45158	0.00583942	-2.23304
NM_000310 /// NM_0011426	0.00428146	1.54817	0.000728238	-2.22407
NM_133465	0.0205419	2.42117	0.02691	-2.22294
NM_178836	0.000219836	3.52614	0.000853994	-2.22242
NM_001261392 /// NM_0012	0.0211745	1.69503	0.00678305	-2.21529
NM_018112	0.00526977	2.20697	0.00520709	-2.21427
NM_003201	0.00197535	1.84649	0.000935911	-2.20381
NM_001012626 /// NM_0226	9.72E-05	1.96184	6.05E-05	-2.20326
NM_003686 /// NM_006027 /	0.00254318	1.8947	0.00137272	-2.19998
NM_000534 /// NM_0011281	0.0108343	1.68593	0.00336926	-2.195
NM_001083585 /// NM_0047	0.00725004	2.66306	0.0136936	-2.18305
NM_001166160 /// NM_0011	0.0293561	1.6864	0.00986797	-2.1829
NM_003201	0.000383644	2.36409	0.000513794	-2.18133
NM_001105573	0.00580465	2.10916	0.00511808	-2.18094
NM_001197297 /// NM_0020	0.0357147	1.7551	0.0150079	-2.18066
NM_004589	0.00870461	1.66539	0.00257087	-2.17989
NM_017947	0.0145637	2.36319	0.0190643	-2.17961
NM_001004346 /// NM_0011	0.0441356	1.81415	0.0221481	-2.17653
NM_000946	0.00113159	1.94073	0.000712531	-2.17103
NM_000819 /// NM_0011360	0.0132359	2.04685	0.0106446	-2.16986
NM_018518 /// NM_182751	0.00384356	1.5335	0.000671021	-2.16921
NM_001160305 /// NM_0248	0.000518084	1.78333	0.000217428	-2.16889
NM_152547	0.0258773	1.55856	0.00563067	-2.15939
NM_001014972 /// NM_0012	0.00515123	2.42339	0.0076992	-2.15755
NM_018518 /// NM_182751	0.000594626	2.05625	0.000491883	-2.15631
NM_001008394	0.00112389	2.50578	0.00190546	-2.15513
NM_032367	0.000582068	2.56049	0.0010679	-2.15137
NM_001042490 /// NM_0010	0.00354691	1.72248	0.00129999	-2.15133
NM_002454 /// NM_024010	0.00890394	1.63759	0.00251837	-2.14901
NM_001515	0.000776009	2.0234	0.000616353	-2.14186
NM_001136557 /// NM_0011	0.0054936	2.33577	0.00753759	-2.13686
NM_001144920 /// NM_0011	0.00636774	2.90437	0.0164916	-2.13581
NM_006252	0.00218389	3.17969	0.0073931	-2.13527
NM_182705	3.13E-05	10.8573	0.000955389	-2.13526
NM_152405	0.00448527	5.04529	0.0363281	-2.13041
NM_001207025 /// NM_0012	2.09E-05	9.71903	0.000561762	-2.12836
NM_054027	0.00282206	2.14022	0.00289069	-2.12689
NM_002033	0.00186109	2.20711	0.00216835	-2.12016
NM_001256798 /// NM_0806	0.00134455	2.0951	0.00130972	-2.109
NM_006896	0.00355725	2.76325	0.00866587	-2.10634
NM_144695	0.0119262	1.74609	0.00528927	-2.10196

NM_001077708 /// NM_0196	0.00417888	2.19327	0.00491402	-2.10115
NM_030780	0.00276938	1.80031	0.00139815	-2.10067
NM_001203 /// NM_0012567	0.00038466	2.29274	0.000545195	-2.09164
NM_001032281 /// NM_0062	0.000200654	4.82939	0.00190125	-2.09143
NM_001077440 /// NM_0010	0.0274594	2.19617	0.0324525	-2.09126
NM_014285	0.0241844	1.68482	0.00937035	-2.09035
NM_002915 /// NM_181558	0.00933654	2.13383	0.0101011	-2.08961
NM_020386	0.0313722	1.64809	0.0109988	-2.08874
XR_110490 /// XR_133252	0.00680193	1.8571	0.00413322	-2.08819
NM_032367	8.40E-05	2.62677	0.000191925	-2.0804
NM_001178091 /// NM_0011	0.000144623	2.90728	0.000445728	-2.0787
NM_001207025 /// NM_0012	9.21E-05	5.97117	0.0013153	-2.07795
NM_001080393	0.0126859	2.64536	0.027539	-2.07554
NM_001207025 /// NM_0012	0.00680063	2.29608	0.00989971	-2.07066
NM_016612	0.000559677	2.28797	0.000820848	-2.06978
NM_001135575	0.00504942	1.85077	0.00315126	-2.0638
NM_144658	0.00324889	2.96744	0.0104124	-2.06236
NR_039993 /// NR_039994 //	0.000798802	1.7685	0.000394067	-2.06104
NM_006646	0.00208229	2.47422	0.00401489	-2.0609
NR_040027 /// NR_040028	0.0273336	2.30729	0.0397199	-2.06071
NM_001166345 /// NM_0011	0.00200686	2.23524	0.00274159	-2.06057
NR_027301	0.00227337	1.89306	0.00159857	-2.05352
NM_001085379 /// NR_01543	0.00239448	3.83693	0.0143804	-2.04928
NM_001171904 /// NM_0147	0.00685567	1.73514	0.00324132	-2.04376
NM_001142853 /// NM_0186	0.0261356	2.3132	0.0395846	-2.04209
NM_152432	0.00693117	2.37481	0.0119164	-2.04114
NM_198461	4.92E-05	6.3997	0.000865848	-2.03385
NM_017518 /// NM_080701 /	0.0171989	1.70603	0.00780566	-2.03308
NM_001203 /// NM_0012567	3.37E-05	3.30775	0.000161656	-2.03033
NM_001098729 /// NR_03341	0.013009	1.67437	0.00534859	-2.02602
NM_001165412 /// NM_0039	0.0263847	1.53305	0.00662263	-2.02483
NM_003201	0.000256245	2.32318	0.000440958	-2.01887
NM_001164271 /// NM_0060	0.0106211	2.59132	0.0243686	-2.0186
NM_181655 /// NM_181656	0.0167084	1.75939	0.00913869	-2.01825
NM_000077 /// NM_0011951	0.000168763	7.01954	0.00354181	-2.0063
NM_001134830 /// NM_0011	0.00869819	1.55571	0.00235448	-2.00496
NM_006896	0.000201778	2.67862	0.000572769	-2.00204
NM_198461	3.84E-05	22.0423	0.00325389	-2.00145
NM_001018054 /// NM_0046	0.000560213	3.37963	0.00294346	-2.00087
NM_005746 /// NM_182790	0.00119964	1.84134	0.000823987	-2.00003
NM_001172574 /// NM_0011	0.00357842	2.64825	0.00961033	-1.99265
NM_001174166 /// NM_0046	0.000282538	10.8481	0.0106255	-1.99179
NM_001105206 /// NM_0011	0.000932597	3.98443	0.00713946	-1.98873
NM_001039374 /// NM_0328	0.0484309	1.60599	0.0184728	-1.98795
NM_001086	0.00117923	2.56199	0.00296999	-1.98723
NM_152407	0.00584519	1.9184	0.00503191	-1.98656
NM_006291	0.0239911	1.69711	0.0118079	-1.98624

NM_001173982 /// NM_0184	0.00309543	2.4425	0.00666285	-1.98279
NM_021154 /// NM_058179	0.000333293	3.97112	0.00267196	-1.97768
NM_016612	0.000586904	2.4747	0.00136289	-1.97719
NM_003201	0.0439704	1.88703	0.0370734	-1.97305
NR_003013 /// NR_027058	0.0257217	1.50758	0.00648756	-1.96633
NM_001197330 /// NM_0011	0.00482758	1.92208	0.00439507	-1.96409
NM_001616	0.00350817	2.24288	0.00594764	-1.95935
NM_174910	0.0200911	2.20908	0.0312244	-1.95576
NM_014053	0.0186546	1.68485	0.0093172	-1.95549
NM_001006622 /// NM_0010	0.00107238	2.42015	0.0024207	-1.95444
NM_001013620	0.00217616	1.73438	0.00122479	-1.95327
XR_110082 /// XR_112807	0.0221781	1.60864	0.00865756	-1.95219
NM_016612	0.00773949	2.00224	0.00862817	-1.95053
NM_000201	0.00309128	2.79164	0.0106017	-1.94901
NM_144581	0.000102546	3.54868	0.000693825	-1.94833
NM_000462 /// NM_130838 /	0.00704445	1.61659	0.00273909	-1.94722
NM_001142317 /// NM_0011	0.0383444	1.66657	0.0191852	-1.94489
NM_032834	0.0274376	1.84453	0.0220436	-1.94446
NM_000636 /// NM_0010244	3.77E-05	2.85524	0.000147745	-1.94376
NM_017754	0.000488602	1.98071	0.000531843	-1.943
NM_005916 /// NM_182776	0.00779986	2.03222	0.00943362	-1.94049
NM_024094	0.017065	1.89181	0.0153526	-1.94001
NM_001935	0.00455235	2.67987	0.0140541	-1.93798
NM_002577	0.00377446	1.6124	0.00146981	-1.93398
NM_014363	0.0013257	2.31108	0.00268266	-1.93257
NM_001139459 /// NM_1526	0.00617942	2.5087	0.0158372	-1.92984
NM_000077 /// NM_0011951	0.000190417	7.25995	0.00494034	-1.92962
NM_000436	0.000651287	2.86629	0.00263556	-1.92577
NM_006513 /// NR_034072 //	0.0056111	1.79146	0.00402468	-1.92384
NM_002041 /// NM_005254 /	0.000100156	2.26795	0.000196162	-1.92308
NM_001135575	0.0193521	1.85311	0.0165331	-1.92265
NM_001144958 /// NM_0011	0.000697593	5.25193	0.0105706	-1.91701
NM_014388	0.000936701	1.88016	0.000858169	-1.91614
NM_020768	0.00272467	3.71416	0.0199622	-1.9132
NM_001199237 /// NM_0011	0.000926021	2.5158	0.00261223	-1.91269
NM_003455	0.013143	1.57998	0.00489996	-1.91243
NM_004731	0.0130712	2.43743	0.0308082	-1.91089
NM_203302 /// NM_203477 /	0.000159165	1.7799	0.000113582	-1.90687
NM_001018054 /// NM_0046	0.00616657	3.4043	0.0354931	-1.9068
NM_001256279 /// NM_0012	6.05E-05	2.02469	8.00E-05	-1.90118
NM_001012626 /// NR_02684	0.000870614	1.76875	0.000611444	-1.90111
NM_001080502 /// NM_1734	0.000408825	3.92294	0.00380936	-1.89794
NM_003090	0.0108517	1.61247	0.00472607	-1.89672
NM_001034841 /// NR_02802	0.00298622	2.0228	0.00395149	-1.89592
NM_001145343 /// NM_0011	0.00200145	2.08265	0.00299097	-1.8954
NM_007192	0.000705093	2.23633	0.00139672	-1.89411
NM_001032281 /// NM_0062	3.02E-05	6.08242	0.000673972	-1.89288

NM_001018113 /// NM_1526	0.00150255	1.99361	0.00189164	-1.89263
NM_001201545 /// NM_0227	0.0119035	1.625	0.00550624	-1.892
NM_032021	0.0154009	1.58713	0.00624072	-1.8917
NM_002895 /// NM_183404	0.0183636	2.13769	0.0294375	-1.88929
NM_002395	3.00E-05	2.60211	0.000102531	-1.88592
NM_001034841 /// NR_02802	0.0259175	1.55097	0.00953271	-1.88309
NM_003146	0.000209737	1.50377	5.65E-05	-1.88245
NM_014388	0.00113928	3.37772	0.00764186	-1.88216
NM_001173982 /// NM_0184	0.00572589	2.3187	0.0128437	-1.88065
NM_001008708	0.00334497	1.65398	0.00172212	-1.88037
NM_001127395 /// NM_1452	0.00128205	3.74853	0.0109021	-1.87733
NM_024796 /// NR_024321	0.031931	1.86897	0.031635	-1.8732
NM_001139466 /// NM_0011	0.017598	1.6328	0.00890239	-1.87189
NM_001190809 /// NM_0219	0.0463433	1.53892	0.0174776	-1.87163
NM_001193621 /// NM_0011	0.0126846	1.99025	0.0164528	-1.87045
NM_005916 /// NM_182776	0.000992709	2.45556	0.00287333	-1.86959
NM_017664	0.000370882	2.00879	0.000516562	-1.86644
NM_001031713 /// NM_0221	0.000458761	1.96481	0.000584997	-1.86333
NM_032315	0.000805887	4.02767	0.00845967	-1.86118
NM_019022	0.0245526	1.86152	0.0246548	-1.85971
NM_030647	0.00028182	2.17909	0.000559878	-1.85614
NM_001128431 /// NM_0011	6.49E-05	2.7236	0.000274985	-1.85559
NM_004671 /// NM_173206	0.0183079	1.78304	0.0153033	-1.85452
NM_002915 /// NM_181558	0.000594384	1.82594	0.000551192	-1.85444
NM_024524	0.00873766	1.78379	0.00733656	-1.85074
NM_001193424 /// NM_0011	0.00226284	2.00991	0.00326604	-1.85073
XR_110202 /// XR_112909	0.0413879	1.74915	0.0325229	-1.84912
NM_005687	0.0042141	1.69261	0.00269165	-1.84799
NM_001142307 /// NM_0053	0.0282895	2.01099	0.0395128	-1.84677
NR_024490	0.00434356	2.43428	0.0125446	-1.84438
NM_153006	0.00761652	1.75613	0.00601922	-1.84339
NM_014243	5.44E-05	16.2957	0.00488404	-1.84266
NM_001013694	0.0299976	1.6025	0.0150155	-1.84165
NM_001083585 /// NM_0047	0.00365219	1.69364	0.00238021	-1.84099
NM_001010986 /// NM_1736	0.0125925	1.66801	0.00767837	-1.8409
NR_024278	0.00323011	3.55994	0.0253577	-1.83766
NM_016310	0.00147305	1.77277	0.00123507	-1.83639
XR_109888 /// XR_112387	0.00900851	2.28238	0.0210662	-1.83364
NM_006951	0.00115453	2.97818	0.0064552	-1.8301
NM_001014437 /// NM_0010	0.00103995	2.93184	0.00563151	-1.82776
NM_001139459 /// NM_1526	0.00119169	1.94527	0.00159693	-1.82667
NM_001444	0.0036916	1.74034	0.00290451	-1.82528
NM_001137673 /// NM_0045	0.0130936	1.73643	0.0104308	-1.81992
NM_152446	0.000827576	1.65327	0.000493012	-1.81957
NM_001143781 /// NM_0011	0.00365265	1.81068	0.00357012	-1.81921
NM_001789 /// NM_201567	0.00535963	1.87875	0.00623226	-1.81894
NM_001032283 /// NM_0010	0.0099983	2.48869	0.0313207	-1.81869

NM_001159728 /// NM_0169	0.00504254	2.07935	0.00900596	-1.81704
NM_001039618 /// NM_0212	0.0036308	1.59194	0.00174923	-1.81671
NM_013319	0.00141553	2.47236	0.00477727	-1.81593
NM_001134937 /// NM_0011	0.0175268	1.96028	0.0247206	-1.80784
NM_006951	0.000491373	1.82314	0.000512932	-1.80751
NM_018063	0.00159234	2.03713	0.00273354	-1.80709
NM_152608	0.00640093	1.52105	0.00237011	-1.80619
NM_014165	0.00232924	2.56104	0.00887638	-1.80577
NM_022466	0.00381566	2.21183	0.0088876	-1.80533
NM_001193609 /// NM_0011	0.00045316	2.03874	0.000790303	-1.80521
NM_001142307 /// NM_0053	0.00156257	1.96614	0.00233356	-1.80347
NM_018063	0.000368249	2.99828	0.0023154	-1.80338
NM_005729	0.000146035	2.67279	0.000670943	-1.80276
NM_001242804	0.0133752	1.69119	0.0097206	-1.80251
NM_001106	0.00312453	1.8511	0.00356913	-1.80079
NR_024284	0.0152437	1.96773	0.0223481	-1.79982
NM_007007	0.00529879	1.60638	0.00285093	-1.79886
NM_020401	0.000500381	1.51046	0.000174783	-1.79845
NM_005680	0.00746063	1.72308	0.00601599	-1.79821
NM_001098616 /// NM_0154	0.00216243	1.79763	0.0021704	-1.79631
NM_001134779 /// NM_0163	0.00742928	2.04842	0.0131235	-1.79577
NM_001128324 /// NM_1748	0.00387258	1.75824	0.0034822	-1.79567
NM_001080415	0.00193267	1.72988	0.00159463	-1.79519
NM_001080415	0.0275171	1.70059	0.0214421	-1.79207
NM_001077204 /// NM_0247	0.000414536	1.63822	0.00025334	-1.79016
NM_001014437 /// NM_0010	0.00147774	1.9716	0.00232027	-1.78987
NM_001143787 /// NM_0011	0.0375945	1.52269	0.0159601	-1.78858
NM_001102592 /// NM_1445	0.0131974	2.39366	0.038906	-1.78808
NM_001134375 /// NM_0011	0.00483676	2.27121	0.0129339	-1.78507
NM_001193609 /// NM_0011	0.000639126	1.76237	0.000600254	-1.78383
NM_001008544 /// NM_1382	0.00179313	1.57872	0.000895636	-1.78204
NM_014881	0.0083243	1.55125	0.0037942	-1.78174
NM_001256054 /// NM_0183	0.0250256	1.57874	0.0135148	-1.77418
NM_004419	0.00363267	1.61607	0.00216495	-1.77401
NM_016612	0.00112256	1.72073	0.000955853	-1.77372
NM_001160147 /// NM_0011	0.000472704	4.05912	0.00653089	-1.77135
NM_001031684 /// NM_0011	0.00210986	1.51413	0.000821038	-1.77068
NM_016620 /// NM_032186 /	0.00989997	2.08711	0.019963	-1.76887
NM_019083	0.0114498	1.60526	0.00688425	-1.76279
NM_003198	0.0165819	1.55885	0.00842437	-1.76188
NM_001178010 /// NM_0011	0.0092612	1.91559	0.0136506	-1.76051
NM_001100621 /// NM_0011	0.0346992	1.74329	0.0334822	-1.75693
NM_001195303 /// NM_0012	0.0253672	1.68584	0.0209954	-1.75193
NM_030763	0.00369573	4.0031	0.0442541	-1.75154
NM_052951	0.00136162	2.18801	0.00363971	-1.7499
NM_001010862 /// NR_02713	0.00169036	1.52532	0.000735697	-1.74987
NM_000791	0.00642775	2.07509	0.0137892	-1.74437

NM_004241 /// NM_032776	0.00166799	1.93903	0.00278747	-1.74316
NM_001256858 /// NM_0251	0.0404806	1.52725	0.0199748	-1.74217
NM_001142317 /// NM_0011	0.00924718	1.95634	0.0156716	-1.74199
NM_000722	1.30E-05	38.0977	0.00348667	-1.74171
NM_001190818 /// NM_0011	0.00860468	1.5317	0.00405029	-1.7417
NM_004134	0.0117181	1.55151	0.00606868	-1.74101
NM_012260	0.00290217	2.14489	0.00729344	-1.74057
NM_001204402 /// NM_0027	0.00853284	2.00231	0.0160781	-1.73828
NM_000332 /// NM_0011281	0.00269869	2.28074	0.00853174	-1.73781
NM_020165	0.0315474	1.69728	0.0282551	-1.73659
NM_152611	4.59E-05	4.52487	0.000923935	-1.73649
NM_052951	0.00606517	2.67105	0.029733	-1.73537
NM_018451 /// NR_047594 //	0.0175583	1.74854	0.0182311	-1.73515
NM_001204220 /// NM_0332	0.0125593	2.44709	0.0453621	-1.73403
NM_014783 /// NM_199357	0.00769013	2.5401	0.0324139	-1.73299
NM_000064	0.00355541	1.96417	0.006431	-1.73237
NM_006510 /// NM_030950	0.00211844	3.23793	0.0184004	-1.73212
NM_153451	0.0289648	1.89263	0.0429436	-1.72773
NM_001134419 /// NM_0011	5.65E-05	2.63167	0.000311532	-1.72739
NM_001172779 /// NM_0011	0.000528157	5.2077	0.013053	-1.72721
NM_001171905 /// NM_0011	0.00707567	1.78235	0.00833693	-1.72539
NM_001145412 /// NM_0011	0.00832441	1.64225	0.00638456	-1.72395
NM_014331	6.62E-05	4.30096	0.00124993	-1.72278
NM_017782	0.00010423	1.60986	7.01E-05	-1.72223
NM_002296 /// NM_194442	0.000411947	2.02286	0.000889547	-1.72223
NM_001143781 /// NM_0011	0.00260635	2.18932	0.00754754	-1.71933
NM_001109903 /// NM_0328	0.00371185	2.50893	0.0165883	-1.71871
NM_006321	0.00109128	2.18544	0.00321099	-1.7181
NM_001139459 /// NM_1526	0.00244859	2.99384	0.0182448	-1.71669
NM_001082969 /// NM_0010	0.00438994	1.69415	0.00409822	-1.7158
NM_001251874 /// NM_0305	0.00492145	2.24465	0.0154618	-1.71352
NM_176814	0.00516958	2.31341	0.0179284	-1.71303
NM_024900 /// NM_199320	0.000255248	2.5024	0.00124823	-1.71168
NM_004805	0.005666	1.85344	0.00840095	-1.71141
NM_015253 /// NR_040000	0.00142723	4.60425	0.0274714	-1.71101
NM_001102653 /// NM_0174	0.00131332	1.86767	0.00205051	-1.71065
NM_001018025 /// NM_0142	0.0157457	1.71212	0.0159134	-1.70857
NM_018014 /// NM_022893 /	0.00211537	1.78254	0.00264463	-1.70839
NM_001173982 /// NM_0184	0.0012245	1.94519	0.00232428	-1.70749
NM_001199427 /// NM_0033	0.00263809	2.81082	0.0171842	-1.70595
NM_000251 /// NM_0012582	0.00106095	3.04204	0.00894201	-1.70535
NM_006251 /// NM_206907	0.019139	1.53015	0.0102487	-1.70508
NM_015231	0.0163949	1.67072	0.0148802	-1.7019
NM_006510 /// NM_030950	0.00218253	1.92518	0.00400657	-1.70183
NM_018170	0.0177584	1.5139	0.00894518	-1.70086
NM_001145966 /// NM_0024	0.00185411	2.00857	0.00410547	-1.70064
NM_001159596 /// NM_0176	0.00363329	1.80339	0.00494098	-1.69919

NM_153634	0.0221291	1.61245	0.0167226	-1.69891
NM_001203247 /// NM_0012	0.00237953	2.07387	0.00603748	-1.69697
NM_004555 /// NM_173163 /	0.0152631	1.50384	0.00739849	-1.69673
NM_020347	0.000918209	3.37897	0.0103347	-1.69619
NM_002994	2.71E-06	12.0184	0.000280904	-1.69515
NM_000791	0.00441778	1.61409	0.00333263	-1.69505
NM_001142522 /// NM_0121	6.01E-05	3.38543	0.000731044	-1.69497
NM_001080541 /// NM_0011	0.0129366	1.68203	0.0124364	-1.69461
NM_006739	0.00320447	2.72489	0.0196566	-1.69389
NM_004586	0.00166508	2.52393	0.00849562	-1.69389
NM_003401 /// NM_022406 /	0.0356335	1.68864	0.0351692	-1.6932
NM_005085	0.0123252	2.00648	0.0263621	-1.69214
NM_005729	0.00357951	2.03123	0.00841882	-1.69191
NM_031459	8.73E-06	3.27526	9.98E-05	-1.6919
NM_002638	0.00254981	1.81461	0.00367393	-1.69147
NM_001142776 /// NM_0241	0.000829706	2.80573	0.00597604	-1.69036
NM_001270	0.0135032	1.55468	0.00832783	-1.68966
NM_153634	0.00130352	1.59953	0.00094246	-1.68912
NM_052857	0.000598746	2.08272	0.00161825	-1.68909
NM_001277 /// NM_212469	0.0174426	1.71927	0.0191285	-1.68837
NM_001032281 /// NM_0062	0.000188797	7.88497	0.0105257	-1.68736
NM_001098614 /// NM_0010	0.00523292	1.95401	0.0105624	-1.68713
NM_018112	0.000860555	3.93473	0.0139011	-1.68668
NM_022070	0.00282419	2.05795	0.00719791	-1.68489
NM_004184 /// NM_173701 /	0.00113803	2.47219	0.00570311	-1.68353
NM_198514	0.019546	1.79881	0.0269358	-1.6829
NM_006031	0.000130649	1.86546	0.000224709	-1.682
NM_001145822 /// NM_0032	0.00512921	1.64219	0.00449919	-1.68056
NR_026778	1.61E-05	2.83353	0.000130566	-1.6784
NM_001080463 /// NM_0013	0.0131662	2.06531	0.0325128	-1.67807
NM_001256835 /// NM_0012	0.0202259	1.57991	0.0145372	-1.67595
NM_001080124 /// NM_0010	0.00757413	1.59597	0.00571781	-1.67517
NM_005914 /// NM_182746	0.00224807	2.55083	0.012417	-1.67476
NM_001013848 /// NM_0190	0.00507779	2.79705	0.0340014	-1.6736
NM_004181	0.000509403	6.333	0.0202006	-1.67308
NM_016529	0.00148143	4.27085	0.0280921	-1.66988
NM_001083617 /// NM_0147	0.00470432	2.04435	0.0120891	-1.66964
NM_138962 /// NM_170721	0.00327522	1.76125	0.00436779	-1.66944
NM_001013730 /// XR_11003	0.00108092	1.82484	0.00173326	-1.66939
NM_001139459 /// NM_1526	0.00103627	2.0421	0.00276046	-1.66789
NM_019109	0.0104462	1.66241	0.0102678	-1.66763
NM_206908 /// NM_206910 /	0.00309836	3.4743	0.036553	-1.66696
NM_001078166 /// NM_0069	0.00596351	2.72094	0.0373696	-1.66662
NM_001104595 /// NM_0179	0.040242	1.50648	0.02288	-1.66433
NM_001143781 /// NM_0011	0.000119242	2.22396	0.000460359	-1.66234
NM_001270	0.0104605	1.56989	0.00751516	-1.66051
NM_001079516	0.0122345	1.51327	0.00695521	-1.65922

NM_017858	8.36E-05	2.8939	0.00076407	-1.65855
NM_001031812 /// NM_0010	0.007085	1.58938	0.00553073	-1.65749
NM_001173516 /// NM_0011	0.00301623	1.68215	0.00329285	-1.65636
NM_025139	0.000522525	2.39766	0.00265146	-1.6558
NM_001040152 /// NM_0011	0.00889404	1.52309	0.00534599	-1.65388
NM_001163817 /// NM_0013	0.00103094	1.7197	0.00128769	-1.65338
NM_005023	0.0499922	1.50536	0.0297021	-1.65308
NM_001098614 /// NM_0010	0.0283779	1.75716	0.0382835	-1.65168
NM_000140 /// NM_0010125	0.00551416	2.68166	0.0351708	-1.65136
NM_001191322 /// NM_0011	0.000106886	50.8321	0.0397859	-1.64969
NM_001002877 /// NM_0010	0.000192821	1.64532	0.000190454	-1.64872
NM_001243797 /// NM_0012	0.000941362	1.94697	0.00219855	-1.64798
NM_001077440 /// NM_0010	0.0013272	1.53702	0.00085622	-1.64634
NM_004398	0.00052048	1.62292	0.000478289	-1.64575
XR_108279 /// XR_112047 ///	0.0104249	1.57177	0.00798216	-1.64406
NM_001935	7.91E-05	6.11185	0.0036534	-1.64306
NM_004412 /// NM_176081 /	0.00711549	1.82473	0.01232	-1.64014
NM_001040409 /// NM_0066	0.000631878	2.14286	0.00226537	-1.63958
NM_001008239 /// NM_1450	0.0137383	1.65586	0.0145337	-1.63906
NM_032842	0.0107478	1.74967	0.015165	-1.63894
NM_152611	0.000666062	5.40575	0.0226232	-1.63829
NM_015939	0.00057903	2.36385	0.00297932	-1.63789
NM_016299	0.000109506	2.23772	0.000472804	-1.63774
NM_006716	0.0123603	1.9703	0.0293555	-1.63582
NM_001164313 /// NM_0147	0.0137991	1.74063	0.0191052	-1.63559
NM_001170803 /// NM_0011	0.0037431	1.63921	0.00381259	-1.63409
NM_001139466 /// NM_0011	0.00357547	2.1757	0.0132659	-1.63248
NM_001173990 /// NM_0011	0.01664	1.84696	0.0304416	-1.63091
NM_005445	0.00537066	1.7746	0.00848283	-1.62995
NM_001018113 /// NM_1526	0.00367366	2.27655	0.0160643	-1.6296
NM_030928	0.0152226	1.98623	0.037632	-1.62838
NR_024052 /// NR_024053	0.00537728	1.97238	0.0138662	-1.62488
NM_001207025 /// NM_0012	0.0107659	1.95274	0.025965	-1.62306
NM_001270472 /// NM_0023	0.000600553	1.65122	0.000667928	-1.62234
NM_001145208 /// NM_0183	0.000118241	2.01724	0.000359774	-1.6215
NM_031965	0.0252189	1.74973	0.0369458	-1.62073
NR_026751	0.00237003	1.7446	0.0036181	-1.61818
NM_002577	0.00495906	1.94867	0.0125831	-1.61625
NM_001256182 /// NM_0012	6.41E-05	1.89987	0.000152827	-1.61621
NM_004775	0.0223901	1.76316	0.0347124	-1.61546
NM_005914 /// NM_182746	0.00283966	1.72623	0.00414281	-1.61503
NM_002395	0.002179	2.6167	0.0158853	-1.61491
NR_024510 /// NR_024511 //,	0.00172778	1.51711	0.00114811	-1.61417
NM_017915	0.00130469	2.75527	0.0114425	-1.61225
NM_001142279 /// NM_0245	0.0229905	1.70632	0.0309477	-1.61157
NM_015253 /// NR_040000	8.54E-05	26.9902	0.0236274	-1.61027
NM_001017408 /// NM_0203	0.0115488	1.80308	0.0207582	-1.6094

NM_001191322 /// NM_0011	5.15E-05	76.117	0.0311946	-1.60915
NM_004866 /// NM_052822	4.40E-05	1.93861	0.000118744	-1.608
NM_001032283 /// NM_0010	0.00227181	2.71931	0.0188701	-1.60735
NM_006107 /// NM_016424	0.000386463	2.20595	0.00175654	-1.60715
NM_002877 /// NM_133509 /	0.018019	1.97662	0.0464021	-1.60588
NM_032140	0.00916668	1.93274	0.0227439	-1.6054
NM_001083963 /// NM_0010	0.00501599	2.09443	0.0175528	-1.60507
NM_001003398 /// NM_0017	0.000280885	3.36166	0.00449885	-1.60494
NM_002047	0.000946222	2.11967	0.00367965	-1.60458
NM_019083	0.00423235	1.78707	0.00764793	-1.60358
NM_001110798 /// NM_0185	0.000832492	1.59086	0.000795325	-1.60237
NM_004775	0.000362299	1.90075	0.000928323	-1.59658
NM_001164313 /// NM_0147	0.0255384	1.59839	0.0257641	-1.5959
NM_012081	0.00323475	2.11084	0.0123573	-1.59498
NM_001093771 /// NM_0012	4.13E-05	8.99296	0.00407913	-1.59493
NM_001136478 /// NM_0011	0.000734595	2.82448	0.0075681	-1.59478
NM_144632	0.00240364	2.35309	0.0136059	-1.59436
NM_001014796 /// NM_0061	0.000520656	6.27733	0.0264631	-1.59393
NM_003605 /// NM_181672 /	0.000508023	1.6757	0.000687834	-1.59386
NM_003364 /// NM_181597	0.00265557	2.34934	0.0149272	-1.59332
NM_138787	0.00296121	1.63932	0.00352625	-1.59276
NM_001008234 /// NR_02448	0.000320415	3.53015	0.00601853	-1.59176
NM_001032287 /// NM_0011	0.000420976	2.07731	0.00161403	-1.59103
XM_001714385 /// XM_00311	2.88E-05	9.15728	0.00303332	-1.5878
NM_152405	8.15E-05	9.1873	0.00828246	-1.58706
NM_001077204 /// NM_0247	0.0145693	1.76857	0.0259793	-1.58421
NM_000038 /// NM_0011275	0.00674162	1.92199	0.0179673	-1.58359
NM_006111	0.00156352	2.04789	0.00572152	-1.58239
NM_004793	0.00346314	1.72581	0.00577156	-1.57957
NM_001007226 /// NM_0010	0.0026938	2.03545	0.00957133	-1.57937
NM_001166260 /// NM_0042	0.00529259	1.67224	0.00745869	-1.57771
NM_016448	0.00135977	3.98727	0.03116	-1.57769
NM_015049	0.00124878	2.95563	0.0150773	-1.57685
NM_001029991 /// NM_0010	0.0171706	1.55831	0.0160766	-1.57529
NM_015409	2.42E-05	1.78756	5.05E-05	-1.57484
NM_173567	6.23E-06	9.4035	0.000737304	-1.57438
NM_032329	0.00612027	1.80054	0.0127157	-1.57413
NM_001167865 /// NM_0176	0.000546436	1.58533	0.000578037	-1.5717
NM_022840	0.00643627	2.62669	0.0498256	-1.56984
NM_018848 /// NM_170784 /	0.0013799	1.54533	0.0012515	-1.56814
NM_001083585 /// NM_0047	0.00193077	2.00724	0.0068685	-1.56769
NM_015144	0.00255357	2.18269	0.0124072	-1.56692
NM_001204171 /// NM_0012	0.0214313	1.66534	0.0300506	-1.56633
NM_001033559 /// NM_0010	0.00112725	2.62133	0.0103144	-1.56606
NM_001177663 /// NM_0011	0.00764503	2.01539	0.0260536	-1.56604
NM_014851	0.00106237	2.05077	0.00424374	-1.5644
NM_018112	0.000131887	2.47014	0.001073	-1.56375

NR_029701	1.41E-05	58.2943	0.00964676	-1.56329
NM_001164579 /// NM_1735	0.00210682	1.64981	0.0029661	-1.56104
NM_001127394 /// NM_0529	0.000982904	2.50736	0.00810435	-1.5605
NM_024654	0.00250936	1.56349	0.00254453	-1.56017
NM_001099268 /// NM_0165	0.00624792	1.61565	0.00780779	-1.55831
NM_001184734 /// NM_0011	0.00366277	1.68807	0.00592798	-1.55741
NM_018362	0.0115955	1.60991	0.0141787	-1.55711
NM_001142522 /// NM_0121	0.000286638	3.54316	0.00627161	-1.55686
NM_015885	0.0139305	1.51452	0.0117431	-1.55502
NM_001003704 /// NM_0164	0.00488028	1.75017	0.00960255	-1.55469
NM_000161 /// NM_0010240	3.25E-05	4.40449	0.00121078	-1.55398
NM_004405	0.000328844	11.3929	0.0423437	-1.55369
NM_001142617 /// NM_0011	0.0193205	1.63007	0.0255378	-1.55294
NM_001130112 /// NM_0011	0.00960025	1.67088	0.0147588	-1.55238
NM_017754	0.00116627	1.70545	0.00206285	-1.55238
NM_017437	0.00931561	1.55905	0.00962078	-1.55118
NM_001034173 /// NR_0277	0.00257108	2.11529	0.0118804	-1.55096
NM_018137	0.0056133	2.084	0.0236556	-1.54869
NM_005171	6.87E-05	2.10211	0.000337485	-1.54672
NM_001080541 /// NM_0011	0.00905335	1.53047	0.00844888	-1.5467
NM_022118	0.0157332	1.62151	0.0208901	-1.54554
NM_004774	0.0150562	1.76034	0.0303409	-1.5453
NM_001194954 /// NM_0011	0.00468483	2.0151	0.0178779	-1.54495
NM_005124	0.00608477	2.36448	0.0390852	-1.54415
NM_001267594 /// NM_0012	0.00137404	2.09255	0.00651288	-1.54098
NM_005746 /// NM_182790	0.0198042	1.56894	0.0221287	-1.54057
NM_025077	0.00251074	2.17736	0.0135262	-1.53949
NM_007018	0.00322467	2.18952	0.0174981	-1.53886
NM_053042	0.00340985	1.71443	0.00653773	-1.53731
NM_001042414 /// NR_0032	0.00583941	1.62296	0.00823651	-1.53593
NM_001029991 /// NM_0010	0.0141427	1.53537	0.0141223	-1.53572
NM_005387 /// NM_016320 /	0.00521122	2.3762	0.0358977	-1.53432
NM_001008860 /// NM_0010	0.00606597	2.48342	0.0464787	-1.5342
NM_017645	6.30E-05	1.55578	6.93E-05	-1.53418
NM_006510 /// NM_030950	5.12E-05	2.58906	0.000557933	-1.53327
NM_001007245 /// NM_0011	0.000265623	2.3617	0.00210355	-1.53321
NM_001135564 /// NM_0012	0.00149043	2.01742	0.00631119	-1.53294
NM_006275 /// NR_034009	0.00248658	2.58237	0.0236104	-1.53261
NM_001002926	0.0162128	1.82016	0.0395544	-1.5326
NM_001325	0.0133177	2.00652	0.0482491	-1.5322
NM_018394	0.00215987	2.62227	0.0217775	-1.53143
NM_007045 /// NM_194429	0.00145344	2.6646	0.0158825	-1.53031
NM_002936	0.00430173	1.63612	0.00655438	-1.52984
NM_207351	0.0088731	1.6194	0.012691	-1.5283
NM_001042482 /// NM_0224	0.00189085	2.62079	0.0195715	-1.52741
NM_004294	0.000117305	3.47015	0.00286971	-1.52677
NR_024510 /// NR_024511 //	0.00537526	1.54171	0.00573942	-1.5267

NM_005614	0.00900041	2.14371	0.0436455	-1.52633
NM_004134	0.00263756	1.6808	0.00479532	-1.52588
NM_203448 /// NR_015363 //	0.00222292	2.8346	0.0281515	-1.52526
NM_001131035 /// NM_0011	0.00439763	1.53897	0.00468902	-1.52444
NM_018262 /// NM_052985 /	0.00811568	1.50966	0.00761447	-1.52387
NM_032146 /// NM_177976	0.000410802	5.15095	0.0207473	-1.52344
NM_001093755 /// NM_0010	0.00303905	2.92645	0.0403626	-1.52327
NM_022496 /// NR_048568 //	0.00193208	1.5153	0.00186756	-1.52265
XM_001128243	0.00821763	1.983	0.0311206	-1.52187
NM_182490	0.00205733	3.20374	0.0355332	-1.52179
NM_000201	0.000193245	5.24269	0.0107858	-1.52101
NM_001042399 /// NM_0161	0.00123215	1.83209	0.00362418	-1.52027
NM_001076683 /// NM_0010	0.000847391	2.00637	0.00376811	-1.52014
NM_001135608 /// NM_0150	0.00129219	3.40105	0.0270508	-1.52002
NM_018944	0.00690302	1.69472	0.0132329	-1.51959
NM_018944	0.013868	1.52903	0.0144487	-1.51946
NM_001205028 /// NM_0012	0.000806137	3.88096	0.0233597	-1.51896
NM_032505	0.000290064	2.78984	0.00410738	-1.51836
NM_013329 /// NM_016631 /	0.0035214	1.61198	0.00518583	-1.51829
NM_001159651 /// NM_1383	0.000973825	1.60086	0.00138723	-1.51802
NM_004586	0.00247377	1.69696	0.00493951	-1.51695
NM_020861	0.00233154	2.60135	0.024314	-1.51629
NM_001166356 /// NM_0011	0.000740403	1.82066	0.00216895	-1.51619
NM_001184906 /// NM_0328	0.0130097	1.73211	0.0276551	-1.51506
NR_029383	0.000949192	3.29063	0.019486	-1.5146
NM_052947	0.000163412	2.18989	0.00108344	-1.51437
NM_014188	0.0015565	1.89382	0.00546204	-1.51421
NM_030816	0.0215313	1.64863	0.0351374	-1.51391
NM_001159699 /// NM_0011	0.000348314	1.66204	0.000639741	-1.51304
NM_001001323 /// NM_0016	0.00233429	2.18538	0.0144113	-1.51166
NM_001191028 /// NM_0124	0.00378685	1.57763	0.00507527	-1.50975
NM_031923	0.00253032	2.31691	0.0191888	-1.50836
NM_001256182 /// NM_0012	0.00729822	1.60509	0.0109011	-1.50742
NM_017886	0.0246132	1.66862	0.0436872	-1.50629
NM_001099678	0.00323749	1.88534	0.0112836	-1.50612
NM_001185118 /// NM_0011	0.007014	1.71625	0.0152516	-1.50564
NM_001079516	0.00380819	2.6807	0.0426792	-1.50456
NM_017426	0.00232302	1.89509	0.00844907	-1.50448
NM_004990	0.000464368	2.13904	0.00290521	-1.50442
NM_001135608 /// NM_0150	0.00194909	2.71141	0.0243845	-1.50396
NM_001018089 /// NM_0246	0.0026262	2.09044	0.0141982	-1.50376
NM_001164665 /// NM_0209	0.00287405	1.89886	0.010594	-1.50175
NM_025138 /// NM_170719	0.00306428	1.67878	0.00617387	-1.50145
NM_001242826 /// NM_0057	0.00280012	2.11769	0.0160058	-1.50115
NM_001048249	0.00146558	1.54246	0.00177517	-1.50087
NM_004990	0.000991115	2.85147	0.01523	-1.5004
NM_001024647 /// NM_0224	0.00325009	2.08984	0.0176104	-1.50013

Supplementary Table 3 highly expressed genes in both xenograft FTSCt and HGSC (2 fold and p < 0.05, 2395

Probeset ID	Gene Symbol	Gene Title
223278_at	GJB2	gap junction protein, beta 2, 26kDa
211719_x_at	FN1	fibronectin 1
207039_at	CDKN2A	cyclin-dependent kinase inhibitor 2A
225681_at	CTHRC1	collagen triple helix repeat containing 1
212464_s_at	FN1	fibronectin 1
216442_x_at	FN1	fibronectin 1
204268_at	S100A2	S100 calcium binding protein A2
210495_x_at	FN1	fibronectin 1
219918_s_at	ASPM	asp (abnormal spindle) homolog, microcephaly associated (Droso
203186_s_at	S100A4	S100 calcium binding protein A4
228335_at	CLDN11	claudin 11
222608_s_at	ANLN	anillin, actin binding protein
201387_s_at	UCHL1	ubiquitin carboxyl-terminal esterase L1 (ubiquitin thiolesterase)
208025_s_at	HMGA2	high mobility group AT-hook 2
209773_s_at	RRM2	ribonucleotide reductase M2
219148_at	PBK	PDZ binding kinase
202345_s_at	FABP5	fatty acid binding protein 5 (psoriasis-associated)
201645_at	TNC	tenascin C
218662_s_at	NCAPG	non-SMC condensin I complex, subunit G
203764_at	DLGAP5	discs, large (Drosophila) homolog-associated protein 5
204170_s_at	CKS2	CDC28 protein kinase regulatory subunit 2
204331_s_at	MRPS12	mitochondrial ribosomal protein S12
218585_s_at	DTL	denticleless E3 ubiquitin protein ligase homolog (Drosophila)
222958_s_at	DEPDC1	DEP domain containing 1
AFFX-HUMGAPDH/	GAPDH /// GAPDH	glyceraldehyde-3-phosphate dehydrogenase /// glyceraldehyde-3
204822_at	TTK	TTK protein kinase
218663_at	NCAPG	non-SMC condensin I complex, subunit G
201890_at	RRM2	ribonucleotide reductase M2
201291_s_at	TOP2A	topoisomerase (DNA) II alpha 170kDa
210559_s_at	CDK1	cyclin-dependent kinase 1
236313_at	CDKN2B	cyclin-dependent kinase inhibitor 2B (p15, inhibits CDK4)
206445_s_at	PRMT1	protein arginine methyltransferase 1
201292_at	TOP2A	topoisomerase (DNA) II alpha 170kDa
202503_s_at	KIAA0101	KIAA0101
223490_s_at	EXOSC3	exosome component 3
209714_s_at	CDKN3	cyclin-dependent kinase inhibitor 3
228273_at	PRR11	proline rich 11
203554_x_at	PTTG1	pituitary tumor-transforming 1
211071_s_at	MLLT11	myeloid/lymphoid or mixed-lineage leukemia (trithorax homolog,
202870_s_at	CDC20	cell division cycle 20 homolog (S. cerevisiae)
219493_at	SHCBP1	SHC SH2-domain binding protein 1
202095_s_at	BIRC5	baculoviral IAP repeat containing 5
214710_s_at	CCNB1	cyclin B1

235545_at	DEPDC1	DEP domain containing 1
228053_s_at	TOMM5	translocase of outer mitochondrial membrane 5 homolog (yeast)
218542_at	CEP55	centrosomal protein 55kDa
218009_s_at	PRC1	protein regulator of cytokinesis 1
209642_at	BUB1	budding uninhibited by benzimidazoles 1 homolog (yeast)
209644_x_at	CDKN2A	cyclin-dependent kinase inhibitor 2A
223381_at	NUF2	NUF2, NDC80 kinetochore complex component, homolog (S. cere
224428_s_at	CDCA7	cell division cycle associated 7
222680_s_at	DTL	denticleless E3 ubiquitin protein ligase homolog (Drosophila)
203276_at	LMNB1	lamin B1
222037_at	MCM4	minichromosome maintenance complex component 4
218039_at	NUSAP1	nucleolar and spindle associated protein 1
219295_s_at	PCOLCE2	procollagen C-endopeptidase enhancer 2
207165_at	HMMR	hyaluronan-mediated motility receptor (RHAMM)
205046_at	CENPE	centromere protein E, 312kDa
206884_s_at	SCEL	sciellin
223229_at	UBE2T	ubiquitin-conjugating enzyme E2T (putative)
218755_at	KIF20A	kinesin family member 20A
201105_at	LGALS1	lectin, galactoside-binding, soluble, 1
201505_at	LAMB1	laminin, beta 1
202954_at	UBE2C	ubiquitin-conjugating enzyme E2C
218883_s_at	MLF1IP	MLF1 interacting protein
214437_s_at	SHMT2	serine hydroxymethyltransferase 2 (mitochondrial)
203214_x_at	CDK1	cyclin-dependent kinase 1
209709_s_at	HMMR	hyaluronan-mediated motility receptor (RHAMM)
220651_s_at	MCM10	minichromosome maintenance complex component 10
208002_s_at	ACOT7	acyl-CoA thioesterase 7
207828_s_at	CENPF	centromere protein F, 350/400kDa (mitosin)
208079_s_at	AURKA	aurora kinase A
238756_at	GAS2L3	growth arrest-specific 2 like 3
209825_s_at	MIR3658 /// UCK2	microRNA 3658 /// uridine-cytidine kinase 2
203560_at	GGH	gamma-glutamyl hydrolase (conjugase, folylpolygammaglutamyl
229332_at	HPDL	4-hydroxyphenylpyruvate dioxygenase-like
204026_s_at	ZWINT	ZW10 interactor
213599_at	OIP5	Opa interacting protein 5
220295_x_at	DEPDC1	DEP domain containing 1
220083_x_at	UCHL5	ubiquitin carboxyl-terminal hydrolase L5
225655_at	UHRF1	ubiquitin-like with PHD and ring finger domains 1
225834_at	FAM72A /// FAM72B	family with sequence similarity 72, member A /// family with seq
205394_at	CHEK1	checkpoint kinase 1
204092_s_at	AURKA	aurora kinase A
203213_at	CDK1	cyclin-dependent kinase 1
225687_at	FAM83D	family with sequence similarity 83, member D
209679_s_at	SMAGP	small cell adhesion glycoprotein
239579_at	EPHX4	epoxide hydrolase 4
230165_at	SGOL2	shugoshin-like 2 (S. pombe)
206550_s_at	NUP155	nucleoporin 155kDa

201577_at	NME1	NME/NM23 nucleoside diphosphate kinase 1
213007_at	FANCI	Fanconi anemia, complementation group I
236641_at	KIF14	kinesin family member 14
201714_at	TUBG1	tubulin, gamma 1
226980_at	DEPDC1B	DEP domain containing 1B
213113_s_at	SLC43A3	solute carrier family 43, member 3
209900_s_at	SLC16A1	solute carrier family 16, member 1 (monocarboxylic acid transpor
201663_s_at	SMC4	structural maintenance of chromosomes 4
218073_s_at	TMEM48	transmembrane protein 48
227928_at	PARPBP	PARP1 binding protein
221521_s_at	GINS2	GINS complex subunit 2 (Psf2 homolog)
202718_at	IGFBP2	insulin-like growth factor binding protein 2, 36kDa
204962_s_at	C2orf18 /// CENPA	chromosome 2 open reading frame 18 /// centromere protein A
209434_s_at	PPAT	phosphoribosyl pyrophosphate amidotransferase
218336_at	PFDN2	prefoldin subunit 2
222077_s_at	RACGAP1	Rac GTPase activating protein 1
202705_at	CCNB2	cyclin B2
205034_at	CCNE2	cyclin E2
203755_at	BUB1B	budding uninhibited by benzimidazoles 1 homolog beta (yeast)
232231_at	RUNX2	runt-related transcription factor 2
204444_at	KIF11	kinesin family member 11
219979_s_at	C11orf73	chromosome 11 open reading frame 73
209891_at	SPC25	SPC25, NDC80 kinetochore complex component, homolog (S. cere
217755_at	HN1	hematological and neurological expressed 1
205129_at	NPM3	nucleophosmin/nucleoplasmin 3
204146_at	RAD51AP1	RAD51 associated protein 1
235609_at	BRIP1	BRCA1 interacting protein C-terminal helicase 1
210052_s_at	TPX2	TPX2, microtubule-associated, homolog (Xenopus laevis)
202234_s_at	SLC16A1	solute carrier family 16, member 1 (monocarboxylic acid transpor
232056_at	SCEL	sciellin
221730_at	COL5A2	collagen, type V, alpha 2
219306_at	KIF15	kinesin family member 15
204709_s_at	KIF23	kinesin family member 23
222036_s_at	MCM4	minichromosome maintenance complex component 4
219555_s_at	CENPN	centromere protein N
226237_at	COL8A1	collagen, type VIII, alpha 1
228323_at	CASC5	cancer susceptibility candidate 5
204825_at	MELK	maternal embryonic leucine zipper kinase
228069_at	FAM54A	family with sequence similarity 54, member A
224870_at	DANCR	differentiation antagonizing non-protein coding RNA
201742_x_at	SRSF1	serine/arginine-rich splicing factor 1
205361_s_at	PFDN4	prefoldin subunit 4
235022_at	FAM210A	family with sequence similarity 210, member A
218252_at	CKAP2	cytoskeleton associated protein 2
225799_at	LINC00152 /// LOC541	long intergenic non-protein coding RNA 152 /// uncharacterized L
219410_at	TMEM45A	transmembrane protein 45A
213226_at	CCNA2	cyclin A2

1555772_a_at	CDC25A	cell division cycle 25 homolog A (S. pombe)
201202_at	PCNA	proliferating cell nuclear antigen
202206_at	ARL4C	ADP-ribosylation factor-like 4C
223570_at	MCM10	minichromosome maintenance complex component 10
227211_at	PHF19	PHD finger protein 19
1555225_at	C1orf43	chromosome 1 open reading frame 43
200634_at	PFN1	profilin 1
226661_at	CDCA2	cell division cycle associated 2
204887_s_at	PLK4	polo-like kinase 4
218726_at	HJURP	Holliday junction recognition protein
224913_s_at	TIMM50	translocase of inner mitochondrial membrane 50 homolog (S. cere
218235_s_at	UTP11L	UTP11-like, U3 small nucleolar ribonucleoprotein, (yeast)
1554572_a_at	SUV39H2	suppressor of variegation 3-9 homolog 2 (Drosophila)
224972_at	ROMO1	reactive oxygen species modulator 1
209796_s_at	CNPY2	canopy 2 homolog (zebrafish)
222443_s_at	RBM8A	RNA binding motif protein 8A
223403_s_at	POLR1B	polymerase (RNA) I polypeptide B, 128kDa
227212_s_at	PHF19	PHD finger protein 19
211981_at	COL4A1	collagen, type IV, alpha 1
220865_s_at	PDSS1	prenyl (decaprenyl) diphosphate synthase, subunit 1
212364_at	MYO1B	myosin IB
221987_s_at	TSR1	TSR1, 20S rRNA accumulation, homolog (S. cerevisiae)
207507_s_at	ATP5G3	ATP synthase, H+ transporting, mitochondrial Fo complex, subuni
223307_at	CDCA3	cell division cycle associated 3
202246_s_at	CDK4	cyclin-dependent kinase 4
213011_s_at	TPI1	triosephosphate isomerase 1
204836_at	GLDC	glycine dehydrogenase (decarboxylating)
206364_at	KIF14	kinesin family member 14
217728_at	S100A6	S100 calcium binding protein A6
212949_at	NCAPH	non-SMC condensin I complex, subunit H
202998_s_at	LOXL2	lysyl oxidase-like 2
226936_at	CENPW	centromere protein W
229551_x_at	ZNF367	zinc finger protein 367
222740_at	ATAD2	ATPase family, AAA domain containing 2
210466_s_at	SERBP1	SERPINE1 mRNA binding protein 1
222803_at	PRTFDC1	phosphoribosyl transferase domain containing 1
203022_at	RNASEH2A	ribonuclease H2, subunit A
218782_s_at	ATAD2	ATPase family, AAA domain containing 2
202613_at	CTPS1	CTP synthase 1
219978_s_at	NUSAP1	nucleolar and spindle associated protein 1
212094_at	PEG10	paternally expressed 10
223032_x_at	PRELID1	PRELI domain containing 1
214512_s_at	SUB1	SUB1 homolog (S. cerevisiae)
228977_at	LOC729680	uncharacterized LOC729680
201014_s_at	PAICS	phosphoribosylaminoimidazole carboxylase, phosphoribosylamin
228729_at	CCNB1	cyclin B1
223556_at	HELLS	helicase, lymphoid-specific

212022_s_at	MKI67	antigen identified by monoclonal antibody Ki-67
221685_s_at	CCDC99	coiled-coil domain containing 99
210983_s_at	MCM7	minichromosome maintenance complex component 7
205909_at	POLE2	polymerase (DNA directed), epsilon 2, accessory subunit
208627_s_at	YBX1	Y box binding protein 1
206102_at	GINS1	GINS complex subunit 1 (Psf1 homolog)
225161_at	GFM1	G elongation factor, mitochondrial 1
203145_at	SPAG5	sperm associated antigen 5
225300_at	C15orf23	chromosome 15 open reading frame 23
206632_s_at	APOBEC3B	apolipoprotein B mRNA editing enzyme, catalytic polypeptide-like
201930_at	MCM6	minichromosome maintenance complex component 6
202635_s_at	POLR2K	polymerase (RNA) II (DNA directed) polypeptide K, 7.0kDa
202094_at	BIRC5	baculoviral IAP repeat containing 5
209026_x_at	TUBB	tubulin, beta class I
201138_s_at	SSB	Sjogren syndrome antigen B (autoantigen La)
208767_s_at	LAPTM4B	lysosomal protein transmembrane 4 beta
204886_at	PLK4	polo-like kinase 4
209408_at	KIF2C	kinesin family member 2C
224345_x_at	FAM162A	family with sequence similarity 162, member A
202589_at	TYMS	thymidylate synthetase
208758_at	ATIC	5-aminoimidazole-4-carboxamide ribonucleotide formyltransferas
202207_at	ARL4C	ADP-ribosylation factor-like 4C
206074_s_at	HMGA1	high mobility group AT-hook 1
212782_x_at	POLR2J	polymerase (RNA) II (DNA directed) polypeptide J, 13.3kDa
204126_s_at	CDC45	cell division cycle 45 homolog (S. cerevisiae)
201478_s_at	DKC1 /// SNORA56	dyskeratosis congenita 1, dyskerin /// small nucleolar RNA, H/ACA
224637_at	OST4	oligosaccharyltransferase 4 homolog (S. cerevisiae)
200039_s_at	PSMB2	proteasome (prosome, macropain) subunit, beta type, 2
201072_s_at	SMARCC1	SWI/SNF related, matrix associated, actin dependent regulator of
201688_s_at	TPD52	tumor protein D52
224753_at	CDCA5	cell division cycle associated 5
211714_x_at	TUBB	tubulin, beta class I
217946_s_at	SAE1	SUMO1 activating enzyme subunit 1
212891_s_at	GADD45GIP1	growth arrest and DNA-damage-inducible, gamma interacting pro
212694_s_at	PCCB	propionyl CoA carboxylase, beta polypeptide
203931_s_at	MRPL12	mitochondrial ribosomal protein L12
223193_x_at	FAM162A	family with sequence similarity 162, member A
1554667_s_at	METTL8	methyltransferase like 8
208103_s_at	ANP32E	acidic (leucine-rich) nuclear phosphoprotein 32 family, member E
221437_s_at	MRPS15	mitochondrial ribosomal protein S15
228597_at	MIS18A	MIS18 kinetochore protein homolog A (S. pombe)
202647_s_at	NRAS	neuroblastoma RAS viral (v-ras) oncogene homolog
208628_s_at	YBX1	Y box binding protein 1
204510_at	CDC7	cell division cycle 7 homolog (S. cerevisiae)
212563_at	BOP1	block of proliferation 1
200822_x_at	TPI1	triosephosphate isomerase 1
222883_at	SELRC1	Sel1 repeat containing 1

201725_at	CDC123	cell division cycle 123 homolog (S. cerevisiae)
225402_at	TP53RK	TP53 regulating kinase
201555_at	MCM3	minichromosome maintenance complex component 3
211519_s_at	KIF2C	kinesin family member 2C
209053_s_at	WHSC1	Wolf-Hirschhorn syndrome candidate 1
219787_s_at	ECT2	epithelial cell transforming sequence 2 oncogene
226545_at	CD109	CD109 molecule
200665_s_at	LOC100505813 /// SP	uncharacterized LOC100505813 /// secreted protein, acidic, cyste
203046_s_at	TIMELESS	timeless homolog (Drosophila)
216228_s_at	WDHD1	WD repeat and HMG-box DNA binding protein 1
208967_s_at	AK2	adenylate kinase 2
200832_s_at	SCD	stearoyl-CoA desaturase (delta-9-desaturase)
205680_at	MMP10	matrix metallopeptidase 10 (stromelysin 2)
203358_s_at	EZH2	enhancer of zeste homolog 2 (Drosophila)
219000_s_at	DSCC1	defective in sister chromatid cohesion 1 homolog (S. cerevisiae)
226835_s_at	ZNFX1-AS1	ZNFX1 antisense RNA 1 (non-protein coding)
204023_at	RFC4	replication factor C (activator 1) 4, 37kDa
218605_at	TFB2M	transcription factor B2, mitochondrial
218027_at	MRPL15	mitochondrial ribosomal protein L15
203511_s_at	TRAPPC3	trafficking protein particle complex 3
201112_s_at	CSE1L	CSE1 chromosome segregation 1-like (yeast)
204127_at	RFC3	replication factor C (activator 1) 3, 38kDa
202309_at	MTHFD1	methylenetetrahydrofolate dehydrogenase (NADP+ dependent) 1
218512_at	WDR12	WD repeat domain 12
223774_at	SNHG12 /// SNORA16	small nucleolar RNA host gene 12 (non-protein coding) /// small n
222216_s_at	MRPL17	mitochondrial ribosomal protein L17
214431_at	GMPS	guanine monphosphate synthetase
211971_s_at	LRPPRC	leucine-rich pentatricopeptide repeat containing
226456_at	RMI2	RMI2, RecQ mediated genome instability 2, homolog (S. cerevisia
205436_s_at	H2AFX	H2A histone family, member X
224752_at	C7orf73 /// LOC10028	chromosome 7 open reading frame 73 /// chromosome 7 open re
221922_at	GPSM2	G-protein signaling modulator 2
217949_s_at	VKORC1	vitamin K epoxide reductase complex, subunit 1
218051_s_at	NT5DC2	5'-nucleotidase domain containing 2
203889_at	SCG5	secretogranin V (7B2 protein)
201689_s_at	TPD52	tumor protein D52
218355_at	KIF4A	kinesin family member 4A
223993_s_at	CNIH4	cornichon homolog 4 (Drosophila)
202856_s_at	SLC16A3	solute carrier family 16, member 3 (monocarboxylic acid transpor
202690_s_at	SNRPD1	small nuclear ribonucleoprotein D1 polypeptide 16kDa
225099_at	FBXO45	F-box protein 45
238075_at	CHEK1	checkpoint kinase 1
222701_s_at	CHCHD7	coiled-coil-helix-coiled-coil-helix domain containing 7
212320_at	TUBB	tubulin, beta class I
228559_at	CENPN	centromere protein N
212013_at	PXDN	peroxidasin homolog (Drosophila)
224217_s_at	FAF1	Fas (TNFRSF6) associated factor 1

202580_x_at	FOXM1	forkhead box M1
201629_s_at	ACP1	acid phosphatase 1, soluble
223062_s_at	PSAT1	phosphoserine aminotransferase 1
201096_s_at	ARF4	ADP-ribosylation factor 4
201897_s_at	CKS1B	CDC28 protein kinase regulatory subunit 1B
225827_at	EIF2C2	eukaryotic translation initiation factor 2C, 2
227350_at	HELLS	helicase, lymphoid-specific
208581_x_at	MT1X	metallothionein 1X
224523_s_at	C3orf26	chromosome 3 open reading frame 26
239002_at	ASPM	asp (abnormal spindle) homolog, microcephaly associated (Drosop
231855_at	KIAA1524	KIAA1524
235425_at	SGOL2	shugoshin-like 2 (S. pombe)
222039_at	KIF18B	kinesin family member 18B
213133_s_at	GCSH	glycine cleavage system protein H (aminomethyl carrier)
229442_at	C18orf54	chromosome 18 open reading frame 54
204165_at	WASF1	WAS protein family, member 1
224320_s_at	MCM8	minichromosome maintenance complex component 8
203119_at	CCDC86	coiled-coil domain containing 86
213427_at	RPP40	ribonuclease P/MRP 40kDa subunit
218586_at	C20orf20	chromosome 20 open reading frame 20
205024_s_at	RAD51	RAD51 homolog (S. cerevisiae)
212141_at	MCM4	minichromosome maintenance complex component 4
1555878_at	RPS24	Ribosomal protein S24
207508_at	ATP5G3	ATP synthase, H+ transporting, mitochondrial Fo complex, subuni
218695_at	EXOSC4	exosome component 4
203270_at	DTYMK	deoxythymidylate kinase (thymidylate kinase)
225943_at	NLN	neurolysin (metallopeptidase M3 family)
202591_s_at	MIR5096 /// SSBP1	microRNA 5096 /// single-stranded DNA binding protein 1, mitoch
229305_at	MLF1IP	MLF1 interacting protein
202296_s_at	RER1	RER1 retention in endoplasmic reticulum 1 homolog (S. cerevisiae
221520_s_at	CDCA8	cell division cycle associated 8
204641_at	NEK2	NIMA (never in mitosis gene a)-related kinase 2
1553984_s_at	DTYMK	deoxythymidylate kinase (thymidylate kinase)
228868_x_at	CDT1	Chromatin licensing and DNA replication factor 1
228564_at	LOC375295	uncharacterized LOC375295
200975_at	PPT1	palmitoyl-protein thioesterase 1
201848_s_at	BNIP3	BCL2/adenovirus E1B 19kDa interacting protein 3
201263_at	TARS	threonyl-tRNA synthetase
212458_at	SPRED2	sprouty-related, EVH1 domain containing 2
222843_at	FIGNL1	fidgetin-like 1
204695_at	CDC25A	cell division cycle 25 homolog A (S. pombe)
201231_s_at	ENO1	enolase 1, (alpha)
205402_x_at	PRSS2	protease, serine, 2 (trypsin 2)
212789_at	NCAPD3	non-SMC condensin II complex, subunit D3
211762_s_at	KPNA2	karyopherin alpha 2 (RAG cohort 1, importin alpha 1)
216470_x_at	PRSS2	protease, serine, 2 (trypsin 2)
200658_s_at	PHB	prohibitin

227942_s_at	CRIPT	cysteine-rich PDZ-binding protein
220011_at	C1orf135	chromosome 1 open reading frame 135
228931_at	COQ4	coenzyme Q4 homolog (S. cerevisiae)
223480_s_at	MRPL47	mitochondrial ribosomal protein L47
219544_at	BORA	bora, aurora kinase A activator
204610_s_at	CCDC85B	coiled-coil domain containing 85B
221692_s_at	MRPL34	mitochondrial ribosomal protein L34
205499_at	SRPX2	sushi-repeat containing protein, X-linked 2
238996_x_at	ALDOA	aldolase A, fructose-bisphosphate
223055_s_at	XPO5	exportin 5
202666_s_at	ACTL6A	actin-like 6A
205167_s_at	CDC25C	cell division cycle 25 homolog C (S. pombe)
225439_at	NUDCD1	NudC domain containing 1
213008_at	FANCI	Fanconi anemia, complementation group I
AFFX-HUMGAPDH/	GAPDH /// GAPDH	glyceraldehyde-3-phosphate dehydrogenase /// glyceraldehyde-3
224714_at	MKI67IP	MKI67 (FHA domain) interacting nucleolar phosphoprotein
203625_x_at	SKP2	S-phase kinase-associated protein 2, E3 ubiquitin protein ligase
212680_x_at	PPP1R14B	protein phosphatase 1, regulatory (inhibitor) subunit 14B
204162_at	NDC80	NDC80 kinetochore complex component homolog (S. cerevisiae)
202310_s_at	COL1A1	collagen, type I, alpha 1
203818_s_at	SF3A3	splicing factor 3a, subunit 3, 60kDa
225853_at	GNPNAT1	glucosamine-phosphate N-acetyltransferase 1
212816_s_at	CBS	cystathionine-beta-synthase
205122_at	MSANTD3-TMEFF1 ///	MSANTD3-TMEFF1 readthrough /// transmembrane protein with
228468_at	MASTL	microtubule associated serine/threonine kinase-like
205733_at	BLM	Bloom syndrome, RecQ helicase-like
214095_at	SHMT2	serine hydroxymethyltransferase 2 (mitochondrial)
200744_s_at	GNB1	guanine nucleotide binding protein (G protein), beta polypeptide
201664_at	SMC4	structural maintenance of chromosomes 4
224376_s_at	C20orf24 /// TGIF2-C2	chromosome 20 open reading frame 24 /// TGIF2-C20orf24 readt
213647_at	DNA2	DNA replication helicase 2 homolog (yeast)
219311_at	CEP76	centrosomal protein 76kDa
211980_at	COL4A1	collagen, type IV, alpha 1
200925_at	COX6A1	cytochrome c oxidase subunit VIa polypeptide 1
226943_at	C12orf73	chromosome 12 open reading frame 73
227477_at	ZMYND19	zinc finger, MYND-type containing 19
202107_s_at	MCM2	minichromosome maintenance complex component 2
218984_at	PUS7	pseudouridylate synthase 7 homolog (S. cerevisiae)
209781_s_at	KHDRBS3	KH domain containing, RNA binding, signal transduction associate
229742_at	C15orf61	chromosome 15 open reading frame 61
208875_s_at	PAK2	p21 protein (Cdc42/Rac)-activated kinase 2
224232_s_at	PRELID1	PRELI domain containing 1
224331_s_at	MRPL36	mitochondrial ribosomal protein L36
218187_s_at	C8orf33	chromosome 8 open reading frame 33
202839_s_at	NDUFB7	NADH dehydrogenase (ubiquinone) 1 beta subcomplex, 7, 18kDa
202806_at	DBN1	drebrin 1
205449_at	SAC3D1	SAC3 domain containing 1

204584_at	L1CAM	L1 cell adhesion molecule
225036_at	TOMM5	translocase of outer mitochondrial membrane 5 homolog (yeast)
203417_at	MFAP2	microfibrillar-associated protein 2
222702_x_at	CRIPT	cysteine-rich PDZ-binding protein
236075_s_at	LOC100506676	uncharacterized LOC100506676
212296_at	PSMD14	proteasome (prosome, macropain) 26S subunit, non-ATPase, 14
201564_s_at	FSCN1 /// LOC100653	fascin homolog 1, actin-bundling protein (Strongylocentrotus purp
227165_at	SKA3	spindle and kinetochore associated complex subunit 3
229097_at	DIAPH3	diaphanous homolog 3 (Drosophila)
221676_s_at	CORO1C	coronin, actin binding protein, 1C
220060_s_at	PARPBP	PARP1 binding protein
232238_at	ASPM	asp (abnormal spindle) homolog, microcephaly associated (Droso
202667_s_at	SLC39A7	solute carrier family 39 (zinc transporter), member 7
201774_s_at	NCAPD2	non-SMC condensin I complex, subunit D2
211456_x_at	MT1P2	metallothionein 1 pseudogene 2
202715_at	CAD	carbamoyl-phosphate synthetase 2, aspartate transcarbamylase,
218479_s_at	XPO4	exportin 4
223020_at	CLPTM1L	CLPTM1-like
223839_s_at	SCD	stearoyl-CoA desaturase (delta-9-desaturase)
203347_s_at	MTF2	metal response element binding transcription factor 2
217829_s_at	USP39	ubiquitin specific peptidase 39
223413_s_at	LYAR	Ly1 antibody reactive homolog (mouse)
211318_s_at	RAE1	RAE1 RNA export 1 homolog (S. pombe)
1558750_a_at	LOC100288637	OTU domain containing 7A pseudogene
225291_at	PNPT1	polyribonucleotide nucleotidyltransferase 1
217398_x_at	GAPDH	glyceraldehyde-3-phosphate dehydrogenase
203577_at	GTF2H4	general transcription factor IIH, polypeptide 4, 52kDa
202016_at	MEST	mesoderm specific transcript homolog (mouse)
234464_s_at	EME1	essential meiotic endonuclease 1 homolog 1 (S. pombe)
213088_s_at	DNAJC9	DnaJ (Hsp40) homolog, subfamily C, member 9
204033_at	TRIP13	thyroid hormone receptor interactor 13
223461_at	TBC1D7	TBC1 domain family, member 7
221436_s_at	CDCA3	cell division cycle associated 3
220094_s_at	CCDC90A	coiled-coil domain containing 90A
200770_s_at	LAMC1	laminin, gamma 1 (formerly LAMB2)
202311_s_at	COL1A1	collagen, type I, alpha 1
218982_s_at	MRPS17	mitochondrial ribosomal protein S17
228281_at	C11orf82	chromosome 11 open reading frame 82
201672_s_at	USP14	ubiquitin specific peptidase 14 (tRNA-guanine transglycosylase)
222497_x_at	NMD3	NMD3 homolog (S. cerevisiae)
221845_s_at	CLPB	ClpB caseinolytic peptidase B homolog (E. coli)
225788_at	RRP36	ribosomal RNA processing 36 homolog (S. cerevisiae)
218193_s_at	GOLT1B	golgi transport 1B
204724_s_at	COL9A3	collagen, type IX, alpha 3
218080_x_at	FAF1	Fas (TNFRSF6) associated factor 1
229886_at	C5orf34	chromosome 5 open reading frame 34
225593_at	LSM10	LSM10, U7 small nuclear RNA associated

200657_at	SLC25A5	solute carrier family 25 (mitochondrial carrier; adenine nucleotide
200910_at	CCT3	chaperonin containing TCP1, subunit 3 (gamma)
202706_s_at	UMPS	uridine monophosphate synthetase
205339_at	STIL	SCL/TAL1 interrupting locus
204728_s_at	WDHD1	WD repeat and HMG-box DNA binding protein 1
228990_at	SNHG12 /// SNORA16	small nucleolar RNA host gene 12 (non-protein coding) /// small n
200966_x_at	ALDOA	aldolase A, fructose-bisphosphate
224623_at	LOC728554 /// THOC3	THO complex 3 pseudogene /// THO complex 3
218399_s_at	CDCA4	cell division cycle associated 4
201074_at	SMARCC1	SWI/SNF related, matrix associated, actin dependent regulator of
201417_at	SOX4	SRY (sex determining region Y)-box 4
1554101_a_at	TMTC4	transmembrane and tetratricopeptide repeat containing 4
220789_s_at	SNORA5B /// TBRG4	small nucleolar RNA, H/ACA box 5B /// transforming growth facto
218308_at	TACC3	transforming, acidic coiled-coil containing protein 3
223880_x_at	C20orf24 /// TGIF2-C2	chromosome 20 open reading frame 24 /// TGIF2-C20orf24 readt
206461_x_at	MT1H	metallothionein 1H
232065_x_at	CENPL	centromere protein L
241937_s_at	WDR4	WD repeat domain 4
204957_at	ORC5	origin recognition complex, subunit 5
211576_s_at	SLC19A1	solute carrier family 19 (folate transporter), member 1
222714_s_at	LACTB2	lactamase, beta 2
210766_s_at	CSE1L	CSE1 chromosome segregation 1-like (yeast)
211594_s_at	MRPL9	mitochondrial ribosomal protein L9
213523_at	CCNE1	cyclin E1
203502_at	BPGM	2,3-bisphosphoglycerate mutase
235509_at	LOC100506538 /// ND	uncharacterized LOC100506538 /// NADH dehydrogenase (ubiqui
210976_s_at	PFKM	phosphofructokinase, muscle
219510_at	POLQ	polymerase (DNA directed), theta
228733_at	PUSL1	pseudouridylate synthase-like 1
216237_s_at	MCM5	minichromosome maintenance complex component 5
204853_at	ORC2	origin recognition complex, subunit 2
217834_s_at	SYNCRIP	synaptotagmin binding, cytoplasmic RNA interacting protein
58696_at	EXOSC4	exosome component 4
1568873_at	ZNF519	zinc finger protein 519
235704_at	DAZAP2	DAZ associated protein 2
220607_x_at	TH1L	TH1-like (Drosophila)
225693_s_at	CAMTA1	calmodulin binding transcription activator 1
230954_at	C20orf112	chromosome 20 open reading frame 112
216222_s_at	MYO10	myosin X
200644_at	MARCKSL1	MARCKS-like 1
208308_s_at	GPI	glucose-6-phosphate isomerase
219420_s_at	SELRC1	Sel1 repeat containing 1
225657_at	LOC152217	uncharacterized LOC152217
225638_at	C1orf31	chromosome 1 open reading frame 31
201322_at	ATP5B	ATP synthase, H+ transporting, mitochondrial F1 complex, beta p
210933_s_at	FSCN1 /// LOC100653	fascin homolog 1, actin-bundling protein (Strongylocentrotus pur
200818_at	ATP5O	ATP synthase, H+ transporting, mitochondrial F1 complex, O subu

227896_at	BCCIP	BRCA2 and CDKN1A interacting protein
201757_at	NDUFS5	NADH dehydrogenase (ubiquinone) Fe-S protein 5, 15kDa (NADH-
224579_at	SLC38A1	solute carrier family 38, member 1
209482_at	POP7	processing of precursor 7, ribonuclease P/MRP subunit (S. cerevis
229139_at	JPH1	junctophilin 1
201976_s_at	MYO10	myosin X
200607_s_at	RAD21	RAD21 homolog (S. pombe)
1553956_at	TMEM237	transmembrane protein 237
217165_x_at	MT1F	metallothionein 1F
214687_x_at	ALDOA	aldolase A, fructose-bisphosphate
223452_s_at	ATL3	atlastin GTPase 3
202598_at	S100A13	S100 calcium binding protein A13
214086_s_at	PARP2	poly (ADP-ribose) polymerase 2
204767_s_at	FEN1	flap structure-specific endonuclease 1
219105_x_at	ORC6	origin recognition complex, subunit 6
227545_at	BARD1	BRCA1 associated RING domain 1
212023_s_at	MKI67	antigen identified by monoclonal antibody Ki-67
227587_at	KRI1	KRI1 homolog (S. cerevisiae)
224468_s_at	C19orf48	chromosome 19 open reading frame 48
226059_at	TOMM40L	translocase of outer mitochondrial membrane 40 homolog (yeast
225933_at	CCDC137	coiled-coil domain containing 137
211042_x_at	MCAM	melanoma cell adhesion molecule
225261_x_at	TH1L	TH1-like (Drosophila)
202190_at	CSTF1	cleavage stimulation factor, 3' pre-RNA, subunit 1, 50kDa
213453_x_at	GAPDH	glyceraldehyde-3-phosphate dehydrogenase
218580_x_at	AURKAIP1	aurora kinase A interacting protein 1
222417_s_at	SNX5	sorting nexin 5
209172_s_at	CENPF	centromere protein F, 350/400kDa (mitosin)
202679_at	NPC1	Niemann-Pick disease, type C1
204315_s_at	GTSE1	G-2 and S-phase expressed 1
221535_at	LSG1	large subunit GTPase 1 homolog (S. cerevisiae)
226909_at	ZNF518B	zinc finger protein 518B
211960_s_at	RAB7A	RAB7A, member RAS oncogene family
52285_f_at	CEP76	centrosomal protein 76kDa
200783_s_at	STMN1	stathmin 1
1555501_s_at	RSRC1	arginine/serine-rich coiled-coil 1
223491_at	COMMD2	COMM domain containing 2
209836_x_at	BOLA2 /// BOLA2B	bolA homolog 2 (E. coli) /// bolA homolog 2B (E. coli)
212581_x_at	GAPDH	glyceraldehyde-3-phosphate dehydrogenase
219217_at	NARS2	asparaginyl-tRNA synthetase 2, mitochondrial (putative)
226006_at	PET100	PET100 homolog (S. cerevisiae)
226296_s_at	MRPS15	mitochondrial ribosomal protein S15
222989_s_at	UBQLN1	ubiquilin 1
200846_s_at	PPP1CA	protein phosphatase 1, catalytic subunit, alpha isozyme
235253_at	RAD1	RAD1 homolog (S. pombe)
222622_at	PGP	phosphoglycolate phosphatase
202514_at	DLG1	discs, large homolog 1 (Drosophila)

225100_at	FBXO45	F-box protein 45
213175_s_at	SNRPB	small nuclear ribonucleoprotein polypeptides B and B1
209609_s_at	MRPL9	mitochondrial ribosomal protein L9
208962_s_at	FADS1 /// MIR1908	fatty acid desaturase 1 /// microRNA 1908
201818_at	LPCAT1	lysophosphatidylcholine acyltransferase 1
233588_x_at	PFDN6	prefoldin subunit 6
203039_s_at	NDUFS1	NADH dehydrogenase (ubiquinone) Fe-S protein 1, 75kDa (NADH-
222593_s_at	SPATS2	spermatogenesis associated, serine-rich 2
225401_at	C1orf85	chromosome 1 open reading frame 85
213787_s_at	EBP	emopamil binding protein (sterol isomerase)
206316_s_at	KNTC1	kinetochore associated 1
221522_at	ANKRD27	ankyrin repeat domain 27 (VPS9 domain)
223234_at	MAD2L2	MAD2 mitotic arrest deficient-like 2 (yeast)
225841_at	HENMT1	HEN1 methyltransferase homolog 1 (Arabidopsis)
220642_x_at	GPR89A /// GPR89B //	G protein-coupled receptor 89A /// G protein-coupled receptor 8
203209_at	RFC5	replication factor C (activator 1) 5, 36.5kDa
202183_s_at	KIF22	kinesin family member 22
222700_at	ATL2	atlastin GTPase 2
223231_at	TATDN1	TatD DNase domain containing 1
204326_x_at	MT1X	metallothionein 1X
218712_at	C1orf109	chromosome 1 open reading frame 109
201896_s_at	PSRC1	proline/serine-rich coiled-coil 1
204700_x_at	DIEXF	digestive organ expansion factor homolog (zebrafish)
200075_s_at	GUK1	guanylate kinase 1
235572_at	SPC24	SPC24, NDC80 kinetochore complex component, homolog (S. cere
224521_s_at	CCDC77	coiled-coil domain containing 77
204173_at	MYL6B	myosin, light chain 6B, alkali, smooth muscle and non-muscle
227517_s_at	GAS5 /// SNORD44 ///	growth arrest-specific 5 (non-protein coding) /// small nucleolar R
38158_at	ESPL1	extra spindle pole bodies homolog 1 (S. cerevisiae)
217025_s_at	DBN1	drebrin 1
216088_s_at	PSMA7	proteasome (prosome, macropain) subunit, alpha type, 7
224439_x_at	RNF7	ring finger protein 7
208964_s_at	FADS1 /// MIR1908	fatty acid desaturase 1 /// microRNA 1908
215165_x_at	UMPS	uridine monophosphate synthetase
202737_s_at	LSM4	LSM4 homolog, U6 small nuclear RNA associated (S. cerevisiae)
225018_at	SPIRE1	spire homolog 1 (Drosophila)
202857_at	CNPY2	canopy 2 homolog (zebrafish)
201180_s_at	GNAI3	guanine nucleotide binding protein (G protein), alpha inhibiting ac
225552_x_at	AURKAIP1	aurora kinase A interacting protein 1
239413_at	CEP152	centrosomal protein 152kDa
228970_at	ZBTB8OS	zinc finger and BTB domain containing 8 opposite strand
202330_s_at	UNG	uracil-DNA glycosylase
201853_s_at	CDC25B	cell division cycle 25 homolog B (S. pombe)
222981_s_at	RAB10	RAB10, member RAS oncogene family
222029_x_at	PFDN6	prefoldin subunit 6
225880_at	TOR1AIP2	torsin A interacting protein 2
202128_at	KIAA0317	KIAA0317

201790_s_at	DHCR7	7-dehydrocholesterol reductase
212654_at	TPM2	tropomyosin 2 (beta)
201584_s_at	DDX39A	DEAD (Asp-Glu-Ala-Asp) box polypeptide 39A
230060_at	CDCA7	cell division cycle associated 7
1554390_s_at	ACTR2	ARP2 actin-related protein 2 homolog (yeast)
235463_s_at	CERS6	ceramide synthase 6
221538_s_at	PLXNA1	plexin A1
204558_at	RAD54L	RAD54-like (S. cerevisiae)
217943_s_at	MAP7D1	MAP7 domain containing 1
203190_at	MIR4691 /// NDUFS8	microRNA 4691 /// NADH dehydrogenase (ubiquinone) Fe-S prote
203105_s_at	DNM1L	dynamin 1-like
1555764_s_at	TIMM10	translocase of inner mitochondrial membrane 10 homolog (yeast)
204752_x_at	PARP2	poly (ADP-ribose) polymerase 2
215227_x_at	ACP1	acid phosphatase 1, soluble
213334_x_at	HAUS7	HAUS augmin-like complex, subunit 7
206032_at	DSC3	desmocollin 3
203234_at	UPP1	uridine phosphorylase 1
202824_s_at	TCEB1	transcription elongation factor B (SIII), polypeptide 1 (15kDa, elon
201970_s_at	NASP	nuclear autoantigenic sperm protein (histone-binding)
212165_at	TMEM183A /// TMEM	transmembrane protein 183A /// transmembrane protein 183B
222992_s_at	NDUFB9	NADH dehydrogenase (ubiquinone) 1 beta subcomplex, 9, 22kDa
201587_s_at	IRAK1	interleukin-1 receptor-associated kinase 1
219402_s_at	DERL1	derlin 1
223524_s_at	TMEM108	transmembrane protein 108
234311_s_at	GTPBP10	GTP-binding protein 10 (putative)
200980_s_at	PDHA1	pyruvate dehydrogenase (lipoamide) alpha 1
201433_s_at	PTDSS1	phosphatidylserine synthase 1
238964_at	FIGN	fidgetin
228245_s_at	LOC100509445 /// LO	uncharacterized LOC100509445 /// ovostatin homolog 2-like /// c
208941_s_at	SEPHS1	selenophosphate synthetase 1
225006_x_at	TH1L	TH1-like (Drosophila)
218286_s_at	RNF7	ring finger protein 7
217733_s_at	TMSB10	thymosin beta 10
203228_at	PAFAH1B3	platelet-activating factor acetylhydrolase 1b, catalytic subunit 3 (
226473_at	CBX2	chromobox homolog 2
202961_s_at	ATP5J2	ATP synthase, H+ transporting, mitochondrial Fo complex, subuni
209744_x_at	ITCH	itchy E3 ubiquitin protein ligase
224932_at	CHCHD10	coiled-coil-helix-coiled-coil-helix domain containing 10
221711_s_at	BABAM1	BRISC and BRCA1 A complex member 1
213843_x_at	SLC6A8	solute carrier family 6 (neurotransmitter transporter, creatine), m
235266_at	ATAD2	ATPase family, AAA domain containing 2
221909_at	RNFT2	ring finger protein, transmembrane 2
201114_x_at	PSMA7	proteasome (prosome, macropain) subunit, alpha type, 7
214096_s_at	SHMT2	serine hydroxymethyltransferase 2 (mitochondrial)
210115_at	RPL39L	ribosomal protein L39-like
209680_s_at	KIFC1	kinesin family member C1
201390_s_at	CSNK2B	casein kinase 2, beta polypeptide

209882_at	RIT1	Ras-like without CAAX 1
226616_s_at	NDUFV3	NADH dehydrogenase (ubiquinone) flavoprotein 3, 10kDa
226947_at	GUSBP1 /// GUSBP4	glucuronidase, beta pseudogene 1 /// glucuronidase, beta pseud
204839_at	POP5	processing of precursor 5, ribonuclease P/MRP subunit (S. cerevis
204745_x_at	MT1G	metallothionein 1G
201064_s_at	PABPC4	poly(A) binding protein, cytoplasmic 4 (inducible form)
225317_at	ACBD6	acyl-CoA binding domain containing 6
210854_x_at	SLC6A8	solute carrier family 6 (neurotransmitter transporter, creatine), m
218590_at	C10orf2	chromosome 10 open reading frame 2
239710_at	FIGN	fidgetin
202633_at	TOPBP1	topoisomerase (DNA) II binding protein 1
227455_at	C6orf136	chromosome 6 open reading frame 136
213906_at	MYBL1	v-myb myeloblastosis viral oncogene homolog (avian)-like 1
222894_x_at	NDUFAF5	NADH dehydrogenase (ubiquinone) complex I, assembly factor 5
201441_at	COX6B1	cytochrome c oxidase subunit VIb polypeptide 1 (ubiquitous)
206261_at	ZNF239	zinc finger protein 239
201379_s_at	TPD52L2	tumor protein D52-like 2
226161_at	SLC30A6	solute carrier family 30 (zinc transporter), member 6
201727_s_at	ELAVL1	ELAV (embryonic lethal, abnormal vision, Drosophila)-like 1 (Hu a
235694_at	TCFL5	transcription factor-like 5 (basic helix-loop-helix)
221591_s_at	FAM64A	family with sequence similarity 64, member A
222640_at	DNMT3A	DNA (cytosine-5-)-methyltransferase 3 alpha
228049_x_at	LOC100507303	uncharacterized LOC100507303
203025_at	NAA10	N(alpha)-acetyltransferase 10, NatA catalytic subunit
210213_s_at	EIF6	eukaryotic translation initiation factor 6
225865_x_at	TH1L	TH1-like (Drosophila)
201310_s_at	NREP	neuronal regeneration related protein homolog (rat)
223374_s_at	B3GALNT1	beta-1,3-N-acetylgalactosaminyltransferase 1 (globoside blood gr
222763_s_at	SFT2D3 /// WDR33	SFT2 domain containing 3 /// WD repeat domain 33
223244_s_at	NDUFA12	NADH dehydrogenase (ubiquinone) 1 alpha subcomplex, 12
202279_at	C14orf2	chromosome 14 open reading frame 2
204228_at	PPIH	peptidylprolyl isomerase H (cyclophilin H)
204256_at	ELOVL6	ELOVL fatty acid elongase 6
200625_s_at	CAP1	CAP, adenylate cyclase-associated protein 1 (yeast)
209015_s_at	DNAJB6	DnaJ (Hsp40) homolog, subfamily B, member 6
1555241_at	C8orf59	chromosome 8 open reading frame 59
225427_s_at	APOA1BP	apolipoprotein A-I binding protein
226452_at	PDK1	pyruvate dehydrogenase kinase, isozyme 1
218408_at	TIMM10	translocase of inner mitochondrial membrane 10 homolog (yeast)
209589_s_at	EPHB2	EPH receptor B2
208029_s_at	LAPTM4B	lysosomal protein transmembrane 4 beta
212175_s_at	AK2	adenylate kinase 2
218770_s_at	TMEM39B	transmembrane protein 39B
212791_at	C1orf216	chromosome 1 open reading frame 216
202059_s_at	KPNA1	karyopherin alpha 1 (importin alpha 5)
201091_s_at	CBX3	chromobox homolog 3
204348_s_at	AK4 /// LOC10050785	adenylate kinase 4 /// adenylate kinase isoenzyme 4, mitochondri

212058_at	U2SURP	U2 snRNP-associated SURP domain containing
212411_at	IMP4	IMP4, U3 small nucleolar ribonucleoprotein, homolog (yeast)
216026_s_at	POLE	polymerase (DNA directed), epsilon, catalytic subunit
208795_s_at	MCM7	minichromosome maintenance complex component 7
204817_at	ESPL1	extra spindle pole bodies homolog 1 (S. cerevisiae)
235029_at	GINS4	GINS complex subunit 4 (Sld5 homolog)
227852_at	RP9	retinitis pigmentosa 9 (autosomal dominant)
207714_s_at	SERPINH1	serpin peptidase inhibitor, clade H (heat shock protein 47), memb
222606_at	ZWILCH	Zwilch, kinetochore associated, homolog (Drosophila)
219119_at	NAA38	N(alpha)-acetyltransferase 38, NatC auxiliary subunit
208698_s_at	NONO	non-POU domain containing, octamer-binding
208743_s_at	YWHAB	tyrosine 3-monooxygenase/tryptophan 5-monooxygenase activat
221962_s_at	UBE2H	ubiquitin-conjugating enzyme E2H
225963_at	KLHDC5	kelch domain containing 5
223024_at	AP1M1	adaptor-related protein complex 1, mu 1 subunit
204766_s_at	NUDT1	nudix (nucleoside diphosphate linked moiety X)-type motif 1
218897_at	TMEM177	transmembrane protein 177
218481_at	EXOSC5	exosome component 5
200771_at	LAMC1	laminin, gamma 1 (formerly LAMB2)
220864_s_at	NDUFA13	NADH dehydrogenase (ubiquinone) 1 alpha subcomplex, 13
40148_at	APBB2	amyloid beta (A4) precursor protein-binding, family B, member 2
217835_x_at	C20orf24 /// TGIF2-C2	chromosome 20 open reading frame 24 /// TGIF2-C20orf24 readt
229666_s_at	CSTF3	cleavage stimulation factor, 3' pre-RNA, subunit 3, 77kDa
224578_at	RCC2	regulator of chromosome condensation 2
204668_at	RNF24	ring finger protein 24
201770_at	SNRPA	small nuclear ribonucleoprotein polypeptide A
214005_at	GGCX	gamma-glutamyl carboxylase
223560_s_at	C2orf56	chromosome 2 open reading frame 56
202475_at	TMEM147	transmembrane protein 147
1558692_at	C1orf85	chromosome 1 open reading frame 85
228252_at	PIF1	PIF1 5'-to-3' DNA helicase homolog (S. cerevisiae)
200692_s_at	HSPA9	heat shock 70kDa protein 9 (mortalin)
220942_x_at	FAM162A	family with sequence similarity 162, member A
219522_at	FJX1	four jointed box 1 (Drosophila)
1557945_at	TCTE3	T-complex-associated-testis-expressed 3
232398_at	CCDC150	coiled-coil domain containing 150
208821_at	SNRPB	small nuclear ribonucleoprotein polypeptides B and B1
200862_at	DHCR24	24-dehydrocholesterol reductase
220223_at	ATAD5	ATPase family, AAA domain containing 5
218507_at	HILPDA	hypoxia inducible lipid droplet-associated
1553972_a_at	CBS	cystathionine-beta-synthase
202219_at	SLC6A8	solute carrier family 6 (neurotransmitter transporter, creatine), m
212621_at	TMEM194A	transmembrane protein 194A
236718_at	MYO10	myosin X
203736_s_at	PPFIBP1	PTPRF interacting protein, binding protein 1 (liprin beta 1)
223690_at	LTBP2	latent transforming growth factor beta binding protein 2
200608_s_at	RAD21	RAD21 homolog (S. pombe)

209104_s_at	NHP2	NHP2 ribonucleoprotein homolog (yeast)
213696_s_at	MED8	mediator complex subunit 8
214804_at	CENPI	centromere protein I
234926_s_at	C20orf43	chromosome 20 open reading frame 43
228671_at	TMEM201	transmembrane protein 201
212877_at	KLC1	kinesin light chain 1
228401_at	ATAD2	ATPase family, AAA domain containing 2
201111_at	CSE1L	CSE1 chromosome segregation 1-like (yeast)
215812_s_at	LOC653562 /// SLC6A1	sodium- and chloride-dependent creatine transporter 1-like /// sc
227997_at	IL17RD	interleukin 17 receptor D
231517_at	ZYG11A	zyg-11 homolog A (C. elegans)
1554020_at	BICD1	bicaudal D homolog 1 (Drosophila)
222514_at	RRAGC	Ras-related GTP binding C
213671_s_at	MARS	methionyl-tRNA synthetase
225991_at	TMEM41A	transmembrane protein 41A
201264_at	COPE	coatomer protein complex, subunit epsilon
224448_s_at	MNF1	mitochondrial nucleoid factor 1
201692_at	SIGMAR1	sigma non-opioid intracellular receptor 1
214321_at	NOV	nephroblastoma overexpressed
212625_at	STX10	syntaxin 10
235384_at	NUDT19	nudix (nucleoside diphosphate linked moiety X)-type motif 19
224610_at	SNHG1 /// SNORD22 /	small nucleolar RNA host gene 1 (non-protein coding) /// small nu
224791_at	ASAP1	ArfGAP with SH3 domain, ankyrin repeat and PH domain 1
201521_s_at	NCBP2	nuclear cap binding protein subunit 2, 20kDa
214073_at	CTTN	cortactin
230424_at	NREP	neuronal regeneration related protein homolog (rat)
225540_at	MAP2	microtubule-associated protein 2
210811_s_at	DDX49	DEAD (Asp-Glu-Ala-Asp) box polypeptide 49
212985_at	APBB2	amyloid beta (A4) precursor protein-binding, family B, member 2
202208_s_at	ARL4C	ADP-ribosylation factor-like 4C
203578_s_at	SLC7A6	solute carrier family 7 (amino acid transporter light chain, y+L syst
218237_s_at	SLC38A1	solute carrier family 38, member 1
225676_s_at	DCAF13	DDB1 and CUL4 associated factor 13
203536_s_at	CIAO1	cytosolic iron-sulfur protein assembly 1
214039_s_at	LAPTM4B	lysosomal protein transmembrane 4 beta
236565_s_at	LARP6	La ribonucleoprotein domain family, member 6
226255_at	ZBTB33	zinc finger and BTB domain containing 33
207746_at	POLQ	polymerase (DNA directed), theta
201298_s_at	MOB1A	MOB kinase activator 1A
204649_at	TROAP	trophinin associated protein (tastin)
210416_s_at	CHEK2	checkpoint kinase 2
226847_at	FST	follistatin
224564_s_at	RTN3	reticulon 3
225424_at	GPAM	glycerol-3-phosphate acyltransferase, mitochondrial
230696_at	LOC100289092	uncharacterized LOC100289092
217861_s_at	PREB	prolactin regulatory element binding
244427_at	KIF23	Kinesin family member 23

212800_at	STX6	syntaxin 6
241453_at	LOC100653024 /// LO	uncharacterized LOC100653024 /// uncharacterized LOC1006531
217094_s_at	ITCH	itchy E3 ubiquitin protein ligase
227651_at	NACC1	nucleus accumbens associated 1, BEN and BTB (POZ) domain cont
203422_at	POLD1	polymerase (DNA directed), delta 1, catalytic subunit
224684_at	SNX12	sorting nexin 12
228238_at	GAS5 /// SNORD44 ///	growth arrest-specific 5 (non-protein coding) /// small nucleolar R
229647_at	NDUFS1	NADH dehydrogenase (ubiquinone) Fe-S protein 1, 75kDa (NADH-
220051_at	PRSS21	protease, serine, 21 (testisin)
212405_s_at	METTL13	methyltransferase like 13
225143_at	SFXN4	sideroflexin 4
218133_s_at	NIF3L1	NIF3 NGG1 interacting factor 3-like 1 (S. cerevisiae)
213310_at	EIF2C2 /// LOC286109	Eukaryotic translation initiation factor 2C, 2 /// Uncharacterized L
204480_s_at	C9orf16	chromosome 9 open reading frame 16
204608_at	ASL	argininosuccinate lyase
217926_at	C19orf53	chromosome 19 open reading frame 53
225081_s_at	CDCA7L	cell division cycle associated 7-like
201250_s_at	SLC2A1	solute carrier family 2 (facilitated glucose transporter), member 1
200827_at	PLOD1	procollagen-lysine, 2-oxoglutarate 5-dioxygenase 1
226938_at	DCAF4	DDB1 and CUL4 associated factor 4
202918_s_at	HSPE1-MOB4 /// MOB	HSPE1-MOB4 readthrough /// MOB family member 4, phocein
225468_at	PATL1	protein associated with topoisomerase II homolog 1 (yeast)
202804_at	ABCC1	ATP-binding cassette, sub-family C (CFTR/MRP), member 1
226355_at	POC1A	POC1 centriolar protein homolog A (Chlamydomonas)
222530_s_at	MKKS	McKusick-Kaufman syndrome
224598_at	MGAT4B	mannosyl (alpha-1,3-)-glycoprotein beta-1,4-N-acetylglucosaminy
217784_at	YKT6	YKT6 v-SNARE homolog (S. cerevisiae)
229671_s_at	MIS18A	MIS18 kinetochore protein homolog A (S. pombe)
219348_at	USE1	unconventional SNARE in the ER 1 homolog (S. cerevisiae)
217860_at	NDUFA10	NADH dehydrogenase (ubiquinone) 1 alpha subcomplex, 10, 42kD
223389_s_at	ZNF581	zinc finger protein 581
225864_at	FAM84B	family with sequence similarity 84, member B
200868_s_at	RNF114	ring finger protein 114
231784_s_at	DCAF13	DDB1 and CUL4 associated factor 13
203588_s_at	TFDP2	transcription factor Dp-2 (E2F dimerization partner 2)
227103_s_at	ECE2	endothelin converting enzyme 2
218388_at	PGLS	6-phosphogluconolactonase
204407_at	TTF2	transcription termination factor, RNA polymerase II
201791_s_at	DHCR7	7-dehydrocholesterol reductase
232596_at	DIAPH3	diaphanous homolog 3 (Drosophila)
224615_x_at	HM13	histocompatibility (minor) 13
224890_s_at	C7orf59	chromosome 7 open reading frame 59
222451_s_at	ZDHHC9	zinc finger, DHHC-type containing 9
201066_at	CYC1	cytochrome c-1
202888_s_at	ANPEP	alanyl (membrane) aminopeptidase
200979_at	PDHA1	pyruvate dehydrogenase (lipoamide) alpha 1
230032_at	OSGEPL1	O-sialoglycoprotein endopeptidase-like 1

211964_at	COL4A2	collagen, type IV, alpha 2
204717_s_at	SLC29A2	solute carrier family 29 (nucleoside transporters), member 2
212020_s_at	MKI67	antigen identified by monoclonal antibody Ki-67
218003_s_at	FKBP3 /// LOC100652	FK506 binding protein 3, 25kDa /// uncharacterized LOC1006528
220189_s_at	MGAT4B	mannosyl (alpha-1,3-)-glycoprotein beta-1,4-N-acetylglucosaminy
201690_s_at	TPD52	tumor protein D52
219531_at	CEP72	centrosomal protein 72kDa
242828_at	FIGN	fidgetin
201710_at	MYBL2	v-myb myeloblastosis viral oncogene homolog (avian)-like 2
211031_s_at	CLIP2	CAP-GLY domain containing linker protein 2
229268_at	FAM105B	family with sequence similarity 105, member B
235648_at	ZNF567	zinc finger protein 567
218343_s_at	GTF3C3	general transcription factor IIIC, polypeptide 3, 102kDa
212541_at	FLAD1	FAD1 flavin adenine dinucleotide synthetase homolog (S. cerevisia
226032_at	CASP2	caspase 2, apoptosis-related cysteine peptidase
201754_at	COX6C	cytochrome c oxidase subunit VIc
222155_s_at	SLC52A2	solute carrier family 52, riboflavin transporter, member 2
230249_at	KHDRBS3	KH domain containing, RNA binding, signal transduction associate
213127_s_at	MED8	mediator complex subunit 8
241908_at	BROX	BRO1 domain and CAAX motif containing
229665_at	CSTF3	cleavage stimulation factor, 3' pre-RNA, subunit 3, 77kDa
201479_at	DKC1 /// SNORA56	dyskeratosis congenita 1, dyskerin /// small nucleolar RNA, H/ACA
201275_at	FDPS	farnesyl diphosphate synthase
238273_at	C7orf73 /// LOC10028	chromosome 7 open reading frame 73 /// chromosome 7 open re
243531_at	ORAOV1	oral cancer overexpressed 1
222987_s_at	TMEM9	transmembrane protein 9
209054_s_at	WHSC1	Wolf-Hirschhorn syndrome candidate 1
226649_at	PANK1	pantothenate kinase 1
205395_s_at	MRE11A	MRE11 meiotic recombination 11 homolog A (S. cerevisiae)
39729_at	PRDX2	peroxiredoxin 2
208934_s_at	LGALS8	lectin, galactoside-binding, soluble, 8
203167_at	TIMP2	TIMP metallopeptidase inhibitor 2
210290_at	ZNF174	zinc finger protein 174
224185_at	WRAP53	WD repeat containing, antisense to TP53
226630_at	MIS18BP1	MIS18 binding protein 1
228972_at	PITPNA-AS1	PITPNA antisense RNA 1 (non-protein coding)
210685_s_at	UBE4B	ubiquitination factor E4B
213754_s_at	PAIP1	poly(A) binding protein interacting protein 1
225196_s_at	MRPS26	mitochondrial ribosomal protein S26
202847_at	PCK2	phosphoenolpyruvate carboxykinase 2 (mitochondrial)
219004_s_at	MIS18A	MIS18 kinetochore protein homolog A (S. pombe)
227160_s_at	NDUFAF5	NADH dehydrogenase (ubiquinone) complex I, assembly factor 5
200734_s_at	ARF3	ADP-ribosylation factor 3
210418_s_at	IDH3B	isocitrate dehydrogenase 3 (NAD+) beta
210470_x_at	NONO	non-POU domain containing, octamer-binding
65588_at	LOC388796	uncharacterized LOC388796
206273_at	SLMO1	slowmo homolog 1 (Drosophila)

222018_at	NACA	nascent polypeptide-associated complex alpha subunit
212072_s_at	CSNK2A1 /// CSNK2A1	casein kinase 2, alpha 1 polypeptide /// casein kinase 2, alpha 1 p
201068_s_at	PSMC2	proteasome (prosome, macropain) 26S subunit, ATPase, 2
213419_at	APBB2	amyloid beta (A4) precursor protein-binding, family B, member 2
32723_at	CSTF1	cleavage stimulation factor, 3' pre-RNA, subunit 1, 50kDa
211056_s_at	SRD5A1	steroid-5-alpha-reductase, alpha polypeptide 1 (3-oxo-5 alpha-ste
225303_at	KIRREL	kin of IRRE like (Drosophila)
218829_s_at	CHD7	chromodomain helicase DNA binding protein 7
203728_at	BAK1	BCL2-antagonist/killer 1
202554_s_at	GSTM3	glutathione S-transferase mu 3 (brain)
1555760_a_at	RBM15	RNA binding motif protein 15
213610_s_at	KLHL23 /// PHOSPHO2	kelch-like 23 (Drosophila) /// PHOSPHO2-KLHL23 readthrough
219345_at	BOLA1	bolA homolog 1 (E. coli)
233058_at	GPSM2	G-protein signaling modulator 2
232881_at	GNAS-AS1	GNAS antisense RNA 1 (non-protein coding)
224580_at	SLC38A1	solute carrier family 38, member 1
225925_s_at	USP48	ubiquitin specific peptidase 48
209171_at	ITPA	inosine triphosphatase (nucleoside triphosphate pyrophosphatase
218497_s_at	RNASEH1	ribonuclease H1
1553099_at	TIGD1	tigger transposable element derived 1
225777_at	SAPCD2	suppressor APC domain containing 2
227385_at	PPAPDC2	phosphatidic acid phosphatase type 2 domain containing 2
57703_at	SENP5	SUMO1/sentrin specific peptidase 5
217895_at	PTCD3	pentatricopeptide repeat domain 3
1558508_a_at	C1orf53	chromosome 1 open reading frame 53
214173_x_at	URI1	URI1, prefoldin-like chaperone
204514_at	DPH2	DPH2 homolog (S. cerevisiae)
219880_at	LOC100507619	uncharacterized LOC100507619
203550_s_at	FAM189B	family with sequence similarity 189, member B
202382_s_at	GNPDA1	glucosamine-6-phosphate deaminase 1
218538_s_at	MRS2	MRS2 magnesium homeostasis factor homolog (S. cerevisiae)
220525_s_at	AUP1	ancient ubiquitous protein 1
220399_at	LINC00115	long intergenic non-protein coding RNA 115
219491_at	LRFN4	leucine rich repeat and fibronectin type III domain containing 4
222233_s_at	DCLRE1C	DNA cross-link repair 1C
214700_x_at	RIF1	RAP1 interacting factor homolog (yeast)
220160_s_at	KPTN	kaptin (actin binding protein)
223513_at	CENPJ	centromere protein J
1554408_a_at	TK1	thymidine kinase 1, soluble
212832_s_at	CKAP5	cytoskeleton associated protein 5
213571_s_at	EIF4E2 /// LOC100507	eukaryotic translation initiation factor 4E family member 2 /// un
212008_at	UBXN4	UBX domain protein 4
1554063_at	ZHX1-C8ORF76	ZHX1-C8ORF76 readthrough
204849_at	DPH3P1 /// TCFL5	DPH3, KTI11 homolog (S. cerevisiae) pseudogene 1 /// transcripti
219002_at	FASTKD1	FAST kinase domains 1
219061_s_at	LAGE3	L antigen family, member 3
201509_at	IDH3B	isocitrate dehydrogenase 3 (NAD+) beta

237005_at	LOC442075	uncharacterized LOC442075
225861_at	FAM195A	family with sequence similarity 195, member A
204871_at	MTERF	mitochondrial transcription termination factor
203390_s_at	KIF3C	kinesin family member 3C
223811_s_at	GET4 /// SUN1	golgi to ER traffic protein 4 homolog (S. cerevisiae) /// Sad1 and U
222654_at	IMPAD1	inositol monophosphatase domain containing 1
202528_at	GALE	UDP-galactose-4-epimerase
202645_s_at	MEN1	multiple endocrine neoplasia I
225692_at	CAMTA1	calmodulin binding transcription activator 1
1554026_a_at	MYO10	myosin X
227094_at	DHTKD1	dehydrogenase E1 and transketolase domain containing 1
209797_at	CNPY2	canopy 2 homolog (zebrafish)
228987_at	FAM49B	family with sequence similarity 49, member B
217950_at	NOSIP	nitric oxide synthase interacting protein
201558_at	RAE1	RAE1 RNA export 1 homolog (S. pombe)
230521_at	C9orf100	chromosome 9 open reading frame 100
217208_s_at	DLG1	discs, large homolog 1 (Drosophila)
218617_at	TRIT1	tRNA isopentenyltransferase 1
227724_at	LOC728190	uncharacterized LOC728190
212012_at	PXDN	peroxidasin homolog (Drosophila)
228543_at	PET117	PET117 homolog (S. cerevisiae)
209899_s_at	PUF60	poly-U binding splicing factor 60KDa
203706_s_at	FZD7	frizzled family receptor 7
226346_at	MEX3A	mex-3 homolog A (C. elegans)
208952_s_at	LARP4B	La ribonucleoprotein domain family, member 4B
227818_at	CEP85	centrosomal protein 85kDa
229981_at	SNX5	sorting nexin 5
211527_x_at	VEGFA	vascular endothelial growth factor A
229538_s_at	IQGAP3	IQ motif containing GTPase activating protein 3
202338_at	TK1	thymidine kinase 1, soluble
221908_at	RNFT2	ring finger protein, transmembrane 2
217043_s_at	MFN1	mitofusin 1
45714_at	HCFC1R1	host cell factor C1 regulator 1 (XPO1 dependent)
1553715_s_at	FAM195A	family with sequence similarity 195, member A
242592_at	GPR137C	G protein-coupled receptor 137C
228066_at	C17orf96	chromosome 17 open reading frame 96
213668_s_at	SOX4	SRY (sex determining region Y)-box 4
226086_at	SYT13	synaptotagmin XIII
224790_at	ASAP1	ArfGAP with SH3 domain, ankyrin repeat and PH domain 1
211165_x_at	EPHB2	EPH receptor B2
238768_at	C2orf68	chromosome 2 open reading frame 68
212757_s_at	CAMK2G	calcium/calmodulin-dependent protein kinase II gamma
218567_x_at	DPP3	dipeptidyl-peptidase 3
31807_at	DDX49	DEAD (Asp-Glu-Ala-Asp) box polypeptide 49
1555274_a_at	EPT1	ethanolaminephosphotransferase 1 (CDP-ethanolamine-specific)
202261_at	VPS72	vacuolar protein sorting 72 homolog (S. cerevisiae)
207098_s_at	MFN1	mitofusin 1

214264_s_at	EFCAB11	EF-hand calcium binding domain 11
223530_at	TDRKH	tudor and KH domain containing
221649_s_at	PPAN /// PPAN-P2RY1	peter pan homolog (Drosophila) /// PPAN-P2RY11 readthrough
209588_at	EPHB2	EPH receptor B2
210014_x_at	IDH3B	isocitrate dehydrogenase 3 (NAD+) beta
202486_at	AFG3L2	AFG3 ATPase family gene 3-like 2 (S. cerevisiae)
229980_s_at	SNX5	sorting nexin 5
212858_at	PAQR4	progestin and adipoQ receptor family member IV
210785_s_at	C1orf38	chromosome 1 open reading frame 38
202758_s_at	RFXANK	regulatory factor X-associated ankyrin-containing protein
218522_s_at	MAP1S	microtubule-associated protein 1S
231967_at	PHF20L1	PHD finger protein 20-like 1
227456_s_at	C6orf136	chromosome 6 open reading frame 136
218016_s_at	POLR3E	polymerase (RNA) III (DNA directed) polypeptide E (80kD)
222759_at	SUV420H1	suppressor of variegation 4-20 homolog 1 (Drosophila)
200778_s_at	SEPT2	septin 2
232740_at	MCM3AP-AS1	MCM3AP antisense RNA 1 (non-protein coding)
217310_s_at	FOXJ3	forkhead box J3
219984_s_at	HRASLS	HRAS-like suppressor
203805_s_at	FANCA	Fanconi anemia, complementation group A
203438_at	STC2	stanniocalcin 2
202735_at	EBP	emopamil binding protein (sterol isomerase)
201341_at	ENC1	ectodermal-neural cortex 1 (with BTB-like domain)
225150_s_at	RTKN	rhotekin
213526_s_at	LIN37	lin-37 homolog (C. elegans)
201548_s_at	KDM5B	lysine (K)-specific demethylase 5B
221082_s_at	NDRG3	NDRG family member 3
228499_at	PFKFB4	6-phosphofructo-2-kinase/fructose-2,6-biphosphatase 4
232652_x_at	SCAND1	SCAN domain containing 1
207571_x_at	C1orf38	chromosome 1 open reading frame 38
1555500_s_at	SLC2A4RG	SLC2A4 regulator
1554348_s_at	CDKN2AIPNL	CDKN2A interacting protein N-terminal like
213378_s_at	DDX11 /// DDX12P ///	DEAD/H (Asp-Glu-Ala-Asp/His) box helicase 11 /// DEAD/H (Asp-G
1555797_a_at	ARPC5	actin related protein 2/3 complex, subunit 5, 16kDa
219556_at	C16orf59	chromosome 16 open reading frame 59
203806_s_at	FANCA	Fanconi anemia, complementation group A
206949_s_at	RUSC1	RUN and SH3 domain containing 1
226569_s_at	CHTF18	CTF18, chromosome transmission fidelity factor 18 homolog (S. ce
204078_at	LEPREL4	leprecan-like 4
1558329_at	TONSL	tonsoku-like, DNA repair protein
200709_at	FKBP1A	FK506 binding protein 1A, 12kDa
223528_s_at	METTL17	methyltransferase like 17
210463_x_at	TRMT1	tRNA methyltransferase 1 homolog (S. cerevisiae)
231146_at	FAM24B	family with sequence similarity 24, member B
204432_at	SOX12	SRY (sex determining region Y)-box 12
218206_x_at	SCAND1	SCAN domain containing 1
209705_at	MTF2	metal response element binding transcription factor 2

227348_at	PARS2	prolyl-tRNA synthetase 2, mitochondrial (putative)
226775_at	ENY2	enhancer of yellow 2 homolog (Drosophila)
1553015_a_at	RECQL4	RecQ protein-like 4
225362_at	FAM122B	family with sequence similarity 122B
228906_at	TET1	tet methylcytosine dioxygenase 1
1558143_a_at	BCL2L11	BCL2-like 11 (apoptosis facilitator)
238333_s_at	MTG1	Mitochondrial GTPase 1 homolog (S. cerevisiae)
34868_at	SMG5	smg-5 homolog, nonsense mediated mRNA decay factor (C. elega
200990_at	TRIM28	tripartite motif containing 28
219080_s_at	CTPS2	CTP synthase 2
223255_at	G2E3	G2/M-phase specific E3 ubiquitin protein ligase
210656_at	EED	embryonic ectoderm development
219615_s_at	KCNK5	potassium channel, subfamily K, member 5
221004_s_at	ITM2C	integral membrane protein 2C
209205_s_at	LMO4	LIM domain only 4
214185_at	KHDRBS1	KH domain containing, RNA binding, signal transduction associate
221906_at	TXNRD3 /// TXNRD3N	thioredoxin reductase 3 /// thioredoxin reductase 3 neighbor
217714_x_at	MIR3917 /// STMN1	microRNA 3917 /// stathmin 1
207812_s_at	GORASP2	golgi reassembly stacking protein 2, 55kDa
203262_s_at	FAM50A	family with sequence similarity 50, member A
212809_at	NFATC2IP	nuclear factor of activated T-cells, cytoplasmic, calcineurin-depen
201948_at	GNL2	guanine nucleotide binding protein-like 2 (nucleolar)
44669_at	SDHAF1	succinate dehydrogenase complex assembly factor 1
200661_at	CTSA	cathepsin A
242560_at	FANCD2	Fanconi anemia, complementation group D2
202282_at	HSD17B10	hydroxysteroid (17-beta) dehydrogenase 10
212276_at	LPIN1	lipin 1
1553220_at	FAM117B	family with sequence similarity 117, member B
224652_at	CCNY	cyclin Y
41047_at	C9orf16	chromosome 9 open reading frame 16
222343_at	BCL2L11	BCL2-like 11 (apoptosis facilitator)
231895_at	SASS6	spindle assembly 6 homolog (C. elegans)
229099_at	C11orf83	chromosome 11 open reading frame 83
229672_at	UQCC	ubiquinol-cytochrome c reductase complex chaperone
61732_r_at	IFT74	intraflagellar transport 74 homolog (Chlamydomonas)
228259_s_at	EPB41L4A-AS1	EPB41L4A antisense RNA 1 (non-protein coding)
240228_at	CSMD3	CUB and Sushi multiple domains 3
204301_at	KBTBD11	kelch repeat and BTB (POZ) domain containing 11
210791_s_at	ARHGAP32	Rho GTPase activating protein 32
1563502_at	ZDHHC2	Zinc finger, DHHC-type containing 2
1569262_x_at	UBE3D	ubiquitin protein ligase E3D
206030_at	ASPA	aspartoacylase
1564372_s_at	CASC2	cancer susceptibility candidate 2 (non-protein coding)
1555352_at	FOXP2	forkhead box P2
205116_at	LAMA2	laminin, alpha 2
219332_at	MICALL2	MICAL-like 2
218483_s_at	IFT46	intraflagellar transport 46 homolog (Chlamydomonas)

225539_at	ZNF295	zinc finger protein 295
219415_at	TTYH1	tweety homolog 1 (Drosophila)
213519_s_at	LAMA2	laminin, alpha 2
203233_at	IL4R	interleukin 4 receptor
225999_at	RIMKLB	ribosomal modification protein rimK-like family member B
238484_s_at	SSBP2	single-stranded DNA binding protein 2
213228_at	PDE8B	phosphodiesterase 8B
1557132_at	WDR17	WD repeat domain 17
200704_at	LITAF	lipopolysaccharide-induced TNF factor
235335_at	ABCA9	ATP-binding cassette, sub-family A (ABC1), member 9
219954_s_at	GBA3	glucosidase, beta, acid 3 (cytosolic)
1554117_at	CCDC60	coiled-coil domain containing 60
205241_at	SCO2	SCO cytochrome oxidase deficient homolog 2 (yeast)
202972_s_at	FAM13A	family with sequence similarity 13, member A
205632_s_at	PIP5K1B	phosphatidylinositol-4-phosphate 5-kinase, type I, beta
201042_at	TGM2	transglutaminase 2 (C polypeptide, protein-glutamine-gamma-glu
203151_at	MAP1A	microtubule-associated protein 1A
231434_at	LOC100505841	zinc finger protein 474-like
224648_at	GPBP1	GC-rich promoter binding protein 1
1561928_s_at	ANKUB1	ankyrin repeat and ubiquitin domain containing 1
238810_at	RFX3	regulatory factor X, 3 (influences HLA class II expression)
201924_at	AFF1	AF4/FMR2 family, member 1
1553798_a_at	FBXL13	F-box and leucine-rich repeat protein 13
242323_at	PLA2G12A	phospholipase A2, group XIIA
234605_at	CDC14B	CDC14 cell division cycle 14 homolog B (S. cerevisiae)
229956_at	NR2C1	nuclear receptor subfamily 2, group C, member 1
220500_s_at	RABL2A /// RABL2B	RAB, member of RAS oncogene family-like 2A /// RAB, member of
1552993_at	DYDC1	DPY30 domain containing 1
208866_at	CSNK1A1	casein kinase 1, alpha 1
1559067_a_at	LOC158402	Uncharacterized LOC158402
230351_at	LOC283481	uncharacterized LOC283481
1557285_at	AREGB	Amphiregulin B
238483_at	SSBP2	single-stranded DNA binding protein 2
202284_s_at	CDKN1A	cyclin-dependent kinase inhibitor 1A (p21, Cip1)
1562301_at	C8orf34	chromosome 8 open reading frame 34
208070_s_at	REV3L	REV3-like, polymerase (DNA directed), zeta, catalytic subunit
204497_at	ADCY9	adenylate cyclase 9
209612_s_at	ADH1B	alcohol dehydrogenase 1B (class I), beta polypeptide
1553228_at	CCDC89	coiled-coil domain containing 89
219970_at	GIPC2	GIPC PDZ domain containing family, member 2
204874_x_at	BAIAP3	BAI1-associated protein 3
202552_s_at	CRIM1	cysteine rich transmembrane BMP regulator 1 (chordin-like)
231961_at	RBPMS	RNA binding protein with multiple splicing
210176_at	TLR1	toll-like receptor 1
235328_at	PLXNC1	Plexin C1
45288_at	ABHD6	abhydrolase domain containing 6
240303_at	TMC5	transmembrane channel-like 5

224165_s_at	IQCH	IQ motif containing H
215321_at	RUNDC3B	RUN domain containing 3B
218730_s_at	OGN	osteoglycin
202588_at	AK1	adenylate kinase 1
201983_s_at	EGFR	epidermal growth factor receptor
229064_s_at	RCAN3	RCAN family member 3
220050_at	C9orf9	chromosome 9 open reading frame 9
229573_at	USP9X	ubiquitin specific peptidase 9, X-linked
206914_at	CRTAM	cytotoxic and regulatory T cell molecule
225747_at	COQ10A	coenzyme Q10 homolog A (S. cerevisiae)
237298_at	FLJ26850	FLJ26850 protein
1559097_at	C14orf64	chromosome 14 open reading frame 64
1553211_at	ANKFN1	ankyrin-repeat and fibronectin type III domain containing 1
230824_at	MARCH10	membrane-associated ring finger (C3HC4) 10, E3 ubiquitin protei
1554708_s_at	SPATA6L	spermatogenesis associated 6-like
242009_at	SLC6A4	solute carrier family 6 (neurotransmitter transporter, serotonin),
35846_at	THRA	thyroid hormone receptor, alpha
242669_at	UFM1	Ubiquitin-fold modifier 1
226646_at	KLF2	Kruppel-like factor 2 (lung)
224175_s_at	TRIM34 /// TRIM6-TRI	tripartite motif containing 34 /// TRIM6-TRIM34 readthrough
217047_s_at	FAM13A	family with sequence similarity 13, member A
202035_s_at	SFRP1	secreted frizzled-related protein 1
221766_s_at	FAM46A	family with sequence similarity 46, member A
204526_s_at	TBC1D8	TBC1 domain family, member 8 (with GRAM domain)
238854_at	LOC100506668	uncharacterized LOC100506668
205583_s_at	ALG13	asparagine-linked glycosylation 13 homolog (S. cerevisiae)
227415_at	LOC283508	uncharacterized LOC283508
1562640_at	HOXA-AS2	HOXA cluster antisense RNA 2 (non-protein coding)
228748_at	CD59	CD59 molecule, complement regulatory protein
226717_at	LRTOMT	leucine rich transmembrane and 0-methyltransferase domain con
212993_at	NACC2	NACC family member 2, BEN and BTB (POZ) domain containing
208707_at	EIF5	eukaryotic translation initiation factor 5
217437_s_at	TACC1	transforming, acidic coiled-coil containing protein 1
204713_s_at	F5	coagulation factor V (proaccelerin, labile factor)
202962_at	KIF13B	kinesin family member 13B
224588_at	XIST	X (inactive)-specific transcript (non-protein coding)
236016_at	SMARCE1	SWI/SNF related, matrix associated, actin dependent regulator of
224391_s_at	SIAE	sialic acid acetylesterase
1557122_s_at	GABRB2	gamma-aminobutyric acid (GABA) A receptor, beta 2
231300_at	C16orf93	chromosome 16 open reading frame 93
213558_at	PCLO	piccolo (presynaptic cytomatrix protein)
219795_at	SLC6A14	solute carrier family 6 (amino acid transporter), member 14
202663_at	WIPF1	WAS/WASL interacting protein family, member 1
1563961_at	FHAD1	forkhead-associated (FHA) phosphopeptide binding domain 1
243413_at	TTC30B	tetratricopeptide repeat domain 30B
1560458_s_at	CAPS2	calcyphosine 2
231051_at	M1	uncharacterized LOC100507027

220218_at	SPATA6L	spermatogenesis associated 6-like
209977_at	PLG	plasminogen
202551_s_at	CRIM1	cysteine rich transmembrane BMP regulator 1 (chordin-like)
220272_at	BNC2	basonuclin 2
228905_at	PCM1	pericentriolar material 1
215806_x_at	TARP /// TRGC2	TCR gamma alternate reading frame protein /// T cell receptor ga
230964_at	FREM2	FRAS1 related extracellular matrix protein 2
1556907_at	ZNF474	zinc finger protein 474
231136_at	MIR30C2	microRNA 30c-2
206010_at	HABP2	hyaluronan binding protein 2
1556325_at	FILIP1	filamin A interacting protein 1
241705_at	ABCA5	ATP-binding cassette, sub-family A (ABC1), member 5
214607_at	PAK3	p21 protein (Cdc42/Rac)-activated kinase 3
205337_at	DCT	dopachrome tautomerase (dopachrome delta-isomerase, tyrosine
1562321_at	PDK4	pyruvate dehydrogenase kinase, isozyme 4
202995_s_at	FBLN1	fibulin 1
233915_at	KIAA0825	KIAA0825
205198_s_at	ATP7A	ATPase, Cu++ transporting, alpha polypeptide
226228_at	AQP4	aquaporin 4
243423_at	TNIP1	TNFAIP3 interacting protein 1
231103_at	KCNN3	potassium intermediate/small conductance calcium-activated cha
227478_at	SETBP1	SET binding protein 1
212225_at	EIF1	eukaryotic translation initiation factor 1
206834_at	HBD	hemoglobin, delta
225102_at	MGLL	monoglyceride lipase
225250_at	STIM2	stromal interaction molecule 2
223905_at	CCDC135	coiled-coil domain containing 135
203787_at	SSBP2	single-stranded DNA binding protein 2
214438_at	HLX	H2.0-like homeobox
1565544_at	RNF141	ring finger protein 141
204674_at	LRMP	lymphoid-restricted membrane protein
225212_at	SLC25A25	solute carrier family 25 (mitochondrial carrier; phosphate carrier),
1556607_at	EHD4	EH-domain containing 4
227934_at	KPNA5	karyopherin alpha 5 (importin alpha 6)
205798_at	IL7R	interleukin 7 receptor
1558815_at	SORBS2	sorbin and SH3 domain containing 2
222892_s_at	TMEM40	transmembrane protein 40
233326_at	CCDC39	coiled-coil domain containing 39
235723_at	BNC2	basonuclin 2
205291_at	IL2RB	interleukin 2 receptor, beta
236745_at	CCDC78	coiled-coil domain containing 78
226956_at	MTMR3	myotubularin related protein 3
202393_s_at	KLF10	Kruppel-like factor 10
230891_at	TUBE1	Tubulin, epsilon 1
200911_s_at	TACC1	transforming, acidic coiled-coil containing protein 1
226992_at	NOSTRIN	nitric oxide synthase trafficker
226576_at	ARHGAP26	Rho GTPase activating protein 26

1553202_at	STOX1	storkhead box 1
223348_x_at	MUM1	melanoma associated antigen (mutated) 1
225624_at	SNX29	sorting nexin 29
219093_at	PID1	phosphotyrosine interaction domain containing 1
1553134_s_at	C9orf72	chromosome 9 open reading frame 72
214681_at	GK	glycerol kinase
230772_at	HNF4A	hepatocyte nuclear factor 4, alpha
228442_at	NFATC2	nuclear factor of activated T-cells, cytoplasmic, calcineurin-depen
213527_s_at	ZNF688	zinc finger protein 688
202747_s_at	ITM2A	integral membrane protein 2A
203508_at	TNFRSF1B	tumor necrosis factor receptor superfamily, member 1B
201288_at	ARHGDIB	Rho GDP dissociation inhibitor (GDI) beta
229994_at	NFIA	Nuclear factor I/A
236833_at	TTC16	tetratricopeptide repeat domain 16
230976_at	AK8	adenylate kinase 8
215046_at	KANSL1L	KAT8 regulatory NSL complex subunit 1-like
203845_at	KAT2B	K(lysine) acetyltransferase 2B
237420_at	ODF2L	outer dense fiber of sperm tails 2-like
229313_at	ANO5	anoctamin 5
228425_at	LOC654433	uncharacterized LOC654433
1558334_a_at	C22orf15	chromosome 22 open reading frame 15
202973_x_at	FAM13A	family with sequence similarity 13, member A
223322_at	RASSF5	Ras association (RalGDS/AF-6) domain family member 5
216109_at	MED13L	Mediator complex subunit 13-like
1552459_a_at	MBD3L1	methyl-CpG binding domain protein 3-like 1
225564_at	SPATA13	spermatogenesis associated 13
226430_at	RELL1	RELT-like 1
226991_at	NFATC2	nuclear factor of activated T-cells, cytoplasmic, calcineurin-depen
235561_at	TXNL1	thioredoxin-like 1
213271_s_at	DOPEY1	dopey family member 1
224999_at	EGFR	epidermal growth factor receptor
227627_at	C8orf44-SGK3 /// SGK	C8orf44-SGK3 readthrough /// serum/glucocorticoid regulated ki
216840_s_at	LAMA2	laminin, alpha 2
219252_s_at	GEMIN8	gem (nuclear organelle) associated protein 8
213572_s_at	SERPINB1	serpin peptidase inhibitor, clade B (ovalbumin), member 1
1563845_at	FAM153B /// LOC1005	family with sequence similarity 153, member B /// uncharacterize
244289_at	ZNF300P1	zinc finger protein 300 pseudogene 1
243539_at	KIAA1841	KIAA1841
235465_at	FAM123A	family with sequence similarity 123A
240771_at	C1orf101	chromosome 1 open reading frame 101
221569_at	AHI1	Abelson helper integration site 1
221029_s_at	WNT5B	wingless-type MMTV integration site family, member 5B
231178_at	SPATA4	spermatogenesis associated 4
1552320_a_at	CCDC65	coiled-coil domain containing 65
228256_s_at	EPB41L4A	erythrocyte membrane protein band 4.1 like 4A
215232_at	ARHGAP44	Rho GTPase activating protein 44
209613_s_at	ADH1B	alcohol dehydrogenase 1B (class I), beta polypeptide

209960_at	HGF	hepatocyte growth factor (hepapoietin A; scatter factor)
230511_at	CREM	cAMP responsive element modulator
213003_s_at	KIAA0146	KIAA0146
237282_s_at	AKAP14	A kinase (PRKA) anchor protein 14
213908_at	WHAMMP2 /// WHAM	WAS protein homolog associated with actin, golgi membranes anc
220324_at	LINC00472	long intergenic non-protein coding RNA 472
37547_at	BBS9	Bardet-Biedl syndrome 9
1553905_at	CXorf22	chromosome X open reading frame 22
212268_at	SERPINB1	serpin peptidase inhibitor, clade B (ovalbumin), member 1
205419_at	GPR183	G protein-coupled receptor 183
212463_at	CD59	CD59 molecule, complement regulatory protein
213832_at	KCND3	potassium voltage-gated channel, Shal-related subfamily, membe
1569225_a_at	SCML4	sex comb on midleg-like 4 (Drosophila)
213400_s_at	TBL1X	transducin (beta)-like 1X-linked
220150_s_at	FAM184A	family with sequence similarity 184, member A
209723_at	SERPINB9	serpin peptidase inhibitor, clade B (ovalbumin), member 9
227747_at	MPZL3	myelin protein zero-like 3
207546_at	ATP4B	ATPase, H+/K+ exchanging, beta polypeptide
1555197_a_at	C21orf58	chromosome 21 open reading frame 58
208305_at	PGR	progesterone receptor
236009_at	PERP	PERP, TP53 apoptosis effector
225656_at	EFHC1	EF-hand domain (C-terminal) containing 1
239468_at	MKX	mohawk homeobox
231223_at	CSMD1	CUB and Sushi multiple domains 1
1555007_s_at	WDR66	WD repeat domain 66
229266_at	SHISA6	shisa homolog 6 (Xenopus laevis)
204037_at	LPAR1	lysophosphatidic acid receptor 1
238840_at	LRRFIP1	leucine rich repeat (in FLII) interacting protein 1
235256_s_at	GALM	galactose mutarotase (aldose 1-epimerase)
223572_at	HHATL	hedgehog acyltransferase-like
205406_s_at	SPA17	sperm autoantigenic protein 17
1554545_at	APOBEC4	apolipoprotein B mRNA editing enzyme, catalytic polypeptide-like
242013_at	BCL2L15	BCL2-like 15
209539_at	ARHGEF6	Rac/Cdc42 guanine nucleotide exchange factor (GEF) 6
223753_s_at	CFC1 /// CFC1B	cripto, FRL-1, cryptic family 1 /// cripto, FRL-1, cryptic family 1B
224110_at	PRO1804	uncharacterized LOC100133319
220648_at	ADARB2	adenosine deaminase, RNA-specific, B2
235764_at	PRDM5	PR domain containing 5
232311_at	B2M	Beta-2-microglobulin
209442_x_at	ANK3	ankyrin 3, node of Ranvier (ankyrin G)
209487_at	RBPMS	RNA binding protein with multiple splicing
1554072_s_at	CCDC67	coiled-coil domain containing 67
215239_x_at	ZNF273	zinc finger protein 273
205298_s_at	BTN2A2	butyrophilin, subfamily 2, member A2
220330_s_at	SAMSN1	SAM domain, SH3 domain and nuclear localization signals 1
235672_at	MAP6	microtubule-associated protein 6
205338_s_at	DCT	dopachrome tautomerase (dopachrome delta-isomerase, tyrosine

222520_s_at	IFT57	intraflagellar transport 57 homolog (Chlamydomonas)
244485_at	HLA-DPB1	major histocompatibility complex, class II, DP beta 1
213684_s_at	PDLIM5	PDZ and LIM domain 5
230839_at	PRMT8	protein arginine methyltransferase 8
201525_at	APOD	apolipoprotein D
230744_at	FSTL1	follistatin-like 1
204202_at	IQCE	IQ motif containing E
223706_at	C22orf23	chromosome 22 open reading frame 23
235048_at	FAM169A	family with sequence similarity 169, member A
229941_at	FAM166B	family with sequence similarity 166, member B
1556630_at	CASC2	cancer susceptibility candidate 2 (non-protein coding)
202902_s_at	CTSS	cathepsin S
1565149_at	DYNC2H1	dynein, cytoplasmic 2, heavy chain 1
211696_x_at	HBB	hemoglobin, beta
209655_s_at	TMEM47	transmembrane protein 47
202727_s_at	IFNGR1	interferon gamma receptor 1
206465_at	ACSBG1	acyl-CoA synthetase bubblegum family member 1
203969_at	PEX3	peroxisomal biogenesis factor 3
215342_s_at	RABGAP1L	RAB GTPase activating protein 1-like
206932_at	CH25H	cholesterol 25-hydroxylase
223059_s_at	FAM107B	family with sequence similarity 107, member B
232262_at	PIGL	phosphatidylinositol glycan anchor biosynthesis, class L
1556579_s_at	IGSF10	immunoglobulin superfamily, member 10
236098_at	C17orf110	chromosome 17 open reading frame 110
206194_at	HOXC4	homeobox C4
227337_at	ANKRD37	ankyrin repeat domain 37
1553423_a_at	SLFN13	schlafen family member 13
202157_s_at	CELF2	CUGBP, Elav-like family member 2
229430_at	C8orf46	chromosome 8 open reading frame 46
206335_at	GALNS	galactosamine (N-acetyl)-6-sulfate sulfatase
212486_s_at	FYN	FYN oncogene related to SRC, FGR, YES
210390_s_at	CCL14 /// CCL14-CCL1	chemokine (C-C motif) ligand 14 /// CCL14-CCL15 readthrough ///
209978_s_at	LPA /// PLG	lipoprotein, Lp(a) /// plasminogen
201694_s_at	EGR1	early growth response 1
1556950_s_at	SERPINB6	serpin peptidase inhibitor, clade B (ovalbumin), member 6
230552_at	LOC100134317 /// LO	uncharacterized LOC100134317 /// uncharacterized LOC284412
211776_s_at	EPB41L3	erythrocyte membrane protein band 4.1-like 3
1559496_at	PPA2	pyrophosphatase (inorganic) 2
236029_at	FAT3	FAT tumor suppressor homolog 3 (Drosophila)
232109_at	UBXN10	UBX domain protein 10
203074_at	ANXA8 /// ANXA8L1 //	annexin A8 /// annexin A8-like 1 /// annexin A8-like 2
226653_at	MARK1	MAP/microtubule affinity-regulating kinase 1
236031_x_at	FREM1	FRAS1 related extracellular matrix 1
1552705_at	DUSP19	dual specificity phosphatase 19
223047_at	CMTM6	CKLF-like MARVEL transmembrane domain containing 6
241843_at	EIF5 /// SNORA28	eukaryotic translation initiation factor 5 /// small nucleolar RNA,
219864_s_at	RCAN3	RCAN family member 3

212779_at	KIAA1109	KIAA1109
219736_at	TRIM36	tripartite motif containing 36
231930_at	ELMOD1 /// LOC6439	ELMO/CED-12 domain containing 1 /// uncharacterized LOC6439
210345_s_at	DNAH9	dynein, axonemal, heavy chain 9
204179_at	MB	myoglobin
1562336_at	CASC2	cancer susceptibility candidate 2 (non-protein coding)
205651_x_at	RAPGEF4	Rap guanine nucleotide exchange factor (GEF) 4
231909_x_at	ODF2L	outer dense fiber of sperm tails 2-like
230722_at	BNC2	basonuclin 2
215092_s_at	NFAT5	nuclear factor of activated T-cells 5, tonicity-responsive
223786_at	CHST6	carbohydrate (N-acetylglucosamine 6-O) sulfotransferase 6
209823_x_at	HLA-DQB1 /// LOC100	major histocompatibility complex, class II, DQ beta 1 /// HLA class
239151_at	LOC399753	uncharacterized LOC399753
1564474_at	ZBED3-AS1	ZBED3 antisense RNA 1 (non-protein coding)
205251_at	PER2	period homolog 2 (Drosophila)
220539_at	TTC40	tetratricopeptide repeat domain 40
218694_at	ARMCX1	armadillo repeat containing, X-linked 1
242482_at	PRKAR1A	protein kinase, cAMP-dependent, regulatory, type I, alpha (tissue
225283_at	ARRDC4	arrestin domain containing 4
201496_x_at	MYH11	myosin, heavy chain 11, smooth muscle
238158_at	MEIG1	meiosis expressed gene 1 homolog (mouse)
243649_at	FBXO7	F-box protein 7
218764_at	PRKCH	protein kinase C, eta
221207_s_at	NBEA	neurobeachin
241808_at	ZC2HC1A	zinc finger, C2HC-type containing 1A
201739_at	SGK1	serum/glucocorticoid regulated kinase 1
242344_at	GABRB2	gamma-aminobutyric acid (GABA) A receptor, beta 2
201721_s_at	LAPTM5	lysosomal protein transmembrane 5
1555112_a_at	C1orf114	chromosome 1 open reading frame 114
202018_s_at	LTF	lactotransferrin
216663_s_at	ZMYND10	zinc finger, MYND-type containing 10
205597_at	SLC44A4	solute carrier family 44, member 4
220908_at	CCDC33	coiled-coil domain containing 33
210538_s_at	BIRC3	baculoviral IAP repeat containing 3
205831_at	CD2	CD2 molecule
237755_s_at	WDR16	WD repeat domain 16
231875_at	KIF21A	kinesin family member 21A
241950_at	WWC1	WW and C2 domain containing 1
232731_x_at	LOC100190938	uncharacterized LOC100190938
212651_at	RHOBTB1	Rho-related BTB domain containing 1
234072_at	SEMA4A	sema domain, immunoglobulin domain (Ig), transmembrane dom
227830_at	GABRB3	gamma-aminobutyric acid (GABA) A receptor, beta 3
232461_at	AHI1	Abelson helper integration site 1
228577_x_at	ODF2L	outer dense fiber of sperm tails 2-like
220105_at	RTDR1	rhabdoid tumor deletion region gene 1
213910_at	IGFBP7	insulin-like growth factor binding protein 7
206693_at	IL7	interleukin 7

1556493_a_at	KDM4C	lysine (K)-specific demethylase 4C
236083_at	BCL2L15	BCL2-like 15
1559322_at	LOC727916	uncharacterized LOC727916
36711_at	MAFF	v-maf musculoaponeurotic fibrosarcoma oncogene homolog F (av
241745_at	LOC100507557	uncharacterized LOC100507557
225939_at	EIF4E3	eukaryotic translation initiation factor 4E family member 3
219222_at	RBKS	ribokinase
207624_s_at	RPGR	retinitis pigmentosa GTPase regulator
237690_at	GPR115	G protein-coupled receptor 115
241731_x_at	ZNF440	zinc finger protein 440
1552448_a_at	C8orf12	chromosome 8 open reading frame 12
227098_at	DUSP18	dual specificity phosphatase 18
201693_s_at	EGR1	early growth response 1
204249_s_at	LMO2	LIM domain only 2 (rhombotin-like 1)
221180_at	YSK4	YSK4 Sps1/Ste20-related kinase homolog (S. cerevisiae)
1552950_at	C15orf26	chromosome 15 open reading frame 26
243582_at	SH3RF2	SH3 domain containing ring finger 2
223608_at	EFCAB2	EF-hand calcium binding domain 2
220003_at	LRRC36	leucine rich repeat containing 36
228476_at	KIAA1407	KIAA1407
210650_s_at	PCLO	piccolo (presynaptic cytomatrix protein)
213888_s_at	TRAF3IP3	TRAF3 interacting protein 3
228448_at	MAP6	microtubule-associated protein 6
212441_at	KIAA0232	KIAA0232
209970_x_at	CASP1	caspase 1, apoptosis-related cysteine peptidase
1556378_a_at	LOC440896	uncharacterized LOC440896
216979_at	NR4A3	nuclear receptor subfamily 4, group A, member 3
231026_at	EFHC1	EF-hand domain (C-terminal) containing 1
35974_at	LRMP	lymphoid-restricted membrane protein
205308_at	ZC2HC1A	zinc finger, C2HC-type containing 1A
212291_at	HIPK1	homeodomain interacting protein kinase 1
230561_s_at	KANSL1L	KAT8 regulatory NSL complex subunit 1-like
207789_s_at	DPP6	dipeptidyl-peptidase 6
1557207_s_at	LOC283177	uncharacterized LOC283177
222486_s_at	ADAMTS1	ADAM metallopeptidase with thrombospondin type 1 motif, 1
238778_at	MPP7	membrane protein, palmitoylated 7 (MAGUK p55 subfamily mem
1552384_a_at	FAM71A	family with sequence similarity 71, member A
220769_s_at	WDR78	WD repeat domain 78
1559756_at	DKFZp667F0711	uncharacterized protein DKFZp667F0711
228642_at	HOTAIRM1	HOXA transcript antisense RNA, myeloid-specific 1 (non-protein c
217671_at	DSERG1	Down syndrome encephalopathy related protein 1
205650_s_at	FGA	fibrinogen alpha chain
205366_s_at	HOXB6	homeobox B6
216356_x_at	BAIAP3	BAI1-associated protein 3
217995_at	SQRDL	sulfide quinone reductase-like (yeast)
232639_at	C3orf25	chromosome 3 open reading frame 25
221185_s_at	IQCG	IQ motif containing G

219777_at	GIMAP6	GTPase, IMAP family member 6
210839_s_at	ENPP2	ectonucleotide pyrophosphatase/phosphodiesterase 2
206363_at	MAF	v-maf musculoaponeurotic fibrosarcoma oncogene homolog (avia
1554980_a_at	ATF3	activating transcription factor 3
218584_at	TCTN1	tectonic family member 1
204057_at	IRF8	interferon regulatory factor 8
1557570_a_at	LOC285084	uncharacterized LOC285084
219563_at	LINC00341	long intergenic non-protein coding RNA 341
219584_at	PLA1A	phospholipase A1 member A
207797_s_at	LRP2BP	LRP2 binding protein
204703_at	IFT88	intraflagellar transport 88 homolog (Chlamydomonas)
1555564_a_at	CFI	complement factor I
220088_at	C5AR1	complement component 5a receptor 1
220271_x_at	EFCAB6	EF-hand calcium binding domain 6
219597_s_at	DUOX1	dual oxidase 1
223611_s_at	LNX1	ligand of numb-protein X 1, E3 ubiquitin protein ligase
238326_at	ODF3B	outer dense fiber of sperm tails 3B
204731_at	TGFBR3	transforming growth factor, beta receptor III
221290_s_at	MUM1	melanoma associated antigen (mutated) 1
230763_at	SPATA17	spermatogenesis associated 17
206974_at	CXCR6	chemokine (C-X-C motif) receptor 6
223731_at	MYCBPAP	MYCBP associated protein
226066_at	MITF	microphthalmia-associated transcription factor
213006_at	CEBPD	CCAAT/enhancer binding protein (C/EBP), delta
242268_at	CELF2	CUGBP, Elav-like family member 2
209616_s_at	CES1 /// LOC10065305	carboxylesterase 1 /// liver carboxylesterase 1-like
1564238_a_at	WDR49	WD repeat domain 49
226553_at	TMPRSS2	transmembrane protease, serine 2
205302_at	IGFBP1	insulin-like growth factor binding protein 1
230261_at	ST8SIA4	ST8 alpha-N-acetyl-neuraminide alpha-2,8-sialyltransferase 4
1553630_at	C10orf107	chromosome 10 open reading frame 107
236674_at	LOC388780	uncharacterized LOC388780
223940_x_at	LOC100507645 /// MA	uncharacterized LOC100507645 /// metastasis associated lung ad
217752_s_at	CNDP2	CNDP dipeptidase 2 (metallopeptidase M20 family)
212331_at	RBL2	retinoblastoma-like 2 (p130)
1559584_a_at	C16orf54	chromosome 16 open reading frame 54
223882_at	FAM172A	family with sequence similarity 172, member A
241495_at	CCNL1	cyclin L1
224021_at	RP1	retinitis pigmentosa 1 (autosomal dominant)
242979_at	IRS1	insulin receptor substrate 1
213784_at	IFT27	intraflagellar transport 27 homolog (Chlamydomonas)
225557_at	CSRNP1	cysteine-serine-rich nuclear protein 1
214734_at	EXPH5	exophilin 5
240033_at	PLG	plasminogen
236965_at	UBQLNL	ubiquilin-like
213186_at	DZIP3	DAZ interacting protein 3, zinc finger
231029_at	F5	coagulation factor V (proaccelerin, labile factor)

233057_at	HSPB8	heat shock 22kDa protein 8
221491_x_at	HLA-DRB1 /// HLA-DR	major histocompatibility complex, class II, DR beta 1 /// major hist
231081_at	C2orf73	chromosome 2 open reading frame 73
230903_s_at	C8orf42	chromosome 8 open reading frame 42
214211_at	FTH1	ferritin, heavy polypeptide 1
228850_s_at	SLIT2	slit homolog 2 (Drosophila)
228316_at	C2orf63	chromosome 2 open reading frame 63
205011_at	VWA5A	von Willebrand factor A domain containing 5A
238909_at	S100A10	S100 calcium binding protein A10
242661_x_at	ALS2CR12	amyotrophic lateral sclerosis 2 (juvenile) chromosome region, can
213998_s_at	DDX17	DEAD (Asp-Glu-Ala-Asp) box helicase 17
235352_at	MR1	major histocompatibility complex, class I-related
227250_at	KREMEN1	kringle containing transmembrane protein 1
228496_s_at	CRIM1	Cysteine rich transmembrane BMP regulator 1 (chordin-like)
1557432_at	RASAL2	RAS protein activator like 2
205568_at	AQP9	aquaporin 9
1566079_at	RPS16P5	ribosomal protein S16 pseudogene 5
236166_at	LOC285147	uncharacterized LOC285147
214043_at	PTPRD	protein tyrosine phosphatase, receptor type, D
215133_s_at	FAM153A /// FAM153	family with sequence similarity 153, member A /// family with se
229953_x_at	LCA5	Leber congenital amaurosis 5
211795_s_at	FYB	FYN binding protein
213142_x_at	PION	pigeon homolog (Drosophila)
209821_at	IL33	interleukin 33
229378_at	STOX1	storkhead box 1
227265_at	FGL2	fibrinogen-like 2
238900_at	HLA-DRB1 /// HLA-DR	major histocompatibility complex, class II, DR beta 1 /// major hist
209194_at	CETN2	centrin, EF-hand protein, 2
204749_at	NAP1L3	nucleosome assembly protein 1-like 3
227210_at	SFMBT2	Scm-like with four mbt domains 2
237328_at	C14orf105	chromosome 14 open reading frame 105
214748_at	N4BP2L2	NEDD4 binding protein 2-like 2
239458_at	ALS2CR12	amyotrophic lateral sclerosis 2 (juvenile) chromosome region, can
204783_at	MLF1	myeloid leukemia factor 1
228461_at	SH3RF3	SH3 domain containing ring finger 3
1553674_at	LRRIQ3	leucine-rich repeats and IQ motif containing 3
1557261_at	WHAMMP2 /// WHAM	WAS protein homolog associated with actin, golgi membranes an
238494_at	TRAF3IP1	TNF receptor-associated factor 3 interacting protein 1
212192_at	KCTD12	potassium channel tetramerisation domain containing 12
220141_at	C11orf63	chromosome 11 open reading frame 63
229254_at	MFSD4	major facilitator superfamily domain containing 4
203881_s_at	DMD	dystrophin
213954_at	FAM169A	family with sequence similarity 169, member A
204686_at	IRS1	insulin receptor substrate 1
242586_at	FSD1L	fibronectin type III and SPRY domain containing 1-like
217623_at	MYLK3	myosin light chain kinase 3
226226_at	TMEM45B	transmembrane protein 45B

230496_at	FAM123A	family with sequence similarity 123A
201843_s_at	EFEMP1	EGF containing fibulin-like extracellular matrix protein 1
242086_at	SPATA6	spermatogenesis associated 6
237285_at	SORBS2	sorbin and SH3 domain containing 2
219182_at	TMEM231	transmembrane protein 231
1563475_s_at	METTL20	methyltransferase like 20
236981_at	C17orf99	chromosome 17 open reading frame 99
219197_s_at	SCUBE2	signal peptide, CUB domain, EGF-like 2
1553765_a_at	KLHL32	kelch-like 32 (Drosophila)
235298_at	WDR27	WD repeat domain 27
1564093_at	NEK1	NIMA (never in mitosis gene a)-related kinase 1
204759_at	RCBTB2	regulator of chromosome condensation (RCC1) and BTB (POZ) dor
1556608_a_at	EHD4	EH-domain containing 4
219578_s_at	CPEB1	cytoplasmic polyadenylation element binding protein 1
238447_at	RBMS3	RNA binding motif, single stranded interacting protein 3
1560119_at	LOC389634	uncharacterized LOC389634
236175_at	TRIM55	tripartite motif containing 55
214633_at	SOX3	SRY (sex determining region Y)-box 3
209897_s_at	SLIT2	slit homolog 2 (Drosophila)
244710_at	LRGUK	leucine-rich repeats and guanylate kinase domain containing
220244_at	LINC00312	long intergenic non-protein coding RNA 312
207961_x_at	MYH11	myosin, heavy chain 11, smooth muscle
232366_at	KIAA0232	KIAA0232
239870_at	SPATS1 /// TMEM151I	spermatogenesis associated, serine-rich 1 /// transmembrane pro
236325_at	KIAA1377	KIAA1377
206076_at	LRRC23	leucine rich repeat containing 23
203518_at	LYST	lysosomal trafficking regulator
210800_at	TIMM8A	translocase of inner mitochondrial membrane 8 homolog A (yeast
208078_s_at	SIK1	salt-inducible kinase 1
1561200_at	VWA3B	von Willebrand factor A domain containing 3B
201328_at	ETS2	v-ets erythroblastosis virus E26 oncogene homolog 2 (avian)
220252_x_at	CXorf21	chromosome X open reading frame 21
201301_s_at	ANXA4	annexin A4
1556477_a_at	LOC283485	uncharacterized LOC283485
231549_at	C1orf158	chromosome 1 open reading frame 158
205529_s_at	RUNX1T1	runt-related transcription factor 1; translocated to, 1 (cyclin D-rela
225502_at	DOCK8	dedicator of cytokinesis 8
242345_at	COL28A1	collagen, type XXVIII, alpha 1
201466_s_at	JUN	jun proto-oncogene
210222_s_at	RTN1	reticulon 1
220072_at	CSPP1	centrosome and spindle pole associated protein 1
1568924_a_at	IQUB	IQ motif and ubiquitin domain containing
211143_x_at	NR4A1	nuclear receptor subfamily 4, group A, member 1
241368_at	PLIN5	perilipin 5
203758_at	CTSO	cathepsin O
203474_at	IQGAP2	IQ motif containing GTPase activating protein 2
202587_s_at	AK1	adenylate kinase 1

207231_at	DZIP3	DAZ interacting protein 3, zinc finger
240282_at	WDR1	WD repeat domain 1
205948_at	PTPRT	protein tyrosine phosphatase, receptor type, T
222253_s_at	POM121L9P	POM121 transmembrane nucleoporin-like 9, pseudogene
227081_at	DNALI1	dynein, axonemal, light intermediate chain 1
243896_at	WDR96	WD repeat domain 96
233971_at	FAM166A	family with sequence similarity 166, member A
243758_at	CCDC37	coiled-coil domain containing 37
206938_at	SRD5A2	steroid-5-alpha-reductase, alpha polypeptide 2 (3-oxo-5 alpha-ste
226856_at	MUSTN1 /// TMEM11	musculoskeletal, embryonic nuclear protein 1 /// TMEM110-MUS
237585_at	C4orf47	chromosome 4 open reading frame 47
242907_at	GBP2	guanylate binding protein 2, interferon-inducible
225344_at	NCOA7	nuclear receptor coactivator 7
214192_at	NUP88	nucleoporin 88kDa
205476_at	CCL20	chemokine (C-C motif) ligand 20
222150_s_at	PION	pigeon homolog (Drosophila)
228600_x_at	FAM221A	family with sequence similarity 221, member A
201473_at	JUNB	jun B proto-oncogene
227690_at	GABRB3	gamma-aminobutyric acid (GABA) A receptor, beta 3
213922_at	TTBK2	tau tubulin kinase 2
206526_at	RIBC2	RIB43A domain with coiled-coils 2
213934_s_at	ZNF23	zinc finger protein 23 (KOX 16)
228056_s_at	NAPSB	napsin B aspartic peptidase pseudogene
240898_at	SPAG16	sperm associated antigen 16
57540_at	RBKS	ribokinase
206115_at	EGR3	early growth response 3
203543_s_at	KLF9	Kruppel-like factor 9
219049_at	CSGALNACT1	chondroitin sulfate N-acetylgalactosaminyltransferase 1
214811_at	RIMBP2	RIMS binding protein 2
242036_x_at	ATP2B3	ATPase, Ca++ transporting, plasma membrane 3
200904_at	HLA-E	major histocompatibility complex, class I, E
230142_s_at	CIRBP	cold inducible RNA binding protein
236519_at	C9orf135	chromosome 9 open reading frame 135
207075_at	NLRP3	NLR family, pyrin domain containing 3
238127_at	GAS6-AS1	GAS6 antisense RNA 1 (non-protein coding)
232777_s_at	C6orf118	chromosome 6 open reading frame 118
238430_x_at	SLFN5	schlafen family member 5
231043_at	PCDP1	primary ciliary dyskinesia protein 1
239043_at	ZNF404	zinc finger protein 404
205528_s_at	RUNX1T1	runt-related transcription factor 1; translocated to, 1 (cyclin D-rela
206811_at	ADCY8	adenylate cyclase 8 (brain)
210032_s_at	SPAG6	sperm associated antigen 6
40284_at	FOXA2	forkhead box A2
218687_s_at	MUC13	mucin 13, cell surface associated
209116_x_at	HBB	hemoglobin, beta
221524_s_at	RRAGD	Ras-related GTP binding D
1559333_at	SRGAP3-AS2	SRGAP3 antisense RNA 2 (non-protein coding)

211200_s_at	EFCAB2	EF-hand calcium binding domain 2
239785_at	DZIP1L	DAZ interacting protein 1-like
1553684_at	PPIL6	peptidylprolyl isomerase (cyclophilin)-like 6
225328_at	FBXO32	F-box protein 32
209619_at	CD74	CD74 molecule, major histocompatibility complex, class II invarian
205068_s_at	ARHGAP26	Rho GTPase activating protein 26
220344_at	C11orf16	chromosome 11 open reading frame 16
204863_s_at	IL6ST	interleukin 6 signal transducer (gp130, oncostatin M receptor)
209921_at	SLC7A11	solute carrier family 7 (anionic amino acid transporter light chain,
229369_at	VSIG2	V-set and immunoglobulin domain containing 2
236421_at	ANKRD45	ankyrin repeat domain 45
231073_at	C1orf168	chromosome 1 open reading frame 168
222904_s_at	TMC5	transmembrane channel-like 5
220293_at	CATSPERB	catsper channel auxiliary subunit beta
1561096_at	LOC285419	uncharacterized LOC285419
224400_s_at	CHST9	carbohydrate (N-acetylgalactosamine 4-0) sulfotransferase 9
204002_s_at	ICA1	islet cell autoantigen 1, 69kDa
205860_x_at	FOLH1 /// FOLH1B	folate hydrolase (prostate-specific membrane antigen) 1 /// folate
1555246_a_at	SCN1A	sodium channel, voltage-gated, type I, alpha subunit
222314_x_at	EGOT	eosinophil granule ontogeny transcript (non-protein coding)
220581_at	CCDC170	coiled-coil domain containing 170
242807_at	FSD1L	fibronectin type III and SPRY domain containing 1-like
207072_at	IL18RAP	interleukin 18 receptor accessory protein
1556666_a_at	LOC100652860 /// LO	tetratricopeptide repeat protein 6-like /// tetratricopeptide repea
209966_x_at	ESRRG	estrogen-related receptor gamma
228969_at	AGR2	anterior gradient 2 homolog (Xenopus laevis)
222220_s_at	TSNAXIP1	translin-associated factor X interacting protein 1
240830_at	SCARNA17	small Cajal body-specific RNA 17
1552325_at	CCDC11	coiled-coil domain containing 11
211471_s_at	RAB36	RAB36, member RAS oncogene family
221886_at	DENND2A	DENN/MADD domain containing 2A
205488_at	GZMA	granzyme A (granzyme 1, cytotoxic T-lymphocyte-associated serin
225516_at	SLC7A2	solute carrier family 7 (cationic amino acid transporter, y+ system
243352_at	ALPK1	alpha-kinase 1
238581_at	GBP5	guanylate binding protein 5
203675_at	NUCB2	nucleobindin 2
202341_s_at	TRIM2	tripartite motif containing 2
205518_s_at	CMAHP	cytidine monophospho-N-acetylneuraminic acid hydroxylase, pseu
1560396_at	KLHL6	kelch-like 6 (Drosophila)
230180_at	DDX17	DEAD (Asp-Glu-Ala-Asp) box helicase 17
205016_at	TGFA	transforming growth factor, alpha
219583_s_at	SPATA7	spermatogenesis associated 7
232027_at	SYNE1	spectrin repeat containing, nuclear envelope 1
211105_s_at	NFATC1	nuclear factor of activated T-cells, cytoplasmic, calcineurin-depen
213217_at	ADCY2	adenylate cyclase 2 (brain)
225061_at	DNAJA4	DnaJ (Hsp40) homolog, subfamily A, member 4
200811_at	CIRBP	cold inducible RNA binding protein

211654_x_at	HLA-DQB1	major histocompatibility complex, class II, DQ beta 1
205101_at	CIITA	class II, major histocompatibility complex, transactivator
226187_at	CDS1	CDP-diacylglycerol synthase (phosphatidate cytidylyltransferase)
1557718_at	PPP2R5C	protein phosphatase 2, regulatory subunit B', gamma
1560426_at	C12orf55 /// C12orf63	chromosome 12 open reading frame 55 /// chromosome 12 open
205821_at	KLRC4-KLRK1 /// KLRK	KLRC4-KLRK1 readthrough /// killer cell lectin-like receptor subfan
230931_at	PLG	plasminogen
220084_at	C14orf105	chromosome 14 open reading frame 105
229724_at	GABRB3	gamma-aminobutyric acid (GABA) A receptor, beta 3
210943_s_at	LYST	lysosomal trafficking regulator
227865_at	IDNK	idnK, gluconokinase homolog (E. coli)
227438_at	ALPK1	alpha-kinase 1
227727_at	MRGPRF	MAS-related GPR, member F
204363_at	F3	coagulation factor III (thromboplastin, tissue factor)
202036_s_at	SFRP1	secreted frizzled-related protein 1
215692_s_at	MPPED2	metallophosphoesterase domain containing 2
207584_at	LPA	lipoprotein, Lp(a)
206552_s_at	TAC1	tachykinin, precursor 1
229723_at	TAGAP	T-cell activation RhoGTPase activating protein
1553159_at	DNAH11	dynein, axonemal, heavy chain 11
205399_at	DCLK1	doublecortin-like kinase 1
216920_s_at	TARP /// TRGC2	TCR gamma alternate reading frame protein /// T cell receptor gar
202191_s_at	GAS7	growth arrest-specific 7
1570289_at	LOC646736	uncharacterized LOC646736
203896_s_at	PLCB4	phospholipase C, beta 4
206169_x_at	ZC3H7B	zinc finger CCCH-type containing 7B
1555993_at	CACNA1D	calcium channel, voltage-dependent, L type, alpha 1D subunit
204813_at	MAPK10	mitogen-activated protein kinase 10
221523_s_at	RRAGD	Ras-related GTP binding D
1552825_at	ZNF396	zinc finger protein 396
222336_at	C4orf34	chromosome 4 open reading frame 34
235350_at	C4orf19	chromosome 4 open reading frame 19
213451_x_at	TNXA /// TNXB	tenascin XA (pseudogene) /// tenascin XB
242162_at	WDR69	WD repeat domain 69
242814_at	SERPINB9	serpin peptidase inhibitor, clade B (ovalbumin), member 9
1569652_at	MLLT3	myeloid/lymphoid or mixed-lineage leukemia (trithorax homolog,
228071_at	GIMAP7	GTPase, IMAP family member 7
211656_x_at	HLA-DQB1 /// LOC100	major histocompatibility complex, class II, DQ beta 1 /// HLA class
1562255_at	SYTL3	synaptotagmin-like 3
203996_s_at	C21orf2	chromosome 21 open reading frame 2
206011_at	CASP1	caspase 1, apoptosis-related cysteine peptidase
209785_s_at	PLA2G4C	phospholipase A2, group IVC (cytosolic, calcium-independent)
1559413_at	TCP11L2	t-complex 11 (mouse)-like 2
204103_at	CCL4	chemokine (C-C motif) ligand 4
214696_at	MIR22 /// MIR22HG	microRNA 22 /// MIR22 host gene (non-protein coding)
223504_at	DNAJC27	DnaJ (Hsp40) homolog, subfamily C, member 27
242916_at	CNTRL	centriolin

228903_at	CES4A	carboxylesterase 4A
212249_at	PIK3R1	phosphoinositide-3-kinase, regulatory subunit 1 (alpha)
229740_at	C17orf109	chromosome 17 open reading frame 109
220361_at	IQCH	IQ motif containing H
220102_at	FOXL2	forkhead box L2
206721_at	C1orf114	chromosome 1 open reading frame 114
213988_s_at	SAT1	spermidine/spermine N1-acetyltransferase 1
227148_at	PLEKHH2	pleckstrin homology domain containing, family H (with MyTH4 do
215078_at	LOC100129518 /// SO	uncharacterized LOC100129518 /// superoxide dismutase 2, mito
207330_at	PZP	pregnancy-zone protein
206496_at	FMO3	flavin containing monooxygenase 3
205902_at	KCNN3	potassium intermediate/small conductance calcium-activated cha
203973_s_at	CEBPD	CCAAT/enhancer binding protein (C/EBP), delta
201952_at	ALCAM	activated leukocyte cell adhesion molecule
211006_s_at	KCNB1	potassium voltage-gated channel, Shab-related subfamily, membe
206417_at	CNGA1	cyclic nucleotide gated channel alpha 1
222549_at	CLDN1	claudin 1
203868_s_at	VCAM1	vascular cell adhesion molecule 1
213802_at	PRSS12	protease, serine, 12 (neurotrypsin, motopsin)
206785_s_at	KLRC1 /// KLRC2	killer cell lectin-like receptor subfamily C, member 1 /// killer cell
230359_at	KNDC1	kinase non-catalytic C-lobe domain (KIND) containing 1
206374_at	DUSP8	dual specificity phosphatase 8
213568_at	OSR2	odd-skipped related 2 (Drosophila)
224590_at	XIST	X (inactive)-specific transcript (non-protein coding)
204440_at	CD83	CD83 molecule
221874_at	KIAA1324	KIAA1324
1554988_at	SLC9C2	solute carrier family 9, member C2 (putative)
206325_at	SERPINA6	serpin peptidase inhibitor, clade A (alpha-1 antiproteinase, antitry
206541_at	KLKB1	kallikrein B, plasma (Fletcher factor) 1
228097_at	MYLIP	myosin regulatory light chain interacting protein
209304_x_at	GADD45B	growth arrest and DNA-damage-inducible, beta
235946_at	RIBC1	RIB43A domain with coiled-coils 1
234732_s_at	EFCAB6	EF-hand calcium binding domain 6
227359_at	OSCP1	organic solute carrier partner 1
239213_at	SERPINB1	serpin peptidase inhibitor, clade B (ovalbumin), member 1
215363_x_at	FOLH1 /// FOLH1B	folate hydrolase (prostate-specific membrane antigen) 1 /// folate
205922_at	VNN2	vanin 2
224568_x_at	LOC100507645 /// MA	uncharacterized LOC100507645 /// metastasis associated lung ad
1553605_a_at	ABCA13	ATP-binding cassette, sub-family A (ABC1), member 13
209687_at	CXCL12	chemokine (C-X-C motif) ligand 12
244144_at	SYNE1	spectrin repeat containing, nuclear envelope 1
1555298_a_at	VWA3B	von Willebrand factor A domain containing 3B
235649_at	ADAMTS8	ADAM metallopeptidase with thrombospondin type 1 motif, 8
229530_at	GUCY1A3	guanylate cyclase 1, soluble, alpha 3
224215_s_at	DLL1	delta-like 1 (Drosophila)
228128_x_at	PAPPA	pregnancy-associated plasma protein A, pappalysin 1
223794_at	ARMC4	armadillo repeat containing 4

213900_at	FAM189A2	family with sequence similarity 189, member A2
219290_x_at	DAPP1	dual adaptor of phosphotyrosine and 3-phosphoinositides
235638_at	RASSF6	Ras association (RalGDS/AF-6) domain family member 6
228882_at	TUB	tubby homolog (mouse)
221834_at	LOC100507577 /// LO	uncharacterized LOC100507577 /// lon peptidase 2, peroxisomal
1566480_x_at	C17orf104	Chromosome 17 open reading frame 104
244401_at	LCA5	Leber congenital amaurosis 5
239123_at	TSC22D1	TSC22 domain family, member 1
228532_at	C1orf162	chromosome 1 open reading frame 162
241359_at	TLCD2	TLC domain containing 2
213537_at	HLA-DPA1	major histocompatibility complex, class II, DP alpha 1
219396_s_at	MIR631 /// NEIL1	microRNA 631 /// nei endonuclease VIII-like 1 (E. coli)
209879_at	SELPLG	selectin P ligand
215266_at	DNAH3	dynein, axonemal, heavy chain 3
201162_at	IGFBP7	insulin-like growth factor binding protein 7
213397_x_at	RNASE4	ribonuclease, RNase A family, 4
219014_at	PLAC8	placenta-specific 8
206093_x_at	TNXA /// TNXB	tenascin XA (pseudogene) /// tenascin XB
1562743_at	ZNF33B	zinc finger protein 33B
206710_s_at	EPB41L3	erythrocyte membrane protein band 4.1-like 3
236710_at	C1orf87	chromosome 1 open reading frame 87
1558792_x_at	AP2A1	Adaptor-related protein complex 2, alpha 1 subunit
243087_at	WDR63	WD repeat domain 63
230924_at	TTLL6	tubulin tyrosine ligase-like family, member 6
205383_s_at	ZBTB20	zinc finger and BTB domain containing 20
242290_at	TACC1	transforming, acidic coiled-coil containing protein 1
230378_at	SCGB3A1	secretoglobin, family 3A, member 1
230391_at	CD84	CD84 molecule
207808_s_at	PROS1	protein S (alpha)
237227_at	NEK10	NIMA (never in mitosis gene a)- related kinase 10
215322_at	LONRF1	LON peptidase N-terminal domain and ring finger 1
229233_at	NRG3	neuregulin 3
209447_at	SYNE1	spectrin repeat containing, nuclear envelope 1
1559400_s_at	PAPPA	pregnancy-associated plasma protein A, pappalysin 1
236331_at	CDKL2	cyclin-dependent kinase-like 2 (CDC2-related kinase)
1553183_at	UMODL1	uromodulin-like 1
218532_s_at	FAM134B	family with sequence similarity 134, member B
213309_at	PLCL2	phospholipase C-like 2
241193_at	ETS2	V-ets erythroblastosis virus E26 oncogene homolog 2 (avian)
1552321_a_at	CCDC65	coiled-coil domain containing 65
204487_s_at	KCNQ1	potassium voltage-gated channel, KQT-like subfamily, member 1
206017_at	KIAA0319	KIAA0319
219687_at	HHAT	hedgehog acyltransferase
229041_s_at	LOC100505746	uncharacterized LOC100505746
203924_at	GSTA1	glutathione S-transferase alpha 1
237719_x_at	RGS7BP	regulator of G-protein signaling 7 binding protein
223737_x_at	CHST9	carbohydrate (N-acetylgalactosamine 4-0) sulfotransferase 9

226917_s_at	ANAPC4	anaphase promoting complex subunit 4
216333_x_at	TNXA /// TNXB	tenascin XA (pseudogene) /// tenascin XB
227346_at	IKZF1	IKAROS family zinc finger 1 (Ikaros)
204894_s_at	AOC3	amine oxidase, copper containing 3 (vascular adhesion protein 1)
64900_at	TMEM231	transmembrane protein 231
216119_s_at	SPEF1	sperm flagellar 1
1552296_at	BEST4	bestrophin 4
221698_s_at	CLEC7A	C-type lectin domain family 7, member A
206483_at	LRRC6	leucine rich repeat containing 6
206101_at	ECM2	extracellular matrix protein 2, female organ and adipocyte specifi
211621_at	AR	androgen receptor
204655_at	CCL5	chemokine (C-C motif) ligand 5
1554919_s_at	C7orf63	chromosome 7 open reading frame 63
239336_at	THBS1	thrombospondin 1
213185_at	KIAA0556	KIAA0556
230287_at	SGSM1	small G protein signaling modulator 1
231728_at	CAPS	calcyphosine
223732_at	SLC23A1	solute carrier family 23 (nucleobase transporters), member 1
217362_x_at	HLA-DRB6	major histocompatibility complex, class II, DR beta 6 (pseudogene
238423_at	SYTL3	synaptotagmin-like 3
209606_at	CYTIP	cytohesin 1 interacting protein
243868_at	RFX3	regulatory factor X, 3 (influences HLA class II expression)
226872_at	RFX2	regulatory factor X, 2 (influences HLA class II expression)
232617_at	CTSS	cathepsin S
224916_at	TMEM173	transmembrane protein 173
219371_s_at	KLF2	Kruppel-like factor 2 (lung)
233312_at	ROPN1L	rhophilin associated tail protein 1-like
209114_at	TSPAN1	tetraspanin 1
219734_at	SIDT1	SID1 transmembrane family, member 1
219455_at	C7orf63	chromosome 7 open reading frame 63
215418_at	PARVA	parvin, alpha
1405_i_at	CCL5	chemokine (C-C motif) ligand 5
234476_at	DNAH7	dynein, axonemal, heavy chain 7
1552957_at	DNAH6	dynein, axonemal, heavy chain 6
202158_s_at	CELF2	CUGBP, Elav-like family member 2
243334_at	CACNA1D	calcium channel, voltage-dependent, L type, alpha 1D subunit
209173_at	AGR2	anterior gradient 2 homolog (Xenopus laevis)
1553789_a_at	C21orf58	chromosome 21 open reading frame 58
237238_at	WWC1	WW and C2 domain containing 1
225941_at	EIF4E3	eukaryotic translation initiation factor 4E family member 3
205114_s_at	CCL3 /// CCL3L1 /// CC	chemokine (C-C motif) ligand 3 /// chemokine (C-C motif) ligand 3
1560397_s_at	KLHL6	kelch-like 6 (Drosophila)
242342_at	GUCY1A2	guanylate cyclase 1, soluble, alpha 2
238763_at	RBM20	RNA binding motif protein 20
1568906_at	LOC728196	uncharacterized LOC728196
237251_at	LRRC71	leucine rich repeat containing 71
242286_at	GRIN2A	glutamate receptor, ionotropic, N-methyl D-aspartate 2A

205890_s_at	GABBR1 /// UBD	gamma-aminobutyric acid (GABA) B receptor, 1 /// ubiquitin D
211726_s_at	FMO2	flavin containing monooxygenase 2 (non-functional)
222102_at	GSTA3	glutathione S-transferase alpha 3
228086_at	STK33	serine/threonine kinase 33
210136_at	MBP	myelin basic protein
228111_s_at	DNAH1	dynein, axonemal, heavy chain 1
220173_at	C14orf45	chromosome 14 open reading frame 45
213385_at	CHN2	chimerin (chimaerin) 2
222858_s_at	DAPP1	dual adaptor of phosphotyrosine and 3-phosphoinositides
220308_at	CCDC19	coiled-coil domain containing 19
207651_at	GPR171	G protein-coupled receptor 171
243495_s_at	ZNF652	Zinc finger protein 652
230807_at	CCDC151	coiled-coil domain containing 151
211896_s_at	DCN	decorin
226218_at	IL7R	interleukin 7 receptor
233463_at	RASSF6	Ras association (RalGDS/AF-6) domain family member 6
206043_s_at	ATP2C2	ATPase, Ca++ transporting, type 2C, member 2
220475_at	SLC28A3	solute carrier family 28 (sodium-coupled nucleoside transporter),
219508_at	GCNT3	glucosaminyl (N-acetyl) transferase 3, mucin type
226248_s_at	KIAA1324	KIAA1324
232099_at	PCDHB16	protocadherin beta 16
228885_at	MAMDC2	MAM domain containing 2
219106_s_at	KBTBD10	kelch repeat and BTB (POZ) domain containing 10
219147_s_at	NMRK1	nicotinamide riboside kinase 1
220064_at	LOC100506124 /// TT	uncharacterized LOC100506124 /// tetratricopeptide repeat doma
223343_at	MS4A7	membrane-spanning 4-domains, subfamily A, member 7
226878_at	HLA-DOA	major histocompatibility complex, class II, DO alpha
205896_at	SLC22A4	solute carrier family 22 (organic cation/ergothioneine transporter
1562815_at	EFCAB6	EF-hand calcium binding domain 6
1568377_x_at	DEFB124	defensin, beta 124
222943_at	GBA3	glucosidase, beta, acid 3 (cytosolic)
203542_s_at	KLF9	Kruppel-like factor 9
1553729_s_at	LRRC43	leucine rich repeat containing 43
223636_at	ZMYND12	zinc finger, MYND-type containing 12
201951_at	ALCAM	activated leukocyte cell adhesion molecule
225299_at	MYO5B	myosin VB
1563814_at	C2orf50	chromosome 2 open reading frame 50
1557417_s_at	RSPH10B /// RSPH10B	radial spoke head 10 homolog B (Chlamydomonas) /// radial spok
205656_at	PCDH17	protocadherin 17
213464_at	SHC2	SHC (Src homology 2 domain containing) transforming protein 2
214798_at	ATP2C2	ATPase, Ca++ transporting, type 2C, member 2
228943_at	MAP6	microtubule-associated protein 6
1553133_at	C9orf72	chromosome 9 open reading frame 72
202376_at	SERPINA3	serpin peptidase inhibitor, clade A (alpha-1 antiproteinase, antitry
229245_at	PLEKHA6	pleckstrin homology domain containing, family A member 6
230033_at	DNAAF3	dynein, axonemal, assembly factor 3
220528_at	VNN3	vanin 3

233198_at	GOLGA2P5	golgin A2 pseudogene 5
237439_at	USP43	ubiquitin specific peptidase 43
224941_at	PAPPA	pregnancy-associated plasma protein A, pappalysin 1
219857_at	PLEKHS1	pleckstrin homology domain containing, family S member 1
210592_s_at	SAT1	spermidine/spermine N1-acetyltransferase 1
205654_at	C4BPA	complement component 4 binding protein, alpha
234974_at	GALM	galactose mutarotase (aldose 1-epimerase)
225207_at	PDK4	pyruvate dehydrogenase kinase, isozyme 4
227775_at	CELF6	CUGBP, Elav-like family member 6
236407_at	KCNE1	potassium voltage-gated channel, Isk-related family, member 1
227474_at	LOC654433	uncharacterized LOC654433
1560147_at	WDR86-AS1	WDR86 antisense RNA 1 (non-protein coding)
212451_at	SECISBP2L	SECIS binding protein 2-like
227226_at	MRAP2	melanocortin 2 receptor accessory protein 2
230499_at	BIRC3	baculoviral IAP repeat containing 3
238720_at	LOC100506582	uncharacterized LOC100506582
201743_at	CD14	CD14 molecule
1552540_s_at	IQCD	IQ motif containing D
237363_at	SPATA6L	spermatogenesis associated 6-like
214735_at	IPCEF1	interaction protein for cytohesin exchange factors 1
212188_at	KCTD12	potassium channel tetramerisation domain containing 12
202643_s_at	TNFAIP3	tumor necrosis factor, alpha-induced protein 3
227812_at	TNFRSF19	tumor necrosis factor receptor superfamily, member 19
201497_x_at	MYH11	myosin, heavy chain 11, smooth muscle
220724_at	CWH43	cell wall biogenesis 43 C-terminal homolog (S. cerevisiae)
231149_s_at	ULK4	unc-51-like kinase 4 (C. elegans)
205945_at	IL6R	interleukin 6 receptor
201289_at	CYR61	cysteine-rich, angiogenic inducer, 61
235308_at	ZBTB20	zinc finger and BTB domain containing 20
228946_at	INTU	inturned planar cell polarity effector homolog (Drosophila)
205714_s_at	ZMYND10	zinc finger, MYND-type containing 10
212327_at	LIMCH1	LIM and calponin homology domains 1
205044_at	GABRP	gamma-aminobutyric acid (GABA) A receptor, pi
230828_at	GRAMD2	GRAM domain containing 2
202435_s_at	CYP1B1	cytochrome P450, family 1, subfamily B, polypeptide 1
1564160_at	DTHD1	death domain containing 1
238721_at	MDH1B	malate dehydrogenase 1B, NAD (soluble)
236293_at	RHOH	ras homolog family member H
230451_at	LOC100506974	uncharacterized LOC100506974
242287_at	CLIP1	CAP-GLY domain containing linker protein 1
228221_at	SLC44A3	solute carrier family 44, member 3
235213_at	ITPKB	Inositol-trisphosphate 3-kinase B
232449_at	BCO2	beta-carotene oxygenase 2
207992_s_at	AMPD3	adenosine monophosphate deaminase 3
226822_at	STOX2	storkhead box 2
226690_at	ADCYAP1R1	adenylate cyclase activating polypeptide 1 (pituitary) receptor typ
230505_at	LOC145474	uncharacterized LOC145474

232972_at	C17orf72	chromosome 17 open reading frame 72
220920_at	ATP10B	ATPase, class V, type 10B
224209_s_at	GDA	guanine deaminase
205898_at	CX3CR1	chemokine (C-X3-C motif) receptor 1
205288_at	CDC14A	CDC14 cell division cycle 14 homolog A (S. cerevisiae)
214261_s_at	ADH6	alcohol dehydrogenase 6 (class V)
229849_at	WIPF3	WAS/WASL interacting protein family, member 3
230273_at	C6orf165	chromosome 6 open reading frame 165
224559_at	LOC100507645 /// MA	uncharacterized LOC100507645 /// metastasis associated lung ad
223217_s_at	NFKBIZ	nuclear factor of kappa light polypeptide gene enhancer in B-cells
204793_at	GPRASP1	G protein-coupled receptor associated sorting protein 1
233375_at	EFCAB2	EF-hand calcium binding domain 2
223623_at	C2orf40	chromosome 2 open reading frame 40
200810_s_at	CIRBP	cold inducible RNA binding protein
232417_x_at	ZDHHC11	zinc finger, DHHC-type containing 11
230092_at	UBXN10	UBX domain protein 10
232611_at	GOLGA2P5	golgin A2 pseudogene 5
228214_at	SOX6	SRY (sex determining region Y)-box 6
1556474_a_at	FLJ38379	uncharacterized FLJ38379
238008_at	PRR18	proline rich 18
1556421_at	LOC286189	uncharacterized LOC286189
238657_at	UBXN10	UBX domain protein 10
228338_at	C11orf93	chromosome 11 open reading frame 93
204714_s_at	F5	coagulation factor V (proaccelerin, labile factor)
204070_at	RARRES3	retinoic acid receptor responder (tazarotene induced) 3
235945_at	SRD5A2	Steroid-5-alpha-reductase, alpha polypeptide 2 (3-oxo-5 alpha-ste
230132_at	LOC100505495	uncharacterized LOC100505495
210742_at	CDC14A	CDC14 cell division cycle 14 homolog A (S. cerevisiae)
205923_at	RELN	reelin
202746_at	ITM2A	integral membrane protein 2A
207981_s_at	ESRRG	estrogen-related receptor gamma
227289_at	PCDH17	protocadherin 17
208131_s_at	PTGIS	prostaglandin I2 (prostacyclin) synthase
244655_at	LOC100507311	uncharacterized LOC100507311
203932_at	HLA-DMB	major histocompatibility complex, class II, DM beta
204365_s_at	REEP1	receptor accessory protein 1
223218_s_at	NFKBIZ	nuclear factor of kappa light polypeptide gene enhancer in B-cells
211368_s_at	CASP1	caspase 1, apoptosis-related cysteine peptidase
220184_at	NANOG	Nanog homeobox
235421_at	MAP3K8	mitogen-activated protein kinase kinase kinase 8
205249_at	EGR2	early growth response 2
231133_at	CCDC164	coiled-coil domain containing 164
238513_at	PRRG4	proline rich Gla (G-carboxyglutamic acid) 4 (transmembrane)
215341_at	DNAH6	dynein, axonemal, heavy chain 6
235746_s_at	PLA2R1	phospholipase A2 receptor 1, 180kDa
214414_x_at	HBA1 /// HBA2	hemoglobin, alpha 1 /// hemoglobin, alpha 2
232196_at	LCA5L	Leber congenital amaurosis 5-like

217478_s_at	HLA-DMA	major histocompatibility complex, class II, DM alpha
214889_at	FAM149A	family with sequence similarity 149, member A
223866_at	ARMC2	armadillo repeat containing 2
218510_x_at	FAM134B	family with sequence similarity 134, member B
205269_at	LCP2	lymphocyte cytosolic protein 2 (SH2 domain containing leukocyte
40665_at	FMO3	flavin containing monooxygenase 3
228325_at	KIAA0146	KIAA0146
224940_s_at	PAPPA	pregnancy-associated plasma protein A, pappalysin 1
1568606_at	C11orf88	chromosome 11 open reading frame 88
228503_at	RPS6KA6	ribosomal protein S6 kinase, 90kDa, polypeptide 6
211458_s_at	GABARAPL1 /// GABAI	GABA(A) receptor-associated protein like 1 /// GABA(A) receptors
226358_at	APH1B	anterior pharynx defective 1 homolog B (C. elegans)
202156_s_at	CELF2	CUGBP, Elav-like family member 2
212914_at	CBX7	chromobox homolog 7
1568698_at	TMEM232	transmembrane protein 232
227404_s_at	LOC100653132	uncharacterized LOC100653132
229918_at	CCDC40	coiled-coil domain containing 40
239722_at	C5orf49	chromosome 5 open reading frame 49
228035_at	STK33	serine/threonine kinase 33
225345_s_at	FBXO32	F-box protein 32
229147_at	RASSF6	Ras association (RalGDS/AF-6) domain family member 6
220232_at	SCD5	stearoyl-CoA desaturase 5
203131_at	PDGFRA	platelet-derived growth factor receptor, alpha polypeptide
239098_at	KCNRG	potassium channel regulator
205997_at	ADAM28	ADAM metallopeptidase domain 28
219833_s_at	EFHC1	EF-hand domain (C-terminal) containing 1
214890_s_at	FAM149A	family with sequence similarity 149, member A
236575_at	ARHGEF26-AS1	ARHGEF26 antisense RNA 1 (non-protein coding)
231044_at	C1orf194	chromosome 1 open reading frame 194
239921_at	COL28A1	collagen, type XXVIII, alpha 1
239185_at	ABCA9	ATP-binding cassette, sub-family A (ABC1), member 9
231565_at	C4orf22	chromosome 4 open reading frame 22
203455_s_at	SAT1	spermidine/spermine N1-acetyltransferase 1
240288_at	KCNRG /// TRIM13	potassium channel regulator /// tripartite motif containing 13
1554141_s_at	WDR78	WD repeat domain 78
227420_at	TNFAIP8L1	tumor necrosis factor, alpha-induced protein 8-like 1
225009_at	CMTM4	CKLF-like MARVEL transmembrane domain containing 4
230104_s_at	TPPP	tubulin polymerization promoting protein
241600_at	WIPF3	WAS/WASL interacting protein family, member 3
226439_s_at	NBEA	neurobeachin
228195_at	C2orf88	chromosome 2 open reading frame 88
226333_at	IL6R	interleukin 6 receptor
226778_at	C8orf42	chromosome 8 open reading frame 42
228546_at	DPP6	dipeptidyl-peptidase 6
223609_at	ROPN1L	rhophilin associated tail protein 1-like
236335_at	GUCY1A2	guanylate cyclase 1, soluble, alpha 2
239828_at	AKD1	adenylate kinase domain containing 1

209959_at	NR4A3	nuclear receptor subfamily 4, group A, member 3
205363_at	BBOX1	butyrobetaine (gamma), 2-oxoglutarate dioxygenase (gamma-but
220156_at	EFCAB1	EF-hand calcium binding domain 1
231710_at	CAPS	calcyphosine
209160_at	AKR1C3	aldo-keto reductase family 1, member C3 (3-alpha hydroxysteroid
243296_at	NAMPT	Nicotinamide phosphoribosyltransferase
233071_at	RSPH4A	radial spoke head 4 homolog A (Chlamydomonas)
1552365_at	SCIN	scinderin
202901_x_at	CTSS	cathepsin S
230792_at	FAAH2	fatty acid amide hydrolase 2
227088_at	PDE5A	phosphodiesterase 5A, cGMP-specific
1553794_at	STOML3	stomatin (EPB72)-like 3
230206_at	DOCK5	Dedicator of cytokinesis 5
238864_at	VWA3A	von Willebrand factor A domain containing 3A
225286_at	ARSD	arylsulfatase D
220125_at	DNAI1	dynein, axonemal, intermediate chain 1
220030_at	STYK1	serine/threonine/tyrosine kinase 1
200974_at	ACTA2	actin, alpha 2, smooth muscle, aorta
202340_x_at	NR4A1	nuclear receptor subfamily 4, group A, member 1
219511_s_at	SNCAIP	synuclein, alpha interacting protein
209795_at	CD69	CD69 molecule
1569675_at	POU2AF1	POU class 2 associating factor 1
1555804_a_at	YSK4	YSK4 Sps1/Ste20-related kinase homolog (S. cerevisiae)
209071_s_at	RGS5	regulator of G-protein signaling 5
213172_at	TTC9	tetratricopeptide repeat domain 9
227758_at	RERG	RAS-like, estrogen-regulated, growth inhibitor
239500_at	EFCAB1	EF-hand calcium binding domain 1
207996_s_at	C18orf1	chromosome 18 open reading frame 1
220389_at	CCDC81	coiled-coil domain containing 81
240809_at	ZNF295-AS1	ZNF295 antisense RNA 1 (non-protein coding)
215085_x_at	DLEC1	deleted in lung and esophageal cancer 1
207655_s_at	BLNK	B-cell linker
243036_at	CCDC30	coiled-coil domain containing 30
219681_s_at	RAB11FIP1	RAB11 family interacting protein 1 (class I)
219747_at	NDNF	neuron-derived neurotrophic factor
229628_s_at	C9orf174 /// LOC1004	chromosome 9 open reading frame 174 /// LOC100499484-C9orf1
209074_s_at	FAM107A /// LOC1005	family with sequence similarity 107, member A /// uncharacterize
224227_s_at	BDP1	B double prime 1, subunit of RNA polymerase III transcription initi
221103_s_at	WDR52	WD repeat domain 52
1557544_at	CCDC147	coiled-coil domain containing 147
1552733_at	KLHDC1	kelch domain containing 1
212999_x_at	HLA-DQB1 /// LOC100	major histocompatibility complex, class II, DQ beta 1 /// HLA class
224929_at	TMEM173	transmembrane protein 173
203029_s_at	PTPRN2	protein tyrosine phosphatase, receptor type, N polypeptide 2
237131_at	RIIAD1	regulatory subunit of type II PKA R-subunit (RIIa) domain containi
231389_at	CXorf41	chromosome X open reading frame 41
206385_s_at	ANK3	ankyrin 3, node of Ranvier (ankyrin G)

1554528_at	C3orf15 /// LOC10065	chromosome 3 open reading frame 15 /// uncharacterized LOC10
204621_s_at	NR4A2	nuclear receptor subfamily 4, group A, member 2
223867_at	TEKT3	tektin 3
210108_at	CACNA1D	calcium channel, voltage-dependent, L type, alpha 1D subunit
241365_at	SATB1	SATB homeobox 1
220623_s_at	TSGA10	testis specific, 10
237151_s_at	PCDP1	primary ciliary dyskinesia protein 1
205768_s_at	SLC27A2	solute carrier family 27 (fatty acid transporter), member 2
214234_s_at	CYP3A5	cytochrome P450, family 3, subfamily A, polypeptide 5
212587_s_at	PTPRC	protein tyrosine phosphatase, receptor type, C
202994_s_at	FBLN1	fibulin 1
1554547_at	FAM13C	family with sequence similarity 13, member C
1552594_at	TMEM190	transmembrane protein 190
207850_at	CXCL3	chemokine (C-X-C motif) ligand 3
213375_s_at	N4BP2L1	NEDD4 binding protein 2-like 1
229021_at	MCTP2	multiple C2 domains, transmembrane 2
210033_s_at	SPAG6	sperm associated antigen 6
203408_s_at	SATB1	SATB homeobox 1
214070_s_at	ATP10B	ATPase, class V, type 10B
214719_at	SLC46A3	solute carrier family 46, member 3
201859_at	SRGN	serglycin
1553734_at	AK7	adenylate kinase 7
232357_at	TTLL9	tubulin tyrosine ligase-like family, member 9
214823_at	ZNF204P	zinc finger protein 204, pseudogene
223695_s_at	ARSD	arylsulfatase D
220351_at	CCRL1	chemokine (C-C motif) receptor-like 1
207636_at	SERPINI2	serpin peptidase inhibitor, clade I (pancpin), member 2
239776_at	TMEM232	transmembrane protein 232
1567627_at	CD74	CD74 molecule, major histocompatibility complex, class II invariar
214222_at	DNAH7	dynein, axonemal, heavy chain 7
228806_at	RORC	RAR-related orphan receptor C
237314_at	ENKUR	enkurin, TRPC channel interacting protein
243900_at	WDR38	WD repeat domain 38
222592_s_at	ACSL5	acyl-CoA synthetase long-chain family member 5
219542_at	NEK11	NIMA (never in mitosis gene a)- related kinase 11
207547_s_at	FAM107A /// LOC1005	family with sequence similarity 107, member A /// uncharacterize
203240_at	FCGBP	Fc fragment of IgG binding protein
230454_at	ICA1L	islet cell autoantigen 1,69kDa-like
212224_at	ALDH1A1	aldehyde dehydrogenase 1 family, member A1
1556711_at	FAM216B	family with sequence similarity 216, member B
204748_at	PTGS2	prostaglandin-endoperoxide synthase 2 (prostaglandin G/H syntha
205769_at	SLC27A2	solute carrier family 27 (fatty acid transporter), member 2
227497_at	SOX6	SRY (sex determining region Y)-box 6
236915_at	C4orf47	chromosome 4 open reading frame 47
221841_s_at	KLF4	Kruppel-like factor 4 (gut)
235956_at	KIAA1377	KIAA1377
1557275_a_at	TLCD2	TLC domain containing 2

230131_x_at	ARSD	arylsulfatase D
201236_s_at	BTG2	BTG family, member 2
225919_s_at	C9orf72	chromosome 9 open reading frame 72
238049_at	GRAMD3	GRAM domain containing 3
223691_at	RGS22	regulator of G-protein signaling 22
1557867_s_at	C9orf117	chromosome 9 open reading frame 117
203824_at	TSPAN8	tetraspanin 8
230997_at	TTC21A	tetratricopeptide repeat domain 21A
232568_at	MGC24103	uncharacterized MGC24103
1558077_s_at	MDH1B	malate dehydrogenase 1B, NAD (soluble)
223823_at	KCNMB2	potassium large conductance calcium-activated channel, subfamil
224370_s_at	CAPS2	calcyphosine 2
201041_s_at	DUSP1	dual specificity phosphatase 1
1559640_at	ANKFN1	Ankyrin-repeat and fibronectin type III domain containing 1
223467_at	RASD1	RAS, dexamethasone-induced 1
212067_s_at	C1R	complement component 1, r subcomponent
206197_at	NME5	NME/NM23 family member 5
213661_at	PAMR1	peptidase domain containing associated with muscle regeneratio
206798_x_at	DLEC1	deleted in lung and esophageal cancer 1
210982_s_at	HLA-DRA	major histocompatibility complex, class II, DR alpha
218380_at	LOC728392	uncharacterized LOC728392
205844_at	VNN1	vanin 1
222722_at	OGN	osteoglycin
201893_x_at	DCN	decorin
220302_at	MAK	male germ cell-associated kinase
242904_x_at	LOC100653229	uncharacterized LOC100653229
228731_at	GUCY1A2	guanylate cyclase 1, soluble, alpha 2
241538_at	CXorf30	chromosome X open reading frame 30
230695_s_at	RSPH9	radial spoke head 9 homolog (Chlamydomonas)
217757_at	A2M	alpha-2-macroglobulin
210809_s_at	POSTN	periostin, osteoblast specific factor
208894_at	HLA-DRA	major histocompatibility complex, class II, DR alpha
201137_s_at	HLA-DPB1	major histocompatibility complex, class II, DP beta 1
228827_at	RUNX1T1	runt-related transcription factor 1; translocated to, 1 (cyclin D-rel
223475_at	CRISPLD1	cysteine-rich secretory protein LCCL domain containing 1
1556003_a_at	LOC100506777	uncharacterized LOC100506777
200878_at	EPAS1 /// LOC100652	endothelial PAS domain protein 1 /// uncharacterized LOC100652
205590_at	RASGRP1	RAS guanyl releasing protein 1 (calcium and DAG-regulated)
236430_at	TMED6	transmembrane emp24 protein transport domain containing 6
221646_s_at	ZDHHC11	zinc finger, DHHC-type containing 11
221667_s_at	HSPB8	heat shock 22kDa protein 8
225280_x_at	ARSD	arylsulfatase D
233011_at	ANXA1	Annexin A1
237020_at	CATSPERD	catsper channel auxiliary subunit delta
202437_s_at	CYP1B1	cytochrome P450, family 1, subfamily B, polypeptide 1
226164_x_at	RIMKLB	ribosomal modification protein rimK-like family member B
205414_s_at	ARHGAP44	Rho GTPase activating protein 44

242903_at	IFNGR1	interferon gamma receptor 1
232166_at	KIAA1377	KIAA1377
239216_at	TEKT1	tektin 1
212671_s_at	HLA-DQA1 /// HLA-DQ	major histocompatibility complex, class II, DQ alpha 1 /// major hi
204041_at	MAOB	monoamine oxidase B
216248_s_at	NR4A2	nuclear receptor subfamily 4, group A, member 2
206228_at	PAX2	paired box 2
212998_x_at	HLA-DQB1 /// LOC100	major histocompatibility complex, class II, DQ beta 1 /// HLA class
219505_at	CECR1	cat eye syndrome chromosome region, candidate 1
240293_at	CCDC153	coiled-coil domain containing 153
229096_at	LIMS3 /// LIMS3-LOC4	LIM and senescent cell antigen-like domains 3 /// LIMS3-LOC4408
227194_at	FAM3B	family with sequence similarity 3, member B
230193_at	WDR66	WD repeat domain 66
243109_at	MCTP2	multiple C2 domains, transmembrane 2
230152_at	WDR52	WD repeat domain 52
202295_s_at	CTSH	cathepsin H
207959_s_at	DNAH9	dynein, axonemal, heavy chain 9
213849_s_at	PPP2R2B	protein phosphatase 2, regulatory subunit B, beta
207574_s_at	GADD45B	growth arrest and DNA-damage-inducible, beta
228648_at	LRG1	leucine-rich alpha-2-glycoprotein 1
228482_at	CDRT4 /// FAM18B2-C	CMT1A duplicated region transcript 4 /// FAM18B2-CDRT4 readth
235086_at	THBS1	thrombospondin 1
230130_at	SLIT2	Slit homolog 2 (Drosophila)
205043_at	CFTR	cystic fibrosis transmembrane conductance regulator (ATP-bindin
236666_s_at	LRRC10B	leucine rich repeat containing 10B
204622_x_at	NR4A2	nuclear receptor subfamily 4, group A, member 2
227917_at	LOC100506990	uncharacterized LOC100506990
220168_at	CASC1	cancer susceptibility candidate 1
209550_at	NDN	necdin homolog (mouse)
204803_s_at	RRAD	Ras-related associated with diabetes
226682_at	RORA	RAR-related orphan receptor A
239499_at	DNAH2	dynein, axonemal, heavy chain 2
222068_s_at	DNAAF1	dynein, axonemal, assembly factor 1
225895_at	SYNPO2	synaptopodin 2
214204_at	PACRG	PARK2 co-regulated
212681_at	EPB41L3	erythrocyte membrane protein band 4.1-like 3
238327_at	ODF3B	outer dense fiber of sperm tails 3B
1554140_at	WDR78	WD repeat domain 78
239733_at	DYDC2	DPY30 domain containing 2
213975_s_at	LYZ	lysozyme
222162_s_at	ADAMTS1	ADAM metallopeptidase with thrombospondin type 1 motif, 1
235527_at	DLGAP1	discs, large (Drosophila) homolog-associated protein 1
229976_at	MORN5	MORN repeat containing 5
243803_at	LOC643037	uncharacterized LOC643037
207896_s_at	DLEC1	deleted in lung and esophageal cancer 1
219564_at	KCNJ16	potassium inwardly-rectifying channel, subfamily J, member 16
222291_at	FAM149A	family with sequence similarity 149, member A

204072_s_at	FRY	furry homolog (Drosophila)
236118_at	LOC100128893	uncharacterized LOC100128893
226197_at	AR	androgen receptor
220591_s_at	EFHC2	EF-hand domain (C-terminal) containing 2
229802_at	WISP1	WNT1 inducible signaling pathway protein 1
238805_at	C11orf52 /// HSPB2 //	chromosome 11 open reading frame 52 /// heat shock 27kDa pro
221541_at	CRISPLD2	cysteine-rich secretory protein LCCL domain containing 2
1556026_at	LOC100131434	uncharacterized LOC100131434
231172_at	C9orf117	chromosome 9 open reading frame 117
202644_s_at	TNFAIP3	tumor necrosis factor, alpha-induced protein 3
238682_at	CCDC96	coiled-coil domain containing 96
203685_at	BCL2	B-cell CLL/lymphoma 2
234970_at	TC2N	tandem C2 domains, nuclear
243386_at	CASZ1	castor zinc finger 1
208147_s_at	CYP2C8	cytochrome P450, family 2, subfamily C, polypeptide 8
232968_at	FANK1	fibronectin type III and ankyrin repeat domains 1
218353_at	RGS5	regulator of G-protein signaling 5
236203_at	HLA-DQA1 /// LOC100	major histocompatibility complex, class II, DQ alpha 1 /// HLA clas
219871_at	FLJ13197	uncharacterized FLJ13197
237654_at	PPP1R36	protein phosphatase 1, regulatory subunit 36
204364_s_at	REEP1	receptor accessory protein 1
229738_at	DNAH10	dynein, axonemal, heavy chain 10
208323_s_at	ANXA13	annexin A13
231380_at	C8orf34	chromosome 8 open reading frame 34
232603_at	DCDC5	doublecortin domain containing 5
230624_at	SLC25A27	solute carrier family 25, member 27
208140_s_at	LRRC48	leucine rich repeat containing 48
205765_at	CYP3A5	cytochrome P450, family 3, subfamily A, polypeptide 5
1569040_s_at	ANKRD36BP2	ankyrin repeat domain 36B pseudogene 2
228726_at	SERPINB1	serpin peptidase inhibitor, clade B (ovalbumin), member 1
207490_at	TUBA4B	tubulin, alpha 4b (pseudogene)
212805_at	PRUNE2	prune homolog 2 (Drosophila)
201531_at	ZFP36	zinc finger protein 36, C3H type, homolog (mouse)
231729_s_at	CAPS	calcyphosine
230323_s_at	TMEM45B	transmembrane protein 45B
219932_at	SLC27A6	solute carrier family 27 (fatty acid transporter), member 6
227091_at	CCDC146	coiled-coil domain containing 146
210002_at	GATA6	GATA binding protein 6
205432_at	OVGP1	oviductal glycoprotein 1, 120kDa
226147_s_at	PIGR	polymeric immunoglobulin receptor
220723_s_at	CWH43	cell wall biogenesis 43 C-terminal homolog (S. cerevisiae)
203413_at	LOC100653018 /// LO	uncharacterized LOC100653018 /// uncharacterized LOC1006532
232381_s_at	DNAH5	dynein, axonemal, heavy chain 5
227697_at	SOCS3	suppressor of cytokine signaling 3
227498_at	SOX6	SRY (sex determining region Y)-box 6
227742_at	CLIC6	chloride intracellular channel 6
218876_at	TPPP3	tubulin polymerization-promoting protein family member 3

229616_s_at	GRAMD2	GRAM domain containing 2
204051_s_at	SFRP4	secreted frizzled-related protein 4
208306_x_at	HLA-DRB1 /// LOC100	major histocompatibility complex, class II, DR beta 1 /// HLA class
213293_s_at	TRIM22	tripartite motif containing 22
1552390_a_at	C8orf47	chromosome 8 open reading frame 47
232984_at	HYDIN	HYDIN, axonemal central pair apparatus protein
214235_at	CYP3A5	cytochrome P450, family 3, subfamily A, polypeptide 5
1557636_a_at	C7orf57	chromosome 7 open reading frame 57
226192_at	AR	androgen receptor
208791_at	CLU	clusterin
239297_at	KIAA1456	KIAA1456
1554298_a_at	WDR49	WD repeat domain 49
218322_s_at	ACSL5	acyl-CoA synthetase long-chain family member 5
240857_at	DNAH9	dynein, axonemal, heavy chain 9
203780_at	MPZL2	myelin protein zero-like 2
223962_at	TTC29	tetratricopeptide repeat domain 29
39248_at	AQP3	aquaporin 3 (Gill blood group)
1552283_s_at	ZDHHC11	zinc finger, DHHC-type containing 11
223235_s_at	SMOC2	SPARC related modular calcium binding 2
204802_at	RRAD	Ras-related associated with diabetes
213308_at	SHANK2	SH3 and multiple ankyrin repeat domains 2
236909_at	C2orf77	chromosome 2 open reading frame 77
235650_at	CDHR3 /// LOC100652	cadherin-related family member 3 /// uncharacterized LOC10065
210323_at	TEKT2	tektin 2 (testicular)
237281_at	AKAP14	A kinase (PRKA) anchor protein 14
206815_at	SPAG8	sperm associated antigen 8
236320_at	CCDC17	coiled-coil domain containing 17
220636_at	DNAI2	dynein, axonemal, intermediate chain 2
200986_at	SERPING1	serpin peptidase inhibitor, clade G (C1 inhibitor), member 1
209189_at	FOS	FBJ murine osteosarcoma viral oncogene homolog
230601_s_at	LRRC46	leucine rich repeat containing 46
228167_at	KLHL6	kelch-like 6 (Drosophila)
227238_at	MUC15	mucin 15, cell surface associated
239477_at	EFHB	EF-hand domain family, member B
204670_x_at	HLA-DRB1 /// HLA-DR	major histocompatibility complex, class II, DR beta 1 /// major his
208096_s_at	COL21A1	collagen, type XXI, alpha 1
209335_at	DCN	decorin
230600_at	LRRC46	leucine rich repeat containing 46
213307_at	SHANK2	SH3 and multiple ankyrin repeat domains 2
209774_x_at	CXCL2	chemokine (C-X-C motif) ligand 2
231582_at	CDHR3 /// LOC100652	cadherin-related family member 3 /// uncharacterized LOC10065
224355_s_at	MS4A8B	membrane-spanning 4-domains, subfamily A, member 8B
207016_s_at	ALDH1A2	aldehyde dehydrogenase 1 family, member A2
209312_x_at	HLA-DRB1 /// HLA-DR	major histocompatibility complex, class II, DR beta 1 /// major his
222043_at	CLU	clusterin
232277_at	SLC28A3	solute carrier family 28 (sodium-coupled nucleoside transporter),
209392_at	ENPP2	ectonucleotide pyrophosphatase/phosphodiesterase 2

228067_at	C2orf55	chromosome 2 open reading frame 55
208268_at	ADAM28	ADAM metallopeptidase domain 28
231969_at	STOX2	storkhead box 2
236717_at	FAM179A	family with sequence similarity 179, member A
205709_s_at	CDS1	CDP-diacylglycerol synthase (phosphatidate cytidylyltransferase)
228100_at	C1orf88	chromosome 1 open reading frame 88
219580_s_at	TMC5	transmembrane channel-like 5
226424_at	CAPS	calcyphosine
203485_at	RTN1	reticulon 1
1553635_s_at	TCTEX1D1	Tctex1 domain containing 1
226185_at	CDS1	CDP-diacylglycerol synthase (phosphatidate cytidylyltransferase)
243681_at	SHANK2	SH3 and multiple ankyrin repeat domains 2
235004_at	RBM24	RNA binding motif protein 24
208451_s_at	C4A /// C4B /// LOC10	complement component 4A (Rodgers blood group) /// compleme
212328_at	LIMCH1	LIM and calponin homology domains 1
231472_at	FBXO15	F-box protein 15
238983_at	NSUN7	NOP2/Sun domain family, member 7
240275_at	ARMC3	armadillo repeat containing 3
1552439_s_at	MEGF11	multiple EGF-like-domains 11
215193_x_at	HLA-DRB1 /// HLA-DR	major histocompatibility complex, class II, DR beta 1 /// major his
223838_at	TSGA10	testis specific, 10
231077_at	C1orf192	chromosome 1 open reading frame 192
208792_s_at	CLU	clusterin
204052_s_at	SFRP4	secreted frizzled-related protein 4
204719_at	ABCA8	ATP-binding cassette, sub-family A (ABC1), member 8
212588_at	PTPRC	protein tyrosine phosphatase, receptor type, C
203397_s_at	GALNT3	UDP-N-acetyl-alpha-D-galactosamine:polypeptide N-acetylgalact
229095_s_at	LIMS3 /// LIMS3-LOC4	LIM and senescent cell antigen-like domains 3 /// LIMS3-LOC4408
211991_s_at	HLA-DPA1	major histocompatibility complex, class II, DP alpha 1
233516_s_at	SPAG17	sperm associated antigen 17
227188_at	FAM176C	family with sequence similarity 176, member C
228554_at	PGR	progesterone receptor
215695_s_at	GYG2	glycogenin 2
228771_at	ADRBK2	adrenergic, beta, receptor kinase 2
1562371_s_at	VWA3B	von Willebrand factor A domain containing 3B
222890_at	CCDC113	coiled-coil domain containing 113
205027_s_at	MAP3K8	mitogen-activated protein kinase kinase kinase 8
202436_s_at	CYP1B1	cytochrome P450, family 1, subfamily B, polypeptide 1
227662_at	SYNPO2	synaptopodin 2
229331_at	SPATA18	spermatogenesis associated 18
229012_at	C9orf24	chromosome 9 open reading frame 24
229816_at	WDR78	WD repeat domain 78
203854_at	CFI	complement factor I
219313_at	GRAMD1C	GRAM domain containing 1C
210168_at	C6	complement component 6
229169_at	TTC18	tetratricopeptide repeat domain 18
205413_at	MPPED2	metallophosphoesterase domain containing 2

240304_s_at	TMC5	transmembrane channel-like 5
223924_at	TTC25	tetratricopeptide repeat domain 25
209829_at	FAM65B	family with sequence similarity 65, member B
210445_at	FABP6	fatty acid binding protein 6, ileal
220614_s_at	ADGB	androglobin
202768_at	FOSB	FBJ murine osteosarcoma viral oncogene homolog B
202672_s_at	ATF3	activating transcription factor 3
227099_s_at	C11orf96	chromosome 11 open reading frame 96
214428_x_at	C4A /// C4B /// LOC10	complement component 4A (Rodgers blood group) /// compleme
1552326_a_at	CCDC11	coiled-coil domain containing 11
239150_at	SNTN	sentan, cilia apical structure protein
236222_at	C3orf15 /// LOC10065	chromosome 3 open reading frame 15 /// uncharacterized LOC10
220269_at	ZBBX	zinc finger, B-box domain containing
226863_at	FAM110C	family with sequence similarity 110, member C
220110_s_at	NXF3	nuclear RNA export factor 3
218901_at	PLSCR4	phospholipid scramblase 4
213792_s_at	INSR	insulin receptor
243610_at	C9orf135	chromosome 9 open reading frame 135
1556158_at	FAM154B	family with sequence similarity 154, member B
223315_at	NTN4	netrin 4
228692_at	PREX2	phosphatidylinositol-3,4,5-trisphosphate-dependent Rac exchange
228241_at	AGR3	factor 2 anterior gradient 3 homolog (Xenopus laevis)
201163_s_at	IGFBP7	insulin-like growth factor binding protein 7
220390_at	AGBL2	ATP/GTP binding protein-like 2
229542_at	C20orf85	chromosome 20 open reading frame 85
238116_at	DYNLRB2	dynein, light chain, roadblock-type 2
233157_x_at	CCDC114	coiled-coil domain containing 114
232745_x_at	SPEF2	sperm flagellar 2
217767_at	C3	complement component 3
226344_at	ZMAT1	zinc finger, matrin-type 1
229831_at	CNTN3	contactin 3 (plasmacytoma associated)
210383_at	SCN1A	sodium channel, voltage-gated, type I, alpha subunit
236085_at	CAPSL	calcyphosine-like
227450_at	ERP27	endoplasmic reticulum protein 27
239916_at	WDR16	WD repeat domain 16
243802_at	DNAH12	dynein, axonemal, heavy chain 12
202948_at	IL1R1	interleukin 1 receptor, type I
238625_at	C1orf168	chromosome 1 open reading frame 168
240065_at	FAM81B	family with sequence similarity 81, member B
231084_at	WDR96	WD repeat domain 96
210262_at	CRISP2	cysteine-rich secretory protein 2
229170_s_at	TTC18	tetratricopeptide repeat domain 18
208498_s_at	ACTG1P4 /// AMY1A /	actin, gamma 1 pseudogene 4 /// amylase, alpha 1A (salivary) ///
230093_at	RSPH1	radial spoke head 1 homolog (Chlamydomonas)
214945_at	FAM153A /// FAM153	family with sequence similarity 153, member A /// family with sec
200795_at	SPARCL1	SPARC-like 1 (hevin)
211990_at	HLA-DPA1	major histocompatibility complex, class II, DP alpha 1

223044_at	SLC40A1	solute carrier family 40 (iron-regulated transporter), member 1
207802_at	CRISP3	cysteine-rich secretory protein 3

genes)

	Xenografted tumor vs. Normal oviduct		Serous cancer vs
RefSeq Transcript ID	p-value	Fold-Change	p-value
NM_004004	5.87E-07	194.15	0.0446097
NM_002026 /// NM_05403	1.82E-07	150.943	0.0001132
NM_000077 /// NM_00119	2.20E-09	146.365	2.63E-06
NM_001256099 /// NM_13	1.41E-06	136.964	1.65E-05
NM_002026 /// NM_05403	2.58E-07	129.223	0.000228229
NM_002026 /// NM_05403	1.11E-07	122.519	0.000212078
NM_005978	1.97E-06	111.322	0.000336779
NM_002026 /// NM_05403	5.67E-08	102.878	0.000180865
NM_001206846 /// NM_01	4.07E-10	86.748	1.19E-07
NM_002961 /// NM_01955	5.57E-07	86.1008	0.000314175
NM_001185056 /// NM_0C	7.77E-08	84.8932	0.000783687
NM_018685	4.17E-07	82.5849	2.17E-06
NM_004181	4.39E-07	79.0854	0.0176215
NM_001015886 /// NM_0C	3.20E-08	76.9694	0.00244253
NM_001034 /// NM_00116	8.27E-08	73.2436	9.71E-06
NM_018492	7.62E-07	71.9627	4.81E-05
NM_001444	6.05E-11	70.4237	1.20E-07
NM_002160	7.24E-06	67.1956	0.0413871
NM_022346	1.06E-09	63.5059	6.73E-08
NM_001146015 /// NM_01	5.23E-09	62.5462	4.50E-08
NM_001827	1.07E-08	59.8806	3.97E-06
NM_021107 /// NM_03336	1.42E-10	58.6994	7.24E-05
NM_016448	6.18E-11	55.1857	1.36E-08
NM_001114120 /// NM_01	3.66E-08	54.8264	2.75E-05
NM_001256799 /// NM_0C	8.01E-09	54.8252	0.00313461
NM_001166691 /// NM_0C	2.20E-12	53.1695	2.02E-11
NM_022346	4.94E-10	53.1519	2.04E-05
NM_001034 /// NM_00116	3.02E-05	52.5865	0.00140245
NM_001067	7.37E-09	52.3716	9.75E-10
NM_001130829 /// NM_0C	3.71E-09	51.1075	8.02E-06
NM_004936 /// NM_07848	7.46E-10	50.3667	0.00496907
NM_001207042 /// NM_0C	8.29E-16	47.9748	5.91E-06
NM_001067	2.56E-08	47.6484	1.61E-07
NM_001029989 /// NM_01	4.21E-07	46.8959	9.42E-06
NM_001002269 /// NM_01	3.63E-09	45.9372	0.0134098
NM_001130851 /// NM_0C	9.15E-11	45.0968	8.25E-07
NM_018304	6.11E-09	44.7991	2.18E-06
NM_004219	7.83E-12	44.0016	7.45E-08
NM_006818	2.38E-12	43.8789	0.000328096
NM_001255	2.84E-06	43.7721	6.30E-06
NM_024745	7.16E-13	42.6672	5.67E-07
NM_001012270 /// NM_0C	3.35E-08	42.0438	2.00E-05
NM_031966	7.24E-08	41.3069	4.42E-06

NM_001114120 /// NM_01	6.40E-09	40.6658	4.96E-05
NM_001001790 /// NM_00	4.47E-09	40.4379	0.000971516
NM_001127182 /// NM_01	9.34E-08	40.3811	1.95E-07
NM_001267580 /// NM_00	1.99E-08	40.1021	1.97E-08
NM_004336	3.89E-09	39.5809	8.46E-08
NM_000077 /// NM_00119	1.83E-11	39.4114	1.06E-05
NM_031423 /// NM_14569	2.02E-11	39.2024	4.90E-12
NM_031942 /// NM_14581	3.29E-06	38.0567	0.000915955
NM_016448	3.02E-12	37.4461	2.27E-07
NM_001198557 /// NM_00	9.62E-09	37.416	2.96E-05
NM_005914 /// NM_18274	2.02E-12	37.0746	2.03E-06
NM_001129897 /// NM_00	2.86E-08	36.6682	9.65E-09
NM_013363	1.18E-08	36.1554	0.00474735
NM_001142556 /// NM_00	3.19E-07	35.3182	9.70E-06
NM_001813	5.33E-14	34.727	1.20E-06
NM_001160706 /// NM_00	6.52E-07	34.0245	0.00658233
NM_014176	1.09E-11	33.933	8.95E-05
NM_005733	6.54E-10	33.0866	1.87E-10
NM_002305	2.75E-10	32.4713	0.0008352
NM_002291	2.63E-06	32.3716	0.0311721
NM_007019 /// NM_18179	1.29E-10	32.3393	5.21E-10
NM_024629	3.85E-10	32.1917	6.61E-08
NM_001166356 /// NM_00	1.40E-08	32.095	0.00011338
NM_001130829 /// NM_00	1.60E-08	32.0495	3.35E-05
NM_001142556 /// NM_00	1.16E-07	32.0253	0.0032725
NM_018518 /// NM_18275	3.75E-07	31.5499	0.0160453
NM_007274 /// NM_18186	1.37E-10	31.3961	5.81E-05
NM_016343	7.88E-10	31.0042	6.16E-09
NM_003600 /// NM_19843	5.10E-10	30.9649	5.60E-12
NM_174942	1.14E-08	30.7088	1.24E-08
NM_012474 /// NR_03743	1.64E-10	30.3586	3.09E-05
NM_003878	1.69E-06	30.2673	1.37E-06
NM_032756	2.97E-10	30.2069	0.000433131
NM_001005413 /// NM_00	6.99E-07	30.1462	2.97E-07
NM_007280	7.48E-11	29.4258	0.000273079
NM_001114120 /// NM_01	2.03E-09	29.2812	0.00113718
NM_001199261 /// NM_00	2.50E-12	28.7377	0.000110883
NM_001048201 /// NM_01	3.96E-07	28.549	0.00232417
NM_001100910 /// NM_00	4.01E-07	28.5277	5.61E-05
NM_001114121 /// NM_00	1.37E-08	28.0585	5.47E-05
NM_003600 /// NM_19843	5.43E-11	28.0358	2.02E-10
NM_001130829 /// NM_00	8.16E-06	27.4298	2.37E-05
NM_030919	7.86E-06	27.3062	1.31E-06
NM_001031628 /// NM_00	2.76E-09	27.2913	0.000736861
NM_173567	4.29E-09	27.0949	0.000395683
NM_001160033 /// NM_00	7.74E-10	26.9468	5.10E-05
NM_004298 /// NM_15348	7.69E-08	26.9426	0.000149792

NM_000269 /// NM_19817	3.63E-09	26.9322	0.000135352
NM_001113378 /// NM_01	6.21E-11	26.6319	4.80E-09
NM_014875	2.47E-08	25.8864	1.88E-08
NM_001070	7.31E-10	25.7397	2.19E-05
NM_001145208 /// NM_01	1.69E-09	25.2949	6.04E-05
NM_014096 /// NM_01761	8.44E-10	25.2498	1.46E-05
NM_001166496 /// NM_00	8.86E-07	25.105	0.00371699
NM_001002799 /// NM_00	6.76E-07	24.856	4.87E-05
NM_001168551 /// NM_01	1.01E-13	24.8376	1.34E-08
NM_017915	2.45E-11	24.7816	5.54E-05
NM_016095	2.53E-10	24.7519	9.86E-07
NM_000597	2.69E-05	24.5338	0.000196035
NM_001042426 /// NM_00	2.44E-06	24.3145	3.35E-06
NM_002703	9.13E-08	24.1661	0.016957
NM_012394	2.89E-11	24.1376	1.71E-05
NM_001126103 /// NM_00	7.42E-08	23.9965	2.53E-07
NM_004701	2.06E-08	23.9216	2.23E-08
NM_004702 /// NM_05773	3.81E-09	23.6354	9.74E-05
NM_001211	1.79E-06	23.536	4.08E-07
NM_001015051 /// NM_00	5.99E-05	23.5275	0.0275818
NM_004523	1.37E-07	23.4655	1.38E-07
NM_016401 /// NR_02459	2.69E-08	23.4505	0.00973226
NM_020675	8.28E-08	23.1727	0.00090201
NM_001002032 /// NM_00	3.93E-12	23.0821	1.32E-05
NM_006993	8.56E-13	22.6309	3.16E-05
NM_001130862 /// NM_00	3.27E-07	22.4118	2.47E-07
NM_032043	1.75E-10	22.2716	1.48E-07
NM_012112	1.01E-08	22.0444	4.57E-08
NM_001166496 /// NM_00	8.99E-06	21.9351	0.0150149
NM_001160706 /// NM_00	1.62E-06	21.8339	0.0190539
NM_000393	2.96E-06	21.0731	0.00302529
NM_020242	2.49E-07	20.9965	2.29E-07
NM_004856 /// NM_13855	1.31E-06	20.7476	4.18E-07
NM_005914 /// NM_18274	1.05E-09	20.6468	1.07E-06
NM_001100624 /// NM_00	5.47E-11	20.4814	2.73E-05
NM_001850 /// NM_02035	0.000880386	20.4601	6.14E-05
NM_144508 /// NM_17058	3.88E-08	20.1857	0.000110029
NM_001256685 /// NM_00	9.76E-06	20.0948	1.34E-06
NM_001099286 /// NM_13	1.34E-10	20.0666	6.90E-08
NR_024031	6.39E-09	20.059	0.00119736
NM_001078166 /// NM_00	8.54E-08	19.9533	0.00791754
NM_002623	5.11E-12	19.8218	6.53E-07
NM_001098801 /// NM_15	7.14E-08	19.7903	0.00104351
NM_001098525 /// NM_01	1.29E-05	19.5518	0.0112875
NM_052871 /// NR_01539	2.08E-09	19.5471	0.000430063
NM_018004	5.17E-06	19.3835	0.000980456
NM_001237	4.02E-07	19.3134	0.00679371

NM_001789 /// NM_20156	1.09E-11	19.2628	3.18E-05
NM_002592 /// NM_18264	4.53E-07	18.8156	0.000115791
NM_005737	6.60E-07	18.7673	9.58E-05
NM_018518 /// NM_18275	3.46E-07	18.7542	1.77E-05
NM_001009936 /// NM_01	3.10E-08	18.653	7.99E-05
NM_001098616 /// NM_01	2.79E-09	18.6266	0.0016783
NM_005022	5.24E-07	18.4364	0.0110857
NM_152562	2.38E-09	18.3738	1.65E-05
NM_001190799 /// NM_0C	5.06E-08	18.2961	0.000671851
NM_018410	2.13E-09	18.1974	1.72E-08
NM_001001563	2.11E-10	18.0096	3.16E-06
NM_016037	4.08E-13	17.9771	6.73E-06
NM_001193424 /// NM_0C	8.83E-09	17.9541	0.000703176
NM_080748	1.06E-10	17.7752	1.45E-05
NM_001190991 /// NM_01	7.34E-10	17.6389	1.83E-07
NM_005105	9.79E-08	17.6105	0.000230946
NM_001137604 /// NM_01	6.23E-08	17.3881	0.000295671
NM_001009936 /// NM_01	8.28E-08	17.3775	0.00128462
NM_001845	6.97E-08	17.3746	0.000269278
NM_014317	1.31E-09	17.1415	1.23E-05
NM_001130158 /// NM_0C	9.23E-08	17.1188	0.000107932
NM_018128	2.90E-10	17.1172	0.000402458
NM_001002258 /// NM_0C	3.20E-06	17.0082	0.00480524
NM_031299	7.19E-10	16.983	2.36E-10
NM_000075 /// NM_05298	2.16E-07	16.9684	0.000317706
NM_000365 /// NM_00115	9.12E-07	16.8595	0.000575207
NM_000170	1.17E-05	16.8509	1.20E-05
NM_014875	1.96E-11	16.8499	1.83E-07
NM_014624	5.41E-08	16.8	0.00135819
NM_015341	3.64E-09	16.7458	1.06E-05
NM_002318	2.15E-08	16.7454	0.000458976
NM_001012507	4.81E-08	16.6607	0.000166421
NM_153695	3.45E-06	16.4385	0.00105107
NM_014109	3.24E-06	16.4375	4.00E-07
NM_001018067 /// NM_0C	1.21E-08	16.4358	0.000556296
NM_020200	3.18E-05	16.4146	0.0238651
NM_006397	3.67E-08	16.3791	1.50E-05
NM_014109	6.72E-08	16.2747	0.000150378
NM_001905	1.22E-06	16.2653	0.000494056
NM_001129897 /// NM_0C	1.36E-08	16.2319	9.28E-08
NM_001040152 /// NM_0C	4.71E-06	16.0033	0.000524252
NM_013237	8.13E-11	15.9216	6.79E-06
NM_006713	9.97E-12	15.8889	1.36E-05
XR_040503	2.12E-06	15.8533	0.00269906
NM_001079524 /// NM_0C	8.87E-05	15.7932	0.0454423
NM_031966	4.68E-08	15.7874	1.83E-07
NM_018063	7.39E-10	15.6299	7.06E-06

NM_001145966 /// NM_00	1.64E-06	15.6074	0.000354249
NM_017785	2.19E-09	15.5705	9.00E-06
NM_005916 /// NM_18277	1.45E-06	15.552	7.44E-05
NM_001197330 /// NM_00	1.16E-12	15.5076	1.56E-07
NM_004559	1.20E-07	15.4581	0.000587199
NM_021067	3.76E-10	15.2466	3.13E-11
NM_024996	5.33E-07	15.2306	0.00110486
NM_006461	5.65E-10	15.1867	3.72E-07
NM_001142761 /// NM_00	2.22E-10	15.1837	2.66E-05
NM_001270411 /// NM_00	1.97E-05	15.1138	0.0183959
NM_005915	1.02E-07	15.095	1.02E-06
NM_005034	1.22E-07	15.0357	0.000152316
NM_001012270 /// NM_00	1.15E-10	14.8851	6.12E-06
NM_178014	2.15E-06	14.8738	0.000549977
NM_003142	4.83E-07	14.8137	0.00818877
NM_018407	2.49E-05	14.7292	0.000931545
NM_001190799 /// NM_00	1.29E-07	14.6136	0.000138719
NM_006845	1.38E-07	14.4754	3.21E-09
NM_014367	9.32E-09	14.2675	2.14E-06
NM_001071	0.000297954	14.1616	0.0022331
NM_004044	1.36E-08	14.1593	0.00112029
NM_005737	3.97E-07	14.1323	2.96E-05
NM_002131 /// NM_14589	7.37E-09	14.1193	0.000307272
NM_006234	4.29E-12	14.0097	4.55E-06
NM_001178010 /// NM_00	4.14E-08	13.9065	0.00132257
NM_001142463 /// NM_00	7.73E-08	13.9015	0.000569094
NM_001134693	1.68E-09	13.8741	0.00036413
NM_001199779 /// NM_00	1.00E-07	13.8076	1.17E-05
NM_003074	3.08E-09	13.7237	0.000515849
NM_001025252 /// NM_00	1.15E-07	13.6939	0.00095701
NM_080668	3.72E-08	13.6521	1.19E-06
NM_178014	1.22E-06	13.5373	0.000454097
NM_001145713 /// NM_00	4.16E-08	13.4628	0.000552009
NM_052850	2.11E-06	13.4536	0.0150484
NM_000532 /// NM_00117	2.03E-06	13.3138	4.07E-05
NM_002949	1.30E-08	13.2763	3.17E-05
NM_014367	1.76E-09	13.1732	7.67E-07
NM_024770	1.11E-06	13.1079	0.00413249
NM_001136478 /// NM_00	3.78E-07	13.0845	0.00360709
NM_031280	4.87E-08	13.0801	5.72E-06
NM_018944	1.45E-06	13.0689	0.000586995
NM_002524	1.26E-06	12.8581	0.000255187
NM_004559	5.71E-06	12.8256	0.000382104
NM_001134419 /// NM_00	9.28E-05	12.7286	0.000277555
NM_015201	7.09E-06	12.6794	7.99E-06
NM_000365 /// NM_00115	3.23E-07	12.5824	0.000775943
NM_023077	2.56E-10	12.4935	8.04E-05

NM_006023	1.33E-06	12.4622	0.00497142
NM_033550	9.45E-07	12.4162	0.00570171
NM_001270472 /// NM_00	4.41E-07	12.3988	0.00158603
NM_006845	1.92E-08	12.3006	9.41E-05
NM_001042424 /// NM_00	2.65E-09	12.2896	3.96E-07
NM_001258315 /// NM_00	0.000167362	12.2313	6.57E-05
NM_001159587 /// NM_00	0.00017269	12.2247	0.0167102
NM_003118 /// XR_110317	0.000203278	12.1374	0.000365182
NM_003920	4.12E-06	12.1269	8.45E-06
NM_001008396 /// NM_00	1.67E-10	12.1163	6.48E-07
NM_001199199 /// NM_00	7.96E-05	12.0647	0.0177409
NM_005063	0.000563744	12.0537	0.000107354
NM_002425	9.39E-06	12.0139	0.00758261
NM_001203247 /// NM_00	5.43E-07	11.9823	1.80E-09
NM_024094	2.18E-06	11.9311	4.07E-05
NR_003604 /// NR_003605	1.31E-08	11.8516	0.000314589
NM_002916 /// NM_18157	1.27E-07	11.8242	2.54E-06
NM_022366	3.63E-06	11.7808	0.0155641
NM_014175	1.62E-06	11.7314	0.00126517
NM_014408	9.65E-07	11.7113	0.000867849
NM_001256135 /// NM_00	1.65E-06	11.7008	0.000158905
NM_002915 /// NM_18155	6.76E-07	11.6909	0.000263607
NM_005956	2.41E-07	11.641	0.00108318
NM_018256	7.24E-09	11.6251	2.56E-06
NM_053040 /// NR_00297	8.50E-08	11.6224	0.00236033
NM_022061	2.60E-08	11.5667	0.00147004
NM_003875	1.38E-10	11.4972	7.80E-07
NM_133259	2.47E-08	11.3777	0.00108183
NM_152308	1.51E-12	11.3364	2.18E-08
NM_002105	1.12E-07	11.2902	0.0010435
NM_001130929 /// XM_00	2.30E-09	11.2823	1.04E-05
NM_013296	5.21E-05	11.2818	3.89E-05
NM_024006 /// NM_20682	5.54E-07	11.267	0.0030102
NM_001134231 /// NM_02	5.27E-09	11.2389	0.000443954
NM_001144757 /// NM_00	0.00100541	11.2111	0.00204246
NM_001025252 /// NM_00	0.00013749	11.1891	0.00985254
NM_012310	4.60E-06	11.1871	0.00255567
NM_014184	3.35E-06	11.1588	0.0101764
NM_001042422 /// NM_00	1.63E-05	11.087	0.0021603
NM_006938	1.64E-09	11.0352	0.000221657
NM_001105573	7.20E-06	11.0227	0.000616816
NM_001114121 /// NM_00	1.32E-09	10.9517	4.31E-05
NM_001011667 /// NM_00	1.73E-08	10.9288	2.72E-07
NM_178014	1.78E-05	10.9233	0.00886206
NM_001100624 /// NM_00	6.40E-13	10.8984	7.32E-09
NM_012293	7.96E-07	10.8981	0.000182296
NM_007051 /// NM_13191	8.42E-08	10.8434	0.000304594

NM_001243088 /// NM_0C	2.40E-07	10.7614	6.21E-07
NM_001040649 /// NM_0C	9.07E-08	10.7344	0.000572196
NM_021154 /// NM_05817	0.000254735	10.7297	0.000131146
NM_001660	4.70E-05	10.7063	0.00280085
NM_001826 /// NR_02416	1.32E-05	10.6633	0.000441453
NM_001164623 /// NM_01	7.34E-07	10.5899	0.00420544
NM_018063	3.11E-07	10.5898	0.000117132
NM_005952	2.42E-05	10.5687	0.0159862
NM_001167924 /// NM_03	7.54E-09	10.5548	0.000392885
NM_001206846 /// NM_01	2.27E-06	10.5212	5.67E-07
NM_020890	8.46E-08	10.4803	0.00138424
NM_001160033 /// NM_0C	5.81E-08	10.4519	1.86E-06
NM_001080443 /// NM_0C	1.10E-09	10.3847	1.92E-10
NM_004483 /// NR_03324	3.42E-06	10.3334	0.0113283
NM_173529	3.41E-05	10.2641	0.00716291
NM_001024934 /// NM_0C	6.25E-06	10.264	0.00762005
NM_032485 /// NM_1828C	7.89E-08	10.2456	3.27E-07
NM_024098	4.66E-10	10.1812	8.28E-05
NM_006638	1.34E-06	10.1638	0.00109895
NM_018270	6.76E-09	10.1564	3.17E-06
NM_001164269 /// NM_0C	4.20E-08	10.1246	2.82E-05
NM_005914 /// NM_18274	1.01E-10	10.0515	6.40E-06
NM_001026 /// NM_00114	9.98E-05	10.0478	0.00511145
NM_001002258 /// NM_0C	5.20E-05	10.0361	0.00130069
NM_019037	1.19E-06	9.97758	0.000644199
NM_001165031 /// NM_01	3.69E-08	9.944	0.000920281
NM_020726	1.80E-07	9.89334	0.00028814
NM_001256510 /// NM_0C	2.81E-05	9.88044	0.0177325
NM_024629	3.14E-05	9.77945	0.000903816
NM_007033	7.05E-07	9.76743	0.00400491
NM_001256875 /// NM_01	1.44E-07	9.72026	5.91E-07
NM_001204182 /// NM_0C	1.50E-05	9.69364	0.000669006
NM_001165031 /// NM_01	1.33E-07	9.67846	0.000107569
NM_030928	1.31E-09	9.67761	6.13E-05
NR_040001	0.000351759	9.62634	0.0307327
NM_000310 /// NM_00114	1.35E-05	9.58299	0.00594439
NM_004052	1.94E-05	9.57858	0.000262759
NM_001258437 /// NM_0C	2.28E-07	9.549	0.00116143
NM_001128210 /// NM_18	5.02E-07	9.53261	0.00192102
NM_001042762 /// NM_02	0.000115937	9.51958	0.00954669
NM_001789 /// NM_20156	4.62E-08	9.50461	8.79E-06
NM_001201483 /// NM_0C	2.81E-05	9.46185	0.00372617
NM_002770	2.17E-06	9.39128	0.00123976
NM_015261	2.81E-06	9.38803	0.00212995
NM_002266	5.93E-05	9.37303	0.00253773
NM_002770	3.25E-07	9.35325	0.00232863
NM_002634	1.56E-05	9.3495	0.0059617

NM_014171	1.47E-06	9.32183	0.000433403
NM_024037	1.22E-09	9.31114	1.25E-08
NM_016035	4.73E-07	9.2694	0.000566425
NM_020409 /// NM_17798	5.03E-10	9.24512	1.54E-05
NM_024808	9.40E-05	9.22064	0.00248125
NM_006848	7.36E-06	9.21135	0.00219912
NM_023937	1.62E-06	9.2026	0.000107653
NM_014467	7.17E-06	9.20018	0.000399589
NM_000034 /// NM_00112	7.70E-05	9.18701	0.00699727
NM_020750	2.23E-10	9.17217	1.34E-05
NM_004301 /// NM_17798	7.08E-06	9.09358	0.000389137
NM_001790 /// NM_0228	2.22E-07	9.09056	8.97E-07
NM_001128211 /// NM_03	0.000131978	9.01149	0.000773952
NM_001113378 /// NM_01	3.34E-08	9.00985	1.35E-06
NM_001256799 /// NM_0	1.02E-05	8.97219	0.0014149
NM_032390	4.34E-08	8.95564	0.0002534
NM_001243120 /// NM_0	6.47E-05	8.95344	0.00283373
NM_138689	8.39E-06	8.94943	0.000496815
NM_006101	6.12E-05	8.92635	8.00E-07
NM_000088	2.26E-06	8.85924	0.000476974
NM_006802	8.37E-06	8.82491	0.00489482
NM_198066	7.52E-05	8.76015	0.0136224
NM_000071 /// NM_00117	0.000147148	8.71307	0.00222914
NM_001198812 /// NM_0	0.000206951	8.6928	6.60E-05
NM_001172303 /// NM_0	3.05E-06	8.68226	0.000455216
NM_000057	9.78E-08	8.62648	6.11E-07
NM_001166356 /// NM_0	1.93E-08	8.62202	2.23E-07
NM_002074	1.65E-06	8.5927	0.000583086
NM_001002799 /// NM_0	0.000298024	8.57285	0.00463527
NM_001199534 /// NM_0	6.24E-06	8.555	0.000130516
NM_001080449	1.15E-07	8.55234	2.96E-06
NM_024899	1.54E-07	8.54779	0.0010084
NM_001845	3.80E-06	8.54282	0.00113215
NM_004373	4.36E-05	8.52075	0.00972443
NM_001135570 /// NR_02	1.96E-05	8.4784	0.00198926
NM_138462	2.29E-06	8.47374	0.00147492
NM_004526	8.53E-06	8.4658	2.18E-05
NM_019042	4.77E-07	8.4411	0.000125268
NM_006558	8.51E-05	8.4241	0.00655065
NM_001143936	4.75E-05	8.36492	0.00347382
NM_002577	2.05E-06	8.36449	0.000121671
NM_013237	6.65E-06	8.3348	0.00303712
NM_032479	2.94E-08	8.32468	0.000156817
NM_023080	0.000396559	8.30749	0.00271216
NM_004146	7.75E-06	8.2795	0.00141556
NM_004395 /// NM_08088	1.17E-06	8.26667	4.92E-07
NM_013299	1.31E-05	8.23892	2.29E-06

NM_000425 /// NM_00114	0.000999044	8.22723	2.98E-06
NM_001001790 /// NM_0C	1.92E-05	8.21173	0.0101217
NM_001135247 /// NM_0C	0.000278273	8.20701	7.93E-06
NM_014171	5.88E-06	8.18042	0.00073109
XR_109352 /// XR_109353	9.78E-07	8.17968	0.00285912
NM_005805	3.09E-05	8.17548	0.0171708
NM_003088 /// XR_132832	1.61E-06	8.17253	3.45E-05
NM_001166017 /// NM_14	2.13E-08	8.07039	1.66E-05
NM_001042517 /// NM_0C	1.93E-05	8.06941	0.0020882
NM_001105237 /// NM_01	1.69E-07	8.05712	0.00030664
NM_017915	1.65E-08	8.01621	6.43E-07
NM_001206846 /// NM_01	2.16E-07	7.994	1.21E-07
NM_001077516 /// NM_0C	1.02E-07	7.93906	0.000241526
NM_014865	0.000353321	7.92715	0.00263073
NM_001039954	3.93E-05	7.92352	0.011369
NM_004341	1.84E-08	7.87212	3.94E-06
NM_022459	2.02E-09	7.82015	1.36E-05
NM_030782	0.000133018	7.80414	0.00200008
NM_005063	0.000574103	7.77791	0.000179549
NM_001164391 /// NM_0C	1.72E-06	7.77559	4.92E-05
NM_001256725 /// NM_0C	4.62E-08	7.76835	0.000269761
NM_001145725 /// NM_01	3.65E-06	7.76108	0.00234654
NM_001015885 /// NM_0C	4.21E-07	7.72119	1.81E-05
NR_038253 /// NR_038254	4.06E-08	7.69968	7.03E-08
NM_033109	4.23E-06	7.69736	0.000326574
NM_001256799 /// NM_0C	1.51E-05	7.55735	0.00179303
NM_001517	2.72E-05	7.54978	0.000790678
NM_001253900 /// NM_0C	0.000322274	7.54569	2.91E-06
NM_001166131 /// NM_15	9.92E-08	7.53626	7.36E-09
NM_015190	2.04E-05	7.51883	0.000304021
NM_001166260 /// NM_0C	0.000229685	7.50922	0.033416
NM_001143964 /// NM_0C	2.38E-05	7.47162	2.92E-05
NM_031299	1.14E-09	7.46256	1.91E-06
NM_001031713 /// NM_02	1.88E-07	7.4542	0.000410814
NM_002293	3.05E-06	7.43828	7.75E-05
NM_000088	4.72E-05	7.3991	0.0110042
NM_015969	5.38E-06	7.38655	0.000944154
NM_145018	4.42E-07	7.37207	0.000315027
NM_001037334 /// NM_0C	4.23E-07	7.36338	0.000583764
NM_015938	7.45E-05	7.35618	0.0176771
NM_001258392 /// NM_0C	1.27E-08	7.34386	1.27E-05
NM_033112	5.84E-05	7.30934	0.00584353
NM_016072	4.01E-05	7.30295	0.000507433
NM_001853	0.0354386	7.23274	0.0176609
NM_007051 /// NM_13191	1.39E-07	7.23199	0.000299323
NM_198566	1.46E-06	7.22182	1.38E-06
NM_032881	8.63E-07	7.21584	0.000892514

NM_001152	0.000501444	7.18788	0.0197753
NM_001008800 /// NM_00	1.14E-05	7.16841	0.00399018
NM_000373 /// NR_033434	4.21E-05	7.14078	0.00284915
NM_001048166 /// NM_00	6.40E-06	7.11008	2.08E-05
NM_001008396 /// NM_00	2.61E-05	7.10511	0.000499648
NM_053040 /// NR_002976	9.64E-05	7.09943	0.0127575
NM_000034 /// NM_00112	6.29E-05	7.09628	0.00233028
NM_032361 /// NR_003615	7.56E-07	7.08486	0.00013073
NM_017955 /// NM_14570	7.97E-08	7.05468	1.16E-05
NM_003074	3.33E-05	7.05221	0.00421035
NM_003107	0.00148803	7.02416	0.00721192
NM_001079669 /// NM_03	0.000100412	7.01266	0.000502035
NM_001261834 /// NM_00	1.01E-05	7.01071	0.000271263
NM_006342	7.19E-05	7.00201	2.40E-06
NM_001199534 /// NM_00	5.99E-05	6.98841	0.000265874
NM_005951	0.000211003	6.98674	0.0150353
NM_001127181 /// NM_00	6.96E-08	6.94256	7.34E-06
NM_001260474 /// NM_00	4.27E-07	6.93479	0.00012781
NM_001197292 /// NM_00	2.94E-05	6.89855	0.00112758
NM_001205206 /// NM_00	9.93E-07	6.86303	1.66E-05
NM_016027	0.00199933	6.84894	0.0306835
NM_001256135 /// NM_00	0.000472848	6.81957	0.00039836
NM_031420	4.62E-07	6.8019	0.000218683
NM_001238 /// NM_05718	0.000150381	6.79781	1.32E-07
NM_001724 /// NM_19918	0.000186928	6.79582	0.0217445
NM_152416 /// XR_108868	0.000501907	6.77023	0.00641851
NM_000289 /// NM_00116	1.30E-07	6.76725	1.18E-05
NM_199420	1.94E-05	6.74497	7.39E-08
NM_153339	1.41E-09	6.74433	1.38E-05
NM_006739	0.00019922	6.73184	0.00668764
NM_006190 /// NR_033915	8.31E-07	6.67255	0.000164614
NM_001159673 /// NM_00	0.00076998	6.66992	0.00464664
NM_019037	4.01E-05	6.66003	0.000618947
NM_145287 /// NR_033354	6.05E-07	6.65597	0.000434341
NM_001136264 /// NM_00	2.69E-05	6.64854	0.00733811
NM_016397 /// NM_19897	2.65E-06	6.63588	0.000426956
NM_001195563 /// NM_00	0.000142545	6.63498	0.0019235
NM_001256798 /// NM_08	0.000184458	6.63222	7.34E-05
NM_012334	0.000581262	6.61682	3.34E-05
NM_023009 /// NR_052852	1.02E-05	6.61307	2.95E-06
NM_000175 /// NM_00118	4.02E-06	6.61233	1.52E-05
NM_023077	3.64E-09	6.58166	4.89E-06
NR_024388	1.38E-05	6.56947	3.33E-05
NM_001012985 /// NM_00	2.17E-05	6.56895	0.00195446
NM_001686	3.29E-05	6.55901	0.00416093
NM_003088 /// XR_132832	1.69E-07	6.55675	0.000238847
NM_001697	0.00160362	6.53291	0.022597

NM_016567 /// NM_07846	4.56E-05	6.52492	0.00152445
NM_001184979 /// NM_00	9.65E-08	6.50628	9.47E-06
NM_001077484 /// NM_03	7.58E-07	6.4934	8.53E-06
NM_005837	6.90E-07	6.4787	0.000928026
NM_020647	0.000236816	6.47645	0.000937137
NM_012334	2.69E-05	6.45122	1.61E-06
NM_006265	9.51E-06	6.44537	0.000288851
NM_001044385 /// NM_15	7.24E-07	6.43354	0.000365912
NM_005949	0.000213695	6.37279	0.00367584
NM_000034 /// NM_00112	8.17E-05	6.37069	0.00251322
NM_015459	6.26E-06	6.33627	0.000121874
NM_001024210 /// NM_00	3.55E-06	6.30081	0.00142175
NM_001042618 /// NM_00	7.95E-07	6.29112	4.86E-05
NM_004111	3.04E-06	6.28725	7.00E-06
NM_014321 /// NR_03762	1.09E-07	6.28132	4.69E-08
NM_000465	5.83E-06	6.25735	7.29E-05
NM_001145966 /// NM_00	1.96E-07	6.25572	2.05E-06
NM_023008 /// NM_17815	3.68E-05	6.24466	0.00157128
NM_199249 /// NM_19925	9.85E-06	6.23958	0.0026748
NM_032174	2.37E-07	6.23803	0.000126517
NM_199287	2.80E-05	6.23668	0.00194555
NM_006500	0.000104543	6.22565	0.00215916
NM_016397 /// NM_19897	1.89E-05	6.18913	0.00109841
NM_001033521 /// NM_00	1.53E-08	6.18674	1.81E-06
NM_001256799 /// NM_00	2.94E-05	6.17178	0.00301906
NM_001127229 /// NM_00	2.60E-06	6.14899	0.000315268
NM_014426 /// NM_15222	1.03E-07	6.14198	4.02E-05
NM_016343	2.15E-05	6.12622	2.01E-09
NM_000271	1.96E-05	6.11955	0.000115787
NM_016426	1.85E-06	6.11924	7.25E-07
NM_018385	1.42E-05	6.10364	0.000414676
NM_053042	2.24E-05	6.10015	0.00324768
NM_004637	5.73E-05	6.0792	0.00207881
NM_024899	0.000205455	6.07861	0.000727947
NM_001145454 /// NM_00	8.25E-08	6.0742	2.79E-10
NM_016625	1.13E-06	6.06727	1.59E-06
NM_016094	2.22E-05	6.06613	4.14E-05
NM_001031827 /// NM_00	1.66E-07	6.05419	2.13E-05
NM_001256799 /// NM_00	7.52E-06	6.02815	0.00118694
NM_001243251 /// NM_02	5.13E-06	5.9996	0.000355568
NM_001171155 /// NR_03	1.37E-07	5.99665	1.30E-05
NM_031280	6.93E-05	5.99322	8.62E-05
NM_013438 /// NM_05306	2.50E-05	5.97406	0.00463059
NM_001008709 /// NM_00	2.95E-06	5.97162	0.000511441
NM_001033673 /// NM_00	2.88E-05	5.93668	0.00316105
NM_001042371	3.74E-05	5.9311	0.000643163
NM_001098424 /// NM_00	1.78E-05	5.92098	0.00138084

NM_001105573	1.94E-05	5.89083	4.67E-05
NM_003091 /// NM_19821	1.10E-06	5.88461	1.03E-07
NM_031420	5.57E-06	5.86508	0.000312334
NM_013402 /// NR_03172	0.000139097	5.86504	0.00074102
NM_024830	5.94E-08	5.8642	1.62E-07
NM_001185181 /// NM_0	5.44E-06	5.85736	0.000466613
NM_001199981 /// NM_0	7.61E-06	5.85331	0.00227409
NM_023071	0.000469537	5.84458	0.00661612
NM_001256604 /// NM_0	5.52E-05	5.82965	0.000376833
NM_006579	1.42E-05	5.82412	0.000343645
NM_014708	2.47E-05	5.82197	6.83E-05
NM_032139	0.000760409	5.78694	0.00218295
NM_001127325 /// NM_0	2.12E-05	5.75812	0.000319226
NM_001102592 /// NM_14	3.14E-05	5.75529	3.19E-06
NM_001097612 /// NM_0	1.36E-05	5.75482	0.0026755
NM_001130112 /// NM_0	0.000531852	5.74619	0.00802145
NM_001256269 /// NM_0	7.97E-07	5.72946	1.05E-06
NM_001135673 /// NM_02	0.00086081	5.72457	0.00603027
NM_001146160 /// NM_03	0.000723107	5.70399	0.00878637
NM_005952	0.000328415	5.69946	0.0162433
NM_017850	6.47E-05	5.6586	0.000911804
NM_001005290 /// NM_0	3.95E-05	5.65156	6.50E-07
NM_014388	2.10E-05	5.64937	0.00391551
NM_000858 /// NM_00115	0.00061228	5.64545	0.0203927
NM_182513	1.25E-05	5.63859	1.21E-07
NM_001130146 /// NM_0	0.000529636	5.63543	0.000248397
NM_001199629 /// NM_0	0.000843475	5.60946	0.0014778
NR_002578 /// NR_002746	7.02E-05	5.60451	0.000726355
NM_012291	1.39E-06	5.60136	4.31E-10
NM_004395 /// NM_08088	1.28E-09	5.59309	2.53E-07
NM_002792 /// NM_15225	0.000340561	5.58533	0.00275967
NM_001201370 /// NM_01	0.000328632	5.5474	0.00423544
NM_013402 /// NR_03172	2.65E-06	5.5437	0.000927845
NM_000373 /// NR_03343	5.23E-06	5.51858	0.000184773
NM_001252129 /// NM_01	0.000476606	5.48928	0.000184469
NM_001128626 /// NM_0	0.000157649	5.4872	0.0048277
NM_001190991 /// NM_01	0.00122084	5.47546	0.00236218
NM_006496	9.93E-05	5.42951	0.00473491
NM_001127229 /// NM_0	5.38E-06	5.41598	0.000606432
NM_001194998 /// NM_01	0.000100559	5.41331	0.00223947
NM_178547	9.70E-06	5.41213	0.00195664
NM_003362 /// NM_08091	0.000502259	5.41189	0.000998251
NM_004358 /// NM_02187	1.39E-05	5.40257	0.000244301
NM_016131	0.00052409	5.40102	0.00525616
NM_001185181 /// NM_0	2.15E-05	5.38559	0.00130755
NM_001199260 /// NM_02	0.00191061	5.37128	0.0350817
NM_001039479 /// NM_01	0.000704058	5.3604	0.00675486

NM_001163817 /// NM_0C	0.000335869	5.33585	0.00104173
NM_001145822 /// NM_0C	1.27E-05	5.33326	0.000904834
NM_001204057 /// NM_0C	1.11E-07	5.31753	9.52E-08
NM_031942 /// NM_14581	0.000140473	5.3091	0.00800785
NM_001005386 /// NM_0C	4.18E-10	5.30506	9.56E-07
NM_001256126 /// NM_20	0.000168436	5.30129	0.000714218
NM_032242	2.00E-07	5.2971	5.67E-08
NM_001142548 /// NM_0C	4.25E-05	5.2934	1.34E-07
NM_018067	2.74E-05	5.2867	0.00160911
NM_002496 /// NR_03984	2.78E-05	5.27343	0.000189932
NM_005690 /// NM_01206	0.00267635	5.26332	0.0259922
NM_012456	0.000201598	5.2469	0.00170441
NM_001042618 /// NM_0C	6.70E-08	5.22448	1.46E-05
NM_001040649 /// NM_0C	6.79E-07	5.22343	1.85E-05
NM_017518 /// NM_20710	4.32E-05	5.2036	0.00378857
NM_001941 /// NM_02442	0.011172	5.19978	0.0293705
NM_003364 /// NM_18159	0.000227056	5.19762	0.00495893
NM_001204857 /// NM_0C	0.000991926	5.18454	0.00488547
NM_001195193 /// NM_0C	0.00147273	5.17843	0.0182266
NM_001079809 /// NM_13	1.44E-07	5.16837	1.42E-05
NM_005005	2.81E-05	5.16582	7.90E-05
NM_001025242 /// NM_0C	1.61E-05	5.16127	0.000303783
NM_001134671 /// NM_02	2.60E-06	5.15771	3.65E-05
NM_001136469 /// NM_02	0.00108724	5.15656	0.00306273
NM_001042717 /// NM_03	2.58E-06	5.14149	0.000107551
NM_000284 /// NM_00117	0.000205223	5.13479	0.000372561
NM_014754	8.07E-06	5.13279	5.09E-05
NM_018086	0.024518	5.11025	0.0028863
NM_001080502 /// NM_17	0.00155633	5.10911	6.64E-07
NM_001195602 /// NM_0C	4.21E-05	5.0979	0.0025997
NM_016397 /// NM_19897	4.68E-06	5.09428	0.00016499
NM_001201370 /// NM_01	0.00110299	5.08755	0.0107557
NM_021103	8.51E-07	5.07527	6.95E-05
NM_001145939 /// NM_0C	5.72E-08	5.06936	2.61E-07
NM_005189 /// NM_03264	0.000302825	5.06819	8.24E-06
NM_001003713 /// NM_0C	0.000947057	5.06489	0.00519154
NM_001257137 /// NM_0C	1.24E-06	5.06193	5.28E-07
NM_213720	0.000391168	5.05791	0.000721802
NM_001033549 /// NM_01	3.76E-07	5.05617	3.06E-07
NM_001142805 /// NM_0C	6.68E-05	5.04308	1.44E-05
NM_014109	0.000206317	5.01992	4.22E-06
NM_001109903 /// NM_03	6.18E-05	5.0035	8.61E-06
NM_002792 /// NM_15225	9.93E-05	4.97334	0.00206053
NM_001166356 /// NM_0C	1.54E-06	4.95916	1.04E-06
NM_052969	2.13E-05	4.94927	1.31E-06
NM_002263	5.84E-08	4.93289	1.29E-05
NM_001320	0.000892431	4.88716	0.00380502

NM_001256820 /// NM_0C	0.000113106	4.88295	0.00054642
NM_001001503 /// NM_02	7.71E-05	4.88047	0.000517602
NM_206908 /// NM_20691	0.000346198	4.86471	0.000187654
NM_015918 /// NM_1982C	0.000390257	4.8601	0.00602586
NM_005950	0.000833189	4.85811	0.011175
NM_001135653 /// NM_0C	2.53E-06	4.8568	1.41E-05
NM_032360	8.42E-07	4.8521	0.00011461
NM_001142805 /// NM_0C	9.88E-05	4.84444	2.50E-05
NM_001163812 /// NM_0C	8.38E-06	4.84332	5.09E-05
NM_018086	0.00175667	4.84128	8.40E-06
NM_007027	0.000116507	4.79756	0.000939402
NM_001109938 /// NM_0C	0.000113216	4.79159	0.00147271
NM_001080416 /// NM_0C	0.00668883	4.78242	0.00465192
NM_001039375 /// NM_02	7.12E-08	4.78017	2.88E-06
NM_001863	3.55E-05	4.77496	5.15E-05
NM_001099282 /// NM_0C	6.88E-06	4.76683	0.000328413
NM_001243891 /// NM_0C	1.46E-05	4.76119	0.000267633
NM_001193513 /// NM_0C	4.83E-06	4.74797	0.000300147
NM_001419	0.0014129	4.74714	0.010918
NM_006602	0.000317217	4.72465	0.00304931
NM_001195228 /// NM_01	1.05E-05	4.71578	3.96E-05
NM_022552 /// NM_15375	2.18E-05	4.71459	8.02E-07
XR_109242 /// XR_111621	0.000768167	4.69198	0.00349431
NM_001256119 /// NM_0C	4.83E-06	4.68907	0.000103507
NM_001267810 /// NM_0C	6.51E-05	4.68609	0.000655966
NM_016397 /// NM_19897	8.76E-06	4.68536	0.000207472
NM_001142474 /// NM_0C	4.18E-05	4.67286	7.54E-06
NM_001038628 /// NM_0C	0.0161805	4.66585	0.0410936
NM_001006622 /// NM_0C	0.00267397	4.66445	0.00489509
NM_001258338 /// NM_01	0.00824853	4.65703	0.0339504
NM_001127393 /// NM_0C	0.00108965	4.64726	0.00937958
NM_006347	7.33E-05	4.61767	0.000600879
NM_001130721 /// NM_02	0.000564557	4.6157	0.00157262
NM_001105530 /// NM_0C	0.000600325	4.602	0.00847569
NM_005494 /// NM_05824	0.00106173	4.59975	0.00180718
NM_001099670 /// NM_0C	9.88E-05	4.59401	0.000548429
NM_144772	2.54E-05	4.59303	0.000100701
NM_002610	0.00581303	4.58019	0.0021737
NM_012456	3.55E-05	4.57541	0.000597544
NM_004442 /// NM_01744	0.000957439	4.56973	6.68E-05
NM_018407	0.0251241	4.55202	0.0232763
NM_001199199 /// NM_0C	0.00226781	4.51892	0.00931295
NM_018056	2.47E-07	4.51874	2.10E-06
NM_152374	0.000100738	4.49951	2.31E-05
NM_002264 /// NR_02669ε	0.000103389	4.49679	0.000988337
NM_007276 /// NM_01658	7.49E-05	4.49486	0.000505177
NM_001005353 /// NM_01	0.0017267	4.49043	0.00294586

NM_001080415	0.000354379	4.48641	0.00138196
NM_033416	4.01E-08	4.48041	4.99E-06
NM_006231	5.61E-05	4.47592	0.00181557
NM_005916 /// NM_18277	9.15E-05	4.47235	2.14E-05
NM_012291	1.46E-05	4.47167	5.86E-09
NM_032336	1.06E-07	4.45557	8.53E-06
NM_203288	0.00176833	4.45219	0.0181816
NM_001207014 /// NM_0C	0.00585986	4.41797	0.0156035
NM_017975 /// NR_00310	0.00317661	4.40978	0.0033077
NM_016200	4.25E-06	4.4049	0.00012479
NM_001145408 /// NM_0C	3.39E-05	4.39734	3.51E-05
NM_003404 /// NM_13932	0.00124982	4.39501	0.00852163
NM_001202498 /// NM_0C	0.000147282	4.36429	0.00122068
NM_020782	0.0102134	4.36405	0.0162177
NM_001130524 /// NM_03	0.000562233	4.36168	0.00950217
NM_002452 /// NM_19894	1.85E-05	4.34971	1.14E-05
NM_001105198 /// NM_0C	0.00103893	4.34851	0.0102236
NM_020158	1.54E-05	4.33987	0.000523834
NM_002293	0.000319123	4.32336	0.00611505
NM_015965	0.00205367	4.31309	0.0222284
NM_001166050 /// NM_0C	0.000100017	4.30342	0.00283825
NM_001199534 /// NM_0C	0.000104392	4.30284	7.89E-05
NM_001033505 /// NM_0C	3.00E-05	4.30096	1.39E-05
NM_001136204 /// NM_01	2.34E-08	4.29256	8.45E-07
NM_001134337 /// NM_0C	1.09E-05	4.28757	0.000140258
NM_004596	0.000360833	4.28481	0.000805824
NM_000821 /// NM_00114	0.0018421	4.28171	0.000106338
NM_001083946 /// NM_01	7.35E-06	4.2756	0.000215406
NM_001242597 /// NM_0C	2.74E-05	4.25308	3.74E-05
NM_001256604 /// NM_0C	0.000593889	4.25261	3.63E-05
NM_025049	8.13E-05	4.228	7.04E-05
NM_004134	0.000510516	4.22615	0.00644384
NM_014367	1.16E-06	4.21649	2.10E-06
NM_014344	4.93E-05	4.21249	0.000121087
NM_174910	0.00147292	4.20814	0.00202614
NM_001080539 /// NM_17	0.000973746	4.20396	2.81E-06
NM_003091 /// NM_19821	0.00010551	4.18839	1.07E-05
NM_014762	0.000349551	4.18403	0.00331796
NM_024857	4.80E-05	4.18331	0.000264878
NM_001098786 /// NM_01	0.00437713	4.18323	0.00926028
NM_000071 /// NM_00117	0.00291774	4.18081	0.00115307
NM_001142805 /// NM_0C	0.00012772	4.15564	0.000406182
NM_001130963 /// NM_01	0.000544423	4.1472	0.00666539
NM_012334	0.00153584	4.12942	0.00267541
NM_001198915 /// NM_0C	1.81E-05	4.07757	2.07E-05
NM_000428	6.19E-05	4.07363	0.000335661
NM_006265	0.00506101	4.07123	0.00832928

NM_001034833 /// NM_01	3.49E-05	4.0555	0.00088001
NM_001001653 /// NM_05	3.28E-05	4.03528	8.01E-05
NM_006733	2.17E-05	4.01095	2.82E-07
NM_016407	0.000517893	3.99772	0.00413558
NM_001010866 /// NM_00	3.02E-06	3.97999	9.40E-05
NM_001130107 /// NM_00	0.000117498	3.97915	0.000589247
NM_014109	0.000439593	3.94904	1.97E-05
NM_001256135 /// NM_00	0.00850796	3.94753	0.00109158
NM_001142805 /// NM_00	6.60E-05	3.94337	2.36E-05
NM_017563	0.00778659	3.93357	0.00292281
NM_001004339	0.00153929	3.92957	0.00169458
NM_001003398 /// NM_00	0.0244205	3.92839	0.00798458
NM_022157	0.000393388	3.92635	0.00195498
NM_004990	1.29E-05	3.92607	0.000259271
NM_080652	8.25E-06	3.8937	2.68E-05
NM_007263 /// NM_19944	0.000908682	3.88505	0.00145926
NM_032340	7.13E-06	3.87567	2.69E-05
NM_005866 /// NM_14715	9.62E-06	3.86621	0.000125989
NM_002514	0.0132277	3.85987	0.00118288
NM_003765	4.37E-06	3.85792	3.44E-06
NM_001105570	0.00221634	3.84693	0.00188982
NR_000008 /// NR_002559	1.48E-05	3.83405	3.08E-05
NM_001247996 /// NM_01	0.0045165	3.80707	0.00361469
NM_001042540 /// NM_00	0.00118579	3.80292	2.50E-06
NM_001184740 /// NM_00	0.000376322	3.79496	9.94E-05
NM_001142474 /// NM_00	0.00407783	3.78253	0.000969146
NM_001039538 /// NM_00	0.000543518	3.78161	0.000122642
NM_019070 /// NR_03367	0.000103849	3.77741	0.000648795
NM_001166050 /// NM_00	0.00830175	3.77474	0.0331506
NM_005737	0.000400399	3.75508	0.000105146
NM_001076785 /// NM_00	0.000227049	3.74721	0.00108541
NM_001077484 /// NM_03	0.00112177	3.74289	0.00180006
NM_015420	0.000649762	3.73862	0.00232691
NM_004804	4.50E-06	3.73311	2.27E-05
NM_018407	0.0146217	3.72976	0.00791789
NM_018357 /// NM_19795	0.0302604	3.72953	0.00579627
NM_001184742 /// NM_00	0.00894066	3.72788	0.0318351
NM_199420	1.00E-05	3.71587	9.81E-08
NM_018221	0.000469104	3.71319	0.00163048
NM_001100620 /// NM_00	0.000114226	3.70764	6.05E-08
NM_001005735 /// NM_00	4.65E-05	3.68593	1.23E-06
NM_006350 /// NM_0134C	0.00125097	3.67947	0.00210039
NM_001265589 /// NM_00	0.00115656	3.67733	0.000285786
NM_001244949 /// NM_02	0.0203698	3.67562	0.0449126
NR_046287 /// NR_046288	7.59E-05	3.66842	0.000292183
NM_013388	0.000666656	3.66613	0.00132941
NM_004856 /// NM_13855	0.000208324	3.66129	0.000224262

NM_005819	0.000763565	3.64823	0.000662148
NM_001199649 /// NM_0C	0.0071631	3.64413	0.00126765
NM_001257137 /// NM_0C	0.0001007	3.61911	0.000929619
NM_052876	9.22E-06	3.61701	1.55E-05
NM_001256849 /// NM_0C	0.00244029	3.61364	0.00236615
NM_001256185 /// NM_0C	0.00405359	3.61167	0.0131277
NR_002578 /// NR_002746	0.00179328	3.5859	0.00173266
NM_001199981 /// NM_0C	0.0022315	3.58393	0.00210703
NM_001270452 /// NM_0C	0.00256241	3.58208	0.00752918
NM_001007239 /// NM_01	0.000654022	3.58025	0.00064355
NM_178867 /// NM_21364	0.00412522	3.57936	0.00453457
NM_001136039 /// NM_0C	0.00654641	3.57469	0.00577675
NM_001164623 /// NM_01	0.0011101	3.57295	0.0038238
NM_024112	0.00028847	3.55273	0.00119623
NM_000048 /// NM_00102	0.00243993	3.55115	0.00827966
NM_014047	0.00016116	3.54972	0.000184363
NM_001127370 /// NM_0C	0.0193097	3.54048	0.0018076
NM_006516	0.0106671	3.53324	0.000592474
NM_000302	0.00308366	3.52355	0.00770414
NM_001163508 /// NM_0C	5.94E-05	3.52333	2.88E-05
NM_001100819 /// NM_0C	0.01127	3.52331	0.0201716
NM_152716	1.66E-07	3.50536	7.75E-08
NM_004996 /// NM_01986	0.000112803	3.50169	4.92E-06
NM_001161580 /// NM_0C	0.00104991	3.50164	0.000679653
NM_018848 /// NM_17078	0.00463129	3.50042	0.00200076
NM_014275 /// NM_05401	0.0206346	3.49152	0.00329981
NM_006555	0.000215756	3.49069	0.00135622
NM_018944	0.000108524	3.49021	0.000178463
NM_018467	0.000144739	3.48105	9.19E-05
NM_004544	0.0225121	3.47436	0.0356726
NM_016535	0.000302152	3.47319	0.00124492
NM_174911	0.0411613	3.46688	0.0370889
NM_018683	1.99E-05	3.46322	9.93E-05
NM_015420	0.0134292	3.45882	0.0331003
NM_001178138 /// NM_0C	0.00106433	3.44781	0.000371447
NM_001037324 /// NM_0C	0.000447193	3.44758	2.80E-05
NM_012088	0.000336541	3.4384	0.00168568
NM_003594	0.000844199	3.42969	9.07E-05
NM_001163817 /// NM_0C	2.46E-05	3.42724	1.56E-07
NM_001042517 /// NM_0C	0.00317186	3.42663	0.00568695
NM_030789 /// NM_17858	4.33E-06	3.41915	1.63E-05
NM_001008395	0.00018411	3.41671	0.000435812
NM_001008222 /// NM_01	0.000478019	3.40444	0.000967503
NM_001916	0.0143152	3.40363	0.00118378
NM_001150	0.0115668	3.38867	0.0136652
NM_000284 /// NM_00117	0.00131395	3.38663	0.00198428
NM_022353	0.00676363	3.38459	0.00267575

NM_001846	0.00593924	3.36398	0.0132856
NM_001532	9.61E-05	3.36004	7.60E-05
NM_001145966 /// NM_00	0.000289329	3.34907	0.000118902
NM_002013 /// XR_13276	0.00821376	3.34168	0.0166502
NM_014275 /// NM_05401	0.00230893	3.31765	0.00157398
NM_001025252 /// NM_00	0.0313241	3.30743	0.0242991
NM_018140	0.000390393	3.30506	9.62E-05
NM_018086	0.0192802	3.30374	0.00096048
NM_002466	0.00120771	3.2807	7.90E-06
NM_003388 /// NM_03242	0.000553297	3.27964	0.00102942
NM_138348	0.00131764	3.27353	0.00177182
NM_152603	0.00514507	3.27021	0.0013994
NM_001206774 /// NM_01	0.0109649	3.25535	0.0229978
NM_001184891 /// NM_00	0.000115734	3.25179	0.000217532
NM_001224 /// NM_03298	0.0148698	3.25024	0.0108862
NM_004374	0.0193182	3.23094	0.00432976
NM_001253815 /// NM_00	0.0134921	3.22236	0.000191046
NM_006558	0.00358896	3.2208	0.00827964
NM_001001653 /// NM_05	0.000295956	3.21842	0.000284403
NM_144695	0.0006344	3.21764	0.000134017
NM_001033505 /// NM_00	3.45E-06	3.21672	1.06E-06
NM_001142463 /// NM_00	0.00114118	3.21032	0.00326772
NM_001135821 /// NM_00	0.0141858	3.20757	0.00198235
NM_001130929 /// NM_01	0.0105507	3.20589	0.00211917
NM_153451	0.000614091	3.20157	1.31E-05
NM_016456	0.000102669	3.18957	0.000219801
NM_001042424 /// NM_00	0.0052781	3.17253	0.0112546
NM_138316 /// NM_14897	0.0167124	3.1543	0.00139965
NM_005590 /// NM_00559	0.00172831	3.13267	0.00159819
NM_005809 /// NM_18173	0.039234	3.12964	0.0206651
NM_006499 /// NM_20154	0.0190645	3.12106	0.0170701
NM_003255	0.00219103	3.11962	6.15E-05
NM_001032292 /// NM_00	0.00172857	3.11864	0.00327552
NM_001143990 /// NM_00	0.00342365	3.10646	4.59E-05
NM_018353	0.00583957	3.10313	0.00250215
NR_028514	0.000174282	3.09571	0.000490317
NM_001105562 /// NM_00	5.51E-05	3.09297	0.000165919
NM_006451 /// NM_18278	0.0321267	3.06377	0.0411293
NM_030811	0.000281967	3.06279	4.76E-05
NM_001018073 /// NM_00	1.61E-05	3.05986	3.54E-05
NM_018944	0.00299447	3.05795	4.69E-05
NM_001039375 /// NM_02	1.10E-05	3.05588	5.25E-06
NM_001659	0.0321961	3.04171	0.00273872
NM_001258384 /// NM_00	0.00400723	3.03777	0.000419124
NM_001145408 /// NM_00	0.00011052	3.02218	0.000134114
NR_015366 /// NR_027241	0.0039025	3.01953	0.00220251
NM_001142405 /// NM_00	0.00481519	3.0158	6.07E-05

NM_001113201 /// NM_00	0.00166535	3.0123	2.94E-05
NM_001256686 /// NM_00	0.00294171	3.01074	4.36E-05
NM_001204453 /// NM_00	0.00454375	3.00992	0.00327254
NM_001166050 /// NM_00	0.00229139	3.00662	0.00347887
NM_001033521 /// NM_00	0.00035384	3.00447	0.000143115
NM_001047	0.00131137	2.99422	0.000111034
NM_018240	0.0055355	2.99391	0.000313931
NM_017780	0.00536157	2.99378	0.000449695
NM_001188	0.000237903	2.99255	0.000155987
NM_000849 /// NR_02453	0.000167988	2.96459	0.000112618
NM_001201545 /// NM_02	2.37E-05	2.94882	1.03E-05
NM_001199290 /// NM_14	0.00668348	2.93066	0.0013151
NM_016074	5.61E-05	2.92846	0.000101123
NM_013296	0.000451888	2.92813	0.000118344
NR_002785	0.0102791	2.92578	0.000237128
NM_001077484 /// NM_03	0.00355477	2.92286	0.00139389
NM_001032730 /// NM_03	0.0140734	2.92055	0.0040458
NM_001267623 /// NM_03	1.07E-05	2.9203	3.43E-06
NM_002936	0.000851502	2.91909	3.62E-05
NM_145702	0.0320349	2.91717	0.000122838
NM_178448	0.000888349	2.90077	7.16E-06
NM_203453	0.0151376	2.88725	0.00558055
NM_152699	0.000556353	2.87658	5.01E-05
NM_017952	0.0165647	2.86986	0.0141862
NM_001024594	0.00966714	2.86602	0.00226845
NM_001252641 /// NM_00	0.0121026	2.85767	0.00439137
NM_001039589 /// NM_00	0.000562666	2.85665	0.000196377
XR_110082 /// XR_112807	0.0112509	2.85571	0.000167397
NM_001267608 /// NM_00	4.59E-05	2.84765	6.33E-06
NM_005471	0.000387656	2.84327	0.000372697
NM_020662	0.0186444	2.84285	0.014838
NM_012103 /// NM_18157	0.00881065	2.8407	0.000673517
NM_024796 /// NR_02432	0.0213211	2.83935	0.00218459
NM_024036	0.00231287	2.82618	0.00157086
NM_001033855 /// NM_00	0.00541553	2.81772	0.00149735
NM_001177663 /// NM_00	0.00747536	2.80211	0.00319688
NM_007059	0.000151459	2.78874	4.24E-05
NM_018451 /// NR_04759	0.0111651	2.78487	6.72E-05
NM_003258	6.16E-05	2.7837	4.50E-05
NM_001008938 /// NM_01	7.71E-05	2.78214	5.96E-05
NM_004846 /// XR_11244	0.000351805	2.77611	8.18E-05
NM_014607	0.0161466	2.77176	0.00685515
NM_001204180	8.18E-06	2.76864	3.07E-09
NM_006602 /// NM_08075	0.0120047	2.76808	0.00688017
NM_024622	0.0172903	2.75812	0.00265831
NM_006014	0.00242948	2.75613	3.22E-06
NM_001258384 /// NM_00	0.00322608	2.75029	7.93E-05

NM_001013730 /// XR_110	0.0111702	2.74382	0.00270185
NM_032371 /// NM_13841	0.00424538	2.74347	0.000141242
NM_006980	0.00285433	2.7377	0.000794649
NM_002254	0.00067988	2.73741	0.000111307
NM_001130965 /// NM_00	0.00278601	2.7372	0.00025803
NM_017813	0.0245251	2.73693	0.00110693
NM_000403 /// NM_00100	0.00243563	2.73429	0.00209677
NM_000244 /// NM_13079	0.00116467	2.72882	0.000441238
NM_001195563 /// NM_00	0.0051406	2.71723	0.00241004
NM_012334	0.0134123	2.71605	0.000745807
NM_018706	0.00521769	2.70574	0.000153549
NM_001190991 /// NM_01	0.00369265	2.68758	4.61E-05
NM_001256763 /// NM_01	0.0115766	2.68394	0.00234919
NM_015953	0.03592	2.67958	0.01475
NM_001015885 /// NM_00	0.000233815	2.67287	3.36E-05
NM_032818	0.00147199	2.67203	8.79E-05
NM_001098424 /// NM_00	0.0433555	2.65653	0.0305176
NM_017646	0.00410256	2.65042	0.000969043
NR_024397	0.00496486	2.64975	2.97E-05
NM_012293	0.00465933	2.6478	0.000557154
NM_001164811	0.017688	2.63661	0.00215088
NM_001136033 /// NM_01	0.00584748	2.63507	0.00116982
NM_003507	0.0175753	2.63069	6.32E-05
NM_001093725	0.000402474	2.62669	3.23E-06
NM_015155	0.00493799	2.61596	0.000848966
NM_022778	0.00502312	2.61428	0.00267398
NM_014426 /// NM_15222	0.0100988	2.61117	0.000130803
NM_001025366 /// NM_00	0.00695236	2.60121	0.000133257
NM_178229	3.40E-05	2.59576	5.07E-13
NM_003258	0.00106387	2.59367	3.31E-06
NM_001109903 /// NM_03	0.0012575	2.59044	8.32E-05
NM_017927 /// NM_03354	0.00961541	2.58194	0.00566464
NM_001002017 /// NM_00	0.000475587	2.57779	0.000147877
NM_032371 /// NM_13841	0.0122843	2.57704	0.000372989
NM_001099652	0.0260202	2.57227	1.90E-05
NM_001130677	0.00466091	2.56175	0.000306874
NM_003107	0.0259326	2.55389	0.000636005
NM_001247987 /// NM_02	0.0349408	2.55176	3.78E-05
NM_001247996 /// NM_01	7.54E-05	2.54405	2.32E-05
NM_004442 /// NM_01744	0.00208323	2.54234	3.34E-05
NM_001013649	0.0222945	2.53611	0.00302361
NM_001204492 /// NM_00	0.0013481	2.52247	6.43E-05
NM_001256670 /// NM_00	5.76E-05	2.50841	8.24E-06
NM_019070 /// NR_03367	0.000125246	2.50682	1.91E-05
NM_033505	0.0122216	2.50652	0.00269497
NM_005997	0.0105441	2.49721	0.000441109
NM_017927 /// NM_03354	0.0227395	2.48932	0.00208488

NM_145231	0.0240059	2.48596	0.00549941
NM_001083963 /// NM_00	0.0131973	2.48034	0.000433102
NM_001040664 /// NM_00	0.00719132	2.46782	0.000152061
NM_004442 /// NM_01744	0.000231369	2.44636	2.24E-05
NM_001258384 /// NM_00	0.00525099	2.44141	0.000134695
NM_006796	0.00587978	2.42822	0.000496276
NM_014426 /// NM_15222	0.00895797	2.40945	0.00234194
NM_152341	0.00757604	2.40877	0.000986576
NM_001039477 /// NM_00	0.0443508	2.40365	0.0174253
NM_003721 /// NM_13444	0.0143483	2.40016	0.00254392
NM_018174	0.0289731	2.39212	0.00606325
NM_016018 /// NM_02487	0.00547544	2.38855	0.000141053
NM_001109938 /// NM_00	0.00994332	2.38565	0.00051123
NM_001258033 /// NM_00	0.00680477	2.37989	0.00150437
NM_016028 /// NM_01763	0.0241129	2.37215	0.00109897
NM_001008491 /// NM_00	0.00794681	2.37142	0.00012502
NR_002776	0.00248674	2.35634	0.000118334
NM_001198850 /// NM_00	0.00175653	2.35092	0.000179211
NM_020386	0.0282001	2.34524	0.00102848
NM_000135 /// NM_00101	0.00016353	2.34484	3.49E-06
NM_003714	0.0483855	2.34211	0.00522508
NM_006579	0.00117407	2.33231	3.11E-06
NM_001256574 /// NM_00	0.00700322	2.32804	5.11E-05
NM_001015055 /// NM_00	0.0307408	2.32518	2.08E-05
NM_019104	0.0372472	2.3192	0.00101841
NM_006618	0.0372274	2.31711	0.00197485
NM_022477 /// NM_03201	0.00150349	2.31636	0.000143866
NM_004567	0.0109774	2.31533	3.30E-05
NM_016558 /// NM_03363	0.0205612	2.31225	0.00187022
NM_001039477 /// NM_00	0.0349297	2.3087	0.00279409
NM_020062	0.047564	2.30708	0.00121847
NM_080656	0.00537181	2.30643	0.0010731
NM_001257144 /// NM_00	0.00886148	2.3019	1.65E-05
NM_001270439 /// NM_00	0.0014331	2.301	6.79E-05
NM_025108	0.000179554	2.29448	1.77E-07
NM_000135 /// NM_00101	0.00222142	2.28841	8.74E-05
NM_001105203 /// NM_00	0.000306743	2.28819	6.11E-08
NM_022092	0.0308305	2.28732	2.70E-06
NM_006455	0.00239734	2.28175	5.20E-05
NM_013432	0.00252919	2.27734	1.45E-05
NM_000801 /// NM_00119	0.0181998	2.27205	0.00296202
NM_001029991 /// NM_00	0.0281712	2.26914	0.00700075
NM_001136035 /// NM_00	0.0458729	2.26895	0.00133049
NM_001204364 /// NM_15	0.000360152	2.26129	9.55E-09
NM_006943	0.00170733	2.25829	1.18E-05
NM_016558 /// NM_03363	0.0180044	2.25449	0.00312224
NM_001164391 /// NM_00	0.0202809	2.24901	0.00400399

NM_152268	0.00183071	2.2463	7.49E-05
NM_001193557 /// NM_02	0.0169498	2.23782	0.000355252
NM_004260	0.0114038	2.23154	5.42E-05
NM_001166599 /// NM_00	0.0477747	2.22489	0.000377973
NM_030625	0.0140239	2.20846	0.000120588
NM_001204106 /// NM_00	0.00166686	2.20688	1.90E-05
NM_138384	0.0118147	2.19766	0.000285136
NM_015327	0.00853369	2.1957	0.00027145
NM_005762	0.0110702	2.19206	0.00105357
NM_001144002 /// NM_01	0.00637082	2.19038	0.000698744
NM_017769	0.0171758	2.18996	0.0011136
NM_003797 /// NM_15299	0.0344162	2.18758	0.00194473
NM_003740	0.0149678	2.18163	0.000579025
NM_001012514 /// NM_00	0.0177222	2.18132	0.00116445
NM_006769	0.031934	2.17403	0.00644385
NM_006559	0.00071141	2.17389	3.39E-05
NM_001039783 /// NM_00	0.00230862	2.15553	0.000123408
NM_001145454 /// NM_00	0.000321074	2.14612	5.55E-06
NM_001201428 /// NM_01	0.0449453	2.13684	0.00689629
NM_004699	0.0435783	2.12711	0.00665859
NM_032815	0.000938462	2.11296	6.95E-06
NM_013285	0.00518732	2.09976	0.000189222
NM_001042631	0.00322677	2.09601	0.000151921
NM_000308 /// NM_00112	0.0147243	2.089	0.000470215
NM_001018115 /// NM_03	0.0117156	2.08041	1.23E-05
NM_001037811 /// NM_00	0.0198788	2.07201	0.000288306
NM_001261427 /// NM_00	0.0166277	2.06143	0.000223129
NM_173511	0.0101943	2.04909	5.60E-05
NM_145012 /// NM_18169	0.0197377	2.04867	0.000169142
NM_024112	0.0143324	2.04566	0.00033741
NM_001204106 /// NM_00	0.0200284	2.02366	0.00107473
NM_194292	0.00847605	2.02179	8.54E-05
NM_001085372	0.0135665	2.01606	0.000147273
NM_001184977 /// NM_01	0.0143888	2.01505	1.05E-05
NM_001099222 /// NM_00	0.00137878	-2.02597	1.84E-05
NM_053000 /// NR_015370	0.0445363	-2.03801	0.00525927
NM_052900 /// NM_19812	0.043518	-2.03994	0.00306063
NM_014867	0.0169534	-2.04477	0.000423071
NM_001142685 /// NM_01	0.0154126	-2.04805	0.000194133
NM_016353	0.0330585	-2.05208	0.00188074
NM_198920	0.0158044	-2.06049	0.000949583
NM_000049 /// NM_00112	0.0258824	-2.06347	0.000490738
NM_178816 /// NM_20137	0.00677375	-2.06863	5.56E-05
NM_001172766 /// NM_00	0.0491818	-2.0928	0.00110792
NM_000426 /// NM_00107	0.0156504	-2.09962	2.07E-06
NM_024723 /// NM_18292	0.0145025	-2.11112	9.77E-05
NM_001168618 /// NM_02	0.0205909	-2.12308	7.38E-05

NM_001098402 /// NM_00	0.0309385	-2.12643	0.000148795
NM_001005367 /// NM_00	0.00186559	-2.12793	8.63E-05
NM_000426 /// NM_00107	0.0107995	-2.13707	8.13E-07
NM_000418 /// NM_00100	0.0485917	-2.13971	0.00371708
NM_020734	0.0185038	-2.14185	0.00112458
NM_001256732 /// NM_00	0.00103473	-2.14745	4.09E-05
NM_001029851 /// NM_00	0.0251409	-2.15436	1.30E-05
NM_170710 /// NM_18126	0.0379251	-2.15487	5.69E-06
NM_001136472 /// NM_00	0.0483293	-2.16212	3.13E-05
NM_080283 /// NM_17238	0.00169874	-2.18976	5.88E-05
NM_001128432 /// NM_02	0.00646131	-2.20278	0.000260008
NM_178499	0.0220811	-2.2066	0.00422569
NM_001169109 /// NM_00	0.0294738	-2.21427	1.32E-06
NM_001015045 /// NM_00	0.00677561	-2.22016	4.94E-05
NM_001031687 /// NM_00	0.0244229	-2.23129	0.000490266
NM_004613 /// NM_19895	0.022703	-2.23957	0.000120943
NM_002373	0.0010806	-2.24885	7.70E-05
NM_001195535	0.000156656	-2.26989	1.39E-07
NM_001127235 /// NM_00	0.0381493	-2.27382	0.0111832
NM_001144960	0.00386188	-2.275	0.000294867
NM_002919 /// NM_13442	0.0335753	-2.27714	3.68E-05
NM_001166693 /// NM_00	0.00202331	-2.28203	4.23E-06
NM_001111038 /// NM_14	0.00484257	-2.28782	1.97E-05
NM_030821	0.0248973	-2.28897	0.000871953
NM_001077181 /// NM_00	0.0472355	-2.30253	0.00393145
NM_001032287 /// NM_00	0.00428576	-2.30859	0.000253767
NM_001003789 /// NM_00	0.0124339	-2.31234	0.000465315
NM_001269053 /// NM_13	0.0227174	-2.31379	0.00162138
NM_001025105 /// NM_00	0.0392068	-2.31504	0.00222511
---	0.0276852	-2.32064	0.00404862
NR_036487	0.0305442	-2.32463	0.00148852
XM_001125684	0.00783062	-2.33546	0.000976223
NM_001256732 /// NM_00	0.00285295	-2.33693	0.000359917
NM_000389 /// NM_00122	0.0299391	-2.34269	4.22E-07
NM_001195639 /// NM_05	0.00606997	-2.35306	0.000885814
NM_002912	0.0117839	-2.38068	0.00037981
NM_001116	0.0490926	-2.38476	0.00257178
NM_000668	0.00351059	-2.38644	0.00054212
NM_152723	0.0396672	-2.38693	0.0116277
NM_017655	0.0282523	-2.40463	0.0076759
NM_001199096 /// NM_00	0.000267241	-2.40938	4.85E-05
NM_016441	0.0364096	-2.42288	0.00586934
NM_001008710 /// NM_00	0.0110631	-2.42486	0.00385031
NM_003263	0.00142513	-2.42533	4.38E-05
NM_005761 /// NR_03768	0.00496711	-2.43864	0.000153534
NM_020676	0.00019809	-2.4402	2.64E-07
NM_001105248 /// NM_00	0.00783602	-2.45457	0.000567958

NM_001031715 /// NM_02	0.0266489	-2.46802	0.00316198
NM_001134405 /// NM_0C	0.0100258	-2.47406	0.00146619
NM_014057 /// NM_02441	0.00468197	-2.47425	0.00104327
NM_000476	2.48E-05	-2.4743	4.17E-07
NM_005228 /// NM_20128	0.0429253	-2.47705	0.0230957
NM_001251977 /// NM_0C	0.0186661	-2.48141	0.00302333
NM_018956	0.000107207	-2.49192	6.00E-06
NM_001039590 /// NM_0C	0.00425431	-2.49309	1.03E-05
NM_019604	0.00639602	-2.49351	0.0023804
NM_001099337 /// NM_14	0.0206813	-2.5002	0.00611079
NM_001001687 /// NR_02	0.010509	-2.50077	0.00198774
NR_015430	0.00109188	-2.50098	0.000305252
NM_153228	0.00449995	-2.50312	0.000588123
NM_001100875 /// NM_15	0.000765126	-2.50893	3.10E-05
NM_001039395 /// NM_01	0.00152194	-2.50963	6.32E-05
NM_001045	0.000742975	-2.51447	3.88E-05
NM_001190918 /// NM_0C	0.000171788	-2.5154	2.71E-05
NM_016617	0.00885548	-2.54424	0.00294288
NM_016270	0.000297541	-2.56933	1.41E-05
NM_001003819 /// NM_0C	0.00110773	-2.56968	0.000112429
NM_001015045 /// NM_0C	0.0248591	-2.56976	0.0019299
NM_003012	0.00378275	-2.57452	0.00011459
NM_017633	0.0385296	-2.58067	7.68E-05
NM_001102426 /// NM_0C	0.00961539	-2.58276	0.000865543
NR_038854	0.00241636	-2.59563	5.34E-05
NM_001039210 /// NM_0C	0.00893351	-2.60249	7.77E-05
---	0.00398051	-2.60315	3.03E-06
XR_108755 /// XR_110657	0.00133221	-2.60334	1.88E-05
NM_000611 /// NM_00112	0.00420863	-2.60752	1.24E-05
NM_001145307 /// NM_0C	0.0120613	-2.60864	0.00111323
NM_144653	0.0465689	-2.61154	0.00848512
NM_001969 /// NM_1830C	0.0051714	-2.6191	0.00011993
NM_001122824 /// NM_0C	0.0124609	-2.61958	4.25E-08
NM_000130	0.0267263	-2.62511	0.000625744
NM_015254	0.0114919	-2.63245	0.000649405
NR_001564	0.02612	-2.63685	0.0013639
NM_003079	0.000392276	-2.6371	9.73E-05
NM_001199922 /// NM_01	0.00494102	-2.63724	0.00203778
NM_000813 /// NM_02191	0.0179987	-2.64001	0.00938966
NM_001014979 /// NM_0C	0.0306526	-2.64307	0.00244117
NM_014510 /// NM_03302	0.035616	-2.64545	0.0161402
NM_007231	0.0196991	-2.64765	0.00516841
NM_001077269 /// NM_0C	0.0414693	-2.6501	0.00424409
NM_052929	0.000837951	-2.65631	0.00024625
NM_152517	0.0298479	-2.65969	0.0153386
NM_032606	0.00167317	-2.66027	0.000430781
NR_038199 /// NR_038200	0.000972902	-2.66277	7.25E-05

NM_001039395 /// NM_01	0.00624734	-2.6687	0.00375484
NM_000301 /// NM_00116	0.00994969	-2.66885	0.000458617
NM_016441	0.0102492	-2.67181	0.000215359
NM_017637	0.0038799	-2.68319	0.000316738
NM_006197	0.0285099	-2.68429	0.000695191
NM_001003799 /// NM_00	0.00183597	-2.68533	0.000220236
NM_207361	0.0128581	-2.68703	7.06E-05
NM_207317	0.00242821	-2.68784	0.000246677
NR_029598	0.0303698	-2.69971	0.0192733
NM_001177660 /// NM_00	0.00941352	-2.70221	0.00638033
NM_015687	0.00821967	-2.7089	0.00199869
NM_018672 /// NM_17223	0.00212933	-2.71344	0.000106954
NM_001128166 /// NM_00	0.0295043	-2.71892	0.0001756
NM_001129889 /// NM_00	0.00974221	-2.7366	0.000453927
NM_002612	0.00988604	-2.74059	0.00303132
NM_001996 /// NM_00648	0.00331138	-2.75126	0.000647835
NM_001145678 /// NM_17	0.000605818	-2.75864	0.00015825
NM_000052	0.0326828	-2.7616	0.0130274
NM_001650 /// NM_00402	0.0014983	-2.76213	0.000176097
NM_001252385 /// NM_00	0.00967559	-2.76658	0.00500005
NM_001204087 /// NM_00	0.0120163	-2.76838	0.00290836
NM_001130110 /// NM_01	0.0383273	-2.78419	0.00549803
NM_005801	0.00117396	-2.78552	8.32E-05
NM_000519	0.00424332	-2.79981	0.00194246
NM_001003794 /// NM_00	0.0129039	-2.80885	0.00154537
NM_001169117 /// NM_00	0.00034273	-2.80947	1.25E-06
NM_032269	0.00379675	-2.81194	0.00215773
NM_001256732 /// NM_00	0.00825622	-2.81518	0.00245099
NM_021958	0.028298	-2.82016	0.00635712
NM_016422	0.00011115	-2.82363	2.15E-05
NM_001204126 /// NM_00	0.000210152	-2.82394	5.98E-05
NM_001006641 /// NM_00	0.00181043	-2.83028	1.51E-05
NM_139265	0.00501849	-2.83173	5.14E-05
NM_002269	0.0378815	-2.8332	0.00332278
NM_002185	0.00943708	-2.83422	0.00319312
NM_001145670 /// NM_00	0.0291515	-2.83633	0.00250088
NM_018306	0.000595363	-2.83838	2.64E-05
NM_181426	0.00722633	-2.84441	0.000126199
NM_017637	0.00274599	-2.84535	0.000880937
NM_000878	2.08E-05	-2.84641	2.79E-05
NM_001031737 /// NM_17	0.00461125	-2.84676	6.41E-05
NM_001013676 /// NM_02	0.000303016	-2.86882	4.37E-05
NM_001032282 /// NM_00	0.0396145	-2.87439	0.0017656
NM_016262	0.00803666	-2.87767	0.00588235
NM_001122824 /// NM_00	0.0010784	-2.88073	4.78E-08
NM_001039724 /// NM_00	0.00508191	-2.88525	0.00263463
NM_001135608 /// NM_01	0.0402685	-2.89288	0.00273028

NM_001130159 /// NM_00	0.00456499	-2.90248	0.00210967
NM_032853 /// NR_02424	0.000129613	-2.9032	8.10E-05
NM_001009607 /// NM_00	0.00351253	-2.90567	0.00173373
NM_001100818 /// NM_01	0.0053009	-2.91369	0.00111809
NM_001256054 /// NM_01	0.00101828	-2.91575	0.000788957
NM_000167 /// NM_00112	0.00322117	-2.9168	6.55E-07
NM_000457 /// NM_00103	0.00048928	-2.91817	0.000110972
NM_001136021 /// NM_00	0.00293569	-2.928	2.43E-05
NM_001024683 /// NM_14	0.00220323	-2.92996	0.00297169
NM_001171581 /// NM_00	0.000858676	-2.93026	6.51E-05
NM_001066	0.000345323	-2.93921	0.000573525
NM_001175	0.00140092	-2.94108	0.00214931
NM_001134673 /// NM_00	0.0181315	-2.94696	0.0175473
NM_144965	0.00234123	-2.94736	0.00105662
NM_152572	0.000298359	-2.94925	0.000142115
NM_152519	0.00113734	-2.95148	0.000275563
NM_003884	0.0111061	-2.96145	0.000284311
NM_001007022 /// NM_00	0.0003816	-2.96489	6.71E-06
NM_001142649 /// NM_21	0.000420318	-2.96577	0.00017049
NR_015377 /// NR_047570	0.000700644	-2.97597	5.74E-05
NM_182520	1.96E-06	-2.97823	5.31E-07
NM_001015045 /// NM_00	0.0121261	-2.97912	0.00129819
NM_031437 /// NM_18266	0.023144	-2.99119	0.00190643
NM_015335	0.00754516	-2.99327	0.0059581
NM_145208	5.91E-05	-2.99634	1.94E-05
NM_001166271 /// NM_15	0.00193795	-2.99659	0.00021692
NM_001085399 /// NM_00	0.010774	-3.01618	0.000933156
NM_001136021 /// NM_00	0.0013851	-3.01902	1.20E-05
NM_004786 /// NR_02454	0.00515752	-3.01996	1.38E-06
NM_001199942 /// NM_01	0.000217755	-3.02883	8.37E-05
NM_005228 /// NM_20128	0.00448466	-3.03582	0.000156312
NM_001033578 /// NM_00	0.00685404	-3.04223	0.00176308
NM_000426 /// NM_00107	0.00565174	-3.04494	2.32E-06
NM_001042479 /// NM_00	0.00311048	-3.04686	0.00311775
NM_030666	0.00650493	-3.04938	9.68E-07
NM_001079529 /// NM_00	0.00017506	-3.04956	0.000138
NR_026867	0.0109684	-3.04998	0.000785492
NM_001129993 /// NM_03	0.011193	-3.05924	0.000644653
NM_152704 /// NM_19913	0.00397975	-3.05925	0.000843482
NM_001130957 /// NM_00	0.00830186	-3.07207	0.0106817
NM_001134830 /// NM_00	2.36E-05	-3.08181	1.69E-07
NM_030775 /// NM_03264	1.52E-05	-3.08196	3.26E-05
NM_144644	0.00404509	-3.0831	0.000340853
NM_033124	0.000123891	-3.08596	8.70E-05
NM_022140	0.00259995	-3.10145	0.00512274
NM_014859	0.020009	-3.10382	0.0208398
NM_000668	0.0185201	-3.11793	0.0022059

NM_000601 /// NM_00101	0.00394823	-3.12115	1.69E-05
NM_001267562 /// NM_0	0.0088958	-3.13076	0.00267395
NM_001080394 /// XM_00	4.86E-05	-3.13445	0.000141967
NM_001008534 /// NM_0	0.0112258	-3.13508	0.00386532
NR_003521 /// NR_026589	0.000591117	-3.14262	0.000312748
NM_024882 /// NR_02680	0.00287234	-3.15	0.0064445
NM_001033604 /// NM_0	0.0380569	-3.15085	0.00330918
NM_152632	0.000802097	-3.15375	0.000493507
NM_030666	0.00424478	-3.15464	2.16E-06
NM_004951	0.00304145	-3.16045	0.00353457
NM_000611 /// NM_00112	0.00096279	-3.1758	0.000667196
NM_004980 /// NM_17219	0.000846114	-3.1766	0.000244791
NM_198081	0.000166141	-3.17723	0.000100238
NM_001139466 /// NM_0	0.0232921	-3.17788	0.0364624
NM_001100411 /// NM_02	0.000864397	-3.17794	0.000108671
NM_004155	0.0113908	-3.18038	0.0140242
NM_198275	0.00023492	-3.1998	2.71E-05
NM_000705	0.00376374	-3.20084	0.000139447
NM_058180 /// NM_19907	0.00479704	-3.20865	0.00428441
NM_000926 /// NM_0012	0.0259025	-3.20954	0.0377844
NM_022121	0.0356953	-3.21674	0.0348304
NM_001172420 /// NM_01	0.00446361	-3.22062	3.08E-05
NM_001242702 /// NM_17	0.0217416	-3.22081	0.0153753
NM_033225	0.00138195	-3.22701	0.000146969
NM_001178003 /// NM_14	5.92E-05	-3.22772	2.06E-08
NM_001173461 /// NM_0	0.000107385	-3.22909	7.51E-06
NM_001401 /// NM_05715	0.00374625	-3.2303	2.09E-05
NM_001137550 /// NM_0	0.00195512	-3.23155	0.00243561
NM_138801	0.00528187	-3.23723	0.000758501
NM_020707 /// NR_02775	5.41E-05	-3.239	2.88E-05
NM_017425	0.0392738	-3.24297	3.35E-05
NM_203454	0.00158472	-3.25377	7.56E-05
NM_001010922 /// NM_0	0.0011035	-3.25741	0.00140152
NM_004840	0.00264063	-3.26134	0.000489614
NM_001079530 /// NM_03	4.12E-05	-3.26591	3.37E-05
XM_001716232 /// XM_00	1.79E-05	-3.26749	9.09E-06
NM_018702	0.000109457	-3.26897	5.60E-05
NM_018699	0.0323911	-3.27198	0.000113896
NM_004048	0.013988	-3.27337	0.00857054
NM_001149 /// NM_0012	0.019022	-3.27471	0.0232108
NM_001008710 /// NM_0	0.0100137	-3.2776	0.00288906
NM_181645	0.00168888	-3.28837	0.000674568
NM_021148 /// NM_03354	0.00157171	-3.29685	7.27E-05
NM_001197237 /// NM_0	3.90E-05	-3.29971	9.75E-05
NM_001256370 /// NM_02	0.0088917	-3.30424	0.0217077
NM_033063 /// NM_20757	4.70E-05	-3.30659	2.01E-05
NM_001129889 /// NM_0	3.50E-05	-3.31719	3.59E-05

NM_018010	0.00116117	-3.31723	2.71E-05
NM_002121	9.07E-06	-3.32203	7.73E-06
NM_001011513 /// NM_00	0.0203459	-3.32685	0.000580662
NM_001256536 /// NM_00	0.000708269	-3.33509	0.00116863
NM_001647	0.0030668	-3.33526	0.00020798
NM_007085	0.000355892	-3.33752	0.001463
NM_001100390 /// NM_15	0.00446949	-3.33956	0.0134469
NM_001207062 /// NM_03	0.000873227	-3.34017	3.31E-06
NM_015566 /// NR_046462	0.0149607	-3.34682	0.0221374
NM_001099951 /// NM_00	5.88E-05	-3.34861	2.76E-05
NM_178816 /// NM_20137	0.0045263	-3.35791	9.36E-05
NM_001199739 /// NM_00	0.000141591	-3.35795	7.95E-07
NM_001080463 /// NM_00	0.0330049	-3.36902	0.0109904
NM_000518	0.0145901	-3.37492	0.004776
NM_031442	0.00260268	-3.37879	0.000741198
NM_000416	4.98E-05	-3.38111	3.21E-06
NM_001199377 /// NM_01	0.00202949	-3.38528	8.50E-05
NM_003630	0.0027804	-3.38626	0.00567663
NM_001035230 /// NM_00	0.000832587	-3.38659	0.00243662
NM_003956	0.00214063	-3.3921	0.000404266
NM_031453	0.0453984	-3.39464	0.0313315
NM_004278	3.05E-05	-3.40219	8.21E-05
NM_001178145 /// NM_00	0.00211059	-3.40388	0.00326104
NM_001162997	0.000295133	-3.40432	8.12E-05
NM_014620 /// NM_15363	0.0150421	-3.41035	0.0191084
NM_181726	0.0038657	-3.41118	8.50E-05
NM_144682	0.0335177	-3.41287	0.0358805
NM_001025076 /// NM_00	0.013983	-3.41539	6.84E-05
NM_152765	0.000849764	-3.42442	0.00346325
NM_000512	9.76E-05	-3.42695	0.000302988
NM_001242779 /// NM_00	0.0317056	-3.43849	0.0155649
NM_004166 /// NM_00416	0.00720889	-3.45609	0.00062594
NM_000301 /// NM_00116	0.00155289	-3.45728	0.000151773
NM_001964	0.0247923	-3.45994	0.000316296
NM_001195291 /// NM_00	0.0127545	-3.46945	0.0297
NR_029389 /// NR_029390	0.000654931	-3.47246	0.00322143
NM_012307	2.17E-06	-3.48046	3.57E-07
NM_001034191 /// NM_00	0.00656107	-3.48352	0.00406649
NM_001008781	0.00311046	-3.48437	0.0111454
NM_152376	0.000357613	-3.49372	0.000482243
NM_001039801 /// NM_00	0.0103598	-3.49514	0.0162399
NM_018650	0.00141554	-3.50388	0.000572068
NM_001177704 /// NM_14	4.61E-05	-3.50469	0.000187852
NM_001142314 /// NM_08	0.0011214	-3.50519	0.000501277
NM_017801	0.011319	-3.5113	0.0102829
NM_001969 /// NM_18300	0.00973001	-3.51383	0.0183932
NM_001251977 /// NM_00	0.00359696	-3.53196	0.00186449

NM_015312 /// NM_0322C	0.000415735	-3.5361	0.000672093
NM_001017397 /// NM_0C	0.0243885	-3.54055	0.00229668
NM_001039772 /// NM_0C	0.0419386	-3.54504	0.000174081
NM_001372 /// NM_00466	0.000175006	-3.54821	5.43E-07
NM_005368 /// NM_20337	0.000144167	-3.55225	0.000112826
NM_178816 /// NM_20137	0.000154848	-3.55609	0.000427459
NM_001100397 /// NM_0C	0.00257821	-3.56029	0.000654504
NM_001007022 /// NM_0C	0.00814151	-3.56306	0.00247264
NM_017637	0.0100937	-3.56969	0.0227163
NM_001113178 /// NM_0C	0.0201723	-3.58225	0.025003
NM_021615	0.00557804	-3.58708	0.0021837
NM_001243961 /// NM_0C	0.000259872	-3.59629	0.000388517
NR_029396	0.00112966	-3.59629	4.38E-05
NR_024398	0.000137823	-3.61354	1.35E-05
NM_003894 /// NM_02281	0.00450866	-3.62286	0.000278931
NM_001200049 /// NM_01	6.07E-08	-3.62376	3.39E-08
NM_016608	0.00085506	-3.62992	0.000789793
NM_002734 /// NM_21247	0.000269988	-3.64053	0.000206759
NM_183376	0.0201581	-3.65633	0.00326503
NM_001040113 /// NM_0C	0.00994108	-3.65953	0.00119562
NM_001080836	0.000249789	-3.66065	4.68E-05
NM_001033024 /// NM_0C	1.74E-05	-3.66445	0.000215923
NM_006255	0.0020497	-3.66812	0.0112418
NM_001204197 /// NM_01	0.00864645	-3.66881	3.84E-07
NM_016010	0.00493807	-3.66998	0.000297791
NM_001143676 /// NM_0C	0.0138485	-3.68213	0.0013566
NM_000813 /// NM_02191	0.00264215	-3.68318	0.00356944
NM_006762	0.0111879	-3.68501	0.0184213
NM_021179	0.0247234	-3.68944	4.59E-05
NM_001199149 /// NM_0C	0.0141214	-3.68965	0.0333333
NM_015896	0.00123314	-3.69089	0.00511284
NM_001178044 /// NM_0C	0.00945536	-3.69359	0.0088899
NM_025055 /// NM_18279	7.42E-06	-3.70033	2.32E-06
NM_001165 /// NM_18296	0.0299424	-3.70181	1.05E-05
NM_001767	0.00191039	-3.7071	0.00603769
NM_001080556 /// NM_14	0.00138298	-3.712	8.72E-05
NM_001173463 /// NM_0C	0.00497476	-3.71624	3.82E-06
NM_001161661 /// NM_0C	0.00128661	-3.71684	0.00103746
NR_024461 /// NR_024462	0.00881733	-3.72767	0.0175482
NM_001242359 /// NM_01	0.00479063	-3.73799	0.00942075
NM_001193300 /// NM_0C	0.0142174	-3.74026	0.0351122
NM_000814 /// NM_0011S	0.000198683	-3.74847	2.07E-05
NM_001134830 /// NM_0C	0.000369873	-3.75242	0.000149332
NM_001007022 /// NM_0C	0.00450849	-3.75487	0.000341879
NM_014433	0.000597239	-3.76579	8.13E-05
NM_001253835 /// NM_0C	1.30E-05	-3.77893	4.36E-06
NM_000880 /// NM_0011S	0.00377308	-3.78221	1.56E-06

NM_001146694 /// NM_00	2.74E-05	-3.78383	0.0001478
NM_001010922 /// NM_00	6.42E-05	-3.78755	5.56E-06
XR_039953 /// XR_039955	0.00108855	-3.78984	2.88E-05
NM_001161572 /// NM_00	0.00614284	-3.79587	0.000336678
NR_038244 /// NR_038245	0.00192196	-3.80404	0.000668548
NM_001134649 /// NM_00	0.00505014	-3.8134	0.0244049
NM_022128	0.0021416	-3.81647	0.00661999
NM_000328 /// NM_00102	0.0154027	-3.81725	0.0392009
NM_153838	0.0108547	-3.81755	0.0108156
NM_152357	0.00336564	-3.82066	0.00163243
NM_054017 /// NR_02681	0.00151254	-3.82821	9.23E-05
NM_152511	0.00180342	-3.84185	0.000163325
NM_001964	0.0156642	-3.84403	8.92E-07
NM_001142315 /// NM_00	0.0164218	-3.84569	0.0352312
NM_001018046 /// NM_02	0.000154019	-3.86003	0.00012962
NM_173528	0.000612077	-3.86005	7.13E-05
NM_152550	0.0022749	-3.86274	0.00182443
NM_001143943 /// NM_03	0.0305517	-3.86321	0.00654536
NM_001161575 /// NM_01	4.79E-06	-3.87237	5.68E-07
NM_020817	0.00179929	-3.87281	0.0002602
NM_014510 /// NM_03302	0.00244303	-3.88575	0.00047226
NM_025228	0.000293792	-3.89512	0.000839743
NM_033063 /// NM_20757	4.63E-05	-3.8998	2.72E-06
NM_001100590 /// NM_01	0.00158276	-3.90781	0.00894831
NM_001223 /// NM_00125	0.000115027	-3.91012	0.000582117
NM_001039940 /// NR_01	0.00680392	-3.91527	0.000583579
NM_006981 /// NM_1731	0.00123657	-3.93549	0.000178151
NM_001172420 /// NM_01	0.000423173	-3.93725	0.00346757
NM_001204126 /// NM_00	0.000420319	-3.93902	0.000379478
NM_016010	0.0034536	-3.95383	0.00722535
NM_152696 /// NM_18135	2.69E-05	-3.95853	3.32E-06
NM_152519	0.00291701	-3.96173	4.50E-05
NM_001039350 /// NM_00	1.93E-05	-3.9661	0.000268673
NR_033852	0.000649266	-3.97421	0.00381958
NM_006988	0.00477187	-3.99349	0.00551778
NM_173496	0.00996594	-3.9945	0.0472841
NM_153606	0.000413434	-3.99712	8.10E-05
NM_024763 /// NM_20701	0.00439377	-3.99745	0.002315
XR_109003 /// XR_111042	5.25E-05	-4.00473	0.000362208
NR_038366 /// NR_038367	0.047945	-4.01447	0.00193089
XR_108924 /// XR_113209	0.000137848	-4.01881	1.33E-06
NM_000508 /// NM_02187	0.00332756	-4.02066	0.000891281
NM_018952 /// NM_15603	0.0375519	-4.02514	0.00658601
NM_001199096 /// NM_00	1.90E-05	-4.02637	9.47E-05
NM_021199	0.00100131	-4.02843	3.57E-05
NM_207307	0.00213771	-4.03458	0.00160178
NM_001134435 /// NM_03	0.0217994	-4.03818	0.000243271

NM_001007224 /// NM_00	0.000848599	-4.03941	0.00566033
NM_001040092 /// NM_00	0.0018771	-4.03981	0.000276799
NM_001031804 /// NM_00	0.000240587	-4.04146	0.000477452
NM_001030287 /// NM_00	0.000173567	-4.04687	0.00118708
NM_001082537 /// NM_00	1.97E-05	-4.06342	2.13E-05
NM_002163	0.000280131	-4.06471	0.000554786
NR_038897	0.00498786	-4.07033	0.011337
NM_024633 /// NR_02677	0.00759523	-4.07282	0.0194724
NM_001206960 /// NM_00	0.00180835	-4.07635	0.00375501
NM_018409	0.00593832	-4.09675	0.00138488
NM_006531 /// NM_1756	4.69E-05	-4.10484	1.15E-05
NM_000204	0.00177877	-4.10727	2.16E-05
NM_001736	2.93E-05	-4.11051	3.87E-06
NM_022785 /// NM_19885	3.15E-06	-4.11285	5.22E-07
NM_017434 /// NM_17594	0.00504833	-4.11949	0.00798345
NM_001126328 /// NM_03	0.0117871	-4.13137	0.0468996
NM_001014440	9.89E-06	-4.13357	3.10E-05
NM_001195683 /// NM_00	0.0068883	-4.14628	0.00766548
NM_032853 /// NR_02424	0.00262557	-4.14642	0.00396288
NM_138796	0.0273343	-4.14644	0.00123497
NM_006564	0.00240549	-4.14822	0.000726243
NM_032133	7.81E-05	-4.16062	8.73E-05
NM_000248 /// NM_00118	0.0183501	-4.16517	0.000773652
NM_005195	0.00118888	-4.16947	0.0027669
NM_001025076 /// NM_00	0.000168216	-4.17211	0.0034968
NM_001025194 /// NM_00	0.00143876	-4.17721	0.000399282
NM_178824	0.00166726	-4.17795	0.00181512
NM_001135099 /// NM_00	0.00427933	-4.18107	0.000323968
NM_000596 /// NM_00101	0.000397351	-4.18808	3.76E-05
NM_005668 /// NM_17505	0.00302595	-4.19683	0.00167188
NM_173554	0.00563538	-4.20916	0.000500207
XR_109642 /// XR_112116	0.00104287	-4.21005	0.000268213
NR_002819 /// XR_110915	0.00239333	-4.21338	0.019941
NM_001168499 /// NM_01	3.61E-05	-4.22583	0.000124703
NM_005611	2.69E-05	-4.2301	6.60E-05
NM_175900	0.00263091	-4.23259	0.00108411
NM_001163417 /// NM_00	0.00252009	-4.2336	0.0139
NM_020307	0.00185241	-4.2411	0.0068424
NM_006269	0.000437974	-4.24321	8.52E-05
NM_005544	0.00218874	-4.24731	0.00284154
NM_001177701 /// NM_00	7.98E-06	-4.25722	1.26E-05
NM_033027	0.00226471	-4.26077	0.000343716
NM_001144763 /// NM_00	8.06E-06	-4.27037	0.000147844
NM_000301 /// NM_00116	4.58E-05	-4.27732	7.87E-06
NM_145053	4.07E-06	-4.27899	0.000104821
NM_014648	0.00204576	-4.28227	0.00029375
NM_000130	0.00258617	-4.28251	0.000106146

NM_014365	7.15E-05	-4.28681	3.08E-06
NM_001243965 /// NM_00	0.0318305	-4.31677	0.0197362
NM_001100396 /// NM_17	6.79E-08	-4.32014	7.98E-07
NM_001256113 /// NM_17	0.000416623	-4.32357	7.75E-06
NM_002032	0.00754486	-4.33418	0.039198
NM_004787	0.0100181	-4.34279	0.0190241
NM_001135598 /// NM_15	0.00568462	-4.34445	0.010658
NM_001130142 /// NM_01	0.000705083	-4.34749	4.42E-05
NM_002966	0.00847192	-4.34806	1.62E-05
NM_001127391 /// NM_13	0.00285967	-4.35209	0.00100155
NM_001098504 /// NM_00	0.00551148	-4.35362	0.00102084
NM_001194999 /// NM_00	0.000441865	-4.35844	0.00155664
NM_001039570 /// NM_03	0.000696121	-4.36018	0.00572805
NM_016441	0.013683	-4.36385	0.026032
NM_004841 /// NM_17069	0.000741931	-4.36991	0.00671701
NM_020980	0.000176838	-4.37247	0.00173405
NR_046241	0.000743327	-4.38519	0.00321328
---	0.000568013	-4.38789	0.000489016
NM_001040712 /// NM_00	0.00659747	-4.39742	0.00657142
NM_001079529 /// NM_00	0.000227811	-4.39869	8.43E-05
NM_001122769 /// NM_18	0.000734562	-4.40031	7.21E-06
NM_001243093 /// NM_00	0.000221426	-4.40242	6.64E-05
NM_017439	0.00544977	-4.40343	0.0022404
NM_001199640 /// NM_00	0.00046527	-4.40531	5.37E-08
NM_001130159 /// NM_00	7.92E-05	-4.40545	0.0017668
NM_006682	0.00585273	-4.41054	0.0064113
NM_001243965 /// NM_00	0.0223145	-4.41088	0.0116216
NM_004344	0.00275518	-4.42394	0.000540416
NM_004538	0.000410356	-4.43366	0.00842909
NM_001018039 /// NM_00	0.00210709	-4.4344	5.59E-05
NM_018168	0.0107874	-4.4398	8.43E-08
NM_014887 /// NM_03311	0.00118353	-4.44934	0.00155703
NM_001127391 /// NM_13	0.000412616	-4.45328	0.000396085
NM_001130156 /// NM_00	0.00579406	-4.46711	0.0218211
NM_001099289	0.000546782	-4.46982	0.00138534
NM_001105659 /// NM_14	3.93E-06	-4.47073	0.000277334
NR_003521 /// NR_026589	0.00219101	-4.47254	0.00845802
NM_001139490 /// NM_01	0.00133672	-4.48158	0.00113077
NM_138444	0.0426204	-4.48217	0.00336347
NM_024806 /// NM_19912	0.000123573	-4.48888	5.05E-05
NM_181644	0.00164057	-4.49092	0.00458706
NM_000109 /// NM_0040	0.00873171	-4.49839	7.05E-07
NM_015566 /// NR_04646	0.0042281	-4.50888	0.0152266
NM_005544	0.040968	-4.5134	0.0339986
NM_001145313 /// NM_03	0.0141924	-4.51538	0.00144847
NM_182493	8.30E-06	-4.51563	8.76E-08
NM_138788	0.000107587	-4.52313	0.00029853

NM_152704 /// NM_19913	0.00214423	-4.52423	0.000154216
NM_001039348 /// NM_0C	0.0293705	-4.52677	6.41E-05
NM_019073	0.0109566	-4.53936	0.0010202
NM_001145670 /// NM_0C	0.000447981	-4.54006	0.000864111
NM_001077416 /// NM_0C	0.00392957	-4.54508	5.67E-05
NM_001135863 /// NM_0C	2.49E-05	-4.54881	0.000351053
NM_001163075	1.97E-05	-4.5707	0.000468791
NM_001170690 /// NM_02	0.000703496	-4.57132	9.16E-05
NM_052904	0.0025414	-4.57474	0.00020211
NM_001202550 /// NM_18	4.59E-05	-4.57483	0.000774529
NM_001199397 /// NM_0C	0.00436131	-4.58074	0.00418935
NM_001268	0.0048873	-4.59453	0.034623
NM_139265	0.000122365	-4.5972	1.02E-05
NM_001079533 /// NM_0C	2.18E-05	-4.59812	1.35E-07
NM_001003792 /// NM_0C	0.00986927	-4.60167	0.000177592
NM_001012988 /// NR_02	0.00266927	-4.60399	0.0308087
NM_033058 /// NM_18408	0.0344661	-4.60482	0.000311009
NM_005634	0.00129238	-4.61092	2.17E-05
NM_004787	0.00217239	-4.61422	0.0141767
NM_144648	0.000618674	-4.61467	0.000836491
NM_013343 /// NR_02406	0.00562057	-4.62091	0.0031258
NM_001040113 /// NM_0C	0.00106682	-4.62527	0.00314341
NM_001100590 /// NM_01	0.00234087	-4.62842	0.0121944
NM_001039704 /// NM_0C	6.72E-05	-4.62889	3.47E-06
NM_020802	0.000807606	-4.6441	1.68E-05
NM_001135217 /// NM_0C	0.00128545	-4.65049	0.000149798
NM_000081 /// NM_0010C	0.00527437	-4.65752	0.00518535
NM_001145951 /// NM_0C	0.000360419	-4.6587	0.00614451
NM_173354	0.0186595	-4.67151	0.00184981
NM_144992	0.000575529	-4.67589	2.60E-05
NM_001256295 /// NM_0C	9.73E-05	-4.69101	2.87E-07
NM_025159	4.56E-06	-4.69767	0.000402758
NM_001153	0.000889361	-4.71763	0.0184164
---	2.20E-05	-4.7197	4.31E-07
NM_152290	0.000109205	-4.7258	9.34E-06
NM_001198625 /// NM_0C	8.82E-05	-4.74991	2.06E-07
NM_001190458 /// NM_0C	0.0023706	-4.75442	0.0138735
NM_001037763	0.00113925	-4.76204	0.00462377
NM_002228	0.00337577	-4.76249	0.0371813
NM_001243115 /// NM_02	1.86E-05	-4.76913	2.30E-05
NM_001077204 /// NM_02	0.00014263	-4.76966	0.00251606
NM_178827	5.04E-05	-4.77658	3.30E-05
NM_001202233 /// NM_0C	0.00100318	-4.79102	0.00191128
NM_001013706	2.03E-06	-4.8072	5.32E-05
NM_001334	0.004717	-4.81126	0.000273768
NM_006633	0.000554563	-4.82025	0.00566488
NM_000476	0.0010715	-4.82172	7.47E-05

NM_014648	0.000732112	-4.82767	1.79E-05
NM_005112 /// NM_01749	0.000148107	-4.82951	0.00070615
NM_007050 /// NM_13317	0.000439522	-4.85087	0.00454172
NM_014549 /// NR_003714	0.00465514	-4.85284	0.0120334
NM_003462	0.024494	-4.85724	0.000691366
NM_025145	0.000922987	-4.85748	8.14E-05
NM_001001710	0.0013085	-4.8582	0.02541
NM_182628	0.00296713	-4.86484	0.000117209
NM_000348	4.72E-05	-4.88426	1.46E-05
NM_001198974 /// NM_20	0.000344635	-4.88696	0.00995334
NM_001114357	0.000311083	-4.88886	6.30E-06
NM_004120	0.000165584	-4.90185	0.000179444
NM_001122842 /// NM_00	0.00055417	-4.90764	9.56E-06
NM_002532	0.000507381	-4.91971	0.00110595
NM_001130046 /// NM_00	0.0120346	-4.91989	0.010802
NM_017439	0.00255228	-4.94463	0.00269797
NM_001127364 /// NM_00	0.000820982	-4.954	0.000315707
NM_002229	0.000202334	-4.96489	0.000139706
NM_000814 /// NM_00119	9.00E-05	-4.96628	1.01E-05
NM_173500	0.0019169	-4.97612	0.000173886
NM_015653	0.00889078	-4.97825	0.00180413
NM_145911	0.000154028	-4.98241	5.24E-05
NR_002798	0.000115006	-4.98982	8.81E-05
NM_001025436 /// NM_02	8.07E-06	-5.0083	9.55E-07
NM_022128	0.0049274	-5.01675	0.0160084
NM_001199880 /// NM_00	0.0422614	-5.02108	5.07E-06
NM_001206	0.00975839	-5.02289	0.015092
NM_001130518 /// NM_01	0.002211	-5.03631	0.000803956
NM_015347	0.000267401	-5.03841	0.00023689
NM_001001344 /// NM_02	0.000150803	-5.03962	0.00621483
NM_005516	0.000303639	-5.04804	0.0117163
NM_001280 /// NR_023312	6.74E-06	-5.04806	9.14E-05
NM_001010940	1.98E-05	-5.04922	9.98E-07
NM_001079821 /// NM_00	0.00846959	-5.05743	0.0271229
NM_001039799 /// NR_044	2.12E-07	-5.07092	8.64E-09
NM_144980	0.00117917	-5.08544	1.55E-06
NM_144975	2.39E-07	-5.09334	8.68E-05
NM_001029996	3.83E-05	-5.09559	0.000166108
NM_001033719	0.00552869	-5.10441	0.0217027
NM_001198625 /// NM_00	0.00108644	-5.10812	0.000776271
NM_001115	0.00363074	-5.12638	0.0129293
NM_001253854 /// NM_00	0.000462172	-5.1353	4.55E-05
NM_021784 /// NM_15367	0.000507499	-5.14251	3.68E-06
NM_033049	2.54E-06	-5.14593	2.14E-07
NM_000518	0.00464053	-5.14989	0.00501718
NM_021244	0.00778591	-5.15983	0.000601234
XR_110029 /// XR_133336	0.000509785	-5.1691	7.56E-05

NM_001143943 /// NM_03	0.010877	-5.20251	0.00283349
NM_001170538 /// NM_17	0.000608971	-5.20443	5.86E-06
NM_001111298 /// NM_17	0.0035917	-5.20746	0.000425257
NM_001242463 /// NM_05	0.0190955	-5.20912	0.00818638
NM_001025158 /// NM_00	4.89E-05	-5.23791	0.000252727
NM_001135608 /// NM_01	6.39E-05	-5.23951	0.00289677
NM_020643	1.45E-05	-5.24222	6.85E-05
NM_001190981 /// NM_00	7.89E-05	-5.24358	2.02E-06
NM_014331	0.00950634	-5.24409	0.000565266
NM_014312	0.000267384	-5.24596	0.00120336
NM_198493	0.000984614	-5.25696	0.000210136
NM_001004303	7.30E-06	-5.26	2.12E-06
NM_001105248 /// NM_00	0.000756173	-5.27187	0.000173885
NM_024764	0.000622845	-5.29344	0.0191701
NR_027105 /// NR_027106	0.007466	-5.30078	0.00106454
NM_001243848 /// NM_00	0.0046195	-5.30562	0.00524105
NM_001136020 /// NM_00	5.77E-09	-5.31628	6.52E-08
NM_001014986 /// NM_00	0.00156039	-5.32451	0.0056952
NM_001165963 /// NM_00	0.00260785	-5.33904	0.000446094
NR_004428	0.00722085	-5.34236	0.0302119
NM_025059	0.000620275	-5.34311	0.000750364
NM_001145313 /// NM_03	0.000428908	-5.34432	1.14E-05
NM_003853	0.00143847	-5.34758	0.00586326
XM_003403521 /// XM_00	0.00104659	-5.35234	0.000181694
NM_001134285 /// NM_00	0.000588726	-5.35616	0.0017975
NM_006408	0.000647935	-5.35983	2.25E-05
NM_018430	0.0003474	-5.38496	0.00058328
NR_003003	0.00232105	-5.40097	0.024489
NM_145020	0.000360031	-5.40987	1.30E-05
NM_004914	1.42E-07	-5.42467	1.54E-06
NM_015689	0.000118019	-5.42731	0.000118217
NM_006144	0.000265617	-5.43601	0.000325809
NM_001008539 /// NM_00	0.00140742	-5.43948	1.51E-08
NM_001102406 /// NM_00	6.51E-05	-5.44016	8.71E-05
NM_001134486 /// NM_05	0.00442711	-5.44263	0.0380487
NM_005013	0.0308436	-5.45252	0.0232975
NM_001130067 /// NM_01	0.00174365	-5.4671	0.000462761
NR_002174 /// NR_027626	0.000859072	-5.47354	0.000802378
NM_130446	1.26E-05	-5.47552	1.82E-05
NM_001098504 /// NM_00	0.00657283	-5.47675	0.00519342
NM_001099691 /// NM_00	0.00280448	-5.48538	0.00193834
NM_001040428 /// NM_01	0.00621799	-5.49527	0.0225875
NM_001099267 /// NM_00	0.000132947	-5.50108	5.50E-05
NM_006162 /// NM_17238	0.000246279	-5.51283	0.00794414
NM_020546	0.00184036	-5.51734	0.000141189
NM_001130182 /// NM_00	0.00291859	-5.51875	2.22E-05
NM_001280 /// NR_02331	1.69E-06	-5.5251	8.59E-06

NM_001243961 /// NM_00	0.00581218	-5.52644	0.00417962
NM_000246	6.90E-05	-5.53138	0.00277493
NM_001263	8.64E-05	-5.54058	0.000719274
NM_001161725 /// NM_00	0.000959167	-5.54285	0.00708675
NM_198520 /// XM_00171	0.00200182	-5.5431	2.64E-05
NM_001199805 /// NM_00	2.30E-06	-5.54685	0.000346706
NM_000301 /// NM_00116	0.000764418	-5.5663	2.68E-05
NM_018168	0.00257563	-5.59001	6.91E-08
NM_000814 /// NM_00119	0.000870233	-5.59069	6.32E-05
NM_000081 /// NM_00100	1.18E-05	-5.59524	0.000633885
NM_001001551 /// NM_00	0.00040087	-5.60619	0.00413702
NM_001102406 /// NM_00	3.18E-06	-5.61726	0.000169273
NM_001098515 /// NM_14	3.17E-06	-5.61828	0.00081076
NM_001178096 /// NM_00	0.00238816	-5.62334	0.000464495
NM_003012	0.000296682	-5.65041	1.19E-06
NM_001145399 /// NM_00	0.00294964	-5.65437	0.0418079
NM_005577	0.00418844	-5.67634	0.000452798
NM_003182 /// NM_01399	0.0185549	-5.69232	0.00319295
NM_054114 /// NM_13881	0.000692604	-5.70746	0.000805627
NM_003777	7.94E-07	-5.74836	8.94E-07
NM_001195415 /// NM_00	0.000649966	-5.75752	0.000582025
NM_001003799 /// NM_00	1.39E-05	-5.76143	1.51E-05
NM_001130831 /// NM_00	0.000228565	-5.76764	6.26E-05
NR_046102 /// XM_933872	0.00189241	-5.79165	0.000505536
NM_000933 /// NM_00117	0.00453076	-5.79639	0.00536709
NM_017590	0.000123797	-5.80309	0.00803712
NM_000720 /// NM_00112	6.01E-06	-5.83835	0.000104439
NM_002753 /// NM_13898	2.81E-05	-5.84239	6.78E-06
NM_021244	0.0282378	-5.84291	0.00140781
NM_145756	0.000265617	-5.84894	0.000725707
NM_174921	0.000139978	-5.87923	0.00213052
NM_001104629 /// NM_01	1.81E-05	-5.88792	0.000112717
NM_007116 /// NM_01910	0.000200396	-5.9039	4.12E-05
NM_178821	0.000777094	-5.92402	4.37E-05
NM_004155	4.11E-06	-5.9273	1.73E-06
NM_004529	0.000131277	-5.93034	1.57E-05
NM_153236	6.76E-06	-5.93344	1.11E-05
NM_001243961 /// NM_00	5.13E-06	-5.95048	1.55E-05
NM_001009991 /// NM_00	0.000284387	-5.95843	0.00041191
NM_004928	9.49E-07	-5.97752	0.000538943
NM_001223 /// NM_00125	1.14E-06	-5.99441	3.70E-05
NM_001159322 /// NM_00	8.18E-06	-5.99645	1.01E-05
NM_152772	0.00105898	-6.00294	0.00483128
NM_002984	1.07E-05	-6.01306	1.63E-05
NM_001001870 /// NM_03	2.01E-05	-6.02452	9.27E-07
NM_001198559 /// NM_01	3.46E-06	-6.04212	0.000241786
NM_007018	0.000115872	-6.04292	7.43E-06

NM_001190201 /// NM_00	7.73E-07	-6.05325	6.05E-07
NM_001242466 /// NM_18	0.00176049	-6.05958	0.0259266
NM_001162995 /// NR_015	6.59E-07	-6.07166	2.06E-05
NM_001031715 /// NM_02	0.00166765	-6.07213	4.36E-05
NM_023067	0.00283258	-6.07928	0.0301919
NM_021179	0.0111343	-6.08819	5.13E-05
NM_002970 /// NR_027783	3.34E-07	-6.09032	5.50E-06
NM_172069	0.00382923	-6.09141	0.000833211
NM_000636 /// NM_00102	0.0123088	-6.09667	0.00457304
NM_002864	2.51E-05	-6.10775	1.25E-05
NM_001002294 /// NM_00	4.78E-06	-6.11156	1.04E-06
NM_001204087 /// NM_00	4.56E-06	-6.11375	0.00215298
NM_005195	0.000262881	-6.13322	0.0013861
NM_001243280 /// NM_00	0.0192131	-6.13397	0.0289767
NM_004975	0.000981399	-6.15255	0.0321825
NM_000087 /// NM_00114	3.64E-06	-6.159	2.29E-05
NM_021101	0.00227907	-6.16281	0.00035475
NM_001078 /// NM_00119	0.0220099	-6.16839	0.000906967
NM_003619	0.00201383	-6.16977	3.41E-05
NM_002259 /// NM_00226	4.91E-05	-6.19084	1.25E-06
NM_152643	3.32E-07	-6.20708	3.47E-07
NM_004420	3.60E-05	-6.22377	0.00363493
NM_001142462 /// NM_05	0.0109399	-6.27368	0.0028817
NR_001564	0.0103542	-6.30367	0.00125762
NM_001040280 /// NM_00	0.00026411	-6.3039	7.32E-06
NM_001267048 /// NM_00	0.0212537	-6.3162	0.0483302
NM_178527	0.000183459	-6.31871	6.15E-06
NM_001756	3.89E-05	-6.32156	2.31E-05
NM_000892	0.000247453	-6.33372	0.000557259
NM_013262	0.000805201	-6.34818	0.0221915
NM_015675	0.000977817	-6.34899	0.00981342
NM_001031745 /// NM_00	4.72E-05	-6.35907	1.71E-05
NM_022785 /// NM_19885	3.71E-05	-6.37722	9.03E-06
NM_145047 /// NM_20683	0.000916127	-6.38992	0.0225337
NM_030666	6.69E-08	-6.39749	7.94E-07
NM_001014986 /// NM_00	0.000227376	-6.39986	0.00439886
NM_001242350 /// NM_00	1.67E-07	-6.40309	1.62E-07
NR_002819 /// XR_110915	0.000145618	-6.40314	0.0172489
NM_152701	0.000587293	-6.4179	1.75E-05
NM_000609 /// NM_00103	0.00126344	-6.43135	4.49E-05
NM_001099267 /// NM_00	1.86E-05	-6.45461	1.57E-07
NM_144992	0.000180517	-6.47126	2.51E-05
NM_007037	5.85E-07	-6.48673	9.17E-06
NM_000856 /// NM_00113	0.000276251	-6.51278	9.86E-06
NM_005618	0.00281377	-6.53253	0.0114133
NM_002581	0.00248966	-6.53397	0.000437903
NM_018076	0.00348075	-6.53445	8.16E-06

NM_001127608 /// NM_00	5.81E-06	-6.5351	0.00213401
NM_014395	2.12E-09	-6.53973	4.62E-06
NM_001270391 /// NM_00	1.15E-05	-6.54251	1.32E-07
NM_003320 /// NM_17797	0.000509948	-6.54857	0.0117307
NM_031490 /// NR_04067	1.73E-06	-6.55714	0.000204493
NM_001033659 /// NM_00	0.00152329	-6.56694	0.0186456
NM_001122769 /// NM_18	0.000556567	-6.56912	0.00105189
NM_001243797 /// NM_00	0.000409307	-6.59297	0.000555192
NM_174896	2.25E-05	-6.61814	0.00718602
NM_001164407	0.00107983	-6.62037	0.00282217
NM_001242524 /// NM_00	7.99E-05	-6.62074	6.01E-05
NM_001256552 /// NM_02	1.16E-07	-6.63141	4.48E-05
NM_001206609 /// NM_00	5.50E-08	-6.63783	4.02E-06
NM_017539	0.000199545	-6.66492	4.70E-05
NM_001253835 /// NM_00	5.66E-05	-6.68502	0.000198292
NM_002937 /// NM_19443	3.31E-05	-6.6881	0.000291652
NM_001130715 /// NM_00	0.00133595	-6.74603	2.10E-06
NM_007116 /// NM_0191	3.15E-05	-6.75806	8.18E-05
NM_006955	3.55E-06	-6.7602	0.000508887
NM_012307	0.000445881	-6.7709	9.49E-05
NM_152377	6.55E-05	-6.77116	6.20E-07
NM_014203 /// NM_13078	0.000343588	-6.78374	0.0064001
NM_145172	0.00145927	-6.78542	9.11E-06
NM_001130918 /// NM_17	2.05E-05	-6.82071	2.71E-06
NM_001164342 /// NM_00	6.25E-05	-6.83161	0.0141681
NM_001122824 /// NM_00	0.000166787	-6.83438	3.89E-05
NM_052863	0.00181971	-6.84023	0.0160659
NM_001184879 /// NM_00	2.45E-05	-6.85153	0.00306037
NM_000313	0.0076936	-6.85305	0.0336922
NM_001031741 /// NM_15	1.02E-05	-6.85413	1.58E-05
NM_152271	1.61E-05	-6.85792	8.10E-05
NM_001010848 /// NM_00	0.000352596	-6.8723	0.000143549
NM_001099267 /// NM_00	0.000511873	-6.89266	8.14E-08
NM_002581	0.0254171	-6.89681	0.00493725
NM_003948	0.00106683	-6.90512	0.0157673
NM_001004416 /// NM_00	0.000464768	-6.91989	0.000115634
NM_001034850 /// NM_01	0.00175417	-6.93	0.0032106
NM_001144382 /// NM_01	0.000645371	-6.93481	0.000146518
NM_001256295 /// NM_00	3.19E-07	-6.94979	2.50E-07
NM_033124	0.000137115	-6.95492	3.32E-05
NM_000218 /// NM_18179	1.38E-08	-6.97664	8.23E-05
NM_001168374 /// NM_00	9.86E-06	-6.9949	6.17E-07
NM_001122834 /// NM_00	2.31E-05	-7.00114	0.000281356
NR_038311 /// NR_038312	0.000120721	-7.00528	0.00813951
NM_145740	2.84E-05	-7.03298	7.27E-05
NM_001029875	1.00E-06	-7.03534	8.10E-08
NM_001243848 /// NM_00	0.00454913	-7.04702	0.00657549

NM_013367	0.000290644	-7.04819	0.0014394
NM_007116 /// NM_0191	2.69E-05	-7.05831	8.62E-05
NM_001220765 /// NM_00	0.002131	-7.07456	0.0300976
NM_003734	0.000298491	-7.09585	0.0222615
NM_001077416 /// NM_00	0.000336895	-7.11867	8.57E-06
NM_015417	9.18E-05	-7.12947	0.000816937
NM_153274	0.0017085	-7.18313	0.00783475
NM_022570 /// NM_19794	5.97E-06	-7.19153	0.000857727
NM_012472	0.000519042	-7.19335	0.0171137
NM_001197295 /// NM_00	0.000322244	-7.19564	0.00286542
NM_000044 /// NM_00101	0.000100589	-7.20021	0.00351045
NM_002985	9.67E-06	-7.21984	0.000821151
NM_001039706 /// NM_00	6.91E-05	-7.24371	7.68E-05
NM_003246	0.000703866	-7.2513	0.0037798
NM_015202	1.96E-06	-7.28771	0.000130899
NM_001039948 /// NM_00	8.11E-06	-7.29193	3.45E-06
NM_004058 /// NM_08059	0.0116539	-7.30487	0.00767003
NM_005847 /// NM_15268	0.00143407	-7.3218	0.0023194
NR_001298	1.93E-05	-7.35774	0.000227348
NM_001009991 /// NM_00	3.50E-08	-7.37057	1.54E-05
NM_004288	0.000304692	-7.40166	0.00830185
NM_002919 /// NM_13442	0.00236768	-7.40225	0.00114519
NM_000635 /// NM_13443	0.000829277	-7.40233	1.55E-05
NM_001199739 /// NM_00	4.28E-06	-7.41416	2.30E-06
NM_198282	1.32E-05	-7.41975	2.81E-05
NM_016270	1.44E-05	-7.42316	1.58E-05
NM_001201466 /// NM_03	2.94E-06	-7.42559	1.21E-06
NM_005727	0.00123627	-7.43629	0.0105965
NM_017699	5.05E-06	-7.43751	4.60E-08
NM_001039706 /// NM_00	2.71E-05	-7.4469	0.00185413
NM_018222	1.15E-06	-7.45192	0.000125391
NM_002985	7.44E-05	-7.46459	0.00147074
NM_018897	2.22E-06	-7.46587	1.42E-06
NM_001370 /// NM_17364	0.000211815	-7.46769	1.34E-05
NM_001025076 /// NM_00	0.000353146	-7.46918	0.000221836
NM_000720 /// NM_00112	7.45E-05	-7.5016	0.00163536
NM_006408	0.00326004	-7.51037	7.37E-08
NM_058180 /// NM_19907	0.00176094	-7.51893	0.00583408
NM_001161661 /// NM_00	0.000196344	-7.52512	0.00905524
NM_001134649 /// NM_00	0.00198616	-7.54862	0.0282364
NM_001001437 /// NM_00	0.000679056	-7.55377	0.000747315
NM_130446	2.45E-06	-7.55487	1.35E-05
NM_000855 /// NM_00125	0.000451399	-7.5579	5.58E-05
NM_001134363	0.000636723	-7.55977	3.58E-05
XR_040780	1.30E-05	-7.57129	7.24E-06
NM_144702	3.98E-06	-7.5832	1.30E-07
NM_000833 /// NM_00113	0.00252652	-7.5878	0.0386345

NM_001470 /// NM_00639	0.00564045	-7.6113	0.0438321
NM_001460	0.016143	-7.63329	0.0394321
NM_000847	1.57E-06	-7.63426	2.13E-07
NM_030906	0.000205467	-7.67853	2.82E-06
NM_001025081 /// NM_00	0.000822197	-7.68541	0.00420404
NM_015512	5.00E-05	-7.69301	0.000982024
NM_025057	0.00101255	-7.69324	0.000951393
NM_001039936 /// NM_00	0.00117187	-7.69936	0.000736467
NM_014395	8.45E-06	-7.71739	0.000201919
NM_012337	0.0015375	-7.73044	2.62E-05
NM_013308	0.000832605	-7.73066	0.00141214
NM_001145365 /// NM_01	0.000715293	-7.76748	0.0336268
NM_145045	0.000176067	-7.77734	0.0298979
NM_001920 /// NM_13350	0.00131874	-7.81523	0.00882708
NM_002185	0.000109863	-7.82528	5.75E-06
NM_001270391 /// NM_00	1.22E-06	-7.84599	3.01E-07
NM_014861	4.22E-06	-7.85372	9.88E-06
NM_001199633 /// NM_02	3.25E-05	-7.85924	7.40E-05
NM_004751	5.40E-06	-7.88014	4.36E-05
NM_001267048 /// NM_00	0.00797869	-7.88468	0.0174149
NM_020957	0.0003204	-7.89211	0.0311343
NM_153267	9.40E-05	-7.90797	6.19E-06
NM_006063	0.000885156	-7.98559	0.0107881
NM_001127603 /// NM_01	6.55E-05	-7.99949	0.0196598
NM_024753 /// NR_04537	2.83E-05	-8.00715	8.76E-05
NM_021201 /// NM_20693	0.000392632	-8.01056	0.0102077
NM_002119	2.26E-05	-8.01237	0.000152428
NM_003059	0.000346655	-8.05806	2.62E-06
NM_022785 /// NM_19885	0.000135295	-8.10895	1.17E-05
NM_001037500	1.35E-05	-8.12989	6.49E-05
NM_001128432 /// NM_02	0.00077688	-8.1565	0.000240739
NM_001206	0.000249108	-8.15894	0.0106346
NM_001098519 /// NM_15	4.28E-05	-8.17174	3.18E-06
NM_001146192 /// NM_03	0.000595417	-8.19358	0.00104437
NM_001243280 /// NM_00	0.00694336	-8.19971	0.00896409
NM_001080467	5.40E-07	-8.20601	6.99E-05
NM_182500	8.08E-05	-8.20878	1.29E-05
NM_001099697 /// NM_17	7.30E-06	-8.22423	8.47E-07
NM_001040429 /// NM_01	0.000805889	-8.22896	0.00881614
NM_012435	1.77E-06	-8.25637	4.60E-05
NM_014861	8.12E-09	-8.26039	1.26E-07
NM_033063 /// NM_20757	1.47E-06	-8.27802	8.32E-08
NM_001256054 /// NM_01	0.00351451	-8.27995	0.00129025
NM_001085	0.00426915	-8.28422	1.12E-05
NM_014935 /// NM_13848	3.76E-05	-8.28598	0.00326299
NM_001031802 /// NM_00	1.84E-05	-8.28676	7.31E-05
NM_018399 /// NM_07862	9.62E-05	-8.3271	1.41E-06

NM_017600 /// NR_02426	4.63E-05	-8.34882	0.00284749
NM_001267576 /// NM_15	0.000139566	-8.35442	0.000211626
NM_002581	7.41E-06	-8.38336	2.18E-05
NM_001193434 /// NM_0	0.00393152	-8.38953	0.048983
NM_002970 /// NR_02778	2.06E-08	-8.42189	7.38E-07
NM_000715	1.95E-05	-8.43361	3.10E-05
NM_138801	7.54E-06	-8.43611	0.00114876
NM_002612	0.00121036	-8.45886	4.16E-06
NM_001172684 /// NM_0	3.10E-06	-8.46072	0.00133203
NM_000219 /// NM_00112	0.000988214	-8.46388	0.000112171
NR_015377 /// NR_047570	2.10E-05	-8.51364	0.000221521
NR_034012 /// NR_034013	0.000180003	-8.52589	4.70E-06
NM_001193489 /// NM_01	3.25E-05	-8.53102	0.00774004
NM_138409	0.00639711	-8.62206	0.002328
NM_001165 /// NM_18296	0.000172485	-8.63478	3.27E-06
XR_109454 /// XR_111677	0.00518014	-8.64842	0.000482511
NM_000591 /// NM_00104	0.000334983	-8.65813	0.0136641
NM_138451	0.000444867	-8.67529	0.00223138
NM_001039395 /// NM_01	1.74E-06	-8.68129	1.11E-07
NM_001130699 /// NM_0	4.05E-05	-8.75233	0.0173095
NM_138444	0.00175791	-8.78668	0.00144355
NM_006290	5.71E-05	-8.80832	0.00040811
NM_001204458 /// NM_0	0.00143956	-8.83669	0.0226359
NM_001040113 /// NM_0	3.73E-06	-8.83787	0.000199129
NM_025087	0.000694501	-8.84041	1.34E-05
NM_017886	3.93E-05	-8.85287	0.00154039
NM_000565 /// NM_0012	0.000164036	-8.8565	0.0114806
NM_001554	0.00099024	-8.85749	0.00494922
NM_001164342 /// NM_0	7.50E-05	-8.87015	0.00772664
NM_015693	0.00181615	-8.88234	0.000199537
NM_015896	0.00145148	-8.92236	0.000119364
NM_001112717 /// NM_0	0.000439766	-8.93603	0.014312
NM_014211	0.00423217	-8.93771	0.0306518
NM_001012642	8.34E-05	-8.94894	0.018175
NM_000104	1.33E-06	-8.95504	3.44E-05
NM_001136536 /// NM_0	6.84E-05	-8.97068	1.65E-06
NM_001039845 /// NM_2	5.50E-06	-8.99984	2.64E-05
NM_004310	7.51E-05	-9.02095	0.000302279
XR_109365 /// XR_111668	6.80E-06	-9.03992	6.01E-05
NM_001247997 /// NM_0	8.60E-06	-9.05639	0.00377279
NM_001114106 /// NM_0	5.13E-05	-9.13421	0.000109188
NM_002221	0.000234046	-9.13645	0.0235181
NM_001037290 /// NM_0	0.000178028	-9.14721	0.00029647
NM_000480 /// NM_00102	5.14E-05	-9.14962	0.000107298
NM_020225	4.32E-08	-9.15903	0.000731081
NM_001118 /// NM_0011	0.000693518	-9.26258	0.000263657
NR_027046	6.68E-08	-9.29354	0.000238534

NM_001164257 /// NM_00	1.44E-07	-9.30234	8.37E-08
NM_025153	0.000198798	-9.30373	0.00051513
NM_001242505 /// NM_00	0.00880551	-9.32858	0.0448283
NM_001171171 /// NM_00	0.00151631	-9.39197	0.0126955
NM_003672 /// NM_03331	0.000255109	-9.39641	0.000150809
NM_000672 /// NM_00110	0.000438064	-9.40483	1.66E-05
NM_001080529	3.11E-05	-9.41658	0.000249196
NM_001031743 /// NM_17	2.59E-05	-9.41901	2.78E-05
NR_002819 /// XR_110915	5.07E-07	-9.42774	0.00237192
NM_001005474 /// NM_03	2.13E-06	-9.44188	1.07E-07
NM_001099410 /// NM_00	1.15E-05	-9.44342	0.00280929
NM_001143943 /// NM_03	0.000702769	-9.46255	0.00136054
NM_032411	0.00529664	-9.46871	0.0316644
NM_001280 /// NR_02331	9.24E-08	-9.51331	3.05E-05
NM_024786	1.74E-06	-9.52737	0.00340169
NM_152376	5.83E-06	-9.53705	3.29E-06
NM_017600 /// NR_02426	2.49E-07	-9.5394	0.000454747
NM_001145811 /// NM_00	1.41E-06	-9.56269	0.00109777
XR_108456	0.000781956	-9.56919	0.0091861
NM_175922	0.000176543	-9.60043	1.09E-05
NR_038877	0.000919218	-9.62902	0.00217758
NM_152376	0.000450347	-9.64026	4.64E-05
NM_001136105	0.000820202	-9.64704	7.37E-05
NM_000130	6.40E-05	-9.68778	1.77E-06
NM_004585	4.87E-05	-9.70238	0.00108961
NM_000348	0.000234138	-9.70691	5.39E-06
NR_040109	0.000427623	-9.71612	1.91E-05
NM_003672 /// NM_03331	2.82E-05	-9.78083	0.000812194
NM_005045 /// NM_17305	8.79E-05	-9.78253	0.0128318
NM_001171581 /// NM_00	0.000137834	-9.80861	6.39E-05
NM_001134285 /// NM_00	0.00207945	-9.82216	0.00613468
NM_001040429 /// NM_01	0.0024324	-9.85095	0.00590646
NM_000961	7.19E-05	-9.89193	0.00560389
XR_109227 /// XR_133091	0.000224925	-9.8948	0.0170891
NM_002118	6.60E-05	-9.93181	0.0124423
NM_001164730 /// NM_00	7.85E-05	-9.93633	1.79E-05
NM_001005474 /// NM_03	3.83E-06	-9.94885	4.53E-07
NM_001223 /// NM_00125	1.16E-05	-9.96	0.000414357
NM_024865	2.99E-05	-9.98179	0.00301072
NM_001244134 /// NM_00	1.57E-06	-9.99812	0.000109954
NM_000399 /// NM_00113	0.00141731	-10.074	0.00246235
NM_145038	5.51E-06	-10.151	1.63E-05
NM_024081	0.000338222	-10.1686	0.0103363
NM_001370 /// NM_17364	0.000104261	-10.2019	8.71E-06
NM_001007267 /// NM_00	0.0003687	-10.2544	0.0151942
NM_000517 /// NM_00055	0.007001	-10.3106	0.00740361
NM_152505	1.01E-06	-10.3119	4.92E-08

NM_006120	4.08E-05	-10.3903	0.000390878
NM_001006655 /// NM_01	0.000221993	-10.4572	3.60E-05
NM_032131	0.000124519	-10.462	1.40E-05
NM_001034850 /// NM_01	4.71E-06	-10.4718	6.02E-05
NM_005565	2.92E-06	-10.4786	6.91E-06
NM_001002294 /// NM_00	6.74E-05	-10.4903	7.79E-06
NM_001080394 /// XM_00	5.12E-06	-10.4914	2.09E-05
NM_002581	0.000157011	-10.5359	0.000149268
NM_001100388 /// NM_20	3.09E-05	-10.612	4.35E-07
NM_014496	0.000225821	-10.6347	0.00432471
NM_031412 /// NR_02828	3.27E-07	-10.6496	0.00194191
NM_001145646 /// NM_03	5.25E-07	-10.7244	1.20E-05
NM_001025076 /// NM_00	1.06E-07	-10.7515	4.41E-05
NM_175709	1.95E-07	-10.7539	0.000145516
NM_001039763	2.30E-07	-10.7767	5.79E-09
XR_133404	2.77E-05	-10.8158	4.78E-06
NM_001243342 /// NM_01	3.77E-08	-10.8514	2.53E-08
NM_001089584	4.19E-05	-10.8864	3.80E-06
NM_030906	6.18E-05	-10.9275	3.25E-06
NM_001242463 /// NM_05	3.47E-05	-10.9832	0.00180351
NM_001270391 /// NM_00	0.000201336	-10.9923	3.69E-06
NM_001037582 /// NM_02	9.38E-06	-10.9976	0.000753929
NM_006206	0.000316829	-11.0029	0.000159065
NM_173605 /// NM_1994	0.000114696	-11.0742	1.27E-06
NM_014265 /// NM_0217	0.000563749	-11.0877	0.00108208
NM_001172420 /// NM_01	7.40E-07	-11.1177	1.82E-06
NM_001006655 /// NM_01	1.98E-05	-11.1543	2.85E-06
NR_037901	3.88E-05	-11.2077	3.38E-06
NM_001122961	1.81E-05	-11.218	1.34E-06
NM_001037763	0.000166335	-11.2275	1.44E-05
NM_080283 /// NM_1723	0.000240286	-11.2428	0.000213834
NM_001206997 /// NM_15	3.28E-05	-11.2519	2.20E-07
NM_002970 /// NR_02778	3.03E-10	-11.2949	9.14E-06
NM_001007278 /// NM_00	0.000151368	-11.3411	1.60E-06
NM_024763 /// NM_2070	8.88E-06	-11.4101	2.64E-05
NM_001167942 /// NM_15	0.000100698	-11.4266	6.92E-05
NM_178818 /// NM_1815	2.67E-07	-11.4758	0.0027691
NM_007030	3.45E-05	-11.4966	0.000530138
NM_001080529	1.33E-07	-11.5519	1.98E-07
NM_001204197 /// NM_01	2.48E-07	-11.5545	1.49E-08
NM_001042519 /// NM_00	0.000667317	-11.574	0.0224574
NM_000565 /// NM_0012	0.000198459	-11.6062	0.00512886
NM_001256113 /// NM_17	6.00E-06	-11.6104	2.13E-05
NM_001039350 /// NM_00	0.000297046	-11.6224	0.000222651
NM_001201466 /// NM_03	0.00160949	-11.6789	0.000647665
NM_000855 /// NM_0012	0.000170077	-11.6881	3.98E-05
NM_001001706 /// NM_00	2.87E-06	-11.7047	4.27E-07

NM_006981 /// NM_17319	0.000218591	-11.7215	0.000313792
NM_003986	0.000272156	-11.8011	0.00305906
NM_001142857 /// NM_02	4.66E-06	-11.8081	5.14E-08
NM_004058 /// NM_08059	5.56E-05	-11.8103	0.000109162
NM_001253908 /// NM_00	0.000290037	-11.8301	1.80E-05
NM_005746 /// NM_18279	8.39E-05	-11.8341	5.77E-07
NM_001010892 /// NM_00	0.000580144	-11.8722	1.51E-05
NM_001112706 /// NM_03	0.00014107	-11.8956	8.60E-06
NM_001199739 /// NM_00	4.05E-06	-11.9055	6.66E-06
NM_174912	4.08E-09	-11.9698	4.33E-05
NM_001083 /// NM_03343	4.29E-06	-12.0119	1.05E-06
NM_001144033 /// NM_14	0.00114305	-12.0417	4.90E-05
NM_024940	4.53E-05	-12.1164	0.000259729
NM_173615 /// NM_17505	5.99E-07	-12.1508	2.07E-07
NM_001669 /// NM_00958	4.26E-07	-12.1734	0.000836802
NM_012144	1.97E-06	-12.2254	1.31E-07
NM_018423	0.000208879	-12.2304	0.00981492
NM_001141945 /// NM_00	0.000358753	-12.2508	0.0209401
NM_001202233 /// NM_00	0.000131522	-12.257	0.00130173
NM_001242935 /// NM_00	2.85E-06	-12.2946	6.96E-05
NM_001781 /// NR_02667	2.46E-06	-12.3527	3.36E-09
NM_006235	0.000187704	-12.3623	4.97E-06
NM_001018046 /// NM_02	4.56E-05	-12.4587	2.51E-06
NM_001195303 /// NM_00	0.000191635	-12.515	0.00023016
NM_015351	1.09E-05	-12.582	0.00945982
NM_001190726 /// NM_03	1.30E-06	-12.6104	0.000567328
NM_001142857 /// NM_02	7.99E-06	-12.686	4.35E-07
NM_001003674 /// NM_00	9.39E-05	-12.6882	0.00711703
NM_001156474 /// NM_02	2.94E-07	-12.6941	8.64E-09
NM_198078 /// NR_02727	0.000404714	-12.7773	0.00145459
NM_007335 /// NM_00733	5.90E-06	-12.7967	2.96E-06
NM_001114094 /// NM_00	1.27E-05	-12.8215	0.010032
NM_001080850	9.68E-06	-12.8285	0.0107224
NM_001002233 /// NM_00	3.54E-05	-12.8451	0.00163819
NM_024574	2.34E-05	-12.9495	1.69E-05
NM_020893 /// NR_03652	3.31E-05	-13.0256	0.000984417
NM_001076778 /// NM_00	6.93E-06	-13.0296	0.00979652
NM_018429	4.91E-05	-13.0447	0.0267189
NM_001164496 /// NM_01	1.44E-05	-13.0974	8.53E-05
NM_001008723	6.40E-05	-13.0985	1.33E-06
NM_172193	0.0001053	-13.1863	0.00135122
NM_001243961 /// NM_00	0.0024713	-13.2167	0.00464605
NM_198282	2.39E-07	-13.2574	2.21E-05
NM_002847 /// NM_13084	3.26E-05	-13.3015	2.91E-05
NM_001144956	7.54E-05	-13.3067	1.15E-06
NM_001169154 /// NM_17	4.84E-05	-13.3092	1.70E-06
NM_001149 /// NM_0012	1.31E-06	-13.3434	0.013086

NM_033364 /// XR_13249	0.000112205	-13.3626	0.00557221
NM_006186 /// NM_17317	3.15E-06	-13.3741	8.19E-06
NM_031898	9.23E-05	-13.3787	1.90E-06
NM_000720 /// NM_00112	2.15E-05	-13.3978	0.0031304
NM_001131010 /// NM_0C	0.000372	-13.4158	7.69E-06
NM_025244 /// NM_18291	4.73E-05	-13.468	8.61E-06
NM_001029996	1.34E-05	-13.6013	1.50E-06
NM_001159629 /// NM_0C	0.000725818	-13.638	3.13E-06
NM_000777 /// NM_0011	3.26E-05	-13.6676	0.00109274
NM_001267798 /// NM_0C	2.82E-06	-13.7008	0.000263889
NM_001996 /// NM_00648	1.37E-06	-13.7281	6.11E-05
NM_001001971 /// NM_0C	7.08E-05	-13.7371	1.93E-05
NM_139172	0.000576014	-13.8348	0.000451422
NM_002090	0.000304404	-13.852	4.51E-05
NM_001079691 /// NM_05	1.71E-07	-13.9109	6.59E-05
NM_001159643 /// NM_0C	5.92E-08	-13.9194	2.65E-05
NM_001253854 /// NM_0C	4.24E-05	-13.9721	1.72E-07
NM_001131010 /// NM_0C	0.000246848	-14.0774	0.000113956
NM_025153	0.0016689	-14.0836	0.0193682
NM_001135919 /// NM_18	7.78E-07	-14.0897	0.000626824
NM_002727 /// NR_03643	0.000103262	-14.1337	0.00224487
NM_152327	2.13E-05	-14.1696	1.70E-05
NM_001008409	0.000175302	-14.1922	0.0100234
NR_002722 /// NR_024553	4.76E-06	-14.1924	8.63E-06
NM_001669 /// NM_00958	2.75E-05	-14.197	0.00047441
NM_016557 /// NM_17844	2.15E-06	-14.2585	5.86E-08
NM_006217	0.000294616	-14.2621	0.000376125
NM_001039763	0.000755146	-14.3132	1.86E-05
NM_001025158 /// NM_0C	7.33E-07	-14.3951	2.56E-06
NM_018897	1.59E-05	-14.4463	2.13E-06
NM_001001523 /// NM_0C	5.00E-07	-14.557	2.66E-05
NM_001270383 /// NM_14	4.39E-05	-14.6823	1.17E-05
NM_001045476	5.89E-06	-14.6842	4.06E-07
NM_016234 /// NM_20337	2.26E-08	-14.6873	1.41E-05
NM_001146003 /// NM_02	3.55E-08	-14.8307	0.000139559
NM_001076778 /// NM_0C	1.60E-06	-14.907	0.00945191
NM_003890	0.000100009	-14.9479	0.0291036
NM_138468 /// NM_17823	1.69E-05	-14.9814	0.000360393
NM_000689	2.70E-07	-14.9966	2.80E-08
NM_182508	0.000766464	-15.0216	4.86E-05
NM_000963	5.38E-06	-15.0244	2.47E-09
NM_001159629 /// NM_0C	6.70E-05	-15.1084	7.54E-08
NM_001145811 /// NM_0C	2.98E-06	-15.1231	0.0112807
NM_001114357	0.000117511	-15.1455	5.85E-05
NM_004235	3.95E-05	-15.1767	7.05E-07
NM_020802	8.58E-05	-15.253	2.73E-06
NM_001164407	2.61E-05	-15.3543	0.0031387

NM_001669 /// NM_0095{8}	5.42E-06	-15.4184	0.000525683
NM_006763	4.03E-05	-15.4279	0.000101711
NM_001256054 /// NM_01	3.02E-07	-15.4331	5.58E-07
NM_001146319 /// NM_00	6.65E-05	-15.4939	0.0433328
NM_015668	1.64E-05	-15.4969	4.29E-06
NM_001012502	1.14E-06	-15.5255	1.68E-07
NM_004616	0.000297612	-15.5514	0.0011123
NM_001105513 /// NM_14	7.58E-05	-15.6444	0.00943173
NM_152576 /// XR_10893	1.47E-05	-15.7815	0.00134501
NM_001039845 /// NM_20	2.91E-07	-15.8287	7.39E-05
NM_005832 /// NM_1813	0.000179821	-15.9058	7.01E-05
NM_032606	0.000124155	-15.9335	4.64E-07
NM_004417	1.08E-05	-15.9636	8.91E-06
NM_153228	3.00E-06	-16.0028	6.25E-08
NM_001199989 /// NM_01	4.86E-05	-16.0373	0.000120973
NM_001733	1.20E-07	-16.1295	0.00696591
NM_003551	3.07E-06	-16.1749	1.42E-06
NM_001001991 /// NM_01	3.12E-07	-16.2852	3.65E-06
NM_007335 /// NM_0073	6.27E-06	-16.2924	7.72E-07
NM_019111	1.79E-05	-16.2929	0.000945978
NM_001162371	0.000121315	-16.3053	0.00420868
NM_004666	4.42E-05	-16.3388	1.89E-07
NM_014057 /// NM_0244	0.000227999	-16.4164	7.12E-06
NM_001920 /// NM_1335	1.36E-05	-16.439	0.0118227
NM_001242385 /// NM_00	1.27E-07	-16.4699	9.21E-09
XR_133482	1.53E-05	-16.4744	2.82E-07
NM_000855 /// NM_0012	0.000129445	-16.5856	1.28E-05
NM_001098843	3.50E-05	-16.6306	5.26E-05
NM_001193341 /// NM_15	1.01E-06	-16.699	1.97E-07
NM_000014	1.22E-05	-16.827	0.0373429
NM_001135934 /// NM_00	0.00842392	-16.8567	0.0049334
NM_019111	3.55E-06	-16.9104	6.41E-05
NM_002121	1.76E-05	-16.9362	0.000522919
NM_001198625 /// NM_00	0.000133635	-16.9711	6.81E-05
NM_031461	0.000529161	-16.9816	0.000575821
XR_110232 /// XR_111449	2.30E-05	-16.9955	1.08E-06
NM_001430 /// XR_13270	8.36E-06	-17.1061	0.00609928
NM_001128602 /// NM_00	5.64E-05	-17.1151	0.00085383
NM_144676	2.09E-05	-17.1536	8.62E-08
NM_024786	2.99E-05	-17.2701	0.00575643
NM_014365	1.35E-06	-17.3629	1.67E-06
NM_001669 /// NM_0095	2.06E-06	-17.3701	0.000614037
NM_000700	0.000633163	-17.518	0.00453511
NM_152784	2.01E-06	-17.5509	1.05E-08
NM_000104	1.10E-05	-17.5993	0.000564276
NM_020734	1.97E-05	-17.6179	0.0427005
NM_014859	1.18E-06	-17.6611	1.65E-05

NM_000416	3.16E-06	-17.7704	0.000881786
NM_020802	6.89E-10	-17.8037	5.96E-12
NM_053285	0.000143758	-17.9309	2.58E-06
NM_002122 /// NM_02005	0.000281988	-17.9649	0.000211915
NM_000898	1.16E-05	-18.097	3.17E-05
NM_006186 /// NM_17317	0.000100252	-18.154	8.39E-05
NM_000278 /// NM_00398	0.00171176	-18.1782	0.00429549
NM_001243961 /// NM_00	7.68E-05	-18.1797	0.000469985
NM_017424 /// NM_17740	7.25E-08	-18.1844	8.40E-05
NM_001033658 /// NM_00	6.36E-05	-18.2079	0.000164184
NM_001205288 /// NM_03	0.00013309	-18.4945	0.0347131
NM_058186 /// NM_20696	2.48E-05	-18.5145	0.00136155
NM_001178003 /// NM_14	6.53E-05	-18.5595	7.09E-06
NM_001159643 /// NM_00	2.38E-05	-18.6732	0.000159714
NM_001164496 /// NM_01	5.61E-08	-18.6734	9.16E-06
NM_004390 /// NM_14897	5.15E-08	-18.9137	0.0025766
NM_001372 /// NM_00466	1.98E-05	-19.0207	7.30E-08
NM_001127381 /// NM_00	0.000111362	-19.0272	0.000508613
NM_015675	3.94E-05	-19.0888	0.00643934
NM_052972	1.20E-06	-19.1217	6.96E-07
NM_001204477 /// NM_00	2.82E-05	-19.1404	0.0370612
NM_003246	4.50E-05	-19.1653	5.03E-06
NM_004787	9.76E-06	-19.3496	0.00292932
NM_000492	0.000204292	-19.3924	0.00459581
NM_001145077	1.93E-05	-19.3925	6.46E-07
NM_006186 /// NM_17317	5.59E-06	-19.5129	2.02E-05
NR_040091 /// NR_040092	3.02E-07	-19.6516	0.00016302
NM_001082972 /// NM_00	3.30E-05	-19.8039	0.00778541
NM_002487	3.01E-05	-19.8714	0.00866296
NM_001128850 /// NM_00	5.71E-05	-19.9522	3.55E-06
NM_002943 /// NM_13426	6.29E-06	-20.03	0.00867568
NM_020877	9.11E-06	-20.0778	4.82E-05
NM_178452	1.12E-07	-20.1865	7.69E-09
NM_001128933 /// NM_00	3.47E-07	-20.4688	1.91E-05
NM_001080378 /// NM_00	1.85E-06	-20.5181	4.96E-06
NM_012307	1.72E-05	-20.7012	2.53E-06
NM_001014440	7.96E-05	-20.7364	4.14E-05
NM_024763 /// NM_20701	3.06E-05	-20.7507	0.000167718
NM_001270041 /// NM_00	7.06E-05	-20.8905	1.15E-05
NM_000239	1.12E-05	-21.0375	0.00380823
NM_006988	1.42E-06	-21.4052	0.000328286
NM_001003809 /// NM_00	0.00026999	-21.6701	0.00126275
NM_198469	5.37E-06	-21.6727	8.95E-07
NM_001190462	3.05E-05	-21.6779	3.00E-07
NM_007335 /// NM_00733	6.15E-06	-21.6806	6.65E-07
NM_001270422 /// NM_01	5.85E-05	-21.7474	0.000139775
NM_001006655 /// NM_01	8.73E-06	-21.8827	2.75E-05

NM_023037	2.33E-05	-21.8939	0.00275597
XR_109470 /// XR_111780	4.65E-08	-21.904	0.00464667
NM_000044 /// NM_00101	3.34E-06	-22.012	0.000468651
NM_025184	1.03E-06	-22.1724	2.12E-06
NM_001204869 /// NM_00	0.000224849	-22.2144	0.0347258
NM_001541 /// NM_08065	2.69E-05	-22.4809	0.00683685
NM_031476	6.10E-06	-22.603	0.00378904
NM_001039766 /// NR_02	2.71E-05	-22.6252	0.00643184
NM_001012502	6.47E-06	-22.7319	2.60E-06
NM_006290	4.12E-08	-22.7608	3.92E-05
NM_153376	3.11E-05	-22.7798	1.44E-05
NM_000633 /// NM_00065	1.44E-05	-22.8051	0.0131311
NM_001128595 /// NM_00	1.18E-05	-22.8312	0.0278602
NM_001039183 /// NM_00	1.99E-06	-22.8807	0.0233671
NM_000770 /// NM_00119	0.00015386	-22.9275	0.000886915
NM_145235	6.55E-07	-22.9348	9.61E-05
NM_001195303 /// NM_00	1.35E-05	-23.0136	0.000305767
NM_002122 /// XM_00311	0.00426421	-23.0892	0.000729735
NM_024614 /// NR_02680	2.44E-06	-23.4758	0.00344101
NM_172365	2.20E-06	-23.4763	1.85E-06
NM_001164730 /// NM_00	4.14E-06	-23.4908	1.38E-07
NM_207437	2.47E-06	-23.7311	5.25E-07
NM_001003954 /// NM_00	9.10E-05	-24.0103	1.07E-05
NM_001195639 /// NM_05	4.40E-05	-24.305	1.57E-05
NM_020869 /// NM_19846	1.11E-05	-24.4379	2.35E-07
NM_001204051 /// NM_00	5.69E-06	-24.6319	0.0419278
NM_001130090 /// NM_00	1.36E-07	-24.634	9.11E-08
NM_000777 /// NM_00119	0.0010862	-24.8372	0.000319805
NR_015424	0.00030897	-24.8511	0.0024341
NM_030666	4.40E-10	-25.1235	1.03E-07
NR_003063	4.12E-06	-25.429	2.59E-07
NM_015225 /// NM_13881	3.79E-06	-25.7145	0.0156305
NM_003407	6.53E-09	-25.7647	5.09E-06
NM_004058 /// NM_08059	0.000412889	-25.9072	0.00291405
NM_138788	4.30E-06	-25.9593	3.93E-06
NM_001017372 /// NM_01	6.65E-05	-26.0132	6.81E-05
NM_020879	2.16E-05	-26.1866	0.0100483
NM_005257	9.38E-05	-26.2112	0.00150572
NM_002557	0.000513459	-26.2942	0.00016527
NM_002644	3.28E-07	-26.4569	3.91E-08
NM_025087	2.00E-06	-26.5114	2.82E-08
NM_001145107 /// NM_00	0.000698089	-26.9296	4.87E-05
NM_001369	4.42E-05	-27.3755	8.75E-07
NM_003955	8.38E-05	-27.4006	0.0206207
NM_001145811 /// NM_00	2.98E-06	-27.4444	0.0197473
NM_053277	0.000253537	-27.6267	0.000294613
NM_015964 /// NM_01614	1.59E-06	-27.6943	1.40E-06

NM_001012642	5.95E-07	-27.7714	0.00733639
NM_003014	7.31E-06	-27.8494	0.000213931
NM_001243965 /// NM_00	3.56E-08	-28.0359	2.22E-05
NM_001199573 /// NM_00	3.62E-08	-28.2653	3.90E-05
NM_001170806 /// NM_17	6.41E-05	-28.6611	0.00129192
NM_001198542 /// NM_00	6.10E-07	-28.7687	3.42E-07
NM_000777 /// NM_00119	1.76E-05	-28.809	0.00068468
NM_001100159 /// NM_00	0.00043475	-28.9804	0.000125715
NM_000044 /// NM_00101	9.88E-06	-29.1522	0.000918005
NM_001831 /// NM_20333	3.62E-07	-29.1919	0.0183023
NM_001099677 /// NM_02	4.29E-05	-29.2517	3.17E-05
NM_178824	4.12E-05	-29.479	1.27E-06
NM_016234 /// NM_20337	1.28E-09	-29.8759	4.34E-08
NM_001372 /// NM_00466	2.16E-05	-30.0155	5.00E-07
NM_005797 /// NM_14476	9.78E-06	-30.5129	0.0422581
NM_031956	1.35E-05	-30.5956	2.60E-07
NM_004925	1.13E-05	-30.6119	0.016608
NM_024786	1.70E-06	-31.0398	0.00246285
NM_001166412 /// NM_02	3.15E-06	-31.0535	0.00255329
NM_001128850 /// NM_00	4.47E-06	-31.0966	1.22E-07
NM_012309 /// NM_13326	2.87E-06	-31.4964	0.0207975
NM_001085447	1.22E-05	-32.1166	1.62E-06
NM_152750 /// XR_132543	1.35E-06	-32.1978	4.47E-08
NM_014466	4.39E-06	-32.3346	0.000140173
NM_001008534 /// NM_00	3.94E-05	-32.5418	4.75E-07
NM_001039592 /// NM_01	4.77E-06	-32.8687	3.66E-06
NM_001114938 /// NM_00	1.66E-06	-32.9932	4.25E-08
NM_001172810 /// NM_02	9.01E-07	-33.0847	3.60E-09
NM_000062 /// NM_00103	1.14E-07	-33.2161	0.0161282
NM_005252	8.72E-06	-33.2807	4.99E-05
NM_033413	2.41E-06	-33.4309	3.75E-08
NM_130446	6.23E-06	-33.4314	1.62E-06
NM_001135091 /// NM_00	0.000217009	-33.4666	0.00264031
NM_144715	1.23E-05	-33.8252	6.20E-07
NM_001243965 /// NM_00	4.92E-07	-34.0139	0.000441615
NM_030820	1.35E-05	-34.0542	4.09E-08
NM_001920 /// NM_13350	1.08E-05	-34.242	0.00166842
NM_033413	3.38E-07	-34.465	5.33E-09
NM_012309 /// NM_13326	1.32E-06	-34.4686	0.00873723
NM_002089	9.70E-05	-35.1846	5.03E-08
NM_152750 /// XR_132543	5.10E-07	-35.7083	1.19E-08
NM_031457	1.81E-05	-35.8343	5.40E-07
NM_001206897 /// NM_00	3.92E-08	-35.8876	1.12E-07
NM_001243965 /// NM_00	2.22E-07	-35.8911	7.22E-05
NM_001831 /// NM_20333	1.10E-07	-36.0344	0.0210951
NM_001199633 /// NM_02	1.53E-06	-36.1055	5.00E-05
NM_001040092 /// NM_00	1.27E-06	-36.4716	3.39E-06

NM_207362	5.03E-06	-36.5015	0.00607348
NM_014265 /// NM_02177	4.86E-06	-36.5621	0.000737601
NM_020225	2.21E-08	-36.7186	0.00813845
NM_199280	5.33E-07	-37.0838	1.66E-07
NM_001263	2.27E-06	-37.7801	0.00143123
NM_181643	1.52E-07	-38.1709	1.99E-07
NM_001105248 /// NM_00	5.22E-06	-38.7019	1.16E-05
NM_004058 /// NM_08059	5.10E-06	-39.272	0.00103517
NM_001243115 /// NM_02	4.09E-05	-39.5179	7.72E-05
NM_152665	4.52E-05	-39.7574	8.98E-07
NM_001263	6.29E-06	-39.8588	0.00232381
NM_012309 /// NM_13326	0.000100395	-39.9057	0.0346321
NM_001143941 /// NM_00	6.65E-05	-40.2316	0.000299831
NM_001002029 /// NM_00	2.24E-06	-40.8773	0.000595415
NM_001112717 /// NM_00	1.11E-08	-41.7871	0.000474851
NM_001142958 /// NM_15	2.18E-06	-41.9092	4.97E-06
NM_024677	4.88E-06	-42.199	0.0427014
NM_173081	2.83E-05	-42.512	9.37E-06
NM_032445	3.85E-06	-43.5731	6.68E-08
NM_001243965 /// NM_00	2.00E-06	-44.0241	0.000469459
NM_025244 /// NM_18291	4.28E-06	-44.1898	1.90E-06
NM_001013625	3.54E-06	-44.643	3.04E-06
NM_001831 /// NM_20333	5.03E-08	-44.8306	0.013923
NM_003014	4.19E-05	-45.3445	8.18E-05
NM_007168	1.60E-05	-45.4576	2.43E-06
NM_001267798 /// NM_00	2.61E-06	-45.6727	0.000156118
NM_004482	3.82E-09	-45.9695	0.00568869
NM_001205288 /// NM_03	9.45E-06	-46.4919	0.0115039
NM_001242524 /// NM_00	6.61E-06	-46.963	0.000306226
NM_206996	1.21E-06	-47.0058	7.39E-06
NM_058187	9.06E-09	-47.0844	0.000165226
NM_000926 /// NM_00120	0.000292803	-47.2619	0.00060646
NM_001079855 /// NM_00	5.71E-06	-52.314	0.0432543
NM_005160	4.96E-08	-52.3613	0.0068473
NM_144992	1.51E-05	-54.099	3.79E-07
NM_001142302 /// NM_01	0.000241993	-54.4723	0.0030382
NM_001244134 /// NM_00	8.86E-09	-54.751	0.000142616
NM_000104	1.76E-08	-56.7041	0.000120721
NM_001128933 /// NM_00	1.78E-06	-56.9467	5.37E-05
NM_145263	6.01E-05	-57.717	1.49E-06
NM_001252195 /// NM_03	3.07E-08	-58.5808	9.98E-10
NM_024763 /// NM_20701	4.44E-05	-58.9127	0.000443031
NM_000204	4.34E-09	-59.0591	5.13E-06
NM_001172105 /// NM_01	7.56E-07	-59.5388	0.0197709
NM_000065 /// NM_00111	4.16E-09	-61.4678	1.34E-11
NM_145170	1.92E-05	-61.7455	0.000132385
NM_001145399 /// NM_00	4.39E-05	-62.6275	0.013254

NM_001105248 /// NM_00	1.02E-06	-63.1097	3.08E-05
NM_031421	1.78E-08	-64.6176	1.50E-08
NM_014722 /// NM_01586	8.91E-08	-67.0458	7.24E-09
NM_001040442 /// NM_00	2.46E-07	-67.4431	1.80E-09
NM_024694	7.31E-07	-68.4132	5.15E-09
NM_001114171 /// NM_00	4.51E-05	-69.1993	6.43E-05
NM_001030287 /// NM_00	3.83E-05	-69.4149	0.000256797
NM_001145033	6.89E-06	-70.8927	0.000539685
NM_001002029 /// NM_00	2.50E-07	-71.1309	0.000477062
NM_145020	4.71E-08	-71.7648	7.54E-08
NM_001080537	1.92E-05	-72.0448	3.83E-07
NM_033364 /// XR_132494	6.16E-11	-73.0893	8.35E-06
NM_001199201 /// NM_00	7.94E-08	-73.1336	3.72E-09
NM_001077710	5.80E-11	-73.8673	2.78E-05
NM_022052	5.44E-07	-75.9611	5.53E-08
NM_001128304 /// NM_00	3.90E-07	-76.474	0.0283374
NM_000208 /// NM_00107	5.73E-12	-77.5206	0.00176242
NM_001010940	7.75E-05	-78.8243	2.95E-05
NM_001008226	3.10E-06	-82.7256	8.82E-08
NM_021229	1.08E-07	-84.3761	0.0396582
NM_024870 /// NM_02517	2.77E-06	-87.5465	0.00194562
NM_176813	2.85E-06	-87.8292	2.00E-07
NM_001253835 /// NM_00	1.84E-07	-90.9671	0.00610231
NM_024783	4.59E-07	-92.5521	2.49E-07
NM_178456	2.25E-07	-94.1098	6.78E-09
NM_130897	1.43E-06	-96.9537	2.21E-07
NM_001135193 /// NM_00	2.05E-08	-102.904	9.66E-06
NM_024867 /// NM_14472	3.58E-07	-106.666	1.10E-06
NM_000064	2.54E-08	-106.906	0.0205606
NM_001011657 /// NR_036	4.36E-09	-107.478	2.43E-05
NM_020872	2.96E-05	-113.843	4.16E-05
NM_001165963 /// NM_00	1.20E-08	-117.312	2.39E-11
NM_001042625 /// NM_14	2.82E-06	-117.775	3.40E-06
NM_152321	9.88E-07	-121.764	0.000221113
NM_001080556 /// NM_14	1.61E-07	-124.428	4.57E-09
NM_178504 /// NM_19856	1.23E-06	-132.326	1.06E-07
NM_000877	8.91E-09	-136.757	0.0123422
NM_001004303	3.19E-06	-143.205	6.02E-07
NM_152548	1.78E-06	-151.774	1.86E-06
NM_025145	9.34E-09	-161.152	1.33E-08
NM_001142407 /// NM_00	2.92E-10	-161.399	8.24E-13
NM_145170	2.01E-08	-176.685	0.000107506
NM_000699 /// NM_00100	2.94E-08	-222.123	0.00185847
NM_080860	3.27E-09	-232.023	3.07E-06
NM_001079527 /// NM_00	7.62E-08	-243.999	1.93E-05
NM_001128310 /// NM_00	9.43E-09	-287.173	0.000598448
NM_001242524 /// NM_00	2.62E-10	-294.793	0.000106144

NM_014585	2.69E-11	-713.82	2.39E-05
NM_001190986 /// NM_0C	6.40E-16	-903.242	1.35E-18

. Normal oviduct
Fold-Change
2.90776
8.15329
8.53629
16.1364
7.02207
6.2772
8.10199
5.59313
8.57691
6.19469
4.27502
14.4994
2.85191
3.24572
8.10545
8.34569
6.28015
2.82505
8.95029
11.7229
6.53706
3.15972
7.30738
5.50563
2.62642
10.9219
3.81935
6.4262
20.7364
4.98484
2.1641
2.01537
10.3303
8.09866
2.03602
4.39391
5.82136
4.5038
2.09694
11.2508
3.14854
5.08233
6.74166

3.85846
2.69361
10.9712
12.305
7.89501
2.95426
14.7949
4.52821
3.56912
4.10717
2.90978
13.682
2.31192
6.66998
2.45095
2.76872
2.33207
12.8617
2.23721
2.33142
8.85718
5.64323
3.43079
3.97646
2.67078
2.29919
2.69176
7.89373
20.1327
10.1186
2.84284
10.5074
2.33652
11.6106
2.26008
2.33485
2.07614
2.93253
4.81095
3.53298
8.19024
7.91385
12.9448
2.42731
2.63586
2.87758
3.56001

2.89117
5.66424
9.47113
3.04742
2.91277
3.16869
2.79861
4.85297
3.0806
2.31881
3.6878
6.2147
8.31957
2.00056
2.52816
7.33961
8.55157
2.86738
10.7702
2.73922
8.52026
2.00895
2.76368
2.30818
2.04128
8.60267
4.07055
6.78027
2.57488
2.22097
2.97168
8.00009
9.28934
3.77684
2.40559
14.1848
3.12971
10.5791
4.06981
2.22892
2.08546
2.733
2.56292
2.67064
2.29215
3.5341
2.27832

2.17426
3.67454
3.88425
4.46772
3.08694
2.04475
2.14936
2.98806
2.56163
5.68553
2.91779
2.04939
2.30409
2.49308
4.01594
2.93966
2.76833
2.42928
2.81404
2.87452
3.13126
2.03709
2.60476
7.77779
2.96351
3.07965
6.79006
3.048
2.33526
3.08145
2.45801
2.83577
3.1522
9.04138
2.32865
2.38883
3.49427
2.90322
3.16162
5.35772
3.50483
2.50355
2.16787
2.6594
2.26638
5.56618
2.80373

3.31406
2.93539
3.94208
2.55273
2.58525
8.41011
2.64769
3.44956
2.35756
2.34762
4.86107
2.92915
2.50973
3.15028
2.09185
3.67719
2.93516
9.90233
3.54325
4.2408
2.11126
3.70409
2.2794
2.15252
2.18239
2.43618
2.08934
3.58338
2.08372
2.36013
4.10414
2.9591
2.3358
2.0438
4.03697
2.77684
3.29953
2.27695
2.17679
3.52994
2.87142
3.09245
3.35058
4.76255
5.52881
2.48489
2.07692

2.21824
2.14207
2.34547
2.52155
3.47214
6.36188
2.62523
4.96257
4.9845
2.77221
2.42417
7.28064
2.3456
11.1876
3.83157
2.21443
3.92703
2.01651
2.55104
2.56315
3.18529
2.82189
2.30259
3.11088
2.03477
2.00653
2.65146
2.04246
2.59546
2.1962
2.56696
5.40654
2.15914
2.03642
4.53589
2.70636
2.48587
2.0786
2.77553
2.0242
3.00932
2.23334
3.90591
2.32029
2.60609
2.87391
2.37226

4.54567
2.24972
5.56178
2.89205
3.25012
2.07832
2.77126
2.16473
2.04762
5.82274
2.06501
3.53903
5.80156
2.00857
2.44191
2.16764
4.22278
2.00026
2.4212
2.86188
2.69861
2.17686
2.76908
3.1365
2.5143
2.02238
2.40477
2.10802
3.09144
2.03246
4.08093
2.98748
2.54502
2.09424
2.2988
2.28438
3.39286
2.13359
2.12279
2.50731
2.90231
2.53301
2.39093
2.30022
2.81613
2.03006
2.28419

2.57579
3.73874
2.33737
2.1552
2.92442
2.42006
2.95041
2.90113
2.49558
2.09224
2.88995
3.91403
3.50265
3.22083
2.56915
2.17185
2.73942
2.83241
7.93509
2.57101
2.19996
2.23433
3.01529
5.1011
2.61354
3.65661
3.49873
2.43902
2.90096
3.11078
3.21465
2.04111
2.40758
2.22592
2.53347
2.26697
3.85046
2.5665
2.44776
2.52465
2.83289
2.23476
2.15021
3.18613
2.43561
4.58749
5.11672

10.8442
2.07629
6.94592
2.54265
2.01209
2.00053
3.09378
2.44982
2.46381
2.20494
3.05176
4.33384
2.17573
3.0785
2.11153
2.66279
2.17675
2.86255
4.77487
2.93115
2.06199
2.15497
2.87414
3.81605
2.61348
2.3921
2.72741
7.6443
5.02069
2.94363
2.01079
3.83237
2.34233
2.10516
2.86962
2.09134
2.35788
2.23612
2.12368
2.02573
2.33189
2.2751
2.90943
4.66852
2.09967
3.85098
2.11253

2.26818
2.11871
2.38838
3.37313
2.76792
2.11787
2.51173
2.43342
2.55117
2.23875
2.9354
3.10825
2.70913
5.63242
3.1675
2.17711
2.59633
2.33446
2.5282
2.89329
2.35322
3.77039
2.23127
9.18114
2.03275
2.5963
2.57209
6.83977
2.02515
2.37057
2.33834
2.81988
2.71188
2.12833
2.0331
2.31167
2.66292
4.04398
5.32281
4.09166
3.18729
2.22051
3.29175
2.28691
2.17364
2.07518
2.37231

2.46604
2.51833
2.90544
2.00037
3.00982
4.79672
2.56954
2.14692
2.5025
2.41596
2.67092
2.077
2.49556
3.23493
3.73449
2.76227
2.88799
2.36955
2.06921
2.16232
2.27435
2.47766
2.33319
2.47074
2.17375
2.28839
2.22672
9.92961
2.88084
3.72025
2.48922
2.11184
2.34765
2.94299
5.61773
3.30689
3.2017
2.37022
2.1604
2.33574
2.41448
3.2984
2.03565
2.18779
2.12581
2.52798
2.22843

3.06639
4.09881
2.34835
2.76839
3.08526
2.26563
2.01808
2.38898
2.72645
2.47253
3.00101
2.87653
2.54779
4.1335
2.03987
2.33719
3.2019
2.53468
2.36585
2.04893
2.48697
4.96169
2.00316
2.07434
5.10006
3.55036
3.0034
2.5479
6.97602
2.32356
2.52246
2.38246
2.01092
2.37011
3.55997
2.20276
2.90938
2.12655
2.13841
2.29628
2.00633
2.90327
2.4457
2.38604
2.17095
2.06042
2.36661

2.74543
2.16102
3.14738
2.0382
2.01341
2.66745
3.41739
5.60172
2.14514
2.59735
2.20766
2.45734
2.15977
2.41245
2.0244
2.56035
2.19977
2.50421
2.18114
2.23756
2.77901
2.36793
2.4806
2.67501
2.28256
2.85402
2.60647
4.69268
8.64878
2.07442
2.28064
2.26227
2.19672
2.71694
4.49176
2.44176
3.2176
2.81047
3.05372
3.4813
4.54231
3.60923
2.2184
3.06008
3.81687
2.10425
2.47193

2.52208
2.45673
3.12787
2.17237
2.14733
2.56824
2.07798
3.33647
2.5264
5.82414
2.37618
2.26975
3.06315
2.28649
2.79895
2.14235
2.27798
2.11001
2.23024
2.26788
2.57752
3.8422
2.40444
2.26698
2.32051
2.23112
3.32332
2.38681
2.62667
2.2515
2.19628
2.34029
2.52869
2.10498
2.65064
2.40712
2.51157
3.24602
2.21429
3.81001
2.84333
2.32324
2.42153
3.18351
2.26205
2.34459
2.59929

2.41431
2.08379
2.05254
3.15969
5.61431
2.11133
2.0626
2.37528
2.72583
2.14872
2.72718
2.18491
2.24074
2.52597
2.0152
2.8229
2.09306
2.0692
2.01908
2.00405
2.00769
2.76302
2.86959
2.18844
2.22051
2.48249
3.76226
2.10062
2.60738
3.57764
2.69643
2.05413
2.55314
2.46675
2.5597
5.08666
3.24557
2.12498
2.30001
2.39113
2.96405
2.37774
2.03739
2.46087
2.57228
2.2621
2.42763

2.01597
2.40696
3.64538
2.09089
2.03971
2.23024
3.42987
3.38273
2.76246
2.90319
2.5074
3.08034
2.17915
2.04741
2.31941
2.39616
2.29127
2.09863
3.57865
2.54341
2.54271
2.36448
2.5494
4.75746
2.79433
2.93494
2.84081
2.12896
2.02389
2.775
2.14561
2.33672
2.16906
2.20238
2.6832
3.26812
2.03894
3.43044
2.17561
4.73044
3.22228
2.29907
2.78542
2.11908
2.18036
2.26539
2.40012

2.44191
3.00265
2.01671
2.3133
2.40164
2.07872
2.3896
2.39483
2.11269
2.38207
2.35193
2.4138
2.1037
2.09929
2.07054
2.33945
3.3659
3.45672
2.12404
2.48217
2.16764
2.44751
3.00113
2.44193
2.58195
3.08677
2.01563
2.25075
2.41793
2.16154
2.07166
2.37354
2.08871
2.03723
2.55982
2.94927
2.0236
2.83423
3.33825
2.16608
2.12693
2.154
2.16413
3.22747
2.24005
2.20198
2.5591

2.06989
2.31787
2.44199
2.07525
2.34734
2.35168
2.52737
3.43327
3.58427
2.1269
2.17746
2.58481
2.02235
2.12873
2.32435
2.73822
3.80869
2.02555
2.21933
2.52137
2.37136
2.00896
2.85169
2.68968
3.05455
2.08432
2.01322
3.02649
2.18799
2.41767
2.20069
3.03712
2.04138
3.32335
2.36694
2.00106
2.00421
2.0563
2.44405
2.03933
3.19579
2.23157
3.0689
2.6655
2.09232
2.24321
3.30583

3.02974
3.15859
2.1862
2.03214
2.25918
2.60214
2.83294
2.718
2.17043
2.1509
2.19216
2.46238
2.0001
2.29355
3.15701
2.26575
2.40747
2.21022
2.66625
4.47522
3.04645
2.32064
2.45809
2.08702
2.39787
2.29335
2.20691
3.24878
2.29901
2.03952
2.09389
2.67019
2.71073
2.09496
2.29271
2.19856
2.18037
3.47943
2.0431
2.03574
2.2145
2.21353
3.20886
2.12595
2.4856
3.54624
2.75834

2.31494
2.70923
2.21427
2.26241
2.43251
2.91646
2.00593
2.13153
2.11798
2.70429
2.72806
2.87932
2.31734
2.2134
2.21143
2.42761
2.04705
2.20228
3.08261
2.34357
2.45212
2.24157
3.59208
2.68081
2.24932
2.03363
2.95542
2.76683
7.32628
2.93689
2.33398
2.00854
2.05576
2.71306
4.41855
2.39655
2.91691
4.39181
2.01484
2.59441
2.36528
2.3382
2.0775
2.08098
2.17216
2.52296
2.42841

2.19942
2.598
2.5982
2.10798
2.4885
2.25107
2.05233
2.17139
2.05385
2.14862
2.16564
2.43709
2.35836
2.04892
2.49935
2.56837
2.23079
2.09206
2.55817
2.21029
2.36763
2.64427
2.66438
3.9068
2.67474
2.48413
2.06853
2.95227
2.24959
2.35348
2.75361
2.00288
3.00327
2.15305
2.60665
2.19295
2.93503
4.76875
2.28481
2.51306
2.08165
2.0276
2.6497
3.35383
2.41874
2.05426
2.03372

2.13836
2.46388
2.71556
3.00121
2.58845
2.28037
2.33282
2.24225
2.07287
2.01353
2.18023
2.30465
2.2544
2.1726
2.00531
2.01603
2.03327
2.08037
2.06726
2.05532
2.20141
2.08111
2.01368
2.18627
2.81063
2.3558
2.32694
2.3975
2.42654
2.18623
2.0618
2.23358
2.27451
2.81676
-2.05655
-2.02691
-2.13156
-2.19641
-2.30919
-2.14529
-2.05666
-2.33831
-2.30003
-2.48857
-3.50863
-2.50776
-2.74772

-2.80143
-2.01781
-3.63249
-2.24304
-2.15262
-2.02936
-3.43985
-4.19446
-3.78613
-2.10659
-2.18371
-2.01217
-4.78009
-2.51731
-2.53599
-2.87233
-2.04263
-2.58244
-2.01905
-2.11154
-3.63911
-2.68362
-2.67801
-2.47601
-2.39466
-2.18769
-2.37729
-2.31857
-2.47463
-2.1853
-2.47389
-2.12276
-2.06976
-6.16253
-2.09443
-2.47598
-2.63883
-2.08426
-2.10828
-2.11066
-2.00821
-2.28515
-2.01853
-2.33027
-2.44158
-2.74999
-2.32747

-2.3636
-2.21984
-2.09805
-2.29557
-2.01649
-2.25576
-2.19301
-3.0789
-2.03149
-2.1372
-2.19036
-2.03777
-2.21266
-2.32388
-2.35834
-2.28655
-2.08782
-2.09695
-2.30789
-2.23992
-2.56739
-2.55287
-4.22011
-2.41251
-2.59648
-3.03398
-3.59323
-2.64213
-3.1933
-2.45344
-2.45304
-2.69601
-7.63736
-3.03568
-2.59443
-2.7705
-2.12051
-2.09411
-2.08639
-2.67484
-2.16109
-2.2683
-2.66463
-2.12189
-2.12392
-2.16227
-2.35743

-2.04553
-2.66348
-2.89109
-2.43936
-3.12089
-2.31859
-3.40851
-2.36698
-2.08949
-2.04643
-2.27016
-2.52208
-3.78784
-2.72474
-2.24837
-2.2986
-2.19671
-2.26953
-2.36894
-2.14299
-2.33717
-2.65406
-2.47228
-2.16618
-2.56359
-3.03715
-2.12755
-2.29551
-2.47921
-2.25016
-2.20357
-3.04757
-3.15919
-2.88725
-2.28312
-2.83308
-2.56911
-3.07966
-2.2527
-2.00131
-3.06854
-2.34789
-3.23753
-2.12096
-4.92681
-2.19331
-3.07821

-2.22543
-2.12813
-2.20688
-2.41836
-2.11208
-4.71308
-2.31429
-3.24178
-2.02054
-2.55294
-2.00477
-2.00661
-2.09294
-2.23993
-2.19981
-2.3463
-3.17914
-2.84499
-2.23953
-2.5606
-2.25235
-2.73184
-2.94816
-2.16211
-2.26539
-2.56458
-2.81438
-3.21514
-5.04986
-2.27463
-2.98796
-2.47022
-4.91684
-2.13115
-5.64856
-2.16923
-2.90991
-2.9967
-2.49891
-2.08135
-2.97964
-2.05228
-2.76091
-2.20381
-2.01944
-2.14617
-2.8793

-3.79579
-2.50109
-2.02597
-2.47869
-2.29311
-2.01027
-3.223
-2.2737
-4.89308
-2.15244
-2.2635
-2.43879
-2.27602
-2.04803
-2.62243
-2.13684
-2.60138
-3.10131
-2.23537
-2.08005
-2.22098
-3.77149
-2.33019
-2.72337
-4.06718
-2.69505
-3.82397
-2.17199
-2.75086
-2.32059
-6.86108
-2.96931
-2.18295
-2.64418
-2.2651
-2.33561
-2.34794
-5.33611
-2.39135
-2.17376
-2.61656
-2.45094
-3.01374
-2.11544
-2.00881
-2.39007
-2.25457

-3.20203
-2.28335
-3.75401
-2.16931
-3.00123
-2.02048
-2.00067
-3.79446
-2.1482
-2.39872
-3.49923
-3.44091
-2.74507
-2.66662
-2.60382
-2.79074
-3.14809
-2.12302
-2.07791
-2.71316
-2.46165
-2.14806
-2.1984
-2.55506
-2.22289
-3.49966
-2.27478
-4.71094
-2.02814
-2.12261
-2.61308
-3.1284
-2.92163
-4.5203
-2.06132
-2.01771
-2.61182
-2.47613
-2.02515
-2.28079
-2.20028
-2.5629
-2.1208
-2.53282
-2.37867
-2.15311
-2.53764

-2.2622
-3.42766
-6.16576
-3.86692
-2.41239
-2.18396
-2.74629
-2.76436
-2.1192
-2.29838
-2.66973
-2.3064
-3.287
-2.89243
-3.32603
-2.47807
-2.41922
-2.46112
-3.20675
-3.2143
-2.78822
-2.03251
-2.00626
-9.42936
-3.39174
-3.38969
-2.34437
-2.25613
-6.62216
-2.12531
-2.09967
-2.45031
-2.63465
-9.19086
-2.14945
-3.24094
-5.92202
-2.49407
-2.21987
-2.25029
-2.12603
-2.98164
-2.66495
-3.35582
-2.97587
-2.66765
-6.37001

-2.18409
-3.00712
-3.58763
-3.58527
-2.7811
-2.01984
-2.18716
-2.13413
-2.48585
-2.70816
-3.35352
-3.24165
-11.2264
-2.2013
-2.54026
-3.08511
-2.56785
-3.31049
-2.91628
-3.1007
-3.0335
-2.2907
-3.16892
-2.08336
-2.20655
-3.50354
-3.115
-2.0782
-2.56258
-2.32216
-2.99936
-4.18302
-2.10207
-2.13852
-2.51372
-2.01098
-2.9967
-2.7817
-2.20135
-4.94597
-3.91962
-3.02316
-3.62416
-2.28499
-3.67034
-2.66736
-5.46277

-2.11659
-3.20859
-2.4263
-2.1808
-2.57754
-2.43344
-2.32347
-2.26253
-2.38839
-3.17357
-2.93141
-4.33819
-3.07647
-2.97464
-2.45918
-2.08885
-2.41152
-2.58817
-2.49894
-4.59807
-3.0334
-2.60948
-4.45681
-2.40249
-2.00629
-3.05122
-2.61584
-3.69415
-3.34218
-2.85332
-3.68966
-3.07921
-2.03675
-2.40841
-2.48089
-2.97171
-2.1504
-2.28304
-3.14694
-2.58822
-2.58546
-3.3609
-2.16763
-3.11741
-2.13697
-3.38757
-3.98218

-3.55689
-2.97741
-2.32694
-4.07773
-2.09564
-2.44687
-2.47837
-3.65623
-6.87171
-3.10167
-3.43471
-2.39091
-2.16583
-2.43549
-2.14156
-2.20067
-2.32841
-2.77431
-2.73665
-3.01192
-4.56061
-3.07567
-3.10274
-7.59613
-2.08639
-2.70473
-3.0977
-3.37788
-2.01133
-4.30251
-18.9671
-2.67118
-2.77022
-2.26794
-2.50599
-2.03892
-2.33065
-2.82544
-4.78593
-3.01504
-2.44819
-12.1147
-2.32
-2.90518
-4.08351
-4.07764
-2.5387

-3.87319
-9.01821
-4.08671
-2.609
-4.97528
-2.25274
-2.17346
-3.51992
-3.88937
-2.20365
-2.82799
-2.10102
-3.57909
-4.44521
-5.30804
-2.02039
-7.30321
-4.614
-2.21193
-2.73426
-3.08293
-2.49353
-2.27811
-3.7321
-4.42729
-3.67355
-2.85107
-2.11056
-4.33428
-4.02104
-5.11945
-2.04856
-2.00084
-4.08035
-3.64623
-5.30004
-2.27321
-2.43738
-2.03783
-2.83832
-2.18661
-3.00682
-2.68541
-2.28726
-4.3862
-2.24153
-4.0101

-4.48828
-2.50033
-2.26152
-2.53587
-5.86323
-3.90406
-2.0029
-4.55308
-3.2723
-2.03988
-4.49558
-2.92077
-4.7
-2.70535
-3.00899
-2.93956
-3.32041
-3.086
-3.68545
-4.07235
-3.86935
-3.32231
-3.05988
-3.58997
-2.49019
-22.5119
-2.77448
-3.43595
-3.03899
-2.05633
-2.01341
-2.43264
-3.95099
-2.4577
-3.85601
-7.12798
-2.0336
-2.64373
-2.42738
-3.15736
-2.50945
-3.96565
-5.45258
-3.7421
-3.00865
-4.63241
-3.80908

-3.88582
-5.37651
-4.19019
-3.63562
-2.63748
-2.13499
-2.69099
-4.49172
-4.98678
-2.6164
-3.7462
-3.43986
-3.7006
-2.03771
-4.28619
-3.04648
-2.65675
-2.61542
-4.01009
-2.43004
-3.05146
-4.79217
-2.58786
-3.90696
-2.73557
-4.72031
-2.95901
-2.22399
-4.63871
-2.65825
-3.15483
-3.08765
-16.8947
-3.07
-2.21943
-3.38204
-3.80259
-3.20109
-3.07147
-3.30317
-3.35531
-2.54868
-3.49824
-2.15665
-4.55516
-6.56797
-2.80187

-3.37333
-2.20973
-2.57823
-2.46523
-5.90424
-2.15311
-4.91657
-16.6081
-4.51084
-2.26717
-2.44448
-2.33337
-2.06243
-4.09721
-6.31328
-2.13077
-4.61409
-4.68356
-3.20338
-3.24919
-3.33061
-3.26091
-3.81554
-3.98297
-3.20919
-2.09801
-2.58371
-3.82321
-6.53691
-2.95383
-2.46945
-2.80523
-4.00969
-4.8915
-3.62348
-4.25467
-3.20427
-3.0435
-3.21783
-2.05196
-2.54474
-3.3112
-2.7418
-3.25195
-4.63363
-2.36094
-4.63224

-3.46934
-2.26244
-2.58659
-5.78349
-2.31894
-9.48554
-2.73815
-4.368
-4.15807
-3.6694
-3.94677
-2.00763
-2.81183
-3.12203
-2.08909
-2.92112
-4.55985
-6.93802
-6.34983
-5.15859
-3.44397
-2.16891
-4.52482
-5.24979
-5.45674
-2.86761
-5.2739
-3.69679
-3.17736
-2.20261
-2.53088
-3.91864
-4.09314
-2.2286
-2.91694
-2.46646
-3.53836
-2.01508
-5.67151
-5.74747
-5.94584
-4.51051
-2.83324
-5.44916
-2.8387
-4.71221
-9.86949

-2.08886
-2.16666
-5.74851
-2.35303
-2.38277
-2.44085
-3.29986
-3.46188
-2.01361
-3.1422
-3.72975
-2.29975
-2.6129
-4.33409
-3.16749
-2.89277
-9.85799
-3.30882
-2.33762
-4.50568
-6.37701
-2.50807
-8.00355
-4.58041
-2.00534
-4.41325
-2.60163
-2.24213
-2.73569
-3.53882
-3.13732
-4.16649
-13.412
-5.5613
-2.47479
-4.49089
-3.38685
-4.58474
-3.81387
-4.44024
-2.03369
-5.02787
-2.88634
-2.26343
-3.39992
-4.79227
-3.52237

-3.06218
-3.32801
-2.41207
-2.12841
-6.23748
-2.93763
-2.9845
-2.36778
-2.32566
-2.85952
-2.50341
-2.46014
-3.7919
-3.01123
-2.6225
-4.21549
-4.23083
-3.58488
-2.98431
-2.43362
-2.4941
-4.40215
-7.08059
-4.15482
-3.60262
-3.86384
-4.26728
-2.77983
-6.53464
-2.46983
-2.56684
-2.75427
-4.09386
-5.65057
-4.17634
-2.727
-29.3316
-3.23009
-2.39062
-2.49356
-3.895
-3.34757
-5.31024
-6.0288
-4.21487
-5.71079
-2.41857

-2.60359
-3.18412
-4.86758
-7.16003
-3.11899
-2.83052
-4.03804
-4.30425
-2.89081
-7.81395
-3.70378
-2.21592
-2.03251
-2.96314
-5.92408
-4.66348
-3.71706
-3.69165
-3.28249
-3.43556
-2.11774
-5.77656
-2.76473
-2.04111
-3.6098
-2.5688
-3.31736
-8.42965
-5.73538
-3.49437
-4.98533
-2.46972
-5.74638
-3.8365
-3.95633
-2.68566
-5.28473
-5.32715
-2.86942
-3.05003
-3.34768
-5.70539
-5.07298
-13.2752
-2.48829
-3.598
-7.43463

-2.57917
-4.00334
-3.77107
-2.53334
-3.14952
-4.03588
-2.50412
-11.1111
-2.33037
-6.06311
-3.26909
-7.16068
-2.24586
-5.34315
-7.58284
-6.98436
-2.50516
-3.40722
-5.85936
-2.07732
-4.53168
-3.42634
-2.69118
-2.90412
-8.28424
-2.81542
-2.43972
-3.36796
-2.42258
-6.51737
-6.81023
-2.58602
-2.92318
-2.17958
-3.20037
-7.33785
-3.74574
-3.71938
-3.50814
-2.28937
-4.082
-2.28014
-4.18715
-4.09585
-2.02032
-5.30404
-2.25962

-4.80381
-3.97166
-3.06108
-3.11013
-4.95071
-7.67444
-3.54688
-4.54749
-2.07615
-6.47439
-2.4527
-4.1321
-3.08933
-2.74377
-2.14576
-4.94528
-2.32277
-2.37264
-3.06099
-6.99627
-4.02255
-6.68282
-6.99403
-7.69729
-3.13577
-8.32281
-7.6916
-3.10165
-2.37556
-5.26472
-3.8381
-3.97692
-2.63819
-2.46553
-2.34828
-5.84183
-6.13398
-3.12754
-2.67317
-3.05874
-4.34218
-4.25728
-2.81222
-6.93812
-2.66944
-4.81611
-6.93379

-3.64461
-6.51808
-6.80186
-3.67761
-4.46851
-6.70142
-4.1883
-4.98917
-9.02166
-3.16351
-2.15195
-3.61484
-2.83251
-2.65143
-7.65616
-6.39056
-5.26383
-7.08248
-7.77309
-3.01858
-9.63781
-3.00229
-5.6986
-10.2627
-4.58635
-4.647
-6.68062
-7.2877
-7.35039
-7.57246
-5.27157
-10.7093
-2.33229
-10.7396
-4.56133
-5.53203
-2.10919
-3.63087
-5.05278
-7.30433
-2.78164
-3.1653
-4.52561
-5.54884
-6.34961
-6.67704
-6.7482

-5.02598
-3.6026
-9.77415
-4.85859
-8.51896
-11.6826
-10.3162
-8.3707
-5.06087
-2.43691
-6.48134
-9.92224
-4.25278
-6.18278
-2.4785
-7.72966
-2.92714
-2.70475
-3.85011
-3.75825
-13.7095
-10.0701
-8.56266
-5.40367
-2.33728
-2.81799
-8.37418
-2.89674
-8.66041
-4.51347
-6.18674
-2.35849
-2.29616
-3.29615
-5.96406
-3.5394
-2.28649
-2.24985
-4.51386
-10.5795
-3.87254
-5.02538
-3.54211
-5.89977
-11.3787
-9.75288
-2.02462

-3.1347
-5.15855
-10.9625
-2.92829
-11.7747
-7.58469
-8.05264
-17.1728
-3.56489
-3.39107
-3.7686
-7.27372
-6.23608
-8.36463
-3.15865
-3.19034
-14.6072
-6.89623
-3.52155
-2.80821
-3.69281
-6.25732
-3.05104
-5.60158
-4.01894
-9.97779
-5.82587
-12.6708
-5.25309
-8.24779
-3.88252
-7.62074
-9.08547
-3.22816
-2.7088
-2.19468
-2.44226
-4.06751
-8.39812
-10.9419
-20.9978
-20.6669
-2.23362
-7.12423
-12.2011
-11.4198
-3.1529

-3.48986
-5.55932
-5.9517
-2.22771
-7.87148
-8.33464
-5.07089
-2.95132
-3.4143
-3.44602
-7.74177
-18.0799
-6.75795
-11.568
-5.69802
-2.03701
-7.3786
-4.93596
-9.06239
-3.71723
-3.626
-16.9962
-12.7821
-2.51339
-9.42204
-12.6436
-10.1591
-6.32945
-8.4651
-2.10043
-7.96198
-4.60482
-4.12251
-7.71163
-6.73413
-11.2411
-2.70873
-4.4194
-17.3133
-3.05012
-6.75536
-3.30584
-4.65059
-15.5787
-3.94489
-2.13863
-4.96765

-3.30612
-12.8576
-15.0847
-7.51613
-6.13772
-7.39525
-5.77283
-5.26059
-3.23385
-6.11429
-2.59278
-3.86928
-10.7456
-5.40015
-4.04617
-2.26056
-19.5594
-5.63467
-3.19754
-8.01816
-2.2956
-10.8716
-3.19729
-4.13208
-13.2933
-6.21678
-3.47443
-3.08787
-3.01041
-12.5906
-2.65582
-5.93914
-11.1699
-4.62951
-6.75195
-10.8079
-8.83343
-5.90326
-10.9937
-3.21198
-3.78806
-5.91098
-10.7738
-18.8052
-11.6044
-6.93282
-6.78194

-3.69471
-2.1977
-3.97159
-7.39196
-2.89616
-3.24869
-3.13056
-3.29406
-9.68062
-3.67871
-9.57484
-2.76337
-2.39194
-2.20618
-5.95769
-4.25723
-5.06867
-13.9633
-2.98504
-8.76132
-15.0644
-10.998
-13.1549
-10.5642
-17.4251
-2.16912
-9.33924
-11.9614
-5.69088
-4.82721
-14.3919
-2.52315
-4.13866
-5.88451
-9.27319
-9.10774
-3.1422
-5.34285
-11.9661
-12.8557
-19.205
-17.7798
-20.6404
-3.15996
-2.43405
-9.22544
-9.74923

-2.55623
-5.47351
-4.23174
-3.98335
-5.44473
-10.7333
-5.13259
-13.1548
-4.57081
-2.2105
-10.5071
-20.0412
-6.44956
-21.0681
-2.36128
-21.8568
-2.85197
-3.35524
-3.52584
-19.9669
-2.4973
-15.4696
-19.2628
-5.9201
-26.8247
-11.2401
-20.7405
-29.3964
-2.18266
-7.91718
-23.332
-13.8774
-6.15591
-19.5687
-3.9883
-36.0359
-4.47158
-22.7596
-2.79681
-67.3686
-22.0073
-23.2021
-9.73127
-4.84987
-2.13621
-6.44019
-9.75023

-3.37248
-4.82489
-2.24619
-14.2013
-4.03495
-11.3718
-10.3471
-4.72212
-10.6504
-29.0414
-4.21927
-3.23535
-8.89013
-4.79963
-3.12698
-10.9038
-2.43592
-16.1386
-29.3655
-5.0874
-15.3365
-13.5921
-2.28159
-11.5483
-19.8727
-6.44575
-2.25781
-3.43567
-6.58849
-9.903
-3.62583
-11.392
-2.58511
-2.61003
-34.4782
-7.80082
-3.87684
-4.25141
-8.23976
-39.1878
-29.9238
-9.38929
-5.6909
-2.70711
-48.5907
-10.7525
-4.34965

-8.83524
-17.5087
-28.2192
-48.5913
-51.3652
-16.3208
-11.3466
-7.22176
-4.88452
-16.7411
-47.7447
-3.97161
-33.851
-3.50127
-30.4949
-2.56689
-2.10632
-25.0385
-45.7399
-2.2821
-5.36778
-38.5578
-3.35219
-24.6396
-46.9619
-34.0703
-7.91715
-18.8878
-2.4743
-5.85672
-22.8112
-103.42
-24.4247
-8.29247
-59.8709
-50.073
-2.65885
-44.4051
-30.0183
-29.3218
-118.828
-6.61764
-4.51097
-10.7133
-12.4828
-5.31656
-4.99204

-6.3995

-568.512

Supplementary Table 4 aberrantly upregulated in common between STIC and invasive cancer (2 fold anc

		Invasive SC vs. Normal oviduct		STIC vs. Norı
Gene Symbol	RefSeq	p-value	Fold-Change	p-value
ASPM	NM_018136	2.60E-06	2.94409	1.33E-05
CCDC144A	ENST00000443444	0.00213885	5.32473	0.0243328
CCNE1	ENST00000262643	0.00572145	2.23008	0.0115957
CDH6	NM_004932	0.00283368	2.1433	0.000295215
CENPF	NM_016343	5.58E-07	3.37557	2.40E-06
CKS2	NM_001827	0.0022546	2.89973	0.001283
CLDN6	ENST00000396925	0.0104175	5.93699	0.00243631
CLIC5	NM_001114086	0.009439	2.46718	0.00139079
CRABP2	NM_001878	0.00755329	2.78862	0.0212031
DBN1	NM_004395	2.24E-05	2.05241	2.64E-05
DEK	ENST00000397239	0.000384725	2.32674	0.000217432
DNAJB6	ENST00000262177	0.000272738	2.54209	0.00312649
ECT2	NM_001258316	0.000212608	2.53965	0.00013513
FIGN	ENST00000333129	0.0097029	2.50304	0.00128213
FN1	ENST00000354785	0.00215023	4.76499	0.0446495
GINS1	NM_021067	0.00684686	2.17969	0.0074439
HIST1H2AE	NM_021052	3.44E-05	3.19263	0.000221535
HIST1H2BC	NM_003526	0.0198544	2.24863	0.0371524
HIST1H2BK	NM_080593	0.000451902	2.85981	0.00053831
HIST1H2BO	NM_003527	0.00192634	2.62733	0.00989244
HIST1H3F	NM_021018	0.00448196	3.10484	0.00305663
HIST1H4C	NM_003542	0.00833898	2.18377	0.00595323
HIST1H4L	NM_003546	0.000243457	3.58937	0.000175076
HIST2H2AB	NM_175065	0.000637198	4.20247	0.000722952
KPNA2	NM_002266	0.00344636	2.34762	0.0129578
LOC441268	AK125166	0.000374969	4.11755	0.000820112
MACC1	NM_182762	0.0304047	2.35567	0.0382608
MKI67	ENST00000368654	0.00039812	2.5419	0.000512702
MMP23B	NM_006983	0.0129185	2.51867	0.00175544
MT1G	ENST00000444837	0.0428614	2.35685	0.00461934
NREP	NM_001142481	0.000485486	3.15952	0.00240787
PHOSPHO2-KLHL23	NM_001199290	0.000554576	2.64251	0.00116485
PRAME	NM_206953	0.0297283	2.12296	0.00542624
PRC1	ENST00000361188	0.000336928	2.21306	0.000736568
PTH2R	NM_005048	0.00495188	2.23137	0.00544872
PTTG1	ENST00000352433	0.00451955	2.80642	0.0390721
PVRL3	NM_015480	0.00765987	2.68279	0.0137273
RPL39L	ENST00000296277	0.0055029	2.62684	0.00333233
RRM2	ENST00000360566	0.00383353	2.68346	0.0128528
SKIL	NM_005414	0.0130943	2.03889	0.00849818
SLC16A1	NM_001166496	0.00557925	2.30772	0.0072816
SLC38A1	NM_030674	0.0010424	2.31448	0.0024103
SMC4	NM_005496	4.93E-05	2.57383	0.000371199

SPINT2	NM_021102	0.000296385	2.21178	0.000238397
STMN1	NM_203401	4.99E-06	3.48098	8.76E-07
TBL1XR1	ENST00000430069	0.0174733	2.05526	0.0189784
TIA1	NM_022037	0.00310822	2.37	0.00490998
TMSB10	NM_021103	3.32E-05	2.60096	2.32E-05
TOP2A	NM_001067	0.0001045	3.28641	0.000712484
TPMT	NM_000367	0.0107081	2.62068	0.0237245
TPX2	NM_012112	4.09E-05	3.27148	0.000258971
TXNDC9	NM_005783	0.00363903	2.0506	0.00286028
UBE2T	ENST00000367274	0.0043026	2.33065	0.00586935
URI1	ENST00000542441	0.0130175	2.43578	0.00507933
WRAP53	ENST00000316024	0.00287094	2.78275	0.00691762
ZC3HAV1L	BC020784	0.00870664	2.10747	0.0106318
ZIC1	ENST00000282928	0.0108722	2.60269	0.00477505
ZNF146	NM_007145	0.00509871	2.49424	0.00149398
ZNF345	NR_038362	0.00010634	2.33358	0.000569311
ZNF566	NM_001145345	0.000363159	2.17544	0.000559765
ZNF850	NM_001193552	0.000890238	2.03178	7.58E-05
ZNF93	NM_031218	0.00124937	3.25181	0.000421892

d $p < 0.05$, 62 genes)

mal oviduct
Fold-Change
2.55218
3.10055
2.04568
2.72304
2.94353
3.14103
9.14572
3.27737
2.35262
2.03034
2.45512
2.00273
2.65618
3.40042
2.52238
2.15762
2.62357
2.03615
2.80158
2.13867
3.30768
2.27842
3.75505
4.11536
2.00124
3.64794
2.25771
2.47644
3.46765
3.62657
2.57426
2.43506
2.76631
2.06902
2.20613
2.01265
2.44664
2.82552
2.26102
2.15188
2.23131
2.12583
2.15717

2.25367
4.23057
2.03246
2.24393
2.68618
2.63066
2.29851
2.67713
2.10144
2.2434
2.81859
2.45958
2.05689
2.97193
2.94787
2.03043
2.09682
2.52018
3.8168

Supplementary Table 5 overlapped genes between immortalized and STIC (123 genes)-upregulated

Gene Symbol	Gene Title
STMN1	stathmin 1
ZNF93	zinc finger protein 93
DCDC2	doublecortin domain containing 2
CENPF	centromere protein F, 350/400kDa (mitosin)
RPL39L	ribosomal protein L39-like
CDH6	cadherin 6, type 2, K-cadherin (fetal kidney)
RBBP4	Retinoblastoma binding protein 4
TPX2	TPX2, microtubule-associated, homolog (Xenopus laevis)
ECT2	epithelial cell transforming sequence 2 oncogene
TOP2A	topoisomerase (DNA) II alpha 170kDa
NREP	neuronal regeneration related protein homolog (rat)
ASPM	asp (abnormal spindle) homolog, microcephaly associated
FN1	(Drosophila) fibronectin 1
CDH2	cadherin 2, type 1, N-cadherin (neuronal)
MKI67	antigen identified by monoclonal antibody Ki-67
ZC3H11A	zinc finger CCCH-type containing 11A
UBE2T	ubiquitin-conjugating enzyme E2T (putative)
SMC4	structural maintenance of chromosomes 4
SKIL	SKI-like oncogene
ARHGAP29	Rho GTPase activating protein 29
CXCR4	chemokine (C-X-C motif) receptor 4
ZNF644	zinc finger protein 644
PRC1	protein regulator of cytokinesis 1
EPB41L5	erythrocyte membrane protein band 4.1 like 5
MSH2	mutS homolog 2, colon cancer, nonpolyposis type 1 (E. coli)
UBE2C	ubiquitin-conjugating enzyme E2C
MASTL	microtubule associated serine/threonine kinase-like
KIF23	kinesin family member 23
BUB1	budding uninhibited by benzimidazoles 1 homolog (yeast)
STAT1	signal transducer and activator of transcription 1, 91kDa
NUSAP1	nucleolar and spindle associated protein 1
PARP14	poly (ADP-ribose) polymerase family, member 14
TTK	TTK protein kinase
KPNA4	karyopherin alpha 4 (importin alpha 3)
ANP32E	acidic (leucine-rich) nuclear phosphoprotein 32 family, member E
CEP55	centrosomal protein 55kDa
CCDC88A	coiled-coil domain containing 88A
KIF20B	kinesin family member 20B
CREB1	cAMP responsive element binding protein 1
SYT11	synaptotagmin XI
IFIT2	interferon-induced protein with tetratricopeptide repeats 2
CDKN3	cyclin-dependent kinase inhibitor 3
PLEKHO1	pleckstrin homology domain containing, family O member 1

NDC80	NDC80 kinetochore complex component homolog (S. cerevisiae)
CHEK1	checkpoint kinase 1
PEA15	phosphoprotein enriched in astrocytes 15
FOXM1	forkhead box M1
KLHL24	kelch-like 24 (Drosophila)
KALRN	kalirin, RhoGEF kinase
SKA3	spindle and kinetochore associated complex subunit 3
CARD16	caspase recruitment domain family, member 16
CKAP2	cytoskeleton associated protein 2
CGGBP1	CGG triplet repeat binding protein 1
IFI44	interferon-induced protein 44
ANLN	anillin, actin binding protein
STAT2	signal transducer and activator of transcription 2, 113kDa
RAI14	retinoic acid induced 14
EMP1	epithelial membrane protein 1
KIF11	kinesin family member 11
CDK1	Cyclin-dependent kinase 1
NUF2	NUF2, NDC80 kinetochore complex component, homolog (S. cerevisiae)
NABP1	nucleic acid binding protein 1
KIF18A	kinesin family member 18A
PRKD3	protein kinase D3
MTHFD2	methylenetetrahydrofolate dehydrogenase (NADP+ dependent) 2
PTMS	parathymosin
SPECC1	sperm antigen with calponin homology and coiled-coil domains 1
EIF2AK2	eukaryotic translation initiation factor 2-alpha kinase 2
PRTFDC1	phosphoribosyl transferase domain containing 1
KIAA1524	KIAA1524
PTBP2	polypyrimidine tract binding protein 2
KIAA0101	KIAA0101
PTPN14	protein tyrosine phosphatase, non-receptor type 14
FBXO28	F-box protein 28
MX2	myxovirus (influenza virus) resistance 2 (mouse)
NCAPG	non-SMC condensin I complex, subunit G
CEP89	centrosomal protein 89kDa
CNPY3	canopy 3 homolog (zebrafish)
RIF1	RAP1 interacting factor homolog (yeast)
ATAD2	ATPase family, AAA domain containing 2
CALU	calumenin
FADS2	fatty acid desaturase 2
SLC16A4	solute carrier family 16, member 4 (monocarboxylic acid transporter 5)
ENPP5	ectonucleotide pyrophosphatase/phosphodiesterase 5 (putative)
BMPR2	bone morphogenetic protein receptor, type II (serine/threonine kinase)
SLC30A6	solute carrier family 30 (zinc transporter), member 6
ARHGAP11A	Rho GTPase activating protein 11A
LMO4	LIM domain only 4
RAB23	RAB23, member RAS oncogene family
BCAP29	B-cell receptor-associated protein 29

DTL	denticleless E3 ubiquitin protein ligase homolog (Drosophila)
CLIC4	chloride intracellular channel 4
TLK2	tousled-like kinase 2
CDC5L	CDC5 cell division cycle 5-like (S. pombe)
CDK2	cyclin-dependent kinase 2
KLHL14	kelch-like 14 (Drosophila)
C12orf4	chromosome 12 open reading frame 4
CCDC77	coiled-coil domain containing 77
DPYSL3	dihydropyrimidinase-like 3
CTHRC1	collagen triple helix repeat containing 1
MLF1IP	MLF1 interacting protein
TRMT6	tRNA methyltransferase 6 homolog (S. cerevisiae)
NCAPH	non-SMC condensin I complex, subunit H
ZNF302	zinc finger protein 302
ZBTB2	zinc finger and BTB domain containing 2
PLEKHG4B	pleckstrin homology domain containing, family G member 4B
SGOL2	shugoshin-like 2 (S. pombe)
FGF12	fibroblast growth factor 12
HERC5	HECT and RLD domain containing E3 ubiquitin protein ligase 5
RFC3	replication factor C (activator 1) 3, 38kDa
FBXO5	F-box protein 5
PARPBP	PARP1 binding protein
DKK3	dickkopf 3 homolog (Xenopus laevis)
STAU2	staufen, RNA binding protein, homolog 2 (Drosophila)
SEC22B	SEC22 vesicle trafficking protein homolog B (S. cerevisiae) (gene/pseudogene)
RAD1	RAD1 homolog (S. pombe)
KIAA0355	KIAA0355
CCNA2	cyclin A2
RNF144A	ring finger protein 144A
STIL	SCL/TAL1 interrupting locus
MSH6	mutS homolog 6 (E. coli)
MCM4	minichromosome maintenance complex component 4
TMPO	thymopoietin

Immnortalized vs. normal SC		STIC vs. normal oviduct	
p-value	Fold-Change	p-value	Fold-Change
0.000283907	3.80725	8.76E-07	4.23057
0.0144245	2.87429	0.000421892	3.8168
0.00716298	13.1974	4.28E-06	2.99104
0.00282425	4.4932	2.40E-06	2.94353
0.0472861	2.37036	0.00333233	2.82552
0.000144791	16.6572	0.000295215	2.72304
0.0360557	2.07024	0.00182861	2.69556
0.0155442	3.41929	0.000258971	2.67713
0.000987003	2.69336	0.00013513	2.65618
0.0384599	3.66365	0.000712484	2.63066
0.049286	3.34473	0.00240787	2.57426
0.00995083	4.19182	1.33E-05	2.55218
0.000815221	7.51886	0.0446495	2.52238
0.00103662	26.8722	0.0442521	2.48339
0.00406514	2.92177	0.000512702	2.47644
0.0440437	2.07644	0.0102092	2.2883
0.0146618	2.60053	0.00586935	2.2434
0.021717	2.65716	0.000371199	2.15717
8.38E-06	6.69368	0.00849818	2.15188
0.000667348	6.11737	0.0160522	2.12452
0.000441767	12.0686	0.0203638	2.07604
0.00479026	2.08711	0.000646319	2.06913
0.0472451	3.40855	0.000736568	2.06902
0.0184493	3.71605	0.00312586	2.05776
0.0384693	3.04204	0.0062282	2.03844
0.00446833	3.63974	0.000282922	2.01489
0.0176956	3.4969	0.000964698	2.00404
0.0424054	3.89455	0.000618361	1.99464
0.00893113	4.51362	0.000357272	1.98425
0.0104007	12.2952	0.00151445	1.9638
0.00123492	4.91539	0.000469143	1.96106
0.000783412	7.93847	0.0084577	1.95012
0.0196974	2.55622	0.000316293	1.94746
0.00158105	3.71015	8.16E-05	1.94129
0.0462063	2.82448	0.00638506	1.91164
0.0390095	4.1117	0.00165101	1.90968
0.000140019	2.80443	2.09E-05	1.88932
0.000216432	2.09166	9.57E-05	1.88057
0.0314904	2.44408	0.00629166	1.87344
0.00807315	12.0806	0.000205062	1.8629
0.00426074	14.3947	0.0229778	1.84615
0.0101394	3.42749	0.0075941	1.84499
0.0253665	2.86124	0.00881319	1.84464

0.0126441	5.27019	7.79E-05	1.83858
0.0191874	2.34074	0.00149298	1.83041
0.000268136	3.21355	0.00114403	1.82733
0.00369879	4.15964	0.00984894	1.8245
0.00407175	9.06502	0.00275194	1.82414
0.00083655	2.66607	0.000161309	1.80456
0.00520891	2.8186	1.07E-05	1.80031
0.0423289	3.741	0.0312376	1.79989
0.00469199	2.15955	0.00958603	1.79114
0.00550966	3.07566	0.0131361	1.78867
0.00161764	29.8796	0.0440225	1.77371
0.0130951	3.04741	0.00422736	1.76301
0.00875975	3.33513	0.00664215	1.75298
0.030317	3.5904	0.0100821	1.75181
0.039396	2.08173	0.0327551	1.74284
0.0428742	3.36452	0.000875107	1.73854
0.000234549	2.73747	0.0112627	1.73794
0.00183276	3.97249	0.00489193	1.737
0.00405556	3.08255	0.00350044	1.72237
0.00648228	2.47888	0.000740851	1.72116
0.00201868	3.3178	0.00488377	1.71706
0.00170041	2.14286	0.0218899	1.71534
0.0420002	2.24513	0.000834693	1.69995
0.0222086	2.49395	0.00973343	1.69965
5.14E-07	4.83426	0.00898711	1.6906
0.0209858	6.32114	5.02E-05	1.69015
0.000189528	6.15731	0.000338866	1.6883
0.00106914	2.11285	0.0205669	1.6871
0.0248471	3.29181	0.0408938	1.68567
0.000925396	2.37864	0.0244379	1.6841
0.0332968	2.00636	0.00621127	1.68318
4.11E-05	36.5634	0.0399436	1.68097
0.00692782	4.49406	0.000777004	1.67433
0.00588523	2.36836	0.00711967	1.67311
0.0111908	2.40382	0.00215059	1.67212
0.0335808	2.02439	0.00316773	1.67174
0.0230576	3.44623	0.00395446	1.66638
0.00520529	4.23804	0.0027015	1.64975
3.08E-06	3.2561	0.00322815	1.64855
1.07E-05	6.74615	0.00813651	1.64756
0.0200538	8.15037	0.0468952	1.64689
0.000752569	2.35956	0.0274736	1.6438
0.0188408	2.02722	0.0017683	1.64325
0.00178417	2.5401	0.00899648	1.63703
0.0476972	2.86426	0.000987487	1.6358
2.44E-06	3.29664	0.00897206	1.63094
0.0410158	2.72067	0.00775898	1.62293

0.000617135	3.98727	0.00333312	1.62264
0.000602153	2.56418	0.0415462	1.6206
0.0436593	2.17529	0.0317785	1.6142
0.00100088	2.80715	0.0137566	1.61287
0.00630406	3.30955	0.0152348	1.61234
0.00367269	7.16821	0.0129579	1.61218
0.00724886	2.49163	0.0120534	1.61084
0.0465192	3.49878	0.000262927	1.60787
0.000118014	6.52417	0.0144391	1.59572
0.00549029	23.5167	0.0435348	1.58698
0.00074259	5.44894	0.00331259	1.57913
0.0147488	2.36385	0.0119903	1.57533
0.0109051	3.06047	0.00160924	1.57371
0.00872522	3.98681	0.00845558	1.57159
0.0254929	2.60135	0.0224159	1.56814
0.0150965	5.70056	0.00541019	1.55604
0.00666477	3.6087	1.00E-05	1.55527
0.0102868	2.52622	0.000725724	1.55182
1.57E-05	36.887	0.000644676	1.55154
0.0149205	2.13383	0.00265562	1.55106
0.046043	3.54316	0.00136405	1.54256
0.00316853	3.11433	0.000703062	1.53346
0.0339119	6.37923	0.0115379	1.52728
0.0387225	3.03602	0.00145672	1.52095
0.00153509	3.00068	0.0302589	1.51537
0.0113217	3.63938	0.00658345	1.51434
0.0117881	2.80383	0.00519076	1.51323
0.00595046	2.98481	0.0429142	1.51204
0.00866395	4.28053	0.00252979	1.51191
0.00235006	4.79982	0.00112532	1.51049
0.00172162	2.58461	0.0267306	1.50822
0.000521248	2.55083	0.0327635	1.50167
0.00251306	2.71931	0.00420601	1.50058

Journal of Pathology
J Pathol 2014; **234:** 478–487

DOI: 10.1002/path.4417

ORIGINAL PAPER

The PAX2-null immunophenotype defines multiple lineages with common expression signatures in benign and neoplastic oviductal epithelium

Gang Ning,[1†] Jonathan G Bijron,[2†] Yusuke Yamamoto,[1] Xia Wang,[1] Brooke E Howitt,[3] Michael Herfs,[4] Eric Yang,[3] Yue Hong,[1] Maxence Cornille,[1] Lingyan Wu,[5] Suchanan Hanamornroongruang,[6] Frank D McKeon,[1†] Christopher P Crum[3†*] and Wa Xian[1,†]

[1] *Jackson Laboratory for Genomic Medicine, Farmington, CT, USA*
[2] *Department of Pathology, University of Utrecht, Utrecht, The Netherlands*
[3] *Department of Pathology, Division of Women's and Perinatal Pathology, Brigham and Women's Hospital, Boston, MA, USA*
[4] *Department of Pathology, University of Liège, Liège, Belgium*
[5] *Genome Institute of Singapore, A*STAR, Singapore*
[6] *Department of Pathology, Siriraj Hospital, Mahidol University, Bangkok, Thailand*

**Correspondence to: Christopher P Crum, Department of Pathology, Division of Women's and Perinatal Pathology, Brigham and Women's Hospital, Boston, MA, USA. e-mail: ccrum@partners.org*

[†] *Shared equal responsibility as first and senior authors.*

Abstract

The oviducts contain high-grade serous cancer (HGSC) precursors (serous tubal intraepithelial neoplasia or STINs), which are γ-H2AX^{p}- and *TP53* mutation-positive. Although they express wild-type p53, secretory cell outgrowths (SCOUTs) are associated with older age and serous cancer; moreover, both STINs and SCOUTs share a loss of PAX2 expression (PAX2^{n}). We evaluated PAX2 expression in proliferating adult and embryonic oviductal cells, normal mucosa, SCOUTs, Walthard cell nests (WCNs), STINs, and HGSCs, and the expression of genes chosen empirically or from SCOUT expression arrays. Clones generated *in vitro* from embryonic gynaecological tract and adult Fallopian tube were Krt7^{p}/PAX2^{n}/EZH2^{p} and underwent ciliated (PAX2^{n}/EZH2^{n}/FOXJ1^{p}) and basal (Krt7^{n}/EZH2^{n}/Krt5^{p}) differentiation. Similarly, non-ciliated cells in normal mucosa were PAX2^{p} but became PAX2^{n} in multi-layered epithelium undergoing ciliated or basal (WCN) cell differentiation. PAX2^{n} SCOUTs fell into two groups: type 1 were secretory or secretory/ciliated with a 'tubal' phenotype and were ALDH1^{n} and β-catenin^{mem} (membraneous only). Type 2 displayed a columnar to pseudostratified (endometrioid) phenotype, with an EZH2^{p}, ALDH1^{p}, β-catenin^{nc} (nuclear and cytoplasmic), stathmin^{p}, LEF1^{p}, RCN1^{p}, and RUNX2^{p} expression signature. STINs and HGSCs shared the type 1 immunophenotype of PAX2^{n}, ALDH1^{n}, β-catenin^{mem}, but highly expressed EZH2^{p}, LEF1^{p}, RCN1^{p}, and stathmin^{p}. This study, for the first time, links PAX2^{n} with proliferating fetal and adult oviductal cells undergoing basal and ciliated differentiation and shows that this expression state is maintained in SCOUTs, STINs, and HGSCs. All three entities can demonstrate a consistent perturbation of genes involved in potential tumour suppressor gene silencing (EZH2), transcriptional regulation (LEF1), regulation of differentiation (RUNX2), calcium binding (RCN1), and oncogenesis (stathmin). This shared expression signature between benign and neoplastic entities links normal progenitor cell expansion to abnormal and neoplastic outgrowth in the oviduct and exposes a common pathway that could be a target for early prevention.

Keywords: Fallopian tube; serous carcinoma; stem cell; PAX2; ALDH1

Received 29 May 2014; Revised 24 July 2014; Accepted 29 July 2014

No conflicts of interest were declared.

Introduction

Recent discoveries have strengthened the relationship between the distal Fallopian tube and epithelial malignancies traditionally attributed to the ovary, specifically high-grade serous carcinomas (HGSCs), the most lethal of ovarian cancers [1–3]. With these discoveries has emerged a collective effort to resolve the sequence of histological and molecular events giving rise to these tumours in the Fallopian tube. The serous carcinogenic sequence involves not only frank malignancies with metastatic spread, but also serous cancer precursors, including latent precursors – the p53 signature – and serous tubal intraepithelial neoplasms (STINs). The latter include intramucosal carcinomas (STICs) and lesser but immunophenotypically similar atypias that are considered premalignant intraepithelial lesions (STILs) [4,5]. Virtually all serous cancer precursors contain mutations in *TP53*, evidence of a DNA damage response (γ-H2AX^p), and predominate in the distal Fallopian tube [4]. Contiguous benign (p53 signatures) and malignant (STICs) epithelia have been documented with shared mutations in specific codons of *TP53* [4,6]. In addition, further studies have unearthed other benign epithelial alterations, termed secretory cell outgrowths (SCOUTs), that do not contain *TP53* mutations or evidence of a DNA damage response, yet share with precursors and carcinomas loss of PAX2 expression [7–9]. SCOUTs do not appear directly linked to HGSC, but have been documented at higher frequency in the normal tubes of postmenopausal women and those with HGSC [8,9]. Based on these properties, we have designated SCOUTs as 'surrogate precursors' and hypothesize that both SCOUTs and serous cancer precursors share properties or similar mechanisms in their pathogenesis, albeit with different potential outcomes.

The shared loss of PAX2 expression in both SCOUTs and many 'true' serous cancer precursors suggests that inactivation of this gene, while integral to neoplasia, has a wider range of associations and may signify a generic pathway common to epithelial cell expansion. The goals of this study were, firstly, to determine the breadth of the PAX2^n immunophenotype in the Fallopian tube by examining 'normal' cell growth and differentiation *in vitro* and *in vivo*. Secondly, we wanted to characterize more fully the alterations in expression that typified SCOUTs by array analysis and employ a biomarker profile to determine whether the SCOUT signature was recapitulated in STINs and HGSCs.

Materials and methods

Case material

This study was approved by the Brigham and Women's Human Investigation Committee and involved the use of discarded fresh and archived tissues. Case material for antibody staining consisted of the following epithelia/lesions: (1) normal salpingeal epithelium ($n = 15$); (2) SCOUTs ($n = 44$) and other outgrowths such as transitional-like metaplasia [Walthard cell nests (WCNs), $n = 5$]; (3) serous tubal intraepithelial neoplasms (STINs) ($n = 18$); and (4) metastatic or invasive serous carcinomas ($n = 39$). In addition, cultured clonogenic cells from normal Fallopian tubes were examined for selected marker expression. Cases for immunohistochemistry were selected by one of us (CPC) using previously described criteria (Figure 1) [10].

Cell culture

Fimbrial tissue was obtained from discarded surgical specimens of women undergoing benign procedures. Discarded fetal oviductal tissues were obtained by parental consent under an approved IRB protocol. Disaggregated cells were cultivated onto a feeder layer

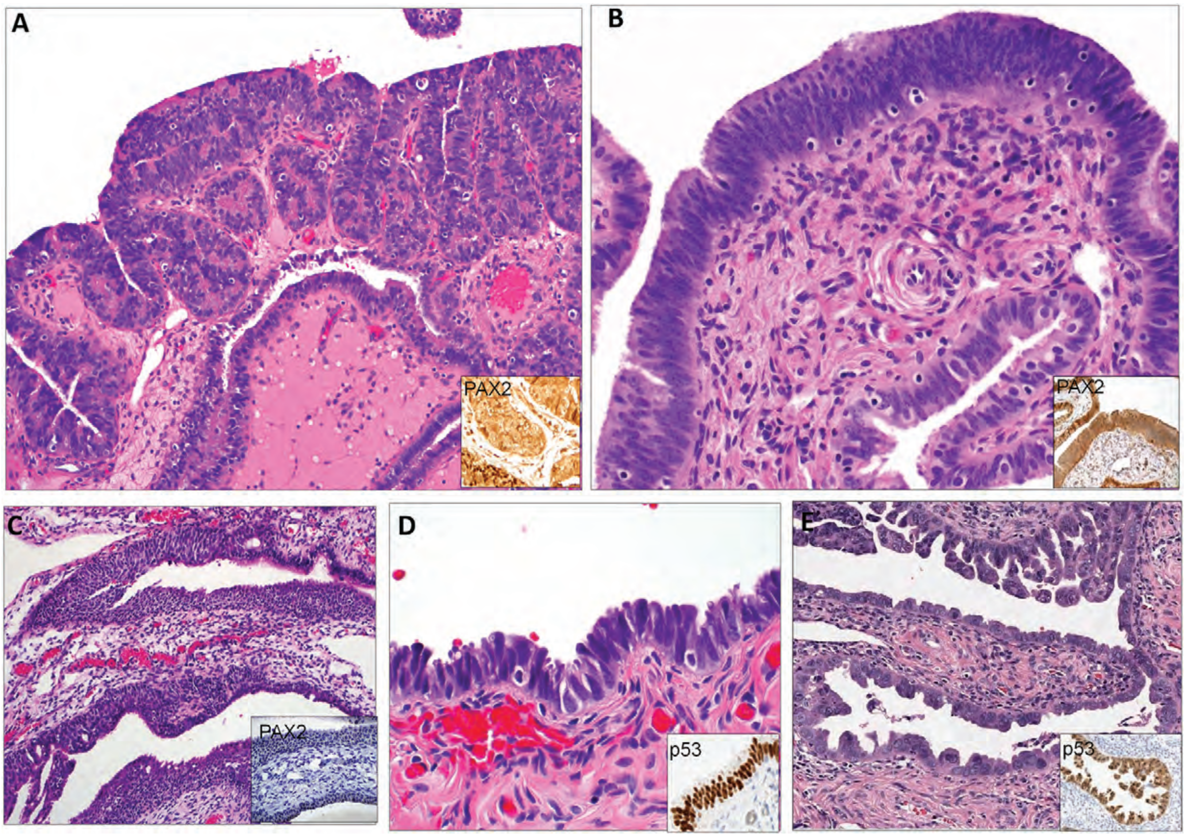

Figure 1. Entities associated with the PAX2^n immunophenotype included (A) type 1 secretory cell outgrowths (SCOUTs), (B) type 2 SCOUTs, (C) Walthard cell nests, and (D) low- and (E) high- (serous tubal intraepithelial carcinoma) grade tubal intraepithelial neoplasia.

of lethally irradiated 3 T3-J2 cells in stem cell culturing media (Jackson Laboratory, scm003). Clonal analysis and *in vitro* 3D differentiation were based on previously described methods for lung epithelial stem cells [11].

Microarray and bioinformatics

In order to identify genes expressed in PAX2^n epithelium, expression arrays were generated from formalin-fixed, laser-capture-micro-dissected (LCM) PAX2^n SCOUTs and benign control oviductal epithelium. RNAs obtained from the LCM procedure were amplified using the Ovation FFPE WTA System, WT-Ovation Exon Module, and Encore Biotin Module (NuGEN Technologies, San Carlos, CA, USA) and hybridized onto GeneChip® Human Exon 1.0 ST Arrays. GeneChip operating software was used to process all the Cel files and calculate probe intensity values. To validate sample quality, hybridization ratios were calculated using Affymetrix Expression Console software. The intensity values were $\log_2$-transformed and imported into the Partek Genomics Suite. Exons were summarized to genes and a one-way ANOVA was performed to identify differentially expressed genes. *p* values and fold change were calculated for each analysis. Heat maps were generated using Pearson's correlation and Ward's method with selected genes based on *p* value. Pathway analyses were performed using Gene Set Enrichment Analysis (GSEA) software. Candidate biomarkers were culled from these arrays and are summarized in Supplementary Table 1.

Immunohistochemistry

Immunostaining was performed with attention to the biomarkers in Supplementary Table 1, in which product information and dilutions are included. When normal-appearing epithelia were scanned for putative PAX2^n secretory cells, sections were immunostained with two antibodies concurrently: PAX2, which stains non-ciliated cells, and FOXJ1, a ciliated cell marker. Antibodies to leukocyte common antigen (LCA) for CD3, as well as FASCIN, were also used to track intraepithelial lymphocytes and dendritic cells, which are normally PAX2^n. Detection was completed with the Vectastain ABC kit (Cat No PK-6102; Vector Laboratories, Inc, Burlingame, CA, USA) with a liquid DAB-plus substrate kit (Cat No 00-2020). Slides were counterstained with Hematoxylin Stain 3 (Cat No CS402-1D). Antibody information is summarized in Supplementary Table 1. Reaction to antibody staining is indicated by superscripted 'p' or 'n' for positive or negative (PAX2, ALDH1, FOXJ1, etc), superscripted 'm' or 'wt' for mutated or wild type (p53), and superscripted 'nc' or 'mem' for nuclear and cytoplasmic versus membrane localization (β-catenin). Immunohistochemistry, immunofluorescence staining, and image acquisition were performed as previously described [9,11]. Proliferating clones were identified and immunostained for PAX2, PAX8, FOXJ1, Krt7, Krt5, p63, EZH2, and Ki67. Evidence of ciliated cell differentiation was identified by immunostaining for FOXJ1 and acetylated alpha-tubulin. Basal cells were identified by Krt5 or p63 immunostaining.

Results

Histological sub-classification of SCOUTs and STINs

The lesions under study are illustrated in Figure 1. Based on previous studies, SCOUTs were subdivided into two general histological categories [8,12]. The first, designated as type 1 SCOUTs, consisted of a typical mono- or bi-phasic tubal epithelial composition with either single layers of tubal non-ciliated cells or (more commonly) a combination of non-ciliated and ciliated cells. The second, arbitrarily labelled type 2 SCOUTs, consisted of proliferations with mildly pseudostratified and closely arranged elongated fusiform nuclei, similar to endometrial epithelium, and also termed 'endometrioid' SCOUTs. Cells with ciliated differentiation (FOXJ1^p) were present, but were typically less than 30% of the cells and scattered throughout the epithelium. Walthard cell nests (WCNs), consisting of basal cell outgrowth with a squamo-transitional phenotype, were also studied because they signify another form of outgrowth derived from columnar epithelial cells, albeit metaplastic. STINs were sub-classified as previously described and contained strong p53 immunostaining and evidence of DNA damage by H2AX staining [5]. Those with mild or moderate atypia and preserved epithelial polarity were classified as low grade and are identical to lesions classified as 'STILs', 'TILTs', and atypical hyperplasia in other reports [13–15]. Those with conspicuous loss of epithelial polarity were classified as high grade, synonymous with serous tubal intraepithelial carcinoma (STIC). The latter have a 0–11% outcome risk of HGSC, based on recent studies [16–18]. The HGSC outcome risk of lower-grade STINs is unknown but presumed to be less than that of high-grade STINs.

In vitro and *in vivo* expression of PAX2 in the Fallopian tube mucosa

Cultured epithelial cells from the gynaecological tract, both in adults and at 20 weeks' gestation, were plated and colonies of clonogenic cells were characterized. The dominant immunophenotype associated with highly-proliferative clonogenic cell outgrowth was Krt7^p/PAX8^p/EZH2^p/ PAX2^n/Krt5^n/p63^n (Figures 2A, 3A, and Supplementary Figure 2A). FOXJ1 expression indicating ciliated cell differentiation was also seen occasionally in the non-proliferative cells that were not stained positively with Ki67 (Figure 2A). To examine the differentiation ability of these cloned cells at the single-cell level, we established single-cell pedigree lines by subsequent rounds of plating and clone selection (Figure 2B). Pedigree lines of these cloned oviductal progenitor cells were differentiated

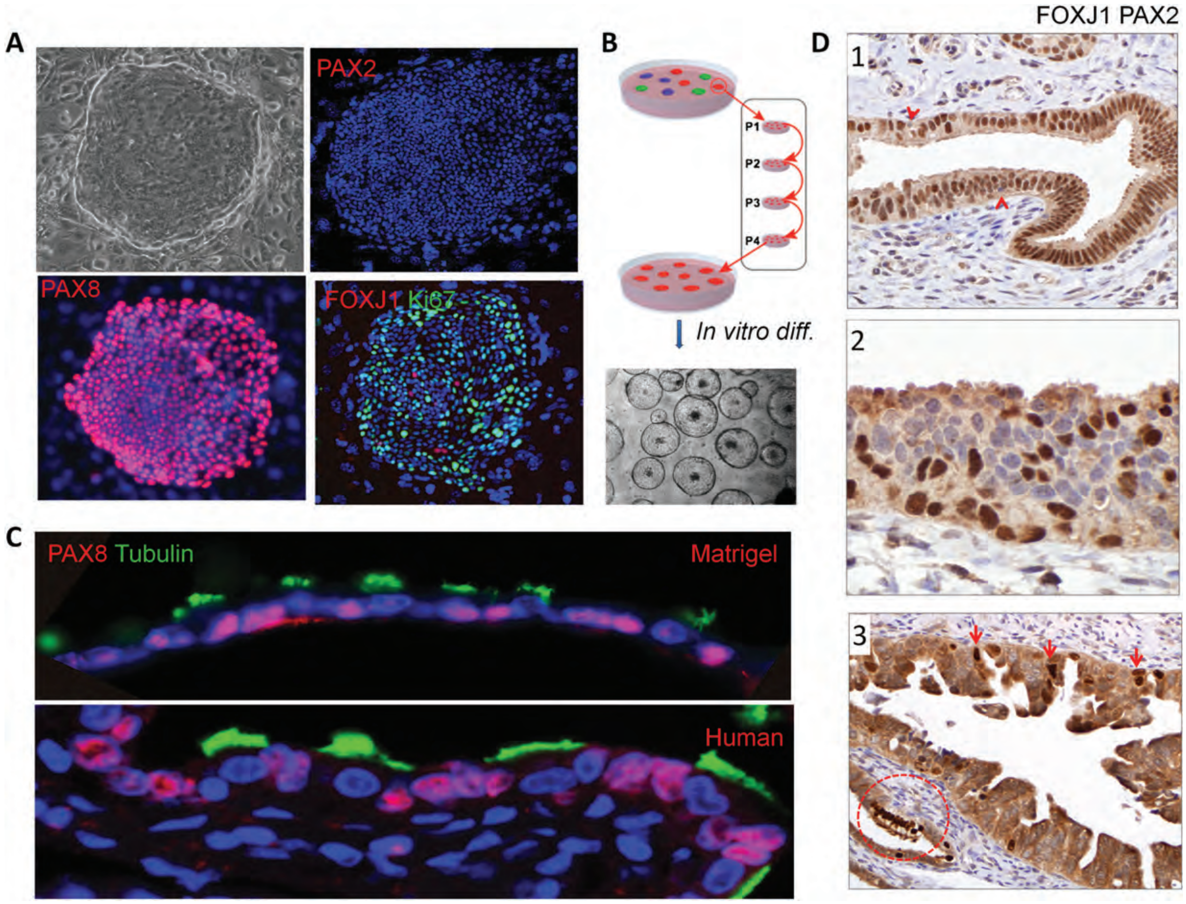

Figure 2. *In vitro* propagation and differentiation of oviductal progenitor cells. (A) The cells cloned from fetal or adult oviduct are PAX2^{n}, PAX8^{p} and occasionally express differentiation marker (FOXJ1) in non-proliferative cells (Ki67^{n}). (B) Schematic diagram of pedigree cell line establishment. (C) Upper panel: representative image of fetal (20-week) oviductal progenitor cells differentiated in 3D Matrigel culture system. Lower panel: immunofluoresence image of human adult oviduct epithelium. Acetyl-alpha-tubulin (green) indicates ciliated cell differentiation. PAX8 (red) indicates non-ciliated cells. DAPI stains nuclei (blue). (D1) Combined staining of histological sections of normal tube with both PAX2 and FOXJ1 reveals widespread nuclear staining, except occasional lymphocytes (arrows). (D2) Occasional foci of multi-layered epithelium undergoing ciliated cell differentiation (positive nuclei) consist of some cells negative for PAX2. (D3) Tubal intraepithelial carcinoma with focal FOXJ1 staining (arrowheads) indicating ciliated cell differentiation. Circled focus of normal ciliated cells is an internal positive control.

in either an air–liquid interface (ALI) cell culture system or 3D Matrigel cultures for 10–20 days. In 3D Matrigel cultures, PAX8^{p} oviductal progenitor cells differentiated into columnar epithelium consisting of acetylated tubulin^{p}/FOXJ1^{p}/PAX8^{n} ciliated cells and PAX8^{p} non-ciliated cells, which resembles the human oviduct histology (Figure 2C). In the ALI culture system, a series of images of acetylated tubulin expression were taken at different time points during the differentiation and showed that the oviductal progenitor cells started to differentiate into ciliated cells at day 3 and became maturely differentiated at day 10 (Supplementary Figure 2B). At day 10 in the ALI culture system, the cloned oviductal progenitor cells formed a simple epithelium with ciliated cells marked by FOXJ1 and acetylated tubulin and non-ciliated cells marked by PAX2 (Supplementary Figure 2C). It is noteworthy that while the proliferating population is PAX2^{n} (Figure 2A), PAX2 expression was reclaimed in some non-ciliated (secretory) cells. This further indicates that the progeny of a single oviductal progenitor cell can give rise to all epithelial lineages typically found in the oviduct, including not only mature ciliated cells but also non-ciliated (secretory) cells.

Immunostaining of both fetal and adult Fallopian tubes was performed to ascertain the distribution of PAX2-expressing cells and address the possibility that the PAX2^{n} immunophenotype was programmed earlier in development. Histological sections of fetal (at 21 weeks) and adult Fallopian tubes were examined. Fetal tubes contained an abundance of PAX2^{p} cells, with occasional interspersed ciliated cells (Supplementary Figure 1A). Expression of PAX8 was similar in distribution (Supplementary Figure 1B). Similarly, in normal adult tubes, PAX2 staining was extensive in cells that were not undergoing ciliated (tubulin^{p}) differentiation (Supplementary Figure 1C). A summary of immunophenotypes for progenitor and adult cells is displayed in Supplementary Table 2.

In the adult tubes, sections were also stained with FOXJ1, and/or LCA to account for other PAX2^{n}

Published by John Wiley & Sons, Ltd. www.pathsoc.org.uk

cells that were either undergoing ciliated differentiation or were non-epithelial. Mono-layered or mildly pseudostratified normal Fallopian tube mucosa typically contained cells expressing either PAX2 or FOXJ1 (Figure 2D1). In occasional foci of prominent multi-layered epithelium with some cells staining positive with FOXJ1, loss of PAX2 nuclear staining could be seen (Figure 2D2), giving the impression that loss of PAX2 expression in non-ciliated cells was coordinated with cell growth in multi-layered epithelium. Albeit less so, FOXJ1 staining was also seen in STINs, supporting ciliated differentiation in PAX2^n neoplastic growth (Figure 2D3).

Metaplastic (WCNs) differentiation of PAX2^n columnar cells *in vitro* and *in vivo*

WCNs are foci of transitional-like metaplasia in the fimbria or adjacent peritoneal surface and are emblematic of basal cell outgrowth that can develop near the junctions of disparate epithelial types [19]. Other sites include the gastro-oesophageal and cervical squamo-columnar junctions. Both have been designated as sites harbouring residual embryonic cells and studies of the latter have suggested that basal or reserve cells emerge from the overlying columnar cells and then undergo squamous metaplasia [20,21]. This process has been termed ‘top-down’ differentiation, ie the progeny (basal cells) emerge from beneath the progenitor population. However, no study has ever displayed this sequence *in vitro*. Fetal tubal cells propagated *in vitro* were strongly positive for both Krt7 and PAX8, in keeping with Müllerian epithelium (Figures 2A and 3A). Moreover, these progenitor cells did not express Krt5 or p63 (Figure 3A). Interestingly, when pedigree lines of these cloned oviductal progenitor cells were differentiated in 3D Matrigel cultures for 10–20 days, in addition to the typical ciliated cell differentiation (Figure 2C), subjacent p63/Krt5^p basal cells emerged (Figure 3B1) and expanded (Figure 3B3) in a pattern similar to that

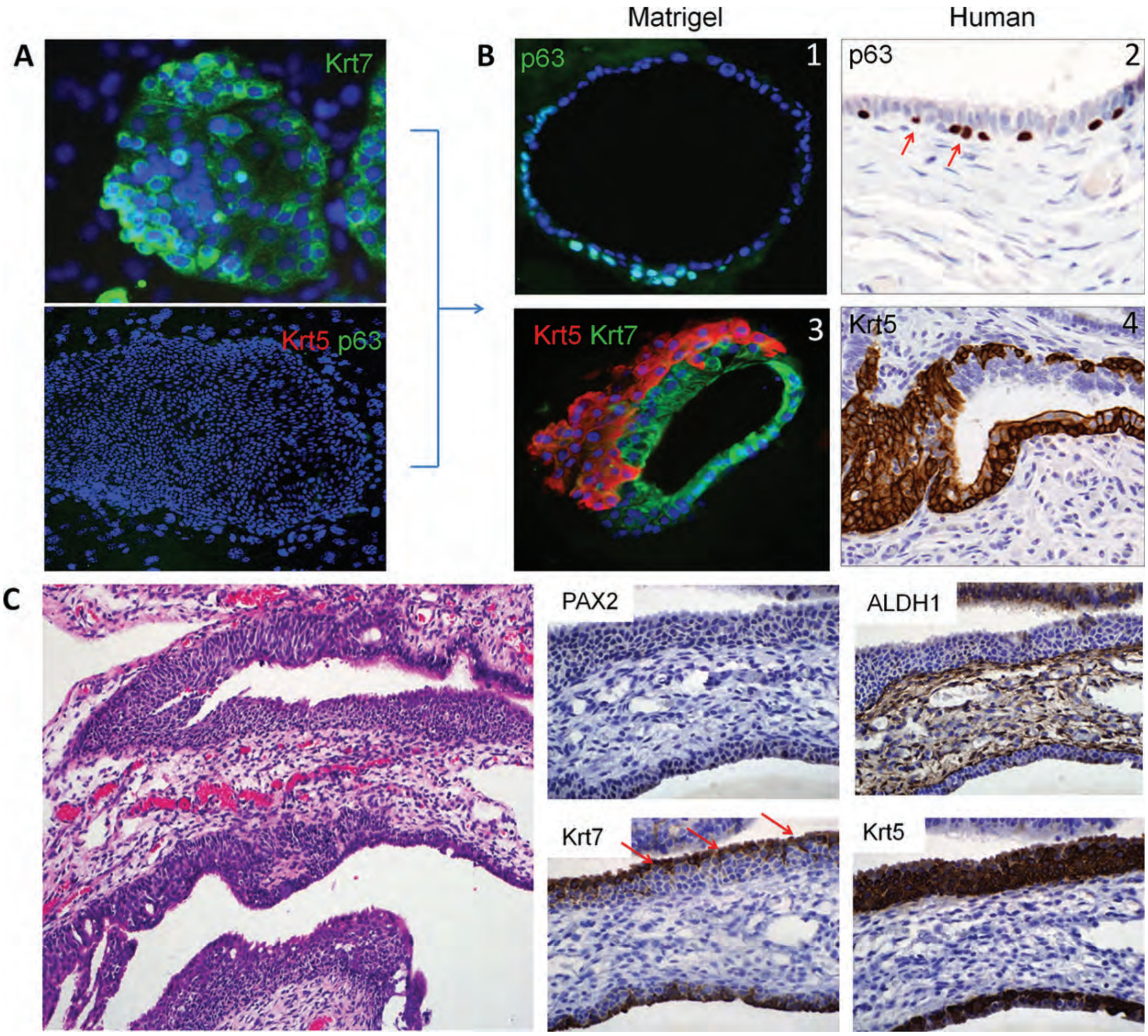

Figure 3. *In vitro* and *in vivo* basal cell differentiation in the oviduct. (A) Colonies of Krt7^p/Krt5^n/p63^n cells from a 20-week-old fetal oviduct. (B1, B3) Single (p63, green) and multi-layered (Krt5, red) basal cell outgrowth seen in Matrigel cultures. (B2, B4) Similar basal cell growth highlighted by p63 and Krt5 in the adult fimbria. (C) Walthard cell nest in the adult tube is typically PAX2 and ALDH1 negative. Residual Krt7-positive cells (arrows) are displaced from beneath by an expanding Krt5 population.

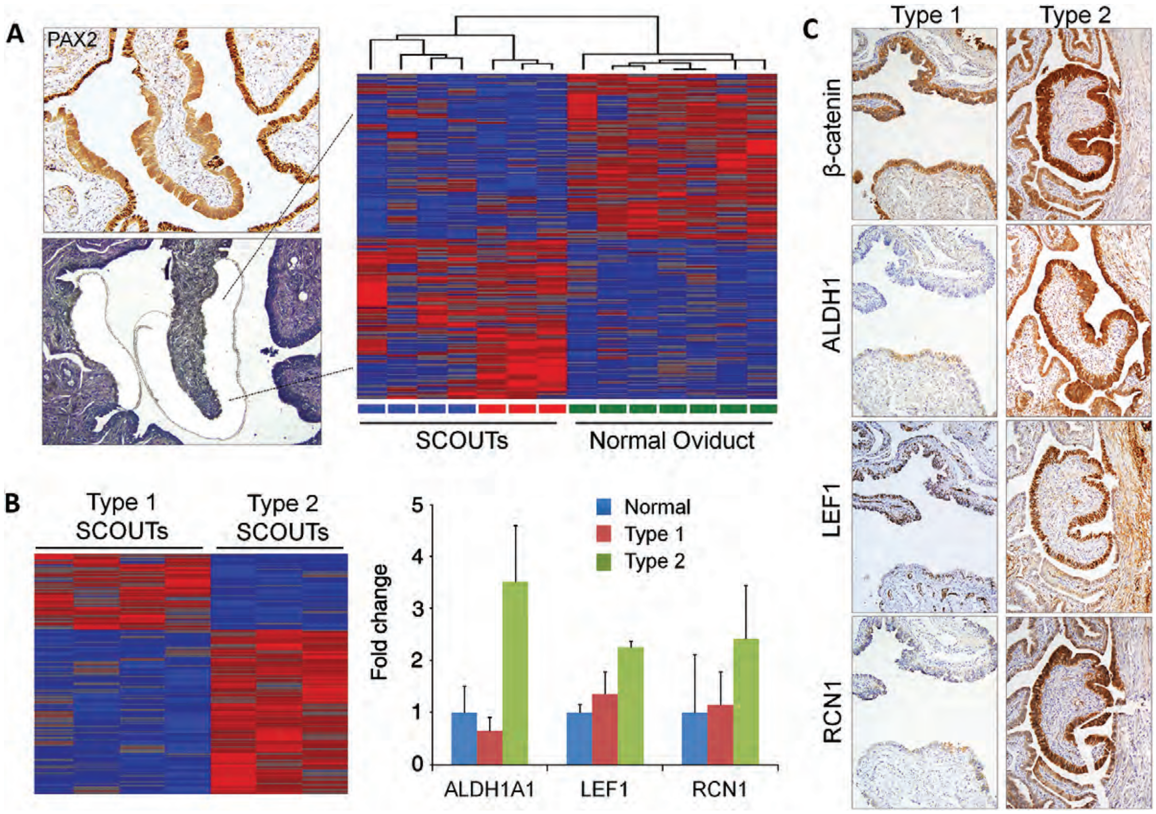

Figure 4. (A) Laser-captured micro-dissected SCOUTs (left) and a heat map comparison of SCOUTs and normal oviduct (right). (B) Arrays generated from PAX2^{n} SCOUTs revealed genes differentially expressed across type 1 and type 2 SCOUTs, including ALDH1, LEF1, and RCN1 (right). (C) Coordinated expression of the above genes distinguish type 1 SCOUTs, which show membraneous β-catenin localization and absent ALDH1 staining plus negative or weak staining for LEF1 and RCN1 staining (left), from type 2 SCOUTs, with nuclear and cytoplasmic β-catenin, strong ALDH1, LEF1, and RCN1 staining (right).

seen in p63/Krt5^{p} cells in WCNs in the adult tube (Figures 3B2 and 3B4). *In vitro*, the Krt5 and p63 immunopositive cells were superimposed, although the Krt5 staining index was higher (Supplementary Figure 2E). Analysis of WCNs in tissue sections (Figure 3C) revealed a strikingly similar pattern of growth and differentiation, arising either from beneath Krt7^{p} epithelial cells or in continuity with columnar epithelium typical of type 1 SCOUTs. The result was a PAX2^{n}/ALDH1^{n} transitional-like outgrowth that was strongly Krt5^{p} but stathmin^{n} (not shown). Taken in the context of the *in vitro* findings, this observation further linked the PAX2^{n} immunophenotype to cell outgrowth and a Krt7^{p} progenitor cell to the development of not only terminal (FOXJ1^{+}) but also metaplastic (Krt5^{+}) differentiation in the Fallopian tube.

Altered gene expression in PAX2^{n} proliferations (SCOUTs, STINs, and HGSCs)

Supplementary Table 3 is a list of genes selected for analysis and found to be differentially expressed in SCOUTs relative to normal-appearing epithelium. Arrays generated from RNA extracted from formalin-fixed laser-capture micro-dissected SCOUTs yielded differentially expressed genes, illustrated in the representative heat map (Figures 4A, 4B, and Supplementary Figures 4 and 5). When stained with selected markers, type 1 SCOUTs varied from strictly secretory to mixed secretory and ciliated, and were ALDH1^{n}, β-catenin^{mem} and stained weakly or negative for LEF1, RCN1, RUNX2, and EZH2 (Figures 4C, 5, and Supplementary Figure 3). Type 2 SCOUTs stained variably for ciliated cell differentiation and were β-catenin^{nc} and ALDH1, LEF1, RCN1, EZH2, RUNX2 (not shown) and stathmin positive (Figures 4C, 5, and Supplementary Figure 3). Basal cell differentiation, signifying WCN development, was associated with PAX2^{n} columnar epithelium, suggesting that this pathway of differentiation might initiate within type 1 PAX2^{n} SCOUTs.

Figure 5 and Supplementary Figure 6 summarize the staining patterns observed in the different lesions. STINs and HGSCs shared expression of several markers with SCOUTs. Expression patterns for ALDH and β-catenin were identical to type 1 SCOUTs (ALDH^{n} and β-catenin^{mem}). In addition, like type 2 SCOUTs, there was increased staining for EZH2, stathmin, LEF1, RCN, Krt5, and RUNX2 (not shown). Not surprisingly, no marker in this group separated STINs or HGSCs from SCOUTs. This is in contrast to other published markers such as Ki67, cyclin E, p16, and others, which are significantly more commonly expressed in STINs and HGSCs relative to benign Fallopian tube mucosa [4,5,15,22].

Published by John Wiley & Sons, Ltd. www.pathsoc.org.uk

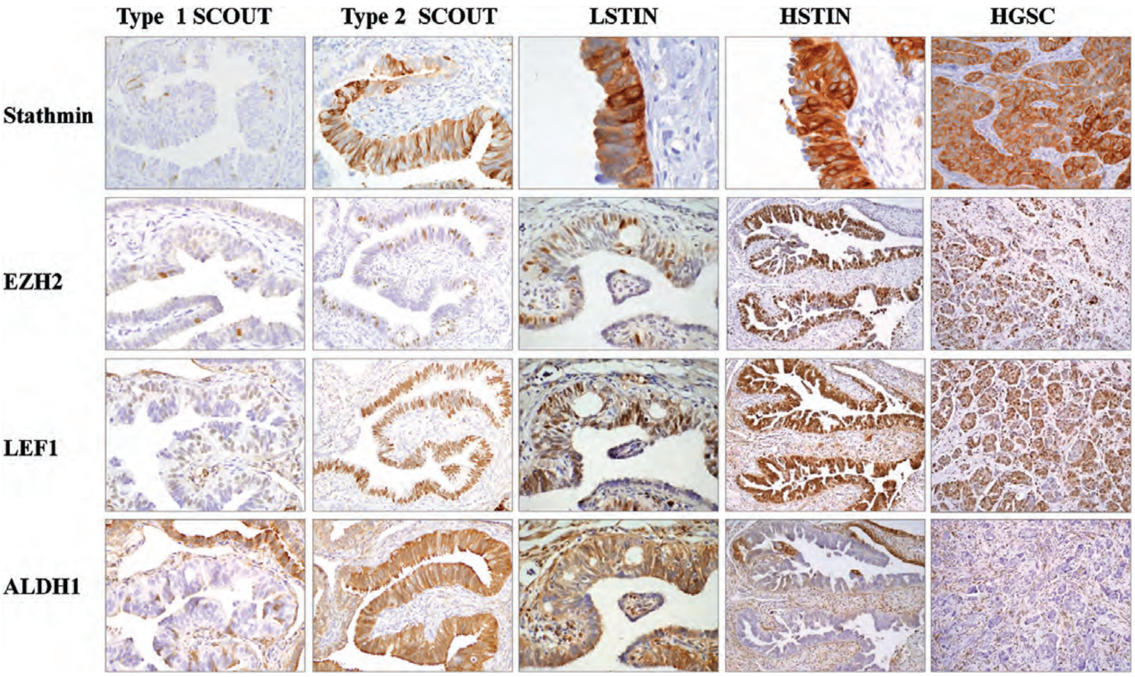

Figure 5. Shared expression of SCOUT markers with low- (LSTIN) and high- (HSTIN or STIC) grade serous tubal intraepithelial neoplasia and high-grade serous carcinoma (HGSC). Neoplasms (STINs, HGSCs) share with type 1 SCOUTs loss of PAX2 and ALDH1, and with type 2 SCOUTs, increased LEF1, EZH2, and stathmin and other markers (see text).

Discussion

Analysis of arrays generated from high-grade serous cancer has confirmed a transcriptome that parallels oviductal epithelium [23]. Given that these tumours are strongly positive for biomarkers (such as PAX8) typically assigned to non-ciliated (so-called secretory) cells, the assumption has been that the secretory cell is the cell of origin [1]. Levanon *et al* showed that PAX8-expressing (secretory) cells of the tube were uniquely susceptible to DNA damage imposed by irradiation, a finding that parallels similar observations in latent precursors (p53 signatures) and STINs that contain *p53* mutations [5,24]. However, with the discovery of PAX2$^{\mathrm{n}}$ SCOUTs and a similar PAX2$^{\mathrm{n}}$ expression pattern in many STINs, it became clear that there may be a relationship between the two entities, despite the fact that SCOUTs are more ubiquitous in the Fallopian tube and do not arise in the setting of a DNA damage response and loss of p53 function. Although altered PAX2 expression has been associated with neoplasia, we hypothesized that the PAX2$^{\mathrm{n}}$ immunophenotype typified a ‘generic’ series of molecular events that were the underpinning of stem cell expansion common to many proliferations.

We addressed PAX2 expression or loss in the Fallopian tube from three perspectives. The first was by analysing expression and differentiation in proliferating normal adult and fetal cells propagated *in vitro*. The second was by comparing the *in vitro* findings to expression in tissue sections from fetal and adult tubes. The third was to look for shared expression across PAX2$^{\mathrm{n}}$ cells in cell proliferation and expansion (SCOUTs, STINs, and HGSCs). We discovered that the PAX2$^{\mathrm{n}}$ immunophenotype was particularly linked to *in vitro* and *in vivo* cell growth, not infrequently with an increase in EZH2 expression. Moreover, in highly clonogenic Krt7$^{\mathrm{p}}$/FOXJ1$^{\mathrm{n}}$ oviductal progenitor cells grown *in vitro*, we demonstrated for the first time that PAX2$^{\mathrm{n}}$ expanding populations were capable of both ciliated (FOXJ1) and basal cell (Krt5) differentiation. This sequence of cell growth and differentiation was recapitulated in SCOUTs, STINs, and HGSCs, with progressively reduced ciliated differentiation in the type 2 SCOUTs, STINs, and HGSCs. We thus concluded that all of these entities were related to a similar progenitor cell.

The next goal was to determine if the cells involved in benign and neoplastic outgrowth shared common expression patterns and we chose to use the least proliferative lesions (SCOUTs) as the reference. One advantage of this approach is to identify events that occur prior to the more dramatic molecular changes that characterize malignancy that may have profound influences on expression. The study delineated two general groups of SCOUTs: the first (type 1) closely resembled normal tubal epithelium, histologically and in their expression profile (Figure 1D). The second (type 2) was composed of proliferations with less pronounced ciliated differentiation, many noticeably ‘endometrial’-like (Figure 1E). Accordingly, there was minimal difference in expression between type 1 SCOUTs and control epithelium, although they were consistently ALDH1$^{\mathrm{n}}$. In contrast, type 2 SCOUTs demonstrated nuclear and cytoplasmic β-catenin staining plus increased BCL2 (see ref 7), ALDH1, and Krt5 staining. This diversity in phenotype underscores the complexity of cell growth and differentiation that can occur in the Fallopian tubes with age. Type 1 SCOUTs appear to signify very minor genomic changes, as evidenced by the similarities in transcription to normal controls. Thus, the alterations in transcription are limited to absence of ALDH1 expression. In contrast, type 2 SCOUTs, which exhibit a more divergent histology, have a common biomarker signature – stathmin, EZH2, LEF1, RCN1, and RUNX2 – that is more similar to premalignant (STINs) and malignant (HGSCs) entities in the tube (Figure 5).

A fundamental question stemming from the above observation is the relevance of the gene signature found in SCOUTs, STINs, and HGSCs to both stem cell biology and neoplasia. ALDH1 has been identified as a marker of epithelial stem cells. Its expression can be both increased or absent, the latter more typical of STINs and HGSCs [25,26]. EZH2 is a polycomb suppressor that is implicated in stem cell maintenance and regulation of differentiation. It is noteworthy that EZH2 expression typically increased in areas of cell expansion, in keeping with the coordinated suppression of PAX2 expression [27]. EZH2 is also a potential suppressor of tumour suppressor genes [28]. LEF1 is likewise expressed during lineage differentiation [29]. The function of RCN1 is less clear but this gene product is a calcium binder that is weakly expressed in renal tubular cells and up-regulated in renal cell carcinomas [30]. *RUNX2* is a gene involved in morphogenesis and osteoblastic differentiation [31]. Functions attributed to stathmin are multiple. It is a marker of P13 kinase activation that has been linked to serous neoplasia in some studies, tumour progression and metastases in others, and regulates p53 stability in still others [32–34]. Its range of expression, including normal epithelium, SCOUTs, and STINs, is similar to that of these other markers, several of which (ALDH1, PAX2, EZH2) have also been linked to not only stem cells but also outcome or resistance to chemotherapy [35–37]. The significance of the unique β-catenin staining in type 2 SCOUTs, with a shift in distribution from the membrane to the cytoplasm and nucleus, is unclear but it is emblematic of Wnt pathway activation, and mutations in β-catenin are commonly found in endometrial and colon carcinomas [38].

Walthard cell nests are a common benign condition seen in the distal Fallopian tube mucosa or the adjacent peritoneal reflection [19]. They bear a close resemblance to the cervical squamo-columnar junction, where columnar cells are undermined by p63-positive basal cells. These cells could be envisioned to either originate from the columnar epithelium or give rise to the overlying Krt7-positive epithelial cells. This study has made two novel observations. First, based on the Matrigel cell culture data, the basal cells emerge from the Krt7-positive columnar cells. Second, this process is marked by not only loss of PAX2 but also ALDH1 expression, similar to that seen in type 1 SCOUTs. The initiating cell, the Krt7^{p} non-ciliated epithelial cell, is remarkably similar to the cells seen in the squamo-columnar (SC) junction of the cervix from which squamous metaplasia is derived and this process is similar to so-called 'top-down' differentiation reported in the SC junction [21]. The fact that

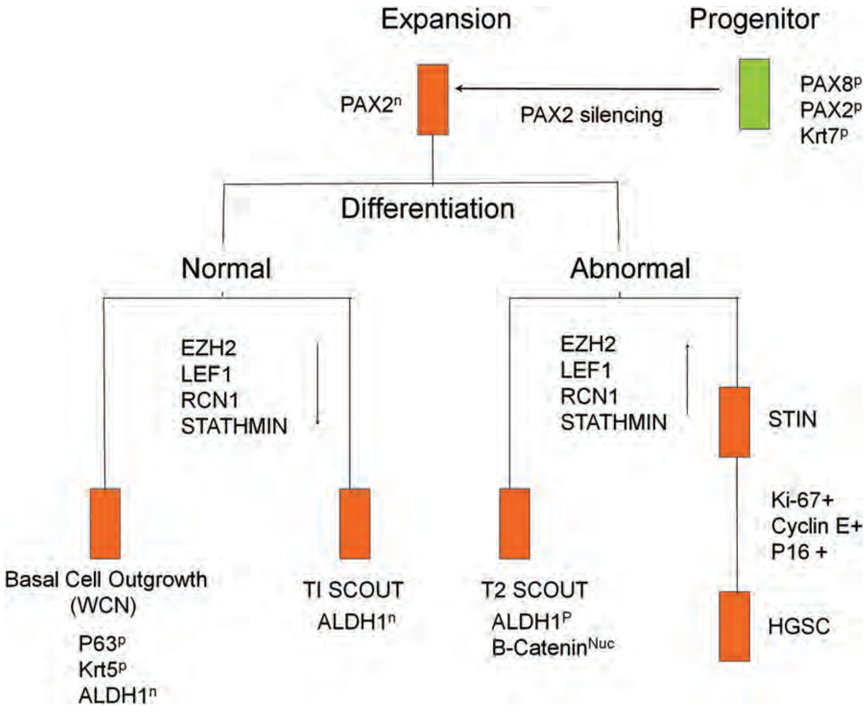

Figure 6. A progenitor cell model for the Fallopian tube in which Krt7 identifies the progenitor cell and PAX2^{n} defines progenitor cell expansion. Expanding PAX2^{n} cells can differentiate into basal or ciliated cells in WCNs or type 1 SCOUTs, both of which approximate normal differentiation pathways, with loss of ALDH1 and normal or minimally increased expression of LEF1, RCN1, stathmin, and EZH2. In contrast, type 2 SCOUTs and STINs (right) share a different expression signature characterized by multiple genes, including EZH2, LEF1, RCN1, and stathmin and others, involved in a divergent pathway of progenitor cell growth.

Published by John Wiley & Sons, Ltd. www.pathsoc.org.uk

WCNs are not considered direct precursors to malignancy is not surprising, in as much as they are terminally differentiated relative to their progenitors. This is similar to the cervix, where the progenitor cells in the SC junction are considered more vulnerable to neoplastic transformation than their metaplastic progeny [21]. What is interesting is the fact that WCNs underscore the existence of multi-potential cells in the distal Fallopian tube [12]. Given that 40–60% of HGSCs do not have a documented source (or STIN) in the Fallopian tube mucosa, coupled with the fact that a subset of HGSCs are strongly Krt5-positive, the possibility that cells involved in alternate differentiation pathways might contribute to a subset of these malignancies deserves further study (Hanamornroongruang S, Howitt BE, Crum CP, unpublished) [5,25].

Epithelia in virtually every organ (breast being a prime example) display a wide range of clonal expansions, some of which may be direct precursors to malignancy and others of which serve as risk factors for a malignant outcome. The model depicted in Figure 6 reflects a similar but novel scenario in the oviduct, with multiple categories of putative monoclonal cell outgrowth and striking similarities in expression across multiple genes between surrogate precursors and lesions that are considered premalignant or pre-metastatic. These findings emphasize the complexity of molecular and phenotypic perturbations that can take place in the Fallopian tubes during and following menopause. This complexity invites caution when considering the role (or diagnostic value) of newly discovered biomarkers as specific indicators of neoplasia. More importantly, it reveals a consistent disturbance in progenitor cell biology in keeping with a common pathway that is triggered by more than one initiating event. Thus, it introduces two approaches to cancer prevention, one directed at the initiating event and the other at the early perturbations in the pathway.

Acknowledgments

This work was supported by grants from the Department of Defense and National Cancer Institute (W81XWH-10-1-0289 and 5R21CA173190-02 to CC). We thank the Division of Gynecologic Oncology at Brigham and Women's Hospital and Dana Farber Cancer Institute for their contribution to the study, and Mei Zheng for assistance with the immunohistochemistry. We are also grateful for the support of this work by the Genome Institute of Singapore of the Agency for Science, Technology and Research, and a Bedside and Bench Grant from Singapore National Medical Research Council.

Author contribution statement

Contributions of the co-authors to design (1), data collection (2), data analysis (3), data interpretation (4), literature search (5), figures (6), and manuscript writing (7) were as follows: GN (1–4, 6, 7); JGB (1–4, 6, 7); YY (1–3, 6); XW (2, 3); BEH (1, 2, 4, 5); MH (1–4); EY (1–3, 5); YH (2–4); MC (2–4); LW (2–4); SH (2–4); FDMcK (1, 4, 7); CPCr (1, 4, 7); and WX (1, 3, 4, 7).

Abbreviations

ALI, air–liquid interface culture; SCOUT, secretory cell outgrowth; STIN, serous tubal intraepithelial neoplasia; WCN, Walthard cell nest

References

1. Piek JM, van Diest PJ, Zweemer RP, *et al.* Dysplastic changes in prophylactically removed Fallopian tubes of women predisposed to developing ovarian cancer. *J Pathol* 2001; **195:** 451–456.
2. Kindelberger DW, Lee Y, Miron A, *et al.* Intraepithelial carcinoma of the fimbria and pelvic serous carcinoma: evidence for a causal relationship. *Am J Surg Pathol* 2007; **31:** 161-169.
3. Finch A, Shaw P, Rosen B, *et al.* Clinical and pathologic findings of prophylactic salpingo-oophorectomies in 159 BRCA1 and BRCA2 carriers. *Gynecol Oncol* 2006; **100:** 58-64.
4. Lee Y, Miron A, Drapkin R, *et al.* A candidate precursor to serous carcinoma that originates in the distal Fallopian tube. *J Pathol* 2007;211:26-35. Erratum in *J Pathol* 2007; **213:** 116.
5. Crum CP, Herfs M, Ning G, *et al.* Through the glass darkly: intraepithelial neoplasia, top-down differentiation and the road to ovarian cancer. *J Pathol* 2013; **231:** 402-412.
6. Carlson JW, Miron A, Jarboe EA, *et al.* Serous tubal intraepithelial carcinoma: its potential role in primary peritoneal serous carcinoma and serous cancer prevention. *J Clin Oncol* 2008; **26:** 4160-4165.
7. Chen EY, Mehra K, Mehrad M, *et al.* Secretory cell outgrowth, PAX2 and serous carcinogenesis in the Fallopian tube. *J Pathol* 2010; **222:** 110-116.
8. Quick CM, Ning G, Bijron J, *et al.* PAX2-null secretory cell outgrowths in the oviduct and their relationship to pelvic serous cancer. *Mod Pathol* 2012; **25:** 449-455.
9. Bijron JG, Ning G, Laury AR, *et al.* Digital quantification of precursor frequency in the Fallopian tube and its significance. *Mod Pathol* 2012; **25:** 1654-1661.
10. Mehrad M, Ning G, Chen EY, *et al.* A pathologist's road map to benign, precancerous, and malignant intraepithelial proliferations in the Fallopian tube. *Adv Anat Pathol* 2010; **17:** 293-302.
11. Kumar PA, Hu Y, Yamamoto Y, *et al.* Distal airway stem cells yield alveoli *in vitro* and during lung regeneration following H1N1 influenza infection. *Cell* 2011; **147:** 525-538.
12. Laury AR, Ning G, Quick CM, *et al.* Fallopian tube correlates of ovarian serous borderline tumors. *Am J Surg Pathol* 2011; **35:** 1759-1765.
13. Vang R, Visvanathan K, Gross A, *et al.* Validation of an algorithm for the diagnosis of serous tubal intraepithelial carcinoma. *Int J Gynecol Pathol* 2012; **31:** 243-253.
14. Ning G, Bijron JG, Yuan J, *et al.* Differential expression of p-ERM, a marker of cell polarity, in benign and neoplastic oviductal epithelium. *Int J Gynecol Pathol* 2013; **32:** 345-352.
15. Lee S, Nelson G, Duan Q, *et al.* Precursor lesions and prognostic factors in primary peritoneal serous carcinoma. *Int J Gynecol Pathol* 2013; **32:** 547-555.
16. Wethington SL, Park KJ, Soslow RA, *et al.* Clinical outcome of isolated serous tubal intraepithelial carcinomas (STIC). *Int J Gynecol Cancer* 2013; **23:** 1603-1611.

17. Lowell CB, Swisher EM, Cass I, *et al.* Long term follow up of *BRCA1* and *BRCA2* mutation carriers with unsuspected neoplasia identified at risk reducing salpingo-oophorectomy. *Gynecol Oncol* 2013; **129:** 364-371.

18. Conner JR, Meserve E, Pizer E, *et al.* Outcome of unexpected adnexal neoplasia discovered during risk reduction salpingo-oophorectomy in women with germ-line *BRCA1* or *BRCA2* mutations. *Gynecol Oncol* 2014; **132:** 280-286.

19. Seidman JD, Yemelyanova A, Zaino RJ, *et al.* The Fallopian tube-peritoneal junction: a potential site of carcinogenesis. *Int J Gynecol Pathol* 2011; **30:** 4-11.

20. Wang X, Ouyang H, Yamamoto Y, *et al.* Residual embryonic cells as precursors of a Barrett's-like metaplasia. *Cell* 2011; **145:** 1023-1035.

21. Herfs M, Yamamoto Y, Laury A, *et al.* A discrete population of squamocolumnar junction cells implicated in the pathogenesis of cervical cancer. *Proc Natl Acad Sci U S A* 2012; **109:** 10516-10521.

22. Sehdev AS, Kurman RJ, Kuhn E, *et al.* Serous tubal intraepithelial carcinoma upregulates markers associated with high-grade serous carcinomas including Rsf-1 (HBXAP), cyclin E and fatty acid synthase. *Mod Pathol* 2010; **23:** 844-855.

23. Marquez RT, Baggerly KA, Patterson AP, *et al.* Patterns of gene expression in different histotypes of epithelial ovarian cancer correlate with those in normal Fallopian tube, endometrium, and colon. *Clin Cancer Res* 2005; **11:** 6116-6126.

24. Levanon K, Ng V, Piao HY, *et al.* Primary *ex vivo* cultures of human Fallopian tube epithelium as a model for serous ovarian carcinogenesis. *Oncogene* 2010; **29:** 1103-1113.

25. Deng S, Yang X, Lassus H, *et al.* Distinct expression levels and patterns of stem cell marker, aldehyde dehydrogenase isoform 1 (ALDH1), in human epithelial cancers. *PLoS One* 2010; **5:** e10277.

26. Flesken-Nikitin A, Hwang CI, Cheng CY, *et al.* Ovarian surface epithelium at the junction area contains a cancer-prone stem cell niche. *Nature* 2013; **495:** 241-245.

27. Chou RH, Yu YL, Hung MC. The roles of EZH2 in cell lineage commitment. *Am J Transl Res* 2011; **3:** 243–250.

28. Deb G, Singh AK, Gupta S. EZH2: not EZHY (easy) to deal. *Mol Cancer Res* 2014; **12:** 639-653.

29. Merrill BJ, Gat U, DasGupta R, *et al.* Tcf3 and Lef1 regulate lineage differentiation of multipotent stem cells in skin. *Genes Dev* 2001; **15:** 1688-1705.

30. Giribaldi G, Barbero G, Mandili G, *et al.* Proteomic identification of Reticulocalbin 1 as potential tumor marker in renal cell carcinoma. *J Proteomics* 2013; **91:** 385-392.

31. Yoshida T, Kanegane H, Osato M, *et al.* Functional analysis of *RUNX2* mutations in Japanese patients with cleidocranial dysplasia demonstrates novel genotype–phenotype correlations. *Am J Hum Genet* 2002; **71:** 724-738.

32. Karst AM, Levanon K, Duraisamy S, *et al.* Stathmin 1, a marker of PI3K pathway activation and regulator of microtubule dynamics, is expressed in early pelvic serous carcinomas. *Gynecol Oncol* 2011; **123:** 5-12.

33. Zheng P, Liu YX, Chen L, *et al.* Stathmin, a new target of PRL-3 identified by proteomic methods, plays a key role in progression and metastasis of colorectal cancer. *J Proteome Res* 2010; **9:** 4897-4905.

34. Sonego M, Schiappacassi M, Lovisa S, *et al.* Stathmin regulates mutant p53 stability and transcriptional activity in ovarian cancer. *EMBO Mol Med* 2014; **6:** 295.

35. Hueber PA, Waters P, Clark P, *et al.* PAX2 inactivation enhances cisplatin-induced apoptosis in renal carcinoma cells. *Kidney Int* 2006; **69:** 1139-1145.

36. Han X, Du F, Jiang L, *et al.* A2780 human ovarian cancer cells with acquired paclitaxel resistance display cancer stem cell properties. *Oncol Lett* 2013; **6:** 1295-1298.

37. Rizzo S, Hersey JM, Mellor P, *et al.* Ovarian cancer stem cell-like side populations are enriched following chemotherapy and overexpress EZH2. *Mol Cancer Ther* 2011; **10:** 325-335.

38. van der Zee M, Jia Y, Wang Y, *et al.* Alterations in Wnt-β-catenin and Pten signalling play distinct roles in endometrial cancer initiation and progression. *J Pathol* 2013; **230:** 48-58.

SUPPORTING INFORMATION ON THE INTERNET

The following supporting information may be found in the online version of this article:

Figure S1. Pax2 and acetyl-alpha-tubulin (cilia) expression in fetal and adult Fallopian tubes.

Figure S2. *In vitro* differentiation of oviduct progenitor cells.

Figure S3. Two types of PAX2^{n} SCOUTs are distinguished in these panels with β-catenin, keratin 5, and LEF1 staining.

Figure S4. Heat map comparing type 1 and type 2 SCOUTs with normal tubal epithelium and high-grade serous cancer.

Figure S5. A depiction, in tabular (A) and graphical format (B), of genes up-regulated with the two-fold change in type 2 relative to type 1 SCOUTs, several of which have been linked to STIN and HGSC.

Figure S6. H&E, p53, and PAX2 staining of cases under study (see Figure 5).

Table S1. Biomarkers selected for analysis of clonogenic cells, SCOUTs, and STINs.

Table S2. Summary of immunophenotypes in cultured progenitor cells and adult cells in tissue sections.

Table S3. Upregulated genes in Type 2 SCOUTs in comparison with Type 1 SCOUTs (3 fold and $p < 0.05$).

doi:10.1038/nature14484

Cloning and variation of ground state intestinal stem cells

Xia Wang[1]*, Yusuke Yamamoto[1]*, Lane H. Wilson[1,2], Ting Zhang[3], Brooke E. Howitt[4], Melissa A. Farrow[5], Florian Kern[3], Gang Ning[1], Yue Hong[1], Chiea Chuen Khor[3,6], Benoit Chevalier[1], Denis Bertrand[3], Lingyan Wu[3], Niranjan Nagarajan[3], Francisco A. Sylvester[7], Jeffrey S. Hyams[8], Thomas Devers[9], Roderick Bronson[10], D. Borden Lacy[5], Khek Yu Ho[11], Christopher P. Crum[4], Frank McKeon[1,3,11,12] & Wa Xian[1,2,4,11,12]

Stem cells of the gastrointestinal tract, pancreas, liver and other columnar epithelia collectively resist cloning in their elemental states. Here we demonstrate the cloning and propagation of highly clonogenic, 'ground state' stem cells of the human intestine and colon. We show that derived stem-cell pedigrees sustain limited copy number and sequence variation despite extensive serial passaging and display exquisitely precise, cell-autonomous commitment to epithelial differentiation consistent with their origins along the intestinal tract. This developmentally patterned and epigenetically maintained commitment of stem cells is likely to enforce the functional specificity of the adult intestinal tract. Using clonally derived colonic epithelia, we show that toxins A or B of the enteric pathogen *Clostridium difficile* recapitulate the salient features of pseudomembranous colitis. The stability of the epigenetic commitment programs of these stem cells, coupled with their unlimited replicative expansion and maintained clonogenicity, suggests certain advantages for their use in disease modelling and regenerative medicine.

While dominating prospective strategies for regenerative medicine, embryonic stem cells and induced pluripotent stem cells (iPSCs) face formidable challenges including risk of teratoma, complex guiding protocols for lineage specificity, and limited regenerative capacity of the lineages ultimately produced[1–8]. The success and promise of iPSCs have largely overshadowed efforts to harness stem cells intrinsic to regenerative tissues. Green and colleagues developed methods for cloning epidermal stem cells[9] that form a stratified epithelium upon engraftment, and these methods have been successfully applied to corneal, thymic and airway epithelia[10–12]. However, stem cells of columnar epithelial tissues resist cloning in a manner that maintains their immaturity during proliferative expansion, and instead must be carried forward as regenerative, differentiating 'organoids'[13–18]. Despite their obvious potential in regenerative medicine and constant improvement[19], the very low percentage of clonogenic cells in organoids limits the kinetics of their propagation as well as their utility for exploring the elemental stem cell.

The present study reports the cloning and propagation of 'ground state' human intestinal stem cells (ISC^{GS}). This technology offers insights into the molecular and functional features of columnar epithelial stem cells and their utility for disease modelling and regenerative medicine.

Cloning human fetal intestinal stem cells

We developed media (herein SCM-6F8) containing novel combinations of growth factors and regulators of TGF-β/BMP (transforming growth factor-β/bone morphogenetic protein), Wnt/β-catenin, EGF (epidermal growth factor), IGF (insulin-like growth factor) and Notch pathways[9,20,21] that supports the maintenance of human intestinal stem cells in a highly clonogenic, ground state form. Thus single-cell suspensions of intestinal epithelia derived from 20- to 21-week-old fetal demise cases yield colonies comprised of highly immature cells in which differentiation markers can be induced by Notch suppression (Fig. 1a). Following induced differentiation via Wnt withdrawal, we were unable to recover ground state stem cells by our methods (Extended Data Fig. 1a–c).

The clonogenicity of cells in the colonies was determined by single-cell transfer to be greater than 50% (Fig. 1b). This high clonogenicity permits the rapid generation of single-cell 'pedigree' lines for expansion and characterization of lineage fates upon differentiation[12] (Fig. 1b). Pedigree lines of ISC^{GS} and tracheobronchial stem cells (TBSC^{GS})[12] grown for several months in culture were differentiated in air–liquid interface (ALI) cultures for 10–30 days (Fig. 1c). The ISC^{GS} formed a highly uniform, 3D serpentine pattern, whereas TBSC^{GS} produced a stratified epithelium with apically positioned ciliated and goblet cells. Histological sections of differentiated ISC^{GS} revealed a columnar epithelium of villus-like structures marked by goblet (Muc2$^+$), endocrine (chromogranin A$^+$), and Paneth cells and polarized villin expression (Fig. 1d; Extended Data Fig. 1d), indicating that the progeny of a single ISC^{GS} can give rise to all epithelial lineages typically found in the small intestine. Importantly, differentiation of these ground state stem cells is accomplished by exposure to an ALI rather than a removal of factors such as Wnt that maintain immaturity.

While principal component analysis (PCA) of differentially expressed genes of ground state stem cells and ALI-differentiated

---

[1]The Jackson Laboratory for Genomic Medicine, Farmington, Connecticut 06032, USA. [2]Department of Genetics and Developmental Biology, University of Connecticut Health Center, Farmington, Connecticut 06032, USA. [3]Genome Institute of Singapore, Agency for Science, Technology and Research, 138672 Singapore. [4]Department of Pathology, Brigham and Women's Hospital, Boston, Massachusetts 02118, USA. [5]Department of Pathology, Microbiology, and Immunology, Vanderbilt University School of Medicine, Nashville, Tennessee 37232, USA. [6]Department of Ophthalmology, Yong Loo Lin School of Medicine, National University of Singapore, 119228 Singapore. [7]Department of Pediatrics, Division of Gastroenterology, The University of North Carolina at Chapel Hill, Chapel Hill, North Carolina 27599, USA. [8]Division of Digestive Diseases, Hepatology, and Nutrition, Connecticut Children's Medical Center, Hartford, Connecticut 06106, USA. [9]Department of Medicine, University of Connecticut Health Center, Farmington, Connecticut 06032, USA. [10]Department of Microbiology and Immunobiology, Harvard Medical School, Boston, Massachusetts 02115, USA. [11]Department of Medicine, National University of Singapore, 119228 Singapore. [12]Multiclonal Therapeutics, Inc., Farmington, Connecticut 06032, USA.
*These authors contributed equally to this work.

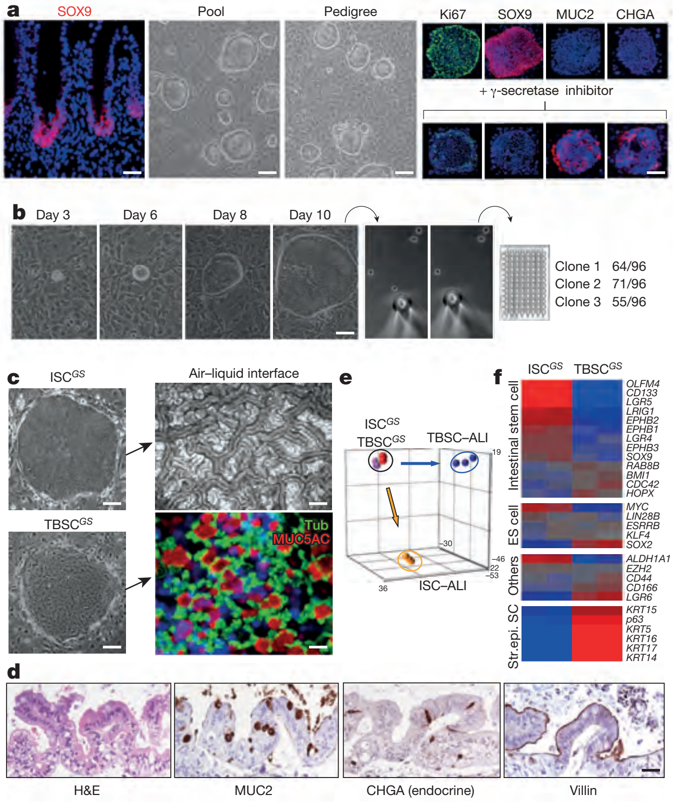

Figure 1 | Cloning stem cells from fetal intestine. a, Left, Sox9 expression in fetal intestine, scale bar, 25 μm; colonies from intestine ($n = 10$ biological replicates; colonies of ISC pedigree ($n = 30$ independent experiments). Scale bar, 75 μm. Right, ISC colonies stained with indicated antibodies. $n = 4$ technical replicates. Bottom, marker expression following Notch inhibition. $n = 4$ technical replicates. **b**, Left, ISC colony growth. Scale bar, 75 μm. Right, clonogenicity of colony cells. $n = 3$ biological replicates. **c**, ISC and TBSC pedigrees and ALI differentiation (tubulin, green; Muc5AC, red). Scale bar, 50 μm left, 25 μm right top, 25 μm bottom right; $n = 7$ biological replicates; $n = 3$ technical replicates; 3 independent experiments. **d**, ALI-differentiated ISC. Scale bar, 50 μm. $n = 7$ biological replicates; $n = 3$ technical replicates; 3 independent experiments. H&E, haematoxylin and eosin staining. **e**, PCA using 2,158 genes (> twofold, $P < 0.05$ by Student's *t*-test) of ISC and TBSC and corresponding ALI-differentiated epithelia. **f**, Expression heat map of markers in ISC and TBSC. Scale, −2.5-fold (extreme blue) to +2.5-fold (extreme red). $n = 3$ technical replicates.

tissue showed great divergence as expected for columnar and stratified epithelia, the gene expression profiles of undifferentiated ISC^{GS} and TBSC^{GS} differed by less than 4% (>2.0-fold, $P < 0.05$) (Fig. 1e). ISC^{GS} showed high expression of intestinal stem-cell markers such as OLFM4, CD133 (ref. 22), Lgr5 (ref. 23) and Lrig1 (ref. 24), whereas those from the airways had the typical stem cells markers of stratified epithelia (Krt14, Krt5 and Tp63 (ref. 11)) (Fig. 1f).

Intestinal stem cell variation

Approximately one in 2,000 cells from duodenum (I^{du}SC), jejunum (I^{je}SC) and ileum (I^{il}SC) of a 21-week-old fetal intestine form a colony (Fig. 2a). Although these colonies were morphologically indistinguishable in culture, whole-genome expression analysis of multiple pedigrees showed a consistent, region-specific signature of 24–178 genes (>1.5-fold, $P < 0.05$; Fig. 2b; Extended Data Fig. 2a).

After 10 days at an ALI, I^{du}SC and I^{je}SC gave rise to a finer pattern of epithelial folds than that produced by I^{il}SC (Fig. 2c). By histology, villi appear progressively more robust along the anterior–posterior axis, with I^{il}SC producing the larger villi and more numerous goblet cells (Fig. 2d, e). Interestingly, the epithelia derived from I^{du}SC expressed markers more typical of gastric epithelium (for example, TFF2 and Muc5AC), consistent with duodenum's location between the stomach and the small intestine (Extended Data Fig. 2b). I^{je}SC-derived epithelium, however, expressed Muc2, consistent with intestinal epithelium (Extended Data Fig. 2c), and I^{il}SC produced an epithelium more akin to colon (Fig. 2f). The pattern of proliferation in the ALI epithelia as measured by Ki67 staining was generally confined to cells proximal to the support membrane (Fig. 2e, f). PCA mapping of gene expression revealed more divergence among ALI-differentiated tissue than among the intestinal stem cells (Fig. 2g).

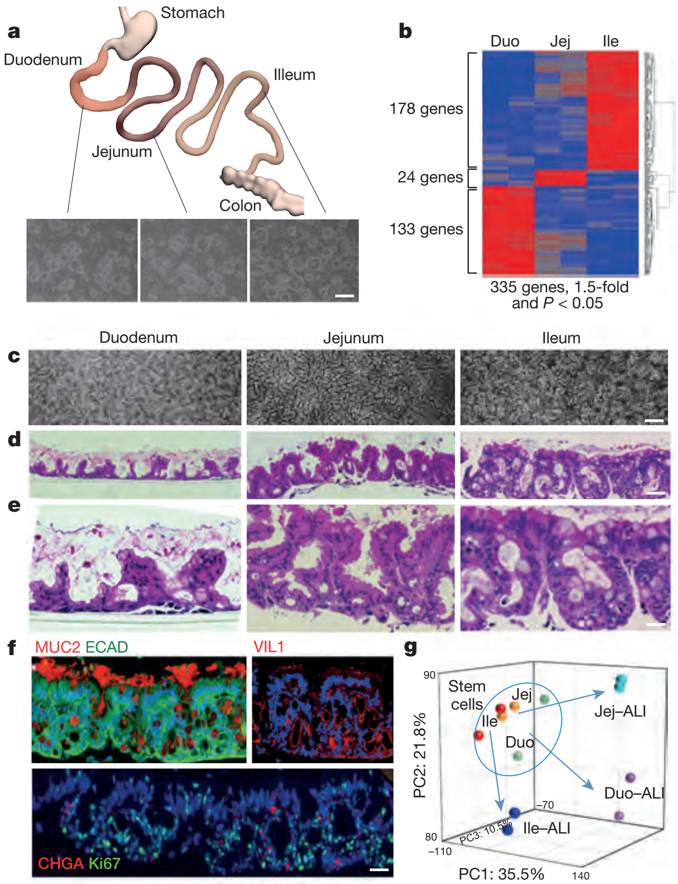

Figure 2 | Stem cells from fetal small intestine. a, Depiction of small intestine and clones derived from each. Scale bar, 400 μm; $n = 3$ biological replicates. **b**, Heat map of pedigrees from duodenum (Duo), jejunum (Jej), and ileum (Ile). **c**, Surface views of ALI cultures. Scale bar, 200 μm; $n = 30$ technical replicates. **d**, **e**, Histological sections through ALI cultures at low (scale bar, 150 μm) and high (scale bar, 50 μm) magnification. **f**, Immunofluorescence on sections of ALI cultures with indicated antibodies. ECAD, E-cadherin. Scale bar, 75 μm; $n = 3$ technical replicates. **g**, PCA map of stem cell gene expression from the three major regions of the small intestine together with their corresponding ALI-differentiated epithelia.

Colon stem cells

We also generated single-cell pedigree lines from the ascending, transverse, and descending colon from the same 21-week fetal demise case (Fig. 3a). The variation in gene expression between the stem cells of these colonic segments was minimal with signatures of 19-28 genes (>1.5-fold, $P < 0.05$; Fig. 3b). As with pedigrees derived from the intestinal epithelium, those from the colon could be propagated for months without loss of clonogenicity (not shown). Differentiation of these colon pedigrees under identical ALI conditions employed for the intestinal stem cells resulted in networks of 3D, large-diameter structures (Fig. 3c). Consistently, the histology of these ALI cultures revealed patterns of broad intestinal glands dominated by goblet cells (Fig. 3d). These ALI-generated tissues showed strong staining for

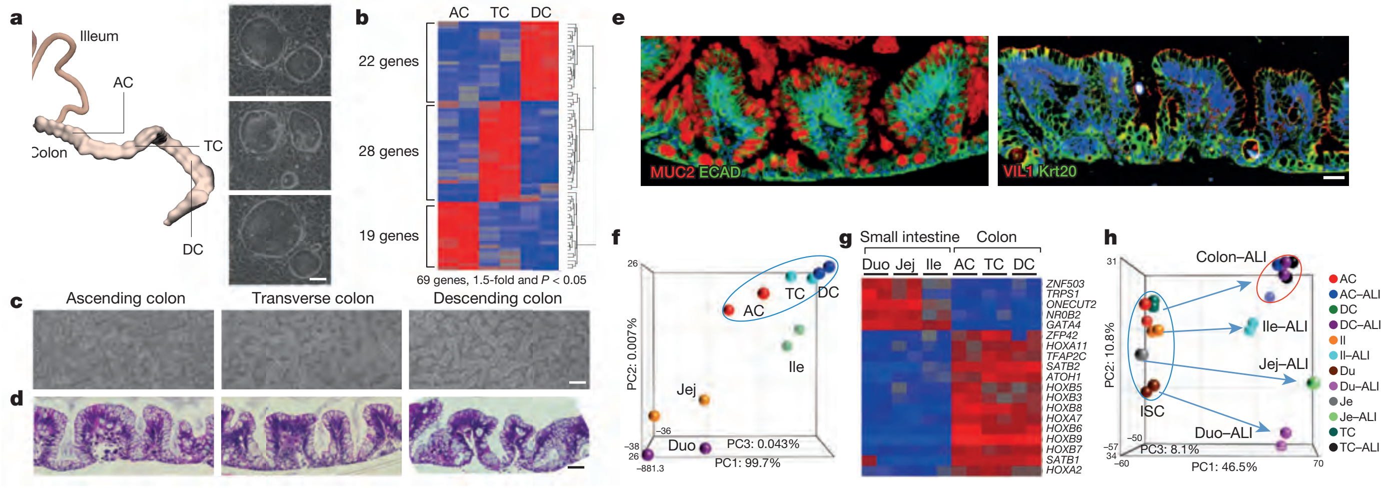

Figure 3 | Stem cells of fetal colon. **a**, Depiction of colon and clones derived from each. Scale bar, 75 μm; $n = 3$ biological replicates. AC, TC and DC, ascending, transverse and descending colon, respectively. **b**, Expression heat map of pedigrees from the three major divisions of the colon. **c**, Surface images of ALI cultures. Scale bar, 100 μm; $n = 20$ technical replicates. **d**, Histological sections through ALI cultures of colon stem cells. Scale bar, 75 μm. **e**, Immunofluorescence on sections through ALI cultures with indicated antibodies. Scale bar, 50 μm. **f**, PCA map of gene expression of colon and intestine stem cells. **g**, Expression heat map of stem cells of small intestine and colon. **h**, PCA map of gene expression profiles of intestinal stem cells and their corresponding ALI-differentiated epithelia.

intestinal goblet cell marker Muc2, as well as polarized villin and Krt20, typical of differentiated colonic epithelium (Fig. 3e). And while the colonic stem cells as a group showed minor differences in gene expression (see Figure 3b), they gave rise to epithelia with more distinct gene expression profiles (Extended Data Fig. 3). PCA mapping of these expression data showed a clustering of the colon stem cells relative to the intestinal stem cells, with increasingly distant spaces occupied by stem cells of the ileum, jejunum and duodenum, respectively (Fig. 3f). This distinction in global gene expression patterns is reflected, for instance, in the differential expression of transcription factors. In particular, *ONECUT2*, *NR0B2*, *TRPS1* and *ZNF503* show relatively high expression in the small intestine stem cells, whereas those of the colon showed a bias for *Hox* genes as well as the global chromatin organizer genes *SATB1* and *SATB2* (Fig. 3g, h).

Columnar versus stratified epithelia

The expression profiles of stem cells of human intestinal tract enabled a detailed comparison with those of stratified epithelia including human epidermis, corneal epithelium, mammary gland, prostate gland and upper airway. From this analysis it is clear that stratified epithelia, all of which depend on the p53-related stem-cell marker p63 for long-term self-renewal[11], occupy a distinct expression space from that of the intestinal stem cells or other columnar epithelial stem cells (Fig. 4a). A survey of genes whose expression is associated with stem cells of one of these two major classes of epithelia revealed a strong bias for *Olfm4*, *CD133* (ref. 22), *Lgr5* (ref. 23), *Nr5a2* (ref. 25), *Id2*, *Lrig1* (ref. 24), *EphB2*, *Ascl2* and *EphB3* in the intestinal stem cells, while the stratified epithelial stem cells expressed *ZNF750*, *TP63* and *KRT5* (Fig. 4b). Many of the markers differentially appearing in the intestinal stem cells, such as Olfm4, Lgr5 and Ascl2, are not general

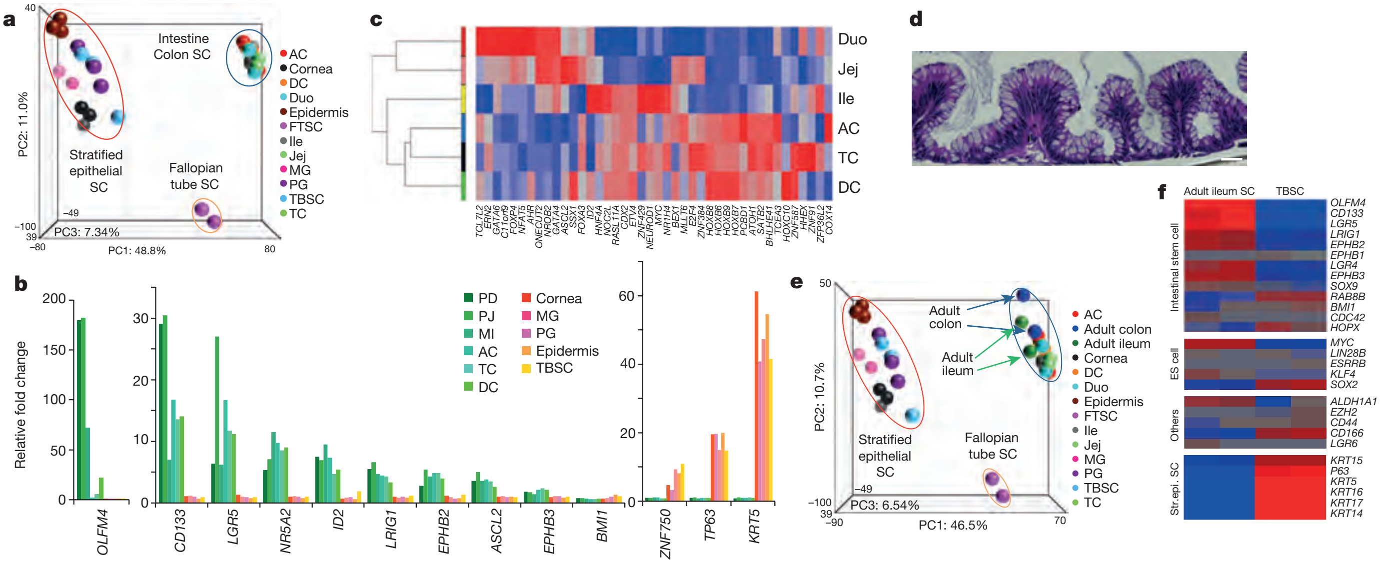

Figure 4 | Differential gene expression in stem cells of stratified and columnar epithelia. **a**, PCA map of stem cells of stratified epithelia (cornea, corneal epithelium; MG, mammary gland; PG, prostate gland; TBSC, tracheobronchial epithelial stem cells) and columnar epithelia (FTSC, fallopian tube epithelium). **b**, Gene expression in stem cells (stratified epithelia $n = 3$ technical replicates; columnar epithelia $n = 2$ technical replicates). **c**, Transcription factors differentially expressed in TBSC and ISC. **d**, ALI-differentiated adult terminal ileum stem cells derived from endoscopic biopsy. Scale bar, 50 μm; $n = 10$ technical replicates. **e**, PCA map of stem cells of adult terminal ileum, colon, fetal ISCs, and stratified epithelia. **f**, Stem cell markers in adult terminal ileum stem cells and TBSCs.

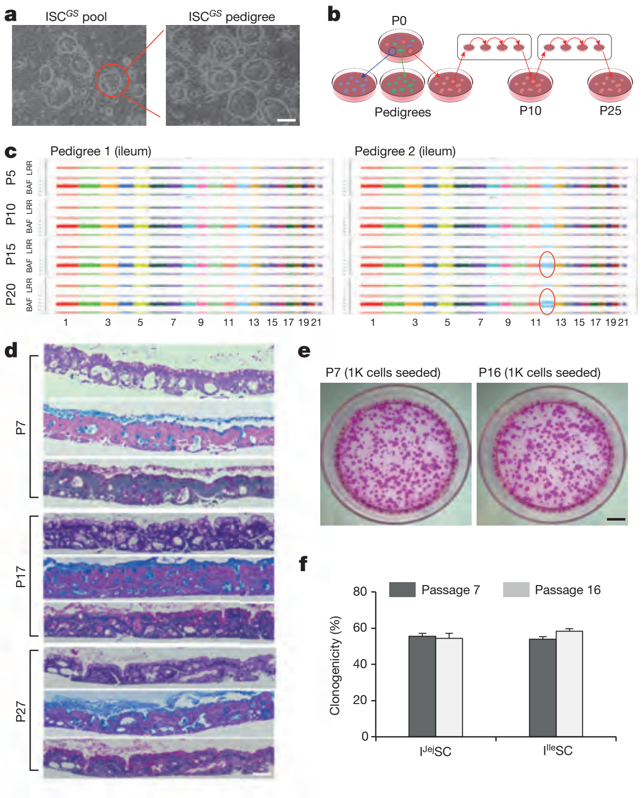

Figure 5 | **Genomic stability of ISC in culture.** **a**, Clone selection for pedigree generation. Scale bar, 200 μm. **b**, Serial passaging of pedigrees. **c**, CNV, BAF (B allele frequency) and LRR (log R ratio) profiles of pedigrees at P5 to P20 and trisomy 12 indicated (circle). **d**, ALI-differentiated pedigree 2 at P7, P17, and P27 stained with H&E (top), Alcian blue (middle), and periodic acid Schiff (bottom). Scale bar, 100 μm; $n = 4$ technical replicates. **e**, Clonogenicity assay revealing Rhodamine red-stained colonies grown 20 days following seeding 1,000 passaged cells. Scale bar, 10mm; $n = 3$ technical replicates. **f**, Quantification of clonogenicity at indicated passage number of ground state stem cells from jejunum ($\text{I}^{\text{Jej}}\text{SC}$) and ileum ($\text{I}^{\text{Ile}}\text{SC}$). $n = 3$ biological replicates; error bars, s.d.

columnar epithelial stem cell markers as evidenced by their absence in fallopian tube stem cells, although Lrig1 is more highly expressed in fallopian tube stem cells than either those of the intestine or the colon (Extended Data Fig. 4a). Notably, Bmi1, a member of the Polycomb group (PcG) PRC1-like complex implicated in self-renewal in both haematopoietic[26] and as reserve cells for proliferating, Lgr5^+ intestinal stem cells[27–29], was not differentially expressed in the cloned intestinal versus stratified epithelial stem cells. And while many of the typical markers of intestinal stem cells such as Lgr5, CD44, Lrig1, EphB2 and ASCL2 show a decrease in expression as the intestinal stem cells are differentiated in ALI cultures, Bmi1 did not (Extended Data Fig. 4b, c). These findings suggest that we are cloning either crypt cells or so-called '+4' cells that have become crypt-like in their expression patterns. We also examined transcription factors differentially expressed in ISC compared to stratified epithelial stem cells in an effort to understand the regiospecificity of commitment programs of stem cells along the intestinal tract (Fig. 4c). In addition to six transcription factors that were uniformly highly expressed in stem cells of the intestinal tract (CREB3L1, Myb, NR5A2, IRF8, HNF4G and Msx2) versus tracheobronchial stem cells, this analysis revealed limited sets of transcription factors differentially expressed in stem cells along the anterior–posterior axis of the intestinal tract that conceivably function in maintaining commitment states. For instance, and consistent with previous observations[30], GATA4 and GATA6 were expressed most strongly in the anterior portions of the intestinal tract (Fig. 4c). Significantly, the selective deletion of GATA4 and GATA6 in the murine duodenum and jejunum promotes ileal properties and a detrimental phenotype[30,31], suggesting a role for these transcription factors in maintaining segmental identity acting at the level of the stem cell. Similarly, the requirement for Onecut2 in the duodenum[32] might be at the level of the duodenal stem cells. It is likely that analyses of cloned stem cells from the various segments of the intestinal tract will help to unravel the roles of such segment-specific transcription factors in the establishment of commitment and differentiation programs. Importantly, the overall properties of ISCs from fetal sources are conserved in those derived from endoscopic biopsies of paediatric and adult cases (Fig. 4d–f).

Genomic and lineage stability

Human embryonic stem cells and iPSC lines acquire with successive passages genomic structural variations, including some that confer a selective advantage[33,34]. To assess the genomic stability of our ISC^{GS}, we examined copy number (CNV) and single nucleotide variation (SNV) in two independent ISC^{GS} pedigrees derived from the ileum of one fetal demise case after 50 (passage 5; P5), 100 (P10), 150 (P15), and 200 days (P20) of continuous proliferation (Fig. 5a, b). At P5, when single ISC^{GS} pedigrees can be amplified to an estimated 300 million to 75 billion cells, no chromosomal aneuploidies were detected, although one pedigree showed three interstitial deletions affecting two genes (Fig. 5c; Extended Data Fig. 5a; Supplementary Information Table 1). This low level of structural variation was maintained though passage 10, although increased by P15 and at P20 one of the pedigrees showed a frank trisomy of chromosome 12 (Fig. 5c; Extended Data Fig. 5a; Supplementary Information Table 1). A similar upward trend in CNV as a function of passage number was observed in five intestinal pedigrees (pedigrees 3–7) derived from a separate fetal demise case (Extended Data Figs 5, 6; Supplementary Information Tables 1, 2).

By exome sequencing, our original two pedigrees showed few (0–1) non-synonymous mutations through passage 10, and these increased modestly (1–2 new non-synonymous mutations) through P15 and P20 (Extended Data Fig. 5a). None of these non-synonymous mutations have been reported as driver genes in human cancers. A similar trend was observed in the five pedigrees from the second fetal demise case followed through P5 and P25. By P25 the range of non-synonymous SNVs increased to 2–10 per clone, and while not involving obvious cancer driver genes, did include genes such as *ECT2L* and *EP300* that might provide a selective growth advantage (Extended Data Fig. 5c). These data indicate that most pedigrees sustain few genomic changes within the first 100 days of proliferative expansion. By P15 and through P25, however, half the pedigrees showed evidence for aneuploidy as well as an increase in interstitial CNV and SNVs with allele frequencies nearing 0.5, suggesting the rise of an advantaged subclone. We asked how these late-passage genomic changes might affect differentiation by comparing early and late passages of pedigree 2 in ALI differentiation. By all histological criteria, including Alcian blue staining for goblet cells and intestinal marker staining, we could not distinguish the ALI-differentiated epithelia derived from P7, P17 and P27 (Fig. 5d; Extended Data Fig. 7). Similarly, we note that these intestinal stem cell pedigrees do not lose (or gain) clonogenicity when tested at P7 and P16, which remain stably above 50% (Fig. 5e, f). Lastly, we found no evidence of tumorigenicity by these ground state intestinal stem cells, including those at P25 harbouring aneuploidies, following their subcutaneous implantation to immunodeficient (NOD.Cg-$\text{Prkdc}^{\text{scid}}$ $\text{Il2rg}^{\text{tm1Wjl}}$/SzJ) mice[35] (Extended Data Fig. 8).

Modelling *Clostridium difficile* infections

C. difficile is a Gram-positive, spore-forming bacterium and the primary cause of nosocomial diarrhoea and pseudomembranous colitis[36]. The pathogenicity of *C. difficile* is linked to its production of two similar, high molecular weight toxins TcdA and TcdB. While together TcdA and TcdB cause fluid secretion, inflammation, and colonic

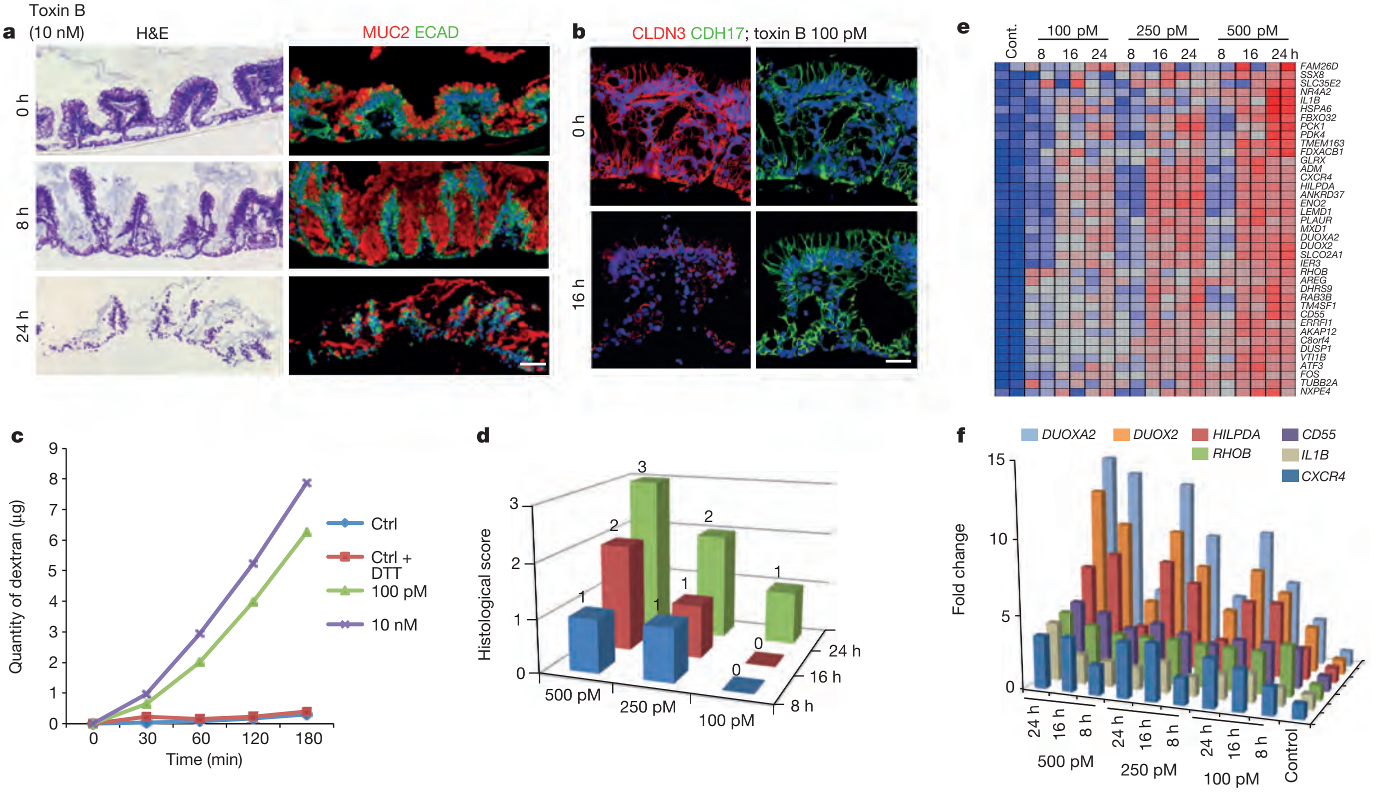

Figure 6 | *C. difficile* toxin B effects on *in vitro*-generated colonic epithelia. **a**, TcdB effects on colonic stem cell-derived epithelia. Scale bar, 100 μm. $n = 4$ technical replicates. **b**, Tight junction protein claudin 3 (CLDN3; red) and adherens junction marker cadherin-17 (CDH17; green) in ALI colonic epithelium treated with TcdB. Scale bar, 50 μm; $n = 4$ biological replicates. **c**, Dextran permeability assay on TcdB-treated ALI colonic epithelia. **d**, 3D plot of histological scoring by gastrointestinal pathologist according to a standard 0–3 rating for colonic epithelial integrity. **e**, Heat map of 39 genes differentially expressed between TcdB (500 pM, 24 h) and controls (> threefold and $P < 0.05$ by Student's *t*-test). **f**, 3D plot of seven selected genes at time points and doses indicated. $n = 2$ technical replicates.

tissue damage, their respective and possible synergistic roles have been difficult to ascertain[37–39]. We therefore challenged colonic epithelia derived from cloned, ground state colonic stem cells with recombinant TcdB (Fig. 6a, b; Extended Data Fig. 9a, b). At higher concentrations or longer time points there is a loss of goblet cells, disruption of the crypt architecture, cell polarity, and a specific loss of tight versus adherens junction proteins that correlates with increased dextran permeability (Fig. 6c). These dose–response changes in the ALI colonic epithelium mirror those of *C. difficile*-associated pseudomembranous colitis (Fig. 6d, Extended Data Fig. 9a, b). Microarray analysis of ALI-generated colonic epithelia following nine TcdB treatment conditions revealed alterations in gene expression in a time- and dose-dependent manner (Fig. 6e, f; Extended Data Fig. 9c–f). Pathway analysis indicated that TcdB triggers changes in gene expression related to inflammation, RhoB-mediated actin regulation, and junctional dynamics previously implicated in *C. difficile* pathology[40,41]. In addition, this analysis revealed that *DUOX2* and *DUOXA2* were consistently the two highest upregulated genes (Fig. 6e, f). These proteins form an enzyme capable of producing hydrogen peroxide and have been implicated in the inflammation of inflammatory bowel disease (IBD)[42]. Finally, we also tested *C. difficile* TcdA in our model. TcdA is reported to be a specific enterotoxin[36,37], and indeed we found that it triggers similar cytopathic and permeability changes in ALI models of human colonic epithelium (Extended Data Fig. 10), albeit at lower doses than those effective for TcdB. Together these findings underscore the potential of this model system to recapitulate and elucidate *C. difficile* pathology.

Discussion

Adult stem cells of the highly regenerative intestinal tract remain largely defined by metabolic, marker profiling, or lineage tracing experiments *in vivo* or transplantation of cells from intestinal organoids[23,43,44]. As stem cells comprise only a minor component of organoids—perhaps less than 1%[45]—the molecular features of stem cells of columnar epithelia such as the intestinal tract have remained unclear. Therefore the selective cloning and proliferative expansion of highly clonogenic, ground state intestinal stem cells described here offers a first glimpse into the molecular properties of these cells. Our inability to convert differentiated cells to clonogenic cells supports the notion that we are cloning resident stem cells rather than somehow 'reprograming' differentiated enterocytes. These resident stem cells possess robust epigenetic programs of commitment to regiospecific intestinal differentiation that are stable despite more than six months of continuous propagation. This cell-autonomous regiospecificity of stem cells along the intestinal tract argues against a unitary 'intestinal stem cell' or even one each for the histologically recognized segments, but rather a developmentally established spectrum of stem cells that ultimately maintains the histological and functional properties that define these segments. A heuristic deciphering of the commitment code from the regiospecific expression patterns presented here will guide parallel efforts with iPSCs to achieve appropriate lineage fates[46]. Interestingly, many inductive signalling pathways and transcription factors implicated in embryonic gut formation[47] may act to reinforce commitment codes via continued expression in stem cells of the intestinal tract.

We anticipate that the ability to maintain these stem cells in their elemental state will enable the discovery of epigenetic mechanisms that underlie properties of very long-term self-renewal, exquisitely precise lineage commitment, and the intrinsically directed, self-assembly of differentiated epithelia. Although we demonstrate the potential of clonally-derived colonic epithelia to model the pathogenesis of *C. difficile* toxins, we anticipate the need to restore complexity in the form of mesenchyme, immune cells, enteric neurons and perhaps components of the microbiome[48] to fully recapitulate disease dynamics. In particular, enteric maladies such as inflammatory bowel disease represent important medical challenges whose aetiologies most likely reside in interactions between the immune system, intestinal mucosa and intestinal flora[49,50]. Finally, the ability to clone patient-specific, ground state stem cells from columnar epithelia via endoscopic biopsies, coupled with their orders-of-magnitude expansion kinetics over organoids, favours their use in regenerative medicine, pre-clinical trials and disease modelling.

Received 20 December 2014; accepted 14 April 2015.

1. Tabar, V. & Studer, L. Pluripotent stem cells in regenerative medicine: challenges and recent progress. *Nature Rev. Genet.* **15,** 82–92 (2014).
2. Okano, H. & Yamanaka, S. iPS cell technologies: significance and applications to CNS regeneration and disease. *Mol. Brain* **7,** 22 (2014).
3. Müller, A. M. & Dzierzak, E. A. ES cells have only a limited lymphopoietic potential after adoptive transfer into mouse recipients. *Development* **118,** 1343–1351 (1993).
4. Helgason, C. D., Sauvageau, G., Lawrence, H. J., Largman, C. & Humphries, R. K. Overexpression of HOXB4 enhances the hematopoietic potential of embryonic stem cells differentiated *in vitro*. *Blood* **87,** 2740–2749 (1996).
5. Bonde, S., Dowden, A. M., Chan, K. M., Tabayoyong, W. B. & Zavazava, N. HOXB4 but not BMP4 confers self-renewal properties to ES-derived hematopoietic progenitor cells. *Transplantation* **86,** 1803–1809 (2008).
6. Iuchi, S., Dabelsteen, S., Easley, K., Rheinwald, J. G. & Green, H. Immortalized keratinocyte lines derived from human embryonic stem cells. *Proc. Natl Acad. Sci. USA* **103,** 1792–1797 (2006).
7. Amabile, G. *et al.* *In vivo* generation of transplantable human hematopoietic cells from induced pluripotent stem cells. *Blood* **121,** 1255–1264 (2013).
8. Suzuki, N. *et al.* Generation of engraftable hematopoietic stem cells from induced pluripotent stem cells by way of teratoma formation. *Mol. Ther.* **21,** 1424–1431 (2013).
9. Rheinwatd, J. G. & Green, H. Serial cultivation of strains of human epidermal keratinocytes: the formation of keratinizing colonies from single cells. *Cell* **6,** 331–343 (1975).
10. Rama, P. *et al.* Limbal stem-cell therapy and long-term corneal regeneration. *N. Engl. J. Med.* **363,** 147–155 (2010).
11. Senoo, M., Pinto, F., Crum, C. P. & McKeon, F. p63 is essential for the proliferative potential of stem cells of stratified epithelia. *Cell* **129,** 523–536 (2007).
12. Kumar, P. A. *et al.* Distal airway stem cells yield alveoli *in vitro* and during lung regeneration following H1N1 influenza infection. *Cell* **147,** 525–538 (2011).
13. Matsuura, R. *et al.* Crucial transcription factors in endoderm and embryonic gut development are expressed in gut-like structures from mouse ES cells. *Stem Cells* **24,** 624–630 (2006).
14. Sato, T. *et al.* Single Lgr5 stem cells build crypt-villus structures *in vitro* without a mesenchymal niche. *Nature* **459,** 262–265 (2009).
15. Ootani, A. *et al.* Sustained *in vitro* intestinal epithelial culture within a Wnt-dependent stem cell niche. *Nature Med.* **15,** 701–706 (2009).
16. Sato, T. *et al.* Paneth cells constitute the niche for Lgr5 stem cells in intestinal crypts. *Nature* **469,** 415–418 (2011).
17. Fordham, R. P. *et al.* Transplantation of expanded fetal intestinal progenitors contributes to colon regeneration after injury. *Cell Stem Cell* **13,** 734–744 (2013).
18. Middendorp, S. *et al.* Adult stem cells in the small intestine are intrinsically programmed with their location-specific function. *Stem Cells* **32,** 1083–1091 (2014).
19. Yin, X. *et al.* Niche-independent high-purity cultures of Lgr5$^+$ intestinal stem cells and their progeny. *Nature Methods* **11,** 106–112 (2014).
20. Kim, K. A. *et al.* Mitogenic influence of human R-spondin1 on the intestinal epithelium. *Science* **309,** 1256–1259 (2005).
21. Dreesen, O. & Brivanlou, A. H. Signaling pathways in cancer and embryonic stem cells. *Stem Cell Rev.* **3,** 7–17 (2007).
22. Zhu, L. *et al.* Prominin 1 marks intestinal stem cells that are susceptible to neoplastic transformation. *Nature* **457,** 603–607 (2009).
23. Barker, N. *et al.* Identification of stem cells in small intestine and colon by marker gene *Lgr5*. *Nature* **449,** 1003–1007 (2007).
24. Powell, A. E. *et al.* The pan-ErbB negative regulator Lrig1 is an intestinal stem cell marker that functions as a tumor suppressor. *Cell* **149,** 146–158 (2012).
25. Botrugno, O. A. *et al.* Synergy between LRH-1 and beta-catenin induces G1 cyclin-mediated cell proliferation. *Mol. Cell* **15,** 499–509 (2004).
26. Lessard, J. & Sauvageau, G. Bmi-1 determines the proliferative capacity of normal and leukaemic stem cells. *Nature* **423,** 255–260 (2003).
27. Sangiorgi, E. & Capecchi, M. R. Bmi1 is expressed *in vivo* in intestinal stem cells. *Nature Genet.* **40,** 915–920 (2008).
28. Tian, H. *et al.* A reserve stem cell population in small intestine renders Lgr5-positive cells dispensable. *Nature* **478,** 255–259 (2011).
29. Metcalfe, C., Kljavin, N. M., Ybarra, R. & de Sauvage, F. J. Lgr5$^+$ stem cells are indispensable for radiation-induced intestinal regeneration. *Cell Stem Cell* **14,** 149–159 (2014).
30. Battle, M. A. *et al.* GATA4 is essential for jejunal function in mice. *Gastroenterology* **135,** 1676–1686 (2008).
31. Walker, E. M., Thompson, C. A. & Battle, M. A. GATA4 and GATA6 regulate intestinal epithelial cytodifferentiation during development. *Dev. Biol.* **392,** 283–294 (2014).
32. Dusing, M. R., Maier, E. A., Aronow, B. J. & Wiginton, D. A. Onecut-2 knockout mice fail to thrive during early postnatal period and have altered patterns of gene expression in small intestine. *Physiol. Genomics* **42,** 115–125 (2010).
33. International Stem Cell Initiative. Screening ethnically diverse human embryonic stem cells identifies a chromosome 20 minimal amplicon conferring growth advantage. *Nature Biotechnol.* **29,** 1132–1144 (2011).
34. Avery, S. *et al.* BCL-XL mediates the strong selective advantage of a 20q11.21 amplification commonly found in human embryonic stem cell cultures. *Stem Cell Rep.* **1,** 379–386 (2013).
35. Shultz, L. D. *et al.* Human cancer growth and therapy in immunodeficient mouse models. *Cold Spring Harb Protoc.* http://dx.doi.org/10.1101/pdb.top073585 (2014).
36. Voth, D. E. & Ballard, J. D. *Clostridium difficile* toxins: mechanism of action and role in disease. *Clin. Microbiol. Rev.* **18,** 247–263 (2005).
37. Carter, G. P., Rood, J. I. & Lyras, D. The role of toxin A and toxin B in the virulence of *Clostridium difficile*. *Trends Microbiol.* **20,** 21–29 (2012).
38. Lyras, D. *et al.* Toxin B is essential for virulence of *Clostridium difficile*. *Nature* **458,** 1176–1179 (2009).
39. Farrow, M. A. *et al.* *Clostridium difficile* toxin B-induced necrosis is mediated by the host epithelial cell NADPH oxidase complex. *Proc. Natl Acad. Sci. USA* **110,** 18674–18679 (2013).
40. Huelsenbeck, J. *et al.* Upregulation of the immediate early gene product RhoB by exoenzyme C3 from *Clostridium limosum* and toxin B from *Clostridium difficile*. *Biochemistry* **46,** 4923–4931 (2007).
41. Aktories, K., Schmidt, G. & Just, I. Rho GTPases as targets of bacterial protein toxins. *Biol. Chem.* **381,** 421–426 (2000).
42. MacFie, T. S. *et al.* DUOX2 and DUOXA2 form the predominant enzyme system capable of producing the reactive oxygen species H2O2 in active ulcerative colitis and are modulated by 5-aminosalicylic acid. *Inflamm. Bowel Dis.* **20,** 514–524 (2014).
43. Cheng, H. & Leblond, C. P. Origin, differentiation and renewal of the four main epithelial cell types in the mouse small intestine. V. Unitarian theory of the origin of the four epithelial cell types. *Am. J. Anat.* **141,** 537–561 (1974).
44. Yui, S. *et al.* Functional engraftment of colon epithelium expanded *in vitro* from a single adult Lgr5$^+$ stem cell. *Nature Med.* **18,** 618–623 (2012).
45. Wang, F. *et al.* Isolation and characterization of intestinal stem cells based on surface marker combinations and colony-formation assay. *Gastroenterology* **145,** 383–395 (2013).
46. Watson, C. L. *et al.* An *in vivo* model of human small intestine using pluripotent stem cells. *Nature Med.* **20,** 1310–1314 (2014).
47. Sheaffer, K. L. & Kaestner, K. H. Transcriptional networks in liver and intestinal development. *Cold Spring Harb. Perspect. Biol.* **4,** a008284 (2012).
48. Nicholson, J. K. *et al.* Host-gut microbiota metabolic interactions. *Science* **336,** 1262–1267 (2012).
49. Brandl, K. & Beutler, B. Creating diseases to understand what prevents them: genetic analysis of inflammation in the gastrointestinal tract. *Curr. Opin. Immunol.* **24,** 678–685 (2012).
50. Lees, C. W., Barrett, J. C., Parkes, M. & Satsangi, J. New IBD genetics: common pathways with other diseases. *Gut* **60,** 1739–1753 (2011).

Acknowledgements This work was supported by grants from Connecticut Innovations (W.X., F.M.), the Joint Council Office of the Agency for Science Technology Research Agency (A*STAR), Singapore (W.X., F.M.), the National Medical Research Council, Singapore (BNB101677A to H.K.Y., F.M., and W.X.; BnB11dec063 to N.N., F.M. and W.X.), the Department of Defense (W81XWH-10-1-0289 to C.P.C.) and the National Institute of Health (AI09575504 to D.B.L.). We thank M. LaLande, B. Lane and B. Seet for support, B. Tennent, B. Knowles and T. McLaughlin for comments on the manuscript, J. Hammer for artwork, L. Lapierre and J. Franklin for histology evaluation. We thank H. Green for advice and support.

Author Contributions Experimental design and conception were done by W.X., F.M., D.B.L., K.Y.H. and C.P.C.; X.W. cloned and differentiated the intestinal stem cells with help from L.H.W., F.K., G.N., B.E.H. and Y.H.; Y.Y., X.W. prepared the genomic and gene expression analyses together with F.K., G.N., C.C.K. and L.W.; T.Z., D.B. and N.N. performed all computational and bioinformatics work. B.H. and C.P.C. obtained fetal tissues and F.A.S., J.S.H. and T.D. provided endoscopic biopsies, and R.B. analysed the xenografts. The *C. difficile* experiments were designed and executed by B.C., L.H.W., M.A.F. and D.B.L.; W.X. and F.M. wrote the manuscript with input from all other authors.

Author Information Data sets generated for this study have been submitted to the National Center for Biotechnology Information Gene Expression Omnibus (GEO) database and the European Nucleotide Archive under accession numbers GSE66749 and SRP056402. Reprints and permissions information is available at www.nature.com/reprints. The authors declare no competing financial interests. Readers are welcome to comment on the online version of the paper. Correspondence and requests for materials should be addressed to W.X. (xianmckeon2014@gmail.com) or F.M. (mckeon.xian@gmail.com).

METHODS

***In vitro* culture of human small intestinal and colonic epithelial stem cells.** Intestinal tissue from 20- to 21-week-old late fetal demise cases were obtained under parent consent as de-identified material under approved institutional review board protocols at the Brigham and Women's Hospital, Boston, MA, USA (2009P002281). Terminal ileum endoscopic biopsies were obtained under informed consent and institutional review board approval at the Connecticut Children's Medical Center, Hartford, Connecticut USA (15-047J-2). Fetal intestinal tissue or 1 mm endoscopic biopsies from terminal ileum were collected into cold F12 media (Gibco, USA) with 5% fetal bovine serum (HyClone, USA) and then minced by sterile scalpel into 0.2–0.5 mm^3 sizes to a viscous and homogeneous appearance. The minced tissue was digested in 2 mg ml^{-1} collagenase type IV (Gibco, USA) at 37 °C for 30–60 min with agitation. Dissociated cells were passed through a 70-μm Nylon mesh (Falcon, USA) to remove aggregates and then were washed four times in cold F12 media, and then seeded onto a feeder layer of lethally irradiated 3T3-J2 cells[9,12] in c-FAD media[9] modified to SCM-6F8 media by the addition of 125 ng ml^{-1} R-spondin1 (R&D systems, USA), 1 μM Jagged-1 (AnaSpec Inc., USA), 100 ng ml^{-1} human Noggin (Peprotech, USA), 2.5 μM Rock-inhibitor (Calbiochem, USA), 2 μM SB431542 (Cayman chemical, USA), and 10 mM nicotinamide (Sigma-Aldrich, USA). Cells were cultured at 37 °C in a 7.5% CO_2 incubator. The culture media was replaced every two days. Colonies were digested by 0.25% trypsin-EDTA solution (Gibco, USA) for 5–8 min and passaged every 7 to 10 days. To obtain single-cell suspensions colonies were trypsinized by TrypLE Express solution (Gibco, USA) for 8–15 min at 37 °C and cell suspensions were passed through 30-μm filters (Miltenyi Biotec, Germany). Approximately 20,000 epithelial cells were seeded to each well of 6-well plate. Cloning cylinder (Pyrex, USA) and high vacuum grease (Dow Corning, USA) were used to select single colonies for pedigrees. Gene expression analyses were performed on cells derived from passage 4–8 (P4–P8) cultures.

Histology and immunostaining. Histology, haematoxylin and eosin (H&E), Alcian blue, periodic acid–Schiff (PAS), rhodamine B staining, immunohistochemistry, and immunofluorescence were performed using standard techniques. For immunofluorescence and immunohistochemistry, 4% paraformaldehyde-fixed, paraffin-embedded tissue sections were subjected to antigen retrieval in citrate buffer (pH 6.0, Sigma-Aldrich, USA) at 120 °C for 20 min, and a blocking procedure was performed with 5% bovine serum albumin (BSA, Sigma-Aldrich, USA) and 0.05% Triton X-100 (Sigma-Aldrich, USA) in phosphate-buffered saline (PBS; Gibco, USA) at room temperature for 1 h. Primary antibodies used in this study and staining condition were listed in Supplementary Information Table 3. All images were captured by using the Inverted Eclipse Ti-Series (Nikon, Japan) microscope with Lumencor SOLA light engine and Andor Technology Clara Interline CCD camera and NIS-Elements Advanced Research v.4.13 software (Nikon, Japan) or LSM 780 confocal microscope (Carl Zeiss, Germany) with LSM software. Bright field cell culture images were obtained on an Eclipse TS100 microscope (Nikon, Japan) with Digital Sight DSFi1camera (Nikon, Japan) and NIS-Elements F3.0 software (Nikon, Japan).

Stem cell differentiation. Air–liquid interface (ALI) culture of TBSCs was performed as described[12,51]. Briefly, for ALI culture of intestinal and colonic epithelial stem cells, Transwell inserts (Corning, USA) were coated with 20% Matrigel (BD Biosciences, USA) and incubated at 37 °C for 30 min to polymerize. 200,000 irradiated 3T3-J2 cells were seeded to each transwell insert and incubated at 37 °C, 7.5% CO_2 incubator overnight. QuadroMACS Starting Kit (LS) (Miltenyi Biotec, Germany) was used to purify the stem cells by removal of feeder cells. 200,000–300,000 stem cells were seeded into each Transwell insert and cultured with SCM-6F8. At confluency (3–7 days), the apical media was removed through careful pipetting and the cultures were continued for an additional 6–12 days before analysis.

***Clostridium difficile* toxin treatment and epithelial permeability assay.** *Clostridium difficile* toxins A and B (TcdA, TcdB) were prepared as described[52]. Intestinal stem cells were differentiated in air–liquid interface cultures as described above and treated with 100, 250, 500 pM and 10 nM TcdA or TcdB for 0, 8, 16, and 24 h). At these time points, membranes with differentiated epithelia were collected for histology and microarray analysis. 4 kDa FITC-dextran (Sigma-Aldrich, USA) was added to the apical chamber of the Transwell chambers for a final concentration of 0.5 mg ml^{-1}. Media was removed from the bottom compartment after different incubation times and fluorescence was read by fluorometer (Infinite M1000 PRO, excitation 490 nm, emission 520 nm, Tecan, USA).

Implantation of intestinal stem cells. Intestinal stem cells (1.5 million cells) from different pedigrees with 50% of Matrigel (BD Bioscience, USA) were subcutaneously implanted into female, six- to eight-week-old immunodeficient (NOD.Cg-Prkdc^{scid} Il2rg^{tm1Wjl}/SzJ) mice[35] under IACUC approval (100533-1115) To test spontaneous transformation of the stem cells, mice were monitored every month (up to 4 months).

RNA and genomic DNA sample preparation. For stem cell colonies, RNA was isolated using PicoPure RNA Isolation Kit (Life Technologies, USA). For ALI-differentiated epithelia, RNA was isolated using TRIzol RNA Isolation Kit (Life Technologies, USA). RNA quality (RNA integrity number, RIN) was measured by analysis Agilent 2100 Bioanalyzer and Agilent RNA 6000 Nano Kit (Agilent Technologies, USA). RNAs having a RIN $>$ 8 were used for microarray analysis. Genomic DNA was extracted with DNeasy Blood & Tissue kit (Qiagen, Netherlands) from intestinal and colonic stem cells for CNV analysis and exome capture sequencing. For genomic DNA extraction, human intestinal and colonic stem cells were isolated from mouse 3T3 feeder layer using QuadroMACS Starting Kit (Miltenyi Biotec, Germany). Genomic DNA concentration was measured with Qubit dsDNA BR Assay Kit (Life Technologies, USA).

Expression microarray and bioinformatics. Total RNAs obtained from immature colonies and ALI-differentiated structure were used for microarray preparation with WT Pico RNA Amplification System V2 for amplification of DNA and Encore Biotin Module for fragmentation and biotin labelling (NuGEN Technologies, USA). RNA quality (RNA integrity number, RIN) was measured by analysis using an Agilent 2100 Bioanalyzer and Agilent RNA 6000 Nano Kit (Agilent Technologies, USA). RNAs having a RIN $>$ 8 were used for microarray analysis. All samples were prepared according to manufacturer's instructions and hybridized onto GeneChip Human Exon 1.0 ST Array (Affymetrix, USA). GeneChip operating software was used to process all the Cel files and calculate probe intensity values. To validate sample quality, quality checks were conducted using Affymetrix Expression Console software. The intensity values were log_2-transformed and imported into the Partek Genomics Suite 6.6 (Partek Incorporated, USA). Exons were summarized to genes and a 1-way ANOVA was performed to identify differentially expressed genes. For two-sample statistics, P values were calculated by Student's t-test for each analysis. Unsupervised clustering and heat map generation were performed with sorted data sets by Euclidean distance based on average linkage clustering, and principal component analysis (PCA) map was conducted using all or selected probe sets by Partek Genomics Suite 6.6. Gene set enrichment analysis (GSEA)[53] was performed for *C. difficile* toxin B treatment. For the region-specific gene signature of small intestine and colon comparison (PD, PJ and MI for Fig. 2b and AC, TC and DC for Fig. 3b), differentially-expressed genes were selected with a cut-off value of 1.5-fold and $P < 0.05$ in each comparison (for example, (1) PD vs. PJ and (2) PD vs. MI) and then intersected genes in 2 gene lists of each comparison were taken as regio-specific gene sets. In the heat maps (Fig. 2b and 3b), 3 regiospecific gene sets (PD, PJ and MI, or AC, TC and DC) were combined, and the heat maps were made with Euclidean distance based on average linkage clustering. For *C. difficile* toxin B treatment data sets, samples from indicated time points and dosages were compared with control (untreated samples). Differentially-expressed genes (two-fold upregulated and downregulated genes) were counted and plotted in 3D column plots (Extended Data Fig. 8c). In comparison of 500 pM 24 h toxin B treatment with control, 39 genes were significantly upregulated (cut-off value: 3-fold and $P < 0.05$) and a heat map (Fig. 6e) was made with 39 genes using all samples. The whole genome expression data of 500 pM 24 h toxin B treatment vs. control were applied to GSEA program to detect significantly enriched pathway in toxin B treatment. Selected pathways (from KEGG) were shown in Fig. 6d. Data sets generated for this study have been submitted to the National Center for Biotechnology Information Gene Expression Omnibus (GEO) database under accession number GSE66749.

No statistical methods were used to predetermine sample size.

Copy number variation. For copy number variation analysis of stem cell pedigrees and passage 0 pooled sample, genomic DNA samples were genotyped with HumanOmniExpress BeadChip Kit for clone 1 and 2 (passage 5, 10, 15 and 20) (Illumina, USA) and Illumina HumanOmniZhonghua BeadChip Kit for clones 3 to 7 (passage 5 and 25) following the manufacturer's instructions. Analysis of BeadChip was performed using GenomeStudio Software (Illumina, USA). Illumina high-density SNP genotyping data was converted to kilobase-resolution detection of copy number variation. CNV detected in passage 0 pooled samples are considered as germline CNVs and removed in the analysis. The data was generated by PennCNV[54]. Genes within 10 kb of CNV regions are reported. The parameter is set as "-expandleft 10k" and "-expandright 10k". Other parameters are default. Confidence score $>$10 was used as a cutoff. The call rates for CNV were all greater than 99%, and two larger CNV amplification and deletion events were validated by quantitative PCR.

Exome capture sequencing. For exome capture and high-throughput sequencing for intestinal stem cells (pedigree 1 and 2), 50 ng of genomic DNA was used to perform Nextera Expanded Exome Kit (Illumina, USA). For pedigree 3 to 7, 1 μg of genomic DNA was sheared using a Covaris S1 Ultrasonicator (Covaris, USA), end-repaired, A-tailed, and Adaptor-ligated. Exome capture was performed using a Tru-seq Exome Enrichment Kit (Illumina, USA) following the manufacturer's instructions. Multiplexed libraries were sequenced on an Illumina HiSeq sequencer using 101-bp paired-end reads. Reads were aligned to the reference genome (UCSC hg19) using Burrows Wheeler Aligner (BWA, 0.6.2)[55]. PCR duplicates were removed using PICARD-1.94 (http://picard.sourceforge.net). The Genome Analysis Toolkit (GATK framework version 2.6.4)[56] was used to realign reads near indels and to recalibrate base quality values.

When running GATK, the minimum phred-scaled confidence threshold at which variants were called (-stand_call_conf) was 50, and the minimum phred-scaled confidence threshold at which variants were emitted (-stand_emit_conf) is 30. The criteria of GATK Variant Filtration is as follows: --clusterWindowSize 10--filterExpression "MQ0 > 4 && ((MQ0/(1.0*DP)) > 0.1)"--filterName "HARD_TO_VALIDATE"--filterExpression "DP < 5"--filterName "LowCoverage"--filterExpression "QUAL < 30"--filterName "VeryLowQual"--filterExpression "QUAL > 30 && QUAL < 50"--filterName "LowQual"--filterExpression "QD < 1.5"--filterName "LowQD"--filterExpression "FS > 150"--filterName "StrandBias". Potential mouse genomic DNA contaminant reads were detected by alignment to the mouse genome (UCSC mm10) and those containing less than 3 mismatches were removed from further analysis. SNVs were called in each sample separately using SAMtools v0.1.19[57] and GATK in the exome capture targeted regions. Variants with at least Q50 confidence, phred-scaled quality score more than 40 and coverage higher than 10 were considered as true SNVs. Variants were annotated with ANNOVAR (version 11 Feb, 2013)[58]. Identical variant calls in intestinal stem cells (passage 5 and higher) when compared to passage 0 pooled samples were used to identify germline SNVs. Sanger sequencing validation was performed using primers designed with Primer3 software version 4.0 (http://frodo.wi.mit.edu/). Extracted genomic DNA was amplified with titanium Taq polymerase (Clontech Laboratories, CA, USA) and purified PCR products were sequenced in the forward directions using ABI PRISM BigDye Terminator Cycle Sequencing Ready Reaction kits and an ABI PRISM 3730 Genetic Analyzer (Applied Biosystems, CA, USA). We validated by PCR and Sanger sequencing 13 of 14 non-synonymous mutations called by our sequencing efforts suggesting a false discovery rate of less than 10%. Other quality control parameters are shown in Supplementary Information Table 4.

51. Schmidt, D., Hübsch, U., Wurzer, H., Heppt, W. & Aufderheide, M. Development of an *in vitro* human nasal epithelial (HNE) cell model. *Toxicol. Lett.* **88,** 75–79 (1996).
52. Chumbler, N. M. *et al. Clostridium difficile* toxin B causes epithelial cell necrosis through an autoprocessing-independent mechanism. *PLoS Pathog.* **8,** e1003072 (2012).
53. Subramanian, A. *et al.* Gene set enrichment analysis: a knowledge-based approach for interpreting genome-wide expression profiles. *Proc. Natl Acad. Sci. USA* **102,** 15545–15550 (2005).
54. Wang, K. *et al.* PennCNV: an integrated hidden Markov model designed for high-resolution copy number variation detection in whole-genome SNP genotyping data. *Genome Res.* **17,** 1665–1674 (2007).
55. Li, H. & Durbin, R. Fast and accurate short read alignment with Burrows-Wheeler Transform. *Bioinformatics* **25,** 1754–1760 (2009).
56. McKenna, A. *et al.* The Genome Analysis Toolkit: a MapReduce framework for analyzing next-generation DNA sequencing data. *Genome Res.* **20,** 1297–1303 (2010).
57. Li, H. *et al.* The Sequence Alignment/Map format and SAMtools. *Bioinformatics* **25,** 2078–2079 (2009).
58. Wang, K., Li, M. & Hakonarson, H. ANNOVAR: functional annotation of genetic variants from high-throughput sequencing data. *Nucleic Acids Res.* **38,** e164 (2010).

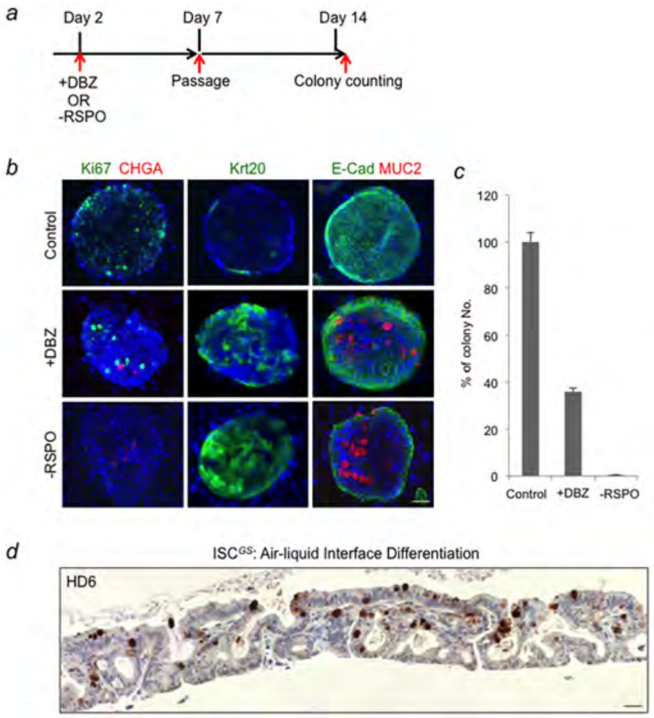

Extended Data Figure 1 | Loss of clonogenicity in differentiated ISC. **a**, Schematic of ISC differentiation using either the γ-secretase inhibitor dibenzazepine (DBZ) or withdrawal of the Wnt regulator R-spondin 1 (Rspo1). ISCs were plated on day 0, DBZ added or Rspo1 removed at day 2, and colonies passaged en masse at day 7. At day 14, after 7 days of continuous growth, colonies were counted. **b**, Micrographs show immunofluorescence at day 7 colonies grown without Rspo1 or in the presence of DBZ for 5 days using antibodies to Ki67, chromogranin A (CHGA), keratin 20 (Krt20), E-cadherin (E-cad), and mucin 2 (Muc2). Scale bar, 50 μm; $n = 4$ technical replicates. **c**, Histogram shows colony formation in each condition normalized to control ISCs. $n = 4$ biological replicates; error bars, s.d. **d**, Staining of ALI-differentiated intestinal stem cells with monoclonal antibody HD6 directed to Paneth cells. Scale bar, 50 μm; $n = 4$ technical replicates.

a

Cell types	Gene symbol										
Du-high	ABCB6	ABHD2	ABHD2	ACOX1	ADAM28	AHNAK	AKR1B10	ALDH3A1	ANXA1	ANXA10	ANXA5	ARHGAP24
133 genes	ARL4C	BACE2	BCAS1	BICC1	BTD	C11orf9	C4orf34	CA2	CAPG	CAPN6	CD24	CD59
	CLDN18	CNOT7	CRIP1	CTSD	CXCL17	CYP2C18	CYP3A5	CYSTM1	DNM2	DPCR1	EHD2	EPB41L1
	FAM110B	FAM177B	FAM189A2	FN1	FOSB	FSIP2	FUT9	FXYD3	GALNT3	GALNT7	GNAQ	GPR87
	GPRC5B	HIPK2	HMGCS2	HOXB8	HS3ST5	HSPB1	HTR1B	IL18R1	IL2RA	KCNE3	KLF4	LEPREL1
	LGMN	LPAR1	LRP1	LYPD6B	MAOB	MEIS2	METTL7A	MFSD1	MITF	MLPH	MSMB	MUC1
	MXD1	MYEOV	NDUFB1P1	NEK6	NFAT5	NKX6-3	NTRK2	OASL	P4HA1	PART1	PCDH7	PGC
	PLA2G10	PLXNA2	PP7080	PPARGC1A	PSCA	PVRIG	PXDC1	QKI	RAB27B	RBMS1	RERG	RETSAT
	RGNEF	RHBDL2	RHOBTB1	RNF128	RNF183	ROBO1	S100P	SCIN	SFTA2	SGK2	SLC16A3	SLC19A3
	SLC26A9	SLC41A2	SLC44A4	SLC45A3	SLC4A4	SLC9A1	SLC9A2	SLC9A3	SMPDL3A	SPINK1	STEAP1	SULT1C2
	SYT9	TFF1	TFF2	TFF3	TM4SF1	TPBG	TRAK1	TSHZ2	TSPAN1	TSPAN31	UGDH	VSIG1
	VSIG2											
Je-high	BDKRB2	C2CD4A	CCR1	CHRM3	CPVL	CYP2A13	EPHB1	FAM47B	FMOD	GLDC	HSD17B7P2	IFITM3
24 genes	LGR5	ODAM	OR8J1	PHYHIPL	RTP4	SESN1	SHPK	SLC26A2	STARD13	TPH1	UNC93A	ZRSR2
Il-high	ABCB1	ABCC2	ABCG2	ACE2	ACOX2	ADH4	ADH6	AKAP7	ALDOB	ANPEP	ANXA2P2	APOB
178 genes	AREG	BTNL3	C17orf72	C1orf201	C1orf21	C3orf26	C3orf52	C4BPB	CACNA1E	CCL25	CCND2	CD52
	CDH17	CDX2	CEACAM1	CEACAM5	CELA3A	CELA3B	CHGA	CIDEC	CLCA1	CLIC5	CLRN3	CPE
	CSF1R	CYBRD1	CYP2A7	DACH1	DENND1A	DHRS11	DKK1	DMBT1	DOK3	DPP4	DSG3	DUSP5
	EFCAB4B	EGR2	EML1	EREG	F2R	FABP2	FABP6	FAM105A	FCGBP	FGF23	FITM2	FOLH1
	FRZB	GALNT8	GBA3	GCET2	GDAP1	GFOD1	GHRL	GIP	GJA1	GLS	GPA33	GSDMB
	GSTA2	GUCY2C	HEPACAM2	HHLA2	HLA-DRB1	HNF4G	HTR1D	IL18	IL2RG	IL32	INE1	IRF8
	ITLN1	JAG1	KIAA0226L	KIRREL	KLF7	KRT20	KRT33B	KRT80	L1TD1	LCT	LEAP2	LGALS2
	LGALS3	LINC00483	LOC100132099	MANBAL	MAOA	MARCH3	MARCH8	MB21D2	MEP1A	MEP1B	MICAL2	MIR17HG
	MLN	MOGAT3	MRPS18A	MUC13	MUC17	MYO1A	MYO1E	MYO7B	NABP1	NELL2	NIPAL1	NME5
	NODAL	NOX1	NPY6R	NR1H4	O3FAR1	OSR2	OSTBETA	OSTalpha	OTC	PADI2	PAPSS2	PDE10A
	PDE3A	PDP1	PI3	PLA2G12B	PLK1S1	PMP22	PRAP1	RASGRF2	RBP2	RGS2	RHOB	RNF182
	RNF217	SARM1	SATB2	SEMA3D	SEMA6D	SERTAD1	SI	SIDT1	SLC17A4	SLC2A5	SLC30A2	SLC46A3
	SLC6A20	SLC7A6	SNX10	TCEANC	TGFBI	THEM4	TM4SF20	TM6SF2	TMEM45B	TRIM36	TUBAL3	TUFT1
	UGT2B15	VTN	XDH	YAE1D1	ZG16	ZNF208	ZNF347	ZNF502	ZNF705G	ZYX		

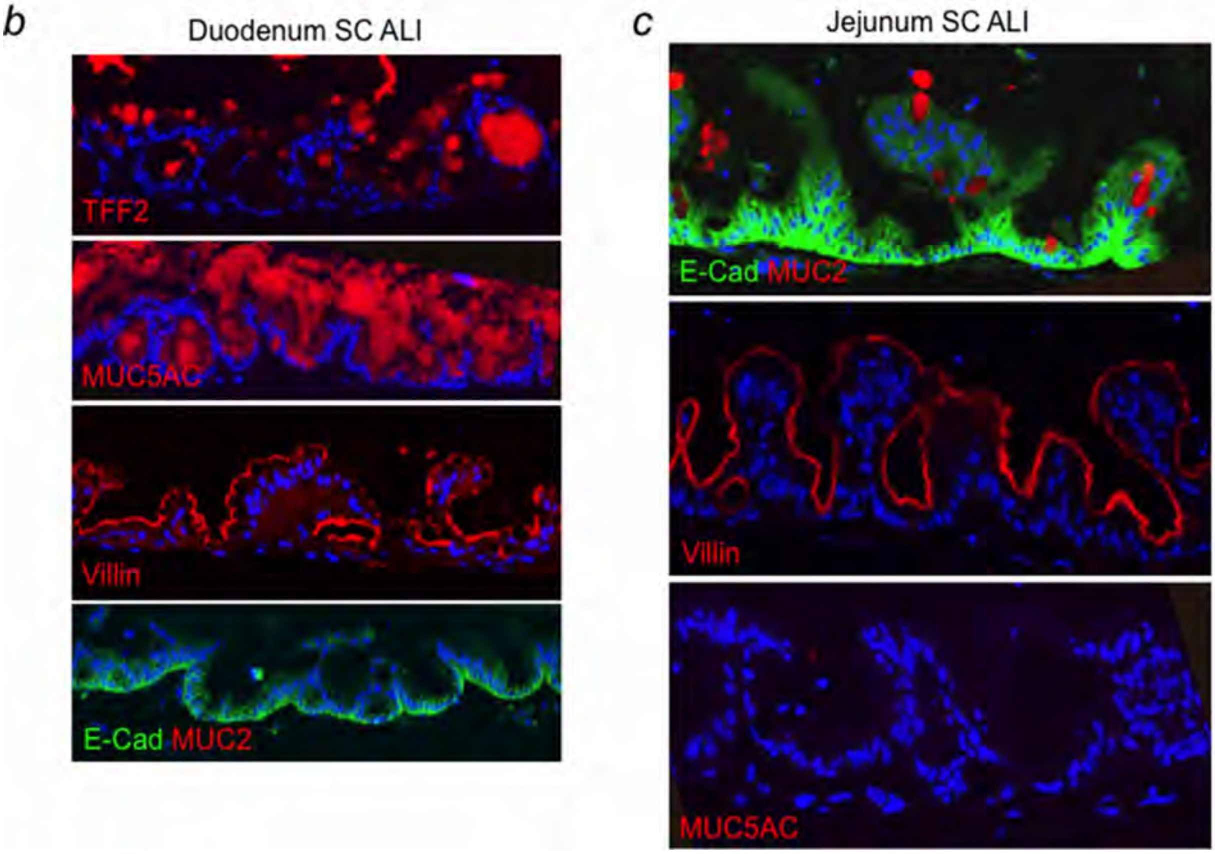

Extended Data Figure 2 | Intestinal stem cell expression profiles. **a**, List of genes differentially expressed in ISC derived from duodenum, jejunum and ileum. These data correspond to heat map of Fig. 2b. **b**, Immunofluorescence labelling of ALI-differentiated ISCs from duodenum with antibodies against Tff2, mucin 5AC, villin, E-cadherin, and mucin 2. **c**, Immunofluorescence labelling of ALI-differentiated epithelia from jejunum stem cells with antibodies to E-cadherin, mucin 2, villin, and mucin 5AC. Scale bar, 50 μm; *n* = 10 technical replicates.

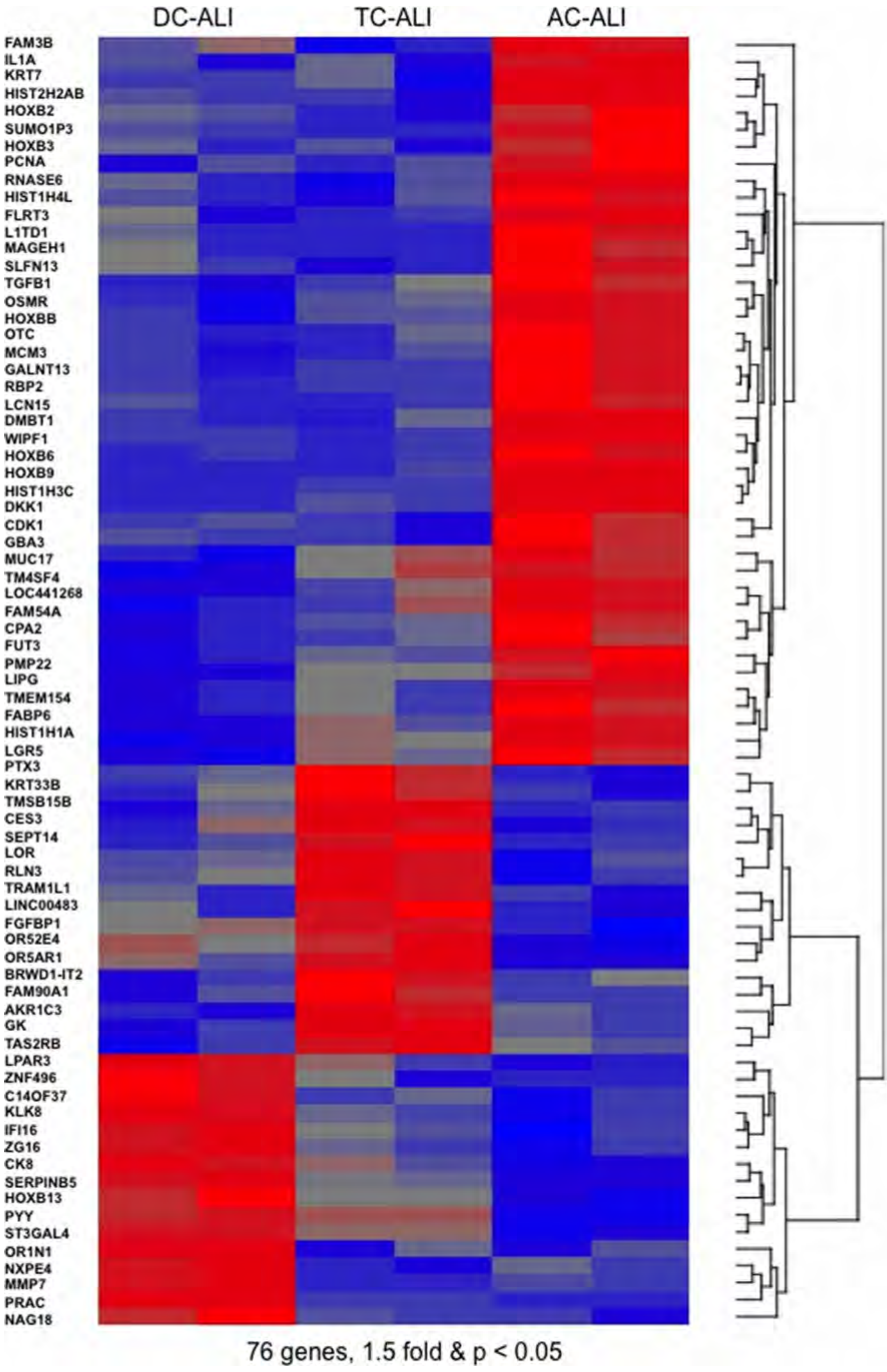

Extended Data Figure 3 | Differential gene expression in epithelia derived from colonic stem cells. Heat map of differentially expressed (>1.5-fold, $P < 0.05$) genes in ALI cultures derived from stem cell pedigrees of ascending, transverse, and descending colon.

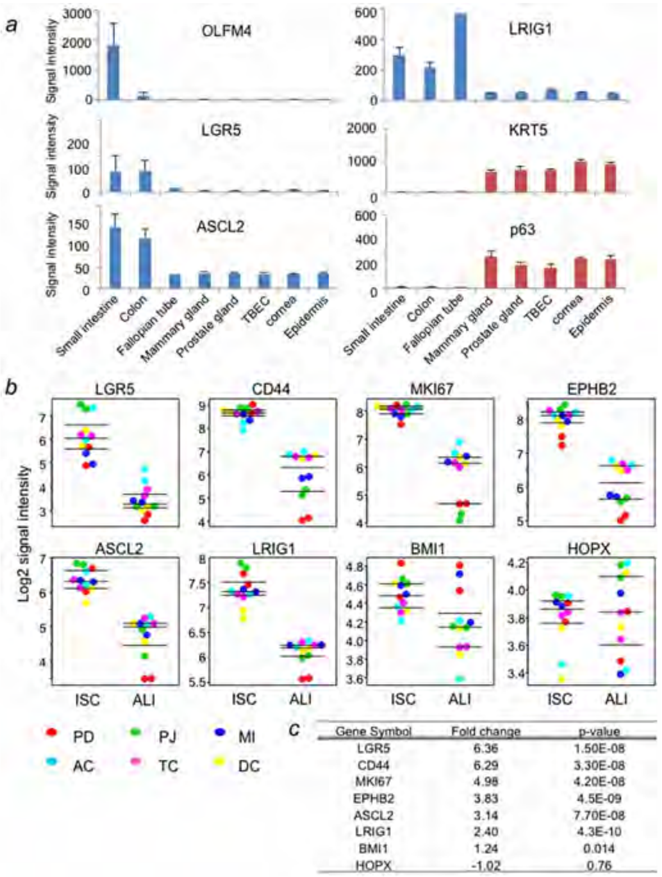

Gene Symbol	Fold change	p-value
LGR5	6.36	1.50E-08
CD44	6.29	3.30E-08
MKI67	4.98	4.20E-08
EPHB2	3.83	4.5E-09
ASCL2	3.14	7.70E-08
LRIG1	2.40	4.3E-10
BMI1	1.24	0.014
HOPX	-1.02	0.76

Extended Data Figure 4 | Differential gene expression across columnar and stratified epithelial stem cells. **a**, Histograms of expression microarray signal intensity of selected genes across averaged intestine and colon ISCs, stratified epithelial stem cells, and stem cells of the fallopian tube (FT). Biological replicas $n = 2$–6 (FT = 2, stratified epithelia = 3, colon, intestine = 6); error bars, s.d. **b**, Dot plot showing expression microarray data of indicated genes for stem cell pedigrees (ISC; Duo, duodenum; Jej, jejunum; Ile, ileum; AC, ascending colon; TC, transverse colon; DC, descending colon) derived from various regions of the intestinal tract before and after air–liquid interface (ALI) differentiation. Biological replicas $n = 2$ (total 12 data sets) for stem cells, technical replicas $n = 2$ for ALI. **c**, Chart of aggregate *P* values by Student's *t*-test for gene expression changes between ground state stem cells and their ALI-differentiated counterparts.

a CNVs and SNVs in 2 clones of Fetus-1

CNV	Pedigree 1				Pedigree 2			
	P5	P10	P15	P20	P5	P10	P15	P20
amp	0 (0)	0 (0)	0 (0)	0 (0)	0 (0)	0 (0)	9 (4)	1 (1) + Chr12^{tri}
del	3 (2)	0 (0)	2 (13)	4 (13)	0 (0)	1 (1)	1 (1)	1 (1)
SNV	Not detected	Not detected	SPEF2 (ns)	SPEF2 (ns)	IL1RAP (ns)	IL1RAP (ns)	IL1RAP (ns), CMYA5 (ns)	IL1RAP (ns), CMYA5 (ns)

b Gene list for CNVs in 5 clones of Fetus-2

Genes affected by amplified region		Gene symbol									
Pedigree 3	P5	No genes									
	P25	C19orf61	CADM4	IRGC	IRGQ	PLAUR	SRRM5	ZNF428	ZNF578	MIR196A2	SATB1
Pedigree 4	P5	ACAP2									
	P25	Chr 11 trisomy									
Pedigree 5	P5	SEPSECS									
	P25	Chr 2, 7, 10 and 12 trisomies									
Pedigree 6	P5	No genes									
	P25	SATB1	Chr 12 trisomy								
Pedigree 7	P5	No genes									
	P25	LOC152225									

Genes affected by deleted region		Gene symbol									
Pedigree 3	P5	GPCRLTM7	NCK1	RIMS2							
	P25	ACAP2	APBB1IP	ASXL2	BMPR2	BNIP2	CFL2	FAM193A	FANCA	FARS2	FHIT
		HERC1	HERC4	IL2RA	IL2RA	LUC7L2	MAPK6	MARVELD2	MIR1288	MYPN	NBEAL1
		NCK1	NFAT5	PHC3	PIGL	RNF150	RNF216	RNF4	RPGRIP1	SIRT1	SKIL
		SLC35F2	SNORA70B	SPPL2A	TMCO7	TMEM116	TMEM22	TRPM7	WWOX	ZFR	
Pedigree 4	P5	No genes									
	P25	FHIT									
Pedigree 5	P5	AGBL2	ARCN1	C16orf73	CLDN3	CLPTM1	GABPB2	HERC4	ITFG3	LOC401109	MLLT11
		NCRNA00254	PIGL	PKD1L2	PTPRJ	SIRT1	WWP2	ZNF604A			
	P25	BNIP2	C1orf129	C4orf34	CBNPV	CFL2	CRYM	FANCA	GPR160	GTF2A2	IL4
		KIF3A	LOC644656	MIR1288	NCK1	NCRNA00169	NFAT5	PHC3	PIGL	SNORA23	TMEM22
		TRPM7	WEE1	ZNF143							
Pedigree 6	P5	AQR	ASH1L	C11orf65	OSBPL1A	PNPT1	POU5F1P4	RAB39	RNF111	SAP30	SCRG1
		SPPL2A	ZNF43								
	P25	FHIT									
Pedigree 7	P5	No genes									
	P25	FHIT									

c Gene list for SNVs in 5 clones of Fetus-2

Clone No.	Passage	Gene symbol of nonsynonymous SNV									
Pedigree 3	Passage 5	BSN									
	Passage 25	KIAA0226	ATP7A								
Pedigree 4	Passage 5	RBMXL1									
	Passage 25	DOCK10	CXCR7	FAM135A	CYP11B2	PTDSS2	CDH8	KRTAP4-5	PSMC5	BPIFC	ANKRD55
Pedigree 5	Passage 5	No SNVs									
	Passage 25	BAI1	CACNA1B	ASUN	LRRC37A3						
Pedigree 6	Passage 5	FAM157A	KCNMA1								
	Passage 25	TMEM48	CCT3	ECEL1	ECT2L	CAMK2B	VIPR2	KCNMA1	DTX4	PVRL2	
Pedigree 7	Passage 5	No SNVs									
	Passage 25	ANKRD17	ADAMTS12	KCNH2	KIF19	KRTAP23-1	EP300				

Extended Data Figure 5 | Genes affected by CNV and SNV events in intestinal stem cell pedigrees during passaging. a, Summary of CNV (events (genes affected)) and non-synonymous SNV in pedigrees 1 and 2 at P5 to P20. **b**, Summary of genes altered by interstitial CNV amplifications (top) or deletions (bottom) in ISC pedigrees 3 to 7 at P5 and P25. **c**, Summary of genes sustaining non-synonymous SNV in five ISC pedigrees at P5 and P25.

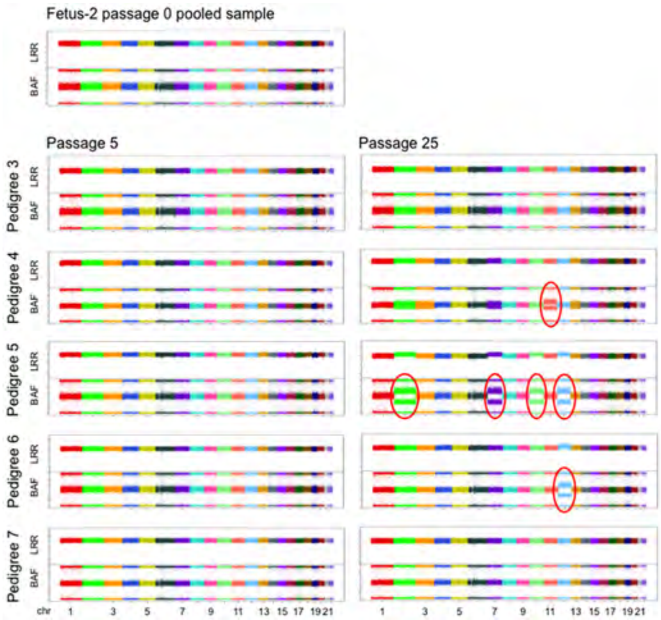

Extended Data Figure 6 | Whole-genome CNV profiles for intestinal stem cell pedigrees 3–7 at P5 and P25. Regions marked by ovals represent aneuploidy.

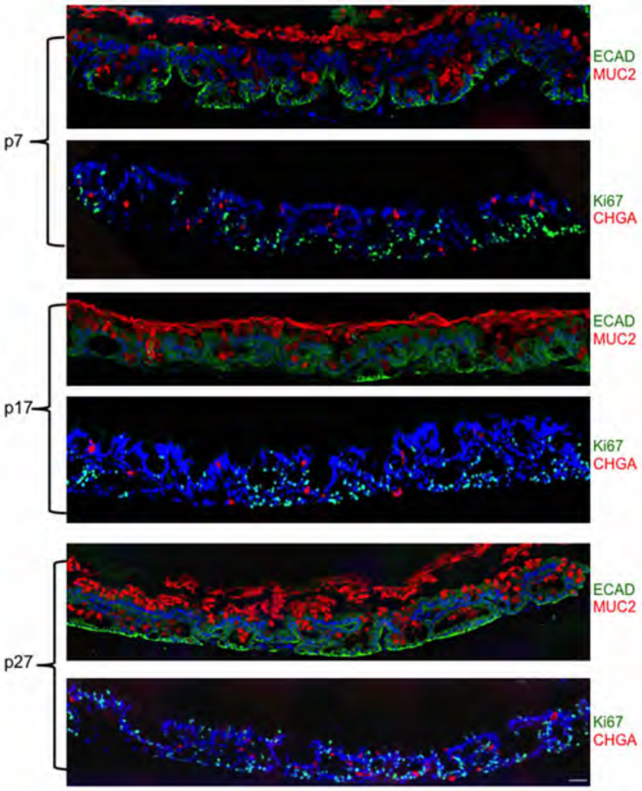

Extended Data Figure 7 | Impact of ISC^{GS} passaging on ALI differentiation. ALI differentiation of intestinal pedigree 2 initiated from cells at the indicated passage number. As indicated, histological sections of differentiated epithelia were stained with antibodies to either E-cadherin (ECAD, green) and mucin 2 (Muc2, red), or Ki67 (green) and chromogranin A (CHGA, red). Scale bar, 75 μm; $n = 4$ technical replicates.

a

Time Name	4 wks	8 wks	12 wks	16 wks
Pedigree 3 P6	0/2	0/2	0/2	0/2
Pedigree 3 P25	0/2	0/2	0/2	0/2
Pedigree 5 P6	0/2	0/2	0/2	0/2
Pedigree 5 P25	0/2	0/2	0/2	0/2
Pedigree 7 P6	0/2	0/2	0/2	0/2
Pool	0/2	0/2	0/2	0/2
Cancer Cells	0/8	2/8	5/8	8/8

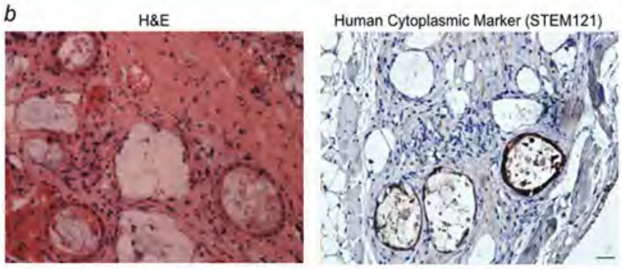

Extended Data Figure 8 | ISC^{GS} tumorigenicity assays in immunodeficient mice. **a**, Quantification of tumour formation assessments at 4–16 weeks following subcutaneous inoculation of two million cells of the indicated ISC pedigrees at passage 6 or passage 25 at 4–16 weeks. ‘Pool’ indicates total set of clones derived from P0 ileum culture before pedigree generation. ‘Cancer cells’ refers to propagating cells from case of high-grade serous ovarian cancer. **b**, Left, histological section through site of injection of 1 million cells from pedigree 3. Right, section of injection site stained with antibody (STEM121) to human epithelial cells (brown) revealing benign cysts. Scale bar, 15 μm.

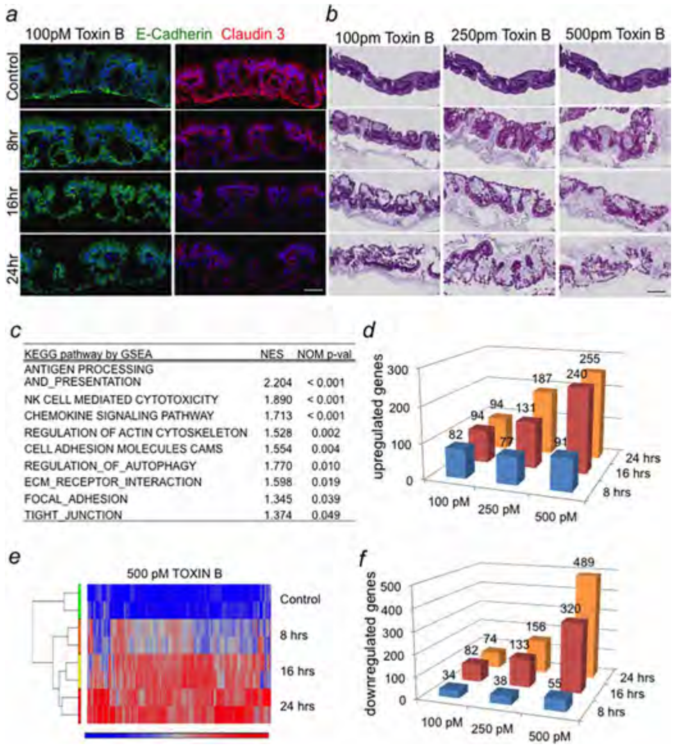

KEGG pathway by GSEA	NES	NOM p-val
ANTIGEN PROCESSING AND_PRESENTATION	2.204	< 0.001
NK CELL MEDIATED CYTOTOXICITY	1.890	< 0.001
CHEMOKINE SIGNALING PATHWAY	1.713	< 0.001
REGULATION OF ACTIN CYTOSKELETON	1.528	0.002
CELL ADHESION MOLECULES CAMS	1.554	0.004
REGULATION_OF_AUTOPHAGY	1.770	0.010
ECM_RECEPTOR_INTERACTION	1.598	0.019
FOCAL_ADHESION	1.345	0.039
TIGHT_JUNCTION	1.374	0.049

Extended Data Figure 9 | Dose- and time-dependency of TcdB pathology in ALI-generated colonic epithelia. **a**, Immunofluorescence localization of adherens junction marker E-cadherin and tight junction marker claudin 3 in ALI-differentiated epithelia derived from transverse colon stem cells following exposure to 100 pM TcdB for the indicated durations. $n = 4$ technical replicates. Scale bar, 100 µm. **b**, Representative H&E images of ALI cultures at indicated times and concentration of TcdB exposure. Scale bar, 250 µm; $n = 4$ technical replicates. **c**, Gene set enrichment analysis of whole-genome expression data from colonic epithelia treated with 500pM TcdB for 24 h and control samples showing enriched KEGG pathway sets. NES, normalized enrichment score; NOM P value, nominal P value. **d**, 3D plot of upregulated genes at the indicated time points and dosages > twofold, $P < 0.05$). $n = 2$ technical replicates. **e**, Heat map of upregulated genes in 500 pM TcdB samples. The genes (237 genes) were chosen by cutoff values (> twofold, $P < 0.05$). Three time points (8, 16 and 24 h) are shown. **f**, 3D plot of downregulated genes at the indicated time points and dosages > twofold, $P < 0.05$). $n = 2$ technical replicates.

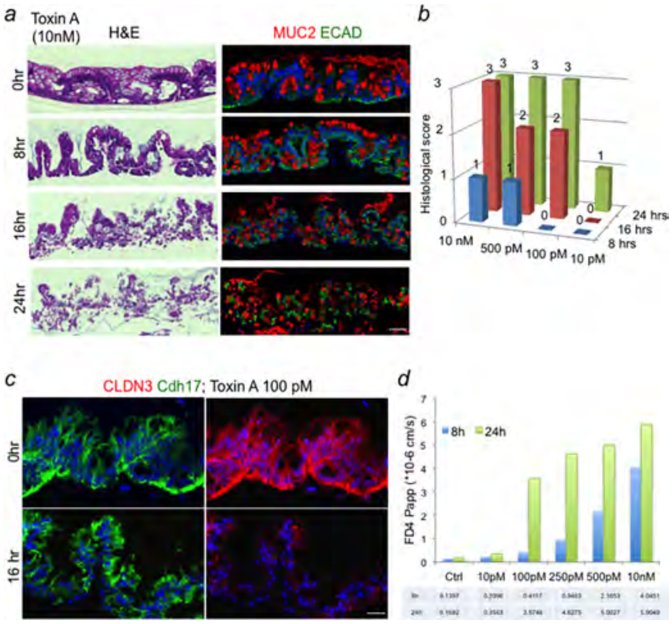

Extended Data Figure 10 | Dose- and time-dependency of TcdA pathology in ALI-generated colonic epithelia. **a**, Left, representative H&E images of ALI cultures at indicated times and concentration of TcdA exposure; right, immunofluorescence localization of adherens junction marker E-cadherin (ECAD; green) and mucin 2 (MUC2; red) in ALI-differentiated epithelia derived from transverse colon stem cells following incubation with 10 nM TcdA for the indicated durations. Scale bar, 100 µm; *n* = 4 technical replicates. **b**, 3D plot of histological scoring of representative H&E time points and concentrations performed by a gastrointestinal pathologist according to a standard 0–3 rating for colonic epithelial integrity. **c**, Distribution of tight junction marker claudin 3 (Cldn3) and adherens junction marker (Cdh17) following treatment of ALI colonic epithelium with TcdA for the indicated times and doses. Scale bar, 50 µm; *n* = 4 technical replicates. **d**, Histogram of permeability of ALI colonic epithelium (Papp) to small molecules (FD4, molecular mass 4,400 Da) following exposure to the indicated doses of TcdA for the indicated times.

AUTHOR QUERY FORM

LIPPINCOTT
WILLIAMS AND WILKINS

JOURNAL NAME: PAS
ARTICLE NO: AJSP_D_14_00447
QUERIES AND / OR REMARKS

QUERY NO.	Details Required	Author's Response
Q1	A running head short title was not supplied; please check if this one is suitable and, if not, please supply a short title of up to 50 characters that can be used instead.	Please see edited short title
Q2	Please confirm whether the conflict of interest statement is correct. If there are any conflicts of interest to be declared, please provide a statement to that effect.	correct.
Q3	As per style all gene names should be in italics. Please italicize all occurrences of gene names in the article.	done.
Q4	Key words included from he title page of the pdf, please confirm.	confirmed, with edits.

Evidence for a Dualistic Model of High-grade Serous Carcinoma

BRCA Mutation Status, Histology, and Tubal Intraepithelial Carcinoma

Brooke E. Howitt, MD, Suchanan Hanamornroongruang, MD,† Douglas I. Lin, MD, PhD,**
James E. Conner, MD, PhD, Stephanie Schulte, MD, PhD,* Neil Horowitz, MD,‡§*
Christopher P. Crum, MD, and Emily E. Meserve, MD, MPH**

Abstract: Most early adnexal carcinomas detected in asymptomatic women with germline ~~BRCA~~ mutations (~~BRCA~~$^+$) present as serous tubal intraepithelial carcinomas (STIC). However, STICs are found in ~~only~~˜~~40%~~ of symptomatic high-grade serous carcinomas (HGSCs) and less frequently in pseudoendometrioid variants of HGSC. Consecutive cases of untreated HGSC from ~~BRCA~~$^+$ and ~~BRCA~~$^-$ women with detailed fallopian tube examination (SEE-FIM protocol) were compared. STIC status (+/−) was determined, and tumors were classified morphologically as SET ("SET", > 50% solid, pseudoendometrioid, or transitional) or classic predominate ("Classic"). SET tumors trended toward a higher frequency in ~~BRCA~~$^+$ versus ~~BRCA~~$^-$ women (50% vs. 28%, $P = 0.11$), had a significantly younger mean age than those with classic HGSC in ~~BRCA~~$^-$ women (mean 56.2 vs. 64.8 y, $P = 0.04$), and displayed a better clinical outcome in both groups combined ($P = 0.024$). STIC was significantly more frequent in tumors from the ~~BRCA~~$^-$ cohort (66% vs. 31%, $P = 0.017$) and specifically the ~~BRCA~~$^-$ tumors with classic morphology (83%) versus those with SET morphology (22%, $P = 0.003$). Overall, several covariables—histology, ~~BRCA~~ status, age, coexisting STIC, and response to therapy—define 2 categories of HGSC with differences in precursor (STIC) frequency, morphology, and outcome. We introduce a dualistic HGSC model that could shed light on the differences in frequency of STIC between symptomatic and asymptomatic women with HGSC. This model emphasizes the need for further study of HGSC precursors to determine their relevance to the prevention of this lethal malignancy.

AQ3

AQ4

Key Words: fallopian tube, neoplasia, serous ~~carcinoma~~BRCA, endometrioid, tubal intraepithelial carcinoma, risk-reduction salpingo-oophorectomy

(*Am J Surg Pathol* 2014;00:000–000)

In the last decade, the origin of ovarian cancer has become the subject of intense study, and the distal fallopian tube has emerged as a potential origin for a significant proportion of high-grade serous carcinomas (HGSCs).[1,2] Evidence in support of the distal fallopian tube as a site of origin has been (1) the discovery of tubal epithelial atypia in women with ~~BRCA1~~ or ~~BRCA2~~ mutations, (2) detection of high-grade serous tubal intraepithelial neoplasia (STIC) in risk-reducing salpingo-oophorectomies (RRSOs), (3) the finding of STIC in fallopian tubes of women with advanced carcinoma, and (4) identification of a credible precursor spectrum spanning both normal and neoplastic tubal mucosa.[1,3–5] The latter has been characterized by evidence of DNA damage, ~~p53~~ mutation, and progressive molecular perturbations that have been reproduced in both cell culture and animal models.[6–8]

The percentage of HGSCs whose origins can be traced to the distal fallopian tube has increased, in part attributable to the use of sampling protocols (SEE-FIM) that more thoroughly examine the distal fallopian tube and fimbria. Identification of STIC supports, if not confirms, a tubal origin in 18% to 60% of cases of advanced or symptomatic HGSCs.[2] Still, in a significant percentage of cases, a tubal carcinogenic sequence has not been confirmed by detection of an intramucosal carcinoma. In contrast, when HGSCs are discovered early or in asymptomatic women (RRSO), approximately 80% coexist with STIC.[9–11]

In recent publications, the spectrum of HGSC has been expanded to include endometrioid or endometrioid-like (pseudoendometrioid) tumors, largely because of the observation of an identical immunophenotype using p53, PTEN, and Pax2 as well as similar rates of ~~p53~~ mutation.[12] Of interest, Roh et al[13] found that the

---

From the *Department of Pathology, Division of Women's and Perinatal Pathology; §Department of Obstetrics and Gynecology, Division of Gynecologic Oncology, Brigham and Women's Hospital; ‡Dana Farber Cancer Institute, Boston MA; and †Department of Pathology, Siriraj Hospital, Mahidol University, Bangkok, Thailand.

Presented at the 103rd United States and Canadian Academy of Pathology Annual Meeting in San Diego, CA.

C.P.C. and E.E.M. contributed equally.

Conflicts of Interest and Source of Funding: Supported by a grant from the Department of Defense (W81XWH-10-1-0289 to C.P.C.). The authors have disclosed that they have no significant relationships with, or financial interest in, any commercial companies pertaining to this article.

AQ2

Correspondence: Christopher P. Crum, MD, Department of Pathology, Brigham and Women's Hospital, Boston, MA 02115 (e-mail: ccrum@partners.org).

endometrioid subset had a lower frequency of associated STIC. This finding was of borderline statistical significance but raised the possibility that certain tumor morphologies might be less likely to arise from STIC. Recently, Soslow et al[14] reported that particular patterns of HGSC ~~differentiation~~, namely solid, pseudoendometrioid, and transitional (SET; Fig. 1), were seen more commonly in association with ~~BRCA1/2~~ mutations. This, combined with the observations of Roh and colleagues, suggested that endometrioid or SET histology might not only be more commonly found in women with ~~BRCA~~ mutations but paradoxically less likely to be associated with a STIC as currently described. The purpose of this study was to examine this paradox from the perspective of symptomatic malignancies in women with (~~BRCA~~$^+$) and without (~~BRCA~~$^-$) germline mutations in the ~~BRCA1~~ or ~~BRCA2~~ genes.

MATERIALS AND METHODS

Patient Samples and Case Selection

This study was approved by the institutional review boards at Brigham and Women's Hospital (BWH) and Dana Farber Cancer Institute (DFCI). All cases of HGSC resected at BWH from 2005 to 2013 were identified from archival records. Careful examination of the tubes and ovaries, including the SEE-FIM protocol, was performed in all cases as previously described.[3] This cohort was cross-indexed with genetic testing records in the Center for Cancer Genetics and Prevention at DFCI to identify 2 cohorts of women with HGSC: those who were confirmed to have ~~BRCA1/2~~ germline mutations and those documented to be negative for these mutations. Patients who received neoadjuvant chemotherapy were excluded from this study. Between 2005 and 2013, 387

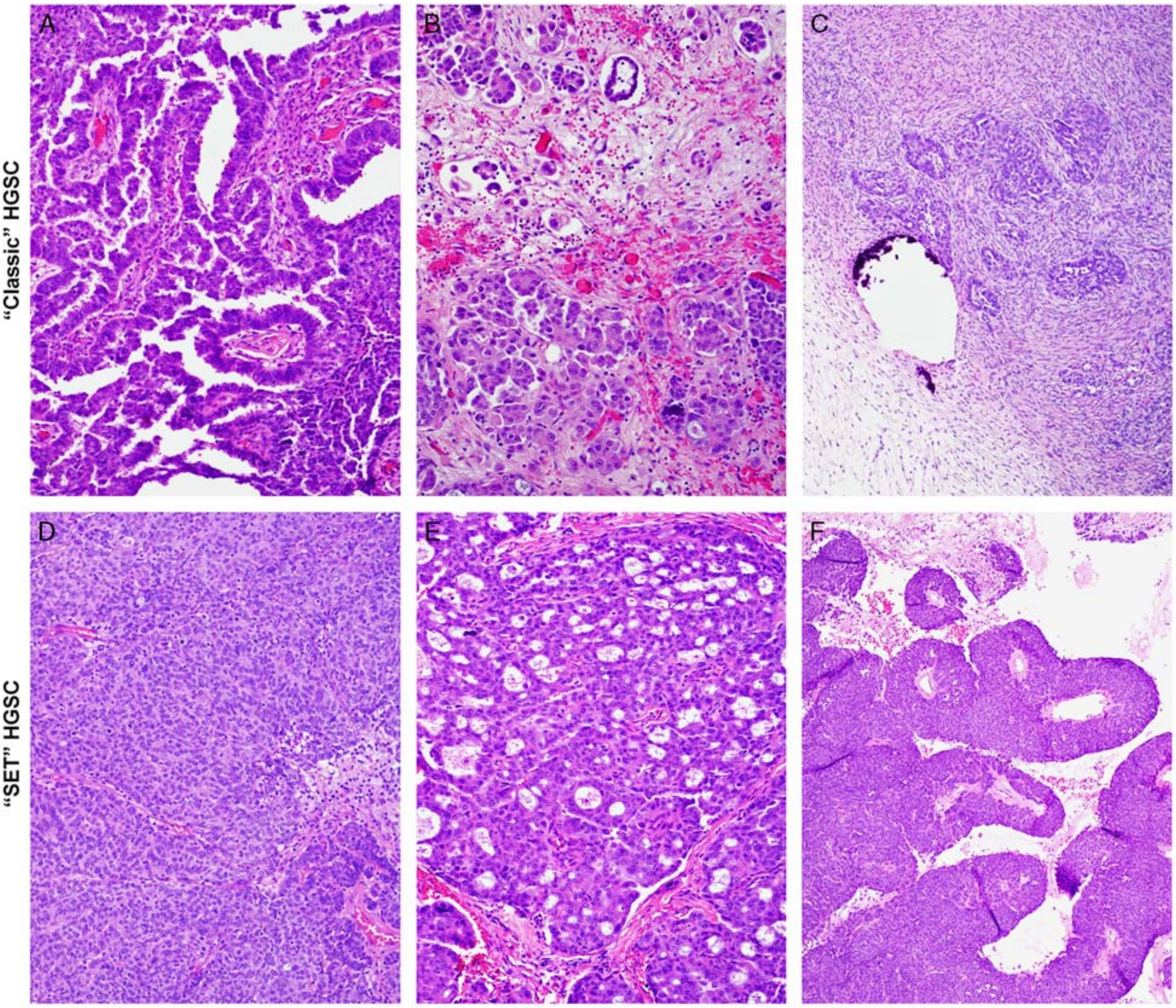

FIGURE 1. Histologic features of HGSC. Classic patterns include papillary (A), micropapillary (B), and infiltrative (C). SET patterns include solid (D), endometrioid-like (E), and transitional (F).

patients underwent surgery at BWH for a diagnosis of HGSC. Within this group, 116 underwent germline testing for ~~BRCA1~~ or ~~BRCA2~~ mutations. A germline mutation in either ~~BRCA1~~ or ~~BRCA2~~ (~~BRCA~~$^{+}$) was detected by direct sequence analysis in 47 patients. No ~~BRCA1~~ or ~~BRCA2~~ germline mutation was detected in 69 patients (~~BRCA~~$^{-}$). Forty-one patients had undergone neoadjuvant chemotherapy treatment (10 ~~BRCA~~$^{+}$, 31 ~~BRCA~~$^{-}$) and were excluded from the study. Slides were unavailable for histologic review in 17 cases (11 ~~BRCA~~$^{+}$, 6 ~~BRCA~~$^{-}$). Clinical outcome data including the time to last follow-up, and clinical status at last follow-up were extracted from the electronic medical record.

Histologic Review and Classification

Invasive Tumors

Tumors were reviewed without knowledge of their ~~BRCA~~ mutation status and classified as previously described into the following groups by 2 coauthors (B.E.H., C.P.C.):

- *Classic Predominate HGSC Histology ("Classic"):* > 50% of the tumor demonstrates papillary, micropapillary, or infiltrative architecture, and often desmoplastic stroma.
- *SET Predominate HGSC Histology ("SET"):* > 50% of the tumor displays 1 or more variant features, including solid growth, gland formation, and papillary transitional patterns.

The percentage of tumor containing SET versus classic histology was estimated in each case (in increments of 10%).

STIC Diagnosis

STIC was identified and confirmed as previously described.[4,5]

Statistical Analysis

Age and predominant morphologic pattern were compared between ~~BRCA~~$^{+}$ and ~~BRCA~~$^{-}$ women by the Student *t* test and χ^2 test. Age was compared between tumors with SET and classic predominant morphology by the Student *t* test. Subgroup analyses of frequency of STIC were performed by the Fisher exact test. Analysis of survival using Kaplan-Meier curves and log rank tests was performed.

RESULTS

Study Population

The study group comprised 26 ~~BRCA~~$^{+}$ cases including 21 advanced (stage 3-4) and 5 early (stage 1-2) carcinomas and 32 advanced ~~BRCA~~$^{-}$ cases, all of which were evaluated by the SEE-FIM protocol. The 5 early carcinomas were all identified in RRSO specimens. Table 1 summarizes the 2 groups.

In 16 (8 ~~BRCA~~$^{+}$ and 8 ~~BRCA~~$^{-}$) of the 58 cases, a grossly normal-appearing portion of distal fallopian tube was sampled (one half of 1 fimbriated end) for research immediately after excision and before processing. In ~~6~~, a STIC was ultimately identified in permanent sections from the main specimen. Ten samples taken for special studies were from specimens in which no STIC was identified in the permanent sections. Of these, 8 were examined by frozen section of the banked tissue, none of which revealed a STIC. No pathologic information was available on the remaining ~~2~~ samples taken for special studies.

TABLE 1. Summary of ~~BRCA~~$^{+}$ and ~~BRCA~~$^{-}$ Tumor Histology, STIC Status, and Age

	Age (y)	No. STIC^{+} Cases (%)
~~BRCA~~$^{+}$ (all; n = 26)	52.9*	8 (31)
SET (n = 13)	49.7	3 (23)
Classic (n = 13)	55.4	5 (38)
~~BRCA~~$^{-}$ (all; n = 32)	62.5*	21 (66)
SET (n = 9)	56.2**	2 (22)***
Classic (n = 23)	64.8**	19 (83)***

*$P = 0.0007$.
**$P = 0.04$.
***$P = 0.003$.

~~BRCA~~$^{+}$ Women With HGSC Are Significantly Younger Than ~~BRCA~~$^{-}$ Women

The study group included 17 women with ~~BRCA1~~ and 9 with ~~BRCA2~~ mutations. The mean age of ~~BRCA~~$^{+}$ women was 52.9 years (range 42 to 76 ~~y~~) and was significantly younger than that of the ~~BRCA~~$^{-}$ population (62.5 y; range 38 to 80 ~~y~~, $P = 0.0007$).

~~BRCA~~$^{+}$ Tumors Trend Toward a Higher Frequency of SET Morphology

Figure 2 and Table 1 summarize the comparison of ~~BRCA~~$^{+}$ and ~~BRCA~~$^{-}$ patients by predominant morphologic pattern. ~~BRCA~~$^{+}$ tumors were more likely to have SET morphology (50%) when compared with ~~BRCA~~$^{-}$ tumors, of which 28% were SET predominate ($P = 0.11$).

In ~~BRCA~~$^{-}$ Tumors, SET Morphology Is Seen in Younger Patients Compared With Those With Classic Morphology

Within the ~~BRCA~~$^{-}$ cohort, tumors with SET morphology had a younger mean age compared with those with classic morphology (56.2 vs. 64.8 ~~y~~, $P = 0.04$). The ~~BRCA~~$^{+}$ patients with SET morphology tended to be younger (mean 49.7 vs. 55.4 ~~y~~), although this difference was not statistically significant ($P = 0.13$).

SET Morphology in ~~BRCA~~$^{-}$ Tumors Is Less Likely to be Associated With STIC

Figure 2 and Table 1 summarize and graphically illustrate the frequency and morphology of STIC in ~~BRCA~~$^{+}$ and ~~BRCA~~$^{-}$ tumors. Eight of 26 (31%) ~~BRCA~~$^{+}$ and 21 of 32 (66%) ~~BRCA~~$^{-}$ tumors contained STIC ($P = 0.017$). In the ~~BRCA~~$^{+}$ group, 38% and 23% of classic and SET tumors, respectively, were associated with STIC ($P = 0.3$). In contrast, 83% and 22% of classic and SET ~~BRCA~~$^{-}$ tumors were associated with STIC, respectively ($P = 0.003$). When both ~~BRCA~~$^{+}$ and ~~BRCA~~$^{-}$ groups were combined, the frequency of STIC in

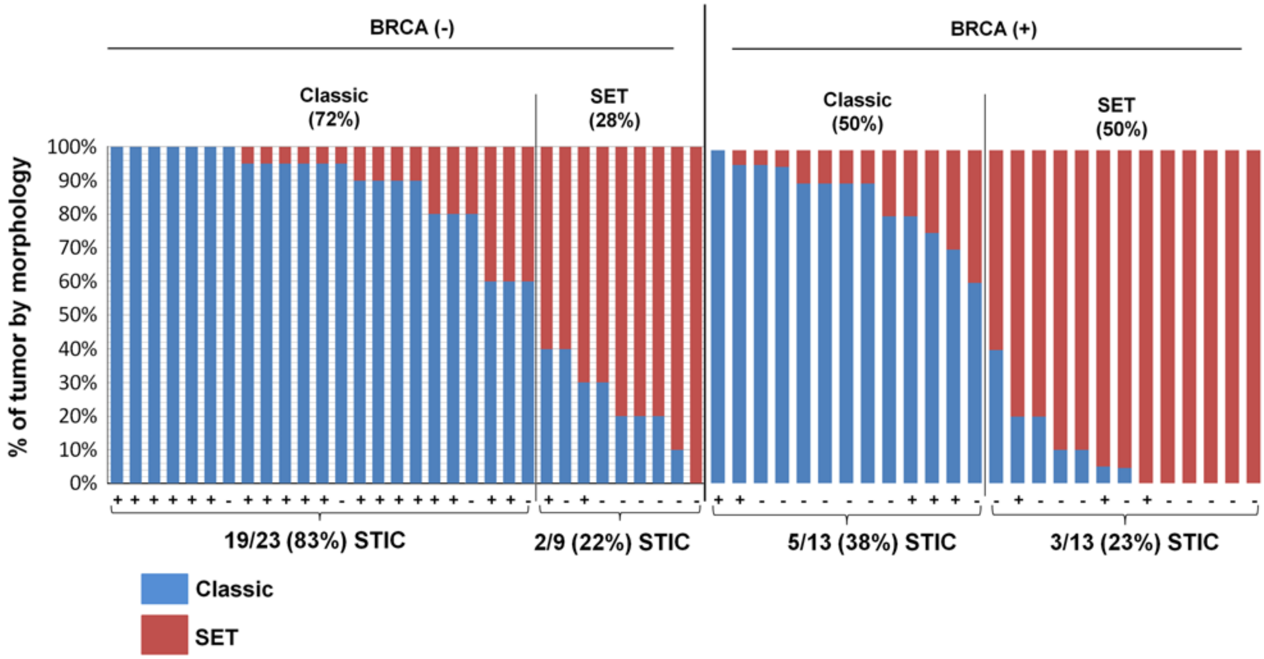

FIGURE 2. Comparison of ~~BRCA~~$^{+}$ and ~~BRCA~~$^{-}$ patients by predominant (>50%) morphologic pattern and STIC status. Each column represents a single patient's tumor, with percent tumor demonstrating SET morphology quantified in red and classic morphology in blue.

classic and SET tumors was 67% and 23%, respectively ($P = 0.003$).

Although most STICs associated with SET tumors were morphologically indistinguishable from those with classic tumors, ~~1~~ ~~BRCA~~$^{+}$ case revealed a STIC with a more solid morphology similar to that seen in the associated SET tumor (Fig. 3). The significance of this is unclear at this point.

Clinical Outcome of Tumors With SET Versus Classic Morphology

Table 2 summarizes the clinical outcome of advanced cases with SET versus classic morphology. In general, ~~BRCA~~$^{+}$ patients were less likely to be dead of disease (DOD) at last clinical follow-up; however, 1 ~~BRCA~~$^{+}$ patient with SET morphology who died also had widely metastatic breast carcinoma and ~~so~~ was excluded from this analysis. Five ~~BRCA~~$^{+}$ HGSCs were early stage and detected in RRSO and were also excluded from the clinical outcome analysis. Of note, 4 of 5 (80%) early HGSCs demonstrated SET predominant morphology, whereas 1 of 5 (20%) demonstrated a predominantly classic pattern. All 5 of these ~~BRCA~~$^{+}$ patients were alive without evidence of disease (ANED) at last follow-up (mean 72.5 ~~mo~~; range 48.3 to 106.5 ~~mo~~). Of the ~~BRCA~~$^{+}$ patients with advanced disease (mean follow-up time 48.5 mo; range 6.4 to 107.2 mo), 5 of 9 (56%) patients with SET tumors were ANED, in contrast to 3 of 12 (25%) patients with classic morphology who were ANED. Within the ~~BRCA~~$^{-}$ cohort (mean follow-up time 30.4 ~~mo~~; range 8.5 to 55.5 ~~mo~~), a favorable effect on clinical outcome was seen in patients with SET predominant tumors when compared with those with classic morphology (1/12 [8%] DOD vs. 8/20 [40%] DOD). After combining both ~~BRCA~~$^{+}$ and ~~BRCA~~$^{-}$ women, SET tumors were significantly more likely to trend toward a less severe outcome ($P = 0.024$, χ^2 test for trend).

DISCUSSION

Beginning in 2000, a wealth of information has progressively linked the distal fallopian tube to the origin of HGSC by the discovery of HGSC precursors in the tubal mucosa. This has produced a paradigm shift in the field of ovarian cancer and prompted recent claims that this disease can be partially prevented by opportunistic salpingectomy. The strongest endorsement of a tubal origin has been studies of early carcinomas~~,~~ which are discovered in approximately 5% to 10% of asymptomatic ~~BRCA~~$^{+}$ women; 80% are associated with a tubal intraepithelial carcinoma (STIC). The distribution of disease in this early "snapshot" of HGSC was heavily weighted toward the fimbria and prompted speculation that the tube was responsible for virtually all HGSCs. However, 2 subsequent observations suggested that the pathogenesis (and possibly origin) of HGSC is more complex. First, a multitude of studies ~~on average~~ have detected STICs in only 40% (on average) of advanced HGSC. Second, a study showed that "endometrioid" variants of HGSC had a lower frequency of STIC (8%) than HGSC with classic morphology, albeit not significant ($P = 0.09$).[13] Another study showed that tumors with SET morphology (solid, pseudoendometrioid, transitional) were more likely to be associated with ~~BRCA~~$^{+}$ status.[14] Taken together, these studies raised the possibilities that the pathway to HGSC

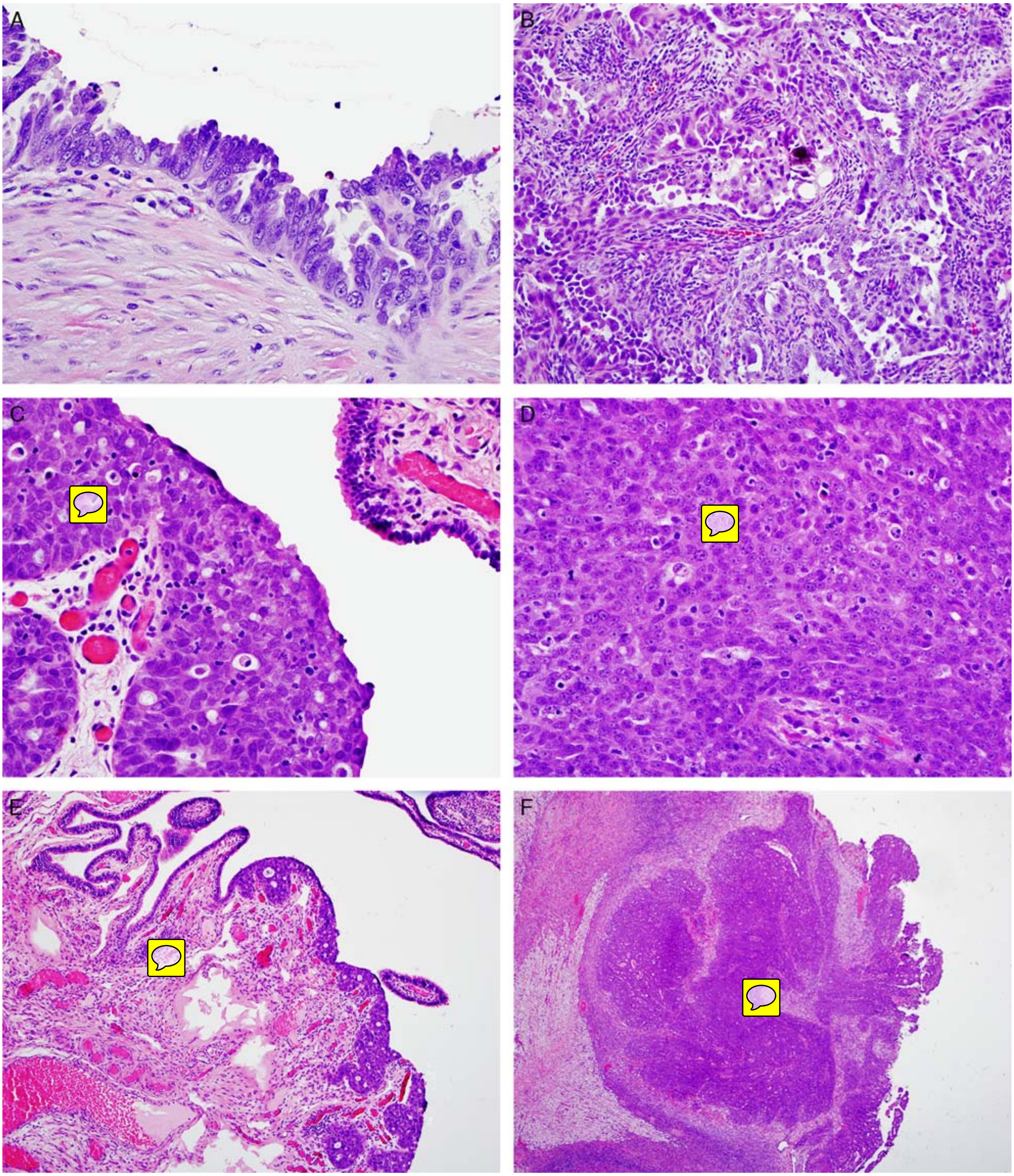

FIGURE 3. Histology of intraepithelial carcinoma (A, C, E) and associated invasive tumor (B, D, F) in a ~~BRCA~~$^{-}$ (A and B) case and ~~BRCA~~$^{+}$ (C–F) case. At higher magnification, the similarity in morphology of 1 ~~BRCA~~$^{+}$ STIC (E) and associated tumor with SET morphology (F) is evident.

might be more diverse than expected, both in precursor and cell type.

This study establishes further that HGSC, in both ~~BRCA~~$^{+}$ and ~~BRCA~~$^{-}$ women, is not a homogenous disease. In our study of ~~BRCA~~$^{+}$ and ~~BRCA~~$^{-}$ groups, we found that several variables, including histology, coexisting STIC, age, and clinical outcome segregated 2 general tumor groups. Further studies will be needed to flesh out the particulars,

TABLE 2. Clinical Outcome in Advanced HGSC by ~~BRCA~~ Status and Tumor Morphology

	~~BRCA~~$^+$		~~BRCA~~$^-$	
	SET	**Classic**	**SET**	**Classic**
ANED	5	3	6	4
AWD	1	7	5	8
DOD	2	2	1	8
Total	9	12	12	20

SET tumors displayed a statistically significant trend toward a more favorable outcome ($P = 0.024$, χ^2 test for trend).
AWD indicates alive with evidence of disease.

but the following observations from this study—witnessed in both ~~BRCA~~$^+$ and/or ~~BRCA~~$^-$ tumors—suggest >1 form of HGSC~~.~~ (1) Multiple histologic patterns are observed in HGSC, and the SET pattern seems more common in ~~BRCA~~$^+$ women albeit the significance of this association varies depending on the criteria for defining SET morphology and the study population.[14] (2) A significant inverse correlation exists between SET histology and STIC in ~~BRCA~~$^-$ tumors. (3) SET histology in ~~BRCA~~$^-$ tumors is associated with a significantly younger mean age. (4) A generally more favorable outcome exists for women with SET histology. Further study is warranted to determine whether there is a consistent association of SET histology with chemo-responsiveness and whether the SET group of HGSCs explains why ~~BRCA~~$^+$ tumors are generally more chemo-responsive.

The negative correlation between SET histology and coexisting STIC observed in both ~~BRCA~~$^+$ and ~~BRCA~~$^-$ tumors in this study suggests that the differences in morphology may reflect different pathways of tumor evolution.[13,14] First, we found that SET tumors were associated with a significantly younger mean age than classic HGSCs. Second, a recent report looking at fallopian tubes from low-risk women who underwent surgery for benign conditions suggests that isolated STICs in asymptomatic women are more common than previously appreciated.[15] Moreover, in ~~BRCA~~$^+$ women STICs in isolation confer a low risk for HGSC, and when HGSC does develop, there is a lag period of 2 to 5 years after discovery of the STIC.[9,10] The implications are that progression from STIC to HGSC does not always occur, and when it does it may take years. The classic tumors—which have high association with STIC—fit nicely into the model proposed by Brown and Palmer[16] that allows an interval of a few years between initiation of carcinogenesis and symptomatic disease, during which a defined precursor (STIC) develops and evolves. With the observed younger mean age of discovery and lower frequency of STIC, SET tumors do not fit as cleanly into this model.

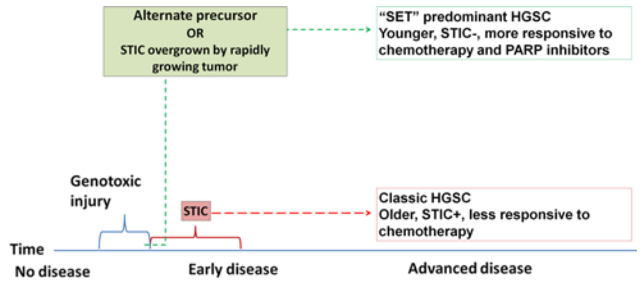

FIGURE 4. A summative model of HGSC pathogenesis with respect to clinical features (age, outcome), precursor lesion, and tumor evolution. In this model, tumor morphology in HGSC could signal a greater likelihood of a certain tumor cell origin and/or biological behavior. The classic pathway involves a STIC and possibly a protracted period from precursor to HGSC. The SET pathway evolves differently as implied by lower frequency of STIC and a younger mean age at discovery. The 2 pathways also seem to differ in terms of responsiveness to chemotherapy and PARP inhibitors.

Figure 4 accounts for the possibility of a second pathway to HGSC and depicts a dualistic model of tumor development in HGSC that incorporates the 2 variables of a defined precursor (STIC) and tumor histology (SET vs. classic). At one pole of this model is classic STIC, which develops and may spread, but demonstrates lag phases both from precursor to STIC and from STIC to symptomatic metastatic tumor, leading to an older average age of clinical presentation. At the other pole are SET tumors that could arise from STIC, from some other tubal precursor, or from elsewhere and become clinically apparent at a younger mean age. This admixture of 2 different tumor biologies would explain ~~1~~ prior observation, which is the rather narrow age gap between ~~BRCA~~$^+$ women with STIC versus women with more advanced disease.[9,10]

This study separated classic and SET tumors on the basis of the assignment of the predominant histologic pattern, and it remains to be determined how this translates biologically and whether the associations seen will be reproduced and consistently reveal 2 separable entities. However, it should be emphasized that type II "ovarian" cancers (HGSCs) are increasingly being subdivided, and the notion that these tumors invariably evolve rapidly may be an oversimplification. ~~For example, in~~ the breast, multiple pathogenetic tumor types have emerged, with ~~BRCA1~~ disease most frequently associated with a basal (including triple negative) breast cancer phenotype and an obscure or particularly high-grade precursor that evolves rapidly.[17,18] Another tumor phenotype, luminal A, is associated with defined precursors, develops more slowly, and as expected is more likely to be detected on screening studies.[19–21] Additional studies are introducing dualistic classifications of HGSC in ~~BRCA~~$^+$ and ~~BRCA~~$^-$ women that correlate molecular profiles with outcome.[22,23] In parallel with arguments for multiple tumor origins, others have divided tumors prognostically into ovarian surface or tubal origin on the basis of expression signatures.[24,25] Such studies beg the correlation of molecular pathways, tumor morphology, and outcome with closer examination of the fallopian tube and its environs to identify novel precursors to explain different biological behaviors within the spectrum of HGSC. The answers bear not only on our understanding of type II HGSCs but also on expectations both from serologic screening and prophylactic salpingectomy.

ACKNOWLEDGMENTS

The authors thank Drs Ross Berkowitz, Michael Muto, Colleen Feltmate, ~~and~~ Donald Goldstein and Ursula Matulonis in the Divisions of Gynecologic Oncology at BWH and DFCI ~~and~~ Dr Judy Garber and Ms Elizabeth Root in the Division of Medical Oncology at the Data Farber Cancer Institute for their contribution to the study, and Mei Zheng and Christine Lam for assistance with the histology and immunohistochemistry. Dr Hanina Hibshoosh of Columbia University provided helpful discussions regarding the comparison of fallopian tube and breast neoplasia.

REFERENCES

1. Piek JM, van Diest PJ, Zweemer RP, et al. Dysplastic changes in prophylactically removed Fallopian tubes of women predisposed to developing ovarian cancer. *J Pathol*. 2001;195:451–456.
2. Crum CP, Herfs M, Ning G, et al. Through the glass darkly: intraepithelial neoplasia, top-down differentiation, and the road to ovarian cancer. *J Pathol*. 2013;231:402–412.
3. Kindelberger DW, Lee Y, Miron A, et al. Intraepithelial carcinoma of the fimbria and pelvic serous carcinoma: evidence for a causal relationship. *Am J Surg Pathol*. 2007;31:161–169.
4. Jarboe E, Folkins A, Nucci MR, et al. Serous carcinogenesis in the fallopian tube: a descriptive classification. *Int J Gynecol Pathol*. 2008;27:1–9.
5. Vang R, Visvanathan K, Gross A, et al. Validation of an algorithm for the diagnosis of serous tubal intraepithelial carcinoma. *Int J Gynecol Pathol*. 2012;31:243–253.
6. Levanon K, Ng V, Piao HY, et al. Primary ex vivo cultures of human fallopian tube epithelium as a model for serous ovarian carcinogenesis. *Oncogene*. 2010;29:1103–1113.
7. Perets R, Wyant GA, Muto KW, et al. Transformation of the fallopian tube secretory epithelium leads to high-grade serous ovarian cancer in Brca;Tp53;Pten models. *Cancer Cell*. 2013;24:751–765.
8. Lee Y, Miron A, Drapkin R, et al. A candidate precursor to serous carcinoma that originates in the distal fallopian tube. *J Pathol*. 2007;211:26–35.
9. Powell CB, Swisher EM, Cass I, et al. Long term follow up of BRCA1 and BRCA2 mutation carriers with unsuspected neoplasia identified at risk reducing salpingo-oophorectomy. *Gynecol Oncol*. 2013;129:364–371.
10. Conner JR, Meserve E, Pizer E, et al. Outcome of unexpected adnexal neoplasia discovered during risk reduction salpingo-oophorectomy in women with germ-line BRCA1 or BRCA2 mutations. *Gynecol Oncol*. 2014;132:280–286.
11. Gilbert L, Basso O, Sampalis J, et al. Assessment of symptomatic women for early diagnosis of ovarian cancer: results from the prospective DOvE pilot project. *Lancet Oncol*. 2012;13:285–291.
12. Köbel M, Kalloger SE, Lee S, et al. Ovarian Tumor Tissue Analysis consortium. Biomarker-based ovarian carcinoma typing: a histologic investigation in the ovarian tumor tissue analysis consortium. *Cancer Epidemiol Biomarkers Prev*. 2013;22:1677–1686.
13. Roh MH, Yassin Y, Miron A, et al. High-grade fimbrial-ovarian carcinomas are unified by altered p53, PTEN and PAX2 expression. *Mod Pathol*. 2010;23:1316–1324.
14. Soslow RA, Han G, Park KJ, et al. Morphologic patterns associated with BRCA1 and BRCA2 genotype in ovarian carcinoma. *Mod Pathol*. 2012;25:625–636.
15. Rabban JT, Garg K, Crawford B, et al. Early detection of high-grade tubal serous carcinoma in women at low risk for hereditary breast and ovarian cancer syndrome by systematic examination of fallopian tubes incidentally removed during benign surgery. *Am J Surg Pathol*. 2014;38:729–742.
16. Brown PO, Palmer C. The preclinical natural history of serous ovarian cancer: defining the target for early detection. *PLoS Med*. 2009;6:e1000114.
17. Anders CK, Carey LA. Biology, metastatic patterns, and treatment of patients with triple negative breast cancer. *Clin Breast Cancer*. 2009;9(suppl 2):S73–S81.
18. Dabbs DJ, Chivukula M, Carter G, et al. Basal phenotype of ductal carcinoma in situ: recognition and immunohistologic profile. *Mod Pathol*. 2006;19:1506–1511.
19. Kurbel S. In search of triple-negative DCIS: tumor-type dependent model of breast cancer progression from DCIS to the invasive cancer. *Tumour Biol*. 2013;34:1–7.
20. Abdel-Fatah TM, Powe DG, Hodi Z, et al. Morphologic and molecular evolutionary pathways of low nuclear grade invasive breast cancers and their putative precursor lesions: further evidence to support the concept of low nuclear grade breast neoplasia family. *Am J Surg Pathol*. 2008;32:513–523.
21. Turashvili G, Hayes M, Gilks B, et al. Are columnar cell lesions the earliest histologically detectable non-obligate precursor of breast cancer? *Virchows Arch*. 2008;452:589–598.
22. Espinosa I, Catasus L, Canet B, et al. Gene expression analysis identifies two groups of ovarian high-grade serous carcinomas with different prognosis. *Mod Pathol*. 2011;24:846–854.
23. George J, Alsop K, Etemadmoghadam D, et al. Nonequivalent gene expression and copy number alterations in high-grade serous ovarian cancers with BRCA1 and BRCA2 mutations. *Clin Cancer Res*. 2013;19:3474–3484.
24. Merritt MA, Bentink S, Schwede M, et al. Gene expression signature of normal cell-of-origin predicts ovarian tumor outcomes. *PLoS One*. 2013;8:e80314.
25. Auersperg N. The stem-cell profile of ovarian surface epithelium is reproduced in the oviductal fimbriae, with increased stem-cell marker density in distal parts of the fimbriae. *Int J Gynecol Pathol*. 2013;32:444–453.

Journal of Pathology
J Pathol 2014; **234:** 478–487

DOI: 10.1002/path.4417

ORIGINAL PAPER

The PAX2-null immunophenotype defines multiple lineages with common expression signatures in benign and neoplastic oviductal epithelium

Gang Ning,[1,†] Jonathan G Bijron,[2,†] Yusuke Yamamoto,[1] Xia Wang,[1] Brooke E Howitt,[3] Michael Herfs,[4] Eric Yang,[3] Yue Hong,[1] Maxence Cornille,[1] Lingyan Wu,[5] Suchanan Hanamornroongruang,[6] Frank D McKeon,[1,†] Christopher P Crum[3,†,*] and Wa Xian[1,†]

[1] *Jackson Laboratory for Genomic Medicine, Farmington, CT, USA*
[2] *Department of Pathology, University of Utrecht, Utrecht, The Netherlands*
[3] *Department of Pathology, Division of Women's and Perinatal Pathology, Brigham and Women's Hospital, Boston, MA, USA*
[4] *Department of Pathology, University of Liège, Liège, Belgium*
[5] *Genome Institute of Singapore, A*STAR, Singapore*
[6] *Department of Pathology, Siriraj Hospital, Mahidol University, Bangkok, Thailand*

**Correspondence to: Christopher P Crum, Department of Pathology, Division of Women's and Perinatal Pathology, Brigham and Women's Hospital, Boston, MA, USA. e-mail: ccrum@partners.org*

[†] *Shared equal responsibility as first and senior authors.*

Abstract

The oviducts contain high-grade serous cancer (HGSC) precursors (serous tubal intraepithelial neoplasia or STINs), which are γ-H2AX^{p}- and *TP53* mutation-positive. Although they express wild-type p53, secretory cell outgrowths (SCOUTs) are associated with older age and serous cancer; moreover, both STINs and SCOUTs share a loss of PAX2 expression (PAX2^{n}). We evaluated PAX2 expression in proliferating adult and embryonic oviductal cells, normal mucosa, SCOUTs, Walthard cell nests (WCNs), STINs, and HGSCs, and the expression of genes chosen empirically or from SCOUT expression arrays. Clones generated *in vitro* from embryonic gynaecological tract and adult Fallopian tube were Krt7^{p}/PAX2^{n}/EZH2^{p} and underwent ciliated (PAX2^{n}/EZH2^{n}/FOXJ1^{p}) and basal (Krt7^{n}/EZH2^{n}/Krt5^{p}) differentiation. Similarly, non-ciliated cells in normal mucosa were PAX2^{p} but became PAX2^{n} in multi-layered epithelium undergoing ciliated or basal (WCN) cell differentiation. PAX2^{n} SCOUTs fell into two groups: type 1 were secretory or secretory/ciliated with a 'tubal' phenotype and were ALDH1^{n} and β-catenin^{mem} (membraneous only). Type 2 displayed a columnar to pseudostratified (endometrioid) phenotype, with an EZH2^{p}, ALDH1^{p}, β-catenin^{nc} (nuclear and cytoplasmic), stathmin^{p}, LEF1^{p}, RCN1^{p}, and RUNX2^{p} expression signature. STINs and HGSCs shared the type 1 immunophenotype of PAX2^{n}, ALDH1^{n}, β-catenin^{mem}, but highly expressed EZH2^{p}, LEF1^{p}, RCN1^{p}, and stathmin^{p}. This study, for the first time, links PAX2^{n} with proliferating fetal and adult oviductal cells undergoing basal and ciliated differentiation and shows that this expression state is maintained in SCOUTs, STINs, and HGSCs. All three entities can demonstrate a consistent perturbation of genes involved in potential tumour suppressor gene silencing (EZH2), transcriptional regulation (LEF1), regulation of differentiation (RUNX2), calcium binding (RCN1), and oncogenesis (stathmin). This shared expression signature between benign and neoplastic entities links normal progenitor cell expansion to abnormal and neoplastic outgrowth in the oviduct and exposes a common pathway that could be a target for early prevention.

Keywords: Fallopian tube; serous carcinoma; stem cell; PAX2; ALDH1

Received 29 May 2014; Revised 24 July 2014; Accepted 29 July 2014

No conflicts of interest were declared.

Introduction

Recent discoveries have strengthened the relationship between the distal Fallopian tube and epithelial malignancies traditionally attributed to the ovary, specifically high-grade serous carcinomas (HGSCs), the most lethal of ovarian cancers [1–3]. With these discoveries has emerged a collective effort to resolve the sequence of histological and molecular events giving rise to these tumours in the Fallopian tube. The serous carcinogenic sequence involves not only frank malignancies with metastatic spread, but also serous cancer precursors, including latent precursors – the p53 signature – and serous tubal intraepithelial neoplasms (STINs). The latter include intramucosal carcinomas (STICs) and lesser but immunophenotypically similar atypias that are considered premalignant intraepithelial lesions (STILs) [4,5]. Virtually all serous cancer precursors contain mutations in *TP53*, evidence of a DNA damage response (γ-H2AX^{p}), and predominate in the distal Fallopian tube [4]. Contiguous benign (p53 signatures) and malignant (STICs) epithelia have been documented with shared mutations in specific codons of *TP53* [4,6]. In addition, further studies have unearthed other benign epithelial alterations, termed secretory cell outgrowths (SCOUTs), that do not contain *TP53* mutations or evidence of a DNA damage response, yet share with precursors and carcinomas loss of PAX2 expression [7–9]. SCOUTs do not appear directly linked to HGSC, but have been documented at higher frequency in the normal tubes of postmenopausal women and those with HGSC [8,9]. Based on these properties, we have designated SCOUTs as 'surrogate precursors' and hypothesize that both SCOUTs and serous cancer precursors share properties or similar mechanisms in their pathogenesis, albeit with different potential outcomes.

The shared loss of PAX2 expression in both SCOUTs and many 'true' serous cancer precursors suggests that inactivation of this gene, while integral to neoplasia, has a wider range of associations and may signify a generic pathway common to epithelial cell expansion. The goals of this study were, firstly, to determine the breadth of the PAX2^{n} immunophenotype in the Fallopian tube by examining 'normal' cell growth and differentiation *in vitro* and *in vivo*. Secondly, we wanted to characterize more fully the alterations in expression that typified SCOUTs by array analysis and employ a biomarker profile to determine whether the SCOUT signature was recapitulated in STINs and HGSCs.

Materials and methods

Case material

This study was approved by the Brigham and Women's Human Investigation Committee and involved the use of discarded fresh and archived tissues. Case material for antibody staining consisted of the following epithelia/lesions: (1) normal salpingeal epithelium ($n = 15$); (2) SCOUTs ($n = 44$) and other outgrowths such as transitional-like metaplasia [Walthard cell nests (WCNs), $n = 5$]; (3) serous tubal intraepithelial neoplasms (STINs) ($n = 18$); and (4) metastatic or invasive serous carcinomas ($n = 39$). In addition, cultured clonogenic cells from normal Fallopian tubes were examined for selected marker expression. Cases for immunohistochemistry were selected by one of us (CPC) using previously described criteria (Figure 1) [10].

Cell culture

Fimbrial tissue was obtained from discarded surgical specimens of women undergoing benign procedures. Discarded fetal oviductal tissues were obtained by parental consent under an approved IRB protocol. Disaggregated cells were cultivated onto a feeder layer

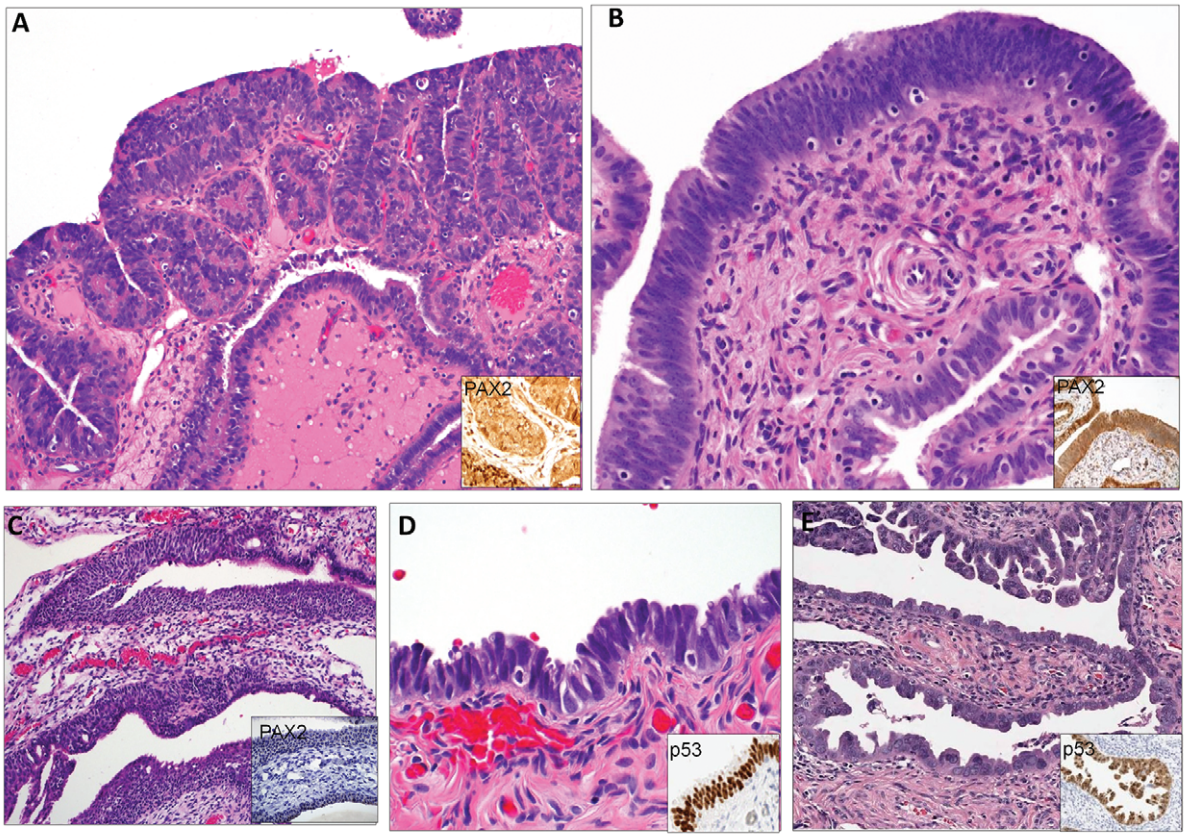

Figure 1. Entities associated with the PAX2^{n} immunophenotype included (A) type 1 secretory cell outgrowths (SCOUTs), (B) type 2 SCOUTs, (C) Walthard cell nests, and (D) low- and (E) high- (serous tubal intraepithelial carcinoma) grade tubal intraepithelial neoplasia.

of lethally irradiated 3 T3-J2 cells in stem cell culturing media (Jackson Laboratory, scm003). Clonal analysis and *in vitro* 3D differentiation were based on previously described methods for lung epithelial stem cells [11].

Microarray and bioinformatics

In order to identify genes expressed in PAX2^n epithelium, expression arrays were generated from formalin-fixed, laser-capture-micro-dissected (LCM) PAX2^n SCOUTs and benign control oviductal epithelium. RNAs obtained from the LCM procedure were amplified using the Ovation FFPE WTA System, WT-Ovation Exon Module, and Encore Biotin Module (NuGEN Technologies, San Carlos, CA, USA) and hybridized onto GeneChip® Human Exon 1.0 ST Arrays. GeneChip operating software was used to process all the Cel files and calculate probe intensity values. To validate sample quality, hybridization ratios were calculated using Affymetrix Expression Console software. The intensity values were $\log_2$-transformed and imported into the Partek Genomics Suite. Exons were summarized to genes and a one-way ANOVA was performed to identify differentially expressed genes. *p* values and fold change were calculated for each analysis. Heat maps were generated using Pearson's correlation and Ward's method with selected genes based on *p* value. Pathway analyses were performed using Gene Set Enrichment Analysis (GSEA) software. Candidate biomarkers were culled from these arrays and are summarized in Supplementary Table 1.

Immunohistochemistry

Immunostaining was performed with attention to the biomarkers in Supplementary Table 1, in which product information and dilutions are included. When normal-appearing epithelia were scanned for putative PAX2^n secretory cells, sections were immunostained with two antibodies concurrently: PAX2, which stains non-ciliated cells, and FOXJ1, a ciliated cell marker. Antibodies to leukocyte common antigen (LCA) for CD3, as well as FASCIN, were also used to track intraepithelial lymphocytes and dendritic cells, which are normally PAX2^n. Detection was completed with the Vectastain ABC kit (Cat No PK-6102; Vector Laboratories, Inc, Burlingame, CA, USA) with a liquid DAB-plus substrate kit (Cat No 00-2020). Slides were counterstained with Hematoxylin Stain 3 (Cat No CS402-1D). Antibody information is summarized in Supplementary Table 1. Reaction to antibody staining is indicated by superscripted 'p' or 'n' for positive or negative (PAX2, ALDH1, FOXJ1, etc), superscripted 'm' or 'wt' for mutated or wild type (p53), and superscripted 'nc' or 'mem' for nuclear and cytoplasmic versus membrane localization (β-catenin). Immunohistochemistry, immunofluorescence staining, and image acquisition were performed as previously described [9,11]. Proliferating clones were identified and immunostained for PAX2, PAX8, FOXJ1, Krt7, Krt5, p63, EZH2, and Ki67. Evidence of ciliated cell differentiation was identified by immunostaining for FOXJ1 and acetylated alpha-tubulin. Basal cells were identified by Krt5 or p63 immunostaining.

Results

Histological sub-classification of SCOUTs and STINs

The lesions under study are illustrated in Figure 1. Based on previous studies, SCOUTs were subdivided into two general histological categories [8,12]. The first, designated as type 1 SCOUTs, consisted of a typical mono- or bi-phasic tubal epithelial composition with either single layers of tubal non-ciliated cells or (more commonly) a combination of non-ciliated and ciliated cells. The second, arbitrarily labelled type 2 SCOUTs, consisted of proliferations with mildly pseudostratified and closely arranged elongated fusiform nuclei, similar to endometrial epithelium, and also termed 'endometrioid' SCOUTs. Cells with ciliated differentiation (FOXJ1^p) were present, but were typically less than 30% of the cells and scattered throughout the epithelium. Walthard cell nests (WCNs), consisting of basal cell outgrowth with a squamo-transitional phenotype, were also studied because they signify another form of outgrowth derived from columnar epithelial cells, albeit metaplastic. STINs were sub-classified as previously described and contained strong p53 immunostaining and evidence of DNA damage by H2AX staining [5]. Those with mild or moderate atypia and preserved epithelial polarity were classified as low grade and are identical to lesions classified as 'STILs', 'TILTs', and atypical hyperplasia in other reports [13–15]. Those with conspicuous loss of epithelial polarity were classified as high grade, synonymous with serous tubal intraepithelial carcinoma (STIC). The latter have a 0–11% outcome risk of HGSC, based on recent studies [16–18]. The HGSC outcome risk of lower-grade STINs is unknown but presumed to be less than that of high-grade STINs.

In vitro and *in vivo* expression of PAX2 in the Fallopian tube mucosa

Cultured epithelial cells from the gynaecological tract, both in adults and at 20 weeks' gestation, were plated and colonies of clonogenic cells were characterized. The dominant immunophenotype associated with highly-proliferative clonogenic cell outgrowth was Krt7^p/PAX8^p/EZH2^p/ PAX2^n/Krt5^n/p63^n (Figures 2A, 3A, and Supplementary Figure 2A). FOXJ1 expression indicating ciliated cell differentiation was also seen occasionally in the non-proliferative cells that were not stained positively with Ki67 (Figure 2A). To examine the differentiation ability of these cloned cells at the single-cell level, we established single-cell pedigree lines by subsequent rounds of plating and clone selection (Figure 2B). Pedigree lines of these cloned oviductal progenitor cells were differentiated

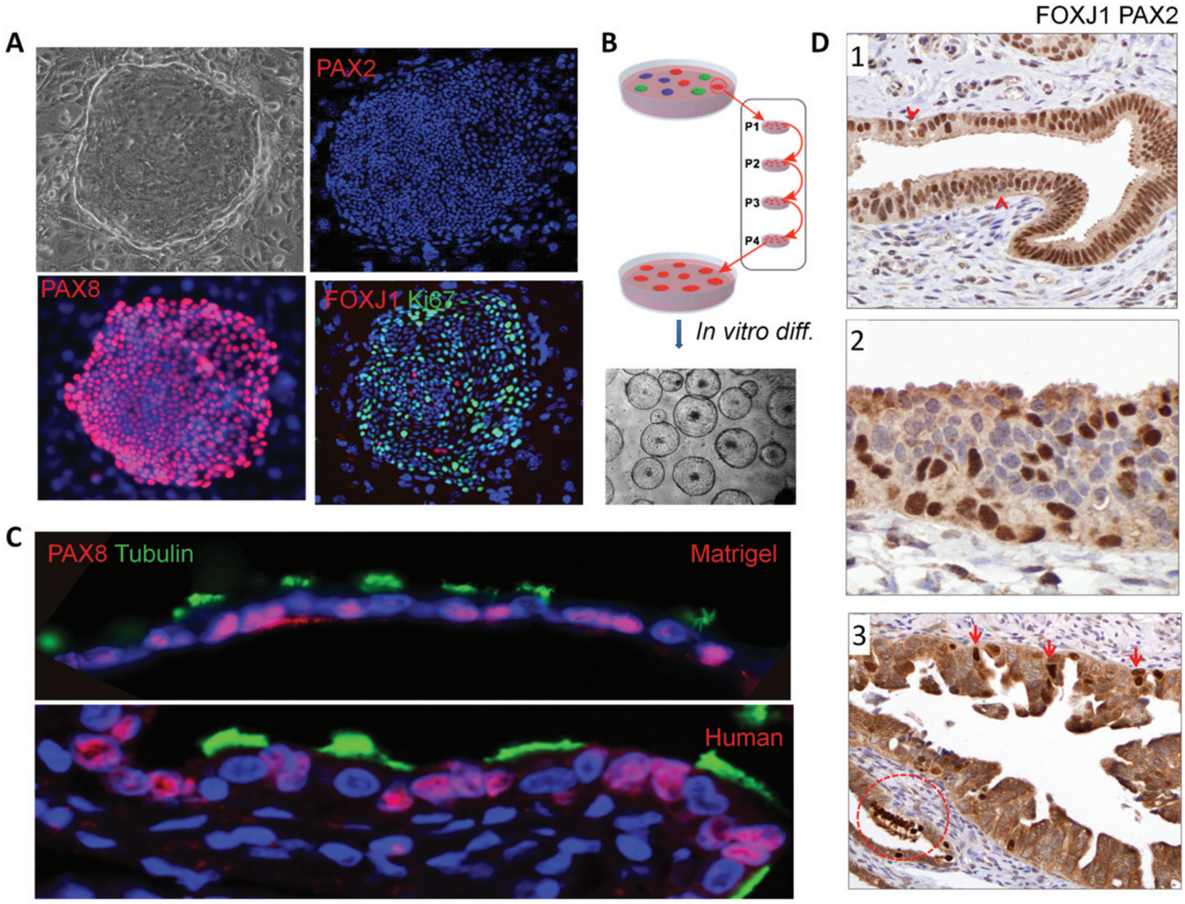

Figure 2. *In vitro* propagation and differentiation of oviductal progenitor cells. (A) The cells cloned from fetal or adult oviduct are PAX2^{n}, PAX8^{p} and occasionally express differentiation marker (FOXJ1) in non-proliferative cells (Ki67^{n}). (B) Schematic diagram of pedigree cell line establishment. (C) Upper panel: representative image of fetal (20-week) oviductal progenitor cells differentiated in 3D Matrigel culture system. Lower panel: immunofluoresence image of human adult oviduct epithelium. Acetyl-alpha-tubulin (green) indicates ciliated cell differentiation. PAX8 (red) indicates non-ciliated cells. DAPI stains nuclei (blue). (D1) Combined staining of histological sections of normal tube with both PAX2 and FOXJ1 reveals widespread nuclear staining, except occasional lymphocytes (arrows). (D2) Occasional foci of multi-layered epithelium undergoing ciliated cell differentiation (positive nuclei) consist of some cells negative for PAX2. (D3) Tubal intraepithelial carcinoma with focal FOXJ1 staining (arrowheads) indicating ciliated cell differentiation. Circled focus of normal ciliated cells is an internal positive control.

in either an air–liquid interface (ALI) cell culture system or 3D Matrigel cultures for 10–20 days. In 3D Matrigel cultures, PAX8^{p} oviductal progenitor cells differentiated into columnar epithelium consisting of acetylated tubulin^{p}/FOXJ1^{p}/PAX8^{n} ciliated cells and PAX8^{p} non-ciliated cells, which resembles the human oviduct histology (Figure 2C). In the ALI culture system, a series of images of acetylated tubulin expression were taken at different time points during the differentiation and showed that the oviductal progenitor cells started to differentiate into ciliated cells at day 3 and became maturely differentiated at day 10 (Supplementary Figure 2B). At day 10 in the ALI culture system, the cloned oviductal progenitor cells formed a simple epithelium with ciliated cells marked by FOXJ1 and acetylated tubulin and non-ciliated cells marked by PAX2 (Supplementary Figure 2C). It is noteworthy that while the proliferating population is PAX2^{n} (Figure 2A), PAX2 expression was reclaimed in some non-ciliated (secretory) cells. This further indicates that the progeny of a single oviductal progenitor cell can give rise to all epithelial lineages typically found in the oviduct, including not only mature ciliated cells but also non-ciliated (secretory) cells.

Immunostaining of both fetal and adult Fallopian tubes was performed to ascertain the distribution of PAX2-expressing cells and address the possibility that the PAX2^{n} immunophenotype was programmed earlier in development. Histological sections of fetal (at 21 weeks) and adult Fallopian tubes were examined. Fetal tubes contained an abundance of PAX2^{p} cells, with occasional interspersed ciliated cells (Supplementary Figure 1A). Expression of PAX8 was similar in distribution (Supplementary Figure 1B). Similarly, in normal adult tubes, PAX2 staining was extensive in cells that were not undergoing ciliated (tubulin^{p}) differentiation (Supplementary Figure 1C). A summary of immunophenotypes for progenitor and adult cells is displayed in Supplementary Table 2.

In the adult tubes, sections were also stained with FOXJ1, and/or LCA to account for other PAX2^{n}

cells that were either undergoing ciliated differentiation or were non-epithelial. Mono-layered or mildly pseudostratified normal Fallopian tube mucosa typically contained cells expressing either PAX2 or FOXJ1 (Figure 2D1). In occasional foci of prominent multi-layered epithelium with some cells staining positive with FOXJ1, loss of PAX2 nuclear staining could be seen (Figure 2D2), giving the impression that loss of PAX2 expression in non-ciliated cells was coordinated with cell growth in multi-layered epithelium. Albeit less so, FOXJ1 staining was also seen in STINs, supporting ciliated differentiation in PAX2^n neoplastic growth (Figure 2D3).

Metaplastic (WCNs) differentiation of PAX2^n columnar cells *in vitro* and *in vivo*

WCNs are foci of transitional-like metaplasia in the fimbria or adjacent peritoneal surface and are emblematic of basal cell outgrowth that can develop near the junctions of disparate epithelial types [19]. Other sites include the gastro-oesophageal and cervical squamo-columnar junctions. Both have been designated as sites harbouring residual embryonic cells and studies of the latter have suggested that basal or reserve cells emerge from the overlying columnar cells and then undergo squamous metaplasia [20,21]. This process has been termed 'top-down' differentiation, ie the progeny (basal cells) emerge from beneath the progenitor population. However, no study has ever displayed this sequence *in vitro*. Fetal tubal cells propagated *in vitro* were strongly positive for both Krt7 and PAX8, in keeping with Müllerian epithelium (Figures 2A and 3A). Moreover, these progenitor cells did not express Krt5 or p63 (Figure 3A). Interestingly, when pedigree lines of these cloned oviductal progenitor cells were differentiated in 3D Matrigel cultures for 10–20 days, in addition to the typical ciliated cell differentiation (Figure 2C), subjacent p63/Krt5^p basal cells emerged (Figure 3B1) and expanded (Figure 3B3) in a pattern similar to that

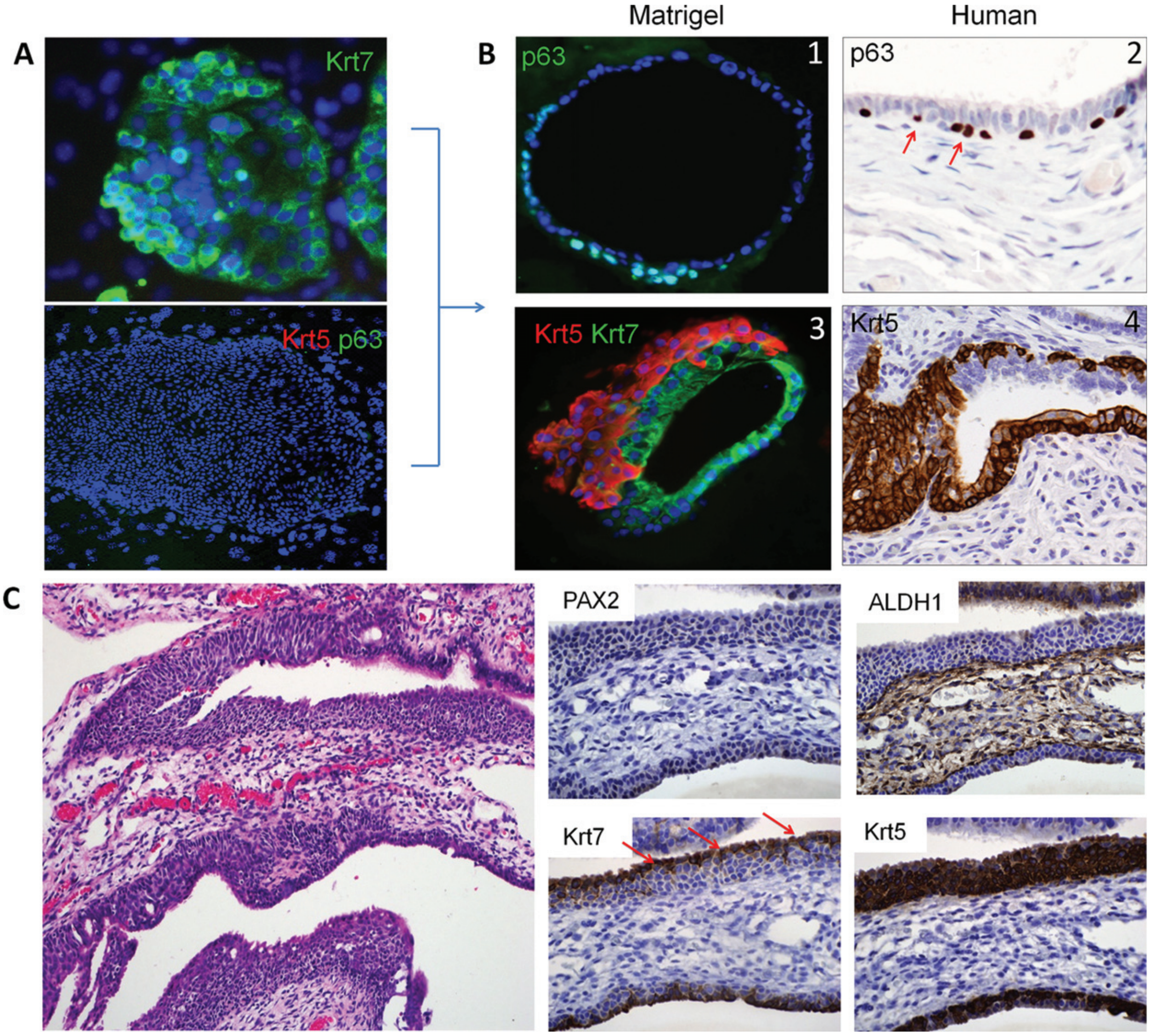

Figure 3. *In vitro* and *in vivo* basal cell differentiation in the oviduct. (A) Colonies of Krt7^p/Krt5^n/p63^n cells from a 20-week-old fetal oviduct. (B1, B3) Single (p63, green) and multi-layered (Krt5, red) basal cell outgrowth seen in Matrigel cultures. (B2, B4) Similar basal cell growth highlighted by p63 and Krt5 in the adult fimbria. (C) Walthard cell nest in the adult tube is typically PAX2 and ALDH1 negative. Residual Krt7-positive cells (arrows) are displaced from beneath by an expanding Krt5 population.

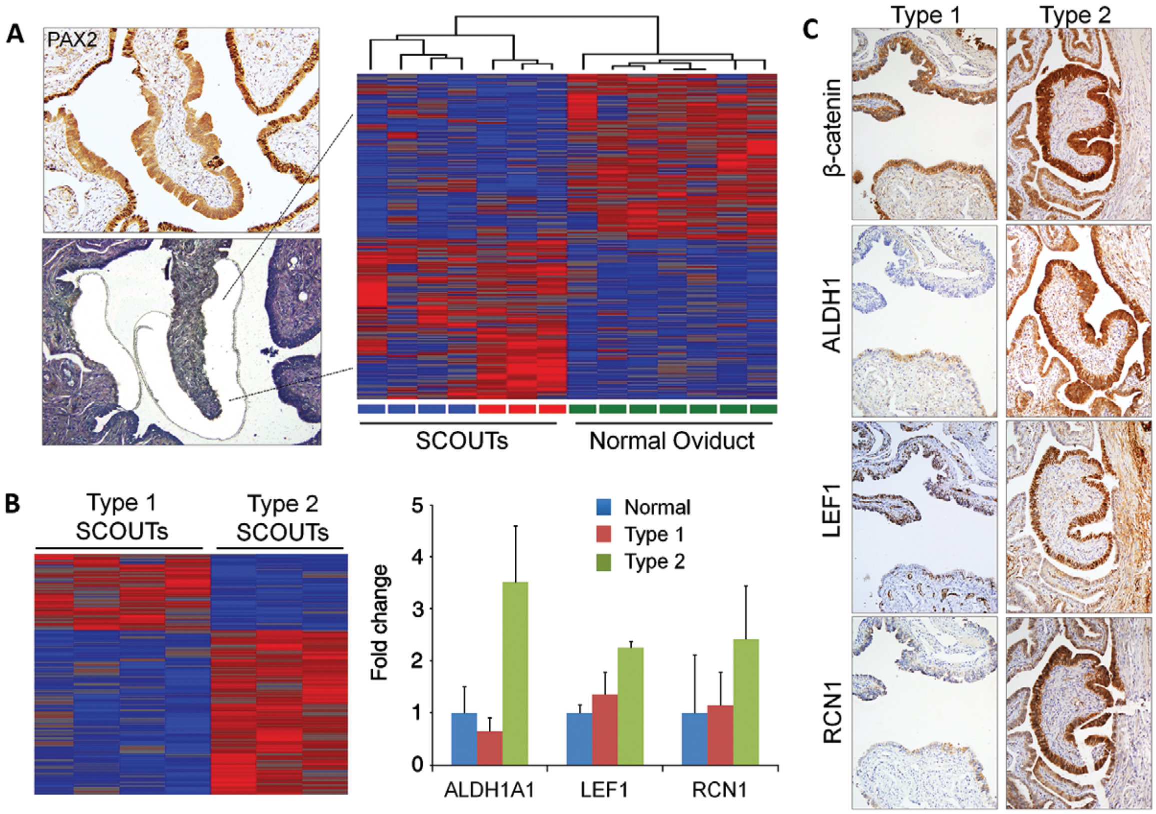

Figure 4. (A) Laser-captured micro-dissected SCOUTs (left) and a heat map comparison of SCOUTs and normal oviduct (right). (B) Arrays generated from PAX2^{n} SCOUTs revealed genes differentially expressed across type 1 and type 2 SCOUTs, including ALDH1, LEF1, and RCN1 (right). (C) Coordinated expression of the above genes distinguish type 1 SCOUTs, which show membraneous β-catenin localization and absent ALDH1 staining plus negative or weak staining for LEF1 and RCN1 staining (left), from type 2 SCOUTs, with nuclear and cytoplasmic β-catenin, strong ALDH1, LEF1, and RCN1 staining (right).

seen in p63/Krt5^{p} cells in WCNs in the adult tube (Figures 3B2 and 3B4). *In vitro*, the Krt5 and p63 immunopositive cells were superimposed, although the Krt5 staining index was higher (Supplementary Figure 2E). Analysis of WCNs in tissue sections (Figure 3C) revealed a strikingly similar pattern of growth and differentiation, arising either from beneath Krt7^{p} epithelial cells or in continuity with columnar epithelium typical of type 1 SCOUTs. The result was a PAX2^{n}/ALDH1^{n} transitional-like outgrowth that was strongly Krt5^{p} but stathmin^{n} (not shown). Taken in the context of the *in vitro* findings, this observation further linked the PAX2^{n} immunophenotype to cell outgrowth and a Krt7^{p} progenitor cell to the development of not only terminal (FOXJ1^{+}) but also metaplastic (Krt5^{+}) differentiation in the Fallopian tube.

Altered gene expression in PAX2^{n} proliferations (SCOUTs, STINs, and HGSCs)

Supplementary Table 3 is a list of genes selected for analysis and found to be differentially expressed in SCOUTs relative to normal-appearing epithelium. Arrays generated from RNA extracted from formalin-fixed laser-capture micro-dissected SCOUTs yielded differentially expressed genes, illustrated in the representative heat map (Figures 4A, 4B, and Supplementary Figures 4 and 5). When stained with selected markers, type 1 SCOUTs varied from strictly secretory to mixed secretory and ciliated, and were ALDH1^{n}, β-catenin^{mem} and stained weakly or negative for LEF1, RCN1, RUNX2, and EZH2 (Figures 4C, 5, and Supplementary Figure 3). Type 2 SCOUTs stained variably for ciliated cell differentiation and were β-catenin^{nc} and ALDH1, LEF1, RCN1, EZH2, RUNX2 (not shown) and stathmin positive (Figures 4C, 5, and Supplementary Figure 3). Basal cell differentiation, signifying WCN development, was associated with PAX2^{n} columnar epithelium, suggesting that this pathway of differentiation might initiate within type 1 PAX2^{n} SCOUTs.

Figure 5 and Supplementary Figure 6 summarize the staining patterns observed in the different lesions. STINs and HGSCs shared expression of several markers with SCOUTs. Expression patterns for ALDH and β-catenin were identical to type 1 SCOUTs (ALDH^{n} and β-catenin^{mem}). In addition, like type 2 SCOUTs, there was increased staining for EZH2, stathmin, LEF1, RCN, Krt5, and RUNX2 (not shown). Not surprisingly, no marker in this group separated STINs or HGSCs from SCOUTs. This is in contrast to other published markers such as Ki67, cyclin E, p16, and others, which are significantly more commonly expressed in STINs and HGSCs relative to benign Fallopian tube mucosa [4,5,15,22].

Published by John Wiley & Sons, Ltd. www.pathsoc.org.uk

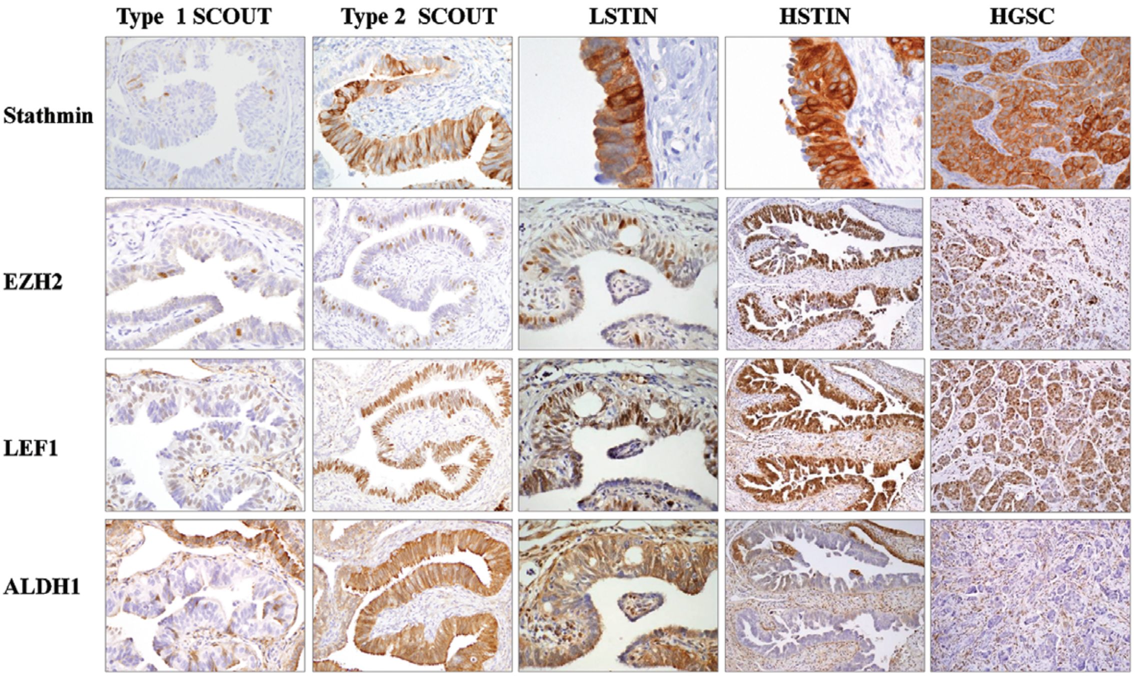

Figure 5. Shared expression of SCOUT markers with low- (LSTIN) and high- (HSTIN or STIC) grade serous tubal intraepithelial neoplasia and high-grade serous carcinoma (HGSC). Neoplasms (STINs, HGSCs) share with type 1 SCOUTs loss of PAX2 and ALDH1, and with type 2 SCOUTs, increased LEF1, EZH2, and stathmin and other markers (see text).

Discussion

Analysis of arrays generated from high-grade serous cancer has confirmed a transcriptome that parallels oviductal epithelium [23]. Given that these tumours are strongly positive for biomarkers (such as PAX8) typically assigned to non-ciliated (so-called secretory) cells, the assumption has been that the secretory cell is the cell of origin [1]. Levanon *et al* showed that PAX8-expressing (secretory) cells of the tube were uniquely susceptible to DNA damage imposed by irradiation, a finding that parallels similar observations in latent precursors (p53 signatures) and STINs that contain *p53* mutations [5,24]. However, with the discovery of PAX2^{n} SCOUTs and a similar PAX2^{n} expression pattern in many STINs, it became clear that there may be a relationship between the two entities, despite the fact that SCOUTs are more ubiquitous in the Fallopian tube and do not arise in the setting of a DNA damage response and loss of p53 function. Although altered PAX2 expression has been associated with neoplasia, we hypothesized that the PAX2^{n} immunophenotype typified a 'generic' series of molecular events that were the underpinning of stem cell expansion common to many proliferations.

We addressed PAX2 expression or loss in the Fallopian tube from three perspectives. The first was by analysing expression and differentiation in proliferating normal adult and fetal cells propagated *in vitro*. The second was by comparing the *in vitro* findings to expression in tissue sections from fetal and adult tubes. The third was to look for shared expression across PAX2^{n} cells in cell proliferation and expansion (SCOUTs, STINs, and HGSCs). We discovered that the PAX2^{n} immunophenotype was particularly linked to *in vitro* and *in vivo* cell growth, not infrequently with an increase in EZH2 expression. Moreover, in highly clonogenic Krt7^{p}/FOXJ1^{n} oviductal progenitor cells grown *in vitro*, we demonstrated for the first time that PAX2^{n} expanding populations were capable of both ciliated (FOXJ1) and basal cell (Krt5) differentiation. This sequence of cell growth and differentiation was recapitulated in SCOUTs, STINs, and HGSCs, with progressively reduced ciliated differentiation in the type 2 SCOUTs, STINs, and HGSCs. We thus concluded that all of these entities were related to a similar progenitor cell.

The next goal was to determine if the cells involved in benign and neoplastic outgrowth shared common expression patterns and we chose to use the least proliferative lesions (SCOUTs) as the reference. One advantage of this approach is to identify events that occur prior to the more dramatic molecular changes that characterize malignancy that may have profound influences on expression. The study delineated two general groups of SCOUTs: the first (type 1) closely resembled normal tubal epithelium, histologically and in their expression profile (Figure 1D). The second (type 2) was composed of proliferations with less pronounced ciliated differentiation, many noticeably 'endometrial'-like (Figure 1E). Accordingly, there was minimal difference in expression between type 1 SCOUTs and control epithelium, although they were consistently ALDH1^{n}. In contrast, type 2 SCOUTs demonstrated nuclear and cytoplasmic β-catenin staining plus increased BCL2 (see ref 7), ALDH1, and Krt5 staining. This diversity in phenotype underscores the complexity of cell growth and differentiation that can occur in the Fallopian tubes with age. Type 1 SCOUTs appear to signify very minor genomic changes, as evidenced by the similarities in transcription to normal controls. Thus, the alterations in transcription are limited to absence of ALDH1 expression. In contrast, type 2 SCOUTs, which exhibit a more divergent histology, have a common biomarker signature – stathmin, EZH2, LEF1, RCN1, and RUNX2 – that is more similar to premalignant (STINs) and malignant (HGSCs) entities in the tube (Figure 5).

A fundamental question stemming from the above observation is the relevance of the gene signature found in SCOUTs, STINs, and HGSCs to both stem cell biology and neoplasia. ALDH1 has been identified as a marker of epithelial stem cells. Its expression can be both increased or absent, the latter more typical of STINs and HGSCs [25,26]. EZH2 is a polycomb suppressor that is implicated in stem cell maintenance and regulation of differentiation. It is noteworthy that EZH2 expression typically increased in areas of cell expansion, in keeping with the coordinated suppression of PAX2 expression [27]. EZH2 is also a potential suppressor of tumour suppressor genes [28]. LEF1 is likewise expressed during lineage differentiation [29]. The function of RCN1 is less clear but this gene product is a calcium binder that is weakly expressed in renal tubular cells and up-regulated in renal cell carcinomas [30]. *RUNX2* is a gene involved in morphogenesis and osteoblastic differentiation [31]. Functions attributed to stathmin are multiple. It is a marker of P13 kinase activation that has been linked to serous neoplasia in some studies, tumour progression and metastases in others, and regulates p53 stability in still others [32–34]. Its range of expression, including normal epithelium, SCOUTs, and STINs, is similar to that of these other markers, several of which (ALDH1, PAX2, EZH2) have also been linked to not only stem cells but also outcome or resistance to chemotherapy [35–37]. The significance of the unique β-catenin staining in type 2 SCOUTs, with a shift in distribution from the membrane to the cytoplasm and nucleus, is unclear but it is emblematic of Wnt pathway activation, and mutations in β-catenin are commonly found in endometrial and colon carcinomas [38].

Walthard cell nests are a common benign condition seen in the distal Fallopian tube mucosa or the adjacent peritoneal reflection [19]. They bear a close resemblance to the cervical squamo-columnar junction, where columnar cells are undermined by p63-positive basal cells. These cells could be envisioned to either originate from the columnar epithelium or give rise to the overlying Krt7-positive epithelial cells. This study has made two novel observations. First, based on the Matrigel cell culture data, the basal cells emerge from the Krt7-positive columnar cells. Second, this process is marked by not only loss of PAX2 but also ALDH1 expression, similar to that seen in type 1 SCOUTs. The initiating cell, the Krt7^{p} non-ciliated epithelial cell, is remarkably similar to the cells seen in the squamo-columnar (SC) junction of the cervix from which squamous metaplasia is derived and this process is similar to so-called 'top-down' differentiation reported in the SC junction [21]. The fact that

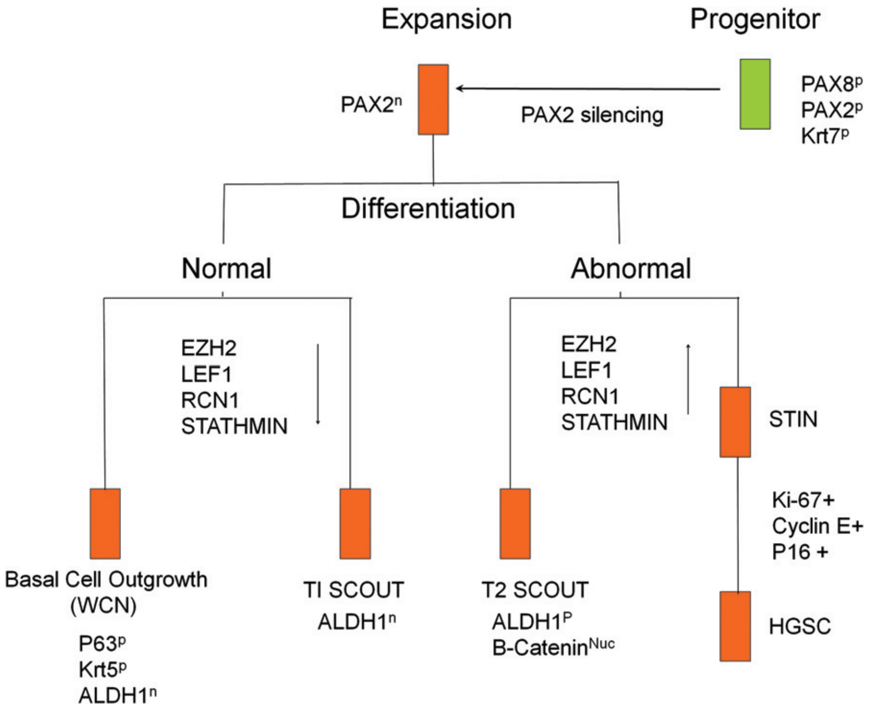

Figure 6. A progenitor cell model for the Fallopian tube in which Krt7 identifies the progenitor cell and PAX2^{n} defines progenitor cell expansion. Expanding PAX2^{n} cells can differentiate into basal or ciliated cells in WCNs or type 1 SCOUTs, both of which approximate normal differentiation pathways, with loss of ALDH1 and normal or minimally increased expression of LEF1, RCN1, stathmin, and EZH2. In contrast, type 2 SCOUTs and STINs (right) share a different expression signature characterized by multiple genes, including EZH2, LEF1, RCN1, and stathmin and others, involved in a divergent pathway of progenitor cell growth.

WCNs are not considered direct precursors to malignancy is not surprising, in as much as they are terminally differentiated relative to their progenitors. This is similar to the cervix, where the progenitor cells in the SC junction are considered more vulnerable to neoplastic transformation than their metaplastic progeny [21]. What is interesting is the fact that WCNs underscore the existence of multi-potential cells in the distal Fallopian tube [12]. Given that 40–60% of HGSCs do not have a documented source (or STIN) in the Fallopian tube mucosa, coupled with the fact that a subset of HGSCs are strongly Krt5-positive, the possibility that cells involved in alternate differentiation pathways might contribute to a subset of these malignancies deserves further study (Hanamornroongruang S, Howitt BE, Crum CP, unpublished) [5,25].

Epithelia in virtually every organ (breast being a prime example) display a wide range of clonal expansions, some of which may be direct precursors to malignancy and others of which serve as risk factors for a malignant outcome. The model depicted in Figure 6 reflects a similar but novel scenario in the oviduct, with multiple categories of putative monoclonal cell outgrowth and striking similarities in expression across multiple genes between surrogate precursors and lesions that are considered premalignant or pre-metastatic. These findings emphasize the complexity of molecular and phenotypic perturbations that can take place in the Fallopian tubes during and following menopause. This complexity invites caution when considering the role (or diagnostic value) of newly discovered biomarkers as specific indicators of neoplasia. More importantly, it reveals a consistent disturbance in progenitor cell biology in keeping with a common pathway that is triggered by more than one initiating event. Thus, it introduces two approaches to cancer prevention, one directed at the initiating event and the other at the early perturbations in the pathway.

Acknowledgments

This work was supported by grants from the Department of Defense and National Cancer Institute (W81XWH-10-1-0289 and 5R21CA173190-02 to CC). We thank the Division of Gynecologic Oncology at Brigham and Women's Hospital and Dana Farber Cancer Institute for their contribution to the study, and Mei Zheng for assistance with the immunohistochemistry. We are also grateful for the support of this work by the Genome Institute of Singapore of the Agency for Science, Technology and Research, and a Bedside and Bench Grant from Singapore National Medical Research Council.

Author contribution statement

Contributions of the co-authors to design (1), data collection (2), data analysis (3), data interpretation (4), literature search (5), figures (6), and manuscript writing (7) were as follows: GN (1–4, 6, 7); JGB (1–4, 6, 7); YY (1–3, 6); XW (2, 3); BEH (1, 2, 4, 5); MH (1–4); EY (1–3, 5); YH (2–4); MC (2–4); LW (2–4); SH (2–4); FDMcK (1, 4, 7); CPCr (1, 4, 7); and WX (1, 3, 4, 7).

Abbreviations

ALI, air–liquid interface culture; SCOUT, secretory cell outgrowth; STIN, serous tubal intraepithelial neoplasia; WCN, Walthard cell nest

References

1. Piek JM, van Diest PJ, Zweemer RP, *et al.* Dysplastic changes in prophylactically removed Fallopian tubes of women predisposed to developing ovarian cancer. *J Pathol* 2001; **195:** 451–456.
2. Kindelberger DW, Lee Y, Miron A, *et al.* Intraepithelial carcinoma of the fimbria and pelvic serous carcinoma: evidence for a causal relationship. *Am J Surg Pathol* 2007; **31:** 161-169.
3. Finch A, Shaw P, Rosen B, *et al.* Clinical and pathologic findings of prophylactic salpingo-oophorectomies in 159 BRCA1 and BRCA2 carriers. *Gynecol Oncol* 2006; **100:** 58-64.
4. Lee Y, Miron A, Drapkin R, *et al.* A candidate precursor to serous carcinoma that originates in the distal Fallopian tube. *J Pathol* 2007;211:26-35. Erratum in *J Pathol* 2007; **213:** 116.
5. Crum CP, Herfs M, Ning G, *et al.* Through the glass darkly: intraepithelial neoplasia, top-down differentiation and the road to ovarian cancer. *J Pathol* 2013; **231:** 402-412.
6. Carlson JW, Miron A, Jarboe EA, *et al.* Serous tubal intraepithelial carcinoma: its potential role in primary peritoneal serous carcinoma and serous cancer prevention. *J Clin Oncol* 2008; **26:** 4160-4165.
7. Chen EY, Mehra K, Mehrad M, *et al.* Secretory cell outgrowth, PAX2 and serous carcinogenesis in the Fallopian tube. *J Pathol* 2010; **222:** 110-116.
8. Quick CM, Ning G, Bijron J, *et al.* PAX2-null secretory cell outgrowths in the oviduct and their relationship to pelvic serous cancer. *Mod Pathol* 2012; **25:** 449-455.
9. Bijron JG, Ning G, Laury AR, *et al.* Digital quantification of precursor frequency in the Fallopian tube and its significance. *Mod Pathol* 2012; **25:** 1654-1661.
10. Mehrad M, Ning G, Chen EY, *et al.* A pathologist's road map to benign, precancerous, and malignant intraepithelial proliferations in the Fallopian tube. *Adv Anat Pathol* 2010; **17:** 293-302.
11. Kumar PA, Hu Y, Yamamoto Y, *et al.* Distal airway stem cells yield alveoli *in vitro* and during lung regeneration following H1N1 influenza infection. *Cell* 2011; **147:** 525-538.
12. Laury AR, Ning G, Quick CM, *et al.* Fallopian tube correlates of ovarian serous borderline tumors. *Am J Surg Pathol* 2011; **35:** 1759-1765.
13. Vang R, Visvanathan K, Gross A, *et al.* Validation of an algorithm for the diagnosis of serous tubal intraepithelial carcinoma. *Int J Gynecol Pathol* 2012; **31:** 243-253.
14. Ning G, Bijron JG, Yuan J, *et al.* Differential expression of p-ERM, a marker of cell polarity, in benign and neoplastic oviductal epithelium. *Int J Gynecol Pathol* 2013; **32:** 345-352.
15. Lee S, Nelson G, Duan Q, *et al.* Precursor lesions and prognostic factors in primary peritoneal serous carcinoma. *Int J Gynecol Pathol* 2013; **32:** 547-555.
16. Wethington SL, Park KJ, Soslow RA, *et al.* Clinical outcome of isolated serous tubal intraepithelial carcinomas (STIC). *Int J Gynecol Cancer* 2013; **23:** 1603-1611.

17. Lowell CB, Swisher EM, Cass I, *et al.* Long term follow up of *BRCA1* and *BRCA2* mutation carriers with unsuspected neoplasia identified at risk reducing salpingo-oophorectomy. *Gynecol Oncol* 2013; **129:** 364-371.
18. Conner JR, Meserve E, Pizer E, *et al.* Outcome of unexpected adnexal neoplasia discovered during risk reduction salpingo-oophorectomy in women with germ-line *BRCA1* or *BRCA2* mutations. *Gynecol Oncol* 2014; **132:** 280-286.
19. Seidman JD, Yemelyanova A, Zaino RJ, *et al.* The Fallopian tube-peritoneal junction: a potential site of carcinogenesis. *Int J Gynecol Pathol* 2011; **30:** 4-11.
20. Wang X, Ouyang H, Yamamoto Y, *et al.* Residual embryonic cells as precursors of a Barrett's-like metaplasia. *Cell* 2011; **145:** 1023-1035.
21. Herfs M, Yamamoto Y, Laury A, *et al.* A discrete population of squamocolumnar junction cells implicated in the pathogenesis of cervical cancer. *Proc Natl Acad Sci U S A* 2012; **109:** 10516-10521.
22. Sehdev AS, Kurman RJ, Kuhn E, *et al.* Serous tubal intraepithelial carcinoma upregulates markers associated with high-grade serous carcinomas including Rsf-1 (HBXAP), cyclin E and fatty acid synthase. *Mod Pathol* 2010; **23:** 844-855.
23. Marquez RT, Baggerly KA, Patterson AP, *et al.* Patterns of gene expression in different histotypes of epithelial ovarian cancer correlate with those in normal Fallopian tube, endometrium, and colon. *Clin Cancer Res* 2005; **11:** 6116-6126.
24. Levanon K, Ng V, Piao HY, *et al.* Primary *ex vivo* cultures of human Fallopian tube epithelium as a model for serous ovarian carcinogenesis. *Oncogene* 2010; **29:** 1103-1113.
25. Deng S, Yang X, Lassus H, *et al.* Distinct expression levels and patterns of stem cell marker, aldehyde dehydrogenase isoform 1 (ALDH1), in human epithelial cancers. *PLoS One* 2010; **5:** e10277.
26. Flesken-Nikitin A, Hwang CI, Cheng CY, *et al.* Ovarian surface epithelium at the junction area contains a cancer-prone stem cell niche. *Nature* 2013; **495:** 241-245.
27. Chou RH, Yu YL, Hung MC. The roles of EZH2 in cell lineage commitment. *Am J Transl Res* 2011; **3:** 243–250.
28. Deb G, Singh AK, Gupta S. EZH2: not EZHY (easy) to deal. *Mol Cancer Res* 2014; **12:** 639-653.
29. Merrill BJ, Gat U, DasGupta R, *et al.* Tcf3 and Lef1 regulate lineage differentiation of multipotent stem cells in skin. *Genes Dev* 2001; **15:** 1688-1705.
30. Giribaldi G, Barbero G, Mandili G, *et al.* Proteomic identification of Reticulocalbin 1 as potential tumor marker in renal cell carcinoma. *J Proteomics* 2013; **91:** 385-392.
31. Yoshida T, Kanegane H, Osato M, *et al.* Functional analysis of *RUNX2* mutations in Japanese patients with cleidocranial dysplasia demonstrates novel genotype–phenotype correlations. *Am J Hum Genet* 2002; **71:** 724-738.
32. Karst AM, Levanon K, Duraisamy S, *et al.* Stathmin 1, a marker of PI3K pathway activation and regulator of microtubule dynamics, is expressed in early pelvic serous carcinomas. *Gynecol Oncol* 2011; **123:** 5-12.
33. Zheng P, Liu YX, Chen L, *et al.* Stathmin, a new target of PRL-3 identified by proteomic methods, plays a key role in progression and metastasis of colorectal cancer. *J Proteome Res* 2010; **9:** 4897-4905.
34. Sonego M, Schiappacassi M, Lovisa S, *et al.* Stathmin regulates mutant p53 stability and transcriptional activity in ovarian cancer. *EMBO Mol Med* 2014; **6:** 295.
35. Hueber PA, Waters P, Clark P, *et al.* PAX2 inactivation enhances cisplatin-induced apoptosis in renal carcinoma cells. *Kidney Int* 2006; **69:** 1139-1145.
36. Han X, Du F, Jiang L, *et al.* A2780 human ovarian cancer cells with acquired paclitaxel resistance display cancer stem cell properties. *Oncol Lett* 2013; **6:** 1295-1298.
37. Rizzo S, Hersey JM, Mellor P, *et al.* Ovarian cancer stem cell-like side populations are enriched following chemotherapy and overexpress EZH2. *Mol Cancer Ther* 2011; **10:** 325-335.
38. van der Zee M, Jia Y, Wang Y, *et al.* Alterations in Wnt-β-catenin and Pten signalling play distinct roles in endometrial cancer initiation and progression. *J Pathol* 2013; **230:** 48-58.

SUPPORTING INFORMATION ON THE INTERNET

The following supporting information may be found in the online version of this article:

Figure S1. Pax2 and acetyl-alpha-tubulin (cilia) expression in fetal and adult Fallopian tubes.

Figure S2. *In vitro* differentiation of oviduct progenitor cells.

Figure S3. Two types of PAX2^n SCOUTs are distinguished in these panels with β-catenin, keratin 5, and LEF1 staining.

Figure S4. Heat map comparing type 1 and type 2 SCOUTs with normal tubal epithelium and high-grade serous cancer.

Figure S5. A depiction, in tabular (A) and graphical format (B), of genes up-regulated with the two-fold change in type 2 relative to type 1 SCOUTs, several of which have been linked to STIN and HGSC.

Figure S6. H&E, p53, and PAX2 staining of cases under study (see Figure 5).

Table S1. Biomarkers selected for analysis of clonogenic cells, SCOUTs, and STINs.

Table S2. Summary of immunophenotypes in cultured progenitor cells and adult cells in tissue sections.

Table S3. Upregulated genes in Type 2 SCOUTs in comparison with Type 1 SCOUTs (3 fold and $p < 0.05$).